Publication No. FHWA-HIF-24-007
March 2024

U.S. Department of Transportation
Federal Highway Administration

Hydraulic Design Series No. 2

Highway Hydrology

Third Edition

Page Intentionally Left Blank

Technical Report Documentation Page

1. Report No. FHWA HIF-24-007	2. Government Accession No.	3. Recipient's Catalog No.	
4. Title and Subtitle Highway Hydrology Third Edition		5. Report Date March 2024	
		6. Performing Organization Code	
7. Author(s) Roger Kilgore, A. Tamim Atayee, George "Rudy" Herrmann, David B. Thompson		8. Performing Organization Report No.	
9. Performing Organization Name and Address Kilgore Consulting and Management 2963 Ash Street Denver, CO 80207		10. Work Unit No. (TRAIS)	
		11. Contract or Grant No. DTFH61-17-D-00035	
12. Sponsoring Agency Name and Address Office of Bridges and Structures Federal Highway Administration 1200 New Jersey Avenue, S.E. Washington, D.C. 20590		13. Type of Report and Period Covered Reference Manual September 2020 – June 2022	
		14. Sponsoring Agency Code	

15. Supplementary Notes
Project Managers: Stan Woronick, National Highway Institute; Cynthia Nurmi, National Highway Institute
Technical Reviewers: Joseph Krolak, Megan Frye, Matt Dillin, Luis Calderon, Daniel Sharar-Salgado
Technical and Editorial Assistance: Liberty Smith, Muhammad Sinjar

16. Abstract

This manual discusses the physical processes of the hydrologic cycle that are important to highway engineers. These processes include the approaches, methods, and assumptions applied in design and analysis of highway drainage structures.

Hydrologic methods of primary interest are frequency analysis for analyzing rainfall and flow data; empirical methods for peak flow estimation; and hydrograph analysis and synthesis. The manual describes the concept and several approaches for determining time of concentration and rainfall-runoff processes. It also provides information on hydrologic data sources and selecting tools for a given application.

The peak flow methods discussed include log-Pearson type III, regression equations, and the Rational Method. The technical discussion of each peak flow approach also includes urban development applications. The manual includes development of design hydrographs and design storms.

The manual presents common storage and channel routing techniques related to highway drainage hydrologic analyses and includes information on hydrologic modeling, uncertainty, and risk in hydrologic analysis applications. Special topics in hydrology include discussions of wetlands hydrology and mitigation design, snowmelt hydrology, and arid lands hydrology.

17. Key Words Hydrology, frequency analysis, peak flow, urban hydrology, hydrograph, storage routing, channel routing, stormwater management, hydrologic modeling, wetland hydrology, snowmelt hydrology, arid lands hydrology		18. Distribution Statement Unlimited distribution	
19. Security Classification (of this report) Unclassified	20. Security Classification (of this page) Unclassified	21. No. of Pages 349	22. Price N/A

Form DOT F 1700.7 (8-72) **Reproduction of completed page authorized**

Page Intentionally Left Blank

Table of Contents

List of Figures

List of Tables

Page Intentionally Left Blank

Acknowledgments

The cover image is State Highway 74 crossing Skeleton Creek north of Oklahoma City, Oklahoma. (Source: Oklahoma Department of Transportation).

In Figure 11.18, the base image is the copyright property of Google® Earth™ and can be accessed from https://www.google.com/earth (Google 2020). The authors developed the overlays and annotations.

Notice

This document is disseminated under the sponsorship of the U.S. Department of Transportation in the interest of information exchange. The U.S. Government assumes no liability for the use of the information contained in this document.

The U.S. Government does not endorse products or manufacturers. Trademarks or manufacturers' names appear in this document only because they are considered essential to the objective of the document. They are included for informational purposes only and are not intended to reflect a preference, approval, or endorsement of any one product or entity.

Unless noted otherwise, FHWA owns all photographs and graphics in this manual. The authors have designated images used from the public domain by their source.

Non-Binding Contents

Except for the statutes and regulations cited, the contents of this document do not have the force and effect of law and are not meant to bind the States or the public in any way. This document is intended only to provide information regarding existing requirements under the law or agency policies.

Quality Assurance Statement

The Federal Highway Administration (FHWA) provides high-quality information to serve Government, industry, and the public in a manner that promotes public understanding. The FHWA uses standards and policies to ensure and maximize the quality, objectivity, utility, and integrity of its information. The FHWA periodically reviews quality issues and adjusts its programs and processes to ensure continuous quality improvement.

Glossary

Accuracy:	The closeness of a statistic or measurements to the true value. It incorporates both bias and precision.
Air Convection Melt:	The portion of snowmelt occurring due to heat transferred from the air above a snowpack to a snowpack.
Albedo:	Fraction of incident radiation that is reflected by a surface or body.
Alluvial:	Soil and rock material deposited by flowing water.
Alluvial Fan:	A fan-shaped deposit of material at the place where a stream issues from a narrow valley of high slope onto a plain or broad valley of low slope. An alluvial cone is made up of the finer materials suspended in flow while a debris cone is a mixture of all sizes and kinds of materials.
Alluvial Stream:	A stream that has formed its channel in cohesive or noncohesive materials that have been and can be transported by the stream.
Annual Exceedance Probability:	The probability that the magnitude of the random variable (e.g., annual maximum flood peak) will be equaled or exceeded each year.
Annual Maximum Flow:	The largest instantaneous peak flow in a year.
Antecedent Moisture:	Water stored in the watershed prior to the start of rainfall.
Attenuation:	Reduction in the peak of a hydrograph as it moves downstream in the watershed, resulting in a broader time base and dampened hydrograph.
Base Flow:	Stream flow arising from the depletion of groundwater storage.
Bias:	A systematic error in a statistic or in measurements. A negative bias indicates underprediction, and a positive bias indicates overprediction.
Binomial Distribution:	A probability mass function used in hydrologic risk studies where there are only two possible outcomes for each trial.
Calibration:	The direct comparison of model results with a standard, reference or observation that allows parameter values to be modified with the goal of improving the comparison outcomes.
Celerity:	Propagation speed of a wave.
Channel Routing:	Mathematical processes that describe movement and attenuation of unsteady flow (normally a hydrograph) upstream to downstream in a stream channel. Normally used to calculate outflow from a stream channel.
Coefficient of Variation:	The ratio of the standard deviation to the mean.
Confidence Limits:	Statistical limits that describe an interval in which the true value of a statistic is expected to lie with the stated probability.

Confluence:	The junction of two or more streams.
Continuity Equation:	Based on conservation of mass, the continuity equation relates that (for incompressible flow) the flow rate equals the product of the flow velocity and the cross-sectional area.
Convolution:	The multiplication-translation-addition process used to route a rainfall-excess hyetograph using the unit hydrograph as the routing model.
Curve Number:	An index that represents the combined effects of soil characteristics, land cover, hydrologic condition, and antecedent soil moisture conditions on runoff.
Dead Storage:	Storage in a reservoir or detention basin below the elevation of the lowest outflow pathway.
Deterministic Methods:	A class of methods that contain no random components (in contrast to stochastic methods).
Dimensionless Hydrograph:	A hydrograph that has ordinates of the ratio of the flow to the peak flow and values on the abscissa of the ratio of time to the time to peak.
Direct Runoff:	The total runoff hydrograph minus base flow.
Drainage Density:	An index of the concentration of streams in a watershed. Frequently reported as the dimensionless ratio of the total length of streams squared to the drainage area.
Energy Grade Line:	The energy state at a channel or conduit section would be the sum of the pressure, velocity, and elevation heads. The energy grade line describes a conceptual link of the energy states between two (or more) channel or conduit locations. The differences in total energy between these two locations would be associated with energy losses. The slope of the energy grade line is often referred to as the friction slope.
Envelope Curves:	Bounds defined approximately by the maximum observed values. The peak flow envelope curve, which is placed on a graph of peak flow versus drainage area, is the upper bound of observed peak flows for any drainage area. The envelope curves are usually established for homogeneous hydrologic regions.
Exceedance probability:	The probability that the magnitude of the random variable (e.g., annual maximum flood peak) will be equaled or exceeded in any one period, often one year.
Froude Number:	The ratio of inertia forces to gravity forces, usually expressed as the ratio of the flow velocity to the square root of the product of gravity and a linear dimension (normally depth). The Froude number is used in the study of fluid motion.
Fusion:	The phase conversion of a solid to a liquid.

Histogram:	A graph that shows the frequency of occurrence of a random variable within class intervals as a function of the value of the random variable. The frequency is the ordinate, and the value of the random variable is the abscissa, which is divided into class intervals.
Hydraulic Grade Line:	A line coinciding with the level of flowing water in an open channel. In a closed conduit flowing under pressure, the HGL is the level to which water would rise in a vertical tube at any point along the pipe. It is equal to the energy grade line elevation minus the velocity head.
Hydraulic Radius:	The cross-sectional flow area of a channel or conduit divided by its wetted perimeter.
Hydrograph:	A plot of flow versus time.
Hydrologic Abstractions:	Portions of the total rainfall that do not contribute to direct runoff, including rainfall intercepted by vegetation, rainwater stored in depressions, and water that enters the watershed surface and remains beyond the duration of the storm.
Hydrologic Cycle:	A representation of the physical processes that control the distribution and movement of water.
Hyetograph:	A plot of the rainfall intensity (or depth) versus time.
Infiltration:	The process by which water on the ground surface enters the soil.
Initial Abstraction:	The portion of the rainfall that occurs prior to the start of direct runoff.
Instantaneous Unit Hydrograph:	The hydrologic response of the watershed to 1 unit (e.g., 1 inch) of rainfall excess concentrated in an infinitesimally small period.
Intensity-duration-frequency:	A graphical, tabular, or mathematical relation between the rainfall intensity, storm duration, and exceedance frequency.
Isohyet:	A line on a map of equal rainfall depth for the same duration, usually the duration of a storm.
Land Cover / Land Use:	Most conventional definitions have land cover relating to the type of feature on the surface of the earth such as rooftop, asphalt surface, grass, and trees. Land use associates the cover with a socio-economic activity such as factory or school, parking lot or highway, golf course or pasture and orchard or forest. Hydrologic modeling often uses the terms land cover and land use interchangeably because the inputs to the models require elements from each definition.
Latent Heat of Fusion:	Heat necessary to change ice to water.
Latent Heat of Sublimation:	Heat necessary to change ice to vapor.
Latent Heat of Vaporization:	Heat necessary to change liquid water to vapor.
Latent Heat:	The amount of heat needed to change the phase of a compound with no change in temperature.

Least-squares Regression:	A procedure for fitting a mathematical function that minimizes the sum of the squares of the differences between the predicted and measured values.
Level of Significance:	A statistical concept that equals the probability of making a specific error, namely of rejecting the null hypothesis when, in fact, it is true. The level of significance is used in statistical decision-making.
Maximum Likelihood Estimation:	A mathematical method of obtaining the parameters of a probability distribution by optimizing a likelihood function that yields the most likely parameters based on the sample information.
Method of Moments Estimation:	A method of fitting the parameters of a probability distribution by equating them to the sample moments.
Moving-average Smoothing:	A statistical method of smoothing a time or space series in which the nonsystematic variation is eliminated by averaging adjacent measurements. The smoothed series represents the systematic variation.
Nonhomogeneity:	A characteristic of time or space series that indicates the moments are not constant throughout the length of the series.
Nonparametric Statistics:	A class of statistical tests that do not require assumptions about the population distribution.
Order-theory Statistics:	A class of statistical methods in which the analysis is based primarily on the order relations among the sample values.
Outlier:	An extreme event in a data sample that has been determined using statistical methods to be from a population different from the remainder of the data.
Parametric Statistics:	A class of statistical tests in which the tests' derivation involved explicit assumptions about the underlying population.
Partial-duration Analysis:	A frequency analysis method that uses all floods of record above a threshold to derive a probability function to represent the data.
Pearson Correlation Coefficient:	An index of association between paired values of two random variables. The value assumes a linear model.
Plotting Position Formula:	An equation used in frequency analysis to compute the probability of an event based on the rank of the event and the sample size.
Power Model:	A mathematical function that relates the criterion (dependent) variable, y, to the predictor (independent) variable, x, raised to an exponent, i.e., y = ax^b.
Precision:	A measure of the nonsystematic variation. It is the ability of an estimator to give repeated estimates that are close together.

Probability Scale:	A tool for graphing the distribution of a random variable in which the ordinate is the value of a random variable, and the abscissa is the probability of the value of the random variable being equaled or exceeded (probability scale). The nature of the probability scale depends on the probability distribution.
Radiation Melt:	The portion of snowmelt occurring due to solar radiation providing energy to a snowpack.
Rainfall Excess:	The portion of rainfall that causes direct flood runoff. It equals the total rainfall minus the initial abstraction and other losses.
Raster Database:	A method for displaying and storing geographic data as a rectangular array of characters where each character represents the dominant feature, such as a land cover or soil type, in a grid cell at the corresponding location on a map.
Rating Curve:	A graph or mathematical equation that relates the stage and flow.
Real-time Modeling:	Hydrologic modeling in which a calibrated model is used with data for a storm event in progress to make predictions of streamflow for the remainder of the storm event.
Return Period:	The average length of time between occurrences in which the value of a random variable (e.g., flood magnitude) is equaled or exceeded. Actual times between occurrences may be longer or shorter.
Sheet Flow:	Shallow flow on the watershed surface that occurs prior to the flow concentrating into rills.
S-hydrograph:	The cumulative hydrograph that results from adding an infinite number of T-hour unit hydrographs, each lagged T-hours.
Skew (statistics):	The third statistical moment, with the mean and variance being the first and second statistical moments. The skew is a measure of the symmetry of either data or a population distribution, with a value of zero indicating a symmetric distribution.
Snow Water Equivalent:	A resulting depth of water obtained by melting the snow from a given snow event.
Spearman Correlation Coefficient:	An index of association between paired values of two random variables. It is computed using the ranks of the data rather than the sample values. It is the nonparametric alternative to the Pearson correlation coefficient.
Specific Energy:	The total energy head measured above the channel bed at a specific section of channel. Calculated as the sum of the velocity head and the depth of flow. The minimum specific energy occurs at critical depth.
Specific Heat:	The amount of heat necessary to raise the temperature of a compound over a given temperature interval without a change in state.

Stage-storage-discharge:	Relationships between stage, storage, and discharge (flow) used in storage routing methods. It is usually computed from the stage-storage and stage-discharge relationships.
Standard Error of Estimate:	The standard deviation of the residuals in a regression analysis. It is based on the number of degrees of freedom associated with the errors.
Sublimation:	The phase conversion of a solid to a gas.
Synthetic Unit Hydrograph:	A unit hydrograph not solely based on measured rainfall and runoff data.
Systematic Record:	Data that are collected at regular, prescribed intervals under a defined protocol. In the context of streamflow, systematic data consist of flow and stage data collected at regular, prescribed intervals, typically at streamflow-gaging stations.
Time of Concentration:	The time for a particle of water to flow from the hydraulically most distant point in the watershed to the outlet or design point.
Time-area Curve:	The relationship between runoff travel time and the portion of the watershed that contributes runoff during that travel time.
Translation:	Movement of a flood wave downstream resulting in a delayed peak while maintaining the same hydrograph shape.
Unit Peak Flow:	The peak flow per unit area.
Vapor Condensation Melt:	The portion of snowmelt occurring due to heat released by water vapor as it condenses on the snowpack and converts to liquid water.
Vaporization:	The phase conversion of a liquid to a gas.
Vector Database:	A method for displaying and storing geographic data as a distribution of vector segments that, when connected, form polygons that enclose homogeneous areas such as a defined land cover or form lines representing features such as roads or streams.
Water Year:	October 1 to September 30, with the water year number taken as the calendar year of the January 1 to September 30 period.
Weighted Skew:	An estimate of the skew based on both the station skew and a regionalized value of skew.
Wetted Perimeter:	The length of contact between the flowing water and the channel or conduit at a specific cross-section.
Zero-flood records:	Annual maximum flood records that include zero values or values below a threshold.

Abbreviations

AASHTO	American Association of State Highway and Transportation Officials
AEP	Annual Exceedance Probability
AMC	Antecedent Moisture Condition
AOP	Aquatic Organism Passage
ARC	Antecedent Runoff Condition
BFE	Base Flood Elevation
BMP	Best Management Practice
CDF	Cumulative Distribution Function
CFR	Code of Federal Regulations
CLOMR	Conditional Letter of Map Revision
CN	Curve Number
CU	Customary Units (English)
CWA	Clean Water Act
DDF	Depth-duration-frequency
DOT	Department of Transportation
DUH	Dimensionless Unit Hydrograph
DEM	Digital Elevation Model
EGL	Energy Grade Line
EMA	Expected Moments Algorithm
EO	Executive Order from the Federal Register
ESA	Endangered Species Act
ET	Evapotranspiration
FAHP	Federal-Aid Highway Program
FDC	Flow Duration Curve
FEMA	Federal Emergency Management Agency
FFC	Flood Frequency Curve
FHWA	Federal Highway Administration
FIRM	Flood Insurance Rate Map
FIS	Flood Insurance Study
GB	Grubbs-Beck
GIS	Geographic Information System
GPS	Global Positioning System
GSSHA	Gridded Surface Subsurface Hydrologic Analysis

H&H	Hydrology and Hydraulics
HDG	Highway Drainage Guidelines
HDS	Hydraulic Design Series
HEC	Hydraulic Engineering Circular (FHWA)
HEC	Hydrologic Engineering Center (USACE)
HEC-1	Hydrologic Engineering Center – Program 1
HEC-HMS	Hydrologic Engineering Center – Hydrologic Modeling System
HGL	Hydraulic Grade Line
HGM	Hydrogeomorphic
HSG	Hydrologic Soil Group
HSPF	Hydrologic Simulation Program Fortran
HWM	High Water Mark
IDF	Intensity-duration-frequency
LiDAR	Light Detection and Ranging
LP3	log-Pearson type III
MAP	Mean Annual Precipitation
MGBT	Multiple Grubbs-Beck Test
MLE	Maximum Likelihood Estimation
MSE	Mean-square Error
NAIP	National Agricultural Imagery Program
NASEM	National Academies of Sciences, Engineering, and Medicine
NCDC	National Climatic Data Center
NCHRP	National Cooperative Highway Research Program
NED	National Elevation Database
NEH	National Engineering Handbook
NEPA	National Environmental Policy Act
NFIP	National Flood Insurance Program
NGP	National Geospatial Program
NHD	National Hydrography Dataset
NHI	National Highway Institute
NHPA	National Historic Preservation Act
NHPP	National Highway Performance Program
NHS	National Highway System
NLCD	National Land Cover Database
NMFS	National Marine Fisheries Service

NOAA	National Oceanic and Atmospheric Administration
NPDES	National Pollutant Discharge Elimination System
NRC	National Research Council
NRCS	National Resources Conservation Service
NSS	National Streamflow Statistics
NWS	National Weather Service
O&M	Operation and Maintenance
PET	Potential Evapotranspiration
PFDS	Precipitation Frequency Data Server
PILF	Potentially Influential Low Flood
PRF	Peak Rate Factor
ROW	Right-of-Way
SCS	Soil Conservation Service (now NRCS)
SE	Standard Error
SFHA	Special Flood Hazard Area
SHPO	State Historic Preservation Officers
SI	System International (Metric)
SIR	Scientific Investigations Report
SSURGO	Soil Survey Geographic Database
SWE	Snow Water Equivalent
SWMM	Storm Water Management Model
UH	Unit Hydrograph
USACE	U.S. Army Corps of Engineers
USBR	U.S. Bureau of Reclamation
USCG	U.S. Coast Guard
USDA	U.S. Department of Agriculture
USDOT	U.S. Department of Transportation
USEPA	U.S. Environmental Protection Agency
USFS	U.S. Forest Service
USFWS	U.S. Fish and Wildlife Service
USGS	U.S. Geological Survey
USWB	U.S. Weather Bureau
WRDA	Water Resources Development Act
WSFO	Weather Service Forecast Office

Page Intentionally Left Blank

Chapter 1 - Introduction

The science of hydrology addresses the physical properties, occurrence, and movement of water in the atmosphere, on the surface of, and in the outer crust of the earth. Individual bodies of science dedicate themselves to the study of various elements contained within this definition. These include, but are not limited to, meteorology, oceanography, and geohydrology. Highway designers primarily focus their hydrologic investigations on the water that moves on the Earth's surface and ultimately crosses infrastructure (i.e., highway stream crossings). Secondarily, designers use hydrology in the provision of drainage for roadways, median areas, and interchanges.

This Highway Hydrology Manual, also referred to as Hydraulic Design Series No. 2 (HDS-2), provides technical information for understanding, assessing, and addressing hydrology for transportation infrastructure. This chapter describes the purpose and scope, organization, target audience, and units used in the manual.

1.1 Purpose and Scope

This Highway Hydrology Manual provides information for developing and using hydrologic estimates to support the design of bridge and roadway transportation infrastructure to protect the public health, safety, and welfare. The manual addresses fundamental aspects of the hydrologic cycle including precipitation, infiltration, runoff, routing, and storage. It includes techniques for estimating design flows on gaged and ungaged watersheds, development of hydrographs, routing, and hydrologic modeling. It describes sources of data needed to support hydrologic and hydraulic (H&H) analyses of bridges, culverts, stormwater management, and other transportation infrastructure assets. It also describes uncertainty in historical and future climate and provides tools for understanding that uncertainty to develop resilient infrastructure.

This manual supports planning, implementation, and stewardship of sustainable, resilient, and reliable transportation networks. The FHWA describes sustainability as considering three primary values or principles: social, environmental, and economic (FHWA 2022b). The goal of sustainability is the satisfaction of basic social and economic needs, both present and future, and the responsible use of natural resources, all while maintaining or improving the well-being of the environment on which life depends. Figure 1.1 illustrates these three values.

Commonly, society views sustainability through a lens of balancing the needs of the environment with the economic needs of roadway and bridge development. This balancing results in the identification of viability, but this is only part of the picture. Balancing the environment with social values results in what is bearable, or acceptable, by both society and the environment, while balancing the social and economic results in what is equitable. "Past Federal transportation investments have too often failed to" consider transportation equity for all community members, including traditionally underserved and underrepresented populations (USDOT 2022). "Underserved populations" include minority and low-income populations but may also include many other demographic categories that face challenges engaging with the transportation process and receiving equitable benefits (See FHWA 2015c). "The U.S. Department of Transportation (USDOT or Department) has committed to pursuing a comprehensive approach to advancing equity for all" (USDOT 2022; see also FHWA 2021; and Executive Order 13985, 86 FR 7009 (2021)). Equity in transportation seeks the consistent and systematic fair, just, and impartial treatment of all individuals, including individuals who belong to traditionally underserved communities or populations (USDOT 2022).

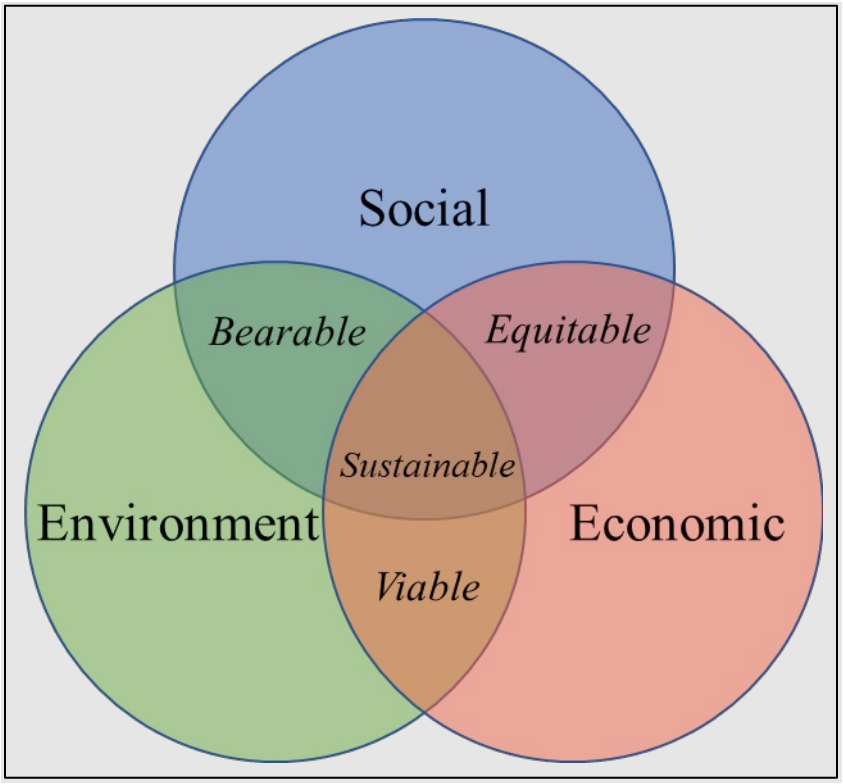

Figure 1.1. Balancing economic, social, and environment aspects for sustainability.

This manual also addresses issues related to hydrologic modeling to facilitate more resilient and reliable hydraulic designs within which potential future hydrologic and meteorologic conditions are identified and accommodated. Reliability is tied to resilience because a resilient transportation network is safer and less susceptible to delays and failures.

Resilient and reliable designs are essential to addressing the significant and growing risk presented by climate change. (USDOT, 2021). In the transportation context, this risk is many-faceted, including risks to the safety, effectiveness, equity, and sustainability of the Nation's transportation infrastructure and the communities it serves. The USDOT recognizes that the United States has a "once-in-a-generation" opportunity to address this risk, which is increasing over time (USDOT 2021; see also Executive Order 14008 on Tackling the Climate Crisis at Home and Abroad, 86 FR 7619 (2021)). Addressing the risk of climate change is also closely interlinked with advancing transportation equity, as discussed above, because of the disproportionate impacts of climate change on vulnerable populations, including older adults, children, low-income communities, and communities of color. The USDOT intends to lead the way in addressing the climate crisis.

The FHWA also encourages the advancement of projects that address climate change and sustainability (FHWA 2021). To enable this, FHWA encourages recipients to consider climate change and sustainability throughout the planning and project development process, including the extent to which Federal-aid projects align with the President's greenhouse gas reduction, climate resilience, and environmental justice commitments.

The FHWA believes that this manual will be useful for aligning and integrating these concepts and components of sustainability within the context of highways and the riverine environment. Such alignments will consist of both direct and indirect interstices and situations.

Resilience

With respect to a project, the FHWA defines "resilience" as a project with the ability to anticipate, prepare for, and or adapt to changing conditions and or withstand, respond to, and or recover rapidly from disruptions, including the ability: (A) to resist hazards or withstand impacts from weather events and natural disasters, or reduce the magnitude or duration of impacts of a disruptive weather event or natural disaster on a project; and (B) to have the absorptive capacity, adaptive capacity, and recoverability to decrease project vulnerability to weather events or other natural disasters. 23 U.S.C. § 101(a)(24) (added by Sec. 11103 of the Bipartisan Infrastructure Law (BIL), enacted as the Infrastructure Investment and Jobs Act, Pub. L. No. 117-58 (Nov. 15, 2021)). See also FHWA Order 5520 (FHWA 2014).

1.2 Changes from Previous Edition

The Federal Highway Administration (FHWA) deleted some topics from the previous edition of this manual (FHWA 2002) because they were outdated and no longer served the purpose and scope of practical highway hydrology. These topics include:

- The FHWA regression equations (outdated and largely replaced by USGS rural regression equations).
- The USGS nationwide urban regression equations (based on the basin development factor whose use is discouraged by the FHWA).
- The graphical peak flow method (effectively replaced by the NRCS dimensionless unit hydrograph in most software applications).
- Design storm by triangular hyetograph (originally developed to support models such as Storm Water Management Model (SWMM) but no longer used for that purpose).

1.3 Hydrology of Highway Stream Crossings

Highway engineers address a diversity of drainage applications that include the design of pavements, bridges, culverts, siphons, and other cross drainage structures for channels varying from small streams to large rivers. They design stable open channels and stormwater collection, conveyance, and detention systems in both urban and rural areas. They also evaluate the impacts of future land use, proposed flood control and water supply projects, and other planned and projected changes on the design of the highway crossing. They consider changes in the watershed (e.g., land use planning maps) and potential changes in climate. In addition, designers assess flood potential and environmental impacts that planned highway and stream crossings may have on the watershed.

Designers typically include three elements in their hydrologic analyses:

- Measurement, recording, compilation, and publication of data.
- Interpretation and analysis of data.
- Application to design or other practical problems.

The level of effort, methods, and detail of analyses depends on:

- Importance and cost of the structure.
- Tolerance for failure.
- Amount of data available for the analysis.
- Additional information and data involved.
- Accuracy.
- Time and other resource constraints.

Depending on the context, engineers may consider failure to be an exceedance of a specific design criteria with little or no damage resulting or where significant damage occurs resulting in costly repairs and loss of service. Choice of effort, methods, and detail of analysis depends on the relevant type of failure.

These factors typically determine the level of analysis appropriate for any design situation. Designers commonly confront issues of insufficient data and limited resources (time, workforce, and funds). They find it impractical in routine design to use analytical methods involving extensive time or data not readily available or that are difficult to acquire. Designers often reserve the more demanding methods and techniques for those special projects where additional data collection and accuracy produce benefits that offset the additional resources involved.

However, engineers have access to several simpler but equally sound and proven methods for analyzing the hydrology for some common design situations. These procedures enable designers to determine peak flows and hydrographs using existing data or, in the absence of data, synthesize methods to develop the design parameters. With care, and often with only limited additional data, designers can use these same procedures to develop the hydrology for the more complex and/or costly design projects.

Among other aspects, hydrologic analysis at a highway stream crossing involves determining either peak flow or the flood hydrograph. Peak flow (instantaneous maximum flow) is common because most highway stream crossings are traditionally designed to pass a given quantity of water with an acceptable level of risk. This capacity is usually specified in terms of the peak rate of flow during passage of a flood. Designers associate a flood severity with a measure of frequency such as annual exceedance probability (AEP) or return period. Table 1.1 provides examples of some typical design frequencies for hydraulic structures associated with different roadway classifications, as identified by the American Association of State Highway and Transportation Officials (AASHTO) (AASHTO 2014). State Departments of Transportation (DOTs), municipalities, and resource agencies may have their own guidelines for situations under their jurisdiction.

Table 1.1. Design storm selection guidelines (AASHTO 2014).

Roadway Classification	Annual Exceedance Probability	Return Period
Rural Principal Arterial System	0.02	50-year
Rural Minor Arterial System	0.04 – 0.02	25-50-year
Rural Collector System, Major	0.04	25-year
Rural Collector System, Minor	0.1	10-year
Rural Local Road System	0.2 – 0.1	5-10-year
Urban Principal Arterial System	0.04 – 0.02	25-50-year
Urban Minor Arterial Street System	0.04	25-year
Urban Collector Street System	0.1	10-year
Urban Local Street System	0.2 – 0.1	5-10-year

Generally, designers determine the peak flows for a range of flood frequencies at a site in a drainage basin. Designers size culverts, bridges, or other structures to convey the design peak flow within other constraints and considerations. If possible, they estimate the peak flow that almost causes highway overtopping and then use this flow to evaluate the risk associated with the crossing.

Hydrograph development plays an important role for projects involving a detailed description of the time variation of runoff rates and volumes. Similarly, urbanization, storage, and other changes in a watershed affect flood flows in many ways. Travel time, time of concentration, runoff duration, peak flow, and the volume of runoff may be changed by significant amounts. Designers primarily evaluate and assess these changes using the flood hydrograph. Additionally, when flows are combined and routed to another point along a stream, hydrographs are essential.

1.4 Organization

This manual consists of 11 chapters, a glossary, list of acronyms, reference section, and an appendix. The organization supports hydrologic analysis at stream crossings by first presenting fundamental information about rainfall-runoff processes and hydrologic data, then information for estimating peak flows and hydrographs, followed by more advanced topics such as routing, hydrologic modeling, and special topics.

Chapter 1 (this chapter) provides discussion of the purpose, background, organization, and units.

Chapter 2 provides an overview of Federal policy as it relates to highway hydrology. This context guides work in the H&H design of transportation infrastructure assets through a series of statutes and regulations.

Chapter 3 describes rainfall-runoff process to provide a context for the tools and procedures that follow. It discusses precipitation, hydrologic abstractions, watershed characteristics, and runoff processes.

Chapter 4 outlines hydrologic data needed to perform hydrologic analysis and design and provides an overview of considerations for choosing the appropriate method or methods for a given situation. The chapter also describes sources of hydrologic data.

Chapters 5, 6, and 7 describe detailed methods and information for estimating peak flows for gaged sites, ungaged sites using statistical methods, and ungaged sites using rainfall-runoff methods, respectively. Each chapter discusses multiple approaches, as well as their strengths and limits.

Chapter 8 outlines situations when a peak flow provides insufficient information, and a full hydrograph is needed to analyze or design an asset. The chapter addresses the development of hydrographs and describes several techniques to create them.

Chapter 9 describes methods for routing hydrographs through detention or retention storage facilities and through natural or constructed channels. The chapter discusses the fundamental principles of routing and outlines computational procedures.

Chapter 10 links the tools and methods from previous chapters into an integrated description of the hydrologic modeling process and available tools. The chapter also discusses uncertainty and risk and describes a framework for understanding these concepts in hydrologic design.

Chapter 11 describes special topics in hydrology that are of regional importance or of a more specialized nature including wetlands hydrology, snowmelt hydrology, and arid lands hydrology. In each case, the chapter discusses the unique context and illustrates tools and methods for performing hydrologic analysis and design.

1.5 Target Audience

The target audience of this manual includes Federal, State, and local highway agencies and consultants with responsibility for developing or using hydrology to support roadway and bridge planning, design, construction, operations, and maintenance. Others responsible for planning, operating, and maintaining roadways and bridges, as well as those interested in the environmental performance and resilience of transportation infrastructure, may also find this a useful reference.

This manual does not have the force and effect of law and it is not meant to bind the States or the public in any way. The FHWA intends any descriptions of processes and approaches to provide illustrative insights into the underlying scientific and engineering concepts and practices, but such descriptions are not intended as requirements.

1.6 Units in This Manual

This manual uses customary (English) units. However, in limited situations both customary units and SI (metric) units are used or only SI units are used because these are the predominant measure used nationwide and globally for such topics. In these situations, the manual provides the rationale for the use of units. An appendix summarizes information on units and unit conversions.

Chapter 2 - Federal Policy for Highway Hydrology

Federal policy related to highway hydrology sets the context for planning, design, construction, and operations and maintenance of roadways and their associated stormwater drainage infrastructure. This chapter provides background on applicable FHWA specific statutes and regulations and provides an overview of other Federal statutes and regulations that may affect roadway projects and hydrology.

Context for Roadways and Hydrology

Federal policy—in the form of statutes and regulations—establishes the context and parameters for the development of transportation infrastructure that serves to facilitate the movement of both people and goods. Taken together, these statutes and regulations, administered by multiple Federal agencies, reflect national values for economic well-being and environmental stewardship. Hydrology plays a role in achieving the goals of these statutes and regulations. For example, hydrologic analyses are needed to establish the overtopping and base flood magnitudes for 23 CFR Part 650.117 (content of design studies) and may be needed to evaluate habitat impacts under the Endangered Species Act of 1973.

2.1 Federal Highways and Hydrology: National Overview

The FHWA has the primary responsibility for U.S. Federal policy on highways. Legislation for the Federal road system dates back over a century. The Federal-Aid Road Act of 1916 created the Federal-Aid Highway Program, which funded State highway agencies so they could make road improvements “to get the farmers out of the mud.” This 1916 Act charged the Bureau of Public Roads with implementing the program. The growth of the Federal highway system, including the addition of the Interstate Highway System and concerns about how all these highways affected the environment, city development, and the ability to provide public mass transit, led to the 1966 establishment of the U.S. Department of Transportation (USDOT). The same enabling legislation renamed the Bureau of Public Roads to the FHWA. Currently, the FHWA continues to administer Federal policy on highways, but also coordinates extensively with other Federal agencies on environmental policies and permits, floodplains, and other compliance issues related to highway program and project delivery.

Other agencies influence hydrology policy. At the Federal level, the Federal Emergency Management Agency (FEMA) oversees the National Floodplain Insurance Program (NFIP). The U.S. Fish and Wildlife Service (USFWS) and the National Oceanic and Atmospheric Administration (NOAA) National Marine Fisheries Service (NMFS) administer and enforce the Endangered Species Act (ESA). Almost every project involving work or activities in rivers is subject to the Clean Water Act (CWA) of 1972, which the U.S. Environmental Protection Agency (USEPA) administers in coordination with State governments.

2.2 FHWA Statutes and Regulations

The FHWA provides financial and technical assistance to State and local governments to ensure that U.S. roads and highways continue to be among the safest and most technologically sound in the world. The FHWA authority for the subject matter of this manual includes the following statutes and regulations. The section below provides a synopsis of these various authorities as well as pertinent Congressional findings and statements, policy, and guidance.

2.2.1 FHWA Statutes

The FHWA operates under the statutory authority of Title 23 (Highways) of the U.S. Code (U.S.C.). For the purposes of this manual, relevant sections include:

- **Standards [23 U.S.C. § 109].** It is the intent of Congress that federally funded projects to resurface, restore, and rehabilitate highways shall "be constructed in accordance with standards to preserve and extend the service life of highways and enhance highway safety." [23 U.S.C. § 109(n)] Designs for new, reconstructed, resurfaced, restored, or rehabilitated highways on the National Highway System must consider, among other criteria, the "constructed and natural environment of the area." [Id. at (c)(1)(a)]
- **Maintenance [23 U.S.C. § 116].** Preventive maintenance is eligible for Federal assistance under Title 23 if a State Department of Transportation (SDOT) can demonstrate that it is a "cost-effective means of extending the useful life of a Federal-aid highway." [23 U.S.C. § 116(e)]
- **National highway performance program [NHPP] [23 U.S.C. § 119].** The NHPP allows FHWA to provide Federal-aid funds for "[c]onstruction, replacement …, rehabilitation, preservation, and protection (including … protection against extreme events) of bridges on the National Highway System." [23 U.S.C. § 119(d)(2)(B)] The NHPP also allows Federal-aid funds for "[c]onstruction, replacement …, rehabilitation, preservation, and protection (including … protection against extreme events) of tunnels on the National Highway System." [Id. at (d)(2)(C)]
- **Surface transportation block grant [STBG] program [23 U.S.C. § 133].** The STBG program allows FHWA to provide Federal-aid funds for protection of "bridges (including approaches to bridges and other elevated structures) and tunnels on public roads" including "painting, scour countermeasures, seismic retrofits, impact protection measures, security countermeasures, and protection against extreme events." [23 U.S.C. § 133(b)(10)] The STBG program also allows Federal-aid funds for "inspection and evaluation of bridges and tunnels and other highway assets." [Id.]
- **Metropolitan transportation planning [23 U.S.C. § 134].** In the context of metropolitan transportation planning, Congress has found that it "is in the national interest … to encourage and promote the safe and efficient management, operation, and development of surface transportation systems … within and between States and urbanized areas" including taking "resiliency needs" into consideration. [23 U.S.C. § 134(a)(1)]
- **National bridge and tunnel inventory and inspection standards [23 U.S.C. § 144]**. Congress has found that "continued improvement to bridge conditions is essential to protect the safety of the traveling public." [23 U.S.C. § 144(a)(1)(A)] Congress has further found that "the systematic preventative maintenance of bridges, and replacement and rehabilitation of deficient bridges, should be undertaken." [Id. at (a)(1)(B)] In addition, Congress has also declared that "it is in the vital national interest" to use a "data-driven, risk-based approach" toward meeting these ends." [Id. at (a)(2)(B)] Considering these findings and declarations, Section 144 requires FHWA to maintain an inventory of bridges and tunnels on public roads both "on and off Federal-aid highways." [Id. at (b)] The FHWA is also required to "establish and maintain inspection standards for the proper inspection and evaluation of all highway bridges and tunnels for safety and serviceability." [Id. at (h)(1)(A)] Section 144 also provides an exception to the requirement to obtain a bridge permit from the U.S. Coast Guard for certain bridges over a limited subset of navigable waters. [Id. at (c)(2)]
- **National goals and performance management measures [23 U.S.C. § 150].** Congress has declared that it is "in the interest" of the U.S. to focus the Federal-aid highway program

on certain national transportation goals including Infrastructure Condition, or the objective to "maintain … highway infrastructure in a state of good repair;" and System Reliability, or the objective to "improve the efficiency of the surface transportation system." [23 U.S.C. § 150(b)]

- **PROTECT Program [23 U.S.C. § 176].** The Promoting Resilient Operations for Transformative, Efficient, and Cost-Saving Transportation (PROTECT) program allows the FHWA to provide grants for resilience improvements through: (i) formula funding distributed to States; (ii) competitive planning grants; and (iii) competitive resilience improvement grants. [23 U.S.C. § 176(b)] Eligible activities under the PROTECT program include, among others, "resurfacing, restoration, rehabilitation, reconstruction, replacement, improvement, or realignment of" certain existing surface transportation facilities and "the incorporation of natural infrastructure." [23 U.S.C. §§ 176(c)(1) and 176(d)(4)(A)(ii)(II)]
- **Bridge Replacement, Rehabilitation, Preservation, Protection, and Construction Program (or Bridge Formula Program) (Division J, title VIII, Highway Infrastructure Program heading, paragraph (1) of BIL).** The Bridge Formula Program provides funding to help repair approximately 15,000 highway bridges. In addition to providing funds to states to replace, rehabilitate, preserve, protect, and construct highway bridges, the Bridge Formula Program has dedicated funding for Tribal transportation facility bridges as well as "off-system" bridges, which are generally locally-owned facilities not on the Federal-aid highway system.
- **Bridge Investment Program (23 U.S.C. § 124).** The Bridge Investment Program provides financial assistance for eligible projects with program goals to improve the safety, efficiency, and reliability of the movement of people and freight over bridges; improve the condition of bridges; and provide financial assistance that leverages and encourages non-Federal contributions from sponsors and stakeholders involved in the planning, design, and construction of eligible projects.
- **National Culvert Removal, Replacement, and Restoration Grants Program (49 U.S.C. § 6703)].** The National Culvert Removal, Replacement, and Restoration Grant program established an annual competitive grant program to award grants to eligible entities for projects for the replacement, removal, and repair of culverts or weirs that would meaningfully improve or restore fish passage for anadromous fish.
- **Research and technology development and deployment [23 U.S.C. § 503].** In carrying out certain highway and bridge infrastructure and research and development activities, FHWA must "study vulnerabilities of the transportation system to … extreme events and methods to reduce those vulnerabilities." [23 U.S.C. § 503(b)(3)(B)(viii)].
- **Statutory Definition of "Resilience." [23 U.S.C. § 101(a)(24)].** Section 11103 of the Bipartisan Infrastructure Law (BIL), enacted as the Infrastructure Investment and Jobs Act, Pub. L. No. 117-58 (Nov. 15, 2021), added a definition of "resilience," which applies throughout Title 23 of the U.S. Code. With respect to a project, "resilience" means a project with the ability to anticipate, prepare for, and or adapt to changing conditions and or withstand, respond to, and or recover rapidly from disruptions, including the ability: (A) to resist hazards or withstand impacts from weather events and natural disasters, or reduce the magnitude or duration of impacts of a disruptive weather event or natural disaster on a project; and (B) to have the absorptive capacity, adaptive capacity, and recoverability to decrease project vulnerability to weather events or other natural disasters. 23 U.S.C. § 101(a)(24).

2.2.2 FHWA Regulations

The FHWA's regulations are found within the Code of Federal Regulations (CFR), Title 23, Highways (23 CFR). The FHWA requires compliance with Federal law and the regulations in Chapter I, Subchapter A, Part 1 of 23 CFR for a project to be eligible for Federal-aid or other FHWA participation or assistance. [23 CFR § 1.36] The following FHWA regulations apply to highway projects and actions interacting with and within rivers and floodplains (in some cases, paraphrased for brevity):

Scope of the statewide and nonmetropolitan transportation planning process [23 CFR § 450.206]. State DOTs must "carry out a continuing, cooperative, and comprehensive statewide transportation planning process that provides for consideration and implementation of projects, strategies, and services that will … improve the resiliency and reliability of the transportation system." [23 CFR § 450.206(a)]

Asset Management Plans [23 CFR Part 515]. Part 515 establishes processes that a SDOT must use to develop a transportation asset management plan (TAMP). Two notable sections include:

- **Section 515.7(b).** "A State DOT shall establish a process for conducting life-cycle planning for an asset class or asset sub-group at the network level (network to be defined by the State DOT). As a State DOT develops its life-cycle planning process, the State DOT should include future changes in demand; information on current and future environmental conditions including extreme weather events, climate change, and seismic activity; and other factors that could impact whole of life costs of assets."
- **Section 515.7(c).** "A State DOT shall establish a process for developing a risk management plan. This process shall, at a minimum, produce the information including: Identification of risks that can affect condition of NHS pavements and bridges and the performance of the NHS, including risks associated with current and future environmental conditions, such as extreme weather events, climate change, seismic activity, and risks related to recurring damage and costs as identified through the evaluation of facilities repeated damaged by emergency events carried out under part 667 of title 23 of the CFR. Additional information that must be produced is specified in the regulation at 23 CFR 515.7(c).

In addition, BIL Section 11105 amended 23 U.S.C. Section 119(e)(4) to require State DOTs to consider extreme weather and resilience as part of the life-cycle planning and risk management analyses within a TAMP (FHWA 2022c).

Design Standards [23 CFR Part 625]. Part 625 describes structural and geometric design standards.

- **Sections 625.3(a)(1), 625.3(b), and 625.4(b)(3).** The FHWA, in cooperation with State DOTs, has approved the American Association of State Highway and Transportation Officials (AASHTO) Load and Resistance Factor Design (LRFD) Bridge Design Specifications. Based on FHWA's approval, National Highway System (NHS) projects must follow those Specifications including sections related to hydrology, hydraulics, and bridge scour.
- **Section 625.3(a)(2).** Non-NHS projects must follow State DOT standard(s) and specifications on drainage, bridges, and other topics.

Location and Hydraulic Design of Encroachments on Flood Plains [23 CFR Part 650, Subpart A]. One of the FHWA's most important river-related regulations, 23 CFR Part 650, Subpart A sets forth policies and procedures for location and hydraulic design of highway encroachments in base (1-percent chance) floodplains. Section 650.111 sets forth requirements for location hydraulic studies to identify the potential impact of the highway alternatives on the

base floodplain; these studies are commonly used during the National Environmental Policy Act (NEPA) process. The regulations prohibit significant encroachment unless FHWA determines that such encroachment is the only practicable alternative. [23 CFR § 650.113(a)] This finding must be included in the NEPA documents for a project and supported information including the reasons for the finding and considered alternatives. [Id.] The procedures also provide minimum standards for Interstate Highways, set freeboard requirements to account for debris and scour, and require highway encroachments to be consistent with certain established design flow standards for hydraulic structures, including standards from FEMA and State and local governments related to administration of the National Flood Insurance Program (NFIP). [23 CFR § 650.115(a)] Notably, the policies and procedures in this Subpart apply to encroachments in all base floodplains, not just the floodplains regulated by the Federal Emergency Management Agency (FEMA) in the NFIP. [23 CFR § 650.107] Additionally, the Subpart incorporates a requirement for project-by-project risk assessments or analyses. [23 CFR § 650.115(a)(1)] Notable sections include:

- **Section 650.103 [Policy].** This section states that "it is the policy of the FHWA: (a) To encourage a broad and unified effort to prevent uneconomic, hazardous or incompatible use and development of the Nation's flood plains, (b) To avoid longitudinal encroachments, where practicable, (c) To avoid significant encroachments, where practicable, (d) To minimize impacts of highway agency actions which adversely affect base flood plains, (e) To restore and preserve the natural and beneficial flood-plain values that are adversely impacted by highway agency actions, (f) To avoid support of incompatible flood-plain development, (g) To be consistent with the intent of the Standards and Criteria of the National Flood Insurance Program, where appropriate, and (h) To incorporate "A Unified National Program for Floodplain Management" of the Water Resources Council into FHWA procedures." [23 CFR § 650.103]
- **Section 650.115 [Hydraulic Design Standards].** This regulation applies to all Federal-aid projects, whether on the NHS or Non-NHS. Federal, State, local, and AASHTO standards may not change or override the design standards set forth under § 650.115 — although certain State and local standards must also be satisfied under the same section. The section also requires development of a "Design Study" for each highway project involving an encroachment on a floodplain. [23 CFR § 650.115(a)]
- **Section 650.117 [Content of Design Studies].** This regulation requires studies to contain the "hydrologic and hydraulic data and design computations." [23 CFR § 650.117(b)] As both hydrologic and hydraulic factors and characteristics lead to scour formation, data and computations applicable to scour should be provided as well. Project plans must show the water surface elevations of the overtopping flood and base flood (i.e., 100-year flood) if larger than the overtopping flood. [23 CFR § 650.117(c)]

Executive Order 14030, Climate-Related Financial Risk, and Executive Order 13690, Establishing a Federal Flood Risk Management Standard and a Process for Further Soliciting and Considering Stakeholder Input (80 FR 6425). As of 2023, USDOT is in the process of developing guidance and rulemaking on floodplain management to include FFRMS, taking into account changing flood hazards resulting from climate change and other processes. At the time of publishing of this manual, there are no requirements to apply FFRMS to actions in the floodplain.

National Bridge Inspection Standards [23 CFR 650 Subpart C]. This regulation implements requirements of 23 U.S.C. § 144. In addition to the inspection and inventory requirements, the regulation specifically focuses on scour at bridges.

Mitigation of Impacts to Wetlands and Natural Habitat [23 CFR Part 777]. This regulation provides policy and procedures for the evaluation and mitigation of adverse environmental impacts to wetlands and natural habitat resulting from Federal-aid funded projects.

2.3 Other Federal Agency Statutes and Regulations

Civil engineering projects in the river environment are subject to numerous Federal laws, policies, and regulations. This section describes some of the common Federal statutes, regulations, and other authoritative guidance that may govern highway projects.

2.3.1 Rivers and Harbors Act of 1899 [33 U.S.C. § 401 and § 403]

River and coastal highway engineering projects are subject to Section 9 [33 U.S.C. § 401] and Section 10 [33 U.S.C. § 403] of the Rivers and Harbors Act of 1899. Section 9 of this act restricts the construction of any bridge, dam, dike, or causeway over or in U.S. navigable waterways. Except for bridges and causeways under Section 9 [33 U.S.C. § 401], the U.S. Army Corps of Engineers (USACE) is responsible for maintaining the standards set by and for issuing permits under the Rivers and Harbors Act. Authority to administer Section 9, applying to bridges and causeways, was redelegated to the U.S. Coast Guard under the provisions of the Department of Transportation Act of 1966 (as discussed below).

2.3.2 General Bridge Act of 1946 [33 U.S.C. § 525 through 533]

The General Bridge Act of 1946 requires the location and plans of bridges and causeways across the navigable waters of the U.S. be submitted to and approved by the U.S. Coast Guard prior to construction. [33 U.S.C. § 525] The USACE may also impose conditions relating to maintenance and operation of the structure. [Id.] The General Bridge Act of 1946 is cited as the legislative authority for bridge construction in most cases. Although the General Bridge Act of 1946 originally provided authority for issuing bridge permits to the USACE, subsequent legislation transferred these responsibilities from the USACE to the U.S. Coast Guard.

2.3.3 Transportation Act of 1966 [Public Law 89-670]

The Transportation Act of 1966 transferred the U.S. Coast Guard (USCG) to USDOT. One of USCG's newly assigned duties was to issue bridge permits. This, along with the Rivers and Harbors Act and General Bridge Act, made the USCG responsible for ensuring that bridges and other waterway obstructions do not interfere with the navigability of waters of the U.S. without express permission of the U.S. Government. Subsequent legislation amended 23 U.S.C. § 144 to provide certain exceptions to USCG's authority under 33 U.S.C. § 401 and 33 U.S.C. § 525 for bridges constructed, reconstructed, rehabilitated, or replaced using Federal-aid funds. [23 U.S.C. § 144(c)(2)]

2.3.4 National Environmental Policy Act [42 U.S.C. § 4321, et seq.]

The National Environmental Policy Act of 1969 (NEPA) establishes the continuing policy of the Federal government to use all practicable means and measures "to foster and promote the general welfare, … create and maintain conditions under which man and nature can exist in productive harmony, and fulfill the social, economic, and other requirements of present and future generations of Americans." [42 U.S.C. § 4331] To achieve this goal, NEPA creates a requirement for Federal agencies to consider the environmental impacts of their actions before undertaking them. [42 U.S.C. § 4332(C)]

Section 102(2)(C) of NEPA requires that Federal agencies develop a detailed statement on proposals for major Federal actions significantly affecting the quality of the human environment. [42 U.S.C. § 4332(C)] Environmental impact statements address items including "the environmental impact of" and "alternatives to" the proposed action." [Id.] FHWA implements NEPA according to the Council on Environmental Quality (CEQ) NEPA regulations at 40 CFR Part 1500 et seq. and the FHWA-FRA-FTA joint regulations at 23 CFR Part 771.

2.3.5 Clean Water Act [33 U.S.C. § 1251-1387]

Almost every project involving work or activities in rivers is subject to the Clean Water Act (CWA) of 1972, which the U.S. Environmental Protection Agency (USEPA) administers in coordination with State governments. The CWA is the primary Federal statute governing protection of the Nation's surface waters. Engineering of highways in the river environment is often subject to Section 404 of the CWA, which regulates the discharge of dredged or fill material in waters of the U.S., including wetlands. [33 U.S.C. § 1344] This includes the use of dredged or fill material for development, water resource projects, and infrastructure development (e.g., roads, bridges, etc.). The USACE handles the day-to-day administration and enforcement of the Section 404 program, including issuing permits. In circumstances where Section 404 is triggered, permit applicants also obtain a Section 401 certification from the State in which the discharge of dredged or fill material originates. [13 U.S.C. § 1341] The Section 401 certification assures that materials discharged to waters of the U.S. will comply with relevant provisions of the CWA, including water quality standards. In addition, Section 402 of the CWA establishes the National Pollutant Discharge Elimination System (NPDES) Program. [33 U.S.C. § 1342] The NPDES Program requires a permit for discharges of pollutants into waters of the United States, including storm water discharges.

2.3.6 Endangered Species Act [16 U.S.C. § 1531-1544]

Highway engineering projects have the potential to impact federally-listed fish, wildlife, and plants. The purposes of the Endangered Species Act of 1973 (ESA) include conserving "the ecosystems upon which endangered species and threatened species depend" and providing "a program for the conservation of such endangered species and threatened species." [16 U.S.C. § 1531] It is the policy of Congress that all Federal agencies shall seek to conserve endangered and threatened species and shall utilize their authorities in furtherance of the purposes of the ESA [16 U.S.C. § 1531] The U.S. Fish and Wildlife Service (USFWS) and the NOAA National Marine Fisheries Service (NMFS) administer the ESA. The USFWS and NMFS conduct consultations with the lead Federal agency when a proposed project may affect federally endangered or threatened species. USFWS or NMFS involvement in a project depends on the affected species and the nature and extent of anticipated impacts (direct and indirect) to that species and its designated critical habitat. If anticipating a "take" of a federally-listed species, USFWS or NMFS will issue a biological opinion, the terms and conditions of which are binding on the lead Federal agency. [16 U.S.C. § 1536]

2.3.7 National Historic Preservation Act [54 U.S.C. 300101 et seq.]

River highway engineering projects are often subject to the National Historic Preservation Act of 1966 (NHPA). Section 106 of the National Historic Preservation Act (NHPA) (commonly called "Section 106") requires Federal agencies to consider the impacts on historic properties of projects that they carry out, approve, or fund. [54 U.S.C. § 306108] The implementing regulations for the Section 106 process are found in 36 CFR Part 800. Those regulations provide that Federal agencies, in consultation with the Advisory Council on Historic Preservation, the State Historic Preservation Officers (SHPO), and certain other interested parties, identify and assess adverse effects to historic properties and seek ways to avoid, minimize, or mitigate those effects. [36 CFR § 800.4-800.6] Under Section 106, "historic property" is defined as any prehistoric or historic district, site, building, structure, or object included in, or eligible to be included in, the National Register of Historic Places. [36 CFR 800.16(l)(1); see also 54 U.S.C. 300311 and 302102] The responsibilities of SHPOs are set forth at 54 U.S.C. § 302303.

In addition to Section 106, Section 4(f) of the U.S. Department of Transportation Act of 1966 [23 U.S.C. 138 and 49 U.S.C. 303] requires that FHWA not approve the use of historic sites for a project unless there is no prudent and feasible alternative and the project incorporates all possible

planning to minimize harm, or any impacts to historic sites are determined to be *de minimis*. The FHWA's regulations for implementation of Section 4(f) are found at 23 CFR Part 774.

2.3.8 National Flood Insurance Act [42 U.S.C. § 4001 et seq.]

The National Flood Insurance Act of 1968 instituted the National Flood Insurance Program (NFIP) to help indemnify and reduce impacts associated with floods. The NFIP adopted the area subject to a 1 percent chance or greater of being flooded in any given year (also known as the 100-year flood) as the standard, or base flood, for mapping U.S. floodplains. See, e.g., 44 CFR § 9.4. The area inundated by the 100-year flood determines the Special Flood Hazard Area (SFHA) on Flood Insurance Rate Maps (FIRMs) developed by FEMA and used to determine flood insurance rates for structures. See, e.g., 44 CFR § 59.1 (defining "area of special flood hazard"). FEMA implements the NFIP using its regulations found in 44 CFR.

The FHWA's policies require projects to be consistent with the Standards and Criteria in the NFIP, where appropriate. 23 CFR § 650.115(a)(5). To assist State DOTs in complying with this policy, FHWA developed coordination procedures for Federal-aid highway projects with encroachments in NFIP regulated floodplains. FEMA agreed to these procedures by signing a 1982 Memorandum of Understanding with FHWA.

2.3.9 Wild and Scenic Rivers Act [16 U.S.C. § 1271 et seq.]

This Act establishes a policy to preserve designated rivers "in free-flowing condition" and to protect "their immediate environments … for the benefit and enjoyment of present and future generations." [16 U.S.C. § 1271] Section 7(a) provides that "no department or agency of the United States shall assist by loan, grant, license, or otherwise in the construction of any water resources project that would have a direct and adverse effect on the values for which such river was established." [16 U.S.C. § 1278(a)] A water resources project is "any dam, water conduit, reservoir, powerhouse, transmission line, or other project works under the Federal Power Act ... or other construction of developments which would affect the free-flowing characteristics of a Wild and Scenic River or Study River." [36 CFR 297.3] "Federal assistance means any assistance by an authorizing agency including, but not limited to, ... [a] license, permit, or other authorization granted by the Corps of Engineers, Department of the Army, pursuant to the Rivers and Harbors Act of 1899 and section 404 of the Clean Water Act (33 U.S.C. 1344)." [Id.]

2.3.10 Fish and Wildlife Coordination Act [16 U.S.C. §§ 661-666c]

The Fish and Wildlife Coordination Act (FWCA) requires adequate consideration for the "conservation, maintenance, and management of wildlife resources" whenever the "waters of any stream or other body of water are impounded, diverted, the channel deepened, or the stream or other body of water otherwise controlled or modified for any purpose … including navigation and drainage, by any department or agency of the United States. [16 U.S.C. § 663(a)] This generally includes consultation with the USFWS, the NMFS, and State wildlife agencies for activities that affect, control, or modify waters of any stream or bodies of water in order to minimize the adverse impacts of such actions on fish and wildlife resources and habitat. This consultation is generally incorporated into the process of complying with Section 404 of the Clean Water Act, NEPA, or other Federal permit, license, or review requirements.

2.3.11 Migratory Bird Treaty Act [16 U.S.C. § 703 et seq.].

The protection of all migratory birds is governed by the Migratory Bird Treaty Act (MBTA) [16 U.S.C. §§ 703-712], which generally prohibits the take of any migratory bird or any part, nest, or eggs of any such bird. [16 U.S.C. § 703(a)]. Under the MBTA, it is illegal to "take, kill, possess, transport, or import migratory birds or any part, nest, or egg of any such bird" unless authorized

by a valid permit from the USFWS. [Id.]. The regulation at 50 CFR 10.13 includes a list of migratory birds protected by the MBTA.

Page Intentionally Left Blank

Chapter 3 - Rainfall-Runoff Processes

The rainfall-runoff process is the collection of interrelated natural processes by which water, as precipitation, enters a watershed and then leaves as runoff. The amount of precipitation that runs off from the watershed is called the “rainfall excess.” “Hydrologic abstractions” commonly describes all the processes that extract water from the original precipitation. "Surface runoff" is the portion of the total precipitation that has not been removed by abstractions." It follows that the volume of surface runoff equals the volume of rainfall excess.

The primary purpose of this chapter is to describe more fully the runoff process placing it in the context of the hydrologic cycle. An understanding of the process enables properly applying hydrologic design methods. This section identifies pertinent aspects of precipitation and discusses each of the hydrologic abstractions in some detail illustrating their respective influence on runoff. The chapter qualitatively discusses the runoff process and specifies the important characteristics of runoff along with how they are influenced by different features of the drainage basin and precipitation. Because the time characteristics of runoff are important in design, the chapter also includes a discussion of runoff travel time parameters.

3.1 The Hydrologic Cycle

Water is one of the most basic and commonly occurring substances and is the only substance on Earth that exists naturally in the three basic forms of matter (i.e., liquid, solid, and gas). The quantity of water varies from place to place and from time to time. At any given moment, the vast majority of the Earth’s water is found in the oceans, but there is a constant interchange of water from the oceans to the atmosphere to the land and back to the ocean. Hydrologists call this interchange, along with transformation of water from one phase to another, the hydrologic cycle.

Hydrologic Cycle

The rainfall-runoff process is also known as the hydrologic cycle. The hydrologic cycle is the continuous movement of water, in the states of liquid, gas and solid, from the atmosphere to the Earth surface and back into the atmosphere. Solar radiation is the driving energy source for precipitation, evaporation, and condensation. Gravity is the driving force for the runoff over the surface of the Earth.

Figure 3.1 illustrates the hydrologic cycle. Beginning with atmospheric moisture, the hydrologic cycle can be described as follows although it does not begin or end at any particular step:

- When warm, moist air is lifted to the level at which condensation occurs, precipitation in the form of rain, hail, sleet, or snow forms and then falls on a watershed.
- Some of the water evaporates as it falls and the rest either reaches the ground or is intercepted by buildings, trees, and other vegetation.
- The intercepted water evaporates directly back to the atmosphere, thus completing a part of the cycle.
- The remaining precipitation reaches the ground’s surface or onto the water surfaces of rivers, lakes, ponds, and oceans.

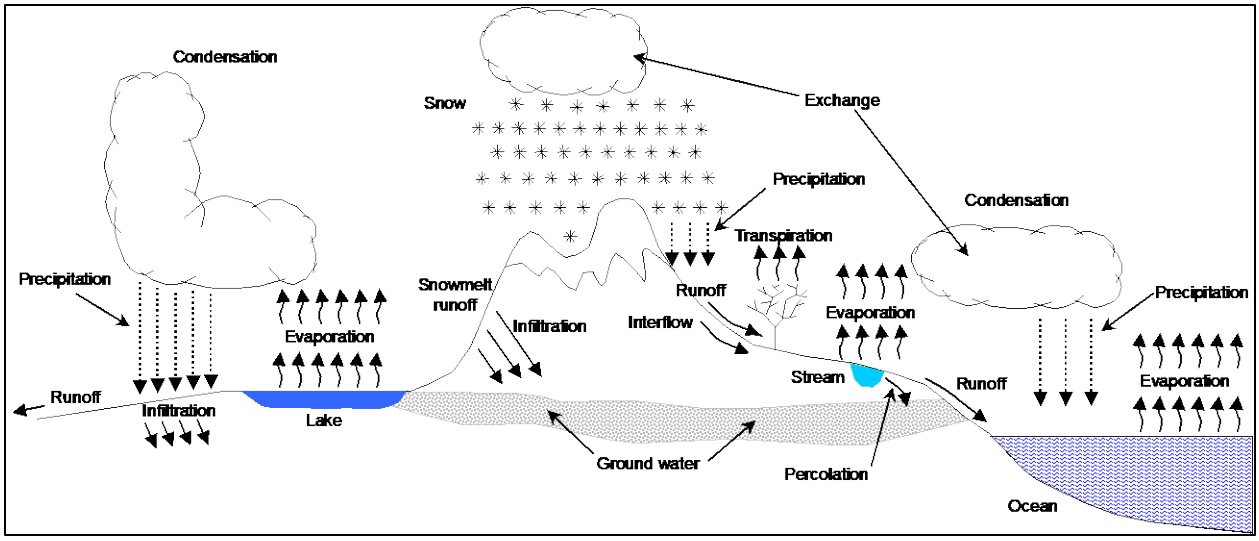

Figure 3.1. The hydrologic cycle.

If the precipitation falls as snow or ice, and the surface or air temperature is sufficiently cold, this frozen water is stored temporarily as snowpack. It is later released when the temperatures increase and melting occurs. While contained in a snowpack, some of the water escapes through sublimation, the process where frozen water (i.e., ice) changes directly into water vapor and returns to the atmosphere without entering the liquid phase. When the temperature exceeds the melting point, the water from snowmelt becomes available to continue in the hydrologic cycle.

The water that reaches the Earth's surface evaporates, infiltrates into the root zone, or flows overland into puddles and depressions in the ground or into swales and streams. The effect of infiltration is to increase the soil moisture. Field capacity is the moisture held by the soil after all gravitational drainage. If the moisture content is less than the field capacity of the soil, water returns to the atmosphere through soil evaporation and by transpiration from plants and trees. If the moisture content becomes greater than the field capacity, the water percolates downward to become groundwater.

The part of precipitation that falls into puddles and depressions can evaporate, infiltrate, or, if it fills the depressions, the excess water flows overland until eventually it reaches natural drainageways. Water held within the depressions is called depression storage and is not available for overland flow or surface runoff.

Before flow can occur overland and in the natural or constructed drainage systems, the flow path must reach its storage capacity. This form of storage, called detention storage, is temporary since most of this water continues to drain after rainfall ceases. The precipitation that percolates into the subsurface is stored as soil moisture or groundwater. It may continue in the hydrologic cycle as seepage into streams and lakes, as capillary movement back into the root zone, or is pumped from wells and discharged into irrigation systems, storm drains, or other drainageways. Water that reaches streams and rivers may be detained in storage reservoirs and lakes or it eventually reaches the oceans. Throughout this path, water is continually evaporated back to the atmosphere, and the hydrologic cycle is repeated.

In highway design, the primary concern is with the surface runoff portion of the hydrologic cycle. The four most important parts of the hydrologic cycle to the highway designer are: 1) precipitation, 2) infiltration, 3) storage, and 4) surface runoff. Depending on local conditions, other elements may be important; however, evaporation and transpiration can generally be discounted.

Precipitation is very important to the development of hydrographs and especially in synthetic unit hydrograph methods. In some peak flow formulas, calculation of excess rainfall, or total

precipitation minus the sum of the infiltration and storage, yields the flood flow estimate. As described above, infiltration is that portion of the rainfall that enters the ground surface to become groundwater or to be used by plants and trees and transpired back to the atmosphere. Some infiltration may find its way back to the tributary system. This element, called interflow, can move slowly beneath the ground surface or as groundwater seepage. The amount of interflow is generally small. HEC-16 (FHWA 2023) discusses in more detail groundwater as it relates to surface water and interflow. Storage is the water held on the surface of the ground in puddles and other irregularities (depression storage) and water stored in more significant quantities often in constructed structures (detention storage). Surface runoff is the water that flows across the surface of the ground into the watershed's tributary system and eventually into the primary watercourse.

The designer determines the quantity and associated time distribution of runoff at a given highway stream crossing, considering each of the pertinent aspects of the hydrologic cycle. In most cases, the designer approximates these factors. In some situations, the designer assigns values to storage and infiltration with confidence, while in others, there may be considerable uncertainty. The final analysis may discount the importance of one or both losses.

3.2 Precipitation

Precipitation is the water that falls from the atmosphere in either liquid or solid form. It results from the condensation of moisture in the atmosphere due to the cooling of a parcel of air. The most common cause of cooling is dynamic or adiabatic lifting of the air. Adiabatic lifting, which is influenced by air pressure, volume, and temperature, means that a given parcel of air is caused to rise with resultant cooling and possible condensation into very small cloud droplets. If these droplets coalesce and become of sufficient size to overcome the air resistance, precipitation in some form results.

3.2.1 Forms of Precipitation

Precipitation occurs in various forms. Rain is precipitation that is in the liquid state when it reaches the Earth. Snow is frozen water in a crystalline state, while hail is frozen water in a "massive" state. Sleet is melted snow that is an intermixture of rain and snow. Of course, precipitation that falls to Earth in the frozen state cannot become part of the runoff process until melting occurs. Much of the precipitation that falls in mountainous areas and in the northerly latitudes falls in the frozen form and is stored as snowpack or ice until warmer temperatures prevail.

3.2.2 Types of Precipitation (by Origin)

The origin of the adiabatic lifting motion allows classification of the type of precipitation. Different spatial and temporal rainfall regimens characterize each of these classifications, typically by storm type. The three major types of storms are classified as convective storms, orographic storms, and cyclonic storms. Certain regions may consider a fourth type of storm, i.e., hurricane or tropical cyclone, although it is a special case of the cyclonic storm. Design storms are discussed in Section 8.2.

3.2.2.1 Convective Storms

Precipitation from convective storms results as warm moist air rises from lower elevations into cooler overlying air as shown in Figure 3.2. The characteristic form of convective precipitation is the summer thunderstorm. The surface of the Earth is warmed considerably by mid-day to late afternoon of a summer day, the surface imparting its heat to the ambient air. The warmed air begins rising through the overlying air, and if proper moisture content conditions are met (condensation level), large quantities of moisture are condensed from the rapidly rising, rapidly

cooling air. The rapid condensation may often result in huge quantities of rain from a single thunderstorm spawned by convective action. Large rainfall rates and depths are quite common beneath slowly moving thunderstorms.

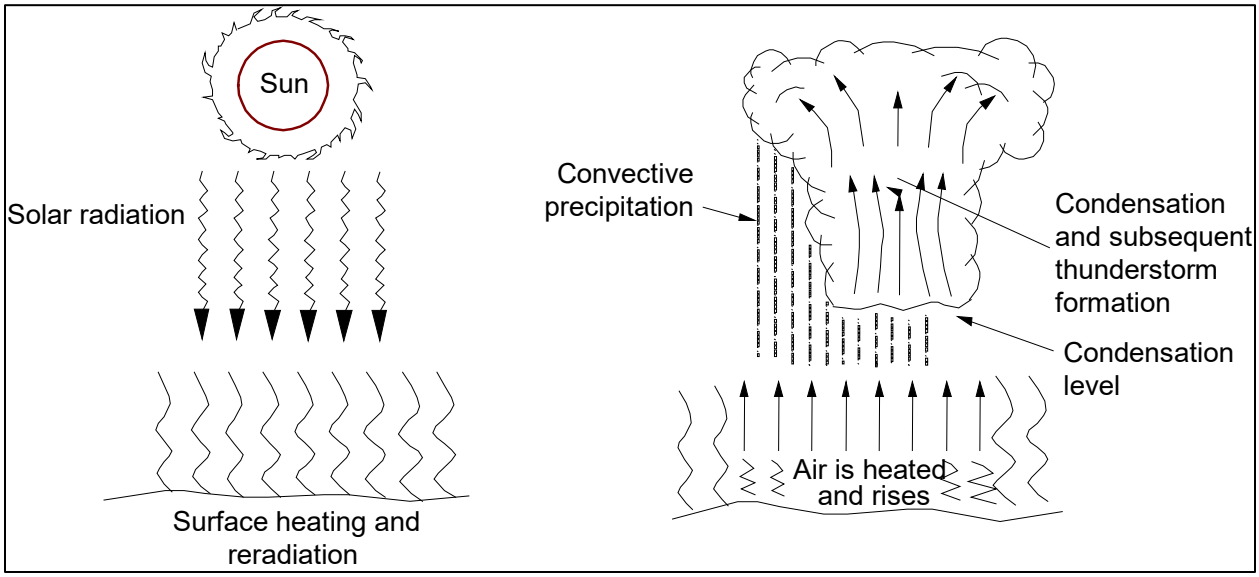

Figure 3.2. Convective storm.

3.2.2.2 Orographic Storms

Orographic precipitation results from air forced to rise over a fixed-position geographic feature such as a range of mountains (see Figure 3.3). The characteristic precipitation patterns of the Pacific Coast States are the result of significant orographic influences. Mountain slopes that face the wind (windward) are much wetter than the opposite (leeward) slopes. In the Cascade Range in Washington and Oregon, the west-facing slopes may receive more than 100 inches of precipitation annually, while the east-facing slopes, only a short distance away over the crest of the mountains, receive about 20 inches of precipitation annually.

3.2.2.3 Cyclonic Storms

The rising or lifting of air as it converges on an area of low pressure causes cyclonic precipitation. Air moves from areas of higher pressure toward areas of lower pressure. In the middle latitudes, cyclonic storms generally move from west to east and have contrasting cold and warm air associated with them. These mid-latitude cyclones are sometimes called extra-tropical cyclones, indicating the loss of their “tropical” characteristics, or continental storms.

Continental storms occur at the boundaries of air of significantly different temperatures. A disturbance in the boundary between the two air parcels can grow, appearing as a wave as it travels from west to east along the boundary. Generally, on a weather map, the cyclonic storm appears as shown in Figure 3.4, with two boundaries or fronts developed. One front has warm air being pushed into an area of cool air, while the other front has cool air pushed into an area of warmer air. This type of air movement, or front, where warm air is the aggressor, is a warm front. Where cold air is the aggressor, it is a cold front (see Figure 3.5). The precipitation associated with a cold front is usually heavy and covers a relatively small area, whereas the precipitation associated with a warm front is more passive, smaller in quantity, but covers a much larger area. Tornadoes and other violent weather phenomena are associated with cold fronts.

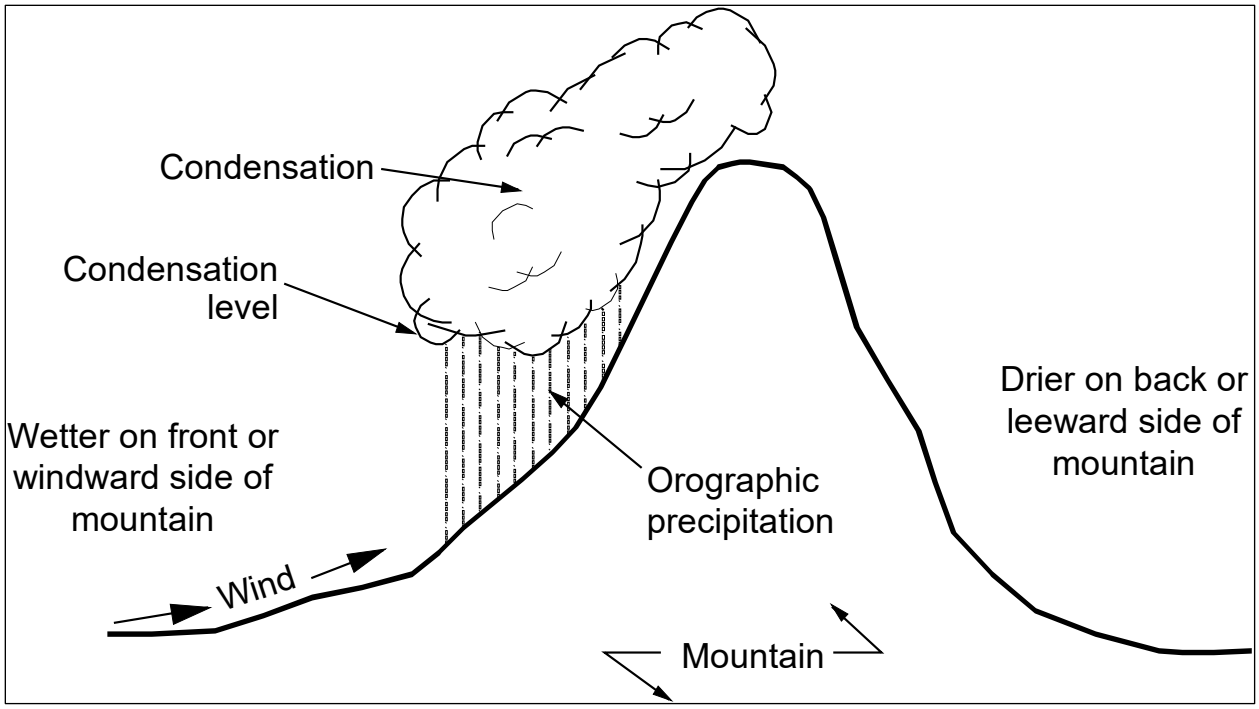

Figure 3.3. Orographic storm.

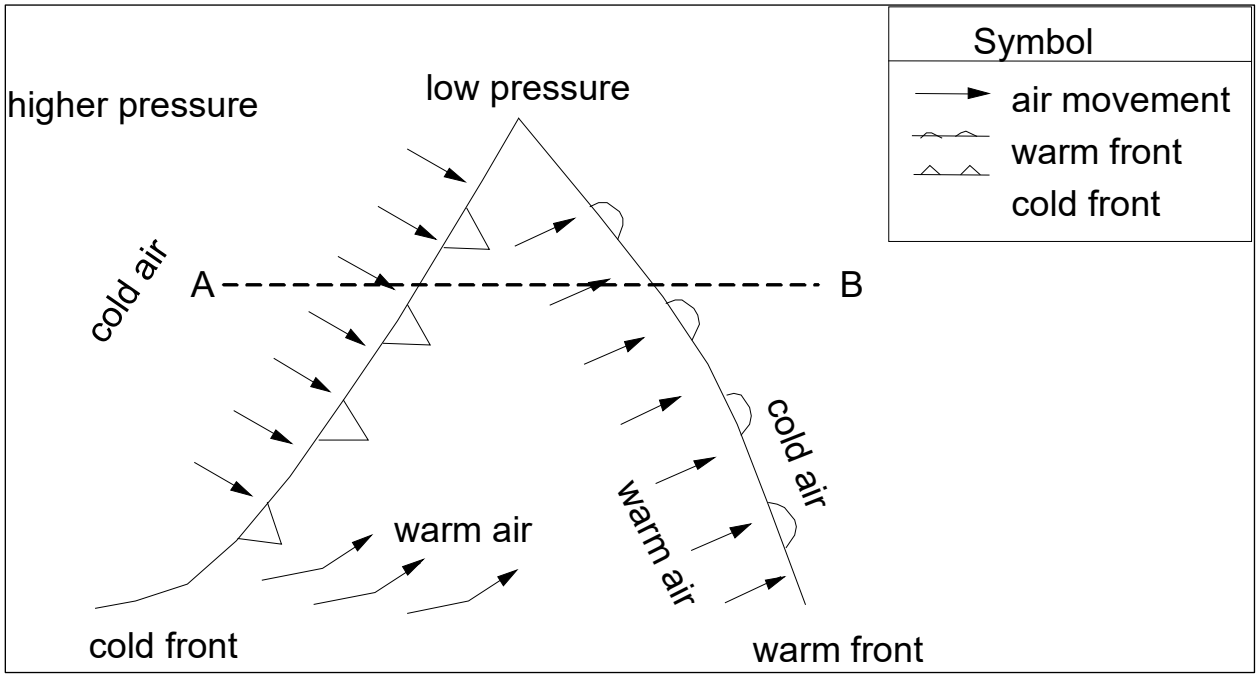

Figure 3.4. Storm as it appears on weather map in the northern hemisphere.

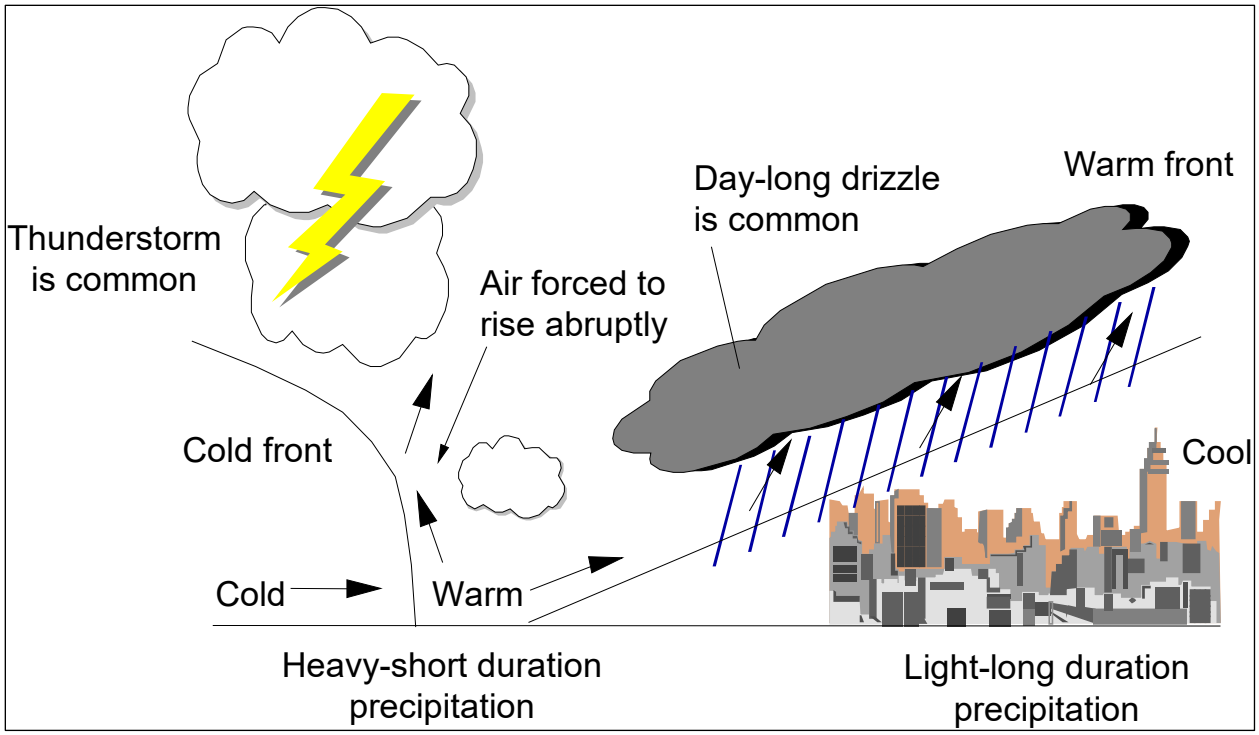

Figure 3.5. Cyclonic storms in mid-latitude; cross-section from A to B of Figure 3.4.

3.2.2.4 Hurricanes and Typhoons

Hurricanes, typhoons, and tropical cyclones develop over tropical oceans with a surface water temperature greater than 84 °F. A hurricane has no trailing fronts, as the air is uniformly warm since the ocean surface from which it was spawned is uniformly warm. Hurricanes can result in tremendous amounts of rainfall in a relatively short time. Rainfall amounts of 14 to 20 inches in less than 24 hours are common in well-developed hurricanes, where sustained winds often exceed 74 mi/h.

3.2.3 Characteristics of Rainfall Events

Rainfall is measured as the vertical depth of water that would accumulate on a level surface if it remained where it fell. A variety of rain gages measure precipitation. All first-order weather stations use gages providing nearly continuous records of accumulated rainfall over time. Highway engineers primarily consider the precipitation characteristics directly impacting highway drainage: intensity (rate of rainfall); duration; time distribution of rainfall; storm shape, size, and movement; and frequency.

Precipitation as Snow

Precipitation in the form of snow is also measured as vertical depth and can be converted to water equivalent. (See Section 11.2)

Figure 3.6 graphically represents the time dependence of rainfall intensity, known as a hyetograph, for two rainfall events at a specific gage location. Rainfall intensity is the time rate of rainfall and is commonly expressed in units of inches per hour. Intensities can vary from misting conditions (where a trace of precipitation may fall) to intense precipitation from cloudbursts. Rainfall data are typically reported in either tabular form or as cumulative mass rainfall curves as shown in Figure 3.7. In any given storm, the instantaneous intensity is the slope of the mass rainfall curve at a particular time.

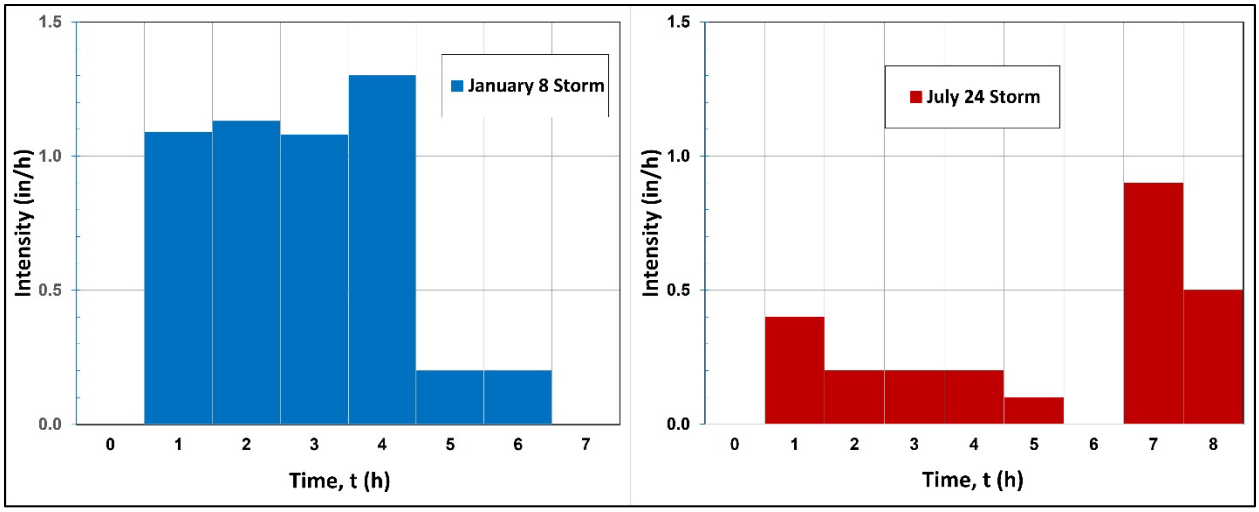

Figure 3.6. Example hyetographs for two rainfall events.

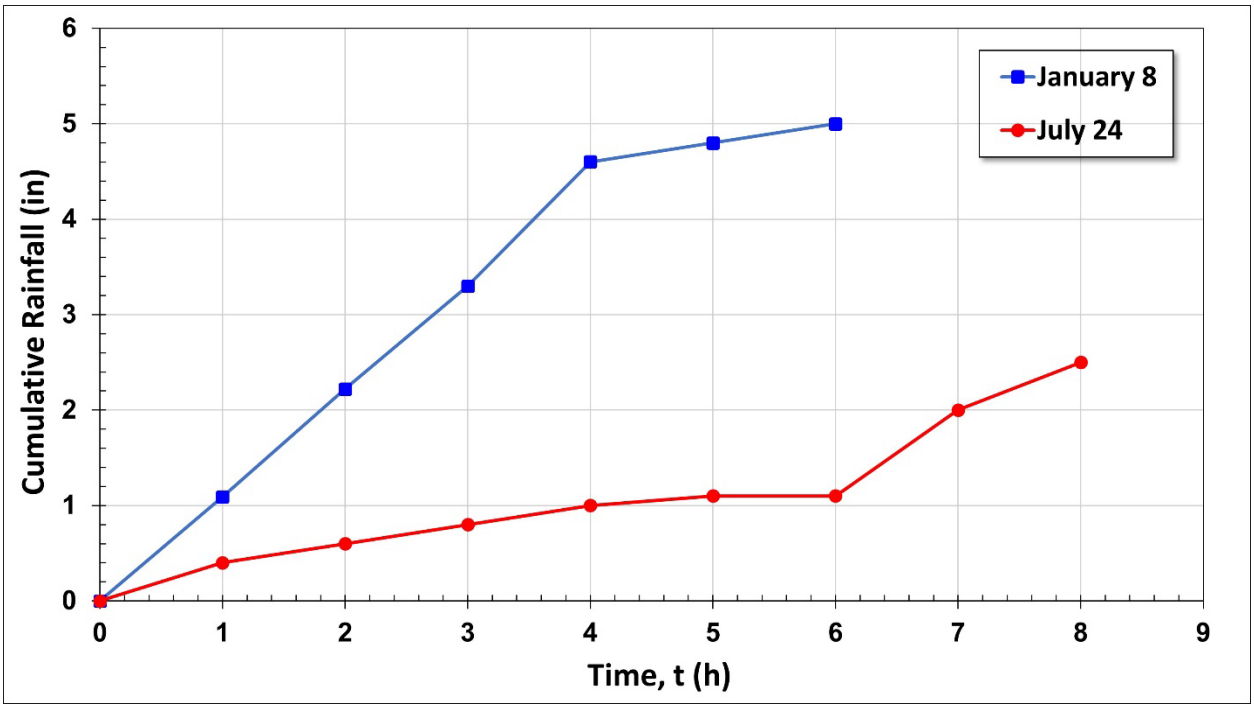

Figure 3.7. Mass rainfall curves for example rainfall events.

Analysts typically divide the storm into convenient time increments and determine the average intensity over each of the selected periods. While the above illustrations use a 1-hour time increment to determine the average intensity, designers can use any time increment compatible with the time scale of the hydrologic event to be analyzed.

Engineers determine the storm duration — or time of rainfall — as the time from the beginning of rainfall to the end of rainfall. For example, in Figure 3.6 the storm duration is simply the width (time base) of the hyetograph. Using Figure 3.7, the duration is from the beginning of the storm to the point where the mass curve becomes horizontal, indicating no further accumulation of precipitation. Storm duration most directly affects the volume of surface runoff, with longer storms producing more runoff than shorter duration storms of the same intensity.

The time distribution of rainfall (hyetograph) influences the corresponding distribution of the surface runoff. As illustrated in Figure 3.8, high intensity rainfall at the beginning of a storm usually results in a rapid rise in the runoff, followed by a long recession of the flow. Conversely, if the more intense rainfall occurs toward the end of the duration the time to peak is typically longer, followed by a rapidly falling recession.

Analysts typically determine the three meteorological factors, storm pattern, areal extent, and movement, by the type of storm (see Section 3.2.2). For example, storms associated with cold fronts (thunderstorms) tend to be more localized, faster moving, and of shorter duration, whereas warm fronts tend to produce slowly moving storms of broad areal extent and longer durations. All three of these factors determine the areal extent of precipitation and how large a portion of the drainage area contributes over time to the surface runoff. As illustrated in Figure 3.9, a small, localized storm of a given intensity and duration, occurring over a part of the drainage area, results in much less runoff than if the same storm covered the entire watershed.

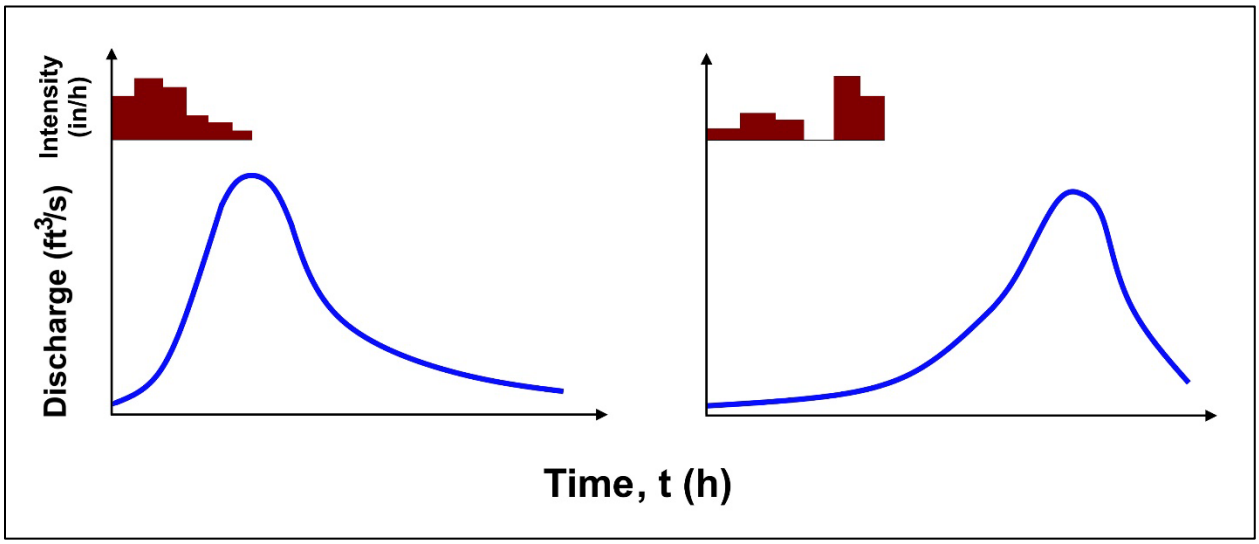

Figure 3.8. Effect of time variation of rainfall intensity on the surface runoff

The location of a localized storm in the drainage basin also affects the time distribution of the surface runoff. A storm near the outlet of the watershed results in the peak flow occurring very quickly and a rapid passage of the flood. If the same storm occurred in a remote part of the basin, the runoff at the outlet resulting from the storm would be longer and the peak flow lower due to storage in the channel.

Storm movement has a similar effect on the runoff distribution, particularly if the basin is long and narrow. Figure 3.10 shows that a storm moving up a basin from its outlet gives a distribution of runoff that is relatively symmetrical with respect to the peak flow. The same storm moving down the basin usually results in a higher peak flow and an asymmetrical distribution with the peak flow occurring later in time.

Frequency is also an important characteristic because it establishes the frame of reference for how often precipitation with given characteristics is likely to occur on average over a period of observation. From the standpoint of highway design, a primary concern is with the frequency of occurrence of the resulting surface runoff, and in particular, the frequency of the peak flow. Although a storm of a given frequency does not always produce a flood of the same frequency, several analytical techniques are based on this assumption, particularly for ungaged watersheds. Section 3.4 discusses some of the factors that determine how closely the frequencies of precipitation and peak flow correlate with one another.

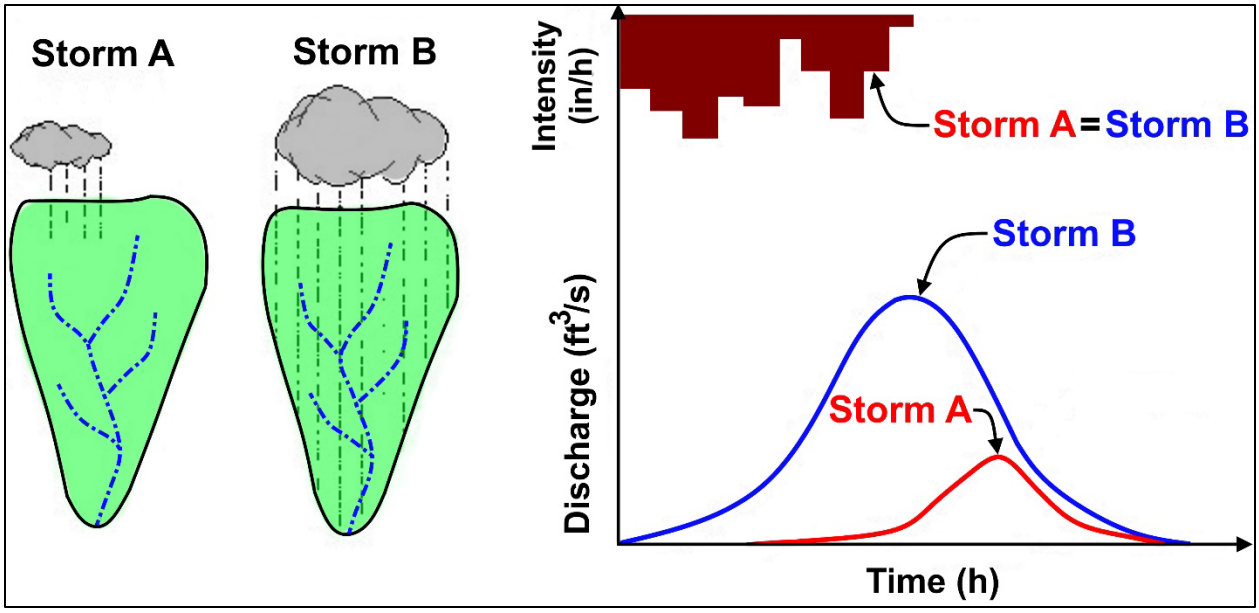

Figure 3.9. Effect of storm size on runoff hydrograph.

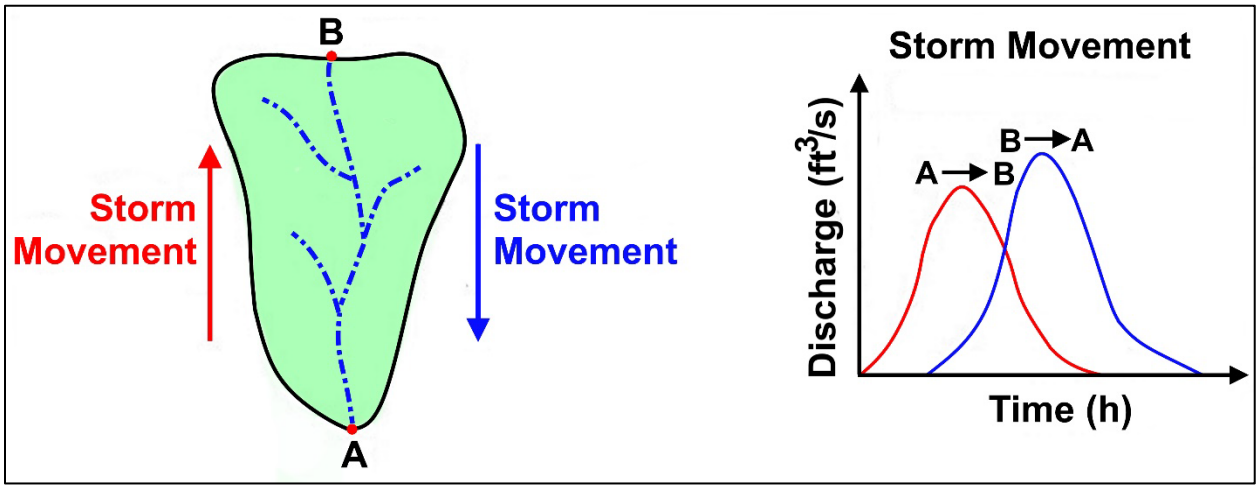

Figure 3.10. Effect of storm movement on runoff hydrograph.

Chapter 4 more fully discusses references and data sources for precipitation. Because of the highly variable and erratic nature of precipitation, highway engineers and designers may wish to become familiar with the different types of storms and the characteristics of precipitation characteristic of their regions. Understanding the seasonal variations prevalent in many areas may be helpful. In addition, highway designers may also benefit from studying reports on historic storms and floods in a region. Such reports can provide information on past storms and the consequences that they may have had on drainage structures.

3.2.4 Intensity-Duration-Frequency Curves

Three rainfall characteristics – intensity, duration, and frequency – are important and interact with each other in many hydrologic design problems. For use in design, highway engineers combine the three characteristics, usually graphically, into the intensity-duration-frequency (IDF) curve. Practitioners plot rainfall intensity versus duration for each exceedance frequency, where the rainfall intensity is the ordinate and duration is the abscissa. IDF curves are location dependent. Because of this location dependency, highway engineers use local IDF curves and NOAA Atlas

14, among other sources, for hydrologic design work. Figure 3.11 illustrates an example of a family of IDF curves.

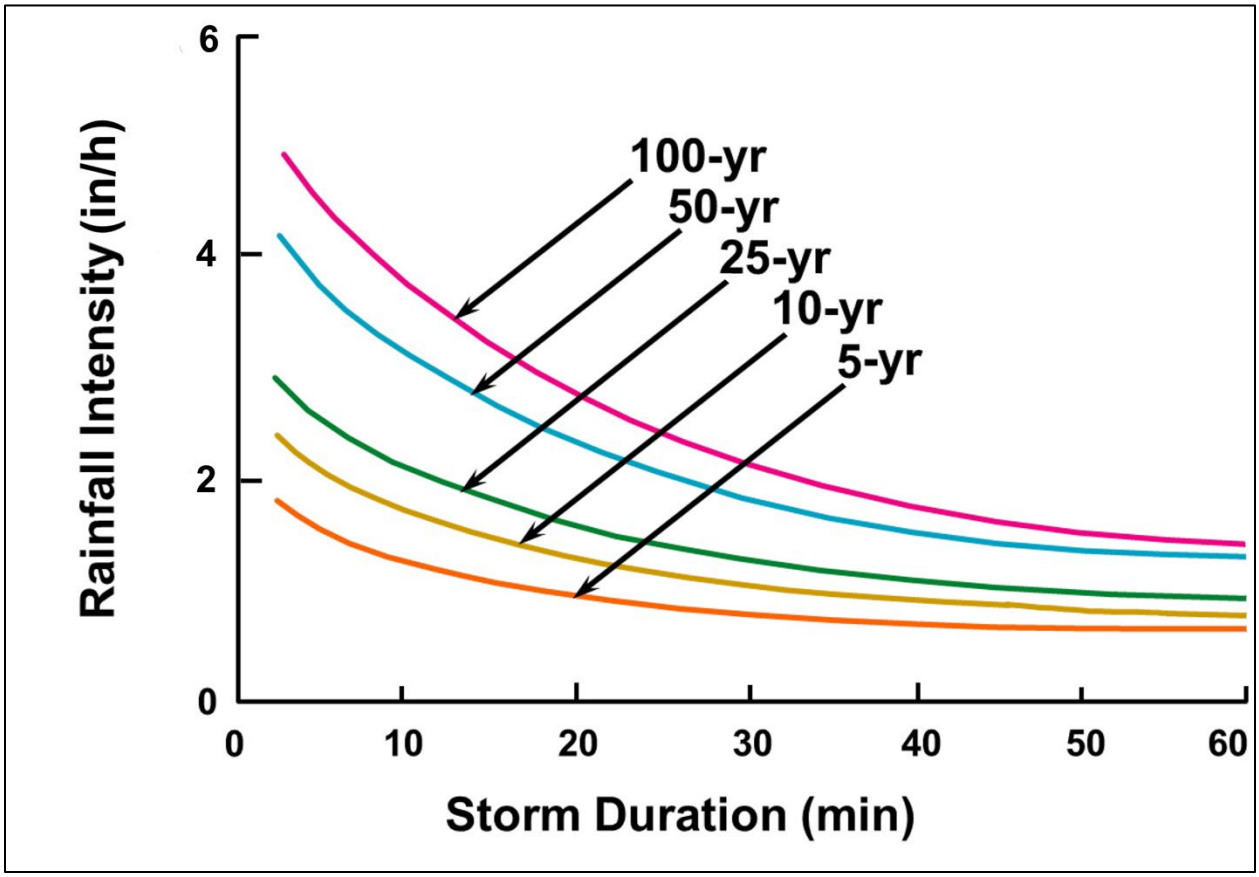

Figure 3.11. Intensity-duration-frequency (IDF) curves.

Typically, the IDF curve for a specific exceedance frequency has a characteristic curve for small durations, usually 2 hours and shorter, and is straight for the longer durations. One model for IDF curves of a given exceedance frequency is:

$$i = \begin{cases} \dfrac{a}{D+b} & \text{for } D \le 2\,h \\ cD^{d} & \text{for } D > 2\,h \end{cases} \qquad (3.1)$$

where:

i	=	Rainfall intensity, in/h (mm/h)
D	=	Rainfall duration, h
a, b, c, and d	=	Empirical constants

Another model for IDF curves is a more generalized version of the short duration portion of the previous model:

$$i = \frac{a}{(D+b)^{m}} \qquad (3.2)$$

where:

i	=	Rainfall intensity, in/h (mm/h)
D	=	Rainfall duration, h
a, b, m	=	Empirical constants

In both models, duration is assumed to be equal to time of concentration in the context of the Rational Method.

Some hydrologic design manuals provide depth-duration-frequency (DDF) curves as an alternative to IDF curves. The DDF curve is like the IDF curve except the depth of rainfall is graphed as the ordinate. Either representation provides the same information. The choice of presentation depends on the application for the rainfall data.

3.3 Hydrologic Abstractions

Abstraction, also known as rainfall loss, is the collective term for the various processes that remove water from the incoming precipitation before it leaves the watershed as runoff. Direct abstractions include infiltration, interception, and depression storage. Indirect abstractions, that is those that primarily occur after the rainfall event, include evaporation and transpiration.

3.3.1 Infiltration

Infiltration is the flow of water from the ground surface into the underlying soil by percolation. The process of infiltration is complex and depends upon many factors such as soil type; vegetal cover; antecedent moisture conditions (discussed in Section 3.5.7), or the amount of time elapsed since the last precipitation event; precipitation intensity; and temperature. Infiltration is usually the most important abstraction in determining the response of a watershed to a given rainfall event. As important as infiltration is, using models to accurately predict infiltration rates or total infiltration volumes for a given watershed has proven to be challenging.

3.3.2 Interception

Interception is the removal of water that wets and adheres to objects above ground such as buildings, trees, and vegetation. When the rainfall first begins, the foliage and other intercepting surfaces are dry. As water adheres to these surfaces, a portion of the initial rainfall is abstracted. This process occurs in a relatively short period of time and, once the initial wetting is complete, the interception losses decrease to zero. This water is subsequently removed from the intercepting surfaces through evaporation. Interception can be as high as 0.08 inches during a single rainfall event, but usually is nearer 0.02 inches. The quantity of water removed through interception is typically not significant for an isolated storm and is often ignored for highway hydrology applications, but over a longer period, it can be significant. After each rainfall event, intercepted water typically evaporates.

3.3.3 Depression Storage

Depression storage is the term applied to water that is lost because it becomes temporarily trapped in the numerous small depressions that are characteristic of any natural surface with no possibility for escape as runoff. Ultimately, water in depression storage either evaporates or infiltrates. Once the depression storage is filled, subsequent rainfall overflows these depressions and becomes runoff. The amount of water lost from depression storage varies greatly with land use. A paved surface does not detain as much water as a recently furrowed field. The relative importance of depression storage in determining the runoff from a given storm depends on the amount and intensity of precipitation in the storm. Typical values for depression storage range

from 0.04 to 0.3 inches with some values as high as 0.6 inches per event. As with evaporation and transpiration, engineers generally do not calculate depression storage in highway design.

3.3.4 Evaporation

Evaporation is the process by which water from the land and water surfaces is converted into water vapor and returned to the atmosphere. It occurs continually whenever the air is unsaturated, and temperatures are sufficiently high. Air is “saturated” when it holds its maximum capacity of moisture at the given temperature. Saturated air has a relative humidity of 100 percent. Evaporation plays a major role in determining the long-term water balance in a watershed. However, evaporation is usually insignificant in small watersheds for single storm events and can be discounted when calculating the discharge from a given rainfall event.

3.3.5 Transpiration

Transpiration is the physical removal of water from the watershed by the life actions associated with the growth of vegetation. In the process of respiration, green plants consume water from the ground and transpire water vapor to the air through their foliage. As with evaporation, this abstraction is only significant for a watershed over a long period. It has minimal effect upon the runoff resulting from a single storm event, which occurs over a shorter period. Transpired water previously infiltrated into the soil.

3.3.6 Total Abstraction Methods

While the volumes of the individual abstractions may be small, their sum can be hydrologically significant. Therefore, hydrologic methods commonly compute a single value for all combined abstractions. For example, the Soil Conservation Service (SCS), now the Natural Resources Conservation Service (NRCS), curve number method combines all abstractions, with the volume equal to the difference between the volumes of rainfall and runoff. The Rational Method uses a single term for total abstraction. The phi-index method assumes a constant rate of abstraction over the duration of the storm. These total abstraction methods simplify the calculation of storm runoff rates.

3.4 Characteristics of Runoff

Water that has not been abstracted from the incoming precipitation leaves the watershed as surface runoff. Therefore, the volume of surface runoff equals the volume of rainfall excess. In the case of the typical highway application, runoff is the original precipitation minus infiltration and storage. While runoff occurs in several stages, highway drainage structure design, i.e., gutters, inlets, and culverts, among others, primarily considers the flow that becomes channelized since it influences the size of a given drainage structure. The rate of flow or runoff at a given instant, in terms of volume per unit of time, is called discharge. The next sections consider characteristics of runoff important to drainage design, in particular: 1) peak discharge or peak rate of flow, 2) discharge variation with time (hydrograph), 3) total volume of runoff, and 4) frequency with which discharges of specified magnitudes are likely to be equaled or exceeded (probability of exceedance).

3.4.1 Peak Flow

The peak flow, often called peak discharge, is the maximum rate of runoff passing a given point during or after a rainfall event. Highway engineers size a given structure to accommodate peak flows for storms in an area. Because the peak flow varies for each storm, the designer is responsible to size a given structure for the magnitude of storm determined to present an acceptable risk in each situation. This risk may be determined by law, by local design manual

and/or by engineering judgment. Peak flow rates can be affected by many factors in a watershed, including rainfall, basin size, and the physiographic features.

3.4.2 Time Variation (Hydrograph)

The flow in a stream varies from time to time, particularly during and in response to storm events. As precipitation falls and moves through the watershed, water levels in streams rise and may continue to do so (depending on position of the storm over the watershed) after the precipitation has ceased. The flood hydrograph characterizes the response of an affected stream through time during a storm event. This response can be pictured by graphing the flow in a stream relative to time. Figure 3.12 illustrates the primary features of a typical hydrograph. These features include the rising and falling limbs, the peak flow, the time to peak, and the time base of the hydrograph. The instantaneous maximum discharge of the hydrograph is the peak flow. Direct runoff is the total runoff hydrograph minus base flow. There are several types of hydrographs, such as flow per unit area and stage hydrographs, but all display the same typical variation through time.

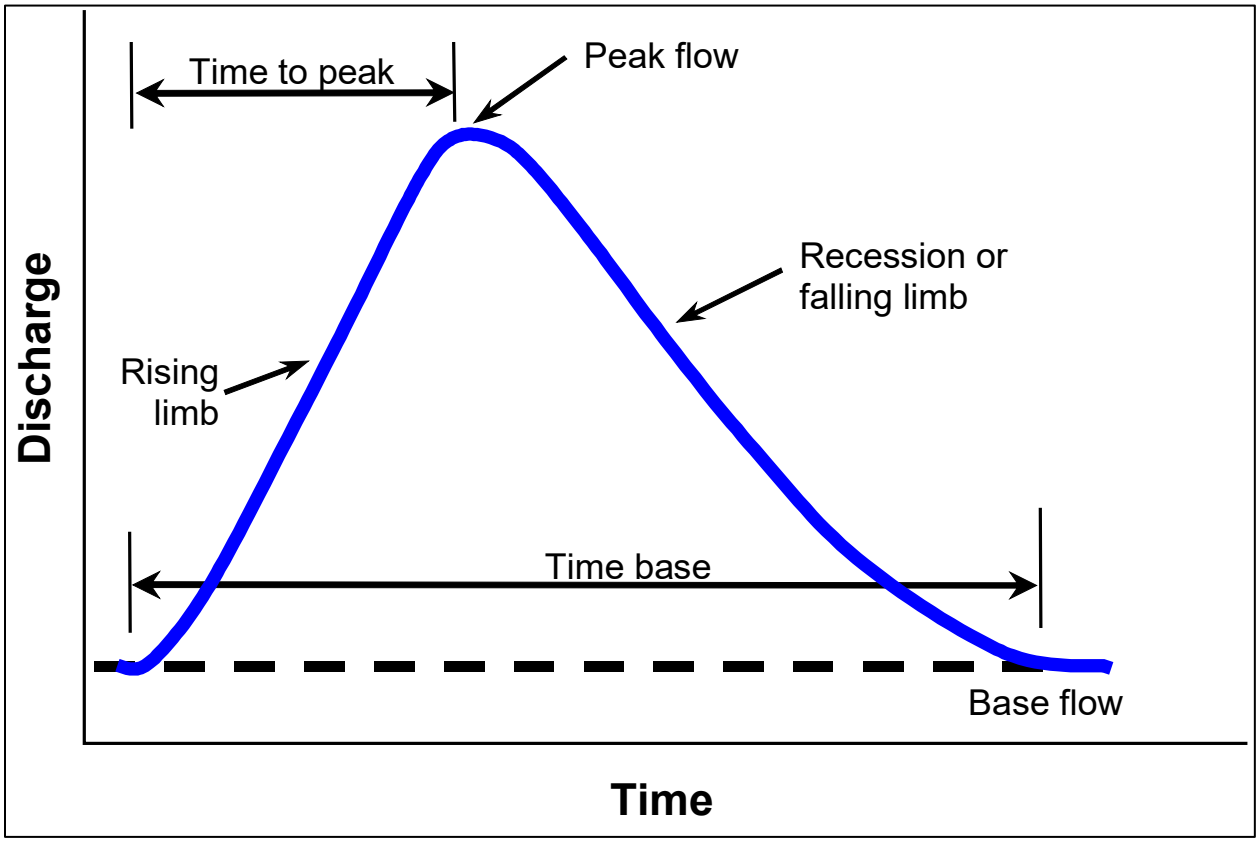

Figure 3.12. Elements of a flood hydrograph.

3.4.3 Total Volume

The total volume of runoff from a given flood is of primary importance to the design of storage facilities and flood control works. Engineers may also consider hydrograph volume at stream crossings where an existing roadway embankment provides detention storage. Engineers most easily determine flood volume as the area under the flood hydrograph (Figure 3.12). It is commonly measured in units of cubic feet (meters). The equivalent depth of net rain over the watershed is determined by dividing the volume of runoff by the watershed area.

3.4.4 Frequency

The exceedance frequency is the relative number of times a flood of a given magnitude can be expected to occur on average over a long period of time. It is usually expressed as a ratio or a percentage. By its definition, frequency is the probability that a flood of a given magnitude may be exceeded in any given year. Exceedance frequency is an important design criterion that identifies the level of risk acceptable for the design of a highway structure. As discussed in Section 1.3, designers use many annual exceedance frequencies (AEPs) for different risk levels associated with roadway classification.

3.4.5 Return Period

Return period is a term commonly used in hydrology. It is the average time interval between the occurrence of storms or floods of a given magnitude. The annual exceedance probability (AEP) (p) and return period (T) are related by:

$$T = \frac{1}{p} \tag{3.3}$$

For example, a flood with an AEP of 0.01 is also referred to as the 100-year flood. The use of the term return period is sometimes discouraged because some people misinterpret it to mean that there will be exactly T years between occurrences of the event. Two 100-year floods can occur in succession or 500 years apart. Such events would affect the probability of occurrence, which may involve revisiting the frequency analysis to incorporate these observed floods. The return period is only the long-term average number of years between occurrences. Refer to Section 10.3 or HEC-17 (FHWA 2016) for more detail on this topic.

3.5 Effects of Basin Characteristics on Runoff

The spatial and temporal variations of precipitation and the concurrent variations of the individual abstraction processes establish the characteristics of the runoff from a given storm. These are not the only factors involved, however. Once the local abstractions have been satisfied for a small area of the watershed, water begins to flow overland and eventually into a natural drainage channel such as a gully or a stream valley. At this point, the hydraulics of the natural drainage channels have a large influence on the character of the total runoff from the watershed.

A few of the many factors determining the hydraulic character of the natural drainage system include: drainage area, slope, hydraulic roughness, natural and channel storage, drainage density, channel length, antecedent moisture conditions, urbanization, and other factors. It is often difficult to quantify the effect of each of these factors on the important characteristics of runoff. The following paragraphs discuss some of the factors affecting the hydraulic character of a given drainage system.

3.5.1 Drainage Area

Drainage area is the most important watershed characteristic affecting runoff. As Figure 3.13a illustrates, the larger the contributing drainage area, the larger the flood runoff given all the other hydrologic parameters are the same. Regardless of the method used to evaluate flood flows, peak flow relates directly to the drainage area.

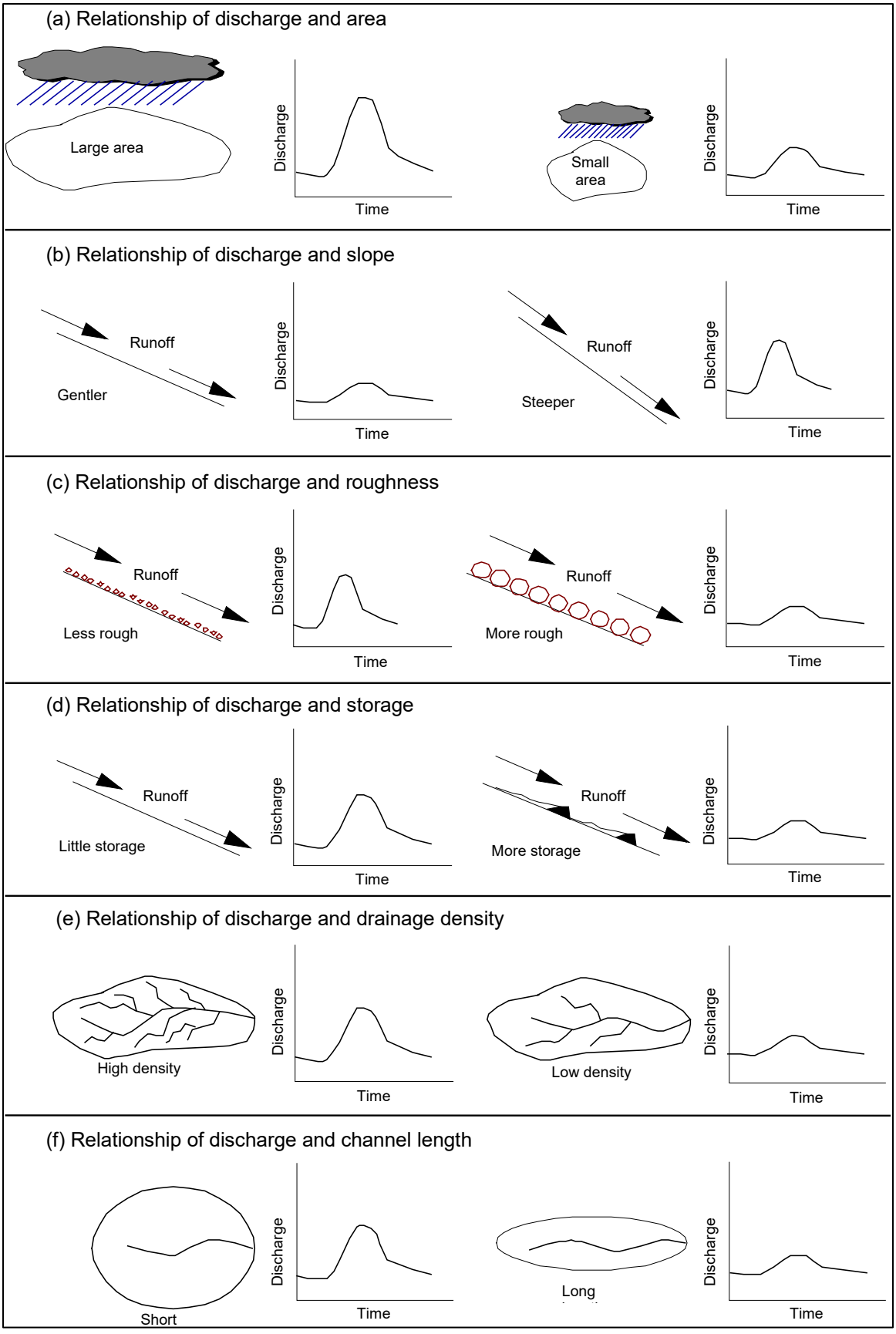

Figure 3.13. Effects of basin characteristics on the flood hydrograph.

3.5.2 Slope

Steep slopes tend to result in rapid runoff responses to local rainfall excess and consequently higher peak flows, as illustrated in Figure 3.13b. The runoff is quickly removed from the watershed, so the hydrograph is short with a high peak. The stage-discharge relationship is highly dependent upon the local characteristics of the drainage channel cross-section. If the slope is sufficiently steep, supercritical flow may prevail. Slope also affects the total volume of runoff. If the slope is very flat, the rainfall is not removed as rapidly. The process of infiltration has more time to affect the rainfall excess, thereby increasing the abstractions and resulting in a reduction of the total volume of rainfall that appears directly as runoff.

Slope is important in how quickly a drainage channel conveys water and, therefore, it influences the sensitivity of a watershed to precipitation events of various time durations. Steeply sloped watersheds rapidly convey incoming rainfall. If the rainfall is convective (characterized by high intensity and relatively short duration), the watershed responds very quickly with the peak flow occurring shortly after the onset of precipitation. If these convective storms occur with a given frequency, the resulting runoff can be expected to occur with a similar frequency. Conversely, the response of mildly sloping watersheds to the same storm is not as rapid and the resulting discharge frequency may be different than the storm frequency.

3.5.3 Hydraulic Roughness

Hydraulic roughness is a composite of the physical characteristics influencing the depth and speed of water flowing across the surface, whether overland or channelized. It affects both the time response of a drainage channel and the channel storage characteristics. Hydraulic roughness markedly affects the characteristics of the runoff resulting from a given storm. The peak rate of discharge is usually inversely proportional to hydraulic roughness (i.e., the lower the roughness, the higher the peak flow). Roughness affects the runoff hydrograph in a manner opposite of slope. The lower the roughness, the more peaked and shorter in time the resulting hydrograph for a given storm, as illustrated in Figure 3.13c.

The stage-discharge relationship for a given section of drainage channel is also dependent on roughness (assuming normal flow conditions and the absence of artificial controls). A higher roughness results in a higher stage for a given discharge.

The total volume of runoff is virtually independent of hydraulic roughness since it does not in itself directly abstract runoff. However, an indirect relationship does exist in that higher roughness slows the watershed response and allows some of the abstraction processes more time to affect runoff. Roughness also influences the frequency of discharges of certain magnitudes by affecting the response time of the watershed to precipitation events of specified frequencies.

3.5.4 Storage

Frequently, a watershed has natural or constructed storage that greatly affects the response to a given precipitation event. Common features contributing to storage within a watershed include lakes; marshes; heavily vegetated overbank areas; natural or engineered constrictions in the drainage channel causing backwater; and the floodplain storage of large, wide rivers. Storage can significantly reduce the peak rate of discharge, although this reduction is not necessarily universal. In cases of stormwater management ponds designed without adequate detention time or outlet controls, storage redistributes the discharges significantly, resulting in higher peak flows than would have occurred without added storage. As shown in Figure 3.13d, storage generally spreads the hydrograph out in time, delays the time to peak, and alters the shape of the resulting hydrograph from a given storm, which is termed attenuation. Section 9.2 details the effect of storage reservoirs.

Storage downstream of channels may create a backwater zone that alters the stage-discharge relationship in the channel such that the stage for a given discharge is higher than if the storage were not present. If the section is downstream of the storage, the stage-discharge relationship may or may not be affected, depending upon the presence of channel controls.

The presence of storage does not directly influence total volume of runoff. Storage redistributes the volume over time but does not directly change the volume. By redistributing the runoff over time, storage may allow other abstraction processes to decrease the runoff (as is the case with slope and roughness).

Changes in storage have a definite effect upon the frequency of discharges of given magnitudes. Storage tends to dampen the response of a watershed to short duration rainfall events. This can alter the relationship between frequency of precipitation and the frequency of the resultant runoff.

3.5.5 Drainage Density

Drainage density represents the capacity of a watershed to be drained by well-established drainage channels. Engineers typically quantify drainage density with a ratio of the total length of continuously flowing streams divided by the drainage area. A dimensionless measure of drainage density is total stream length squared divided by drainage area. Drainage density is somewhat subjective in designating what counts as a stream within the watershed.

Drainage density strongly influences both the spatial and temporal response of a watershed to a given precipitation event. If a watershed is well covered by a pattern of interconnected drainage channels, and the overland flow time is relatively short, the watershed responds more rapidly than if it were sparsely drained and overland flow time was relatively long. The mean velocity of runoff is normally lower for overland flow than it is for flow in a well-established natural channel. High drainage densities are associated with increased response of a watershed leading to higher peak flows and shorter hydrographs for a given precipitation event (see Figure 3.13e).

Drainage density affects the total volume of runoff since some of the abstraction processes relate to how long the rainfall excess exists as overland flow. Therefore, the lower the density of drainage, the lower the volume of runoff from a given precipitation event.

Changes in drainage density, such as with channel improvements in urbanizing watersheds, can affect the frequency of discharges of given magnitudes. By strongly influencing the response of a given watershed to any precipitation input, the drainage density determines in part the frequency of the response. The higher the drainage density, the more closely related the resultant runoff frequency would be to that of the corresponding precipitation event.

3.5.6 Channel Length

Channel length is an important watershed characteristic. The longer the channel, the more time it takes for water to be conveyed from the headwaters of the watershed to the outlet. Consequently, if all other factors are the same, a watershed with a longer channel length usually has a slower response to a given precipitation input than a watershed with a shorter channel length. As the hydrograph travels along a channel, it is attenuated and extended in time from the effects of channel storage and hydraulic roughness. As shown in Figure 3.13f, longer channels result in lower peak flows and longer hydrographs.

Channel length also influences the frequency of discharges of given magnitudes. As is the case for drainage density, highway engineers use channel length in estimating the response time of a watershed to precipitation events of given frequency. However, channel length may not remain constant with discharges of various magnitudes. In the case of a wide floodplain where the main channel meanders appreciably, the higher flood discharges may overtop the banks and essentially flow in a straight line in the floodplain, thus reducing the effective channel length.

The total volume of runoff is practically independent of channel length though it is redistributed in time, similar in effect to storage but less pronounced.

3.5.7 Antecedent Moisture Conditions

As noted earlier, antecedent moisture conditions, or the soil moisture conditions of the watershed at the beginning of a storm, affect infiltration and the volume of runoff generated by a particular storm event. Runoff volumes relate directly to antecedent moisture levels. The smaller the moisture in the ground at the beginning of precipitation, the lower the runoff because of the higher capacity of infiltration. Conversely, higher moisture content in the soil results in lower infiltration rates and the higher runoff attributable to a particular storm.

3.5.8 Urbanization

As a watershed undergoes urbanization, the peak flow typically increases and the hydrograph becomes shorter and rises more quickly unless mitigated. Prior to urbanization, a watershed has developed a natural conveyance system of gullies, streams, ponds, marshes, etc., all in equilibrium with the naturally existing vegetation and physical watershed characteristics. As an area develops, typical changes made to the watershed include: 1) removal of existing vegetation and replacement with impervious surfaces, 2) modification to natural watercourses by channelization, and 3) augmentation of the natural drainage system by storm drains and open channels. These changes tend to reduce infiltration, increase conveyance capacity, and reduce runoff travel times through the urbanized area. Consequently, peak flows and runoff volumes increase, with the time base of hydrographs becoming shorter and the rising limb rising more quickly.

3.5.9 Other Factors

Other factors within a watershed may also determine the characteristics of runoff, among them the extent and type of vegetation, the presence of channel modifications, and the use of flood control structures. These factors modify the runoff by either augmenting or negating some of the basin characteristics described above. It is important to recognize that all the factors discussed exist concurrently within a given watershed, and their combined effects govern runoff peak, volume, and timing.

3.6 Illustration of the Runoff Process

Section 3.3 described several key hydrologic abstractions in general terms. This section illustrates a method for analyzing the runoff process and using the results to obtain a hydrograph. Figure 3.14a through Figure 3.14f show the development of the direct runoff from a typical rainfall event.

Step 1. Select the rainfall input.

Rainfall is randomly distributed in time and space, and the rainfall experienced at a particular point can vary greatly. For simplification, consider the rainfall at only one point in space and assume that the variation of rainfall intensity with time can be approximated by discrete time periods of constant intensity. Figure 3.14a illustrates this simplification. The specific values of intensity and time are not important for this illustrative example since it shows only relative magnitudes and relationships. The rainfall, so arranged, is the input to the runoff process, which accounts for the various abstractions that are removed.

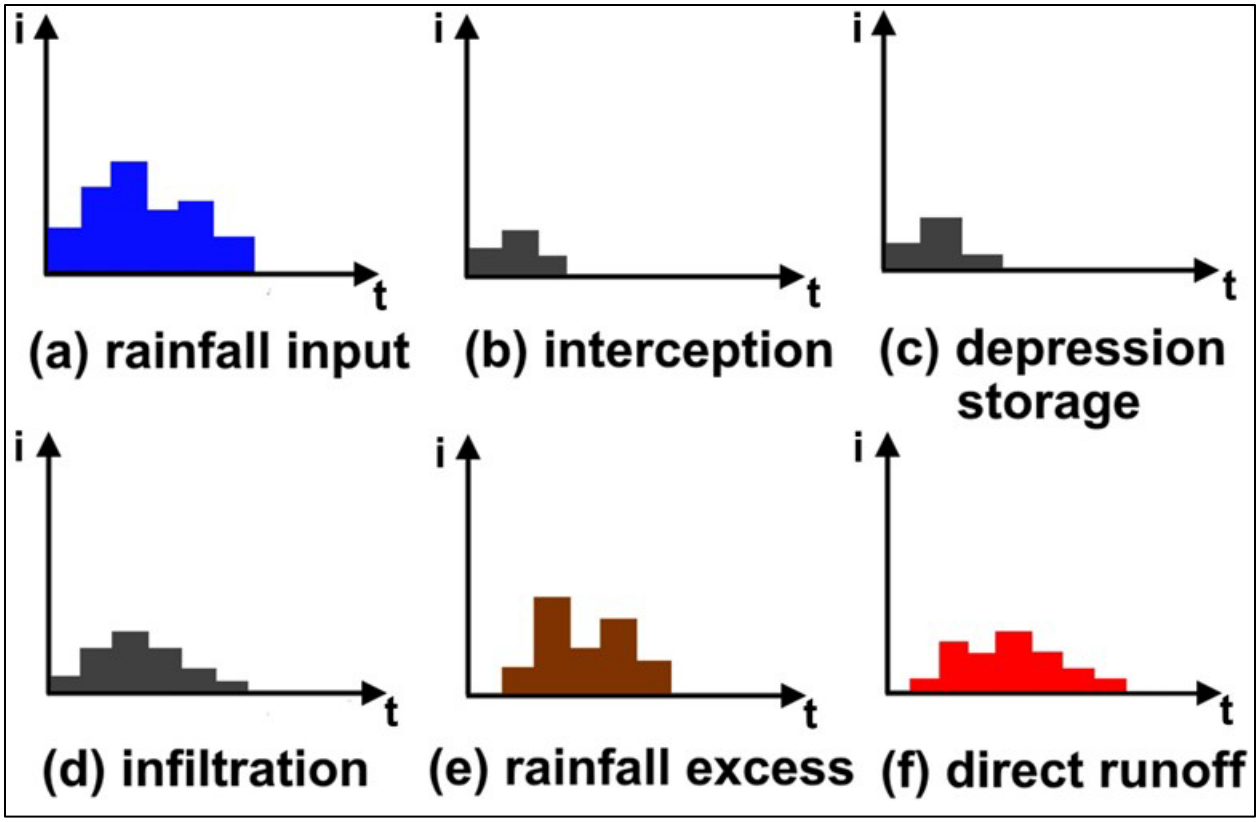

Figure 3.14. Illustration of the runoff process.

Step 2. Estimate interception.

Figure 3.14b illustrates the relative magnitude and time relationship for interception on foliage and other intercepting surfaces. Rainfall that has not been intercepted falls to the ground surface to continue in the runoff process. As described in Section 3.3.2, engineers ignore interception in many situations because it is not significant.

Step 3. Estimate depression storage.

Figure 3.14c illustrates the relative magnitude of depression storage with time. The amount of water going into depression storage varies with differing land uses and soil types, but the curve shown is representative. The smallest depressions fill faster while the larger depressions fill as time as the rainfall supply continues. The curve gradually approaches zero when all the depression storage has been filled. As described in Section 3.3.3, engineers ignore interception in many situations because it is not significant.

Step 4. Estimate infiltration.

Infiltration is a complex process, and the rate of infiltration at any point in time depends on many factors. The important point illustrated in Figure 3.14d is the time dependence of infiltration. It is also important to note the behavior of the infiltration curve after the period of relatively low rainfall intensity near the middle of the storm event. The infiltration rate increases over what it was prior to the period of lower intensity because the upper layers of the soil are drained at a rate independent of the rainfall intensity. Most deterministic models, including the phi-index method for estimating infiltration discussed in Section 7.3.1, do not model the infiltration process accurately in this respect.

Step 5. Calculate the rainfall excess.

The concept of excess rainfall is important in hydrologic analyses. After initial abstractions and other losses have been satisfied, an excess of water is available to run off from the land surface. Figure 3.14e illustrates this rainfall excess. Rainfall excess quantifies the volume of water eventually flowing to the outlet of a drainage basin. When multiplied by the drainage area, it equals the volume under the direct runoff hydrograph. Rainfall excess influences the magnitude of the peak flow, the duration of the flood hydrograph, and the shape of the hydrograph.

Step 6. Determine the direct runoff.

Figure 3.14f illustrates the final direct runoff at the outlet of the watershed. The total volume of the rainfall excess and direct runoff are equal, but the direct runoff is distributed differently and later based on the cumulative effect of all the modifying factors acting on the water as it flows through drainage channels and watershed as discussed in Section 3.5.

The processes discussed in the previous sections act simultaneously to transform the incoming rainfall from that shown in Figure 3.14a to the corresponding outflow direct runoff of Figure 3.14f. This example illustrates the runoff process for a small area. If the watershed is of appreciable size or if the storm is large, areal and time variations and other factors add a new level of complexity to describing the runoff.

3.7 Travel Time

The travel time of runoff is important in hydrologic design. When designing inlets and pipe drainage systems, engineers use estimated travel times of surface runoff. Some peak flow methods apply the time of concentration as an input to obtain rainfall intensities from the IDF curves. Hydrograph times to peak, which in some cases are computed from times of concentration, are used with hydrograph methods (Chapter 8). Channel routing methods (Section 9.3) use computed travel times in routing hydrographs through channel reaches. Thus, estimating travel times is central to a variety of hydrologic design problems.

3.7.1 Time of Concentration

The time of concentration, denoted as t_c, is the time a particle of water takes to flow from the hydrologically most distant point in the watershed to the outlet or design point. Factors affecting the time of concentration are flow length, flow path slope, hydraulic geometry, and flow path roughness. For flow at the upper reaches of a watershed, rainfall characteristics, most notably intensity, may also influence runoff velocity.

Engineers use various methods to estimate the time of concentration of a watershed. When selecting a method to use in design, it is important to select a method that is appropriate for the flow path. Some estimation methods can be classified as “lumped” in that they were designed and calibrated to be used for an entire watershed; some lag formulas are an example of this method, as described in 8.1.3. These methods have t_c as the dependent variable. Other methods are intended for one segment of the principal flow path and produce a flow velocity that can be used with the length of that flow path segment to compute the travel time on that segment. With this segment method, the time of concentration equals the sum of the travel times on each segment of the principal flow path.

In classifying these methods so that the proper method can be selected, it is useful to describe the segments of flow paths. Sheet flow typically occurs in the upper reaches of a watershed. Such flow occurs over short distances and at shallow depths prior to the point where topography and surface characteristics cause the flow to concentrate in rills and swales. The depth of such flow is usually 0.1 feet or less (SCS 1986). Shallow concentrated flow is runoff that occurs in rills and swales and has depths of about 0.1 to 0.5 feet (SCS 1986). Part of the principal flow path may

include pipes or channels. The travel time through these segments would be computed separately. Engineers typically estimate velocities in open channels and pipes assuming bankfull and pipe-full depths, respectively.

3.7.2 Velocity Method

The velocity method (sometimes referred to as the segment method) can be used to estimate travel times for sheet flow, shallow concentrated flow, pipe flow, or channel flow. This method is based on estimating travel time from length and velocity:

$$t_t = \frac{L}{60V} \tag{3.4}$$

where:

t_t = Travel time, min
L = Flow length, ft (m)
V = Flow velocity, ft/s (m/s)

Travel time is computed for the principal flow path. When the principal flow path consists of segments with different slopes or land covers, it is divided into segments and equation 3.4 is used for each flow segment. The time of concentration is then the sum of travel times:

$$t_c = \sum_{i=1}^{k} t_{t_i} = \sum_{i=1}^{k} \left(\frac{L_i}{60V_i} \right) \tag{3.5}$$

where:

k = Number of segments
i = Subscript referring to each flow segment

Velocity is a function of flow type (overland, sheet, rill, and gully flow, channel flow, pipe flow), flow path roughness, and flow path slope. Some methods also include a rainfall index such as the 2-year, 24-hour rainfall depth. Several methods have been developed for estimating velocity.

3.7.2.1 Sheet Flow

Sheet flow is a shallow mass of runoff on a plane surface with uniform depth across the sloping surface. Typically, flow depths do not exceed 2 inches. Such flow occurs over relatively short distances, rarely more than about 300 ft, but most often less than 100 ft (NRCS 2010). Ragan (1971) suggests sheet flow occurs for distances 72 feet or less.

Engineers commonly estimate sheet flow rates using a version of the kinematic wave equation. The original form of the kinematic wave time of concentration is:

$$t_t = \frac{\alpha}{i^{0.4}} \left(\frac{nL}{\sqrt{S}} \right)^{0.6} \tag{3.6}$$

where:

t_t = Travel time, min
n = Roughness coefficient (see Table 3.1)
L = Flow length, ft (m)

i = Rainfall intensity, in/h (mm/h), for a storm with the selected AEP and duration of t_c minutes
S = Slope of the surface, ft/ft (m/m)
α = Unit conversion constant, 0.93 in CU (6.9 in SI).

Table 3.1 provides representative values of Manning's roughness coefficient but they vary by material depending on surface details. Some hydrologic design methods, such as the Rational Method, assume that the storm duration equals the time of concentration. Thus, the time of concentration is entered into the IDF curve to find the design intensity. However, for equation 3.6, i depends on t_c and t_c is not initially known. Therefore, the computation of t_c is an iterative process. An initial estimate of t_c is assumed and used to obtain i from the IDF curve for the locality. The t_c is computed from equation 3.6 and used to check the initial value of i. If they are not the same, the process is repeated until two successive t_c estimates are the same.

Table 3.1. Manning's roughness coefficient for overland and sheet flow (SCS 1986, McCuen 2012).

n	Surface Description
0.011	Smooth asphalt
0.012	Smooth concrete
0.013	Concrete lining
0.014	Good wood
0.014	Brick with cement mortar
0.015	Vitrified clay
0.015	Cast iron
0.024	Corrugated metal pipe
0.024	Cement rubble surface
0.05	Fallow (no residue)
0.06	Cultivated soils: residue cover ≤ 20%
0.17	Cultivated soils: residue cover > 20%
0.13	Cultivated soils: range (natural)
0.15	Short grass prairie
0.24	Dense grasses
0.41	Bermuda grass
0.40	Woods*: light underbrush
0.80	Woods*: dense underbrush

*When selecting n for woody underbrush, consider cover to a height of about 0.1 ft. This is the only part of the plant cover that obstructs sheet flow.

Example 3.1:	Iterative travel time using the kinematic sheet flow equation.
Objective:	Estimate the travel time using the iterative sheet flow equation.

Given: Sheet flow on short grass with the following characteristics:

S_0 = 0. 005 ft/ft (m/m)
L = 164 ft (50 m)
n = 0.15

Figure 3.15 provides the IDF curve for the project location (Baltimore, Maryland) for the 2-year event.

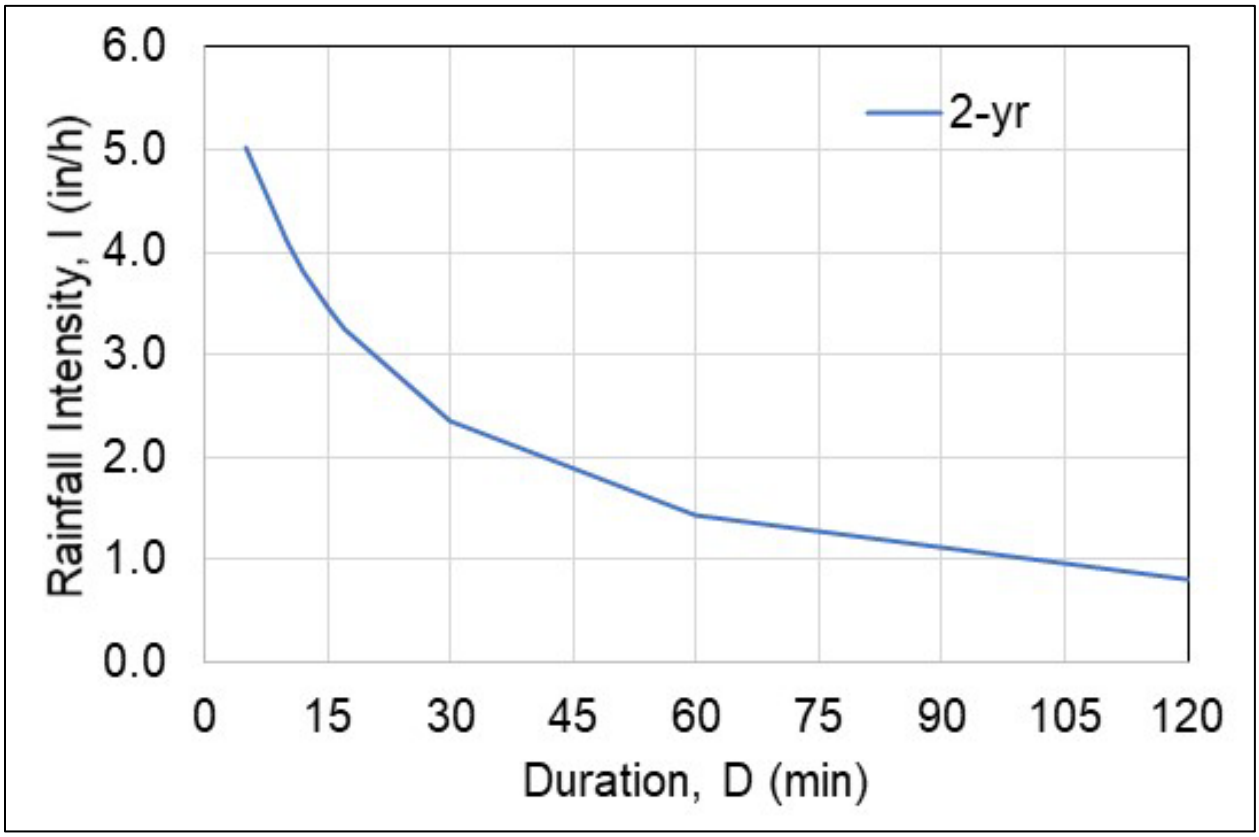

Figure 3.15. Rainfall intensity-duration-frequency curves for the 0.5 AEP (2-year return period).

Step 1. Make initial estimate of the travel time.

Assume initial t_t = 12 min

From Figure 3.15, i = 3.8 in/h

Using equation 3.6, the travel time for this rainfall intensity is:

$$t_t = \frac{\alpha}{i^{0.4}}\left(\frac{nL}{\sqrt{S}}\right)^{0.6} = \frac{0.93}{(3.8)^{0.4}}\left(\frac{0.15(164)}{\sqrt{0.005}}\right)^{0.6} = 18\,\text{min}$$

Since this differs from the assumed t_c of 12 minutes, perform a second iteration.

Step 2. Make a second estimate of time of concentration.

Assume t_t = 18 min

From Figure 3.15, i = 3.2 in/h

Using equation 3.6, the travel time for this rainfall intensity is:

$$t_t = \frac{\alpha}{i^{0.4}}\left(\frac{nL}{\sqrt{S}}\right)^{0.6} = \frac{0.93}{(3.2)^{0.4}}\left(\frac{0.15(164)}{\sqrt{0.005}}\right)^{0.6} = 19.6 \approx 20\,\text{min}$$

Once again, this differs from the assumed value of 17 minutes, so another iteration is indicated.

Step 3. Converge to a solution with a final estimate of time of concentration.

Assume initial t_t = 20 min

From Figure 3.15, i = 3.0 in/h

Using equation 3.6, the travel time for this rainfall intensity is:

$$t_t = \frac{\alpha}{i^{0.4}}\left(\frac{nL}{\sqrt{S}}\right)^{0.6} = \frac{0.93}{(3.0)^{0.4}}\left(\frac{0.15(164)}{\sqrt{0.005}}\right)^{0.6} = 20.1 \approx 20\,\text{min}$$

The assumed value matches the calculated value. No further iterations needed.

Solution: The travel time estimate for this flow path is 20 minutes.

To avoid the necessity to solve for t_c iteratively, the NRCS TR-55 (1986) uses the following variation of the kinematic wave equation:

$$t_t = \frac{\alpha}{P_2^{0.5}}\left(\frac{nL}{\sqrt{S}}\right)^{0.8} \qquad (3.7)$$

where:

P_2 = 2-year, 24-hour rainfall depth, inches (mm)

α = Unit conversion constant, 0.42 in CU (5.5 in SI)

The other variables are as previously described. Equation 3.7 is based on an assumed IDF relationship. TR-55 (SCS 1986) recommends an upper limit of L = 300 ft for this equation.

3.7.2.2 Shallow Concentrated Flow

After short distances, sheet flow tends to concentrate in rills and then gullies of increasing proportions. Such flow is usually referred to as shallow concentrated flow and with depths typically ranging from 0.1 to 0.5 feet (NRCS 2010). The velocity of such flow can be estimated using an empirical relationship between velocity and slope:

$$V = \alpha k S^{0.5} \qquad (3.8)$$

where:

V	=	Velocity, ft/s (m/s)
S	=	Slope, ft/ft (m/m)
k	=	Intercept coefficient (see Table 3.2)
α	=	Unit conversion constant, 33 in CU (10 in SI)

Table 3.2. Intercept coefficients for velocity versus slope relationship (McCuen 2012).

k	Land Cover/Flow Regime
0.076	Forest with heavy ground litter; hay meadow (overland flow)
0.152	Trash fallow or minimum tillage cultivation; contour or strip cropped; woodland (overland flow)
0.213	Short grass pasture (overland flow)
0.274	Cultivated straight row (overland flow)
0.305	Nearly bare and untilled (overland flow); alluvial fans in Western mountain regions
0.457	Grassed waterway (shallow concentrated flow)
0.491	Unpaved (shallow concentrated flow)
0.619	Paved area (shallow concentrated flow); small upland gullies

3.7.2.3 Channel and Pipe Flow

Flow in gullies empties into channels or pipes. In many cases, the transition between shallow concentrated flow and open channels may be assumed to occur by field observations or when the channel is visible on aerial photographs. Channel lengths may be measured directly from the map or georeferenced photograph. However, depending on map scale and the sinuosity of the channel, a map-derived channel length may be an underestimate. Pipe lengths should be taken from as-built drawings for existing systems and design plans for future systems.

Cross-section information (i.e., depth-area and roughness) can be obtained for any channel reach in the watershed. Manning's equation can be used to estimate average flow velocities in pipes and open channels:

$$V = \frac{\alpha}{n} R^{2/3} S^{1/2} \tag{3.9}$$

where:

V	=	Velocity, ft/s (m/s)
n	=	Manning's roughness coefficient
R	=	Hydraulic radius, ft (m)
S	=	Slope, ft/ft (m/m)
α	=	Unit conversion constant, 1.49 in CU (1.0 in SI)

The hydraulic radius equals the cross-sectional area divided by the wetted perimeter. For a circular pipe flowing full, the hydraulic radius equals one-fourth of the diameter. For flow in a wide rectangular channel, the hydraulic radius is approximately equal to the depth of flow. Table 3.3 summarizes typical ranges of Manning's roughness coefficients for channels and pipes.

Table 3.3. Typical range of Manning's roughness coefficient (n) for channels and pipes.

Conduit Category	Conduit Material	Manning's n*
Closed conduits	Concrete pipe	0.010 - 0.015
	CMP	0.011 - 0.037
	Plastic pipe (smooth)	0.009 - 0.015
	Plastic pipe (corrugated)	0.018 - 0.025
Pavement/gutter sections	Concrete, asphalt	0.012 - 0.016
Small open channels	Concrete	0.011 - 0.015
	Rubble or riprap	0.020 - 0.035
	Vegetation	0.020 - 0.150
	Bare soil	0.016 - 0.025
	Rock cut	0.025 - 0.045
Natural channels/streams (top width at flood stage less than 100 ft)	Fairly regular section	0.025 - 0.050
	Irregular section with pools	0.040 - 0.150

*Lower values usually apply to well-constructed and maintained (smoother) pipes and channels.

Example 3.2: Time of concentration with multiple segments.

Objective: Compare time of concentration estimates for: 1) undeveloped versus developed conditions and 2) use of the iterative versus direct sheet flow equation.

Given: Figure 3.16a illustrates the principal flow path for the existing conditions of a small watershed. Table 3.4 summarizes the characteristics of the principal flow paths for the site in Baltimore, Maryland.

For short durations (2 hours or less) the applicable 2-year IDF curve is represented by the following equation:

$$i = \frac{1.85}{0.285 + D}$$

where:

i = Rainfall intensity, in/h
D = Duration, h

The 2-yr 24-hour precipitation depth is 3.2 inches.

Step 1. Estimate the time of concentration for existing conditions.

Figure 3.16 shows an existing conditions flow path with three segments. Compute the individual travel times and sum them for the time of concentration.

Step 1a. Use the shallow concentrated flow equation to estimate velocity and travel time in segment AB.

$V = \alpha k S^{0.5} = 33(0.076)\,(0.07)^{0.5} = 0.66$ ft/s

Thus, the travel time for segment AB is:

t_{AB} = (490 ft) / (0.66 ft/s) / (60 s/min) = 12 min

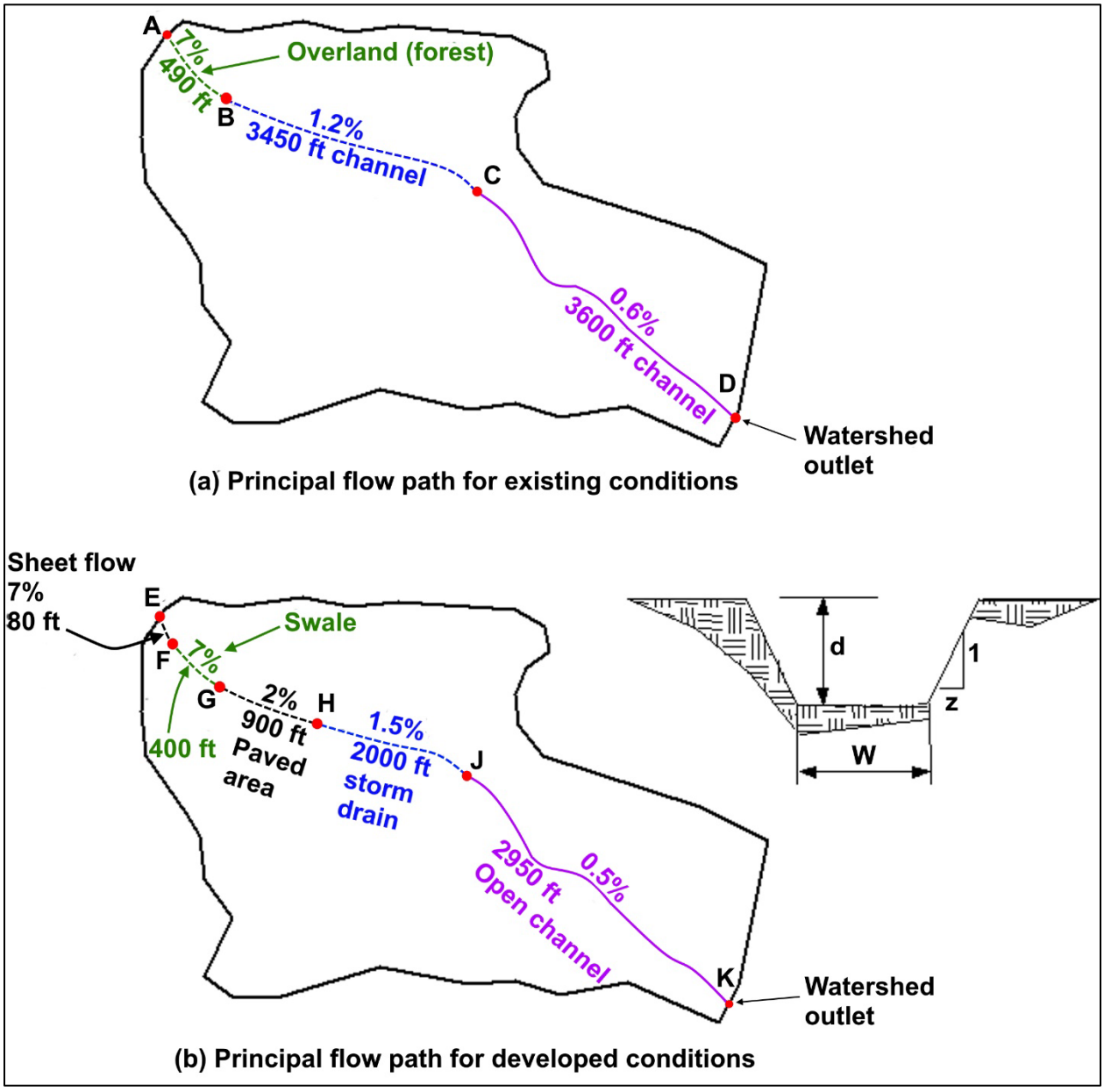

Figure 3.16. Example watershed schematic with segmented flow paths.

Table 3.4. Characteristics of flow paths for the example problem.

Watershed Condition	Flow Segment	Length (ft)	Slope (ft/ft)	n	Land Use/Land Cover
Existing	A to B	490	0.07	—	Overland (forest)
	B to C	3450	0.012	0.040	Natural channel (trapezoidal): w = 1 ft, d = 2.3 ft, z = 2:1
	C to D	3600	0.006	0.030	Natural channel (trapezoidal): w = 4.1 ft, d = 2.3 ft, z = 2:1
Developed	E to F	80	0.07	0.013	Sheet flow: i = 1.85/(0.285 + D) where i [in/h], D [h]
	F to G	400	0.07	—	Grassed swale
	G to H	900	0.02	—	Paved area
	H to J	2000	0.015	0.015	Storm drain, D = 42 inches
	J to K	2950	0.005	0.019	Open channel (trapezoidal): w = 5.2 ft, d = 3.3 ft, z = 1:1

Step 1b. Apply Manning's equation to estimate velocity and travel time in segment BC.

For a trapezoidal channel, the hydraulic radius is:

$$R = A/P = (wd + zd^2)/(w + 2d\sqrt{(1+z^2)}) = (1(2.3) + 2(2.3)^2)/(1 + 2(2.3)\sqrt{(1 + 2^2)}) = 1.14 \text{ ft}$$

Manning's equation yields a velocity of:

$$V = (1.49/0.040)(1.14)^{0.67}(0.012)^{0.5} = 4.45 \text{ ft/s}$$

The travel time is:

t_{BC} = 3450 ft / (4.45 ft/s) / (60 s/min) = 13 min

Step 1c. Apply Manning's equation to estimate velocity and travel time in segment CD.

The hydraulic radius of this trapezoidal channel is:

$$R = (4.1(2.3)+2(2.3)^2)/(4.1+2(2.3)\sqrt{(1+(2)^2)}) = 1.4 \text{ ft}$$

Using Manning's equation, the velocity is:

$$V = (1.49/0.030)(1.4)^{0.67}(0.006)^{0.5} = 4.8 \text{ ft/s}$$

The travel time is:

t_{CD} = (3600 ft) / (4.8 ft/s) / (60 s/min) = 13 min

Step 1d. Estimate time of concentration for the existing condition by summing the segment travel times.

Use equation 3.5 to calculate time of concentration:

$t_c = \Sigma t_t = t_{AB} + t_{BC} + t_{CD}$ = 12 + 13 + 13 = 38 min

Step 2. Estimate the time of concentration for developed conditions using the iterative sheet flow equation.

Figure 3.16 shows a developed conditions flow path with five segments. Compute the individual travel times and sum them for the time of concentration. Since the iterative sheet flow equation uses the estimated time for the entire flow path, estimate the sheet flow segment (EF) last.

Step 2a. Apply the shallow concentrated flow equation to estimate velocity and travel time in segment FG.

This segment consists of grass-lined swales. Use equation 3.8 to compute the velocity:

$V = \alpha k S^{0.5} = 33(0.457)(0.07)^{0.5} = 4.0$ ft/s

The travel time is:

t_{FG} = (400 ft) / (4.0 ft/s) / (60 s/min) = 2 min

Step 2b. Apply the shallow concentrated flow equation to estimate velocity and travel time in segment GH.

This segment consists of paved gutters. Use equation 3.8 and Table 3.2 to estimate velocity:

$V = \alpha k S^{0.5} = 33(0.619)\ (0.02)^{0.5} = 2.9$ ft/s

The travel time is:

t_{GH} = (900 ft) / (2.9 ft/s) / (60 s/min) = 5 min

Step 2c. Use Manning's equation to estimate velocity and travel time in segment HJ.

This segment is a 42-inch pipe. The hydraulic radius is one-fourth the diameter (D/4), so the velocity for full flow is:

$V = (1.49/0.015)(0.875)^{0.67}(0.015)^{0.5} = 11.1$ ft/s

The travel time is:

t_{HJ} = (2000 ft) / (11.1 ft/s) / (60 s/min) = 3 min

Step 2d. Use Manning's equation to estimate velocity and travel time in segment JK.

This segment is an improved trapezoidal channel. The hydraulic radius is:

$R = (wd+zd^2)/(w+2d\sqrt{(1+z^2)}) = (5.2(3.3)+1(3.3)^2)/(5.2+2(3.3)\sqrt{(1+1^2)}) = 1.95$ ft

Manning's equation is used to compute the velocity:

$V = (1.49/0.019)(1.95)^{0.67}(0.005)^{0.5} = 8.7$ ft/s

The travel time is:

t_{JK} = (2950 ft) / (8.7 ft/s) / (60 s/min) = 6 min

Step 2e. Estimate travel time for the developed condition excluding the sheet flow segment (EF).

The total travel time through the four segments (excluding the first segment) is:

$t_t = \Sigma t_t = t_{FG} + t_{GH} + t_{HJ} + t_{JK} = 2 + 5 + 3 + 6 = 16$ min

Step 2f. Use the iterative sheet flow equation to estimate velocity and travel time in segment EF.

Assume a total travel time for the flow path. The time of concentration is 16 minutes plus the travel time over the sheet flow segment EF.

Step 2f1. Iteration 1: Assume that travel time on the sheet flow segment EF is 2 minutes.

Assume t_c = D = 16 + 2 = 18 min = 0.30 h

The corresponding intensity is:

$$i = \frac{1.85}{0.285 + D} = \frac{1.85}{0.285 + 0.3} = 3.2 \text{ in / h}$$

Accordingly, equation 3.6 yields an estimate of the travel time:

$$t_t = \frac{\alpha}{i^{0.4}}\left(\frac{nL}{\sqrt{S}}\right)^{0.6} = \frac{0.93}{(3.2)^{0.4}}\left(\frac{0.013(80)}{\sqrt{0.07}}\right)^{0.6} = 1.2 \approx 1 \text{ min}$$

Since 2 min was assumed for this segment, a second iteration is performed using the new estimate.

Step 2f2. Iteration 2: Make second estimate of travel time in segment EF.

Assume t_c = D = 16 + 1 = 17 min = 0.283 h

The corresponding intensity is:

$$i = \frac{1.85}{0.285 + D} = \frac{1.85}{0.285 + 0.283} = 3.3 \text{ in / h}$$

Accordingly, equation 3.6 yields an estimate of the travel time:

$$t_t = \frac{\alpha}{i^{0.4}}\left(\frac{nL}{\sqrt{S}}\right)^{0.6} = \frac{0.93}{(3.3)^{0.4}}\left(\frac{0.013(80)}{\sqrt{0.07}}\right)^{0.6} = 1.2 \approx 1 \text{ min}$$

Step 2g. Estimate time of concentration for the proposed condition by summing the segment travel times.

Use equation 3.5 to calculate time of concentration:

$t_t = \Sigma t_t = t_{EF} + t_{FG} + t_{GH} + t_{HJ} + t_{JK} = 1 + 2 + 5 + 3 + 6 = 17$ min

Step 3. Estimate the time of concentration for developed conditions using the direct sheet flow equation.

Compute the travel time in sheet flow segment EF using equation 3.7:

$$t_t = \frac{\alpha}{P_2^{0.5}}\left(\frac{nL}{\sqrt{S}}\right)^{0.8} = \frac{0.42}{(3.2)^{0.5}}\left(\frac{0.013(80)}{\sqrt{0.07}}\right)^{0.8} = 0.7 \approx 1 \text{min}$$

The other segment travel times were computed as part of step 2. Therefore, the time of concentration is:

$t_t = \Sigma t_t = t_{EF} + t_{FG} + t_{GH} + t_{HJ} + t_{JK} = 1 + 2 + 5 + 3 + 6 = 17$ min

Solution:	The time of concentrations for undeveloped and developed conditions are 38 and 17 minutes, respectively. Development resulted in a significant decrease in time of concentration. In this example, use of the iterative and direct sheet flow equations both resulted in the same estimate of the sheet flow travel time of 1 minute.

3.7.3 Kerby-Kirpich Method

The Kerby-Kirpich method depends on few input parameters and consists of two components, overland and channel flow, as represented in the following equation:

$$t_c = t_{ov} + t_{ch} \quad (3.10)$$

where:

t_{ov} = Overland flow time (min)
t_{ch} = Channel flow time (min)

The Kerby-Kirpich method for estimating t_c is applicable to watersheds ranging from 0.25 mi^2 to 150 mi^2, main channel lengths between 1 and 50 miles, and main channel slopes between 0.002 and 0.02 (ft/ft) (Roussel et al. 2005). For small watersheds where overland flow is an important component of overall travel time, the Kerby equation for overland flow (maximum length of overland flow is 1,200 ft) is:

$$t_{ov} = \alpha(LN)^{0.467} S^{-0.235} \quad (3.11)$$

where:

L = Overland flow length, ft (m)
N = Dimensionless retardance coefficient
S = Slope of terrain conveying the overland flow, ft/ft (m/m)
α = Unit conversion constant, 0.828 in CU (1.44 in SI)

The dimensionless retardance coefficient used is similar in concept to the Manning's roughness coefficient, n. Table 3.5 lists typical values for the retardance coefficient.

Table 3.5. Kerby equation retardance coefficient values.

Generalized Terrain Description	Dimensionless Retardance Coefficient (N)
Pavement	0.02
Smooth, bare, packed soil	0.10
Poor grass, cultivated row crops, or moderately rough packed surfaces	0.20
Pasture, average grass	0.40
Deciduous forest	0.60
Dense grass, coniferous forest, or deciduous forest with deep litter	0.80

The Kirpich equation was developed for small drainage basins in Tennessee and Pennsylvania, with basin areas from 1 to 112 acres but its use has expanded to applications throughout the United States and for larger watersheds. It applies in watersheds when gullying (including engineered conveyances in fully urbanized watersheds such as curb and gutter, storm drains, and channels) is evident in more than 10 percent of the primary watercourse. For channel flow, the Kirpich equation for travel time is:

$$t_{ch} = \alpha L^{0.77} S^{-0.385} \tag{3.12}$$

where:

L	=	Channel flow length, ft (m)
S	=	Main channel slope, ft/ft (m/m)
α	=	Unit conversion constant, 0.0078 in CU (0.0195 in SI)

The method estimates time of concentration by using equation 3.10 to add the travel times.

Chapter 4 - Hydrologic Data and Choice of Method

As a logical first step in any hydrologic study, engineers identify the data that will be needed as early as possible in the project concept stage. Data needs depend on whether the project is preliminary or detailed, the project's scope and nature, the project's degree of complexity, the source of project funding. Once engineers determine the study purpose, they can usually select a method of analysis for which the type and amount of data can be readily determined.

Engineers may need such data as details of the watershed topography, land use and cover, precipitation information for past storm events, and information on annual peak or partial-duration flood series, or other streamflow records. In some cases, engineers use historical data on floods that occurred prior to the systematic streamflow record.

The availability of data online on websites and in government agency databases has reduced the effort involved in data collection and compilation, while enhancing project understanding. Data typically available in such online data repositories can include both current and historical data, maps, and imagery. Often, using a well-thought-out internet data search engineers can find existing information that meets the needs of a project and reduces the project-specific data collection effort and cost. By acquainting the designer with the data sources available and the procedures involved in accessing the various data sources, subsequent data searches could often be significantly reduced.

4.1 Collection and Compilation of Data

Engineers obtain most of the data and information for the design of highway stream crossings and other hydrologic analyses from some desktop evaluations using existing sources of information and field evaluations to collect site-specific information not otherwise available. Engineers use certain types of data so frequently that some State DOTs have compiled these data into a single document or location to facilitate access. Having data available in a single source supports retrieval of needed data and helps standardize the hydrologic analysis of highway drainage design.

4.1.1 Desktop Data Collection and Evaluation

This section summarizes several data sources useful for hydrologic analysis and modeling. Many databases are compiled and managed by agencies of the Federal Government. In addition, many States and localities maintain websites that include similar or identical data to that from the Federal sites. Some include additional State or local data, such as high-resolution urban aerial imagery, high-resolution LiDAR (Light Detection and Ranging) elevation data, or LiDAR-based digital elevation models (DEMs).

4.1.1.1 Streamflow and Flood Data

The U.S. Geological Survey (USGS) collects and documents streamflow data and is the major source of this information. Its database holds mean daily-discharge data for tens of thousands of locations. USGS compiles and publishes these data in both print publications and on the USGS website. The database contains a peak flow data retrieval capability that provides pertinent characteristics of the station and drainage area and a listing of both peak annual and secondary floods by water year (October through September).

The U.S. Army Corps of Engineers (USACE), the U.S. Bureau of Reclamation (USBR), and the International Boundary and Water Commission also collect streamflow data. Along with the USGS, these agencies account for about 90 percent of the streamflow data available in the United

States. Other sources of this data are local governments, utility companies, water-intensive industries, and academic or research institutions.

Historical records or accounts are another source of flood data. Floods are noteworthy events and, very often, after a flood occurs, specific information such as high water elevations are recorded. Other sources of such information include newspapers, magazines, State historical societies or universities, and publications by any of several Federal agencies. Previous storms or flood events of historic proportion have been very thoroughly documented by the USGS, the USACE, and the National Weather Service (NWS). USGS reports documenting historic floods are summarized by Thomas (1987).

4.1.1.2 Precipitation Data

The major source of precipitation data is the NWS, which is part of the National Oceanic and Atmospheric Administration (NOAA). Precipitation and other measurements are taken at approximately 20,000 locations each day. The measurements are fed through the Weather Service Forecast Offices (WSFOs), which serve each of the 50 States and Puerto Rico. Each WSFO uses these data and information obtained via satellite and other means to forecast the weather for its area of responsibility. In addition to the WSFOs, the NWS maintains a network of River Forecast Centers that prepare river and flood forecasts for about 2,500 communities. The data collected by the NWS and other organizations within NOAA are sent to the National Climatic Data Center (NCDC), which is responsible for collecting, processing, and disseminating environmental data. Online data sources include, but are not limited to:

- NOAA Atlas 14. Precipitation depth-duration-frequency (DDF) information.
- NCDC. Historical climatic data.

4.1.1.3 Land Use/Land Cover and Soils Data

Land use data are available in different forms such as topographic maps, aerial photographs such as those available from the National Agricultural Imagery Program (NAIP), zoning maps, and Landsat images. These different forms of data are available, usually online, from many different sources such as State, regional, or municipal planning organizations, the USGS, and the Natural Resource Economic Division, Water Branch, of the Department of Agriculture.

The Multi-Resolution Land Characteristics (MRLC) consortium developed and maintains the National Land Cover Database (NLCD), which is a collection of datasets of land cover types. The MRLC is a group of Federal agencies who coordinate and generate consistent and relevant land cover information at the national scale for a wide variety of environmental, land management, and modeling applications.

Specific online soils datasets from the Natural Resource Conservation Service (NRCS) include:

- Web Soil Survey. Web service offering detailed soil map data from the Soil Survey Geographic Database (SSURGO).
- gSSURGO. A toolbox for ArcGIS that facilitates the detailed geographic information systems (GIS) mapping of many soil properties (e.g., saturated hydraulic conductivity, hydrologic soil group, detailed textural description) on a State-by-State basis.
- STATSGO: a general soil map of the United States, less detailed than SSURGO.

4.1.1.4 Topographic, Stream Hydrography, and Watershed Boundaries

The USGS National Geospatial Program provides a general geospatial data management program that includes data sources of interest to engineers and hydrologists:

- National Elevation Dataset (NED). A DEM raster representing the ground surface at a minimum resolution of 1 arc-second of latitude/longitude (approximately 30 meters) of the entire United States.
- USGS 3D Elevation Program- Nationwide LiDAR high-resolution elevation data collection program.
- US Topo: Maps for America. Current and historical digital topographic maps.
- National Hydrography Dataset (NHD). A GIS database of streams and stream data.
- Watershed Boundary Dataset. Delineated major and minor stream watersheds as GIS polygons.

4.1.1.5 Aerial Images

Aerial images provide information on historical and current land cover and land use. Sources include:

- NAIP. Georeferenced high-resolution digital aerial imagery acquired periodically (currently on a three-year cycle) from the U.S. Department of Agriculture (USDA) Farm Service Agency.
- Historical Aerial Imagery from the Aerial Photography Field Office. Aerial photos with some available back into the 1950s.
- NOAA satellite imagery.
- NASA Landsat Thematic Mapper. Satellite imagery beginning in 1972 to the present. Used for land use/land cover and other data through remote sensing analysis.

4.1.1.6 Environmental Resources

Hydrologic analysis objectives may include assessment of the impacts on environmental resources such as wetlands, habitat, and others. Online data sources include:

- National Wetlands Inventory from the U.S. Fish and Wildlife Service (USFWS).
- Critical Habitat for endangered species from the USFWS.
- U.S. Environmental Protection Agency (USEPA) Environmental Dataset Gateway.

4.1.1.7 Drainage Complaints and Maintenance Records

Another potential source of information for hydrologic analysis are drainage complaints and maintenance records. These records provide observational information about flood experiences of citizens and landowners as well as records of maintenance types and frequencies. Drainage complaints result from real or perceived deficiencies of stormwater management and flooding that can provide designers with insight into the performance of existing facilities. Designers may also gain insights by contacting the local maintenance personnel about maintenance issues not documented in records.

State and local Departments of Transportation (DOTs) address drainage complaints in a timely and professional manner both to maintain collaborative relationships with stakeholder and to ensure that accurate information is recorded. Complaints may come in the form of a telephone call, email, letter, or personal visit. Drainage complaints lodged by members of the general public are often not well documented by the complainant and may not be well described. It is helpful to have instructions in place for ensuring that the complaint is directed to an appropriate office in a timely manner.

If an investigation is warranted, a qualified engineer experienced in hydrologic and hydraulic design, preferably from another office or area, investigates the complaint. Familiarity with the drainage laws of the State, agency policies, and local issues that may have a bearing on the case are vital. The investigator may contact the complainant and collect details of the complaint to clarify the situation. Designers conduct a site reconnaissance, when appropriate, to preserve any perishable data such as debris lines, flooded structures, or damage. In this case, the investigator bears in mind that the results of the investigation may become evidence in court. Other evidence, such as rainfall or streamflow data from a particular time, may be gathered to enhance the understanding of a particular incident.

The investigator may review design plans, as-built plans, and maintenance records for comparison with the site characteristics, as well as adjacent land development and use information. Depending on the characteristics of the situation, the investigator documents findings in a memorandum or report.

4.1.2 Site Reconnaissance and Field Data Collection

Field surveys or site investigations provide valuable information, even for the most preliminary analysis or simplest designs. Designers use site reconnaissance as a primary source of site data and to gain firsthand experience with the site. Under all circumstances, safety of both the investigating person and the public is of paramount importance; standard safety protocols for site investigations may be developed by an agency if needed.

Before the site visit, a desktop search of the data sources introduced in the previous section typically results in acquiring maps, imagery, elevation and topographic information, information on vegetative cover, potential biological issues including protected animals and plants. With such information, the engineer plans the site visit with less likelihood of surprises on arriving at the site.

During a site visit, the designer identifies, observes, and documents hydrology-related factors including:

- Highwater marks.
- Assessments of the performance of drainage structures.
- Assessments of stream stability and scour potential.
- Location and nature of important physical and cultural features that could affect or be affected by the proposed project.
- Land use compared to that indicated on available maps and imagery.

Follow-up Reconnaissance

During the field visit, the engineer may identify additional data collection to determine precise measurements for:

- The location of stream cross-sections.
- Fluvial geomorphic features.
- Bankfull indicators.
- High-water marks.
- Debris lines.
- Other features.

Marking and photographing features for subsequent measurement reduces uncertainty about the engineer's intent for follow-up data collection.

The designer may anticipate the need for an engineering survey to collect additional information as described in the box. In many cases, topographic surveys are now performed by photogrammetric or laser scanning technology, rather than by traditional survey practices; the site reconnaissance is conducted for information other than topography.

Many digital cameras, including those on many "smart phones," have the capability to geotag photographs with GPS-based location data, along with date, time, and direction of view encoded in the photograph metadata. Geotagged photographs are useful in documenting site features and may be included in GIS maps or web-based map and imagery applications.

To maximize the usefulness of field site survey data, suggested procedures might include:

- Planning the visit to identify data collection objectives and needed equipment.
- Selecting an individual to conduct the drainage aspects of the field site survey with a good working knowledge of drainage design at a minimum.
- Documenting data with written reports and photographs.
- Using a systematic approach to maximize efficiency.
- When possible, having those responsible for the design attend the site visit.

Though the site visit is important, the engineer will wish to augment it with additional information from other reliable sources through desktop analyses before and after the site visit.

4.2 Data Evaluation and Documentation

After collecting data, the engineer evaluates the data for use in hydrologic analysis and design and documents the analysis. GIS tools such as raster maps, DEMs, and vector feature classes are integral to both evaluation and documentation.

4.2.1 Data Evaluation

After data collection, the designer compiles the data into a usable format, evaluating the data for consistency and for unexplained anomalies that might lead to erroneous calculations or results. The aim of this process is to fit the data into a comprehensive and accurate representation of the hydrology at a particular site. For example, most geotagging cameras and phones record coordinates in one datum system (World Geodetic System of 1984, WGS84), while State plane coordinate systems are often in another—the North American Datum of 1983 (NAD83). Translation from one to the other is not difficult within GIS systems, but it is important to first document the datum used for any given dataset before the translation can be done.

Experience, knowledge, and judgment are an important part of data evaluation. The designer ranks the data for reliability and precision and combines historical data with data obtained from measurements. The designer also justifies or, if possible, fills in any gaps in the data record. Some of the methods and techniques discussed later in this manual are useful for this purpose.

Statistics can be useful in data analysis, but an underlying knowledge of hydrology is important for prudent and meaningful application of statistical methods. The engineer should also review previous studies and reports for types and sources of data, how the data were used, and any indications of accuracy and reliability. Reviewing historical data helps determine whether significant changes have occurred in the watershed that might affect its hydrology and whether these data can be used to possibly improve or extend the period of record.

The engineer also evaluates basic data, such as streamflow and precipitation, for hydrologic homogeneity and summarizes them before use. Maps, aerial photographs, Landsat images, and land use studies are compared with each other and with field survey results to resolve inconsistencies. For example, the construction of small reservoirs (such as those constructed by the NRCS) or agricultural terraces may have changed the runoff characteristics of a watershed. A change from cultivation to rangeland or clearing of brush may be identifiable as a change in hydrologic condition. Such changes may be attributable to a given time period, allowing the consideration of runoff data before and after the change. Beginning or cessation of irrigation may

have exerted an effect on hydrologic condition. While much research has been devoted to the effects of urbanization, many changes other than urbanization may occur within a watershed that affect the runoff generation process. The results of this type of data evaluation provide a description of the hydrology of the site within the allotted time and the resources committed to this effort. The designer will want to adequately select the appropriate parameters to design the drainage structures to the indicated reliability.

4.2.2 Data Documentation

If the data needs have been clearly identified, the designer can readily prepare and use results of the analysis in the selected method of hydrologic analysis. The data needs of each method differ, so no single method of presenting the data applies to all situations. The results of the data collection and data evaluation phases should be documented to:

- Provide a record of the data itself.
- Provide references to data that have not been incorporated into the record because of its volume or for other reasons.
- Provide references for the methods of data analysis used.
- Document assumptions, recommendations, and conclusions.
- Present the results in a form compatible with the analytical method used.
- Index the data and analysis for ease of retrieval.
- Provide support of expenditures of public funds by highway agencies.

The format or method used to document the collected data or subsequent analysis may be standardized, so that those unfamiliar with a specific project may readily refer to the needed information. This is especially important in States where there are several different offices or districts performing hydrologic analyses and design. The engineer should either include all data collected in the documentation or adequately reference them for quick retrieval.

The engineer also presents data analyses in the documentation. If several different methods were used, the engineer reports and documents each analysis, even if the results were not included in the final recommendations. Comments explaining why results were either discounted or accepted should also be included in the documentation (see Section 4.3 for selecting hydrologic methods). The engineer references sources such as a State drainage manual, textbook, or other publication, for the selection of methods.

Also important is recording assumptions, conclusions, and recommendations made during or as a result of the data collection and analysis. Since hydrology is not an exact science, it is impossible to adequately collect and analyze hydrologic data without using judgment and making assumptions. By recording these professional judgments, the designer provides a detailed and valuable record of the work.

4.2.3 GIS Analysis and Presentation

Geographic information systems provide powerful tools for analyzing data and presenting the results. The rapid adoption of GIS and Global Positioning Systems (GPS) into the fields of engineering and data management has significantly altered the way State and Federal agencies conduct operations. Because GIS tools store and evaluate georeferenced information, the data can be visualized and processed in hundreds of useful ways. Data presented in georeferenced points, lines, and polygons are used to understand and evaluate watersheds.

Most digital data sources are georeferenced, that is, the location is tied to the image or information so that multiple sources can be overlain for analysis and presentation. For example, Figure 4.1 shows topographic information overlain with a watershed boundary and stream hydrography. Figure 4.2 displays aerial photography and the roadway network at the same location. Similarly, Figure 4.3 and Figure 4.4 illustrate georeferenced soils and topographic data, respectfully, for the same location. These figures illustrate a few of the many types of information readily available in GIS format that the designer of roadway hydraulic structures may find valuable. Section 4.1.1 introduces these and other digital data sources.

Some data sources, such as the USGS quadrangle maps, are in a raster (pixel) format. This format facilitates pixel-by-pixel computations within GIS. Others, such as the elevation contours and hydrologic soil group maps, are stored in "vector" format (points, lines, and polygons) and have attributes that allow calculation of areas, lengths, and other quantities.

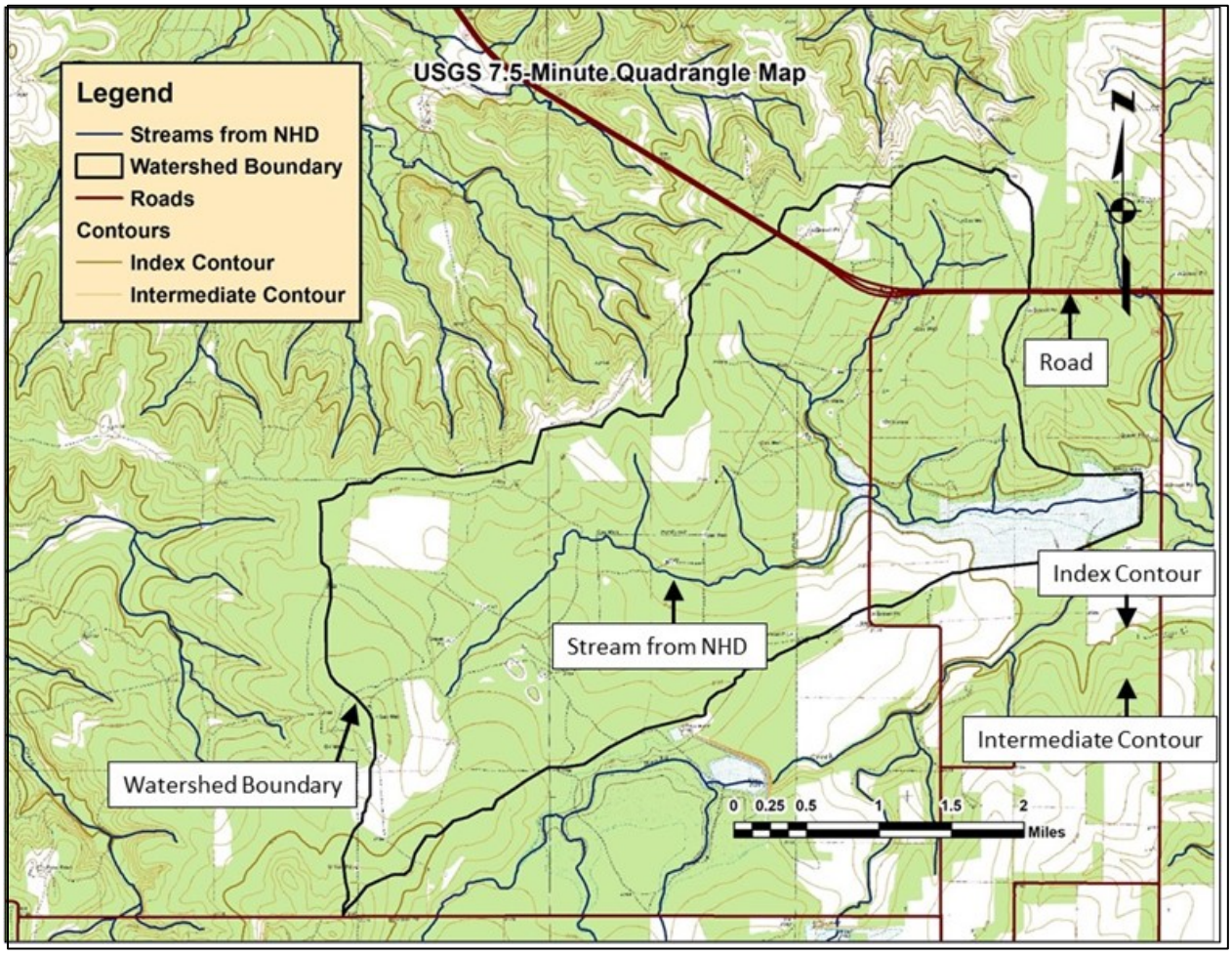

Figure 4.1. USGS map with streams from the USGS-NHD and digitized elevation contours.

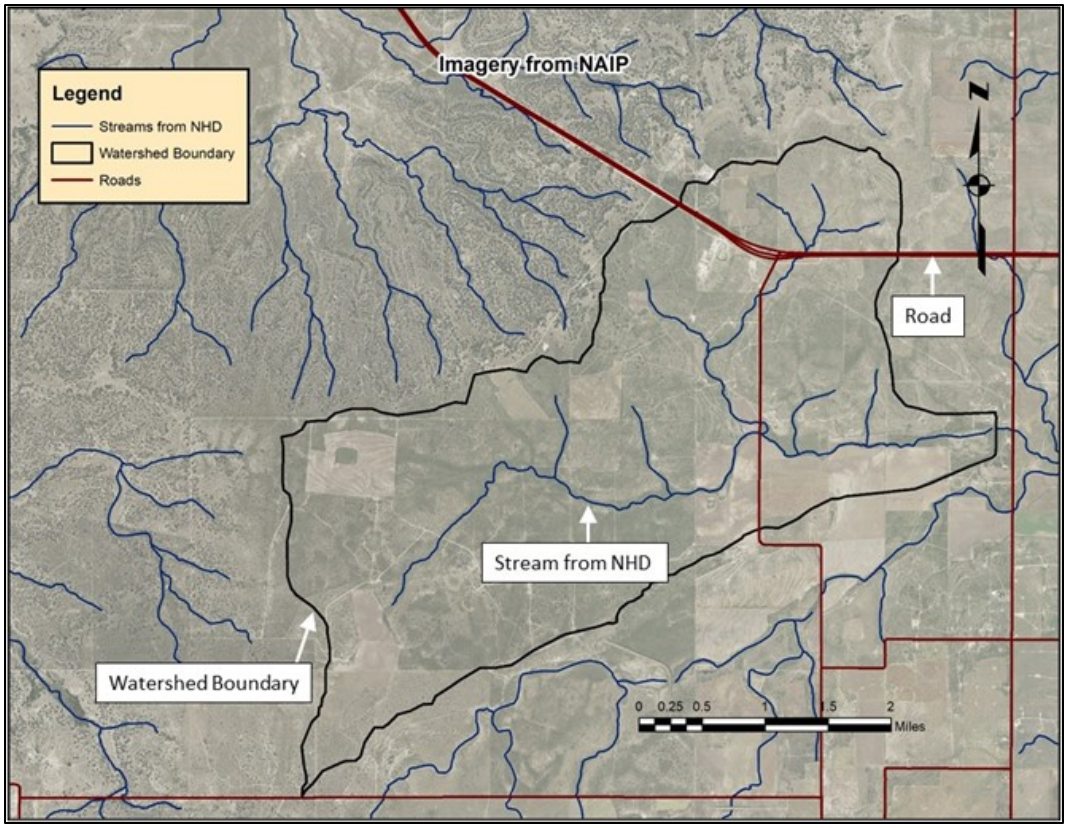

Figure 4.2. Aerial imagery from USDA-NAIP overlaid with roadways.

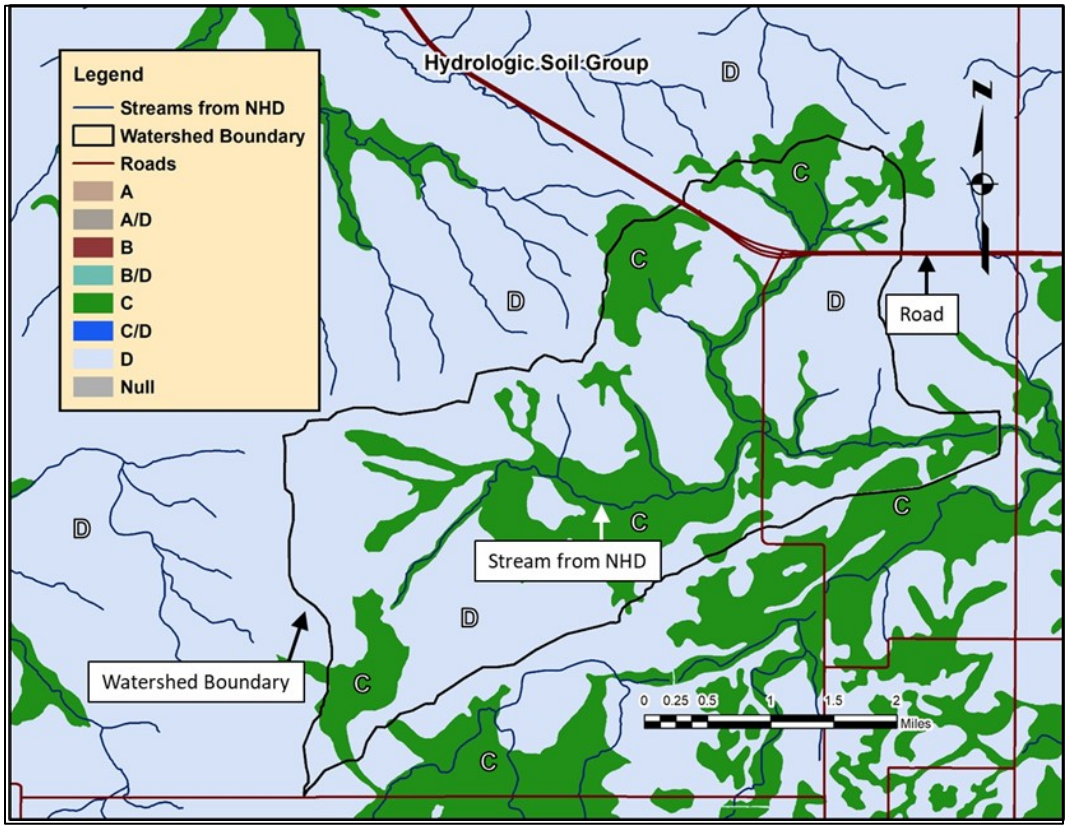

Figure 4.3. Hydrologic soil groups from gSSURGO data with streams from NHD.

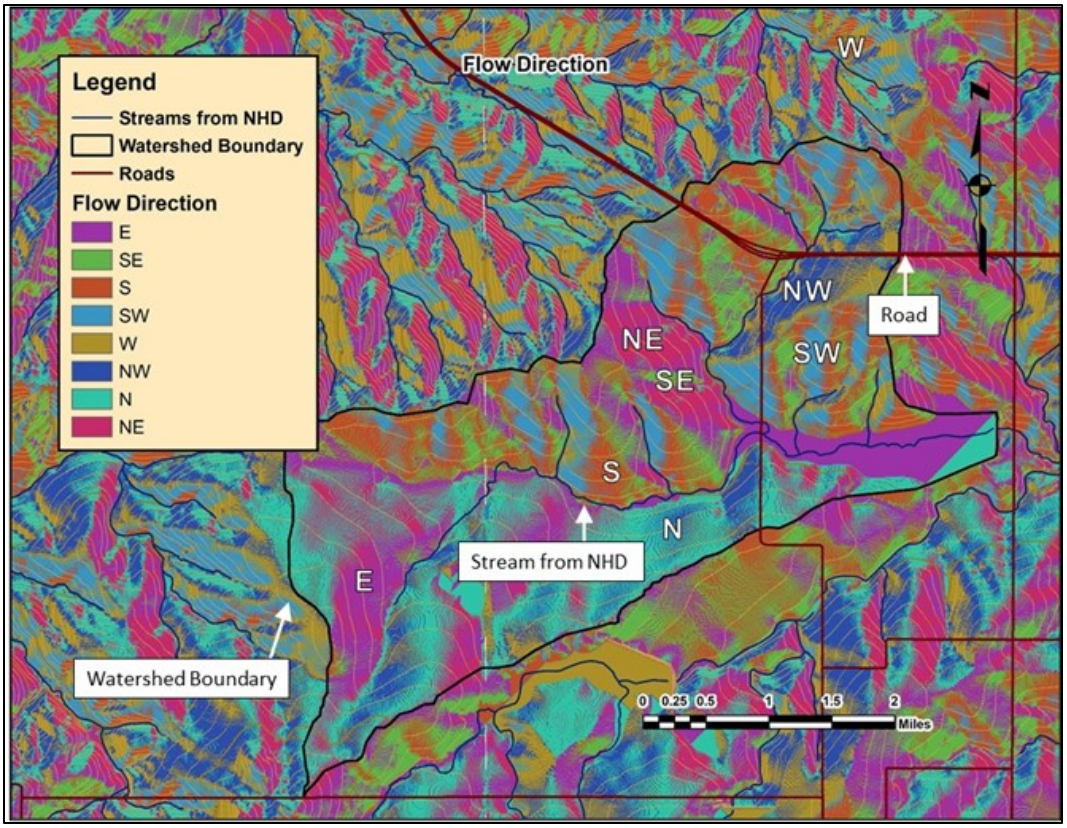

Figure 4.4. Flow direction generated by GIS from a 1/3-arc-second (approximately 10 meter) DEM from USGS-NED, overlaid with elevation contours and roadways.

Like GIS in some ways, computer aided design and drafting (CADD) programs accept georeferenced data, and some State transportation DOTs require that project plans be developed in established coordinate systems (for example, State plane systems) for later inclusion in statewide mapping efforts. Section 10.2 provides more information on the use of spatial data and GIS in hydrologic modeling.

4.3 Selecting Hydrologic Methods

Engineers choose from a variety of different types of hydrologic methods for a given project and location. They may choose multiple methods and compare results for additional insight. Considerations include:

- Hydrologic information needed, e.g., peak flows versus hydrographs for flooding or flow estimates related to wetlands, endangered species, water quality, or other non-flood criteria.
- Applicability of hydrologic methods and State/local guidance for choosing methods.
- Risk factors, e.g., potential consequences of flooding, regulatory floodplains, and impacts to adjacent properties.
- Watershed characteristics such as size and main channel slope.
- Climate characteristics such as precipitation and temperature (snow) patterns.
- Flooding history of the site.
- Land use and land cover (existing and future).

- Availability of stream gages at or near the project.
- Influence of controls in the watershed such as dams or detention storage.

4.3.1 Available Methods

This manual describes several methods applicable to a variety of situations. Table 4.1 summarizes a simplified overview of the methods discussed. Numerous Federal, State, and regional manuals document other methods that may apply nationally or are particular to States, regions, or specific conditions. The FHWA's *Highway Hydrology: Evolving Methods, Tools, and Data* (FHWA 2022a) describes additional approaches for the growing need for hydrologic approaches in less traditional applications.

Table 4.1. Hydrologic method overview.

Method	Drainage Area Limits	Selection Considerations
Gaged Flow Analysis/ Peak Flow Transposition (see Chapter 5)	Gage near or adaptable to design location	Does gage information include sufficient homogeneous record length?
Regression Equations (see Section 6.1)	Limited by the applicable equation	Are the watershed and meteorological characteristics consistent with equation limits?
Index Flood Method (see Section 6.3)	Dependent on the underlying method	Is there an acceptable source for a flood frequency curve to estimate AEP flows beyond the index flood?
Rational Method (see Section 6.2)	Generally, less than 200 acres	Is it reasonable to assume uniform rainfall for a duration equal to the time of concentration?
Unit Hydrographs (see Section 8.1)	Depends on unit hydrograph source	Are an appropriate unit hydrograph and design storm available?

When one or more stream gages are available on the stream or nearby, gaged flow analysis is likely the method of greatest utility. The utility of gage analysis is greatest when the gage series includes a sufficiently long record that can be considered "homogeneous," i.e., when watershed conditions over the gage series life has not been dramatically altered by changes in land use, urbanization, regulation by dams, or diversion for other purposes. Many gages record flow information from rural watersheds though some record the runoff behavior from urban watersheds. Chapter 5 discusses gaged flow analysis.

Nearby gages on similar streams may be suitable for transposition to the project site, or for information transfer by the index flood method. Transposition of gage analysis is most applicable within the same stream or stream system, allowing the designer to make good use of information from gages that are not directly located at the site of interest. Transposition of gage analysis may provide valuable information as a validation technique for other methods, as opposed to being used as a primary method of estimation. Transposition allows the designer to select gages based on proximity and similarity to the site of interest, as compared to the more general analysis of regression equations. Transposition is not limited to one gage, but several nearby gages can be used for comparison. Section 5.4 discusses peak flow transposition.

The USGS publications documenting the development of regression equations contain one or more sections discussing the range of explanatory variables used in the development of the equations and limitations of the equations. In particular, the USGS states the recommended drainage areas for application for each set of equations. Regression equations represent a pooling of information from many watersheds and are often a convenient tool for peak flow estimation. Since regression equations are based on gaged records, they primarily apply to more rural watersheds, but some equations apply to urban situations. Section 6.1 discusses regression equations.

The index flood method is conceptually related to regression equations. It can be considered less direct than gage analysis, but like transposition, the method allows for selection of gages based on proximity and similarity to the site of interest. Section 6.3 presents the index flood method.

Watersheds of less than 200 acres may be best analyzed using the Rational Method. The Rational Method is straight forward and is extensively used in urban situations for the design of storm drains, channels, and small culverts, though designers can apply it to smaller rural watersheds. The Rational Method is usually restricted to contributing areas of 200 acres. However, there may be situations where the Rational Method can be applied to larger areas. Section 6.2 presents the Rational Method.

The modeling of the rainfall-runoff process using unit hydrographs strives to mimic the physical rainfall process and describe how it runs off through the watershed. It is among the most flexible methods available. Rainfall-runoff modeling allows extrapolation beyond the range of watershed characteristics of gaged watersheds, can fill the gaps in the range of contributing area and can simulate the effects of constructed features such as dams and reservoirs, detention basins, and urbanization. The method can be used to project discharges for anticipated changes in conditions such as land use and land cover, post-fire conditions, and changing rainfall. Rainfall-runoff modeling applies to both rural and urban watersheds and applies to watershed drainage areas consistent with underlying assumptions of the particular method. Section 8.1 describes unit hydrographs.

4.3.2 Validation and Comparison

In cases of watersheds with contributing areas larger than what is appropriate for the Rational Method (greater than 200 acres), it is advisable for the designer to compare the results of two or more methods of analysis. Such a comparison provides the designer validation on the approximate magnitude of discharge for the identification of gross errors, and validation of the appropriate selection of methods. Methods that might be considered indirect, such as index flood or gage transposition, often provide considerable value as independent check procedures. Even in cases that demand a hydrograph, independent check of the peak flow against other methods is informative to the designer. Owing to the variety of conditions encountered in hydrology, and the large degree of uncertainty involved, validation of the design discharge is advisable.

For design criteria involving small annual exceedance probability (less than 0.04), validation is of even greater importance. Uncertainty is largest for rare events, and the consequences of the uncertainty may also be greater.

Page Intentionally Left Blank

Chapter 5 - Peak Flow for Gaged Sites

Designing highway drainage structures presents engineers with the common problem of estimating peak flows for various annual exceedance probabilities (AEPs). This chapter describes methods applicable to gaged sites, that is, sites that are at or near a streamflow-gaging station. As discussed in this chapter, to provide estimates of peak flows involves having a nearly complete and sufficiently long streamflow record.

Sites located at or near a gaging station, but that have incomplete or short records, represent special cases. Engineers can estimate peak flows for selected frequencies at such sites either by supplementing the record or transposing data from another site. Alternatively, they can use regression equations or other synthetic methods applicable to ungaged sites (see Chapter 6, 7, and 8).

The USGS publication *Guidelines for Determining Flood Flow Frequency* (England et al. 2019), commonly referred to as **Bulletin 17C,** describes "the data and procedures for computing flood flow frequency where systematic stream gaging records of sufficient length (at least 10 years, with an informative regional skew and [or] record extension) to warrant statistical analysis are available." It was intended for analyzing records of annual flood peak flows, including both systematic records and historic data.

Bulletin 17C presents an approach to estimating the statistical parameters used to fit a flood frequency curve to the annual stream gage record that supersedes Bulletin 17B (Water Resources Council 1982). Bulletin 17C calls the method the Expected Moments Algorithm (EMA), which is implemented in software, primarily the U.S. Army Corps of Engineers (USACE) program HEC-SSP and the U.S. Geological Survey (USGS) program PeakFQ.

This chapter primarily addresses the statistical analysis of gaged data. It presents appropriate solution techniques, discusses their assumptions and limitations, and introduces two common tools. The use of Bulletin 17C and the EMA are part of the subsequent discussions.

5.1 Statistical Character of Floods

Statistical analysis depends on the concepts of populations and samples. Statistics defines a population as the entire collection of all possible occurrences of a given quantity. It may be either finite or infinite. The number of possible outcomes from throwing dice, a fixed number, represents a finite population, while the number of different peak annual discharges possible for a given stream represents an (effectively) infinite population.

In all practical instances, engineers analyze hydrologic data as a sample of an infinite population, and they usually assume the sample is representative of its parent population. In this case, representativeness means that the characteristics of the sample, such as its measures of central tendency and its frequency distribution, are the same as that of the parent population.

Inferential statistics describes the inference of population characteristics and parameters from the characteristics of samples. Engineers often use the techniques of inferential statistics to analyze hydrologic data because samples are used to predict the characteristics of the populations. Not only do the techniques of inferential statistics facilitate estimates of the characteristics of the population from samples, but they also provide tools for the evaluation of the reliability or accuracy of the estimates. The next sections discuss some of the methods available for data analysis, illustrating the methods with actual peak flow data.

5.1.1 Record Length and Historical Data

A key element for inferring the characteristics of a population is the availability of a sufficiently large sample. In the context of streamflow gage data, engineers characterize this as the record length. This regular recording of annual peak flows comprises a record that is called the "systematic record." Engineers analyze gaged data to develop an estimate of the peak flow in terms of its probability or frequency of exceedance at a given site. Bulletin 17C (England et al. 2019) suggests that at least 10 years of record are necessary to warrant a statistical analysis.

At some sites, data that are supplemental or additional to the systematic record are available. These historical data may exist for large floods prior to or after the period over which streamflow data (systematic data) were collected. Engineers can collect this information from inquiries, newspaper accounts, and field surveys for highwater marks. Whenever possible, compiling and documenting these data improves frequency estimates.

When reliable information indicates that one or more large floods occurred outside the period of record, the engineer adjusts the frequency analysis to account for these events. Although estimates of unrecorded historical flood discharges may be inaccurate, it is important to incorporate them into the sample because the error in estimating the flow is small in relation to the random variability in the peak flows from year to year. If, however, there is evidence these floods resulted under different watershed conditions or from situations that differ from the sample, the large floods should be adjusted to reflect current watershed conditions.

Prior to Bulletin 17C, the method for incorporating historical data into the station frequency analysis was a separate component from the development of the statistical parameters used to fit the flood frequency curves. Bulletin 17C provides methods to adjust for historical data based on the assumption that "the data from the systematic (station) record is representative of the intervening period between the systematic and historic record lengths." The engineer enters the historical data into the input data for the software used to execute a Bulletin 17C analysis, considering the historical data as part of the EMA process. That is, separately computing the impact of historical data is not required.

5.1.2 Annual and Partial-Duration Series

Before data analysis, the designer arranges the data systematically. Engineers can arrange data in several ways, depending on the specific characteristics being examined. An arrangement of data by a specific characteristic is called a distribution or a series. Common data groupings include magnitude, time of occurrence, and geographic location.

Engineers most commonly arrange flood data as an annual peak flow series, or simply an annual series. This series is a collection of the largest flood peak in each year. Figure 5.1 displays an example of an annual series for 29 annual peak flows for Mono Creek near Vermilion Valley, California.

Gaging Station Information: Mono Creek near Vermilion Valley, California (11231500)

Basin: USGS 11231500 Mono Creek near Vermilion Valley, California, South Fork of San Joaquin River Basin.

Location: Latitude 37˚22'00" N, Longitude 118˚59'20" W, 1 mile downstream from lower end of Vermilion Valley and 6 miles downstream from North Fork.

Area: 92 mi^2

Remarks: Regulated after October 1954.

Engineers also arrange flood data in the partial-duration series. This procedure uses all peak flows above some base value. For example, the partial-duration series may consider all flows above the discharge of approximately bankfull stage. The U.S. Geological Survey (USGS) sets the base for the partial-duration series so that approximately three peak flows, on average, exceed the base each year. Over a 20-year period of record, this may yield 60 or more floods compared to 20 floods in the annual series. The record contains both annual peaks and partial-duration peaks for unregulated watersheds. Figure 5.2 illustrates a portion of the record for Mono Creek containing both the highest annual floods and other large secondary floods.

Engineers primarily use partial-duration series to define annual flood damages when more than one event causing flood damage can occur in any year. If the base for the partial-duration series conforms approximately to bankfull stage, the peaks above the base are generally flood-damaging events. The partial-duration series avoids a problem with the annual maximum series, specifically that annual maximum series analyses ignore floods other than the highest flood of that year even when they are larger than the highest floods of other years.

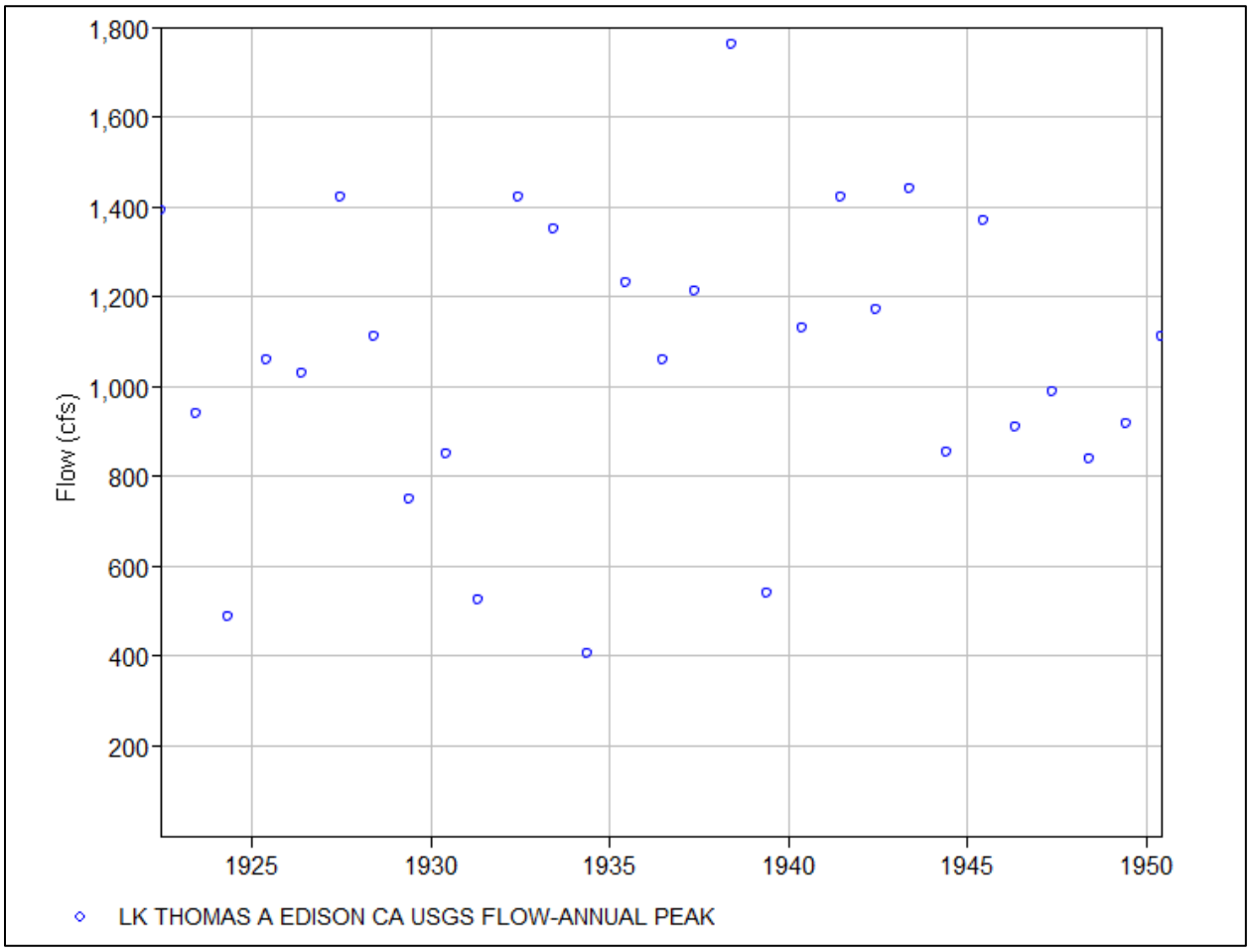

Figure 5.1. Annual maximum flood series, Mono Creek, California.

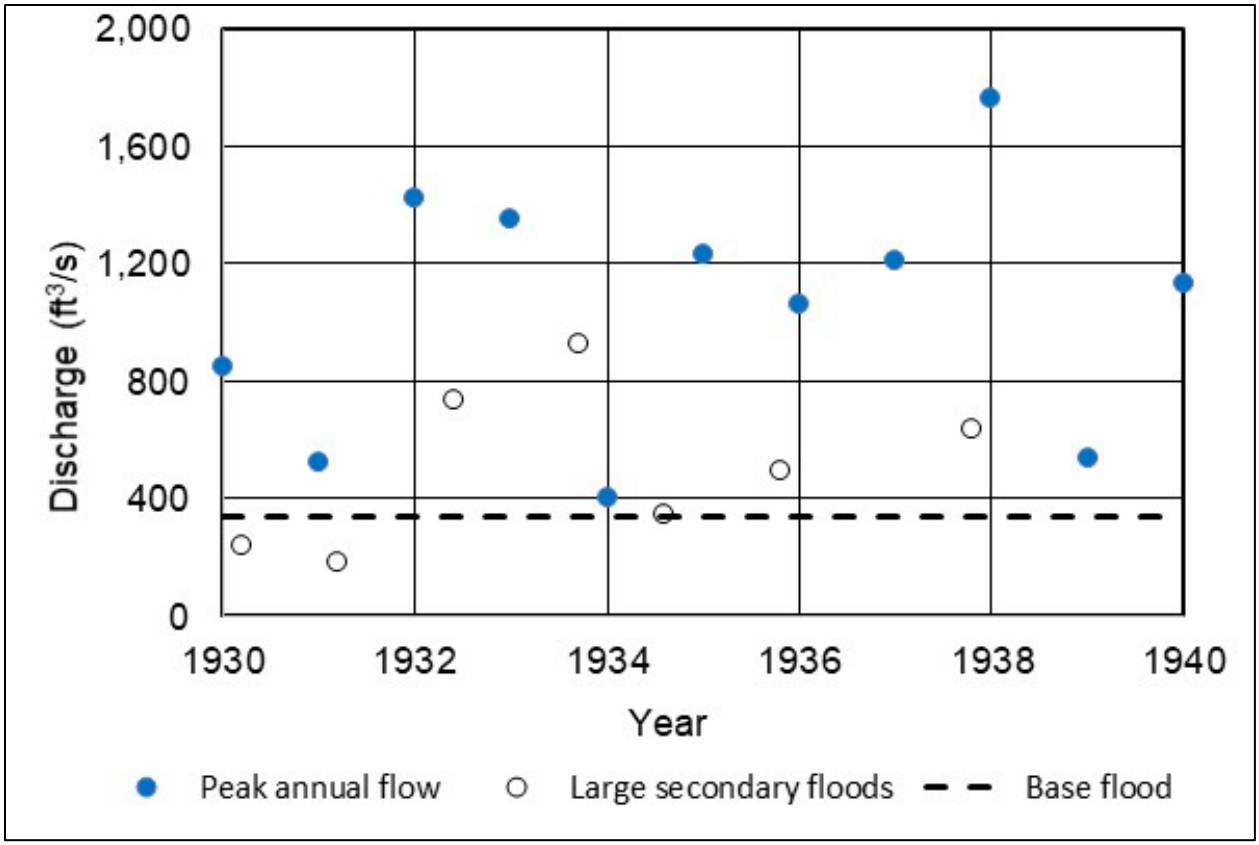

Figure 5.2. Peak annual and other large secondary flows, Mono Creek, California.

If these floods are ordered in the same manner as in an annual series, they can be plotted as illustrated in Figure 5.3. For a given rank (from largest to smallest) order, m, the partial-duration series yields a higher peak flow than the annual series because some of the large secondary flow exceed annual peak flow values. The difference is greatest at the lower flows and becomes small at the higher peak flows. If the return period of these peak flows is computed as the rank order divided by the number of events (not years), the return period of the partial-duration series can be computed in the terms of the annual series by the equation:

$$T_B = \frac{1}{\ln T_A \ \ln(T_A - 1)} \qquad (5.1)$$

where:

T_B = Return period of the partial-duration series, years
T_A = Return period of the annual series, years

Equation 5.1 can also be plotted as shown in Figure 5.4. This curve shows that the maximum deviation between the two series occurs for flows with return periods less than 10 years. At this interval, the deviation is about 5 percent; for the 5-year discharge, the deviation is about 10 percent. For the less frequent floods, the two series approach one another.

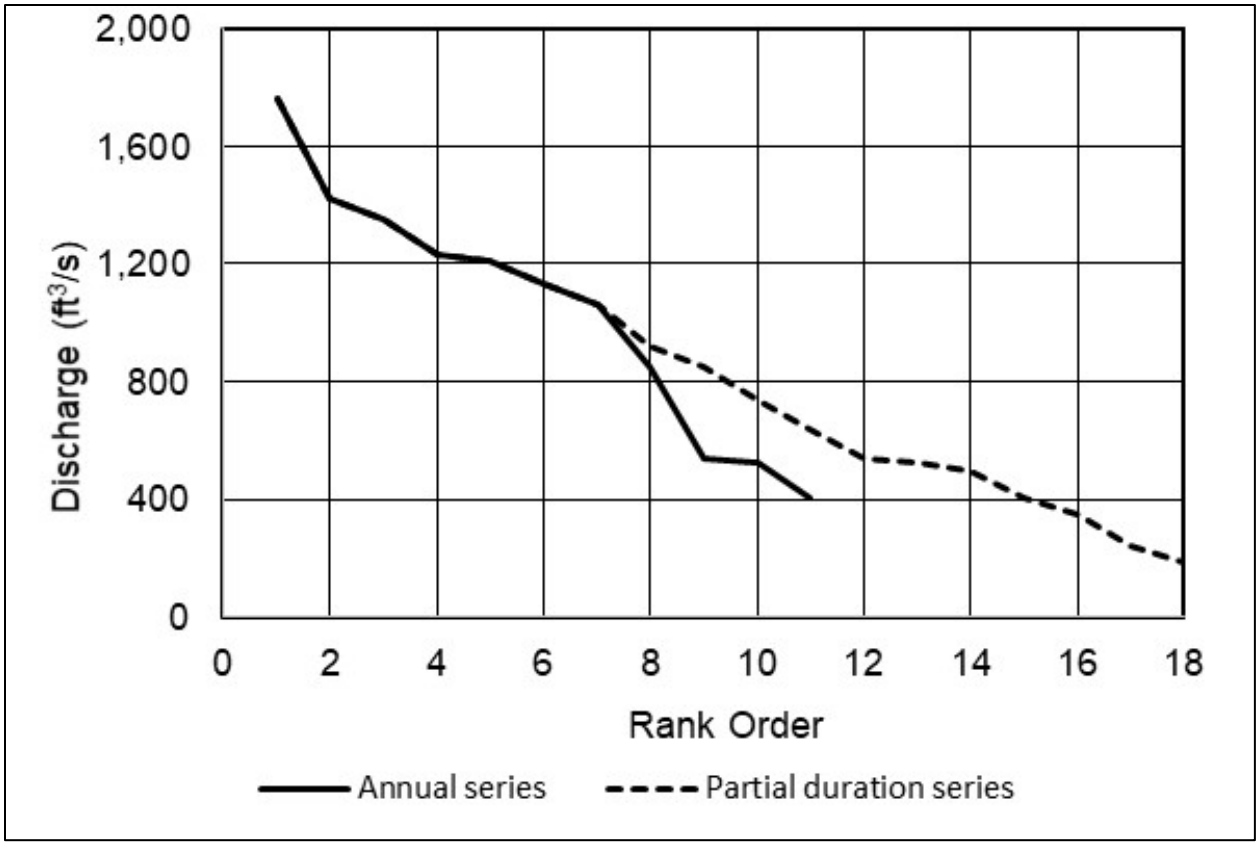

Figure 5.3. Annual and partial-duration series for Mono Creek, California (1930 to 1940).

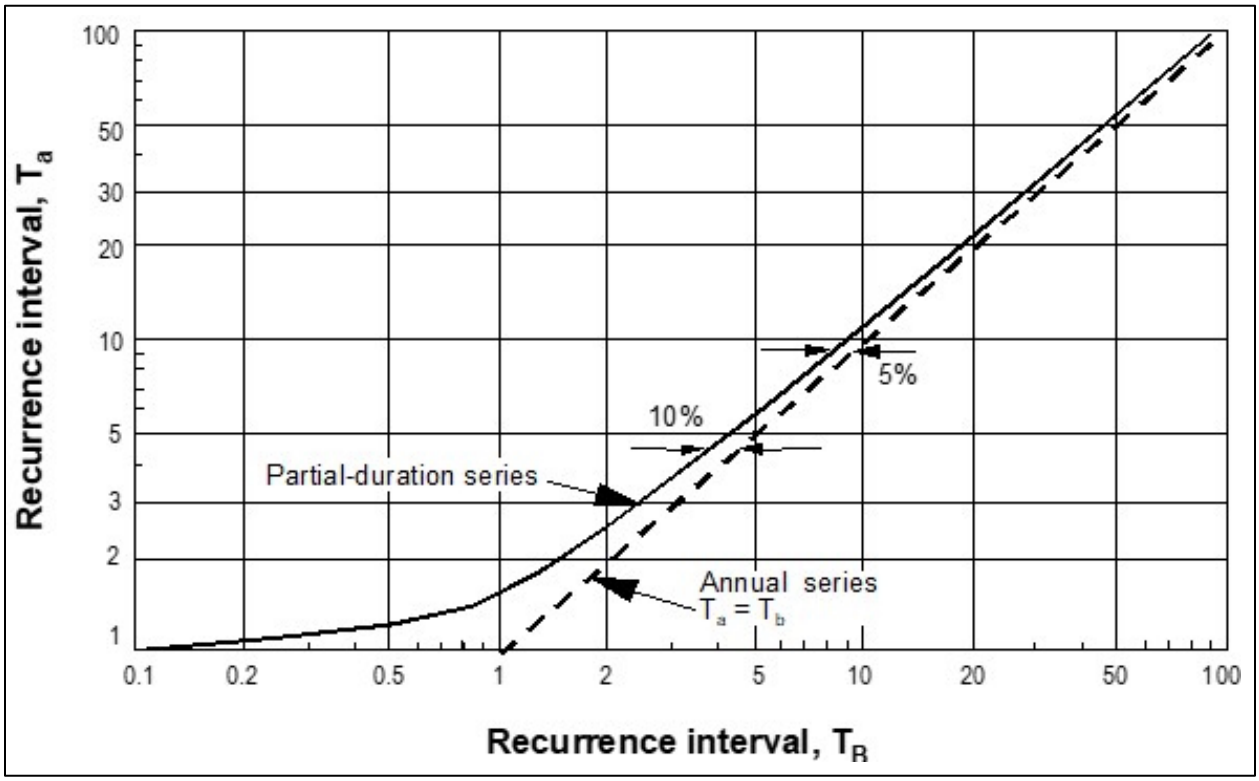

Figure 5.4. Relation between annual and partial-duration series.

When using the partial-duration series, it is important to be especially careful that the selected flood peaks are independent events. That is, there is a tradeoff in using a partial-duration series in that they involve a criterion that defines peak independence. Two large peaks several days apart and separated by a period of lower flows may be part of the same hydrometeorological event. This is challenging in practice because secondary flood peaks may occur during the same flood because of high antecedent moisture conditions. In this case, the secondary flood is not an independent event. It is also important to be cautious with the choice of the lower limit or base flood since it directly affects the computation of the properties of the distribution (i.e., the mean, the variance and standard deviation, and the coefficient of skew), all of which may change the peak flow determinations. For this reason (the difficulty in determining the independence of adjacent peaks), engineers use the annual series and convert the results to a partial-duration series through use of equation 5.1. For the less frequent events (greater than 5 to 10 years), the annual series is appropriate, and no other analysis is indicated.

5.1.3 Common Issues with At-site Data Records

Frequency analysis uses order-theory statistics. The analysis depends on several basic assumptions:

- The data are independent and identically distributed random events.
- The data are from the sample population.
- The data are assumed to be representative of the population.
- The process generating these events is stationary with respect to time.

Using a frequency analysis assumes that no measurement or computational errors were made. When analyzing a dataset, the engineer can statistically evaluate the validity of the four assumptions using tests described in Bulletin 17C. Issues related to these assumptions include nonhomogeneity, outliers, incomplete records, zero flows, and mixed populations.

5.1.3.1 Nonhomogeneity in the Annual Flood Series

Engineers can arrange annual flood series according to their time of occurrence in an arrangement called a time series. By visually examining a time series, such as Figure 5.5, the engineer determines if there is a trend or systematic change in the series with respect to time. Based on visual inspection of Figure 5.5, no trend in the peak flow time series for these data from Mono Creek is evident.

For comparison, Figure 5.6 presents a second time series with 24 years of annual peak floods taken from Pond Creek, Kentucky. The Pond Creek watershed became urbanized in the late 1950s. Therefore, the flood peaks tended to increase. This is evident from the obvious increase in the time series of peak flows during the period of urbanization. As the figure suggests, urbanization caused at least a doubling of flood magnitudes. Other possible causes of the trend should be investigated to provide some assurance that urban development was the cause.

Trend analysis plays an important role in evaluating the effects of changing land use and other time dependent parameters. Bulletin 17C, HEC-17 (FHWA 2016), and Helsel et al. (2020) present techniques for detection of possible trends. The engineer can often use trend analysis to make estimates of future events and to better understand past events.

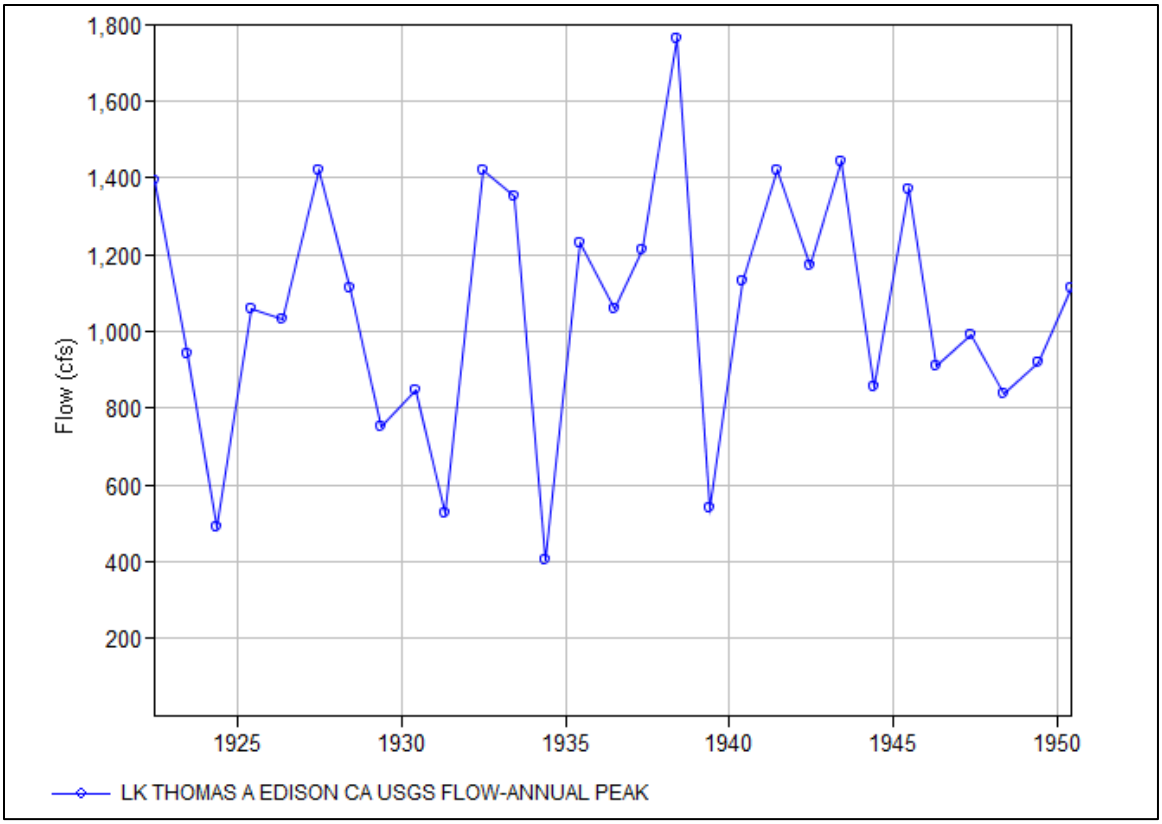

Figure 5.5. Annual peak flow time series from Mono Creek, California.

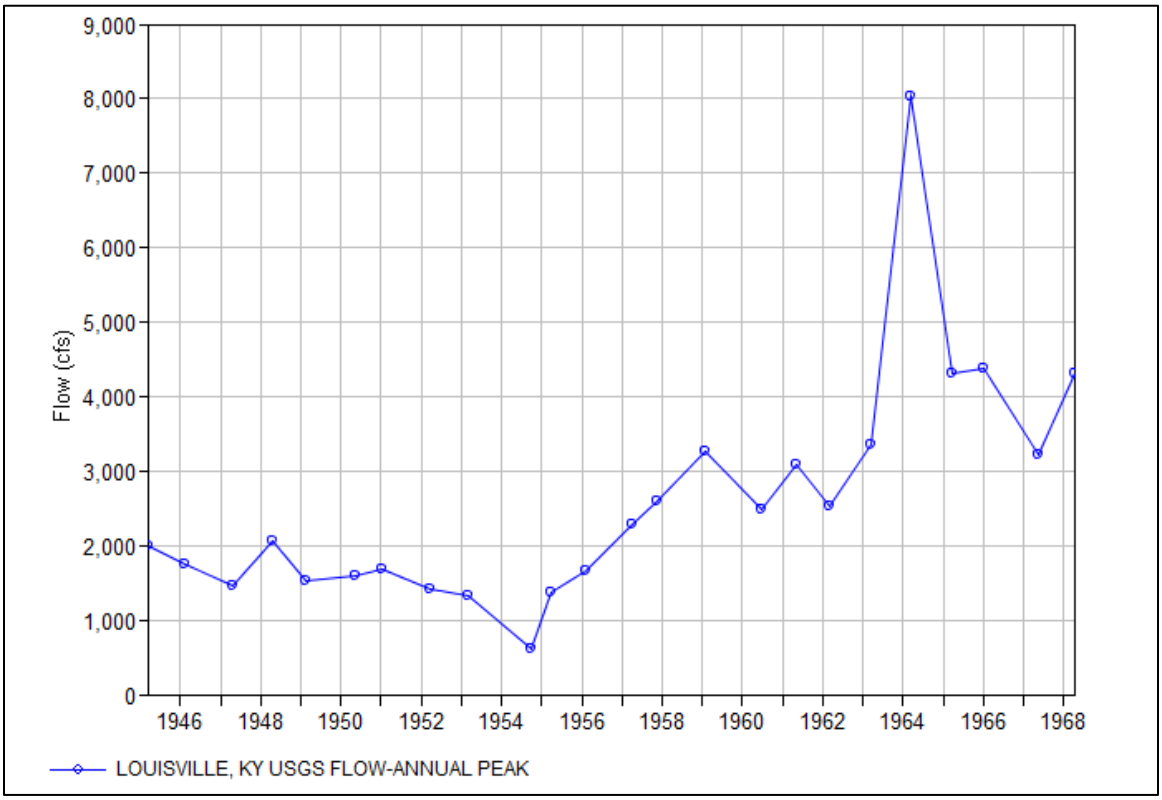

Figure 5.6. Annual peak flow time series from Pond Creek, Kentucky.

5.1.3.2 Outliers

Outliers, which may occur at either or both ends of a frequency distribution, are measured values that occur, but appear to be from a longer sample or different population. This happens when one or more data points do not follow the trend of the remaining data.

In Bulletin 17B (Water Resources Council 1982), the Grubbs-Beck (GB) test was used to identify low outliers. This approach produced a single low outlier and is easily defeated by the presence of multiple low outliers. Multiple low outliers can exert a substantial influence on the fitted frequency curve. In addition, they can increase the standard deviation, resulting in standardized distances between observations that are too small to trigger the GB test.

Therefore, Bulletin 17C presents a generalized version of the GB test, called the Multiple Grubbs-Beck Test (MGBT), to identify multiple small "unusual" or potentially influential low flood (PILF) observations. The MGBT also correctly evaluates cases with one or more observations of zero or below the recording threshold.

The basic approach is to consider the series of logarithms of annual peak floods, $\{X_1, \ldots, X_n\}$. The sorted (from smallest to largest) annual peak series (again, logarithms) is $\{X_{[1:n]}, X_{[2:n]}, \ldots, X_{[n:n]}\}$. The null hypothesis is that all observations emerge from the same population of independent and identically distributed normal deviates. The alternative hypothesis is that the k-th smallest observation, $X_{[k:n]}$, in the dataset is unusually small in comparison to the remainder of the observations. The Bulletin 17C EMA process includes detection of low outliers, so it does not involve a separate computation. Outliers are detected during the iterative solution of the distribution parameters and the results are adjusted accordingly.

5.1.3.3 Incomplete Records and Zero Flows

Streamflow records are often interrupted; this may occur for a variety of reasons. Gages may be out of service or removed for a period, there may be periods of zero flow that are common in the arid regions of the U.S., and there may be periods when a gage is inoperative either because the flow is too low to record or too large (causing a gage malfunction). The input data for the Bulletin 17C EMA analysis includes these parts of the systematic record.

5.1.3.4 Mixed Populations

In some areas of the U.S., multiple types of events cause floods, among them, rainfall and snowmelt in mountainous areas, hurricane events along the Gulf and Atlantic coasts, or other storm mechanisms. Analysts consider records including events from multiple types of events to be mixed populations because they represent the signals from of two (or more) populations. Therefore, the samples from these populations are also mixed. These records are often characterized by large skew coefficients and, when plotted, suggest that two different distributions might be applicable. Bulletin 17C discusses treatment of such cases.

5.1.4 Annual Exceedance Probability and Return Period

As introduced in Section 1.3, engineers often use the AEP of a given flood flow or, more commonly, the flow magnitude for a given AEP. The AEP is the probability that a given peak flow magnitude will be exceeded in any year. The laws of probability determine the statistical analysis of repeated observations of an event (e.g., observations of peak annual flows). Engineers approximate the probability of exceedance of a single peak flow, Q_A, by the relative number of exceedances of Q_A after a long series of observations:

$$P(Q_A) = \frac{n_1}{n} \tag{5.2}$$

where:

$P(Q_A)$ = Probability of exceeding Q_A
n_1 = Number of exceedances of some flood magnitude Q_A
n = Number of observations (if large)

The probability of a nonexceedance (or failure) of an event such as peak flow, Q_A, is given by:

$$P(\text{not } Q_A) = \frac{(n - n_1)}{n} = 1 - \frac{n_1}{n} = 1 - P(Q_A) \quad (5.3)$$

Combining equations 5.2 and 5.3 yields:

$$P(Q_A) + P(\text{not } Q_A) = 1 \quad (5.4)$$

Therefore, the probability of an event being exceeded is between 0 and 1 (i.e., $0 \leq P(Q_A) \leq 1$). If an event is certain to occur, it has a probability of 1, and if it cannot occur at all, it has a probability of 0.

Return period represents an alternative expression of AEP. If the exceedance probability of a given annual peak flow or its relative frequency determined from equation 5.2 is 0.2, this means that there is a 20 percent chance that this flood, over a long period of time, will be exceeded in any one year. Stated another way, this flood will be exceeded an average of once every 5 years. Engineers call that time interval the return period. As introduced in Section 3.4.5, the return period, T, relates to the probability of exceedance by:

Probability Intuition

Most people have an intuitive grasp of the concept of the probability of occurrence, or the probability of exceedance. They know that if a fair coin is tossed, it is equally probable that a head or a tail will result. Again, relying on experience or intuition, when tossing a fair die, any of six equally likely outcomes (the numbers 1 through 6) may result. Each has a probability of occurrence of 1/6. So, the chances that the number 3 will result from a single throw is 1 out of 6. These examples are straightforward because all the possible outcomes are known before the coin is tossed or the die is cast, and the probabilities are readily quantified.

$$T = \frac{1}{P(Q_A)} \quad (5.5)$$

where:

T = Return period
$P(Q_A)$ = Probability of exceeding Q_A

A flood with a return period of 5 years does not mean this flood will occur once every 5 years. Rather, it has a 20 percent probability of being exceeded in any year; two 5-year floods can occur in two consecutive years. There is also a probability that a 5-year flood may not be exceeded in a 10-year period. The same is true for any flood of a specified return period. This important concept leads to use of the binomial probability theorem for estimating various probabilities of

occurrence (or non-occurrence) of events of interest during the lifetime of a project. More information is presented in Section 10.3.

5.1.5 Frequency Analysis Concepts

Future floods cannot be predicted with certainty. Therefore, engineers use probability concepts to project their magnitude and frequency. To do this, they obtain and analyze a sample of flood magnitudes to estimate a population that can represent flooding at that location. Engineers then use the assumed population in making projections of the magnitude and frequency of floods. It is important to recognize that the population is estimated from sample information and that the assumed population, not the sample, is then used for making statements about the likelihood of future flooding. This section introduces concepts for analyzing sample flood data to identify a probability distribution that can represent the occurrence of flooding.

5.1.5.1 Histograms

A histogram contains data arranged by classes or categories with associated frequencies of each class. Engineers use histograms to visualize sample data and reveal basic characteristics of their distribution. The distribution shows the magnitude of past events for certain ranges of the variable. Engineers can also compute sample probabilities by dividing the frequencies of each interval by the sample size.

Engineers construct a histogram by first examining the range of magnitudes (i.e., the difference between the largest and the smallest floods) and dividing this range into several conveniently sized groups, usually between 5 and 20. These groups are called class intervals. The size of the class interval is simply the range divided by the number of class intervals selected.

Histogram Rules of Thumb

Engineers often use rules of thumb when selecting the number of class intervals:

- Select non-overlapping class intervals without gaps between the bounds of the intervals.
- Choose a number of class intervals that will provide most class intervals with at least one event.
- Aim for class intervals of equal width.
- Aim for most class intervals to have at least five occurrences, something that may be impractical for the first and last intervals.

Example 5.1:	Creating a histogram.
Objective:	Create several histograms of peak annual flows for the data from Mono Creek, California.

Given: Data from Table 5.1 as the input data for this example.

Step 1. Using the rules above, place the discharges for the stream gage of interest into a table using the selected class intervals.

The maximum peak flow for Mono Creek is 1,760 ft^3/s and the minimum is 404 ft^3/s. Note that the mean value is 1,060 ft^3/s and the standard deviation is 330 ft^3/s. If a class size of 200 ft^3/s is used, then there are 9 classes. This is consistent with the suggested range of from 5 to 20 classes. Place the count of discharges in each class into Table 5.2.

Table 5.1. Annual peak flow data for Mono Creek.

Year	Annual Maximum (ft^3/s)	Year	Annual Maximum (ft^3/s)	Year	Annual Maximum (ft^3/s)	Year	Annual Maximum (ft^3/s)	Year	Annual Maximum (ft^3/s)
1922	1,390	1928	1,110	1934	404	1940	1,130	1946	910
1923	940	1929	750	1935	1,230	1941	1,420	1947	988
1924	488	1930	848	1936	1,060	1942	1,170	1948	838
1925	1,060	1931	525	1937	1,210	1943	1,440	1949	916
1926	1,030	1932	1,420	1938	1,760	1944	855	1950	1,100
1927	1,420	1933	1,350	1939	540	1945	1,370	n/a	n/a

Table 5.2. Histogram and relative frequency analysis of annual flood data for Mono Creek.

Interval of Annual Floods (ft^3/s)	Frequency	Relative Frequency	Cumulative Frequency
0 – 199	0	0.000	0.000
200 – 399	0	0.000	0.000
400 – 599	4	0.138	0.138
600 – 799	1	0.034	0.172
800 – 999	7	0.241	0.414
1000 – 1199	7	0.241	0.655
1200 – 1399	5	0.172	0.828
1400 – 1599	4	0.138	0.966
1600 – 1799	1	0.034	1.000

Step 2. Use the count of values for each class to create a histogram of the data.

Create the frequency histogram shown in Figure 5.7 using the values in Table 5.2.

Step 3. Compute the relative frequency of events in each class (or bin) as the number of events in each class of events divided by the sample size.

Compute the relative frequency of each class as the number of values in the class (the frequency in Table 5.2) by the total number of observations (in this case 29 observations). Place these values in Table 5.2.

***Step 4.** Create a histogram of the relative frequency of each class.*

This can be done by adding a second ordinate to the previous histogram. The advantage of such a histogram is that it combines both frequency and relative frequency on one display. Add the relative frequency to Figure 5.7 by adding a second ordinate on the right size of the figure.

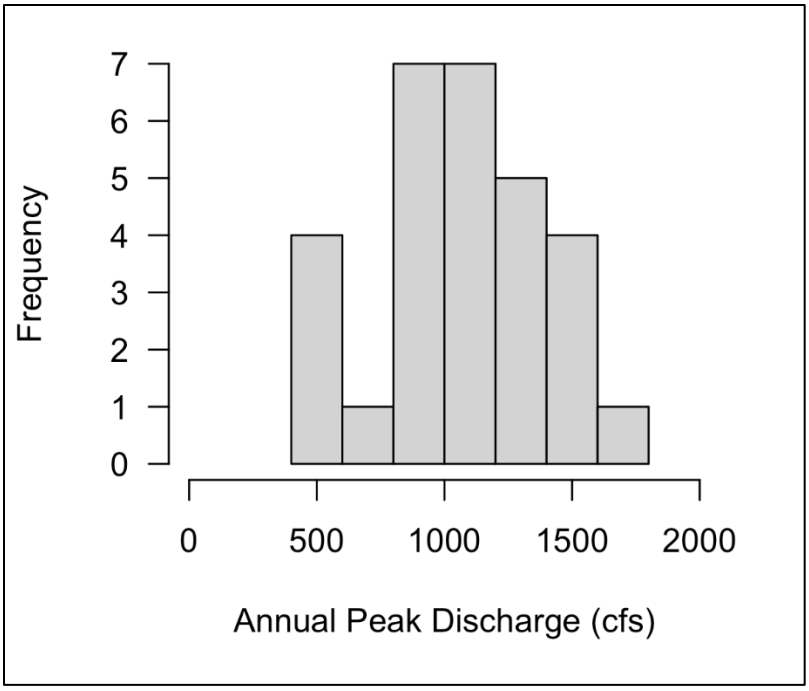

Figure 5.7. Sample frequency histogram and probability, Mono Creek, California.

Solution:	The results in Table 5.2 and the histogram in Figure 5.7 represent the solution. Notice that some ranges of magnitudes occur more frequently than others. Also notice that the data are somewhat spread out and that the distribution of the ordinates is not symmetrical. While an effort was made to have frequencies of five or more, this was not possible with the class intervals selected. Because of the small sample size, it is difficult to assess the distribution of the population using the histogram.

Example 5.2:	Creating alternate histograms from a single dataset.
Objective:	Examine the results of different class sizes on the resulting histogram.

Many flood records have relatively small record lengths. For such records, histograms may not be adequate to assess the shape characteristics of the distribution of floods. The flood record for Pond Creek of Table 5.3 provides a good illustration. With a record length of 24 years, it would be impractical to use more than 5 or 6 intervals when creating a histogram. Therefore, five different class intervals are constructed for comparison.

Step 1. Construct a histogram using five class intervals.

Use a class interval of 1,412 ft^3/s to construct a histogram of peaks from Pond Creek. The second column of Table 5.4 displays the results. The results have a hydrograph-like shape, with few values in the lowest cell and a noticeable peak in the second cell.

Table 5.3. Annual peak flow series from Pond Creek, Kentucky.

Year	Annual Maximum (ft^3/s)
1945	2,002
1946	1,741
1947	1,462
1948	2,062
1949	1,532
1950	1,593
1951	1,691
1952	1,419
1953	1,331
1954	607
1955	1,381
1956	1,660
1957	2,292
1958	2,592
1959	3,263
1960	2,493
1961	3,083
1962	2,521
1963	3,362
1964	8,026
1965	4,311
1966	4,382
1967	3,224
1968	4,322

Table 5.4. Alternative frequency histograms of Pond Creek, Kentucky.

Interval	Histogram 1 Frequency	Histogram 2 Frequency	Histogram 3 Frequency	Histogram 3 Interval (ft^3/s)
1	3	10	10	0 – 1,765
2	13	10	5	1,766 – 2,648
3	4	3	5	2,649 – 3,531
4	3	0	3	3,532 – 5,297
5	1	1	1	> 5,297

Step 2. Construct a second histogram using five class intervals of a different size than Step 1.

Use a class interval of 1,766 ft^3/s to construct a second histogram. The third column of Table 5.4 displays the results. This produces a box-like shape with many observations in the first two cells and the other cells very few, with one intermediate cell not having any occurrences.

Step 3. Construct a third histogram using a variable class interval.

The fifth column of Table 5.4 contains the class interval for this example. It varies with class intervals wider at the low and high end of the data range and narrower class intervals in the middle of the data range. The third histogram displayed in the fourth column of Table 5.4 produces an exponential-decay shape.

Solution: Figure 5.8 displays the three choices of bin size on the shape of the resulting histogram. The results demonstrate that short records make it difficult to identify the distribution of floods.

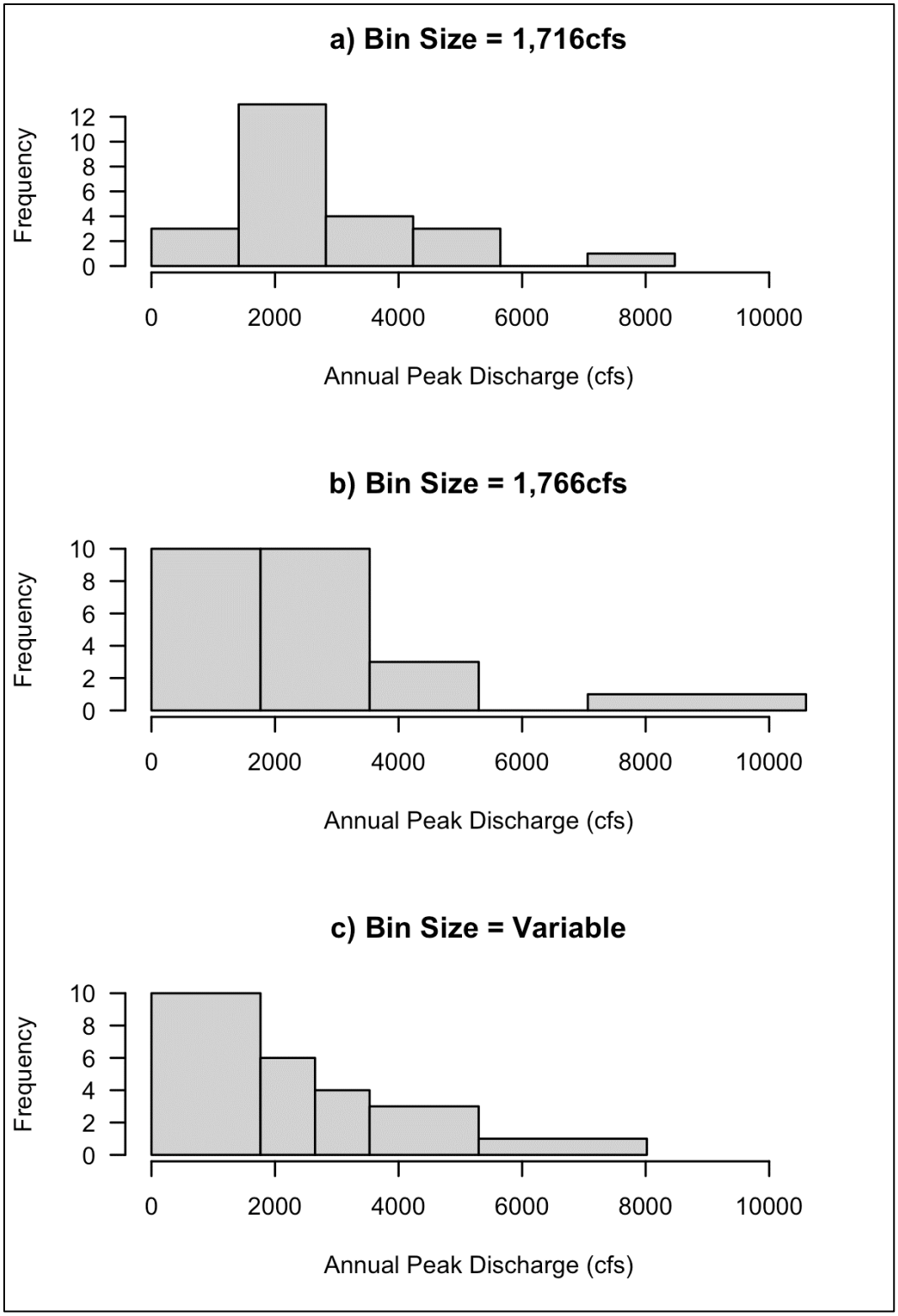

Figure 5.8. Three histograms for Pond Creek, Kentucky.

5.1.5.2 Method of Moments for Parameter Estimation

Flood frequency analysis uses sample information to fit a population to a probability distribution. These distributions have parameters that are estimated to make probability statements about the

likelihood of future flood magnitudes. The method of moments equates the moments of the sample flood record to the moments of the population distribution, yielding equations for estimating the parameters of the population as a function of the sample moments. As an example, if the population is assumed to follow distribution f(x), then the sample mean ($\overline{X}$) could be related to the definition of the population mean (μ):

$$\overline{X} = \int_{-\infty}^{\infty} xf(x)dx \qquad (5.6)$$

The sample variance (S^2) could be related to the definition of the population variance (σ^2):

$$S^2 = \int_{-\infty}^{\infty} (X-\mu)^2 f(x)dx \qquad (5.7)$$

Since f(x) is a function that includes the parameters (μ and σ^2), the solution of equations 5.6 and 5.7 will be expressions that relate the sample parameters $\overline{X}$ and S^2 to the population parameters μ and σ^2.

5.1.5.3 Central Tendency

Central tendency describes the clustering of data about particular magnitudes. The mean value or average is the most frequently used measure of central tendency and is calculated by summing all the individual values of the data and dividing the total by the number of individual data values:

$$\overline{Q} = \frac{\sum_{i=1}^{n} Q_i}{n} \qquad (5.8)$$

where:

$\overline{Q}$	=	Average (mean) peak
Q_i	=	The i^{th} peak
n	=	Number of peak values

Mean, Median, Mode

The mean is more precisely termed arithmetic mean and commonly called the average. The mean is sensitive to very large (or very small) values that are distant from the mean.

The median is not so influenced by very large or very small observations because the median is based only on the ranks of the observations, not the values themselves.

The mode is the most frequently occurring value in the sample.

The mean and median are both used in hydrologic statistics. The mode is not used very often.

The median, another measure of central tendency, is the value of the middle item when the items are arranged according to magnitude. When there is an even number of items, the median is taken as the average of the two central values.

The mode is a third measure of central tendency. The mode is the most frequent or most common value that occurs in a set of data. For continuous variables, such as discharge rates, the mode is defined as the central value of the most frequent class interval.

5.1.5.4 Variability

The spread of the data is called dispersion. The most used measure of dispersion is the standard deviation. The standard deviation, S, is defined as the square root of the mean square of the deviations from the average value. This is shown symbolically as:

$$S = \left[\frac{\sum_{i=1}^{n}(Q_i - \overline{Q})^2}{n-1}\right]^{0.5} = \overline{Q}\left[\frac{\sum_{i=1}^{n}\left(\frac{Q_i}{\overline{Q}} - 1\right)^2}{n-1}\right]^{0.5} \quad (5.9)$$

Another measure of dispersion of the flood data is the variance, or simply the standard deviation squared. A measure of relative dispersion is the coefficient of variation, V, or the standard deviation divided by the mean peak:

$$V = \frac{S}{\overline{Q}} \quad (5.10)$$

5.1.5.5 Skew

The symmetry of the frequency distribution, or more accurately the asymmetry, is called skew. One common measure of skew is the coefficient of skew, G. The skew coefficient is calculated by:

$$G = \frac{n\sum_{i=1}^{n}(Q_i - \overline{Q})^3}{(n-1)(n-2)S^3} = \frac{n\sum_{i=1}^{n}\left(\frac{Q_i}{\overline{Q}} - 1\right)^3}{(n-1)(n-2)V^3} \quad (5.11)$$

If a frequency distribution is symmetrical, the skew coefficient is zero. For example, the normal distribution (discussed in Section 5.2.1) is a symmetrical distribution and has a zero skew coefficient. If the distribution has a longer “tail” to the right of the central maximum than to the left, the distribution has a positive skew and G is positive. If the longer tail is to the left of the central maximum, the distribution has a negative skew coefficient.

Example 5.3: Method of moments calculation.

Objective: Calculate the sample moments for an annual peak flow series.

Given: Table 5.5 lists the annual peak flow series for the unregulated period of record for Mono Creek, California.

Find: The mean, standard deviation, coefficient of variation, and skew coefficient.

The computations below illustrate the computation of measures of central tendency, standard deviation, and coefficient of skew for the Mono Creek frequency distribution shown in Figure 5.7 based on the data provided in Table 5.5.

Step 1. Compute the mean annual peak flow.

Use equation 5.6 and the data in Table 5.5 to compute the mean. Notice that the bottom of Table 5.5 includes the sums.

$$\overline{X} = \frac{\sum_{i=1}^{n} X_i}{n} = \frac{30672}{29} = 1058 \text{ ft}^3/\text{s}$$

Table 5.5. Annual peak flows and statistics computation for Mono Creek, California.

Year	Rank	Annual Maximum (ft^3/s)	$[(X/\overline{X})]$	$[(X/\overline{X})-1]$	$[(X/\overline{X})-1]^2$	$[(X/\overline{X})-1]^3$
1938	1	1,760	1.664	0.664	0.441	0.2929
1943	2	1,440	1.362	0.362	0.131	0.0473
1927	3	1,420	1.343	0.343	0.117	0.0402
1932	4	1,420	1.343	0.343	0.117	0.0402
1941	5	1,420	1.343	0.343	0.117	0.0402
1922	6	1,390	1.314	0.314	0.099	0.0310
1945	7	1,370	1.295	0.295	0.087	0.0257
1933	8	1,350	1.276	0.276	0.076	0.0211
1935	9	1,230	1.163	0.163	0.027	0.0043
1937	10	1,210	1.144	0.144	0.021	0.0030
1942	11	1,170	1.106	0.106	0.011	0.0012
1940	12	1,130	1.068	0.068	0.005	0.0003
1928	13	1,110	1.049	0.049	0.002	0.0001
1950	14	1,100	1.040	0.040	0.002	0.0001
1925	15	1,060	1.002	0.002	0.000	0.0000
1936	16	1,060	1.002	0.002	0.000	0.0000
1926	17	1,030	0.974	-0.026	0.001	0.0000
1947	18	988	0.934	-0.066	0.004	-0.0003
1923	19	940	0.889	-0.111	0.012	-0.0014
1949	20	916	0.866	-0.134	0.018	-0.0024
1946	21	910	0.860	-0.140	0.019	-0.0027
1944	22	855	0.808	-0.192	0.037	-0.0070
1930	23	848	0.802	-0.198	0.039	-0.0078
1948	24	838	0.792	-0.208	0.043	-0.0090
1929	25	750	0.709	-0.291	0.085	-0.0246
1939	26	540	0.511	-0.489	0.240	-0.1173
1931	27	525	0.496	-0.504	0.254	-0.1277
1924	28	488	0.461	-0.539	0.290	-0.1562
1934	29	404	0.382	-0.618	0.382	-0.2361
Total		30,672			2.677	-0.1449

Step 2. Compute the standard deviation of the annual peak flows.

Use equation 5.7 and the data in Table 5.5 to compute the standard deviation.

$$S = \overline{X}\left[\frac{\sum_{i=1}^{n}\left(\frac{X_i}{\overline{X}} - 1\right)^2}{n-1}\right]^{0.5} = 1058\left[\frac{2.677}{28}\right]^{0.5} = 327 \text{ ft}^3 / \text{s}$$

Step 3. Compute the coefficient of variation of the annual peak flows.

Use equation 5.11 and the data in Table 5.5 to compute the coefficient of variation.

$$V = \frac{S}{\overline{X}} = \frac{327}{1058} = 0.31$$

Step 4. Compute the skew coefficient of the annual peak flows.

Use equation 5.10 and the data in Table 5.5 to compute the skew coefficient.

$$G = \frac{n\sum_{i=1}^{n}\left(\frac{X_i}{\overline{X}} - 1\right)^3}{(n-1)(n-2)V^3} = \frac{29(-0.1448)}{28(27)(0.31)^3} = -0.19$$

Solution:	The mean annual peak is 1,058 ft^3/s. The standard deviation of the peaks is 327 ft^3/s, the coefficient of variation is 0.31 (dimensionless), and the skew coefficient is -0.19.

5.1.5.6 Regional and Weighted Skew

Engineers can use three methods to represent the skew coefficient. These include the station skew (the skew coefficient computed from the gage data), a regional skew, and a weighted skew. Since the skew coefficient is sensitive to extreme values, the station skew may not be accurate if the sample size is small. Regional skew estimates and the regional skew coefficient mean square error estimates may be obtained from studies completed by the USGS that use Bayesian weighted least squares (B-WLS) or Bayesian general least squares (B-GLS). The technical background for these procedures is beyond the scope of this document but is presented in Bulletin 17C along with information on where to locate regional skew estimates. Values for the regional skew and the mean square error can be obtained from current USGS reports or by contacting the local USGS office. Bulletin 17C specifically recommends against using the legacy generalized skew and mean squared error estimates from Bulletin 17B.

Bulletin 17C recommends computation of station skew and use of a regional skew coefficient determined by other studies (as described above) or obtained directly from USGS personnel. The EMA automates this process. When the station skew differs from the regional skew by more than 0.5, then engineer conducts additional analyses to determine whether to give station skew greater weight in estimating the skew coefficient for the flood frequency curve.

In general, the station skew and regional skew can be combined to provide a better estimate for a given sample of flood data. Bulletin 17C combines estimation of the station skew (and other distribution parameters), the mean squared error of the station skew, and computation of weighted skew in the EMA process. However, for an analysis of a systematic record with no PILFs, a weighted skew can be computed using:

$$G_W = \frac{MSE_{\bar{G}}(G) + MSE_G(\bar{G})}{MSE_{\bar{G}} + MSE_G} \quad (5.12)$$

where:

G_W	=	Weighted skew
G	=	Station skew
$\bar{G}$	=	Regional skew
MSE_G	=	Mean square error for the station skew
$MSE_{\bar{G}}$	=	Mean square error for the regional skew

The concept is that the mean-square error (MSE) of the weighted skew is minimized by weighting the station and generalized skews in inverse proportion to their individual MSE. MSE is defined as the sum of the squared differences between the true and estimated values of a quantity divided by the number of observations.

Equation 5.12 assumes that station and regional skew are independent. If they are independent, the weighted estimate will have a lower variance than either the station or regional skew. Appendix 7 of Bulletin 17C describes the application of skew.

In Bulletin 17C, the value of MSE_G is computed as part of the EMA process. However, for the purposes of use in a subsequent example, Table 5.6 (from Bulletin 17B) presents MSE_G as a function of skew coefficient and record length.

5.1.6 Probability Distribution Function

A histogram from a large population of floods with small class intervals tends to approach a smooth curve as the population increases. Figure 5.9 provides an example of such a curve, which is called the probability distribution function, f(Q). As with a histogram it encloses an area of 1.0 or:

$$\int_{-\infty}^{\infty} f(Q)dQ = 1 \quad (5.13)$$

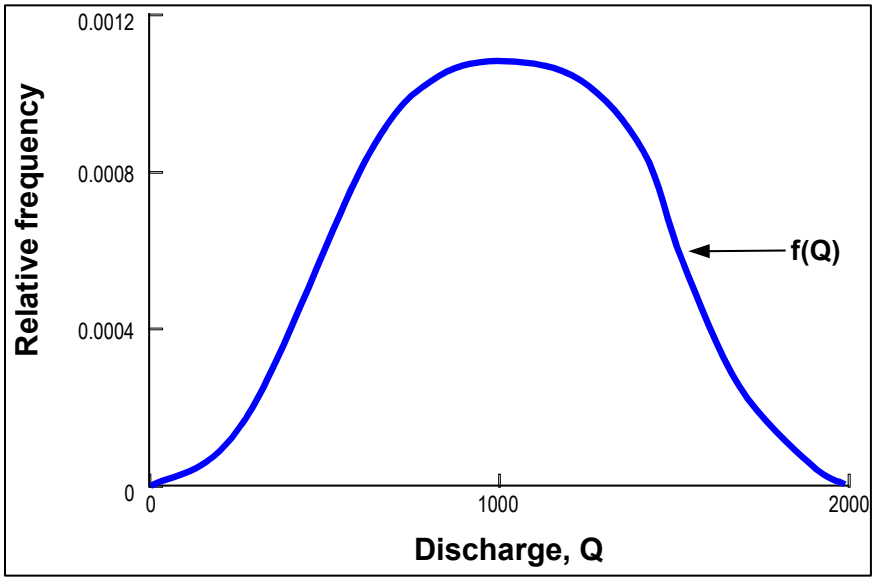

Figure 5.9. Probability distribution function.

Table 5.6. Mean square error of station skew as a function of record length and station skew.

Skew	Record Length, N or H (years)									
	10	20	30	40	50	60	70	80	90	100
0.0	0.468	0.244	0.167	0.127	0.103	0.087	0.075	0.066	0.059	0.054
0.1	0.476	0.253	0.175	0.134	0.109	0.093	0.080	0.071	0.064	0.058
0.2	0.485	0.262	0.183	0.142	0.116	0.099	0.086	0.077	0.069	0.063
0.3	0.494	0.272	0.192	0.150	0.123	0.105	0.092	0.082	0.074	0.068
0.4	0.504	0.282	0.201	0.158	0.131	0.113	0.099	0.089	0.080	0.073
0.5	0.513	0.293	0.211	0.167	0.139	0.120	0.106	0.095	0.087	0.079
0.6	0.522	0.303	0.221	0.176	0.148	0.128	0.114	0.102	0.093	0.086
0.7	0.532	0.315	0.231	0.186	0.157	0.137	0.122	0.110	0.101	0.093
0.8	0.542	0.326	0.243	0.196	0.167	0.146	0.130	0.118	0.109	0.100
0.9	0.562	0.345	0.259	0.211	0.181	0.159	0.142	0.130	0.119	0.111
1.0	0.603	0.376	0.285	0.235	0.202	0.178	0.160	0.147	0.135	0.126
1.1	0.646	0.410	0.315	0.261	0.225	0.200	0.181	0.166	0.153	0.143
1.2	0.692	0.448	0.347	0.290	0.252	0.225	0.204	0.187	0.174	0.163
1.3	0.741	0.488	0.383	0.322	0.281	0.252	0.230	0.212	0.197	0.185
1.4	0.794	0.533	0.422	0.357	0.314	0.283	0.259	0.240	0.224	0.211
1.5	0.851	0.581	0.465	0.397	0.351	0.318	0.292	0.271	0.254	0.240
1.6	0.912	0.623	0.498	0.425	0.376	0.340	0.313	0.291	0.272	0.257
1.7	0.977	0.667	0.534	0.456	0.403	0.365	0.335	0.311	0.292	0.275
1.8	1.047	0.715	0.572	0.489	0.432	0.391	0.359	0.334	0.313	0.295
1.9	1.122	0.766	0.613	0.523	0.463	0.419	0.385	0.358	0.335	0.316
2.0	1.202	0.821	0.657	0.561	0.496	0.449	0.412	0.383	0.359	0.339
2.1	1.288	0.880	0.704	0.601	0.532	0.481	0.442	0.410	0.385	0.363
2.2	1.380	0.943	0.754	0.644	0.570	0.515	0.473	0.440	0.412	0.389
2.3	1.479	1.010	0.808	0.690	0.610	0.552	0.507	0.471	0.442	0.417
2.4	1.585	1.083	0.866	0.739	0.654	0.592	0.543	0.505	0.473	0.447
2.5	1.698	1.160	0.928	0.792	0.701	0.634	0.582	0.541	0.507	0.479
2.6	1.820	1.243	0.994	0.849	0.751	0.679	0.624	0.580	0.543	0.513
2.7	1.950	1.332	1.066	0.910	0.805	0.728	0.669	0.621	0.582	0.550
2.8	2.089	1.427	1.142	0.975	0.862	0.780	0.716	0.666	0.624	0.589
2.9	2.239	1.529	1.223	1.044	0.924	0.836	0.768	0.713	0.669	0.631
3.0	2.399	1.638	1.311	1.119	0.990	0.895	0.823	0.764	0.716	0.676

Equation 5.13 is a mathematical statement that the sum of the probabilities of all events is equal to unity. Figure 5.10a shows that the probability of a flow Q falling between two known flows, Q_1 and Q_2, is the area under the probability distribution curve between Q_1 and Q_2. Figure 5.10b shows the probability that a flood Q exceeds Q_1 is the area under the curve from Q_1 to infinity. This probability is given by $F(Q > Q_1) = 1 - F(Q < Q_1)$.

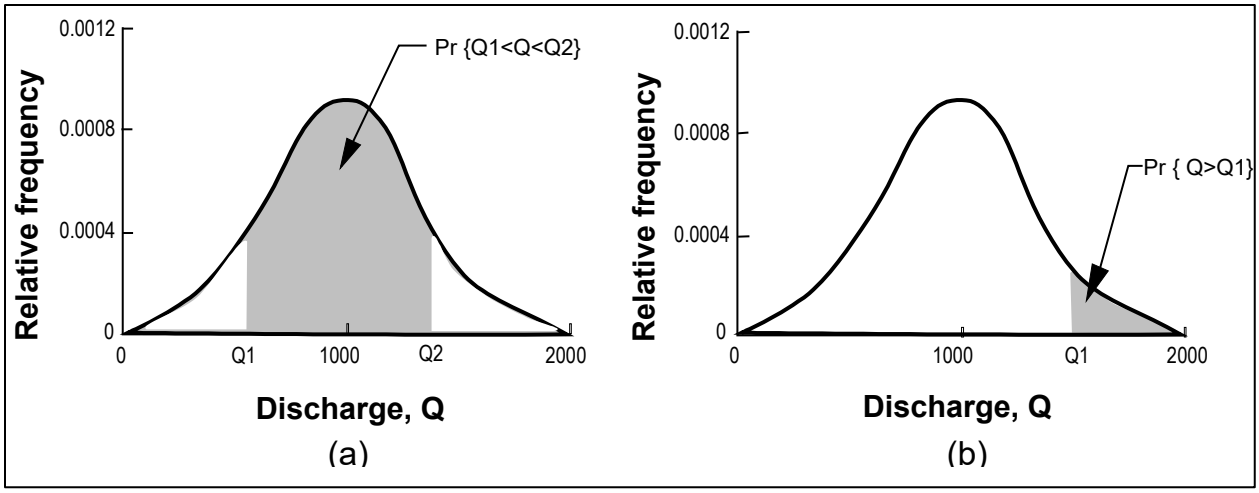

Figure 5.10. Hydrologic probability from probability distribution functions.

From Figure 5.10, the calculation for probability from the probability distribution function is tedious. A further refinement of the frequency distribution is the cumulative frequency distribution. The cumulative distribution function (CDF), F(Q), equals the area under the probability distribution function, f(Q), from -∞ to Q:

$$F(Q) = \int_{-\infty}^{Q} f(Q)dQ \tag{5.14}$$

Table 5.2 illustrates the development of a cumulative frequency distribution as part of histogram development. The CDF is simply the cumulative total of the relative frequencies by class interval. For each range of flows, Table 5.2 defines the number of times that floods equal or exceed the lower limit of the class interval and gives the cumulative frequency.

Using the CDF, the analyst can compute directly the nonexceedance probability for a given magnitude. The nonexceedance probability is defined as the probability that the specified value will not be exceeded. The exceedance probability is 1.0 minus the nonexceedance probability. Figure 5.11 shows the sample cumulative frequency histogram for the Mono Creek, California, annual flood series.

Again, for a sample sufficiently large to define small class intervals, the histogram becomes a smooth curve defined as the CDF, F(Q), shown in Figure 5.12a. This figure shows the area under the curve to the left of each Q of Figure 5.9 and defines the probability that the flow will be less than some stated value, i.e., the nonexceedance probability.

Another convenient representation for hydrologic analysis is the complementary probability function, G(Q), defined as:

$$G(Q) = 1 - F(Q) = P_r(Q \geq Q_1) \tag{5.15}$$

The function, G(Q), shown in Figure 5.12b, is the exceedance probability (i.e., the probability that a flow of a given magnitude will be equaled or exceeded).

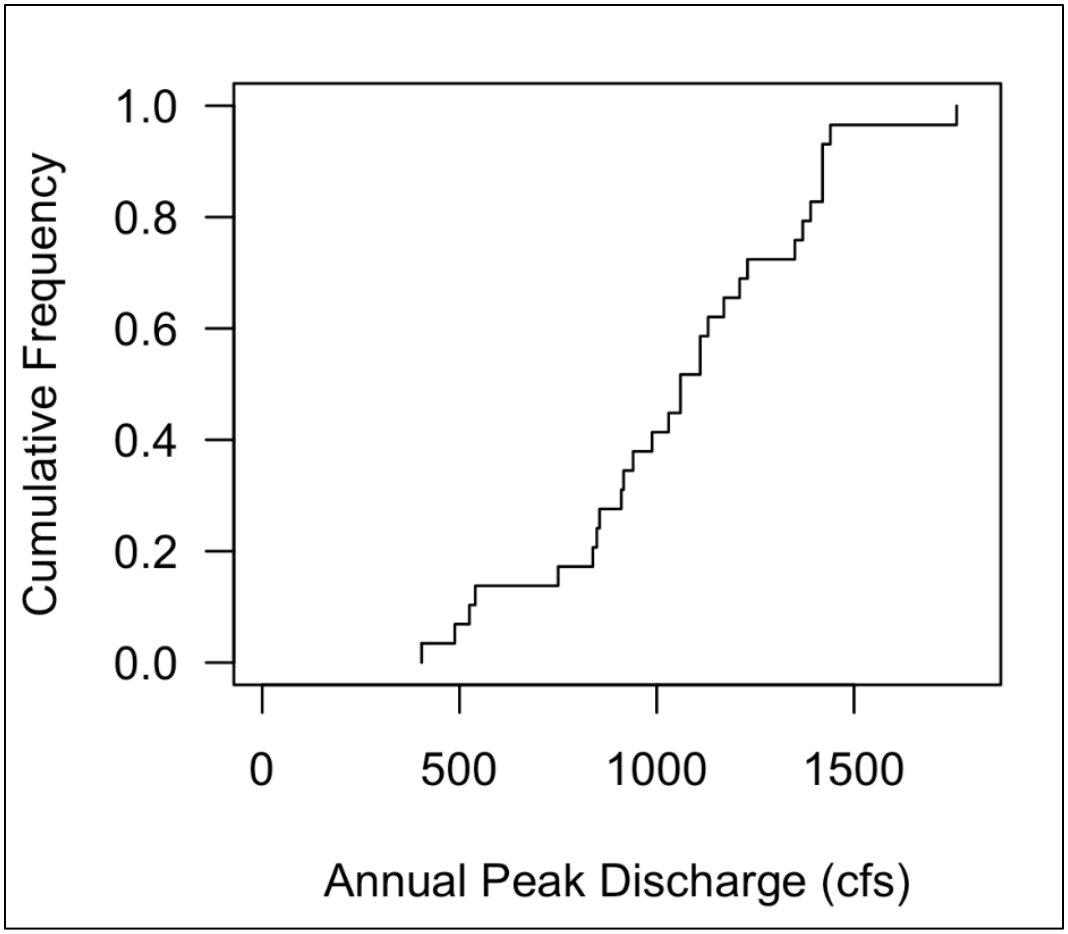

Figure 5.11. Cumulative frequency histogram, Mono Creek, California.

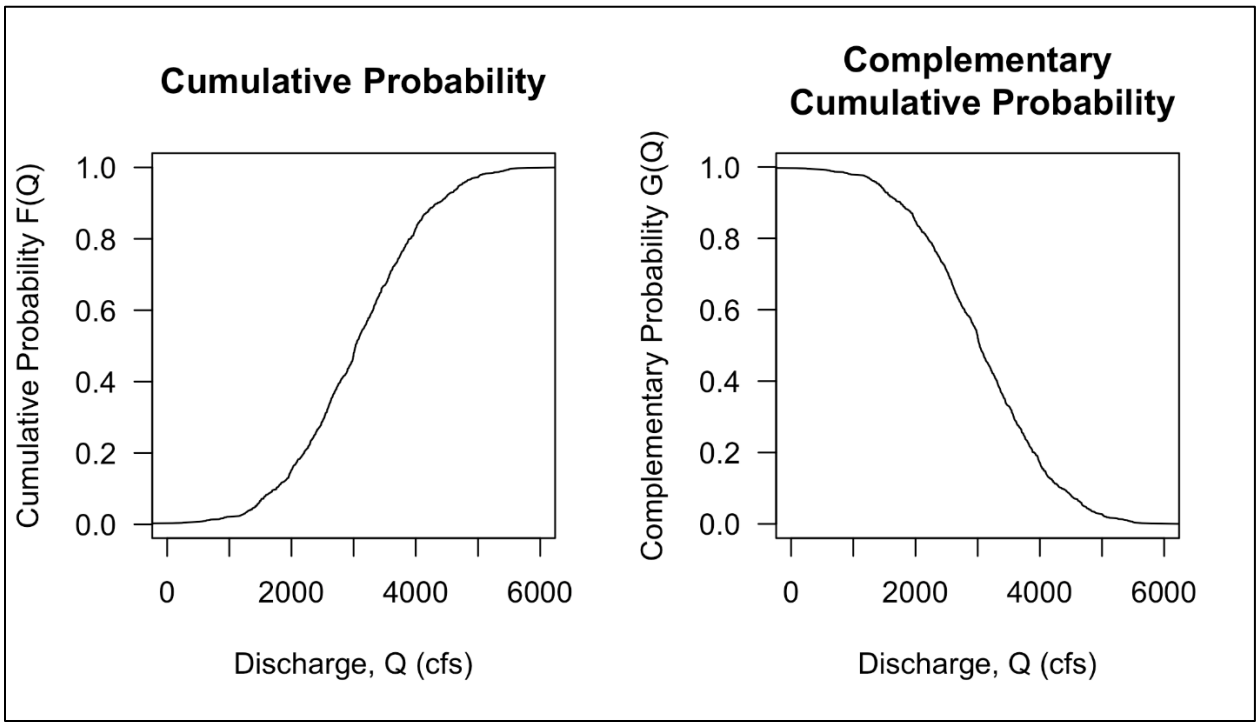

Figure 5.12. Cumulative and complementary CDFs.

5.1.7 Plotting Sample Data with Plotting Position Formulas

When making a flood frequency analysis, the engineer commonly plots quantiles from a fitted distribution function and the observed peak flows (the sample) on the same plot to evaluate the fit. To plot the sample values on a probability scale abscissa, the engineer assigns an exceedance probability to each observation using a plotting position formula.

Many different plotting position formulas have been proposed for estimating the probability of observed peak flows, with no unanimity on the preferred method. However, engineers commonly use a few of them for hydrologic statistical analysis. Bulletin 17C presents a general formula for computing plotting positions:

$$P = \frac{i - a}{(n + 1 - 2a)} \tag{5.16}$$

where:

i	=	Rank order of the ordered flood magnitudes, with the largest flood having a rank of 1
n	=	Record length
a	=	Constant for a particular plotting position formula

Three possibilities arise from equation 5.16, the Weibull, P_w (a = 0), Hazen, P_h (a = 0.5), and Cunnane, P_c (a = 0.4):

$$P_w = \frac{i}{n + 1} \tag{5.17}$$

$$P_h = \frac{i - 0.5}{n} \tag{5.18}$$

$$P_c = \frac{i - 0.4}{n + 0.2} \tag{5.19}$$

The engineer plots the data by placing a point for each value of the flood series at the intersection of the flood magnitude and the exceedance probability computed with the plotting position formula. The plotted data will likely approximate the population line if the assumed population model is a reasonable assumption.

For the partial-duration series where the number of floods exceeds the number of years of record, Beard (1962) recommends:

$$P = \frac{2i - 1}{2n} = \frac{i - 0.5}{n} \tag{5.20}$$

Before engineers use a computed frequency curve to estimate either flood magnitudes or exceedance probabilities, they verify the assumed population by plotting the data. To plot the data:

1. Rank the flood series in descending order, with the largest flood having a rank of 1 and the smallest flood having a rank of n.
2. Use the rank (i) with a plotting position formula such as equation 5.16 and compute the plotting probabilities for each flood.
3. Plot the flood magnitude X against the corresponding plotting probability.

The sample points on the upper and lower ends often deviate from the curve derived from a fitted probability distribution. Engineers use experience rather than an objective criterion to decide whether to accept the fitted probability distribution as the population. The following section describes common probability distributions used in hydrology.

5.2 Standard Frequency Distributions

Engineers commonly use several cumulative frequency distributions in the analysis of hydrologic data including the normal distribution, the log-normal distribution, the Gumbel extreme value distribution, and the log-Pearson type III distribution. This section presents the characteristics and application of each of these distributions.

5.2.1 Normal Distribution

The normal, or Gaussian, distribution is a classical mathematical distribution commonly used in the analysis of natural phenomena. The normal distribution has a symmetrical, unbounded, bell-shaped curve with the maximum value at the central point and extending from $-\infty$ to $+\infty$. Figure 5.13a shows the normal distribution.

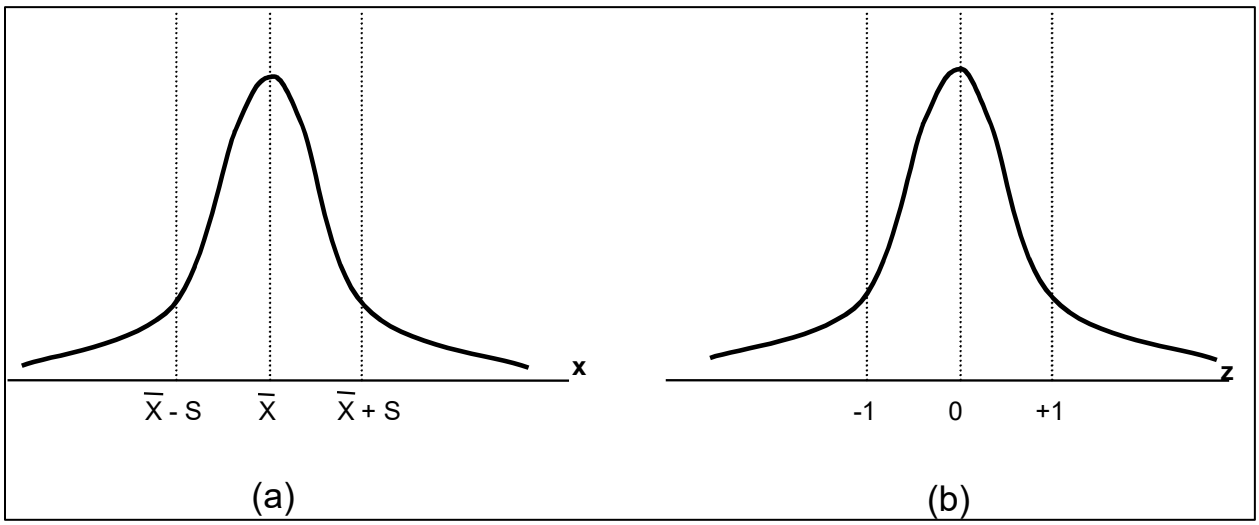

Figure 5.13. (a) Normal probability distribution; (b) Standard normal distribution.

For the normal distribution, the maximum value occurs at the mean. Because of symmetry, half of the flows are below the mean and half are above. Another characteristic of the normal distribution curve is that 68.3 percent of the events fall between ±1 standard deviation (S), 95 percent of the events fall within ±2S, and 99.7 percent fall within ±3S. In a sample of flows, these percentages will be approximated.

For the normal distribution, the coefficient of skew is zero. The function describing the normal distribution curve is:

$$f(X) = \frac{e^{-\left[(x-\bar{x})^2/2S^2\right]}}{S\sqrt{2\pi}} \quad (5.21)$$

Only two parameters are used to describe the normal distribution: the mean value, $\bar{X}$, and the standard deviation, S.

One disadvantage of the normal distribution is that it is unbounded in the negative direction, whereas most hydrologic variables are bounded and can never be less than zero. For this reason and because many hydrologic variables exhibit a pronounced skew, the normal distribution usually has limited applications. However, these problems can sometimes be overcome by performing a log transform on the data. Often the logarithms of hydrologic variables are normally distributed.

5.2.1.1 Standard Normal Distribution

A special case of the normal distribution is the standard normal distribution and is represented by the variate z (see Figure 5.13b). The standard normal distribution always has a mean of 0 and a standard deviation of 1. If the random variable X has a normal distribution with mean $\bar{X}$ and standard deviation S, values of X can be transformed so that they have a standard normal distribution using the following transformation:

$$z = \frac{X - \bar{X}}{S} \quad (5.22)$$

where:

z = Standard normal deviate for the cumulative normal distribution

Table 5.7 summarizes selected values of z. If $\bar{X}$, S, and z for a given frequency are known, then the value of X corresponding to the frequency can be computed by:

$$X = \bar{X} + zS \quad (5.23)$$

Table 5.7. Selected values of the standard normal deviate (z) for the cumulative normal distribution.

Exceedance Probability	Return Period (years)	z
0.5	2	0.0000
0.2	5	0.8416
0.1	10	1.2816
0.04	25	1.7507
0.02	50	2.0538
0.01	100	2.3264
0.002	500	2.8782

Example 5.4:	Computations with the standard normal distribution.
Objective:	To illustrate estimating a 10-year discharge using a standard normal distribution and to estimate the probability of a discharge of 6,390 ft^3/s using the standard normal distribution.

Given: The annual peak flows fit a normal distribution with:

$\overline{X}$ = 4,240 ft^3/s

S = 1,230 ft^3/s

Find: The 10-year discharge and the probability of a discharge of 6,390 ft^3/s.

Step 1. Compute the 10-year discharge.

The 10-year event has an exceedance probability of 0.10 (10 percent) or a nonexceedance probability of 0.90 (90 percent). Thus, the corresponding value of z from Table 5.7 is 1.2816. Compute the 10-year flood with equation 5.23:

$$X = \overline{X} + zS = 4240 + 1.2816(1230) = 5{,}816 \text{ ft}^3/\text{s}$$

Step 2. Compute the probability of a flood of 6,390 ft^3/s.

Use equation 5.22 to compute the standard normal variate, z:

$$z = \frac{x - \overline{x}}{S} = \frac{6390 - 4240}{1230} = 1.75$$

Using Table 5.7 look up z = 1.75. The exceedance probability for z = 1.75 is 0.04, which is the 25-year flood.

Solution:	The 10-year flood is 165 ft^3/s, and the probability of a 6,390 ft^3/s flood is 0.04, or a 25-year event.

5.2.1.2 Frequency Analysis for a Normal Distribution

An arithmetic-probability graph has a specially transformed horizontal probability scale. The horizontal scale is transformed in such a way that the CDF for data that follow a normal distribution will plot as a straight line. If a series of peak flows that are normally distributed are plotted against the cumulative frequency function or the exceedance frequency on the probability scale, the data will plot as a straight line with the equation:

$$X = \overline{X} + K S \qquad (5.24)$$

where:

X = Flood flow at a specified frequency
K = Frequency factor of the distribution

For the normal distribution, K equals z where z is taken from Table 5.7. Table 5.8 provides a detailed table of nonexceedance probabilities for the cumulative standard normal distribution for values of the standard normal deviate (z). If the annual peak flow series is distributed normally, the engineer can estimate the probability of nonexceedance for a given flow rate using the following procedure:

1. Calculate the mean ($\overline{X}$) and standard deviation (S) of the annual peak flow series.

2. Use equation 5.22 to compute the value of the standard normal deviate for the flow rate of interest.
3. Enter Table 5.8 with the value of z and obtain the nonexceedance probability.
4. Compute the AEP by subtracting the nonexceedance probability from one.

Table 5.8. Nonexceedance probabilities of the cumulative standard normal distribution for values of the standard normal deviate (z).

z	0	0.01	0.02	0.03	0.04	0.05	0.06	0.07	0.08	0.09
-3.4	0.0003	0.0003	0.0003	0.0003	0.0003	0.0003	0.0003	0.0003	0.0003	0.0002
-3.3	0.0005	0.0005	0.0005	0.0004	0.0004	0.0004	0.0004	0.0004	0.0004	0.0003
-3.2	0.0007	0.0007	0.0006	0.0006	0.0006	0.0006	0.0006	0.0005	0.0005	0.0005
-3.1	0.0010	0.0009	0.0009	0.0009	0.0008	0.0008	0.0008	0.0008	0.0007	0.0007
-3.0	0.0013	0.0013	0.0013	0.0012	0.0012	0.0011	0.0011	0.0011	0.0010	0.0010
-2.9	0.0019	0.0018	0.0018	0.0017	0.0016	0.0016	0.0015	0.0015	0.0014	0.0014
-2.8	0.0026	0.0025	0.0024	0.0023	0.0023	0.0022	0.0021	0.0021	0.0020	0.0019
-2.7	0.0035	0.0034	0.0033	0.0032	0.0031	0.0030	0.0029	0.0028	0.0027	0.0026
-2.6	0.0047	0.0045	0.0044	0.0043	0.0041	0.0040	0.0039	0.0038	0.0037	0.0036
-2.5	0.0062	0.0060	0.0059	0.0057	0.0055	0.0054	0.0052	0.0051	0.0049	0.0048
-2.4	0.0082	0.0080	0.0078	0.0075	0.0073	0.0071	0.0069	0.0068	0.0066	0.0064
-2.3	0.0107	0.0104	0.0102	0.0099	0.0096	0.0094	0.0091	0.0089	0.0087	0.0084
-2.2	0.0139	0.0136	0.0132	0.0129	0.0125	0.0122	0.0119	0.0116	0.0113	0.0110
-2.1	0.0179	0.0174	0.0170	0.0166	0.0162	0.0158	0.0154	0.0150	0.0146	0.0143
-2.0	0.0228	0.0222	0.0217	0.0212	0.0207	0.0202	0.0197	0.0192	0.0188	0.0183
-1.9	0.0287	0.0281	0.0274	0.0268	0.0262	0.0256	0.0250	0.0244	0.0239	0.0233
-1.8	0.0359	0.0351	0.0344	0.0336	0.0329	0.0322	0.0314	0.0307	0.0301	0.0294
-1.7	0.0446	0.0436	0.0427	0.0418	0.0409	0.0401	0.0392	0.0384	0.0375	0.0367
-1.6	0.0548	0.0537	0.0526	0.0516	0.0505	0.0495	0.0485	0.0475	0.0465	0.0455
-1.5	0.0668	0.0655	0.0643	0.0630	0.0618	0.0606	0.0594	0.0582	0.0571	0.0559
-1.4	0.0808	0.0793	0.0778	0.0764	0.0749	0.0735	0.0721	0.0708	0.0694	0.0681
-1.3	0.0968	0.0951	0.0934	0.0918	0.0901	0.0885	0.0869	0.0853	0.0838	0.0823
-1.2	0.1151	0.1131	0.1112	0.1093	0.1075	0.1056	0.1038	0.1020	0.1003	0.0985
-1.1	0.1357	0.1335	0.1314	0.1292	0.1271	0.1251	0.1230	0.1210	0.1190	0.1170
-1.0	0.1587	0.1562	0.1539	0.1515	0.1492	0.1469	0.1446	0.1423	0.1401	0.1379
-0.9	0.1841	0.1814	0.1788	0.1762	0.1736	0.1711	0.1685	0.1660	0.1635	0.1611
-0.8	0.2119	0.2090	0.2061	0.2033	0.2005	0.1977	0.1949	0.1922	0.1894	0.1867
-0.7	0.2420	0.2389	0.2358	0.2327	0.2296	0.2266	0.2236	0.2206	0.2177	0.2148
-0.6	0.2743	0.2709	0.2676	0.2643	0.2611	0.2578	0.2546	0.2514	0.2483	0.2451
-0.5	0.3085	0.3050	0.3015	0.2981	0.2946	0.2912	0.2877	0.2843	0.2810	0.2776
-0.4	0.3446	0.3409	0.3372	0.3336	0.3300	0.3264	0.3228	0.3192	0.3156	0.3121
-0.3	0.3821	0.3783	0.3745	0.3707	0.3669	0.3632	0.3594	0.3557	0.3520	0.3483
-0.2	0.4207	0.4168	0.4129	0.4090	0.4052	0.4013	0.3974	0.3936	0.3897	0.3859
-0.1	0.4602	0.4562	0.4522	0.4483	0.4443	0.4404	0.4364	0.4325	0.4286	0.4247
-0.0	0.5000	0.4960	0.4920	0.4880	0.4840	0.4801	0.4761	0.4721	0.4681	0.4641

Table 5.8 (continued). Nonexceedance probabilities of the cumulative standard normal distribution for values of the standard normal deviate (z).

z	0	0.01	0.02	0.03	0.04	0.05	0.06	0.07	0.08	0.09
0.0	0.5000	0.5040	0.5080	0.5120	0.5160	0.5199	0.5239	0.5279	0.5319	0.5359
0.1	0.5398	0.5438	0.5478	0.5517	0.5557	0.5596	0.5636	0.5675	0.5714	0.5753
0.2	0.5793	0.5832	0.5871	0.5910	0.5948	0.5987	0.6026	0.6064	0.6103	0.6141
0.3	0.6179	0.6217	0.6255	0.6293	0.6331	0.6368	0.6406	0.6443	0.6480	0.6517
0.4	0.6554	0.6591	0.6628	0.6664	0.6700	0.6736	0.6772	0.6808	0.6844	0.6879
0.5	0.6915	0.6950	0.6985	0.7019	0.7054	0.7088	0.7123	0.7157	0.7190	0.7224
0.6	0.7257	0.7291	0.7324	0.7357	0.7389	0.7422	0.7454	0.7486	0.7517	0.7549
0.7	0.7580	0.7611	0.7642	0.7673	0.7704	0.7734	0.7764	0.7794	0.7823	0.7852
0.8	0.7881	0.7910	0.7939	0.7967	0.7995	0.8023	0.8051	0.8078	0.8106	0.8133
0.9	0.8159	0.8186	0.8212	0.8238	0.8264	0.8289	0.8315	0.8340	0.8365	0.8389
1.0	0.8413	0.8438	0.8461	0.8485	0.8508	0.8531	0.8554	0.8577	0.8599	0.8621
1.1	0.8643	0.8665	0.8686	0.8708	0.8729	0.8749	0.8770	0.8790	0.8810	0.8830
1.2	0.8849	0.8869	0.8888	0.8907	0.8925	0.8944	0.8962	0.8980	0.8997	0.9015
1.3	0.9032	0.9049	0.9066	0.9082	0.9099	0.9115	0.9131	0.9147	0.9162	0.9177
1.4	0.9192	0.9207	0.9222	0.9236	0.9251	0.9265	0.9279	0.9292	0.9306	0.9319
1.5	0.9332	0.9345	0.9357	0.9370	0.9382	0.9394	0.9406	0.9418	0.9429	0.9441
1.6	0.9452	0.9463	0.9474	0.9484	0.9495	0.9505	0.9515	0.9525	0.9535	0.9545
1.7	0.9554	0.9564	0.9573	0.9582	0.9591	0.9599	0.9608	0.9616	0.9625	0.9633
1.8	0.9641	0.9649	0.9656	0.9664	0.9671	0.9678	0.9686	0.9693	0.9699	0.9706
1.9	0.9713	0.9719	0.9726	0.9732	0.9738	0.9744	0.9750	0.9756	0.9761	0.9767
2.0	0.9772	0.9778	0.9783	0.9788	0.9793	0.9798	0.9803	0.9808	0.9812	0.9817
2.1	0.9821	0.9826	0.9830	0.9834	0.9838	0.9842	0.9846	0.9850	0.9854	0.9857
2.2	0.9861	0.9864	0.9868	0.9871	0.9875	0.9878	0.9881	0.9884	0.9887	0.9890
2.3	0.9893	0.9896	0.9898	0.9901	0.9904	0.9906	0.9909	0.9911	0.9913	0.9916
2.4	0.9918	0.9920	0.9922	0.9925	0.9927	0.9929	0.9931	0.9932	0.9934	0.9936
2.5	0.9938	0.9940	0.9941	0.9943	0.9945	0.9946	0.9948	0.9949	0.9951	0.9952
2.6	0.9953	0.9955	0.9956	0.9957	0.9959	0.9960	0.9961	0.9962	0.9963	0.9964
2.7	0.9965	0.9966	0.9967	0.9968	0.9969	0.9970	0.9971	0.9972	0.9973	0.9974
2.8	0.9974	0.9975	0.9976	0.9977	0.9977	0.9978	0.9979	0.9979	0.9980	0.9981
2.9	0.9981	0.9982	0.9982	0.9983	0.9984	0.9984	0.9985	0.9985	0.9986	0.9986
3.0	0.9987	0.9987	0.9987	0.9988	0.9988	0.9989	0.9989	0.9989	0.9990	0.9990
3.1	0.9990	0.9991	0.9991	0.9991	0.9992	0.9992	0.9992	0.9992	0.9993	0.9993
3.2	0.9993	0.9993	0.9994	0.9994	0.9994	0.9994	0.9994	0.9995	0.9995	0.9995
3.3	0.9995	0.9995	0.9995	0.9996	0.9996	0.9996	0.9996	0.9996	0.9996	0.9997
3.4	0.9997	0.9997	0.9997	0.9997	0.9997	0.9997	0.9997	0.9997	0.9997	0.9998

Conversely, the engineer can estimate the peak flow estimate that corresponds to a specific AEP using the following procedure:

1. Calculate the mean ($\overline{X}$) and standard deviation (S) of the annual peak flow series.
2. Compute the nonexceedance probability of interest by subtracting the AEP from one.
3. Enter Table 5.8 with the nonexceedance probability and obtain the corresponding value of z.
4. Use equation 5.23 to compute the magnitude X.

Example 5.5:	Fit a normal distribution to an annual peak flow series.
Objective:	Estimate distribution parameters using sample statistics from a stream gage record and evaluate the fit of the data to the normal distribution.

Given: The annual peak runoff series from the stream gage on the Nueces River below Uvalde, Texas. Table 5.9 presents the data for the Nueces River stream gage and the computations to support the following analysis.

Gaging Station Information: Nueces River below Uvalde, Texas (08192000)

Basin: Nueces River below Uvalde, Texas (USGS 08192000), on right bank 5.7 miles upstream from a bridge on U.S. Highway 83, 8.8 miles southwest of Uvalde, 18.2 miles downstream of Uvalde, and at mile 338.7.

Location: Latitude 29°07'25" N, Longitude 99°53'40" W

Area: 1,861 mi^2

Remarks: Part of the flow of the Nueces River and its headwater tributaries enters the Edwards and associated limestones in the Balcones Fault Zone crossing the basin between Nueces River at Laguna (station 08190000) and this station. No known regulation. There are many small diversions above station for irrigation. No flow at times. Some records listed in the "Period of Record" for surface water and water quality may not be available electronically.

Record: 1939-present.

Step 1. Compute the mean and standard deviation.

$$\overline{X} = \frac{\sum_{i=1}^{n} X_i}{n} = \frac{3,363,176}{93} = 36,163 \text{ ft}^3 / \text{s}$$

$$S = \overline{X}\left[\frac{\sum_{i=1}^{n}\left(\frac{X_i}{\overline{X}} - 1\right)^2}{n-1}\right]^{0.5} = 36,186\left[\frac{417.159}{93-1}\right]^{0.5} = 77,006 \text{ ft}^3 / \text{s}$$

Table 5.9. Frequency analysis computations for the normal distribution: Nueces River below Uvalde, Texas (Gage 08192000).

Year	Rank	Plotting Probability	Annual Maximum (ft^3/s)	$X/\bar{X}$	$(X/\bar{X})-1$	$[(X/\bar{X})-1]^2$	$[(X-\bar{X})-1]^3$
1935	1	0.011	616000	17.034	16.034	257.086	4122.090
1932	2	0.021	207000	5.724	4.724	22.317	105.425
1997	3	0.032	201000	5.558	4.558	20.777	94.703
1955	4	0.043	189000	5.226	4.226	17.862	75.489
1964	5	0.053	188000	5.199	4.199	17.629	74.017
1958	6	0.064	146000	4.037	3.037	9.225	28.018
1974	7	0.074	144000	3.982	2.982	8.892	26.516
2019	8	0.085	105000	2.904	1.904	3.623	6.897
1971	9	0.096	90600	2.505	1.505	2.266	3.411
1939	10	0.106	89000	2.461	1.461	2.135	3.119
1998	11	0.117	83200	2.301	1.301	1.692	2.200
2007	12	0.128	80100	2.215	1.215	1.476	1.793
1936	13	0.138	74800	2.068	1.068	1.141	1.220
2016	14	0.149	70400	1.947	0.947	0.896	0.849
1930	15	0.160	68200	1.886	0.886	0.785	0.695
1987	16	0.170	67200	1.858	0.858	0.737	0.632
2002	17	0.181	65300	1.806	0.806	0.649	0.523
1949	18	0.191	63000	1.742	0.742	0.551	0.409
1982	19	0.202	58500	1.618	0.618	0.382	0.236
1985	20	0.213	44600	1.233	0.233	0.054	0.013
1972	21	0.223	44100	1.219	0.219	0.048	0.011
2005	22	0.234	42000	1.161	0.161	0.026	0.004
1966	23	0.245	39900	1.103	0.103	0.011	0.001
1960	24	0.255	37500	1.037	0.037	0.001	0.000
1991	25	0.266	36600	1.012	0.012	0.000	0.000
2004	26	0.277	35000	0.968	-0.032	0.001	0.000
1961	27	0.287	28600	0.791	-0.209	0.044	-0.009
1931	28	0.298	27000	0.747	-0.253	0.064	-0.016
1981	29	0.309	25900	0.716	-0.284	0.081	-0.023
1965	30	0.319	25200	0.697	-0.303	0.092	-0.028
1970	31	0.330	23700	0.655	-0.345	0.119	-0.041
1948	32	0.340	23600	0.653	-0.347	0.121	-0.042
1975	33	0.351	22300	0.617	-0.383	0.147	-0.056
1990	34	0.362	22000	0.608	-0.392	0.153	-0.060
1963	35	0.372	19500	0.539	-0.461	0.212	-0.098
1954	36	0.383	18400	0.509	-0.491	0.241	-0.119
1938	37	0.394	18200	0.503	-0.497	0.247	-0.123
1959	38	0.404	17300	0.478	-0.522	0.272	-0.142
1976	39	0.415	14900	0.412	-0.588	0.346	-0.203
1929	40	0.426	14500	0.401	-0.599	0.359	-0.215
2001	41	0.436	13700	0.379	-0.621	0.386	-0.240
1968	42	0.447	12100	0.335	-0.665	0.443	-0.295
1986	43	0.457	11600	0.321	-0.679	0.461	-0.313
1942	44	0.468	11200	0.310	-0.690	0.477	-0.329
2015	45	0.479	11200	0.310	-0.690	0.477	-0.329
1999	46	0.489	10200	0.282	-0.718	0.515	-0.370
1928	47	0.500	10000	0.277	-0.723	0.523	-0.379

Table 5.9 (continued). Frequency analysis computations for the normal distribution: Nueces River below Uvalde, Texas (Gage 08192000).

Year	Rank	Plotting Probability	Annual Maximum (ft^3/s)	$X/\bar{X}$	$(X/\bar{X})-1$	$[(X/\bar{X})-1]^2$	$[(X-\bar{X})-1]^3$
2018	48	0.511	9720	0.269	-0.731	0.535	-0.391
1992	49	0.521	9040	0.250	-0.750	0.563	-0.422
1978	50	0.532	8270	0.229	-0.771	0.595	-0.459
1977	51	0.543	7450	0.206	-0.794	0.630	-0.501
1953	52	0.553	6160	0.170	-0.830	0.688	-0.571
1979	53	0.564	6040	0.167	-0.833	0.694	-0.578
1996	54	0.574	6000	0.166	-0.834	0.696	-0.580
1994	55	0.585	5760	0.159	-0.841	0.707	-0.594
1952	56	0.596	5020	0.139	-0.861	0.742	-0.639
1940	57	0.606	4990	0.138	-0.862	0.743	-0.641
1947	58	0.617	4490	0.124	-0.876	0.767	-0.672
1944	59	0.628	3370	0.093	-0.907	0.822	-0.746
1957	60	0.638	3090	0.085	-0.915	0.836	-0.765
1946	61	0.649	3010	0.083	-0.917	0.840	-0.771
1983	62	0.660	2390	0.066	-0.934	0.872	-0.815
1943	63	0.670	2380	0.066	-0.934	0.873	-0.815
1995	64	0.681	1960	0.054	-0.946	0.895	-0.846
1973	65	0.691	1790	0.049	-0.951	0.903	-0.859
2017	66	0.702	1440	0.040	-0.960	0.922	-0.885
1962	67	0.713	728	0.020	-0.980	0.960	-0.941
2003	68	0.723	626	0.017	-0.983	0.966	-0.949
1950	69	0.734	384	0.011	-0.989	0.979	-0.968
1937	70	0.745	330	0.009	-0.991	0.982	-0.973
1933	71	0.755	246	0.007	-0.993	0.986	-0.980
1941	72	0.766	212	0.006	-0.994	0.988	-0.983
1980	73	0.777	189	0.005	-0.995	0.990	-0.984
1988	74	0.787	153	0.004	-0.996	0.992	-0.987
1993	75	0.798	125	0.003	-0.997	0.993	-0.990
1967	76	0.809	83	0.002	-0.998	0.995	-0.993
2006	77	0.819	74	0.002	-0.998	0.996	-0.994
1945	78	0.830	70	0.002	-0.998	0.996	-0.994
2020	79	0.840	63.2	0.002	-0.998	0.997	-0.995
2008	80	0.851	60	0.002	-0.998	0.997	-0.995
1969	81	0.862	56	0.002	-0.998	0.997	-0.995
1989	82	0.872	55	0.002	-0.998	0.997	-0.995
2000	83	0.883	51	0.001	-0.999	0.997	-0.996
1951	84	0.894	46	0.001	-0.999	0.997	-0.996
1934	85	0.904	45	0.001	-0.999	0.998	-0.996
1984	86	0.915	37	0.001	-0.999	0.998	-0.997
2010	87	0.926	25	0.001	-0.999	0.999	-0.998
2009	88	0.936	19	0.001	-0.999	0.999	-0.998
1956	89	0.947	14	0.000	-1.000	0.999	-0.999
2011	90	0.957	8.3	0.000	-1.000	1.000	-0.999
2012	91	0.968	6.2	0.000	-1.000	1.000	-0.999
2013	92	0.979	0.07	0.000	-1.000	1.000	-1.000
2014	93	0.989	0	0.000	-1.000	1.000	-1.000
Total			3363176			417.159	4505.599

Step 2. Compute the typical quantiles for plotting the fitted distribution.

Table 5.10 presents results of computations using equation 5.22 and the sample estimates for the distribution parameters for the Nueces River. The plotting positions are determined using the Weibull plotting position formula.

Table 5.10. Quantile estimates for a normal distribution fit to the Nueces River below Uvalde, Texas.

Exceedance Probability	Return Period (years)	z	X_{RI} (ft^3/s)
0.5	2	0.0000	36,163
0.2	5	0.8416	100,971
0.1	10	1.2816	134,854
0.04	25	1.7507	170,977
0.02	50	2.0538	194,318
0.01	100	2.3264	215,310
0.002	500	2.8782	257,801

Step 3. Plot the sample from Table 5.9 and the quantiles from Table 5.10 on the same log-probability graph.

Figure 5.14 is the result, using HEC-SSP.

Step 4. Compute the coefficient of variation and the skew coefficient for the sample.

Based on Figure 5.14, the correspondence between the normal frequency curve and the actual data is poor. Therefore, these annual maximum peak flow data are not normally distributed. Using equations 5.10 and 5.11 to estimate the coefficient of variation and the skew coefficient, it becomes clear that the data have a large skew while the normal distribution has a skew of zero. This explains the poor correspondence in this case.

$$V = \frac{S}{\overline{X}} = \frac{77{,}066 ft^3/s}{36{,}163 ft^3/s} = 2.129$$

$$G = \frac{n\sum\left(\frac{X_i}{\overline{X}} - 1\right)^3}{(n-1)(n-2)V^3} = \frac{93(4505.6)}{(92)(91)(2.129)^3} = 5.18$$

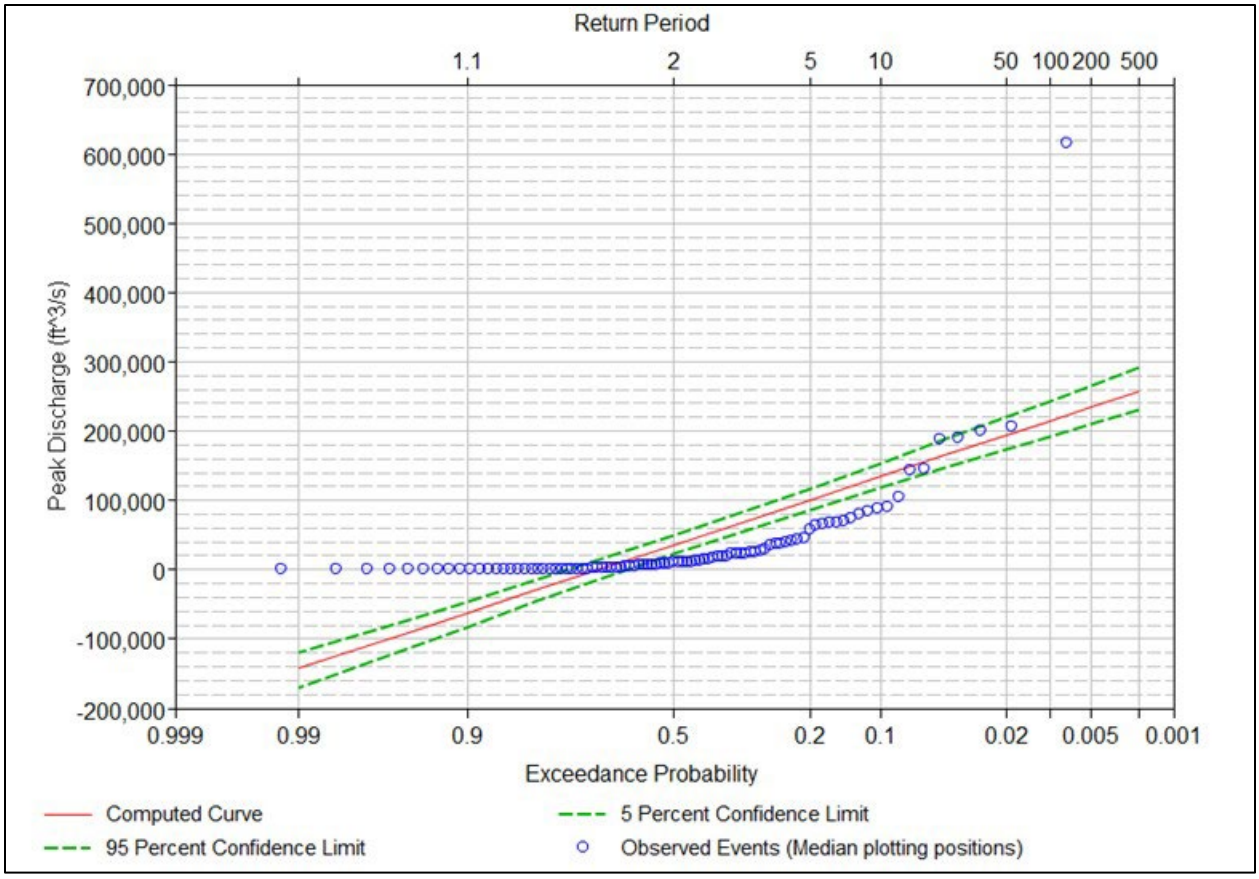

Figure 5.14. Normal distribution frequency curve and observed annual peak flows, Nueces River below Uvalde, Texas (USGS 08192000).

Solution:	The sample parameter estimates are presented above. Table 5.10 presents typical quantile estimates. Figure 5.14 presents the data and fitted distribution. The data do not fit a normal distribution.

5.2.2 Log-Normal Distribution

The log-normal distribution has the same characteristics as the normal distribution except that the dependent variable, X, is replaced with its base-10 logarithm. The characteristics of the log-normal distribution are that it is bounded on the left by zero and it has a pronounced positive skew. These are both characteristics of many of the frequency distributions resulting from an analysis of hydrologic data.

If the engineer performs a logarithmic transformation on the normal distribution function, the resulting logarithmic distribution is normally distributed. This enables the engineer to use the z values tabulated in Table 5.7 and Table 5.8 for a standard normal distribution in a log-normal frequency analysis. As was the case with the normal distribution, log-normal probability scales have been developed where the plot of the CDF is a straight line. This scale uses a transformed horizontal scale based upon the probability function of the normal distribution and a logarithmic vertical scale. If the logarithms of the peak flows are normally distributed, the data will plot as a straight line according to the equation:

$$Y = \log X = \overline{Y} + K S_y \tag{5.25}$$

where:

$\overline{Y}$ = Average of the logarithms of X

S_y = Standard deviation of the logarithms

5.2.2.1 Fitting the Distribution

The procedure for fitting the log-normal distribution is similar to that for the normal distribution, with the difference that the peak flows are transformed by taking the logarithm:

1. Transform the values of the flood series X by taking logarithms: $Y = \log_{10} X$.
2. Compute the log mean ($\overline{Y}$) and log standard deviation (S_y) using the logarithms.
3. Using $\overline{Y}$ and S_y, compute $10^{\overline{Y} + S_y}$ and $10^{\overline{Y} - S_y}$ for the quantiles of interest. Plot these values on log-probability coordinates (usually in software).
4. Because a log-normal distribution plots as a straight line on log-probability coordinates, the result should be a straight line.
5. Compute the plotting positions of the observations (data points in the sample).
6. Plot the observations (data points) on the same coordinate system.
7. Review the observations and distribution for fit.

5.2.2.2 Estimating Flood Magnitudes

Graphical estimates of either flood magnitudes or probabilities can be taken directly from the line representing the assumed log-normal distribution. To obtain a probability for the logarithm of a given magnitude ($Y = \log_{10} X$) compute:

$$z = \frac{Y - \overline{Y}}{S_y} \tag{5.26}$$

To obtain a magnitude for a given probability compute:

$$Y = \overline{Y} + z\,S_y \tag{5.27}$$

The value (Y) is transformed to estimate discharge:

$$X = 10^{Y} \tag{5.28}$$

Example 5.6:	Fit a log-normal distribution to an annual peak flow series.
Objective:	Estimate distribution parameters using sample statistics from a stream gage record.

Given: Use the annual peak flow series from the Nueces River below Uvalde, Texas, stream gage. The gage description is the same as for example 5.5.

Step 1. Use the stream gage data in Table 5.12 to compute the logarithms of the annual peak flow series.

Note that for this example, the lowest observation of peak flow was a zero value. The logarithm of zero is undefined. For this example, that value is eliminated from the record. Because there are a relatively large number of observations in the sample, this does not

seriously impact the analysis (and is sufficient for an example). In practice, engineers use more sophisticated tools (such as in Bulletin 17C) to treat zero values.

Step 2. Compute the mean and standard deviation of the logarithms of peak flow.

$$\overline{Y} = \frac{\sum_{i=1}^{n} Y_i}{n} = \frac{331.474}{92} = 3.603 ft^3 / s$$

$$S_y = \overline{Y}\left[\frac{\sum_{i=1}^{n}\left(\frac{Y_i}{\overline{Y}} - 1\right)^2}{n-1}\right]^{0.5} = 3.603\left(\frac{12.66}{91}\right)^{0.5} = 1.334 ft^3 / s$$

Step 3. Compute the quantiles of interest.

Table 5.11 shows the results from these computations.

Table 5.11. Quantile estimates for a log-normal distribution fit to the Nueces River below Uvalde, Texas, stream gage data.

Exceedance Probability	Return Period (years)	z	Y_{RI} (log-ft^3/s)	X_{RI} (ft^3/s)
0.5	2	0.0000	3.603	4,008
0.2	5	0.8416	4.725	53,120
0.1	10	1.2816	5.312	205,120
0.04	25	1.7507	5.938	866,082
0.02	50	2.0538	6.342	2,196,581
0.01	100	2.3264	6.705	5,072,981
0.002	500	2.8782	7.441	27,611,921

Step 4. Plot the results on log-probability coordinates.

Figure 5.15 displays the results of the computations.

Table 5.12. Frequency analysis computations for the log-normal distribution, Nueces River below Uvalde, Texas.

Year	Rank	Plotting Probability	Annual Maximum (x) (ft^3/s)	Y = Log(X)	$Y/\bar{Y}$	$[(Y/\bar{Y})-1]$	$[(Y/\bar{Y})-1]^2$	$[(Y/\bar{Y})-1]^3$
1935	1	0.011	616000	5.7896	1.607	0.607	0.368	0.224
1932	2	0.022	207000	5.3160	1.475	0.475	0.226	0.107
1997	3	0.032	201000	5.3032	1.472	0.472	0.223	0.105
1955	4	0.043	189000	5.2765	1.464	0.464	0.216	0.100
1964	5	0.054	188000	5.2742	1.464	0.464	0.215	0.100
1958	6	0.065	146000	5.1644	1.433	0.433	0.188	0.081
1974	7	0.075	144000	5.1584	1.432	0.432	0.186	0.080
2019	8	0.086	105000	5.0212	1.394	0.394	0.155	0.061
1971	9	0.097	90600	4.9571	1.376	0.376	0.141	0.053
1939	10	0.108	89000	4.9494	1.374	0.374	0.140	0.052
1998	11	0.118	83200	4.9201	1.366	0.366	0.134	0.049
2007	12	0.129	80100	4.9036	1.361	0.361	0.130	0.047
1936	13	0.140	74800	4.8739	1.353	0.353	0.124	0.044
2016	14	0.151	70400	4.8476	1.345	0.345	0.119	0.041
1930	15	0.161	68200	4.8338	1.342	0.342	0.117	0.040
1987	16	0.172	67200	4.8274	1.340	0.340	0.115	0.039
2002	17	0.183	65300	4.8149	1.336	0.336	0.113	0.038
1949	18	0.194	63000	4.7993	1.332	0.332	0.110	0.037
1982	19	0.204	58500	4.7672	1.323	0.323	0.104	0.034
1985	20	0.215	44600	4.6493	1.290	0.290	0.084	0.024
1972	21	0.226	44100	4.6444	1.289	0.289	0.084	0.024
2005	22	0.237	42000	4.6232	1.283	0.283	0.080	0.023
1966	23	0.247	39900	4.6010	1.277	0.277	0.077	0.021
1960	24	0.258	37500	4.5740	1.270	0.270	0.073	0.020
1991	25	0.269	36600	4.5635	1.267	0.267	0.071	0.019
2004	26	0.280	35000	4.5441	1.261	0.261	0.068	0.018
1961	27	0.290	28600	4.4564	1.237	0.237	0.056	0.013
1931	28	0.301	27000	4.4314	1.230	0.230	0.053	0.012
1981	29	0.312	25900	4.4133	1.225	0.225	0.051	0.011
1965	30	0.323	25200	4.4014	1.222	0.222	0.049	0.011
1970	31	0.333	23700	4.3747	1.214	0.214	0.046	0.010
1948	32	0.344	23600	4.3729	1.214	0.214	0.046	0.010
1975	33	0.355	22300	4.3483	1.207	0.207	0.043	0.009
1990	34	0.366	22000	4.3424	1.205	0.205	0.042	0.009
1963	35	0.376	19500	4.2900	1.191	0.191	0.036	0.007
1954	36	0.387	18400	4.2648	1.184	0.184	0.034	0.006
1938	37	0.398	18200	4.2601	1.182	0.182	0.033	0.006
1959	38	0.409	17300	4.2380	1.176	0.176	0.031	0.005
1976	39	0.419	14900	4.1732	1.158	0.158	0.025	0.004
1929	40	0.430	14500	4.1614	1.155	0.155	0.024	0.004
2001	41	0.441	13700	4.1367	1.148	0.148	0.022	0.003
1968	42	0.452	12100	4.0828	1.133	0.133	0.018	0.002
1986	43	0.462	11600	4.0645	1.128	0.128	0.016	0.002

Table 5.12 (continued). Frequency analysis computations for the log-normal distribution, Nueces River below Uvalde, Texas.

Year	Rank	Plotting Probability	Annual Maximum (x) (ft^3/s)	Y = Log(X)	$Y/\bar{Y}$	$[(Y/\bar{Y})-1]$	$[(Y/\bar{Y})-1]^2$	$[(Y/\bar{Y})-1]^3$
1942	44	0.473	11200	4.0492	1.124	0.124	0.015	0.002
2015	45	0.484	11200	4.0492	1.124	0.124	0.015	0.002
1999	46	0.495	10200	4.0086	1.113	0.113	0.013	0.001
1928	47	0.505	10000	4.0000	1.110	0.110	0.012	0.001
2018	48	0.516	9720	3.9877	1.107	0.107	0.011	0.001
1992	49	0.527	9040	3.9562	1.098	0.098	0.010	0.001
1978	50	0.538	8270	3.9175	1.087	0.087	0.008	0.001
1977	51	0.548	7450	3.8722	1.075	0.075	0.006	0.000
1953	52	0.559	6160	3.7896	1.052	0.052	0.003	0.000
1979	53	0.570	6040	3.7810	1.049	0.049	0.002	0.000
1996	54	0.581	6000	3.7782	1.049	0.049	0.002	0.000
1994	55	0.591	5760	3.7604	1.044	0.044	0.002	0.000
1952	56	0.602	5020	3.7007	1.027	0.027	0.001	0.000
1940	57	0.613	4990	3.6981	1.026	0.026	0.001	0.000
1947	58	0.624	4490	3.6522	1.014	0.014	0.000	0.000
1944	59	0.634	3370	3.5276	0.979	-0.021	0.000	0.000
1957	60	0.645	3090	3.4900	0.969	-0.031	0.001	0.000
1946	61	0.656	3010	3.4786	0.965	-0.035	0.001	0.000
1983	62	0.667	2390	3.3784	0.938	-0.062	0.004	0.000
1943	63	0.677	2380	3.3766	0.937	-0.063	0.004	0.000
1995	64	0.688	1960	3.2923	0.914	-0.086	0.007	-0.001
1973	65	0.699	1790	3.2529	0.903	-0.097	0.009	-0.001
2017	66	0.710	1440	3.1584	0.877	-0.123	0.015	-0.002
1962	67	0.720	728	2.8621	0.794	-0.206	0.042	-0.009
2003	68	0.731	626	2.7966	0.776	-0.224	0.050	-0.011
1950	69	0.742	384	2.5843	0.717	-0.283	0.080	-0.023
1937	70	0.753	330	2.5185	0.699	-0.301	0.091	-0.027
1933	71	0.763	246	2.3909	0.664	-0.336	0.113	-0.038
1941	72	0.774	212	2.3263	0.646	-0.354	0.126	-0.044
1980	73	0.785	189	2.2765	0.632	-0.368	0.136	-0.050
1988	74	0.796	153	2.1847	0.606	-0.394	0.155	-0.061
1993	75	0.806	125	2.0969	0.582	-0.418	0.175	-0.073
1967	76	0.817	83	1.9191	0.533	-0.467	0.218	-0.102
2006	77	0.828	74	1.8692	0.519	-0.481	0.232	-0.111
1945	78	0.839	70	1.8451	0.512	-0.488	0.238	-0.116
2020	79	0.849	63.2	1.8007	0.500	-0.500	0.250	-0.125
2008	80	0.860	60	1.7782	0.494	-0.506	0.257	-0.130
1969	81	0.871	56	1.7482	0.485	-0.515	0.265	-0.136
1989	82	0.882	55	1.7404	0.483	-0.517	0.267	-0.138
2000	83	0.892	51	1.7076	0.474	-0.526	0.277	-0.146
1951	84	0.903	46	1.6628	0.461	-0.539	0.290	-0.156
1934	85	0.914	45	1.6532	0.459	-0.541	0.293	-0.158
1984	86	0.925	37	1.5682	0.435	-0.565	0.319	-0.180
2010	87	0.935	25	1.3979	0.388	-0.612	0.375	-0.229
2009	88	0.946	19	1.2788	0.355	-0.645	0.416	-0.268
1956	89	0.957	14	1.1461	0.318	-0.682	0.465	-0.317
2011	90	0.968	8.3	0.9191	0.255	-0.745	0.555	-0.413
2012	91	0.978	6.2	0.7924	0.220	-0.780	0.609	-0.475
2013	92	0.989	0.07	-1.1549	-0.321	-1.321	1.744	-2.303
Total				331.4737			12.466	-4.229

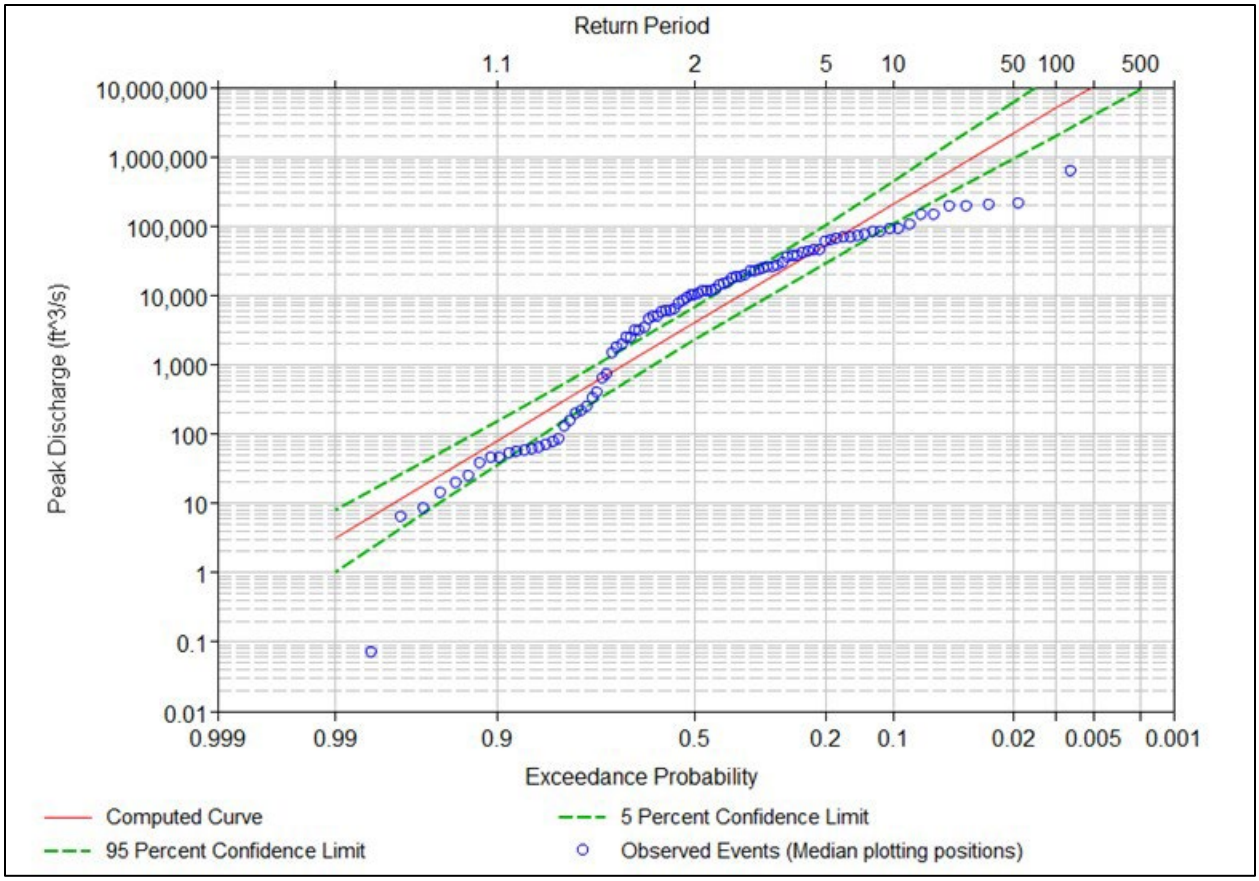

Figure 5.15. Log-normal distribution frequency curve and observed annual peak flows, Nueces River below Uvalde, Texas (USGS 08192000).

Step 5. Compute the coefficient of variation and the skew coefficient for the sample.

Compute the coefficient of variation and the skew coefficient.

$$V = \frac{S}{\overline{Y}} = \frac{1.334 \log ft^3/s}{3.603 \log ft^3/s} = 0.370$$

$$G = \frac{n\sum\left(\frac{Y_i}{\overline{Y}} - 1\right)^3}{(n-1)(n-2)V^3} = \frac{92(-4.229)}{(91)(90)(0.370)^3} = -0.937$$

The skew coefficient is not near zero. This is also apparent on Figure 5.15 because of the curvature in the observed data.

Solution: The computations, tables, and distribution plot present results. The log-normal distribution does not fit the data well.

5.2.3 Gumbel Extreme Value Distribution

The Gumbel extreme value distribution (Gumbel 1941), sometimes called the double-exponential distribution of extreme values, can also be used to describe the distribution of hydrologic variables, especially peak flows. It is based upon the assumption that the cumulative frequency distribution of the largest values of samples drawn from a large population can be described by:

$$F(X) = e^{-e^{-\alpha(X-\beta)}} \quad (5.29)$$

The distribution parameters are:

$$\alpha = \frac{1.281}{S} \quad (5.30)$$

$$\beta = \overline{X} - 0.450\,S \quad (5.31)$$

Values of the Gumbel distribution function are computed from equation 5.28, similar to the process used for the normal and log-normal distributions. Table 5.13 tabulates the frequency factor values K.

Characteristics of the Gumbel extreme value distribution are that the mean flow, $\overline{X}$, occurs at the return period of T = 2.33 years and that it has a positive skew (i.e., it is skewed toward the high flows or extreme values).

Table 5.13. Frequency factors (K) for the Gumbel extreme value distribution.

Sample Size n	Exceedance Probability						
	0.5	0.2	0.1	0.04	0.02	0.01	0.002
10	-0.1355	1.0581	1.8483	2.8468	3.5876	4.3228	6.0219
15	-0.1433	0.9672	1.7025	2.6315	3.3207	4.0048	5.5857
20	-0.1478	0.9186	1.6247	2.5169	3.1787	3.8357	5.3538
25	-0.1506	0.8879	1.5755	2.4442	3.0887	3.7285	5.2068
30	-0.1525	0.8664	1.5410	2.3933	3.0257	3.6533	5.1038
35	-0.1540	0.8504	1.5153	2.3555	2.9789	3.5976	5.0273
40	-0.1552	0.8379	1.4955	2.3262	2.9426	3.5543	4.9680
45	-0.1561	0.8280	1.4795	2.3027	2.9134	3.5196	4.9204
50	-0.1568	0.8197	1.4662	2.2831	2.8892	3.4907	4.8808
55	-0.1574	0.8128	1.4552	2.2668	2.8690	3.4667	4.8478
60	-0.1580	0.8069	1.4457	2.2529	2.8517	3.4460	4.8195
65	-0.1584	0.8019	1.4377	2.2410	2.8369	3.4285	4.7955
70	-0.1588	0.7973	1.4304	2.2302	2.8236	3.4126	4.7738
75	-0.1592	0.7934	1.4242	2.2211	2.8123	3.3991	4.7552
80	-0.1595	0.7899	1.4186	2.2128	2.8020	3.3869	4.7384
85	-0.1598	0.7868	1.4135	2.2054	2.7928	3.3759	4.7234
90	-0.1600	0.7840	1.4090	2.1987	2.7845	3.3660	4.7098
95	-0.1602	0.7815	1.4049	2.1926	2.7770	3.3570	4.6974
100	-0.1604	0.7791	1.4011	2.1869	2.7699	3.3487	4.6860

Example 5.7:	Fit the Gumbel distribution to an annual peak flow series.
Objective:	Using information from previous examples, fit a Gumbel distribution to the data and examine the fit of the distribution to the data.

Given: Use the data for the Nueces River below Uvalde, Texas, as in the previous examples. The mean annual peak flow is 36,163 ft^3/s and the standard deviation is 77,006 ft^3/s.

Step 1. Compute the sample statistics (mean and standard deviation) of the observed annual peaks.

This was completed in the previous example for the normal distribution (example 5.5) and the resulting sample statistics are presented as givens.

Step 2. Use Table 5.13 to determine the Gumbel frequency factors (K) for the quantiles of interest.

Table 5.14 summarizes the quantile estimates.

Table 5.14. Quantile estimates for a Gumbel distribution fit to the Nueces River below Uvalde, Texas, data.

Exceedance Probability	Return Period (years)	K	X_{RI} (ft^3/s)
0.5	2	-0.160	23,842
0.2	5	0.784	96,536
0.1	10	1.409	144,664
0.04	25	2.199	205,476
0.02	50	2.785	250,586
0.01	100	3.366	295,365
0.002	500	4.710	398,845

Step 3. Plot the resulting Gumbel distribution and observed data on log-probability coordinates.

The results are plotted on Figure 5.16.

Solution:	Results are presented in the computations, tables, and distribution plot. The Gumbel distribution does not fit the data well.

The skew coefficient for the untransformed Nueces River data is positive (G = 5.18) as is the skew coefficient for the Gumbel distribution (G = 1.139). The much greater skew of the data is such that the Gumbel distribution does not fit these data well.

A motivating question is “why?” this is the case; subsequent sections address this question. The next item is to describe (and fit) a log-Pearson type III distribution and then apply the Bulletin 17C (EMA) to the same data.

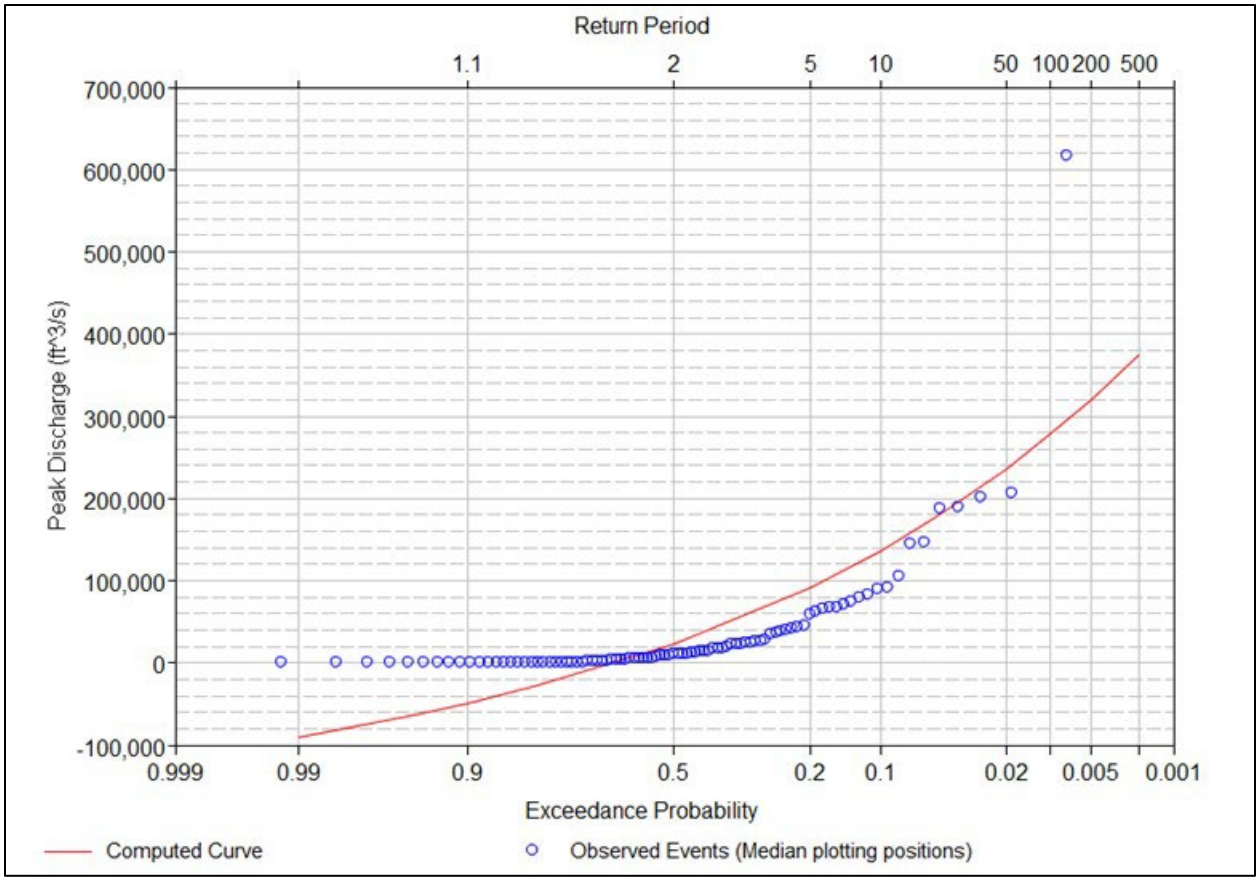

Figure 5.16. Gumbel extreme value distribution frequency curve, Nueces River.

5.2.4 Log-Pearson Type III Distribution

The Pearson type III distribution fitted to the logarithms of the annual peak series has wide application in hydrologic analysis. Engineers often call this distribution the log-Pearson type III (LP3). It is a three-parameter gamma distribution with a logarithmic transform of the dependent variable (annual peak flows). Because of the three parameters, the LP3 distribution can be fitted to a wide variety of data. For this reason, engineers use it widely for flood analyses because the gage data quite frequently fit the assumed population. This flexibility led the Interagency Advisory Committee on Water Data to recommend its use as the standard distribution for flood frequency studies by all Federal agencies. Thomas (1985) provides background on the adoption of the LP3 distribution by Federal agencies in a series of documents including Bulletin 15 (Water Resources Council 1967) and Bulletin 17B. This choice has carried through to continued use of the LP3 distribution in Bulletin 17C.

The log-Pearson type III distribution differs from most of the distributions discussed above in that three parameters (mean, standard deviation, and skew coefficient) describe the distribution. The LP3 distribution, by virtue of three parameters, fits a variety of peak flow datasets. Bulletin 17C presents an extensive treatment on the use of this distribution in the determination of flood frequency distributions. The Bulletin 17C procedure assumes the logarithms of the annual peak flows are Pearson type III distributed rather than assuming the untransformed data are log-Pearson type III. Table 5.15 provides an abbreviated table of the log-Pearson type III distribution function.

Table 5.15. Frequency factors (K) for the log-Pearson type III distribution.

Prob.	Skew						
	-2.0	-1.9	-1.8	-1.7	-1.6	-1.5	-1.4
0.9999	-8.21034	-7.98888	-7.76632	-7.54272	-7.31818	-7.09277	-6.86661
0.9995	-6.60090	-6.44251	-6.28285	-6.12196	-5.95990	-5.79673	-5.63252
0.9990	-5.90776	-5.77549	-5.64190	-5.50701	-5.37087	-5.23353	-5.09505
0.9980	-5.21461	-5.10768	-4.99937	-4.88971	-4.77875	-4.66651	-4.55304
0.9950	-4.29832	-4.22336	-4.14700	-4.06926	-3.99016	-3.90973	-3.82798
0.9900	-3.60517	-3.55295	-3.49935	-3.44438	-3.38804	-3.33035	-3.27134
0.9800	-2.91202	-2.88091	-2.84848	-2.81472	-2.77964	-2.74325	-2.70556
0.9750	-2.68888	-2.66413	-2.63810	-2.61076	-2.58214	-2.55222	-2.52102
0.9600	-2.21888	-2.20670	-2.19332	-2.17873	-2.16293	-2.14591	-2.12768
0.9500	-1.99573	-1.98906	-1.98124	-1.97227	-1.96213	-1.95083	-1.93836
0.9000	-1.30259	-1.31054	-1.31760	-1.32376	-1.32900	-1.33330	-1.33665
0.8000	-0.60944	-0.62662	-0.64335	-0.65959	-0.67532	-0.69050	-0.70512
0.7000	-0.20397	-0.22250	-0.24094	-0.25925	-0.27740	-0.29535	-0.31307
0.6000	0.08371	0.06718	0.05040	0.03344	0.01631	-0.00092	-0.01824
0.5704	0.15516	0.13964	0.12381	0.10769	0.09132	0.07476	0.05803
0.5000	0.30685	0.29443	0.28150	0.26808	0.25422	0.23996	0.22535
0.4296	0.43854	0.43008	0.42095	0.41116	0.40075	0.38977	0.37824
0.4000	0.48917	0.48265	0.47538	0.46739	0.45873	0.44942	0.43949
0.3000	0.64333	0.64453	0.64488	0.64436	0.64300	0.64080	0.63779
0.2000	0.77686	0.78816	0.79868	0.80837	0.81720	0.82516	0.83223
0.1000	0.89464	0.91988	0.94496	0.96977	0.99418	1.01810	1.04144
0.0500	0.94871	0.98381	1.01973	1.05631	1.09338	1.13075	1.16827
0.0400	0.95918	0.99672	1.03543	1.07513	1.11566	1.15682	1.19842
0.0250	0.97468	1.01640	1.06001	1.10537	1.15229	1.20059	1.25004
0.0200	0.97980	1.02311	1.06864	1.11628	1.16584	1.21716	1.26999
0.0100	0.98995	1.03695	1.08711	1.14042	1.19680	1.25611	1.31815
0.0050	0.99499	1.04427	1.09749	1.15477	1.21618	1.28167	1.35114
0.0020	0.99800	1.04898	1.10465	1.16534	1.23132	1.30279	1.37981
0.0010	0.99900	1.05068	1.10743	1.16974	1.23805	1.31275	1.39408
0.0005	0.99950	1.05159	1.10901	1.17240	1.24235	1.31944	1.40413
0.0001	0.99990	1.05239	1.11054	1.17520	1.24728	1.32774	1.41753

Table 5.15 (continued). Frequency factors (K) for the log-Pearson type III distribution.

Prob.	Skew						
	-1.3	-1.2	-1.1	-1.0	-0.9	-0.8	-0.7
0.9999	-6.63980	-6.41249	-6.18480	-5.95691	-5.72899	-5.50124	-5.27389
0.9995	-5.46735	-5.30130	-5.13449	-4.96701	-4.79899	-4.63057	-4.46189
0.9990	-4.95549	-4.81492	-4.67344	-4.53112	-4.38807	-4.24439	-4.10022
0.9980	-4.43839	-4.32263	-4.20582	-4.08802	-3.96932	-3.84981	-3.72957
0.9950	-3.74497	-3.66073	-3.57530	-3.48874	-3.40109	-3.31243	-3.22281
0.9900	-3.21103	-3.14944	-3.08660	-3.02256	-2.95735	-2.89101	-2.82359
0.9800	-2.66657	-2.62631	-2.58480	-2.54206	-2.49811	-2.45298	-2.40670
0.9750	-2.48855	-2.45482	-2.41984	-2.38364	-2.34623	-2.30764	-2.26790
0.9600	-2.10823	-2.08758	-2.06573	-2.04269	-2.01848	-1.99311	-1.96660
0.9500	-1.92472	-1.90992	-1.89395	-1.87683	-1.85856	-1.83916	-1.81864
0.9000	-1.33904	-1.34047	-1.34092	-1.34039	-1.33889	-1.33640	-1.33294
0.8000	-0.71915	-0.73257	-0.74537	-0.75752	-0.76902	-0.77986	-0.79002
0.7000	-0.33054	-0.34772	-0.36458	-0.38111	-0.39729	-0.41309	-0.42851
0.6000	-0.03560	-0.05297	-0.07032	-0.08763	-0.10486	-0.12199	-0.13901
0.5704	0.04116	0.02421	0.00719	-0.00987	-0.02693	-0.04397	-0.06097
0.5000	0.21040	0.19517	0.17968	0.16397	0.14807	0.13199	0.11578
0.4296	0.36620	0.35370	0.34075	0.32740	0.31368	0.29961	0.28516
0.4000	0.42899	0.41794	0.40638	0.39434	0.38186	0.36889	0.35565
0.3000	0.63400	0.62944	0.62415	0.61815	0.61146	0.60412	0.59615
0.2000	0.83841	0.84369	0.84809	0.85161	0.85426	0.85607	0.85703
0.1000	1.06413	1.08608	1.10726	1.12762	1.14712	1.16574	1.18347
0.0500	1.20578	1.24313	1.28019	1.31684	1.35299	1.38855	1.42345
0.0400	1.24028	1.28225	1.32414	1.36584	1.40720	1.44813	1.48852
0.0250	1.30042	1.35153	1.40314	1.45507	1.50712	1.55914	1.61099
0.0200	1.32412	1.37929	1.43529	1.49188	1.54886	1.60604	1.66325
0.0100	1.38267	1.44942	1.51808	1.58838	1.66001	1.73271	1.80621
0.0050	1.42439	1.50114	1.58110	1.66390	1.74919	1.83660	1.92580
0.0020	1.46232	1.55016	1.64305	1.74062	1.84244	1.94806	2.05701
0.0010	1.48216	1.57695	1.67825	1.78572	1.89894	2.01739	2.14053
0.0005	1.49673	1.59738	1.70603	1.82241	1.94611	2.07661	2.21328
0.0001	1.51752	1.62838	1.75053	1.88410	2.02891	2.18448	2.35015

Table 5.15 (continued). Frequency factors (K) for the log-Pearson type III distribution.

Prob.	Skew						
	-0.6	-0.5	-0.4	-0.3	-0.2	-0.1	0.0
0.9999	-5.04718	-4.82141	-4.59687	-4.37394	-4.15301	-3.93453	-3.71902
0.9995	-4.29311	-4.12443	-3.95605	-3.78820	-3.62113	-3.45513	-3.29053
0.9990	-3.95567	-3.81090	-3.66608	-3.52139	-3.37703	-3.23322	-3.09023
0.9980	-3.60872	-3.48737	-3.36566	-3.24371	-3.12169	-2.99978	-2.87816
0.9950	-3.13232	-3.04102	-2.94900	-2.85636	-2.76321	-2.66965	-2.57583
0.9900	-2.75514	-2.68572	-2.61539	-2.54421	-2.47226	-2.39961	-2.32635
0.9800	-2.35931	-2.31084	-2.26133	-2.21081	-2.15935	-2.10697	-2.05375
0.9750	-2.22702	-2.18505	-2.14202	-2.09795	-2.05290	-2.00688	-1.95996
0.9600	-1.93896	-1.91022	-1.88039	-1.84949	-1.81756	-1.78462	-1.75069
0.9500	-1.79701	-1.77428	-1.75048	-1.72562	-1.69971	-1.67279	-1.64485
0.9000	-1.32850	-1.32309	-1.31671	-1.30936	-1.30105	-1.29178	-1.28155
0.8000	-0.79950	-0.80829	-0.81638	-0.82377	-0.83044	-0.83639	-0.84162
0.7000	-0.44352	-0.45812	-0.47228	-0.48600	-0.49927	-0.51207	-0.52440
0.6000	-0.15589	-0.17261	-0.18916	-0.20552	-0.22168	-0.23763	-0.25335
0.5704	-0.07791	-0.09178	-0.11154	-0.12820	-0.14472	-0.16111	-0.17733
0.5000	0.09945	0.08302	0.06651	0.04993	0.03325	0.01662	0.00000
0.4296	0.27047	0.25558	0.24037	0.22492	0.20925	0.19339	0.17733
0.4000	0.34198	0.32796	0.31362	0.29897	0.28403	0.26882	0.25335
0.3000	0.58757	0.57840	0.56867	0.55839	0.54757	0.53624	0.52440
0.2000	0.85718	0.85653	0.85508	0.85285	0.84986	0.84611	0.84162
0.1000	1.20028	1.21618	1.23114	1.24516	1.25824	1.27037	1.28155
0.0500	1.45762	1.49101	1.52357	1.55527	1.58607	1.61594	1.64485
0.0400	1.52830	1.56740	1.60574	1.64329	1.67999	1.71580	1.75069
0.0250	1.66253	1.71366	1.76427	1.81427	1.86360	1.91219	1.95996
0.0200	1.72033	1.77716	1.83361	1.88959	1.94499	1.99973	2.05375
0.0100	1.88029	1.95472	2.02933	2.10394	2.17840	2.25258	2.32635
0.0050	2.01644	2.10825	2.20092	2.29423	2.38795	2.48187	2.57583
0.0020	2.16884	2.28311	2.39942	2.51741	2.63672	2.75706	2.87816
0.0010	2.26780	2.39867	2.53261	2.66915	2.80786	2.94834	3.09023
0.0005	2.35549	2.50257	2.65390	2.80889	2.96698	3.12767	3.29053
0.0001	2.52507	2.70836	2.89907	3.09631	3.29921	3.50703	3.71902

Table 5.15 (continued). Frequency factors (K) for the log-Pearson type III distribution.

Prob.	Skew						
	0.1	0.2	0.3	0.4	0.5	0.6	0.7
0.9999	-3.50703	-3.29921	-3.09631	-2.89907	-2.70836	-2.52507	-2.35015
0.9995	-3.12767	-2.96698	-2.80889	-2.65390	-2.50257	-2.35549	-2.21328
0.9990	-2.94834	-2.80786	-2.66915	-2.53261	-2.39867	-2.26780	-2.14053
0.9980	-2.75706	-2.63672	-2.51741	-2.39942	-2.28311	-2.16884	-2.05701
0.9950	-2.48187	-2.38795	-2.29423	-2.20092	-2.10825	-2.01644	-1.92580
0.9900	-2.25258	-2.17840	-2.10394	-2.02933	-1.95472	-1.88029	-1.80621
0.9800	-1.99973	-1.94499	-1.88959	-1.83361	-1.77716	-1.72033	-1.66325
0.9750	-1.91219	-1.86360	-1.81427	-1.76427	-1.71366	-1.66253	-1.61099
0.9600	-1.71580	-1.67999	-1.64329	-1.60574	-1.56740	-1.52830	-1.48852
0.9500	-1.61594	-1.58607	-1.55527	-1.52357	-1.49101	-1.45762	-1.42345
0.9000	-1.27037	-1.25824	-1.24516	-1.23114	-1.21618	-1.20028	-1.18347
0.8000	-0.84611	-0.84986	-0.85285	-0.85508	-0.85653	-0.85718	-0.85703
0.7000	-0.53624	-0.54757	-0.55839	-0.56867	-0.57840	-0.58757	-0.59615
0.6000	-0.26882	-0.28403	-0.29897	-0.31362	-0.32796	-0.34198	-0.35565
0.5704	-0.19339	-0.20925	-0.22492	-0.24037	-0.25558	-0.27047	-0.28516
0.5000	-0.01662	-0.03325	-0.04993	-0.06651	-0.08302	-0.09945	-0.11578
0.4296	0.16111	0.14472	0.12820	0.11154	0.09478	0.07791	0.06097
0.4000	0.23763	0.22168	0.20552	0.18916	0.17261	0.15589	0.13901
0.3000	0.51207	0.49927	0.48600	0.47228	0.45812	0.44352	0.42851
0.2000	0.83639	0.83044	0.82377	0.81638	0.80829	0.79950	0.79002
0.1000	1.29178	1.30105	1.30936	1.31671	1.32309	1.32850	1.33294
0.0500	1.67279	1.69971	1.72562	1.75048	1.77428	1.79701	1.81864
0.0400	1.78462	1.81756	1.84949	1.88039	1.91022	1.93896	1.96660
0.0250	2.00688	2.05290	2.09795	2.14202	2.18505	2.22702	2.26790
0.0200	2.10697	2.15935	2.21081	2.26133	2.31084	2.35931	2.40670
0.0100	2.39961	2.47226	2.54421	2.61539	2.68572	2.75514	2.82359
0.0050	2.66965	2.76321	2.85636	2.94900	3.04102	3.13232	3.22281
0.0020	2.99978	3.12169	3.24371	3.36566	3.48737	3.60872	3.72957
0.0010	3.23322	3.37703	3.52139	3.66608	3.81090	3.95567	4.10022
0.0005	3.45513	3.62113	3.78820	3.95605	4.12443	4.29311	4.46189
0.0001	3.93453	4.15301	4.37394	4.59687	4.82141	5.04718	5.27389

Table 5.15 (continued). Frequency factors (K) for the log-Pearson type III distribution.

Prob.	Skew						
	0.8	0.9	1.0	1.1	1.2	1.3	1.4
0.9999	2.18448	-2.02891	-1.88410	-1.75053	-1.62838	-1.51752	-1.41753
0.9995	-2.07661	-1.94611	-1.82241	-1.70603	-1.59738	-1.49673	-1.40413
0.9990	-2.01739	-1.89894	-1.78572	-1.67825	-1.57695	-1.48216	-1.39408
0.9980	-1.94806	-1.84244	-1.74062	-1.64305	-1.55016	-1.46232	-1.37981
0.9950	-1.83660	-1.74919	-1.66390	-1.58110	-1.50114	-1.42439	-1.35114
0.9900	-1.73271	-1.66001	-1.58838	-1.51808	-1.44942	-1.38267	-1.31815
0.9800	-1.60604	-1.54886	-1.49188	-1.43529	-1.37929	-1.32412	-1.26999
0.9750	-1.55914	-1.50712	-1.45507	-1.40314	-1.35153	-1.30042	-1.25004
0.9600	-1.44813	-1.40720	-1.36584	-1.32414	-1.28225	-1.24028	-1.19842
0.9500	-1.38855	-1.35299	-1.31684	-1.28019	-1.24313	-1.20578	-1.16827
0.9000	-1.16574	-1.14712	-1.12762	-1.10726	-1.08608	-1.06413	-1.04144
0.8000	-0.85607	-0.85426	-0.85161	-0.84809	-0.84369	-0.83841	-0.83223
0.7000	-0.60412	-0.61146	-0.61815	-0.62415	-0.62944	-0.63400	-0.63779
0.6000	-0.36889	-0.38186	-0.39434	-0.40638	-0.41794	-0.42899	-0.43949
0.5704	-0.29961	-0.31368	-0.32740	-0.34075	-0.35370	-0.36620	-0.37824
0.5000	-0.13199	-0.14807	-0.16397	-0.17968	-0.19517	-0.21040	-0.22535
0.4296	0.04397	0.02693	0.00987	-0.00719	-0.02421	-0.04116	-0.05803
0.4000	0.12199	0.10486	0.08763	0.07032	0.05297	0.03560	0.01824
0.3000	0.41309	0.39729	0.38111	0.36458	0.34772	0.33054	0.31307
0.2000	0.77986	0.76902	0.75752	0.74537	0.73257	0.71915	0.70512
0.1000	1.33640	1.33889	1.34039	1.34092	1.34047	1.33904	1.33665
0.0500	1.83916	1.85856	1.87683	1.89395	1.90992	1.92472	1.93836
0.0400	1.99311	2.01848	2.04269	2.06573	2.08758	2.10823	2.12768
0.0250	2.30764	2.34623	2.38364	2.41984	2.45482	2.48855	2.52102
0.0200	2.45298	2.49811	2.54206	2.58480	2.62631	2.66657	2.70556
0.0100	2.89101	2.95735	3.02256	3.08660	3.14944	3.21103	3.27134
0.0050	3.31243	3.40109	3.48874	3.57530	3.66073	3.74497	3.82798
0.0020	3.84981	3.96932	4.08802	4.20582	4.32263	4.43839	4.55304
0.0010	4.24439	4.38807	4.53112	4.67344	4.81492	4.95549	5.09505
0.0005	4.63057	4.79899	4.96701	5.13449	5.30130	5.46735	5.63252
0.0001	5.50124	5.72899	5.95691	6.18480	6.41249	6.63980	6.86661

Table 5.15 (continued). Frequency factors (K) for the log-Pearson type III distribution.

Prob.	Skew					
	1.5	1.6	1.7	1.8	1.9	2.0
0.9999	-1.32774	-1.24728	-1.17520	-1.11054	-1.05239	-0.99990
0.9995	-1.31944	-1.24235	-1.17240	-1.10901	-1.05159	-0.99950
0.9990	-1.31275	-1.23805	-1.16974	-1.10743	-1.50568	-0.99900
0.9980	-1.30279	-1.23132	-1.16534	-1.10465	-1.04898	-0.99800
0.9950	-1.28167	-1.21618	-1.15477	-1.09749	-1.04427	-0.99499
0.9900	-1.25611	-1.19680	-1.14042	-1.08711	-1.03695	-0.98995
0.9800	-1.21716	-1.16584	-1.11628	-1.06864	-1.02311	-0.97980
0.9750	-1.20059	-1.15229	-1.10537	-1.06001	-1.01640	-0.97468
0.9600	-1.15682	-1.11566	-1.07513	-1.03543	-0.99672	-0.95918
0.9500	-1.13075	-1.09338	-1.05631	-1.01973	-0.98381	-0.94871
0.9000	-1.01810	-0.99418	-0.96977	-0.94496	-0.91988	-0.89464
0.8000	-0.82516	-0.81720	-0.80837	-0.79868	-0.78816	-0.77686
0.7000	-0.64080	-0.64300	-0.64436	-0.64488	-0.64453	-0.64333
0.6000	-0.44942	-0.45873	-0.46739	-0.47538	-0.48265	-0.48917
0.5704	-0.38977	-0.40075	-0.41116	-0.42095	-0.43008	-0.43854
0.5000	-0.23996	-0.25422	-0.26808	-0.28150	-0.29443	-0.30685
0.4296	-0.07476	-0.09132	-0.10769	-0.12381	-0.13964	-0.15516
0.4000	0.00092	-0.01631	-0.03344	-0.05040	-0.06718	-0.08371
0.3000	0.29535	0.27740	0.25925	0.24094	0.22250	0.20397
0.2000	0.69050	0.67532	0.65959	0.64335	0.62662	0.60944
0.1000	1.33330	1.32900	1.32376	1.31760	1.31054	1.30259
0.0500	1.95083	1.96213	1.97227	1.98124	1.98906	1.99573
0.0400	2.14591	2.16293	2.17873	2.19332	2.20670	2.21888
0.0250	2.55222	2.58214	2.61076	2.63810	2.66413	2.68888
0.0200	2.74325	2.77964	2.81472	2.84848	2.88091	2.91202
0.0100	3.33035	3.38804	3.44438	3.49935	3.55295	3.60517
0.0050	3.90973	3.99016	4.06926	4.14700	4.22336	4.29832
0.0020	4.66651	4.77875	4.88971	4.99937	5.10768	5.21461
0.0010	5.23353	5.37087	5.50701	5.64190	5.77549	5.90776
0.0005	5.79673	5.95990	6.12196	6.28285	6.44251	6.60090
0.0001	7.09277	7.31818	7.54272	7.76632	7.98888	8.21034

Using the mean, standard deviation, and skew coefficient for any set of log-transformed annual peak flow data, in conjunction with Table 5.15, the flood with any exceedance frequency can be computed from the equation:

$$\hat{Y} = \log X = \overline{Y} + KS_y \quad (5.32)$$

$\hat{Y}$ is the predicted value of log X, $\overline{Y}$ and S_y are as previously defined, and K is a function of the exceedance probability and the coefficient of skew. The computed discharge is estimated by detransforming the previous estimate:

$$\hat{X} = 10^{\hat{Y}} \quad (5.33)$$

Results from fitting a LP3 distributions are typically plotted on log-normal probability scales even though the plotted frequency distribution is not a straight line. The LP3 distribution plots as a straight line only when the skew of the logarithms is zero.

5.2.4.1 Fitting the Distribution

The procedure for fitting the log-Pearson type III distribution is similar to that for the normal and log-normal. Bulletin 17C refers to this approach to the log-Pearson type III distribution as the "Simple Case" where the data only includes the systematic record and there are no PILFs. The specific steps for making a basic log-Pearson type III analysis without any of the optional adjustments are as follows:

1. Create the annual series of logarithms from the observations in the annual peak flow series ($Y_i = \log X_i$).
2. Compute the sample statistics, mean ($\overline{Y}$), standard deviation (S_y), and skew coefficient (G) of the logarithms. Round the skew to the nearest tenth (e.g., 0.32 is rounded to 0.3).
3. Compute the logarithmic value $\hat{Y}$ for each exceedance frequency needed using equation 5.32.
4. Detransform the quantiles computed in step 3 to discharges using equation 5.33 in which $\hat{X}$ is the computed discharge for the assumed log-Pearson type III population.
5. Plot the quantiles from the fitted distribution (step 4) on log-probability coordinates and draw a smooth curve through the points.
6. Compute the plotting position of the observations and plot them on the same coordinates as the fitted distribution. This provides a visual confirmation of whether the LP3 provides a good fit to the data.

In the Bulletin 17C approach, the optional adjustments are embedded in the EMA computational approach. Therefore, the optional adjustments of the Bulletin 17C process are not amenable to hand computation (or computation with a spreadsheet) and are not included herein.

5.2.4.2 Estimating Flood Magnitudes

In addition to graphical estimation, engineers can make estimates with the mathematical model of equation 5.33. To compute a magnitude for a given probability, the suggested procedure is the same as that in steps 3 and 4 above. To estimate the probability for a given magnitude X, the value is transformed using the logarithm (Y = log X). Solve equation 5.32 for K, and then compute the value of K for the Y (the logarithm of X) of interest:

$$K = \frac{Y - \overline{Y}}{S_y} \quad (5.34)$$

Use Table 5.15 and the computed K for the discharge of interest using the skew coefficient for the fitted distribution to estimate the probability of X. Linear interpolation in Table 5.15 is acceptable.

Example 5.8:	Fit the log-Pearson type III to an annual peak flow series.
Objective:	Using data from the previous examples, fit a log-Pearson type III distribution to the data and examine the fit of the distribution to the data.

Given: Use the data from the Nueces River below Uvalde, Texas, and the previous examples. The mean logarithm of peaks is 3.603 log ft^3/s, the standard deviation of the logarithms is 1.334 log ft^3/s, and the station skew coefficient of the logarithms is -0.937. As in example 5.7, drop the 2014 peak (which is zero) because the logarithm of zero is undefined.

Find: Flood frequency quantiles with AEP values of 0.50, 0.20, 0.10, 0.04, 0.02, 0.01, and 0.002 using a) station skew, b) regional skew, and c) weighted station and regional skew.

Step 1. Sample statistics were computed in previous examples. Use the station skew coefficient to determine the values of K for the desired quantiles.

Using the station skew coefficient of -0.937, round the value to -0.9. Then use this value and Table 5.15 to look up the frequency factors, K, for the desired quantiles (0.5, 0.2, 0.1, 0.04, 0.02, 0.01, and 0.005). Place those values into the second column of Table 5.16.

Step 2. Compute the logarithms of the desired quantiles.

Compute the suite of Y using equation 5.32 and the frequency factors from step 1 to compute the logarithms of the desired quantiles. Place these results in the third column of Table 5.16.

Step 3. Compute the desired quantiles.

Compute the suite of quantiles using the values of Y from step 2 and equation 5.33. Place these values in the fourth column of Table 5.16.

Step 4. Use the station statistics to repeat the above process. Instead of station skew coefficient, use the regional skew coefficient.

Using the regional skew coefficient of -0.4 and Table 5.15, look up the frequency factors, K, for the desired quantiles (0.5, 0.2, 0.1, 0.04, 0.02, 0.01, and 0.005). Place those values into the fifth column of Table 5.16.

Step 5. Compute the logarithms of the desired quantiles.

Compute the suite of Y using equation 5.32 and the frequency factors from step 4 to compute the logarithms of the desired quantiles. Place these results in the sixth column of Table 5.16.

Step 6. Compute the desired quantiles.

Compute the suite of quantiles using the values of Y from step 5 and equation 5.33. Place these values in the seventh column of Table 5.16.

Step 7. Compute the weighted skew coefficient.

The MSE_G for the station skew is estimated using Table 5.6. Use the station skew of -0.9 and 92 years of record. The MSE_G for the station skew is 0.119. The regional skew coefficient is -0.4 and $MSE_{\bar{G}}$ is 0.216 (Asquith 2021). With these data, compute the weighted skew coefficient using equation 5.12:

$$G_w = \frac{0.216(-0.4) + 0.119(-0.9)}{0.216 + 0.119} = -0.57$$

The result is rounded to -0.6.

Step 8. Use the results of step 7 and the weighted skew coefficient, look up the frequency factors, K, in Table 5.15 for the desired quantiles.

Using the weighted skew coefficient of -0.6 and Table 5.15, look up the frequency factors, K, for the desired quantiles (0.5, 0.2, 0.1, 0.04, 0.02, 0.01, and 0.005). Place those values into the eighth column of Table 5.16.

Step 9. Compute the logarithms of the desired quantiles.

Compute the suite of Y values using equation 5.32 and the frequency factors from step 8 to compute the logarithms of the desired quantiles. Place these results in the ninth column of Table 5.16.

Table 5.16. Calculation of log-Pearson type III discharges for the Nueces River below Uvalde, Texas (08192000).

Exceedance Probability	Station Skew (G=-0.9)			Regional Skew (G=-0.4)			Weighted Skew (G=-0.6)		
	K	Y	X (ft^3/s)	K	Y	X (ft^3/s)	K	Y	X (ft^3/s)
0.50	0.148	3.800	6,316	0.067	3.692	4,917	0.099	3.736	5,440
0.20	0.854	4.742	55,226	0.855	4.743	55,365	0.857	4.746	55,723
0.10	1.147	5.133	135,855	1.231	5.245	175,678	1.200	5.204	159,796
0.04	1.407	5.479	301,645	1.764	5.956	902,931	1.528	5.641	437,507
0.02	1.549	5.668	466,018	1.834	6.048	1,117,173	1.720	5.897	788,969
0.01	1.660	5.817	655,575	2.029	6.309	2,037,587	1.880	6.110	1,289,345
0.002	1.842	6.060	1,147,877	2.399	6.803	6,347,994	2.169	6.495	3,127,193

Step 10. Compute the desired quantiles.

Compute the suite of quantiles using the values of Y from step 8 and equation 5.33. Place these values in the tenth (last) column of Table 5.16.

Step 11. Plot the resulting flood frequency curves and the data on log-probability coordinates.

The result from these computations is a set of three flood frequency curves. Figure 5.17 is a graph of all three flood frequency curves and the observed data. The solid line is the fitted distribution using the station skew coefficient. The dashed line is the fitted distribution using the regional skew coefficient. The dotted line is the fitted distribution using the weighted skew coefficient. Open circles are the observed data points. Note that the left tail of the fitted

distributions was extended using computations not in Table 5.16 for comparison with other figures in this chapter.

Plotting the curves on the same graph as the observations makes evident the impact of the various ways of computing the skew coefficient. For this example, the sample size is reasonably large (approaching 100 observations). In general, larger sample sizes result in improved estimates of station skew.

However, comparison of the fitted distributions with the observed data shows that there remains a problem with the fits.

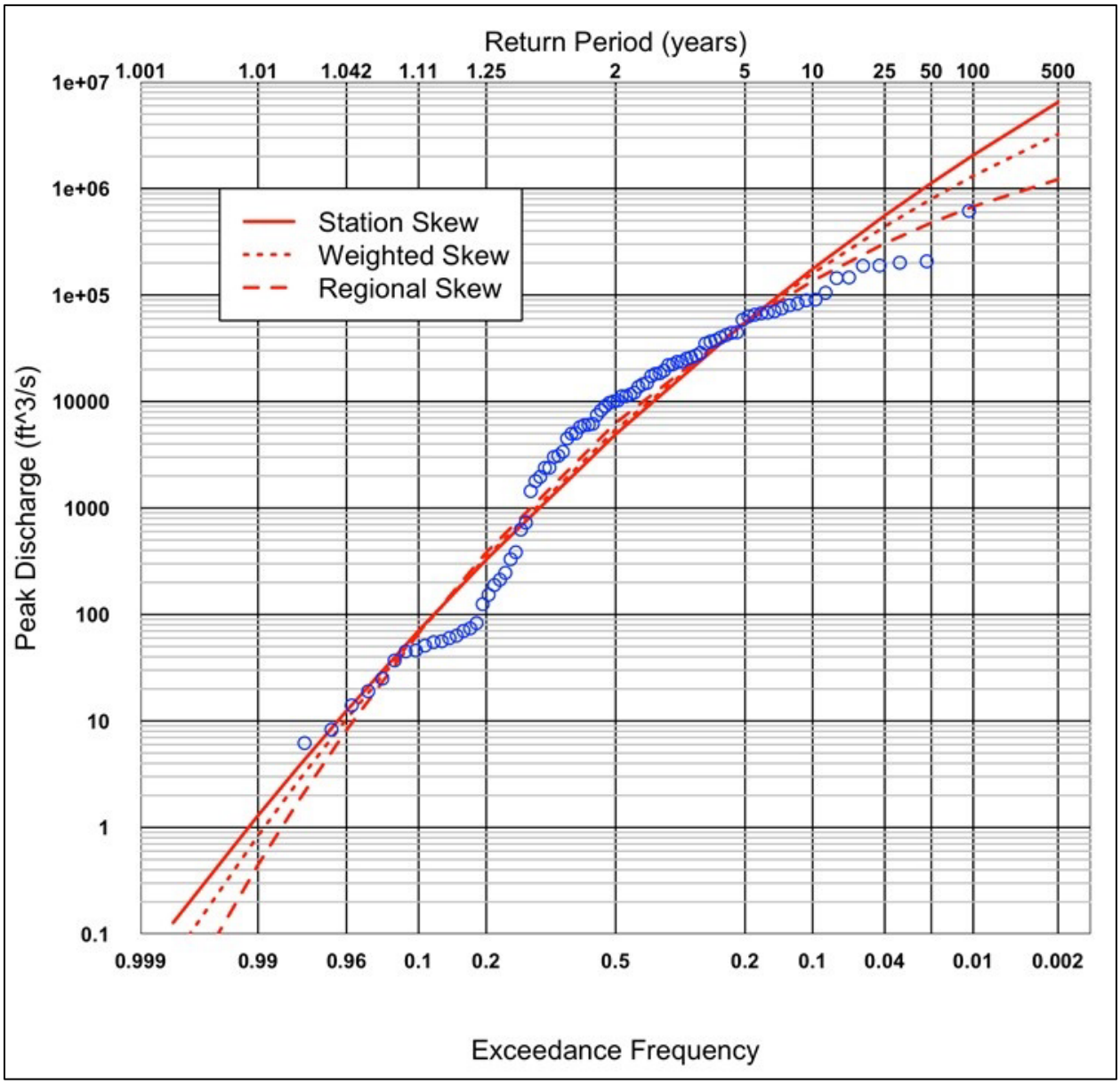

Figure 5.17. Log-Pearson type III distribution frequency curve, Nueces River.

Solution: Figure 5.17 and Table 5.16 display results from the three different estimates of the skew coefficient.

Example 5.9:	Fit a log-Pearson type III distribution using Bulletin 17C.
Objective:	Use the data from the previous example to fit a log-Pearson type III distribution to a dataset using the Bulletin 17C EMA process.

Given: The dataset for the Nueces River below Uvalde, Texas and HEC-SSP (Version 2.2 or later) from the USACE (Bartles et al. 2019).

Find: Use the Bulletin 17C EMA procedure to fit a log-Pearson type III distribution to the data.

Step 1. Start HEC-SSP and create a new project.

Once HEC-SSP is open, select *File* | *New Study* to create a new project. Any meaningful project name can be used.

Step 2. Create a new dataset using the integrated portal to USGS data.

Select *Data* | *New* to open the data importer dialogue. Choose a meaningful dataset name and Short ID. Add a description to the dataset if desired.

Step 3. Find and import the dataset.

Be sure that “USGS Website” is checked, “Annual Peak Data” is the data type, and “Flow” is checked in the data importer. Then select “Get USGS Station ID’s by State” and choose the State in the dropdown (Texas). This will populate the table at the bottom of the data importer. Choose Station ID 08192000 and then select “Import to Study DSS File” near the center right of the data importer dialogue.

This will download and import the study data.

Step 4. Create a new Bulletin 17 Analysis and populate the fields.

Select (right click) “Bulletin 17 Analysis” and select “New.” This will open Bulletin 17 editor and the “General” tab. Choose “17C EMA,” “Use Station Skew,” “Multiple Grubbs-Beck,” and notice that “Hirsch/Stedinger” is the only option for plotting position.

Select the “Options” tab. On the far right is a table of “Output Frequency Ordinates.” In general, the 25-year event is of more interest than the 20-year event, so replace the 5.0 percent frequency with 4.0 percent.

No other options are indicated for this example problem.

Step 5. Compute the fitted distribution.

Select “Compute” button at the bottom of the Bulletin 17 Editor dialogue. This will execute the computations. If there are no errors, then open a display by selecting “Plot Curve” to produce a figure like Figure 5.18. Select “View Report” at the bottom of the Bulletin 17 editor to see details of the results in a report. Figure 5.18 depicts the influence of low outliers on the distribution fit.

Table 5.17. Results from Bulletin 17C EMA analysis of the annual peak flow series for the Nueces River below Uvalde, Texas (08192000).

AEP	X (ft^3/s)
0.5	9,309
0.2	49,530
0.1	102,500
0.04	200,900
0.02	294,300
0.01	401,100
0.002	686,000

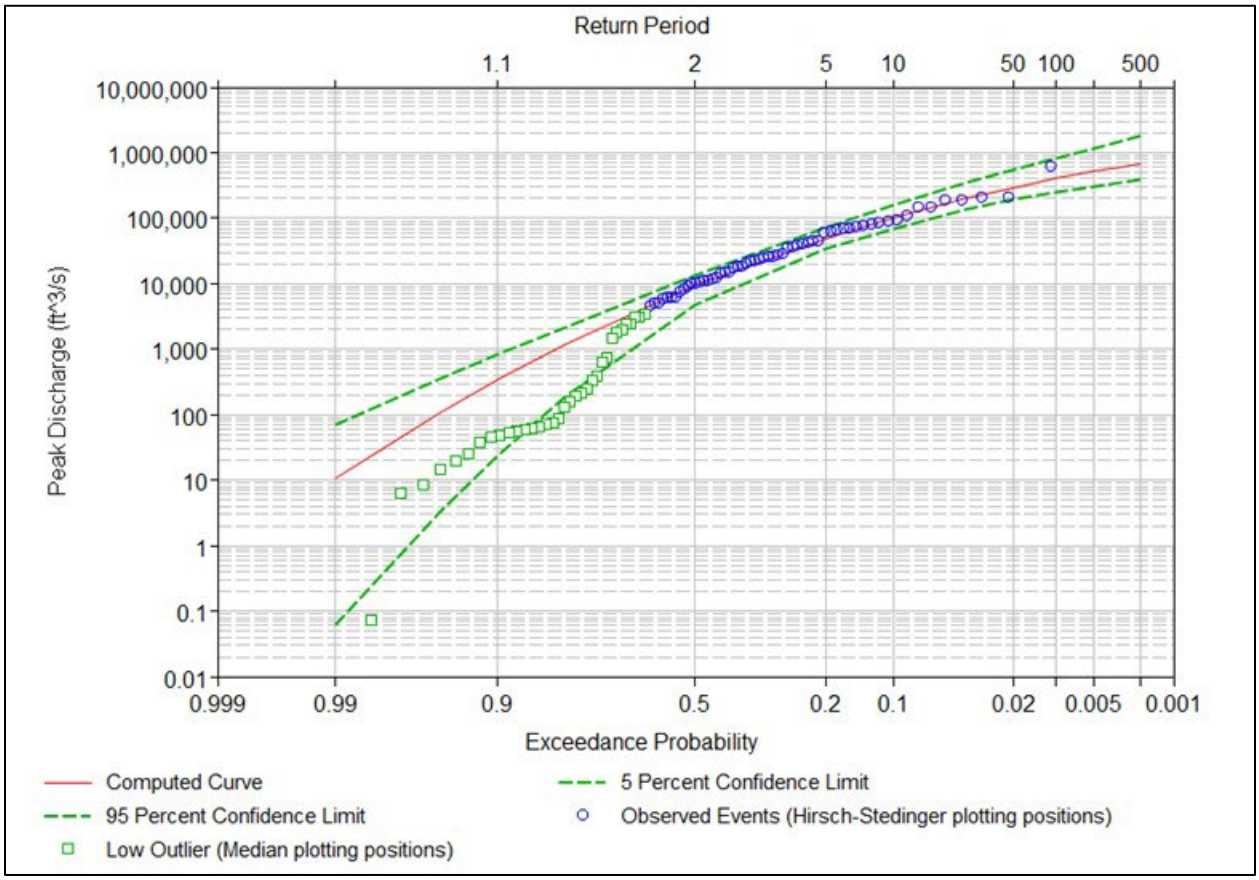

Figure 5.18. Log-Pearson type III distribution frequency curve fit with the Bulletin 17C (EMA) procedure to the Nueces River below Uvalde, Texas (08192000), annual peak flow series.

Solution: Table 5.17 and Figure 5.18 display the results from the Bulletin 17C fit of the Nueces River data.

5.2.5 Evaluation of Flood Frequency Estimates

The process of fitting a distribution to a sample is not a mechanical process. To ensure a reasonable frequency curve it is important to review the results in comparison to the data. Example 5.5 through example 5.9 illustrated fitting four different distributions (normal log-normal, Gumbel, and the log-Pearson type III) to the peak flow data for the Nueces River gage. For the log-Pearson type III distribution, four different approaches were used – three based on the Simple Case (referred to in Bulletin 17C) and one using the EMA approach of Bulletin 17C (using software). Table 5.18 summarizes the 10-year and 100-year quantiles from each approach.

The two-parameter log-normal distribution is a special case of the log-Pearson type III distribution, specifically when the skew is zero. The normal and Gumbel distributions assume fixed skews of zero and 1.139, respectively, for the untransformed data. Because the log-Pearson type III distribution uses a third parameter, it frequently results in better fits of the data compared with the two-parameter distributions.

The estimates in Table 5.18 display substantial variation, especially for the 100-year flood, where the values range from 215,300 to 2,038,000 ft^3 /s. The highway designer faces the obvious question of which is the appropriate distribution to use for the given set of data. The engineer can gain insight into this question by comparing a plot of the observations superimposed on the fitted frequency distribution, using standard probability scales. Based on this preliminary graphical analysis, as well as judgment, some standard distributions might be eliminated before beginning the frequency analysis.

On occasion, more than one distribution or, in the case of the log-Pearson type III, more than one skew option, will seem to fit the data reasonably. When this occurs, the engineer uses a quantitative measure to determine whether one curve or distribution is better than another. The next sections discuss two common techniques, the standard error of estimate and confidence limits.

Table 5.18. Comparison of discharges from the fitted distributions to the Nueces River below Uvalde, Texas, stream gage (08192000).

Distribution	Skew	Estimated Flow (ft^3/s)	
		0.1 AEP	0.01 AEP
Normal	Zero	134,000	215,300
Log-normal	Special case of LP3 with G = 0	205,100	4,073,000
Gumbel	Fixed at 1.139	144,700	295,400
Log-Pearson type III	Station Skew (G = -0.9)	135,900	1,365,000
Log-Pearson type III	Regional Skew ($\overline{G}$ = -0.4)	135,700	2,038,000
Log-Pearson type III	Weighted Skew (G_W = -0.6)	159,800	1,289,000
Log-Pearson type III (Bulletin 17C)	Station Skew (G = -0.9)	102,500	401,100

5.2.5.1 Standard Error of Estimate

The standard error of estimate or the root-mean square error provides a measure of statistical reliability. Beard (1962) gives the standard error of estimate for the mean (S_{TM}), standard deviation (S_{TS}), and coefficient of skew (S_{TG}) as:

$$S_{TM} = \frac{S}{n^{0.5}} \quad (5.35)$$

$$S_{TS} = \frac{S}{(2n)^{0.5}} \quad (5.36)$$

$$S_{TG} = \left[\frac{6n(n-1)}{(n-2)(n+1)(n+3)}\right]^{0.5} \quad (5.37)$$

where:

S = Standard deviation of the sample
n = Number of observations in the sample

These equations show that the standard error of estimate is inversely proportional to the square root of the period of record. In other words, the shorter the record, the larger the standard errors. For example, standard errors for a short record will be approximately twice as large as those for a record four times as long.

The standard error of estimate measures the variance that could be expected in a predicted AEP event if the event were estimated from each of a large number of equally good samples of equal length. Because of its critical dependence on the period of record, engineers may have difficulty interpreting the standard error, and a large value may reflect a short record.

Example 5.10:	Compute the standard error of estimate for the mean, standard deviation, and skew coefficient for the Nueces River below Uvalde, Texas, dataset.
Objective:	Apply the standard error of estimate equations to a dataset and assess the results.

Given: The Bulletin 17C approach was used to fit the LP3 distribution to the annual peak series from the gage. The mean logarithm of flow is 3.847695, the standard deviation is 0.988839, and the skew coefficient is -0.741814. The number of observations in the dataset is 93. Of the 93 observations, 35 were identified as low outliers.

Find: S_{TM}, S_{TS}, S_{TG}

Using the Medina River annual flood series as an example, the standard errors for the parameters of the log-Pearson type III computed from equations 5.35, 5.36, and 5.37 for the logarithms are:

$S_{TM} = 0.989/(93)^{0.5} = 0.103$

$S_{TS} = 0.989/(2(93))^{0.5} = 0.0725$

$S_{TG} = [6(93)(92)/((91)(94)(96))]^{0.5} = 0.250$

Solution:	The standard error for the skew coefficient of 0.250 is somewhat large. The 93-year period of record is relatively long, but there are 35 low outliers in the dataset, based on the Multiple Grubbs-Beck Test. The result is a reduced equivalent record length to the station and suggests that a weighted skew coefficient should be investigated.

5.2.5.2 Confidence Limits

Engineers use confidence limits to estimate the uncertainties associated with the determination of floods of specified AEPs from frequency distributions. A given frequency distribution only estimates the distribution of the population, with that estimate developed from a sample of a population. Therefore, a different sample taken at the same location and of equal length but taken from a different period would likely yield a different frequency distribution. Confidence limits, or more correctly, confidence intervals, define the range within which these frequency curves could be expected to fall with a specified confidence level.

Bulletin 17B (Water Resources Council 1982) outlined a method for developing upper and lower confidence intervals based on the assumption that the confidence intervals were normally distributed about the fitted distribution. The general forms of these confidence limits are:

$$U_{p,c}(Q) = \overline{Q} + S\ K^{U}_{p,c} \tag{5.38}$$

$$L_{p,c}(Q) = \overline{Q} + S\ K^{L}_{p,c} \tag{5.39}$$

where:

c	=	Level of confidence
p	=	Exceedance probability
$U_{p,c}(Q)$	=	Upper confidence limit corresponding to the values of p and c, for flow Q
$L_{p,c}(Q)$	=	Lower confidence limit corresponding to the values of p and c, for flow Q
$K^{U}_{p,c}$	=	Upper confidence coefficient corresponding to the values of p and c
$K^{L}_{p,c}$	=	Lower confidence coefficient corresponding to the values of p and c

Table 5.19 provides values of $K^{U}_{p,c}$ and $K^{L}_{p,c}$ for the normal distribution for the commonly used confidence levels of 0.05 and 0.95. Bulletin 17B, from which Table 5.19 was abstracted, contains a more extensive table covering other confidence levels. Bulletin 17C does not contain this approach, instead taking a completely different approach to confidence limits for LP3 fits. However, this approach for confidence limits applies to distributions other than LP3.

Confidence limits defined in this manner and with the values of Table 5.19 are called one-sided because each defines the limit on just one side of the frequency curve; for 95 percent confidence only one of the values is computed. The one-sided limits can be combined to form a two-sided confidence interval such that the combination of 95 percent and 5 percent confidence limits define a two-sided 90 percent confidence interval. Practically, this means that at a specified exceedance probability, there is a 5 percent chance the flow will exceed the upper confidence limit and a 5 percent chance the flow will be less than the lower confidence limit. Stated another way, it can be expected that, 90 percent of the time, the specified frequency flow will fall within the two confidence limits.

In Bulletin 17C, confidence intervals are computed after the EMA process completes and produces the distribution parameters for the fitted frequency distribution. The confidence intervals are computed by the software and are based on a Student's T distribution. Appendix 7 of Bulletin 17C contains more details.

Confidence intervals were computed for the Nueces River flood series using the Bulletin 17B procedures for both the log-normal and the Bulletin 17C method for the LP3 distribution. The weighted skew of 0.1 was used with the log-Pearson type III analysis. Table 5.20 and Table 5.21 provide the computations for the confidence intervals for the log-normal and log-Pearson type III, respectively. Figure 5.15 and Figure 5.17 show the confidence intervals for the log-normal and log-Pearson type III, respectively.

Table 5.19. Confidence limit deviate values for normal and log-normal distributions.

Confidence Level	Systematic Record n	Exceedance Probability								
		0.002	0.010	0.020	0.040	0.100	0.200	0.500	0.800	0.990
0.05	10	4.862	3.981	3.549	3.075	2.355	1.702	0.580	-0.317	-1.563
	15	4.304	3.520	3.136	2.713	2.068	1.482	0.455	-0.406	-1.677
	20	4.033	3.295	2.934	2.534	1.926	1.370	0.387	-0.460	-1.749
	25	3.868	3.158	2.809	2.425	1.838	1.301	0.342	-0.497	-1.801
	30	3.755	3.064	2.724	2.350	1.777	1.252	0.310	-0.525	-1.840
	40	3.608	2.941	2.613	2.251	1.697	1.188	0.266	-0.556	-1.896
	50	3.515	2.862	2.542	2.188	1.646	1.146	0.237	-0.592	-1.936
	60	3.448	2.807	2.492	2.143	1.609	1.116	0.216	-0.612	-1.966
	70	3.399	2.765	2.454	2.110	1.581	1.093	0.199	-0.629	-1.990
	80	3.360	2.733	2.425	2.083	1.559	1.076	0.186	-0.642	-2.010
	90	3.328	2.706	2.400	2.062	1.542	1.061	0.175	-0.652	-2.026
	100	3.301	2.684	2.380	2.044	1.527	1.049	0.166	-0.662	-2.040
0.95	10	1.989	1.563	1.348	1.104	0.712	0.317	-0.580	-1.702	-3.981
	15	2.121	1.677	1.454	1.203	0.802	0.406	-0.455	-1.482	-3.520
	20	2.204	1.749	1.522	1.266	0.858	0.460	-0.387	-1.370	-3.295
	25	2.264	1.801	1.569	1.309	0.898	0.497	-0.342	-1.301	-3.158
	30	2.310	1.840	1.605	1.342	0.928	0.525	-0.310	-1.252	-3.064
	40	2.375	1.896	1.657	1.391	0.970	0.565	-0.266	-1.188	-2.941
	50	2.421	1.936	1.694	1.424	1.000	0.592	-0.237	-1.146	-2.862
	60	2.456	1.966	1.722	1.450	1.022	0.612	-0.216	-1.116	-2.807
	70	2.484	1.990	1.745	1.470	1.040	0.629	-0.199	-1.093	-2.765
	80	2.507	2.010	1.762	1.487	1.054	0.642	-0.186	-1.076	-2.733
	90	2.526	2.026	1.778	1.500	1.066	0.652	-0.175	-1.061	-2.706
	100	2.542	2.040	1.791	1.512	1.077	0.662	-0.166	-1.049	-2.684

Example 5.11:	Compute the confidence limits (confidence interval) for the Nueces River log-normal distribution fit.
Objective:	Apply the method for estimating confidence limits to a dataset.

Given: The log-normal distribution fit to the Nueces River gage data. The record length is 93 years, the mean logarithm is 3.603, and the standard deviation of logarithms is 1.334.

Find: Estimate the 5- and 95-percent confidence limits for the log-normal distribution fit to the Nueces River below Uvalde, Texas, peak flow series.

Step 1. For the quantiles of interest (0.50, 0.20, 0.10, 0.04, 0.02, 0.01, and 0.002), determine the K factors for the upper and lower confidence limits.

Using the record length of 93 years and Table 5.19, look up the K factors for the quantiles of interest and post in Table 5.20.

Step 2. Compute the logarithms of the confidence limits.

Using the K factors determined in step 1, populate the columns for the logarithms of the upper and lower confidence limits using equations 5.38 and 5.39. For example, for the 2-year event, $K^L = -0.175$ from Table 5.19, so the lower confidence limit is:

$$L = 3.603 + 1.334(-0.175) = 3.370$$

$$X_L = 10^{3.370} = 2,342 \text{ft}^3 / \text{s}$$

Similarly, for the upper confidence limit, $K^U = 0.174$ from Table 5.19, so the upper confidence limit is:

$$U = 3.603 + 1.334(0.175) = 3.836$$

$$X_U = 10^{3.836} = 6,862 \text{ ft}^3 / \text{s}$$

Place these values into Table 5.19.

Step 3. Detransform the logarithms of the confidence limits.

Using the equation $X=10^Y$, detransform the confidence limits and post in Table 5.20.

Step 4. Plot the results onto the same coordinates as the fitted distribution and observed data. Then compare the fitted distribution and observed data to the confidence limits (confidence interval).

Finish the computations and plot the results. Compare with the observed data.

Solution:	Table 5.20 displays the results of the computations. Plot these on the same coordinates as the distribution and data. Figure 5.15 shows the results. Notice that the observations plot outside the 90-percent confidence interval. This visual inspection indicates that the log-normal distribution fit to the observed data is not a good fit. As discussed above, this is attributable to the large number of low outliers in the observations (35 low outliers). Furthermore, this demonstrates the importance of being careful with fitting distributions to observed data and the utility of the MGBT low-outlier check in Bulletin 17C.

Table 5.20. Computation of two-sided, 90 Percent Confidence Interval for the Log-normal Analysis of the Nueces River annual peak flow series.

AEP	Y (log(ft^3/s))	X (ft^3/s)	K^L	L	X_L (ft^3/s)	K^U	U	X_u (ft^3/s)
0.5	3.603	4,008	-0.175	3.370	2,342	0.175	3.836	6,862
0.2	4.725	53,120	0.652	4.473	29,701	1.061	5.018	104,322
0.1	5.312	205,120	1.066	5.025	105,936	1.542	5.660	457,118
0.04	5.938	866,082	1.500	5.604	401,791	2.062	6.354	2,257,917
0.02	6.342	2,196,581	1.778	5.975	943,739	2.400	6.805	6,376,759
0.01	6.705	5,072,981	2.026	6.306	2,021,548	2.706	7.213	16,323,151
0.002	7.441	27,611,921	2.526	6.973	9,390,398	3.328	8.043	110,294,029

Table 5.21. Quantiles and upper and lower confidence limits for a 90-percent confidence interval from Bulletin 17C EMA computations for the Nueces River below Uvalde, Texas, annual peak flow series.

AEP	X (ft^3/s)	X^L (ft^3/s)	X^U (ft^3/s)
0.5	9,309	4,731	13,600
0.2	49,530	34,300	73,500
0.1	102,500	70,200	160,200
0.04	200,900	134,100	346,400
0.02	294,300	190,700	550,500
0.01	401,100	250,000	820,000
0.002	686,000	382,400	1,797,000

It appears that a log-Pearson type III fitted using the Bulletin 17C EMA procedure is the most acceptable distribution for the Nueces River data. The actual data follow the distribution very well, and all the data lie within the confidence intervals except the low outliers. Based on this analysis, the log-Pearson type III is the preferred standard distribution. Because of the impact of low outliers on the fitting of the other distributions, they are not appropriate for the Nueces River data.

5.2.6 Record Extension with Nearby Sites

Bulletin 17C presents an extended approach to Bulletin 17B for statistical analysis of stream gage flow data. This is because the computation of sample parameters is an iterative process in EMA and the two-station comparison process is a process called Record Extension with Nearby Sites. As with the Bulletin 17B approach, this method has the objective of improving estimates of the mean and standard deviation of the logarithms at a short-record station (Y) using the statistics from a nearby long-record station (X). If appropriate, correlation between the common peak flows of the two sites is used to extend the systematic record of the short-record station (Y).

Appendix 8 of Bulletin 17C presents the record extension method. The assumption is that the entire period of record of the short-record station is contained within the period of record of the long-record station. The general procedure for record augmentation of the mean and variance of the short-record site and the construction of a record extension with new observations is:

1. Select a nearby record site that is both hydrologically similar and has a longer period of record than the short-record site. The correlation of peak flows between the two records is critical to computing a record extension and should be as large as possible. This is not a mechanical procedure and judgment is important.
    a. Construct a time series plot containing both records (with appropriate delineation so that the different records are apparent).
    b. Examine the plot for differences and similarities for the overlapping periods of record.
    c. Assess whether the overlapping records are similar. Assess whether the longer-record station provides what appears to be a longer record of the hydrologic events observed in the shorter record.
2. Using the mathematical relations in Appendix 8 of Bulletin 17C, investigate the statistical properties and regression relation between the two records.
    a. If the correlation coefficient between the two records exceeds a critical value ($r \geq 0.8$), then record extension might be appropriate. The analysis can proceed.
    b. If the correlation coefficient is less than the critical value, then record extension is probably not appropriate. Alternative approaches include using a weighted skew coefficient or a regional skew coefficient with the short record might be appropriate.
3. Compute the sample statistics for the concurrent records, and then the mean and variance estimators for the short-record site based on the entire period of record for the long-record site.
4. Compute the total effective record length of the short-record series. This determines the number of observations to add to the short-record series.
5. Compute the extension parameters and use the extension model to generate the needed flow values to extend the record for the short-record site. Use the most recent values from the long-record station that are not concurrent with observations from the short-record station. Examine the extended record problems.
    a. For example, if the generated values are computed from a portion of the long-record station that includes the first or second greatest peaks, then the extended record likely contains values that will misrepresent the station skew coefficient.
    b. A solution for this problem would be to adjust the segment in the long-record station series to avoid these peaks.
6. Use the resulting record for the short-record station as input for the Bulletin 17C procedure.

The previous description is a general overview of the detailed procedure described in Bulletin 17C. Bulletin 17C presents the details and an example.

5.2.7 Other Methods for Estimating Flood Frequency Distribution Parameters

The techniques of fitting an annual series of flood data by the standard frequency distributions described above are all samples of the application of the method of moments. Population moments are estimated from the sample moments with the mean taken as the first moment about the origin, the variance as the second moment about the mean, and the skew as the third moment about the mean. Engineers use three other recognized methods to determine frequency curves: the method of maximum likelihood, the L-moments or probability weighted moments, and a graphical method.

The method of maximum likelihood is a statistical technique based on the principle that the values of the statistical parameters of the sample are maximized so that the probability of obtaining an

observed event is as high as possible. The method is somewhat more efficient for highly skewed distributions if efficient estimates of the statistical parameters exist. On the other hand, the method is complicated to use and its practical use in highway design is not justified in view of the wide acceptance and use of the method of moments for fitting data with standard distributions.

The method of maximum likelihood (maximum likelihood estimation [MLE]) (Kite 1988, Helsel et al. 2020) is not used in Bulletin 17C and is more involved than the method of moments. However, it is instructive to put MLE in perspective. MLE defines a likelihood function that expresses the probability of obtaining the population parameters given that the measured flood record has occurred. For example, if μ and σ are the population parameters and the flood record X contains N events, the likelihood function is:

$$L(\mu,\sigma \mid X_1, X_2, \ldots, X_N) = \prod_{i=1}^{N} f(X_i \mid \mu,\sigma) \tag{5.40}$$

where:

$f(X_I \mid \mu, \sigma)$ = The probability distribution of X as a function of the parameters

The solution of equation 5.40 yields expressions for estimating μ and σ from the flood record X.

Another approach to estimating population parameters is called the method of L-moments. The L-moment method uses the order statistics of the sample to estimate the sample statistics. The sample statistics are used to determine the population parameters just as with the other methods of fitting distributions to samples (Hosking 1990, Hosking 1992).

Graphical methods involve simply fitting a curve to the sample data by eye. Typically, the engineer transforms the data by plotting them on probability or log-probability graph paper such that the plotted data approximate a straight line. This procedure is no longer commonly used because resource agencies prefer use of statistically fitted distributions. However, the tool might be useful for checking results from other methods. As noted in Sanders (1980), some improvement is obtained by ensuring that the maximum positive and negative deviations from the selected line are approximately equal and that the maximum deviations are made as small as possible.

5.2.8 Low Flow Frequency Analysis

While hydrologic engineers use instantaneous maximum discharges for flood frequency analyses, they are frequently interested in low flows. Engineers use low flow frequency analyses in water quality studies and the design of culverts where fish passage is a design criterion. For low flow frequency analyses, engineers commonly specify both a return period and a flow duration. For example, a low flow frequency curve may be computed for a 7-day duration. In this case, the 10-year event would be referred to as the 7-day, 10-year low flow.

Engineers compile a data record for a low flow frequency analysis by identifying the lowest mean flow rate in each year of record for the given duration. For example, if the 21-day low flow frequency curve is needed, the record for each year is analyzed to find the 21-day period in which the mean flow is the lowest. A moving-average smoothing analysis with a 21-day smoothing interval could be used to identify this flow. For a record of N years, such an analysis will yield N low flows for the needed duration.

The computational procedure for making a low flow frequency analysis is like that for a flood frequency analysis. The engineer first specifies the probability distribution, commonly using the log-normal distribution, although another distribution could be used.

To make a log-normal analysis, a logarithmic transform of each of the N low flows is made. The mean and standard deviation of the logarithms are computed. Up to this point, the analysis is the

same as for an analysis of peak flood flows. However, for a low flow analysis, the governing equation is as follows:

$$Y = \overline{Y}_L - z S_L \quad (5.41)$$

where:

$\overline{Y}_L$ = Logarithmic mean
S_L = Logarithmic standard deviation
z = Standard normal deviate

Equation 5.41 includes a minus sign rather than the plus sign of equation 5.25. The low flow frequency curve will have a negative slope rather than the positive slope typical of peak flow frequency curves. Also, computed low flows for the less frequent events (e.g., the 100-year low flow) will be less than the mean. The FHWA's HEC-19 reference manual (FHWA 2022a) includes additional information on low flow methods.

Example 5.12: Low flow analysis.

Objective: Compute an estimate of the 7-day, 50-year low flow.

Given: Average and standard deviation of the base-10 logarithms of the annual series of 7-day low flows:

$\overline{Q}_L = 1.1$

$S_L = 0.2$

Equation 5.41 is used to compute the required estimate. For the 50-year event, the AEP is 0.02. The nonexceedance probability for the 50-year event is 0.98.

Step 1. Determine the standard normal deviate for a nonexceedance probability of 0.98 (50-year event).

The standard normal deviate from Table 5.8 is 2.054 (using linear interpolation).

Step 2. Apply equation 5.41 using the given information.

$\log Y = 1.1 - 2.054(0.2) = 0.6892$

$Q = 10^{(0.6892)} = 4.9$ ft^3/s

Solution: The 7-day, 50-year low flow for the site is estimated at 4.9 ft^3/s.

5.2.9 Common Tools for the Statistical Analysis of Gage Data

Although many statistical analysis software tools are available, engineers commonly use two for the statistical analysis of gage data: 1) the U.S. Army Corps of Engineers (USACE) HEC-SSP and 2) the USGS PeakFQ.

The USACE HEC-SSP package (Bartles et al. 2019) is a general-purpose statistical analysis tool that processes gage data using a variety of methods. These methods include those presented in this chapter, including the methods in Bulletin 17C as of Version 2.2 or later. HEC-SSP contains a module that downloads USGS stream gage data directly from the USGS data portal, which aids ready access to gage data for processing.

The USGS PeakFQ package (Flynn et al. 2006) is a statistical analysis tool for developing estimates of annual maximum flood frequency curve. The program fits the Pearson type III distribution to the logarithms of the annual maximum series. As of Version 7.3 PeakFQ

implements Bulletin 17C even though the published documentation references Bulletin 17B. To use PeakFQ, the user downloads the annual peak flow data from the USGS data portal.

5.3 Index Adjustment of Flood Records for Watershed Changes

The flood frequency methods discussed in this chapter assume that the flood record is a series of events from the same population. In statistical terms, the events should be independent and identically distributed. In hydrologic terms, the events should result from the same meteorological and runoff processes. The year-to-year variation should only be due to the natural variation such as that of the volumes and durations of rainfall events.

Watershed changes, such as afforestation, deforestation, and urbanization, change the runoff processes controlling the watershed response to rainfall. In statistical terms, the events are no longer identically distributed because the population changes with land use changes. Afforestation might decrease the mean flow. Urbanization would probably increase the mean flow but decrease the variation of the peak flows. If the watershed change takes place over an extended period, each event during the period of change is from a different population. Thus, magnitudes and exceedance probabilities obtained from the flood record could not represent future events. Before using such a record for a frequency analysis, the engineer adjusts measured events to reflect homogeneous watershed conditions. One method of adjusting a flood record is referred to as the index adjustment method (which should not be confused with the index flood method of Section 6.3).

Flood records can be adjusted using an index variable, such as the percentage of imperviousness or the fraction of a channel reach that has undergone channelization, to adjust the flood peaks. Index methods use values of the index variables over time and a model that relates the change in peak flow, the index variable, and the exceedance probability. In addition to urbanization, index methods could be calibrated to adjust for the effects of deforestation, surface mining activity, agricultural management practices, or climate change. HEC-17 (FHWA 2016) and HEC-19 (FHWA 2022a) specifically address methods for addressing potential impacts of climate change.

FHWA encourages consideration of climate change and sustainability throughout the planning and project development process, including the extent to which projects align with the President's greenhouse gas reduction, climate resilience, and environmental justice commitments (FHWA 2021; USDOT 2021; USDOT 2022). These considerations can help ensure the transportation network is resilient and reliable for all users despite the risk associated with a changing climate (USDOT 2021; FHWA 2021).

It is important to consider climate change impacts and adaptation early in the project development process to ensure that climate resilience is incorporated into the project design to the extent possible and appropriate. Exploratory engineering-informed adaptation evaluations can have the greatest impact on the design features of the project when conducted early in the project development process (FHWA 2017).

Since urbanization commonly causes nonhomogeneity in flood records, it will be used to illustrate index adjustment of floods. The literature does not identify a single method as best for adjusting an annual flood series when only the time record of urbanization is available. Furthermore, urbanization may be defined by several parameters, which include, but are not limited to:

- Percent imperviousness.
- Percent urbanized land cover (residential, commercial, and industrial).
- Population density.

Each method depends on the data used to calibrate the prediction process, and the data used to calibrate the methods are usually very sparse. However, the sensitivities of measured peak flows

suggest that a 1 percent increase in percent imperviousness causes an increase in peak flow of about 1 to 2.5 percent for the 100-year and the 2-year events, respectively (McCuen 2012). Using data from USGS stream gages, Blum et al. (2020) estimated that increases in impervious area results in increases of annual flood magnitude from 3.3 to 4.7 percent, depending on what data are used. The point is that increases in impervious area result in increased runoff from the affected watershed.

Based on the general trends of results published in available urban flood frequency studies, McCuen (2012) developed a method of adjusting a flood record for the effects of urbanization. Urbanization refers to the introduction of impervious surfaces or changes to drainage patterns that increase runoff peaks and volumes. Figure 5.19 shows the peak adjustment factor as a function of the exceedance probability for percentages of imperviousness up to 60 percent. The greatest effect is for the more frequent events and the highest percentage of imperviousness. For this discussion, percent imperviousness is used as the measure of urbanization.

Given the AEP of a flood peak for a nonurbanized watershed, the effect of an increase in urbanization can be assessed by multiplying the discharge by the peak adjustment factor, which is a function of the AEP and the percentage of urbanization. When adjusting a discharge to another watershed condition, the measured discharge can be divided by the peak adjustment factor for the existing condition to produce a “rural” discharge. This computed discharge is then multiplied by the peak adjustment factor for the second watershed condition. The first operation (i.e., division) adjusts the discharge to a magnitude representative of a nonurbanized condition, while the second operation (i.e., multiplication) adjusts the new discharge to a computed discharge for the second watershed condition. This process is represented as:

$$Q_a = \frac{f_2}{f_1} Q \tag{5.42}$$

where:

Q_a = Adjusted peak flow
Q = Unadjusted (measured) peak flow
f_1 = Peak adjustment factor to adjust measured peak to nonurbanized condition
f_2 = Peak adjustment factor to adjust nonurbanized peak to target level of urbanization

The adjustment method of Figure 5.19 uses an exceedance probability. For a flood record, the best estimate of the probability is obtained from a plotting position formula. The following procedures can be used to adjust a flood record for which the individual flood events have occurred on a watershed undergoing continuous change in the level of urbanization:

Step 1. Identify the percentage of urbanization for each event in the flood record.

Because of the nature of flood series and lack of other information about a watershed, the progression of change may not be completely evident. Percentage change in impervious area might not be available for every year of record. If this is the case, interpolate or extrapolate these changes from existing estimates, to assign each flood event of record a percentage.

Step 2. Identify the target percentage of urbanization for which an adjusted flood record is needed.

Determine the urbanization level to which all flood events in the record will be adjusted, thus producing a record assumed to include independent and identically distributed events.

Step 3. Compute the rank (i) and exceedance probability (p) for each event in the flood record.

Use a plotting position formula to compute the probability.

Step 4. Find peak adjustment factor (f_1) to a nonurbanized condition.

Using the exceedance probability and the percentage of urbanization from step 1, find the peak adjustment factor (f_1) from Figure 5.19 to transform the measured peak from the actual level of urbanization to a nonurbanized condition.

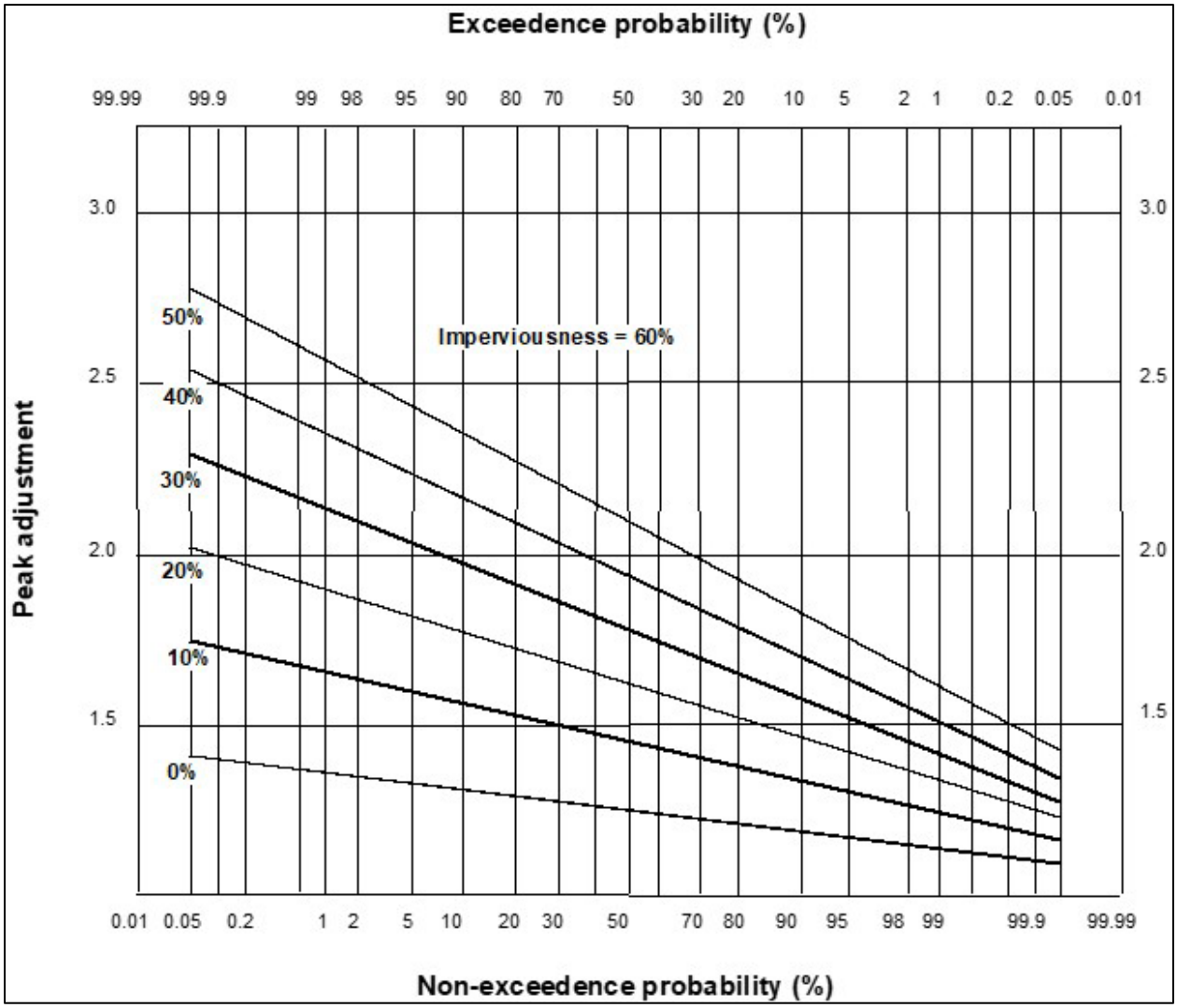

Figure 5.19. Peak adjustment factors for correcting a flood discharge magnitude for the change in imperviousness (McCuen 2012).

Step 5. Find the peak adjustment factor (f_2) for the target urbanized condition.

Using the exceedance probability and the target percentage of urbanization from step 2 from Figure 5.19, find the peak adjustment factor (f_2) that will successfully transform the nonurbanized peak of step 4 to a discharge for the targeted level of urbanization of step 2.

Step 6. Compute the adjusted discharge (Q_a).

Compute the adjusted discharge using equation 5.42 and the peak adjustment factors from steps 4 and 5 and the measured discharge for each discharge in the series.

Step 7. Rank the floods in the adjusted series and check for reordering.

Assign new ranks based on the adjusted discharges. If the ranks have not changed, the adjusted series is the final series.

Step 8. Repeat steps 3 through 7 until ranks stabilize.

If the ranks of the events in the adjusted series differ from the ranks of the previous series, which would be the measured events after one iteration of steps 3 to 7, then repeat the iteration process until the ranks do not change.

Example 5.13: Apply the index adjustment method.

Objective: Estimate flood quantiles for the current watershed imperviousness of Rubio Wash.

Table 5.22 contains the 48-year record of annual maximum peak flows for the Rubio Wash watershed in Los Angeles. The log moments for discharge are summarized as:

- Log mean: 3.252
- Log standard deviation: 0.191
- Station skew: -0.7
- Regional skew: -0.45

The procedure given above was used to adjust the flood record for the period from 1929 to 1963 to current impervious cover conditions. Imperviousness is used as the index variable as a measure of urbanization.

Step 1. Identify the percentage of urbanization for each event in the flood record.

Table 5.22 summarizes the percent impervious cover for the flood record. For example, the peak flows for 1931 and 1945 occurred when the percent impervious cover was 19 and 34 percent, respectively.

Step 2. Identify the percentage of urbanization for which an adjusted flood record is needed.

The values were adjusted to a common percentage of 40 percent, which is the watershed state after 1964.

Step 3. Compute the rank (i) and exceedance probability (p) for each event in the flood record.

Table 5.22 summarizes the initial rank and exceedance probability for each flood.

Step 4. Find peak adjustment factor (f_1).

Table 5.22 summarizes the peak adjustment factor to adjust the peak to a nonurbanized condition.

Step 5. Find the peak adjustment factor (f_2)

Table 5.22 summarizes the peak adjustment factor to adjust the nonurbanized peak to an urbanized condition with the target percent imperviousness of 40 percent.

Step 6. Compute the adjusted discharge (Q_a).

Using equation 5.42, compute the adjusted urbanized peak summarized in Table 5.22.

Step 7. Rank the floods in the adjusted series and check for reordering.

Table 5.22 summarizes the ranks of the adjusted series. After each iteration, compare the adjusted rank with the rank prior to the iteration to determine if the computations are complete. Since some of the ranks changed, e.g., the flood of 1930, subsequent iterations are indicated.

Step 8. Repeat steps 3 through 7 until ranks stabilize.

Two additional iterations are indicated and summarized in Table 5.23 and Table 5.24. The iterative process is appropriate because the ranks for some of the earlier events changed considerably from the initial ranks. For example, the rank of the 1930 peak changed from 30 to 22 and the rank of the 1933 event went from 20 to 14. Changes in the rank result in changes in the exceedance probabilities, and therefore, changes in the adjustment factors.

Table 5.22. Urbanization adjustment of the Rubio Wash annual maximum floods (Iteration 1).

Year	Imperviousness (%)	Measured Discharge (ft^3/s)	Rank	Exceedance Probability	f_1	f_2	Adjusted Discharge (ft^3/s)	Adjusted Rank
1929	18	660	47	0.959	1.560	2.075	878	47
1930	18	1,690	30	0.612	1.434	1.846	2,176	22
1931	19	800	46	0.939	1.573	2.044	1,040	44
1932	20	1,510	34	0.694	1.503	1.881	1,890	32
1933	20	2,070	20	0.408	1.433	1.765	2,550	13
1934	21	1,680	31	0.633	1.506	1.855	2,069	24
1935	21	1,370	35	0.714	1.528	1.890	1,695	34
1936	22	1,180	40	0.816	1.589	1.956	1,453	36
1937	23	2,400	14	0.286	1.448	1.713	2,839	8
1938	25	1,720	29	0.592	1.568	1.838	2,016	28
1939	26	1,000	43	0.878	1.690	1.984	1,174	42
1940	28	1,940	26	0.531	1.603	1.814	2,195	20
1941	29	1,200	38	0.776	1.712	1.931	1,354	37
1942	30	2,780	7	0.143	1.508	1.648	3,038	5
1943	31	1,930	27	0.551	1.663	1.822	2,115	23
1944	33	1,780	28	0.571	1.705	1.830	1,910	31
1945	34	1,630	32	0.653	1.752	1.863	1,733	33
1946	34	2,650	10	0.204	1.585	1.672	2,795	10
1947	35	2,090	19	0.388	1.675	1.757	2,192	21
1948	36	530	48	0.980	2.027	2.123	555	48
1949	37	1,060	42	0.857	1.907	1.969	1,094	43
1950	38	2,290	17	0.347	1.708	1.740	2,333	16
1951	38	3,020	4	0.082	1.557	1.583	3,070	4
1952	39	2,200	18	0.367	1.732	1.748	2,220	19
1953	39	2,310	15	0.306	1.706	1.722	2,332	17
1954	39	1,290	36	0.735	1.881	1.900	1,303	38
1955	39	1,970	25	0.510	1.788	1.806	1,990	29
1956	39	2,980	5	0.102	1.589	1.602	3,004	6
1957	39	2,740	9	0.184	1.646	1.660	2,763	11
1958	39	2,780	8	0.163	1.620	1.634	2,804	9
1959	39	990	44	0.898	1.979	2.001	1,001	45
1960	39	900	45	0.918	1.999	2.020	909	46
1961	39	1,200	39	0.796	1.911	1.931	1,213	40
1962	39	1,180	41	0.837	1.935	1.956	1,193	41
1963	39	1,570	33	0.673	1.853	1.872	1,586	35
1964	40	2,040	22	0.449	1.781	1.781	2,040	27
1965	40	2,300	16	0.327	1.731	1.731	2,300	18
1966	40	2,040	23	0.469	1.790	1.790	2,040	26
1967	40	2,460	13	0.265	1.703	1.703	2,460	15
1968	40	2,890	6	0.122	1.619	1.619	2,890	7
1969	40	2,540	12	0.245	1.693	1.693	2,540	14
1970	40	3,700	1	0.020	1.480	1.480	3,700	1
1971	40	1,240	37	0.755	1.910	1.910	1,240	39
1972	40	3,160	3	0.061	1.559	1.559	3,160	3
1973	40	1,980	24	0.490	1.798	1.798	1,980	30
1974	40	3,180	2	0.041	1.528	1.528	3,180	2
1975	40	2,070	21	0.429	1.773	1.773	2,070	25
1976	40	2,610	11	0.224	1.683	1.683	2,610	12

Table 5.23. Urbanization adjustment of the Rubio Wash annual maximum floods (Iteration 2).

Year	Imperviousness (%)	Measured Discharge (ft^3/s)	Adjusted Rank	Adjusted Exceedance Probability	f_1	f_2	Adjusted Discharge (ft^3/s)	Adjusted Rank
1929	18	660	47	0.959	1.560	2.075	878	47
1930	18	1,690	22	0.449	1.399	1.781	2,151	22
1931	19	800	44	0.898	1.548	2.001	1,034	44
1932	20	1,510	32	0.653	1.493	1.863	1,884	32
1933	20	2,070	13	0.265	1.395	1.703	2,527	14
1934	21	1,680	24	0.490	1.475	1.806	2,057	25
1935	21	1,370	34	0.694	1.522	1.881	1,693	34
1936	22	1,180	36	0.735	1.553	1.900	1,444	36
1937	23	2,400	8	0.163	1.405	1.648	2,815	8
1938	25	1,720	28	0.571	1.562	1.830	2,015	28
1939	26	1,000	42	0.857	1.680	1.969	1,172	42
1940	28	1,940	20	0.408	1.573	1.773	2,187	21
1941	29	1,200	37	0.755	1.695	1.910	1,352	37
1942	30	2,780	5	0.102	1.472	1.602	3,026	5
1943	31	1,930	23	0.469	1.637	1.790	2,110	23
1944	33	1,780	31	0.633	1.726	1.855	1,913	31
1945	34	1,630	33	0.673	1.760	1.872	1,734	33
1946	34	2,650	10	0.204	1.585	1.672	2,795	10
1947	35	2,090	21	0.429	1.690	1.773	2,193	20
1948	36	530	48	0.980	2.027	2.123	555	48
1949	37	1,060	43	0.878	1.921	1.984	1,095	43
1950	38	2,290	16	0.327	1.708	1.740	2,333	16
1951	38	3,020	4	0.082	1.557	1.583	3,070	4
1952	39	2,200	19	0.388	1.741	1.757	2,220	19
1953	39	2,310	17	0.347	1.724	1.740	2,331	17
1954	39	1,290	38	0.776	1.901	1.920	1,303	38
1955	39	1,970	29	0.592	1.820	1.838	1,989	29
1956	39	2,980	6	0.122	1.606	1.619	3,004	6
1957	39	2,740	11	0.224	1.668	1.683	2,765	11
1958	39	2,780	9	0.184	1.646	1.660	2,804	9
1959	39	990	45	0.918	1.999	2.020	1,000	45
1960	39	900	46	0.939	2.022	2.044	910	46
1961	39	1,200	40	0.816	1.923	1.943	1,212	40
1962	39	1,180	41	0.837	1.935	1.956	1,193	41
1963	39	1,570	35	0.714	1.871	1.890	1,586	35
1964	40	2,040	27	0.551	1.822	1.822	2,040	26
1965	40	2,300	18	0.367	1.748	1.748	2,300	18
1966	40	2,040	26	0.531	1.822	1.822	2,040	27
1967	40	2,460	15	0.306	1.722	1.722	2,460	15
1968	40	2,890	7	0.143	1.634	1.634	2,890	7
1969	40	2,540	14	0.286	1.713	1.713	2,540	13
1970	40	3,700	1	0.020	1.480	1.480	3,700	1
1971	40	1,240	39	0.796	1.931	1.931	1,240	39
1972	40	3,160	3	0.061	1.559	1.559	3,160	3
1973	40	1,980	30	0.612	1.846	1.846	1,980	30
1974	40	3,180	2	0.041	1.528	1.528	3,180	2
1975	40	2,070	25	0.510	1.806	1.806	2,070	24
1976	40	2,610	12	0.245	1.693	1.693	2,610	12

Table 5.24. Urbanization adjustment of the Rubio Wash annual maximum floods (Iteration 3).

Year	Imperviousness (%)	Measured Discharge (ft^3/s)	Adjusted Rank-iteration 2	Adjusted Exceedance Probability	f_1	f_2	Adjusted Discharge (ft^3/s)	Adjusted Rank-iteration 3
1929	18	660	47	0.959	1.560	2.075	878	47
1930	18	1,690	22	0.449	1.399	1.781	2,151	22
1931	19	800	44	0.898	1.548	2.001	1,034	44
1932	20	1,510	32	0.653	1.493	1.863	1,884	32
1933	20	2,070	14	0.286	1.401	1.713	2,531	14
1934	21	1,680	25	0.510	1.475	1.806	2,057	25
1935	21	1,370	34	0.694	1.522	1.881	1,693	34
1936	22	1,180	36	0.735	1.553	1.900	1,444	36
1937	23	2,400	8	0.163	1.405	1.648	2,815	8
1938	25	1,720	28	0.571	1.562	1.830	2,015	28
1939	26	1,000	42	0.857	1.680	1.969	1,172	42
1940	28	1,940	21	0.429	1.573	1.773	2,187	21
1941	29	1,200	37	0.755	1.695	1.910	1,352	37
1942	30	2,780	5	0.102	1.472	1.602	3,026	5
1943	31	1,930	23	0.469	1.637	1.790	2,110	23
1944	33	1,780	31	0.633	1.726	1.855	1,913	31
1945	34	1,630	33	0.673	1.760	1.872	1,734	33
1946	34	2,650	10	0.204	1.585	1.672	2,795	10
1947	35	2,090	20	0.408	1.683	1.765	2,192	20
1948	36	530	48	0.980	2.027	2.123	555	48
1949	37	1,060	43	0.878	1.921	1.984	1,095	43
1950	38	2,290	16	0.327	1.708	1.740	2,333	16
1951	38	3,020	4	0.082	1.557	1.583	3,070	4
1952	39	2,200	19	0.388	1.741	1.757	2,220	19
1953	39	2,310	17	0.347	1.724	1.740	2,331	17
1954	39	1,290	38	0.776	1.901	1.920	1,303	38
1955	39	1,970	29	0.592	1.820	1.838	1,989	29
1956	39	2,980	6	0.122	1.606	1.619	3,004	6
1957	39	2,740	11	0.224	1.668	1.683	2,765	11
1958	39	2,780	9	0.184	1.646	1.660	2,804	9
1959	39	990	45	0.918	1.999	2.020	1,000	45
1960	39	900	46	0.939	2.022	2.044	910	46
1961	39	1,200	40	0.816	1.923	1.943	1,212	40
1962	39	1,180	41	0.837	1.935	1.956	1,193	41
1963	39	1,570	35	0.714	1.871	1.890	1,586	35
1964	40	2,040	26	0.531	1.822	1.822	2,040	26
1965	40	2,300	18	0.367	1.748	1.748	2,300	18
1966	40	2,040	27	0.551	1.822	1.822	2,040	27
1967	40	2,460	15	0.306	1.722	1.722	2,460	15
1968	40	2,890	7	0.143	1.634	1.634	2,890	7
1969	40	2,540	13	0.265	1.703	1.703	2,540	13
1970	40	3,700	1	0.020	1.480	1.480	3,700	1
1971	40	1,240	39	0.796	1.931	1.931	1,240	39
1972	40	3,160	3	0.061	1.559	1.559	3,160	3
1973	40	1,980	30	0.612	1.846	1.846	1,980	30
1974	40	3,180	2	0.041	1.528	1.528	3,180	2
1975	40	2,070	24	0.490	1.798	1.798	2,070	24
1976	40	2,610	12	0.245	1.693	1.693	2,610	12

The adjusted series has a mean and standard deviation of 3.280 and 0.178, respectively. The mean increased, but the standard deviation decreased. Thus, the adjusted flood frequency curve will, in general, be higher than the curve for the measured series, but will have a smaller slope. Table 5.25 summarizes the adjusted and unadjusted (measured) flood frequency curves with the AEP quantiles computed from:

- Measured $Q = 10^{3.252 + 0.191\ K}$
- Adjusted $Q = 10^{3.280 + 0.179K}$

Table 5.25. Computed discharges for log-Pearson type III with regional skew for measured series and series adjusted to 40 percent imperviousness.

AEP	K (G = -0.45)	Measured Series (ft^3/s)	Adjusted Series (ft^3/s)	Increase (%)
0.5	0.07476	1,850	1,960	6
0.2	0.85580	2,600	2,710	4
0.1	1.22366	3,060	3,150	3
0.04	1.58657	3,590	3,650	2
0.02	1.80538	3,950	3,990	1
0.01	1.99202	4,290	4,310	0

Since the measured series was not homogeneous, the generalized skew of -0.45 was used to compute the values for the flood frequency curve. Table 5.25 also gives the percent increase in each AEP flood magnitude. The change is relatively minor because the imperviousness did not change after 1964 and the change was small (i.e., 10 percent) from 1942 to 1964. In addition, most of the larger storm events occurred after the watershed had reached the developed condition. The adjusted series represents the annual flood series for a constant urbanization condition (i.e., 40 percent imperviousness).

Solution: Table 5.25 summarizes the increases in the AEP discharges ranging for virtually no change for the 0.01 AEP and a 6 percent increase for the 0.5 AEP.

5.4 Peak Flow Transposition

Peak flow transposition allows gaged flow data to be applied at design locations near, but not coincident with, the gage location. Peak flow transposition is the process of adjusting the peak flow determined at the gage to a downstream or upstream location. If the design location is between two gages, peak flow transposition may also be accomplished using an interpolation process.

Best practice is for the design location to be located on the same stream channel near the gage with no major tributaries draining to the channel in the intervening reach. The definition of “near” depends on the method applied and the changes in the contributing watershed between the gage and the design location.

Engineers commonly can choose from multiple methos of peak flow transposition. The area-ratio method is described by:

$$Q_d = Q_g \left(\frac{A_d}{A_g} \right)^c \quad (5.43)$$

where:

Q_d = Peak flow at the design (ungaged) location
Q_g = Peak flow at the gage location
A_d = Watershed area at the design (ungaged) location
A_g = Watershed area at the gage location
C = Transposition exponent

The area-ratio method applies to a wide range of situations, but engineers use caution when applying the method to design locations with drainage areas differing from the gage location by more than 25 percent. The transposition exponent is frequently taken as the exponent for watershed area in an applicable peak flow regression equation for the site and is generally less than 1. (See Section 6.1 for more information on peak flow regression equations.) Asquith and Thompson (2008) found exponents ranging from 0.50 to 0.52 for various AEPs in Texas watersheds.

An alternative method, the Sauer method (1974) first computes a weighted discharge at the gage from the log-Pearson type III analysis of the gage record and the regression equation estimate at the gage location. Then, Sauer uses the gage drainage area, the design location drainage area, the weighted gage discharge, and regression equation estimates at the gage and design locations to determine the appropriate flow at the design location. Sauer (1974) and McCuen and Levy (2000) contain more detailed descriptions of Sauer's method.

Gages to be transposed warrant careful consideration and selection. As with an ungaged site, engineers might consider such characteristics as geographic proximity, stream nature (single main channel, stream order), geology, topography, mean annual rainfall, and land use. Transposition from several gages (to one another and to the ungaged site) and comparison of the results may be revealing. Engineers might weigh estimates from different gages in some manner, e.g., inverse distance weighting, or inverse area weighting.

Transposition Made Easy

USGS often publishes the flood quantile discharges from the statistical analysis of gage data used to develop regional regression equations in the reports accompanying the equations. This information can be readily extracted from the publications and used as a reference for selecting stations for transposition. The same publications usually contain the latitude and longitude of each station.

A GIS feature class or shape file containing the flood frequency discharges, watershed characteristics, and flood ratios can easily be assembled from that information for fast and easy use in transposition. Once created, it can be made available for use by all of those doing similar design. GIS also allows easy comparison of the physical similarities and differences between the ungaged watershed under investigation and gaged watersheds.

While engineers may not view transposition as providing as reliable magnitude of discharge as other methods, by transposing flood ratios, it can provide local information and validation with respect to the overall shape of the flood frequency curve, and growth of discharge with decreasing AEP.

Page Intentionally Left Blank

Chapter 6 - Peak Flow for Ungaged Sites

While State and local agencies use the frequency approaches discussed in Chapter 5 to determine a peak flow when measured data are available, many stream crossings may have insufficient reliable stream gaging records, or often no records at all. This chapter introduces several statistically based techniques to address these situations.

Adapting data from nearby watersheds with comparable hydrologic and physiographic features is referred to as regional analysis and includes regional regression equations and index flood methods. Watershed area plays an important role for each of these ungaged watershed peak flow determination methods. As described in Chapter 3, watershed area is the single most important characteristic for determining runoff peaks. The area of the watershed also provides a basis for determining the limits of applicability for many of these methods.

6.1 Regional Regression Equations

Highway engineers commonly use regional regression equations to estimate peak flows at ungaged sites or sites with insufficient gaged data. These equations relate the peak flow or some other flood characteristic at a specified AEP to the physiographic, hydrologic, and meteorological characteristics of the watershed.

6.1.1 Analysis Procedure

Regional regression equations can adopt a variety of equation formats. However, a typical multiple-regression model used in regional flood studies has the power model structure:

$$Y_T = a X_1^{b_1} X_2^{b_2} \ldots X_p^{b_p} \quad (6.1)$$

where:

Y_T	=	Dependent variable
$X_1, X_2, \ldots, X_p$	=	Independent variables
a	=	Intercept coefficient
$b_1, b_2, \ldots, b_p$	=	Regression exponents

The dependent variable is usually the peak flow for a given AEP or some other property of the flood frequency, and the independent variables are selected to characterize the watershed and its meteorological conditions. The analysts determine the parameters a, b_1, b_2, ..., b_p using a regression analysis as described in detail by Sanders (1980), Riggs (1968), McCuen (1993), and Helsel et al. (2020). The typical procedure for performing a regional regression analysis is:

1. Obtain the annual maximum flood series for each of the gaged sites in the region.
2. Perform a separate flood frequency analysis (e.g., log-Pearson type III) on each of the flood series obtained in step 1 and determine the peak flows for selected AEPs (commonly, the 0.5, 0.2, 0.1, 0.04, 0.02, 0.01, and 0.002 discharges).
3. Determine the values of watershed and meteorological characteristics for each watershed for which a flood series was collected in step 1.
4. Form an (n by p) matrix of all the data collected in step 3, where n is the number of watersheds from step 1 and p is the number of watershed characteristics from step 3.

5. Form a one-dimensional vector with n peak flows for the specific AEP selected.
6. Regress the vector of n peak flows from step 5 on the data matrix from step 4 to obtain the prediction equation.

For other AEPs, the analyst repeats the procedure, developing a separate equation for each AEP. It is important to closely review the regression coefficients to ensure that they are rational and consistent across the various AEPs. Because of sampling variation, the regression analyses have the potential to produce a set of coefficients that, under certain sets of values for the predictor variables, produces unreasonable results. For example, engineers typically recognize a computed 10-year discharge greater than the computed 25-year discharge as unreasonable. In such cases, the analyst developing the regression equations can eliminate irrational results by smoothing the coefficients. The analyst will also recompute the goodness-of-fit statistics using the smoothed coefficients. Analysts typically avoid irrational results by using the same predictor variables for all equations for the region.

Engineers can use as many independent variables as desired in a regression analysis, although they would be unlikely to include more than one measure of any characteristic. Engineers can determine the statistical significance of each independent variable, eliminating those that are statistically insignificant at a specified level of significance (e.g., five percent). In addition to statistical criteria, it is also important for all coefficients to be reasonable so that unreasonable results discussed previously are avoided.

Drainage Area and Other Characteristics

The most important watershed characteristic is usually the drainage area and almost all regression equations include it. The choice of other watershed characteristics is more varied and can include measurements of the main channel (e.g., slope and length), the watershed (e.g., shape, perimeter, aspect, elevation, and elevation range), land use, and others. Meteorological characteristics often considered as independent variables include various rainfall parameters, snowmelt, evaporation, temperature, and wind.

Analysts typically select the specific predictor variables included in a regression equation using a stepwise regression analysis. They include only those variables that are statistically significant, for example, at a five percent level of significance. Analysts also consider whether users of the regression equations can readily obtain the data for the predictor variables. When analysts use stepwise regression analysis to select variables for a set of equations for different AEPs, they use the same independent variables in all the equations. In a few cases, this may cause some equations in the set to be less accurate than would otherwise be possible, but ensuring consistency across the set of equations remains important.

6.1.2 USGS Regression Equations

In an ongoing series of studies, the U.S. Geological Survey (USGS), the Federal Highway Administration (FHWA), and State Departments of Transportation (DOTs) have developed regression equations throughout the U.S. In addition, for the past 60 years, State DOTs have funded USGS stream gaging stations, providing streamflow data used to estimate peak flows for common AEPs varying from 0.5 to 0.002. Typically, these studies divide each State into regions of similar hydrologic, meteorologic, and physiographic characteristics as determined by various hydrological and statistical measures.

The USGS applies multiple-regression techniques on the logarithmically transformed values of the variables to obtain regression equations for peak flows of selected AEPs. Only those independent variables that were statistically significant at a predetermined level of significance were retained in the final equations. The current equations are available through the National Streamflow Statistics (NSS) Program and StreamStats, which are discussed in Section 6.1.4.

6.1.2.1 Hydrologic Flood Regions

In most statewide flood frequency reports, analysts developing the regression equations divided the State into separate hydrologic regions. Generally, they determined regions of homogeneous flood characteristics by using major watershed boundaries and an analysis of the areal distribution of the regression residuals, which are the differences between regression and station (observed) AEP estimates. In some instances, they also differentiate the hydrologic regions by particular variables, such as the mean elevation of the watershed, or by statistical tests such as the Wilcoxon signed-rank test.

State Spotlight: Maine Peak Flow Regression Equations

Maine is a single hydrologic region. In cooperation with the Maine DOT, USGS developed equations for estimating peak flows with return periods that range from 1 to 500 years. The equations below apply to small watersheds (less than 12 square miles). The explanatory basin variables are drainage area (A), in square miles, and basin wetlands (W), as a percentage of total drainage area. The range of average standard error of prediction (in percent) for each equation is also shown. (See Section 6.1.2.2 for description of standard error.) USGS used peak flow records from up to 70 gages with at least 10 years of record (Hodgkins 1999, Lombard and Hodgkins 2015).

$$Q_{10} = 131.5(A)^{0.811}\,10^{-0.017(W)} \quad -30 \text{ to } 42.9$$

$$Q_{25} = 171.8(A)^{0.814}\,10^{-0.017(W)} \quad -31.5 \text{ to } 46.0$$

$$Q_{50} = 204.2(A)^{0.816}\,10^{-0.018(W)} \quad -32.4 \text{ to } 48.0$$

$$Q_{100} = 238.8(A)^{0.817}\,10^{-0.018(W)} \quad -33.3 \text{ to } 50.0$$

Example 6.1: Application of USGS regional regression equations.

Objective: Estimate peak flows for a given location.

A project team is developing plans for a highway crossing of Ranch Creek, near Fraser, Colorado. The site is ungaged and the design AEP is 0.04 (25-year return period).

Step 1. Identify the applicable regression equation.

Capesius and Stephens (2009) define the applicable regression equations for Colorado (Mountain Region) that have the following form with the limits for each variable given in parentheses following the variable definition:

$$Q_T = a\,A^{b_1}\,S^{b_2}\,P^{b_3} \qquad (6.2)$$

where:

Q_T = Peak annual flow for the specified return periods, ft^3/s
A = Drainage area (1 to 1,060), mi^2
S = Mean basin slope from 10 m digital elevation model (DEM) (7.6 to 60.2), percent
P = Mean annual precipitation (18 to 47), inches
a, b_i = Regression constants

Table 6.1 summarizes the regression constants of equation 6.2 for each AEP. For this example, the regression constants for the 0.04 AEP (25-year return period) are applicable.

Table 6.1. Regression constants for Colorado (Mountain Region) regression equations (Capesius and Stephens 2009).

Annual Exceedance Probability	Return Period (years)	a	b_1	b_2	b_3
0.5	2	0.0089	0.78	0.17	2.10
0.2	5	0.031	0.77	0.16	1.85
0.1	10	0.063	0.77	0.14	1.71
0.04	25	0.126	0.75	0.16	1.55
0.02	50	0.209	0.75	0.16	1.45
0.01	100	0.347	0.75	0.14	1.35

Step 2. Collect the data for the regression equation.

The project team develops the inputs needed manually or using an automated tool:

- Drainage area: 66.4 mi^2
- Mean annual precipitation: 28.8 inches
- Mean basin slope (from a 10 m DEM): 26 percent

Note: USGS specified that the regression equation works best when estimating the mean basin elevation from a DEM with a 10 m resolution.

Step 3. Apply the equation.

$$Q_{25} = a\, A^{b_1} S^{b_2} P^{b_3} = (0.126)\, 66.4^{0.75}\, 26^{0.16}\, 28.8^{1.55} = 900 \text{ ft}^3/\text{s}$$

Solution: The estimated 25-year design flow for the site using the applicable USGS regression equation is 900 ft^3/s.

6.1.2.2 Assessing Peak Flow Accuracy

In most cases, the developers of regional regression equations provide the associated indicators of accuracy that may include the standard error of estimate, the standard error of prediction, the equivalent years of record, or prediction intervals. The standard error of estimate quantifies how accurately the regression equation predicts the observed data used in their development by computing the deviation of the observed data from the corresponding predicted values:

$$SE = \left[\frac{\sum(\hat{Q}_i - Q_i)^2}{n - q} \right]^{0.5} \quad (6.3)$$

where:

SE	=	Standard error
Q_i	=	Observed value of the dependent variable (discharge)
$\hat{Q}_i$	=	Corresponding value predicted by the regression equation
n	=	Number of watersheds used in developing the regression equation
q	=	Number of regression coefficients (i.e., a, b_1, ..., b_p)

In a manner analogous to the variance, the standard error can be expressed as a percentage by dividing the standard error (SE) by the mean value ($\overline{Q_T}$) of the dependent variable:

$$V_e = \frac{SE}{\overline{Q_T}} \times 100\% \quad (6.4)$$

where:

V_e	=	Coefficient of error variation

V_e of equation 6.4 has the form of the coefficient of variation of equation 5.10. The standard error of estimate (SE) has a very similar meaning to that of the standard deviation, equation 5.9, for a normal distribution in that approximately 68 percent of the observed data are contained within ±1 standard error of estimate.

Standard error is reported in a variety of ways including: 1) in log units, 2) with a single percentage value, and 3) with upper and lower percentage values. For example, Capesius and Stephens (2009) report the standard error for the equations used in example 6.1 with a single percentage value. Alternatively, Hodgkins (1999) and Lombard and Hodgkins (2015) reported the standard error for equations in Maine with upper and lower percentages. Many older studies report a single percent standard error.

Prediction Interval

In addition to standard error and confidence intervals (see Chapter 5), a prediction interval is a statistical concept for quantifying uncertainty. A prediction interval expresses the likely range within which the next observation of a series of data will occur.

Table 6.2 summarizes the equivalency between these reporting methods for selected values of standard error in common (base 10) log units. For example, a reported standard error of 0.2 log units is equivalent to a single percentage standard error of 49 percent. Both are also equivalent to reporting upper and lower percentages of 58 and -37 percent.

Table 6.2. Equivalency of alternative standard error reporting methods.

Standard Error (log units)	Standard Error (%)	Standard Error (+%)	Standard Error (-%)
0.1	23	26	-21
0.2	49	58	-37
0.3	78	100	-50
0.4	116	151	-60

The following equations can be used to convert from standard error in log units to the other reporting approaches:

$$SE(\%) = 100\left(e^{5.303\ SE^2} - 1\right)^{0.5} \quad (6.5)$$

$$SE(+\%) = 100\left(10^{SE} - 1\right) \quad (6.6)$$

$$SE(-\%) = 100\left(10^{-SE} - 1\right) \quad (6.7)$$

where:

SE (%)	=	Standard error in percent
SE (+%)	=	Upper standard error in percent
SE (-%)	=	Lower standard error in percent
SE	=	Standard error in common log units
e	=	Natural log base

Standard error provides a measure of accuracy of flow estimates derived from regression equations. Increasingly, USGS reports regression equation accuracy based on 90-percent prediction intervals (e.g., Paretti et al. 2014). The statistical principles are related to those used for the standard error, but the prediction interval allows additional information such as gage record lengths and site-specific basin information to inform the estimate of the prediction interval. The prediction interval uses equations analogous to equations 6.6 and 6.7. An important difference is that equations 6.6 and 6.7 use a 68 percent probability (plus or minus one standard deviation) to define the upper and lower limits. As the name indicates, the 90-percent prediction intervals use a 90 percent probability to define the upper and lower limits. All other factors being equivalent, a higher probability results in a wider gap between the upper and lower limits.

Regardless of the accuracy measure used, the result from applying a regression equation is the most likely estimate for the design flow for the given AEP for the watershed being analyzed based on the information used by the developers of the regression equation. However, the actual design flow could be higher or lower than the estimate computed from the regression equation. Knowing a potential range is generally useful information for the designer seeking to develop robustly designed projects. A large standard error or prediction interval leads to a large range of potential flows, implying greater uncertainty regarding the estimated design flow.

Example 6.2:	Application of standard error.
Objective:	Estimate the range of design flows implied by 1 standard error.

In example 6.1, using the applicable USGS regression equation, the project team estimated the 25-year design flow for the bridge rehabilitation project to be 900 ft^3/s.

Step 1. Find the standard error for the regression equation.

The USGS report (Capesius and Stephens 2009) reported the standard error for the 0.04 annual exceedance probability (AEP) as 40 percent.

Step 2. Convert to log units by solving equation 6.5.

$$40 = 100\left(e^{5.3026\ SE^2} - 1\right)^{0.5}$$

$$(40/100)^2 + 1 = e^{5.3026\,SE^2}$$

$$e^{5.3026\ SE^2} = 1.16$$

Taking the natural logarithm of both sides:

$$5.3026\ SE^2 = 0.148$$

SE = 0.167 in common log units

Step 3. Using equations 6.6 and 6.7, calculate the upper and lower standard error percentages.

$$SE(+\%) = 100\left(10^{SE} - 1\right) = 100\left(10^{0.167} - 1\right) = 47\%$$

$$SE(-\%) = 100\left(10^{-SE} - 1\right) = 100\left(10^{-0.167} - 1\right) = -31\%$$

Step 4. Apply percentages to the regression equation flow.

Upper value: 900 (1+0.47) = 1300 ft^3/s

Lower value: 900 (1-0.31) = 600 ft^3/s

Note: Because the percentage standard error is not symmetrical around the estimate, the upper and lower estimates should be used to compute a flow range rather than the single percent standard error.

Solution:	Based on the regression equation, the 25-year design flow is most likely to be 900 ft^3/s but could range between 600 and 1,300 ft^3/s and be within 1 standard error. This information may be relevant for the bridge rehabilitation project.

6.1.2.3 Comparison with Gaged Estimates

Engineers evaluate peak flow estimates from USGS regression equations using the standard error as described in the previous section. They can also evaluate the results by comparing peak flows estimated from these equations with results obtained from a flood frequency analysis as described in Chapter 5 or other methods. Engineers can gain added insight into possible flood behavior at a given location by applying multiple methods.

This section illustrates a comparison for a gaged watershed of the Medina River near Pipe Creek, Texas (USGS station 08179000). This gage has 42 years of record, drains an area of 474 mi^2, is unregulated, and has station and regional skews of -0.005 and -0.234, respectively. Table 6.3

summarizes the results of the log-Pearson type III distribution analyses using Bulletin 17C (England et al. 2019) with the weighted skew option (G_L = -0.086) and with the station skew.

Table 6.3. Comparison of peak flows from log-Pearson type III distribution and USGS regional regression equations.

Return Period (years)	Log-Pearson Type III Weighted Skew (ft^3/s)	Log-Pearson Type III Station Skew (ft^3/s)	USGS Regression Equations (ft^3/s)
10	49,700	50,300	48,600
25	86,000	89,000	76,400
50	122,000	129,000	102,400
100	167,000	179,000	134,000

Table 6.3 also summarizes the estimates from the applicable USGS regression equations for this location (Asquith and Roussel 2009). In addition to the drainage area, these equations use:

- The main channel slope (0.0031 ft/ft).
- Mean annual precipitation (31 inches).
- Residual adjustment factor, OmegaEM (0.33).

The peak flows estimated from the regression equations are all lower than the comparable values determined from the log-Pearson type III analysis, although all are within the Bulletin 17C 5 and 95 percent confidence limits. (See Chapter 5 for description of confidence limits.)

Further review of the data at this station indicates that a frequency curve constructed using the gaged record with the station skew (and to a lesser extent with the weighted skew) generates higher estimates than regression equations that are based on multiple gages. This is partially a result of a peak flow in 1978 (281,000 ft^3/s), which, according to the log-Pearson type III analysis, is an event approaching the 500-year peak flow.

While this is a single example, it reflects some of the considerations involved in approach selection. Generally, when a project has gaged data available that can be analyzed by the methods described in Chapter 5, designers use the gaged record as at least one source for estimating design discharges. The site-specific information from a gaged record reflects what has occurred at the site over the period of record for the particular meteorological and watershed characteristics. A longer period of record contains more of this valuable information than a shorter record. Two potential limitations of the gage record are that: 1) it does not reflect future events and 2) it could be influenced by outliers.

Looking at Multiple Gages

Adjacent watersheds with comparable characteristics may experience the same storm patterns over a long period but may not experience the same pattern of recorded major floods because of short gage records or the temporal and spatial variation of storm patterns. Examining multiple gages use of regression equation can be beneficial to understanding flood patterns in a watershed.

Because regression equations are based on records from multiple gages over an expanded geographic area, they have the capacity to represent flood frequency relationships that might not be captured in the analysis of a single

gaged record. However, regression equations focus on a relatively small number of explanatory variables.

At a minimum, designers use regression equations as a basis for comparison of statistically determined peak flows of specified frequencies and to further evaluate the results of a frequency analysis. Designers also sometimes use them to add credence to historical flood data or to identify the need for additional analysis of the historical records. Regression equations can also provide insight into the treatment of outliers beyond the purely statistical methods discussed in Chapter 5. Comparison of the peak flows obtained by different methods may indicate the need to review data from other comparable watersheds within a region and the desirability of transposing or extending a given record using data from other gages.

Sauer (1974) proposed a method for using information from both the gage record and similar gaged watersheds in the region using regression equations to improve estimates at gaged locations. The method weights the log-Pearson type III result with the regression equation estimate for the gaged watershed based on the gage record length and the equivalent record length for the regression equation as follows:

$$Q_{gw} = \frac{\left(Q_g N_g + Q_r N_r\right)}{\left(N_g + N_r\right)} \tag{6.8}$$

where:

Q_{gw} = Weighted peak flow estimate at the gage
Q_g = Log-Pearson type III peak flow estimate at the gage
Q_r = Regression equation peak flow estimate at the gage
N_g = Number of years of record at the gage
N_r = Equivalent record length of the regression equation

Others have expanded on this approach using alternative weighting schemes based on the variance of prediction (e.g., Paretti et al. 2014) or the mean square error (e.g., Mastin et al. 2016). The USGS regression report documenting the applicable equations provides information on the weighting scheme and supporting information needed to perform the weighting whether that is equivalent record length as used for equation 6.8 or other weighting parameters. These reports also provide information on when designers may choose to perform weighting to improved estimates of peak flows at gaged sites, such as when the gaged flow record length is short (less than 10 years).

6.1.2.4 Application and Limitations

Generally, hydrologists have developed regional regression equations for peak flow in unregulated, natural, nonurbanized watersheds, striving to separate mixed populations (i.e., rain produced floods from snowmelt floods or hurricane associated storms). Because the equations are regionalized, the user identifies the hydrologic region within which the watershed of interest falls and defines the independent variables in the exact manner specified for each set of regional equations.

In each regional regression report, the USGS provides limits of applicability for the equations in terms of the range of values that each independent variable may take. Typically, the engineer applies the equations only to watersheds within these applicability limits. For example, equation 6.2 recommends that it only be used for drainage areas between 1 and 1060 square miles. Use outside of the recommended limits increases the potential for a misleading result. Under some circumstances, the engineer may determine that application outside the limits would be

informative. In these cases, the standard error of the flow estimates is uncertain, and the results are used with caution.

In some situations, the ungaged watershed of interest may not be wholly contained in a single regional regression hydrologic region. This occurs when a stream or river within the watershed of interest crosses a State border or another hydrologic boundary. In this case, the engineer investigates the hydrologic region in which the outlet of the watershed of interest lies to determine if the watershed parameters fall within the range of values acceptable for that hydrologic region. The engineer also investigates if one or more gaged watersheds included in the development of the regression equations also cross the same boundaries. If so, the engineer applies the regression equations associated with the hydrologic region where the watershed outlet is located. If not, the engineer investigates the watershed parameters and their acceptable ranges for the other hydrologic region in which the watershed of interest is located. Based on the evaluation of the applicability of the regression equations in both hydrologic regions, the engineer selects one as most appropriate or a drainage area weighted estimate from both. If the evaluation determines that the regression equations from both hydrologic regions are unsuitable, the engineer does not use either.

Users of regional regression equations will also consider that:

- Rural equations apply only to rural watersheds and not urban areas unless the effects of urbanization are insignificant.
- Regression equations apply to unregulated watersheds that are not affected by dams, flood-detention structures, and other constructed facilities that have a significant effect on peak flows.
- Some hydrologic regions might not have equations for AEPs of interest particularly for larger discharges such as the 0.01 AEP peak flow. In such cases, the engineer evaluates the flood frequency curve for the AEPs available to determine if interpolation or extrapolation to other AEP peak flows is appropriate. Especially for extrapolation to larger peak flow values, the engineer may apply the flood index method described in Section 6.2.

6.1.3 Regression Equations for Urban Watersheds

The regression equations discussed in Section 6.1.2 primarily apply to rural watersheds. However, many watersheds are partially or fully urbanized. The challenges for extending the regression approach to urban watersheds are identifying appropriate variables to represent the extent of urbanization and determining how to incorporate that information into methods for estimating peak flows. This section focuses on measures of urbanization and State and local urban equations.

6.1.3.1 Measures of Urbanization

Researchers continue to evaluate other approaches to incorporate the effects of urbanization on peak flows developed using regression equations. Measures of urbanization include impervious area, population density, housing density, urbanized land cover, and other indicators of development. Assessing the effects of urbanization requires analysts to consider the changes in watersheds over time and the spatial distribution of urbanization.

Moglen and Shivers (2006) used impervious area and population density and concluded these indicators of urbanization performed well based on analysis of 78 urbanized or partially urbanized gaged streams. Because urbanization takes many forms across the country and runoff is affected by numerous watershed characteristics, use of proxies such as impervious area, population density, or other indicators are limited in their ability to capture these complex effects.

The USGS evaluated several indices of urbanization including percentage of basin occupied by impervious surfaces, population and population density, basin response time, and other indicators of urbanization. In the 1980s, the USGS selected the basin development factor (BDF), which provides a measure of the efficiency of the drainage system within an urbanizing watershed (Sauer et al. 1983). The BDF is still used in some State and local urban equations.

Researchers have examined the effects of impervious cover and urban land uses on annual flood magnitudes and peak streamflow trends nationally (e.g., Blum et al. 2020, Dudley et al. 2018, Hecht and Vogel 2020)). Others have explored relations for more limited geographical areas such as Northeaster Illinois based on the fraction of developed land (Over et al. 2017) and in Delaware based on impervious area and housing density (Ries and Dillow 2006). Some measures and methods have been incorporated into the tools described in Section 6.1.4.

6.1.3.2 State and Local Urban Equations

Many USGS regression studies include additional equations for cities and metropolitan areas developed for local use in those designated areas only. USGS has also completed several statewide urban studies including, for example, Alabama (Hedgecock and Lee 2007), Georgia (Gotvald and Knaak 2011), and Ohio (Sherwood 1994). These studies investigated several measures of urbanization including percent impervious, percent developed, and the BDF and relied on the National Land Cover Database (NLCD) and other resources to establish objective descriptions of percent impervious or percent developed. Application of these equations includes verifying the definition of regression equation variables and using the same or similar databases for quantifying values of the independent variables.

State and local urban equations can be used as an alternative to the nationwide urban equations, or they can be used for comparison purposes. It would be highly coincidental for the local equations and the nationwide equations to give identical results. Therefore, it is suggested to compare results of two (or more) sets of urban equations as well as to compare the urban results to the equivalent rural results. Ultimately, the engineer decides which urban results to use. In addition, some of the rural reports contain estimation techniques for urban watersheds. Several of the rural reports suggest the use of the nationwide equations given by Sauer et al. (1983).

6.1.4 Regression Equations for the Southwestern United States

The USGS (Thomas et al. 1997) provides regression equations for the southwestern United States. The NSS Program (see Section 6.1.5.1) also includes these equations or individual State updates for these equations.

6.1.4.1 Purpose and Scope

The report (Thomas et al. 1997) describes the results of a study to improve the understanding of flood hydrology and develop reliable methods for estimating the magnitude and frequency of floods for gaged and ungaged streams in the southwestern United States. The large study area encompasses all of Arizona, Nevada, and Utah, and parts of California, Colorado, Idaho, New Mexico, Oregon, Texas, and Wyoming. The authors further divided the study area into 16 flood regions shown in Figure 6.1.

The data examined in the study include sites with drainage areas of less than 2,000 mi^2 and mean annual precipitation of less than 68.1 inches. However, the study focused on drainage areas of less than about 200 mi^2 and arid areas with less than 20 inches of mean annual precipitation. Flow regulation does not affect the series of annual peak flows for sites used in this study, and the individual sites have at least 10 years of record through water year 1986. The lower end of applicability of the equations varies by region.

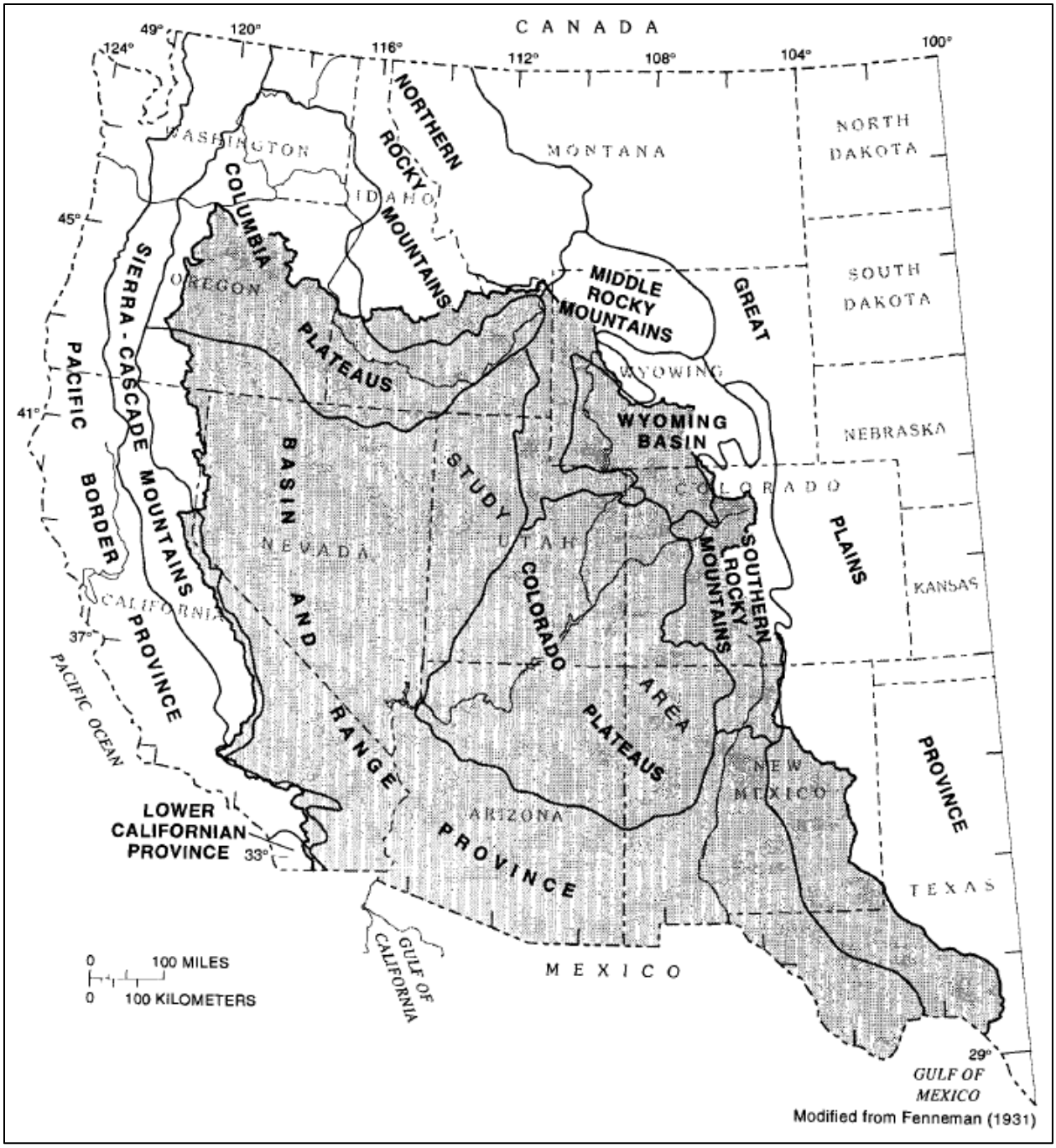

Figure 6.1. Flood regions in study area (Thomas et al. 1997).

The authors determined flood frequency relations at gaged sites using the procedures described in Bulletin 17B (Water Resources Council 1982). The authors related the gaged site flood frequency curves to basin and climatic characteristics using ordinary and generalized least-squares, multiple-regression analyses.

Compared with previous statewide regional studies, this regional study offers several advantages. The time-sampling error of flood estimates can be a problem with small datasets in the southwestern United States. The large database of more than 1,300 gaged sites with about 40,000 station years of annual maximum peaks can decrease this issue. Some of the recent regional studies developed for single States have significant differences in the estimated flood

frequency relations at State boundaries. This study removed these different estimates of flood magnitudes at State boundaries. Regional relations derived from the large database with a large range of values may be more reliable than those from smaller databases and their use for ungaged streams generally involves less extrapolation.

6.1.4.2 Description of Study Area

The study area is over 580,000 mi^2. The area is bounded by the Rocky Mountains on the east, the northern slopes of the Snake River basin on the north, the Cascade-Sierra Mountains on the west, and the border with Mexico on the south. The Basin and Range Province in the western and southern part of the study area has mostly isolated block mountains separated by aggraded desert plains. The mountains commonly rise abruptly from the valley floors and have piedmont plains extending downward to neighboring basin floors. Several large flat desert areas are interspersed between the mountains, including some old lake bottoms that have not been covered with water for hundreds of years. Many of the piedmont plains contain distributary-flow areas composed of material deposited by mountain-front runoff.

Most of the streams in the study area flow only in direct response to rainfall or snowmelt. In the northern latitudes and in the cooler and more humid climate at the higher elevations, most of the streams flow continuously. Streams in alluvial valleys and base-level plains are perennial or intermittent where the stream receives ground water outflow. Small streams in the southern latitudes commonly flow only a few hours during a year.

An arid or semiarid climate in the middle latitudes exists where potential evaporation from the soil surface and from vegetation exceeds the average annual precipitation. About 90 percent of the study area is arid or semiarid and has a mean annual precipitation of less than 20 inches. In addition to the generally meager precipitation, extreme variations in precipitation and temperature characterize the climate of the study area. Mean annual precipitation ranges from more than 50 inches in the Cascade-Sierra Mountains in California to less than 3.1 inches in the deserts of southwestern Arizona and southeastern California. Temperatures range from about 109 °F in the southwestern deserts in the summer to below 0 °F in the northern latitudes and mountains in the winter. Precipitation in the study area varies temporally and spatially. In some extremely arid parts of the study area, the rainfall from one or two summer thunderstorms has exceeded the mean annual precipitation.

6.1.4.3 Peak Flow Equations

The USGS study authors developed equations for estimating 2-, 5-, 10-, 15-, 50-, and 100-year peak flows at ungaged sites in the southwestern United States using generalized least-squares, multiple-regression techniques, and a hybrid method the authors developed in this study. The equations apply to unregulated streams that drain basins of less than about 200 mi^2. The equations use the basin and climatic characteristics of drainage area, mean basin elevation, mean annual precipitation, mean annual evaporation, latitude, and longitude. Table 6.4 gives the equations for one region as an illustration.

The authors made detailed flood frequency analyses of more than 1,300 gaging stations with a combined 40,000 station years of annual peak flows through water year 1986. They used the log-Pearson type III distribution and the method of moments to develop flood frequency relations. The authors applied a low-discharge threshold to about half of the sites to adjust the relations for low outliers. With few exceptions, the use of the low-discharge threshold resulted in markedly better appearing fits between the computed relations and the plotted annual peak flows. After the authors made all adjustments, they judged 80 percent of the gaging stations to have adequate fits of computed relations to the plotted data. The authors judged individual flood frequency relations to be unreliable for the remaining 20 percent of the stations because of extremely poor fits of the computed relations to the data, and they did not use these relations in the generalized

least-squares regional regression analysis. Most of the stations with unreliable relations were from extremely arid areas, with 43 percent of the stations having no flow for more than 25 percent of the years of record. The authors developed a new regional flood frequency method, named the hybrid method, for those more arid regions.

The authors analyzed regional skew coefficient for the study area. The methods of attempting to define the variation in skew by geographic areas or by regression with basin and climatic characteristics all failed to improve on a mean of zero for the sample. Therefore, for the regional skew in the study, the authors used a mean of zero with an associated error equal to the sample variance of 0.31 log units.

The general form for the equations for High-Elevation Region 1 is typical of many of the equations:

$$Q_T = a_T A^{b_{1T}} P^{b_{2T}} \quad (6.9)$$

where:

Q_T = Peak flow for return period T, ft^3/s (m^3/s)
A = Drainage area, mi^2 (km^2)
P = Mean annual precipitation, inches (mm)
a_T = Constant summarized in Table 6.4
b_{1T}, b_{2T} = Exponents summarized in Table 6.4

Table 6.4. Generalized least-squares regression equations for estimating regional flood-frequency relations for the high-elevation region 1 (Thomas et al. 1997).

Return Period, T (years)	a_T	b_{1T}	b_{2T}	Average Standard Error (%)	Equivalent Record Length (years)
2	0.124	0.845	1.44	59	0.16
5	0.629	0.807	1.12	52	0.62
10	1.43	0.786	0.958	48	1.34
25	3.08	0.768	0.811	46	2.50
50	4.75	0.758	0.732	46	3.37
100	6.78	0.750	0.668	46	4.19

6.1.5 Application Tools

The USGS develops and publishes regression equations for estimating streamflow statistics for every State, the Commonwealth of Puerto Rico, and several metropolitan areas in the U.S. These can be applied directly as illustrated in previous sections or using an application tool. Two tools are described in this section: the NSS program and StreamStats.

6.1.5.1 National Streamflow Statistics Program

The USGS has compiled its regression equations into the NSS program (Ries 2006). The NSS program is a useful tool for engineers, hydrologists, and others for planning, management, and design applications.

The regression equations included in NSS can be used to transfer streamflow statistics from gaged to ungaged sites using watershed and climatic characteristics as explanatory or predictor variables. Generally, the equations were developed on a statewide or metropolitan-area basis as

part of cooperative study programs. Equations are available for estimating rural and urban flood frequency statistics, such as the 100-year flood, for every State, the Commonwealth of Puerto Rico, and the island of Tutuila, American Samoa. Equations are available for estimating other statistics, such as the mean annual flow, monthly mean flows, flow duration percentiles, and low flow frequencies (such as the 7-day, 10-year low flow (7Q10)) for many of the States.

Each equation used in the NSS program has limitations that should be understood by the user. This information can be found in the latest report listed on the NSS publications page. The NSS output provides indicators of the accuracy of the estimated streamflow statistics. The indicators may include any combination of the standard error of estimate, the standard error of prediction, the equivalent years of record, or 90-percent prediction intervals.

6.1.5.2 StreamStats

StreamStats provides access to spatial analytical tools, including the USGS peak flow regression equations, for water resources planning and management, and for engineering and design purposes. When the USGS develops new peak flow regression equations for a State or region, USGS generally incorporates these into StreamStats.

This web application accesses an assortment of geographic information systems (GIS) analytical tools through a map-based user interface. The application can delineate drainage areas for user-selected sites on streams, and then extract basin characteristics and estimates of flow statistics for the sites where this functionality is available. StreamStats users also can select the locations of USGS data collection stations and retrieve flow statistics and other information for the stations. The types of flow statistics and other information available vary from State to State. Additional tools are available.

6.2 Rational Method

One of the most commonly used equations for the calculation of peak flows from small drainage areas is the Rational Method, which is given as:

$$Q = CiA / \alpha \qquad (6.10)$$

where:

Q	=	Peak flow, ft^3/s (m^3/s)
i	=	Rainfall intensity for the design storm, in/h (mm/h)
A	=	Drainage area, ac (ha)
C	=	Dimensionless runoff coefficient assumed to be a function of the cover of the watershed
α	=	Unit conversion constant, 1.0 in CU (360 in SI)

6.2.1 Assumptions

The assumptions in the Rational Method are:

- The drainage area is typically 200 ac (80 ha) or smaller.
- The peak flow occurs when the entire watershed is contributing.
- A storm that has a uniform intensity based on a duration equal to t_c produces the highest peak flow for any given frequency.
- The rainfall intensity is uniform over a storm time duration equal to the time of concentration, t_c. The time of concentration is the time for water to travel from the hydrologically most remote point of the basin to the outlet or point of interest.

- The frequency of the computed peak flow is equal to the frequency of the rainfall intensity. In other words, the 10-year rainfall intensity, i, is assumed to produce the 10-year peak flow.

6.2.2 Estimating Input Requirements

The runoff coefficient, C, is a function of surface conditions including slope, soil type, and presence of vegetation. These conditions affect infiltration and other hydrologic abstractions and, therefore, the value of C. Some typical values of C for the Rational Method are given in Table 6.5.

Table 6.5. Runoff coefficients for the Rational Method (ASCE 1960).

Land Use Category	Type of Drainage Area	Runoff Coefficient, C
Business	Downtown area	0.70 – 0.95
	Neighborhood areas	0.50 – 0.70
Residential	Single-family areas	0.30 – 0.50
	Multi-units, detached	0.40 – 0.60
	Multi-units, attached	0.60 – 0.75
	Suburban	0.25 – 0.40
	Apartment dwelling areas	0.50 – 0.70
Industrial	Light areas	0.50 – 0.80
	Heavy areas	0.60 – 0.90
Open	Parks, cemeteries	0.10 – 0.25
	Playgrounds	0.20 – 0.40
	Railroad yard areas	0.20 – 0.40
	Unimproved areas	0.10 – 0.30
Lawns	Sandy soil, flat, < 2%	0.05 – 0.10
	Sandy soil, average, 2 to 7%	0.10 – 0.15
	Sandy soil, steep, > 7%	0.15 – 0.20
	Heavy soil, flat, < 2%	0.13 – 0.17
	Heavy soil, average 2 to 7%	0.18 – 0.22
	Heavy soil, steep, > 7%	0.25 – 0.35
Streets	Asphalt	0.70 – 0.95
	Concrete	0.80 – 0.95
	Brick	0.70 – 0.85
Other impervious	Drives and walks	0.75 – 0.85
	Roofs	0.75 – 0.95

To select values from within the range, designers consider the watershed slope, hydrologic soil group (HSG) (see Section 7.1.3), and the presence of vegetation. Many local, State, and Federal agencies maintain their own values for runoff coefficient which designers can use when applicable. Some tables of C provide for variation with the AEP of the design discharge. In practice, C is usually derived from volumetric balance that relates the peak flow to the "theoretical peak" or 100 percent runoff and an ideal peak rate, occurring when runoff matches the net rain rate.

If the basin contains varying amounts of different covers, a weighted runoff coefficient for the entire basin can be determined as:

$$\text{Weighted } C = \frac{\sum C_i A_i}{A} \tag{6.11}$$

where:

C_i = Runoff coefficient for cover type i that covers area A_i
A = Total area.

6.2.3 Check for Critical Design Condition

When the Rational Method is used to design multiple drainage elements (i.e., inlets and pipes), the design process proceeds from upstream to downstream. For each design element, a time of concentration is computed, the corresponding intensity determined, and the peak flow computed. For pipes that drain multiple flow paths, the engineer determines the longest time of concentration from all the contributing areas. If upstream pipes exist, the engineer also includes travel times in these pipes in the calculation of time of concentration.

In most cases, especially as computations proceed downstream, the contributing area with the longer time of concentration also contributes the greatest flow. Taking the case of two contributing areas, as shown in Figure 6.2, the longest time of concentration of the two areas is used to determine the time of concentration for the combined area. When the rainfall intensity corresponding to this time of concentration is applied to the rational equation for the combined area and runoff coefficient, the appropriate design discharge, Q, results:

$$Q = (1/\alpha)(C_1 A_1 + C_2 A_2)i_1 \tag{6.12}$$

However, it may be possible for the larger contributing flows to be generated from the contributing area with a shorter time of concentration. If this occurs, it is also possible that, if the longer time of concentration is applied to the combined drainage area, the resulting design flow would be an underestimate. Therefore, the engineer conducts a check for a critical design condition:

$$Q' = (1/\alpha)(C_1 A_1(t_2/t_1) + C_2 A_2)i_2 \tag{6.13}$$

where:

Q' = Design check discharge
t_1 = Time of concentration for area 1 (longer)
t_2 = Time of concentration for area 2 (shorter)

If Q' > Q, choose Q' design; otherwise, choose Q. Equation 6.13 uses the rainfall intensity for the contributing area with the shorter time of concentration (area 2) and reduces the contribution of area 1 by the ratio of the times of concentration. This ratio approximates the fraction of the area

that would contribute within the shorter duration. This is equivalent to reducing the contributing area as shown by the dashed line in Figure 6.2.

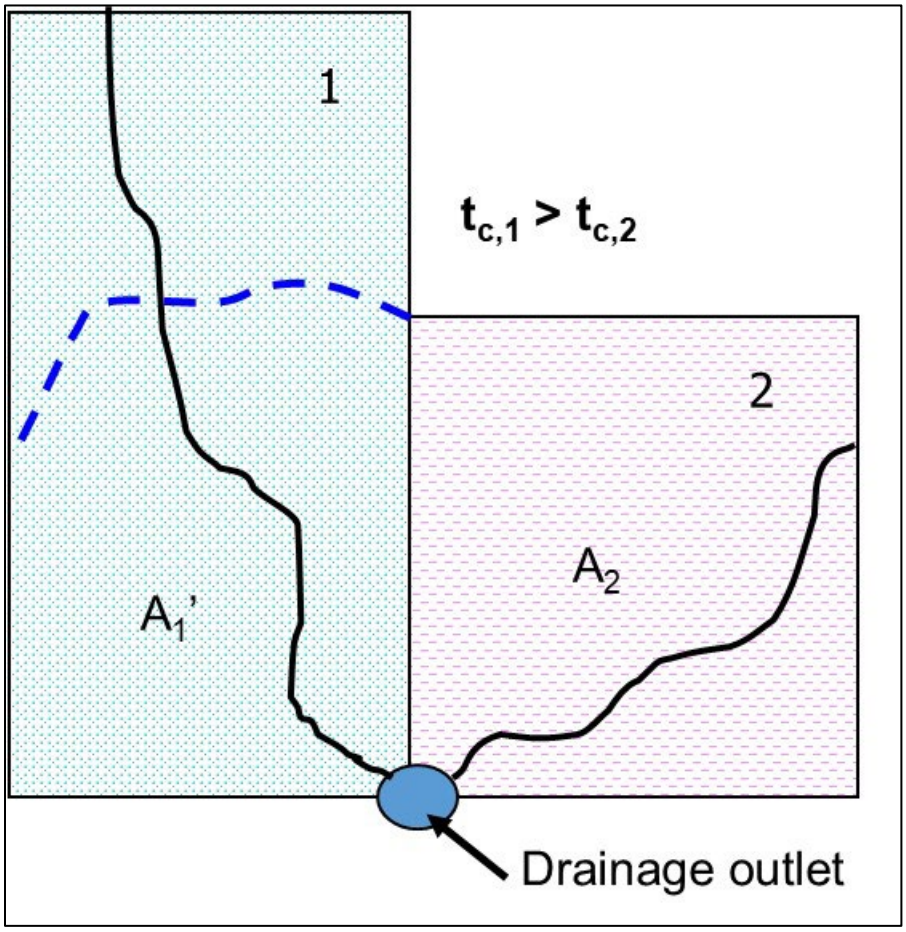

Figure 6.2. Multiple drainage area system schematic.

Example 6.3.	A flooding problem exists along a road near Memphis, Tennessee. A low water crossing is to be replaced by a culvert installation to improve road safety during rainstorms.
Objective:	Estimate the maximum discharge that the culvert must pass for the indicated design storm.

Given: A contributing watershed with the following characteristics:

A = 108 acres (43.7 ha)
RP = 25 years (as stipulated by local authorities)

The watershed current land use consists of parkland, commercial property, and single-family residential housing, the data for which is provided in the table below. The principal flow path is comprised of a grassed waterway. Use the following steps to compute the peak flow with the Rational Method.

Step 1. Compute a weighted runoff coefficient.

Table 6.6 summarizes runoff coefficients for the example based on runoff coefficients from Table 6.5. The average value is used for the parkland and the residential areas, but the highest value is used for the commercial property because it is completely impervious.

Table 6.6. Runoff coefficients for the example.

Description	C Value	Area (acres)	C_iA_i
Park	0.20	53.9	10.8
Commercial (100% impervious)	0.95	3.7	3.5
Single-family	0.40	50.4	20.2
Total	--	108.0	34.5

Weighted C = $(\Sigma C_iA_i) / A = 34.5 / 108.0 = 0.32$

Step 2. Estimate time of concentration.

The 25-year intensity is taken from an intensity-duration-frequency (IDF) curve for Memphis and shown in Figure 6.3. To obtain the intensity, the engineer first estimates the time of concentration, t_c. In this example, the velocity method for t_c is used to compute t_c. Table 6.7 summarizes the flow path characteristics.

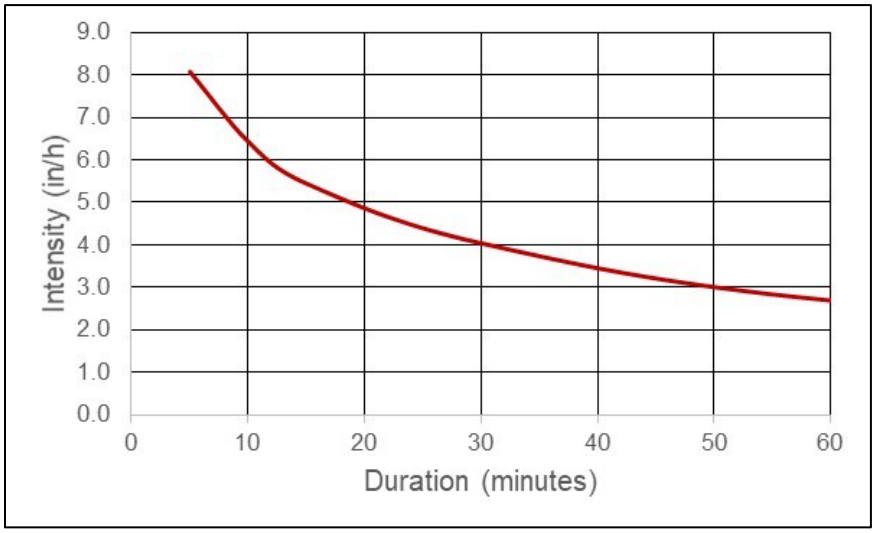

Figure 6.3. IDF curve for example.

Table 6.7. Flow path characteristics for the example.

Flow Path	Slope (%)	Length (ft)	Velocity (ft/s)
Overland (Short grass)	2	295	1.0
Grassed waterway	2	985	2.1
Grassed waterway	1	2,130	1.5

Calculate the time of concentration:

$t_c = \Sigma(L / V) = (295 / 1.0) + (985 / 2.1) + (2{,}130 / 1.5) = 36$ min

Step 3. Calculate 25-year rainfall intensity.

The intensity is obtained from the IDF curve in Figure 6.3 using a storm duration equal to a time of concentration of 36 min which is approximately:

$i_{25} = 3.6$ in/h

Step 4. Estimate 25-year peak flow.

$Q_{25} = CiA = (0.32)(3.6)(108) = 124$ ft^3/s

Solution: The 25-year design flow is 124 ft^3/s.

6.3 Index Flood Method

Where data about the watershed of interest are limited or entirely unavailable, the U.S. Geological Survey (USGS) index flood method can help determine peak flows for various exceedance frequencies using regional statistical methods. The method facilitates estimation of design discharges at ungaged sites based on flood frequency analysis of historical data at gaged sites.

The index flood method is based on flood frequency curves (FFCs). This section describes the index flood method and how designers can use it where other methods are not applicable, where human influences may be suspected, or where climate change may be considered. Designers also use FFCs for validation and comparison with other methods.

The FFC for each watershed can be considered unique to that watershed, but all FFCs:

- Monotonically increase with decreasing probability of exceedance.
- Relate to watershed characteristics.
- Relate to nearby, similar watersheds.

Given these similarities between all FFCs, designers can gain useful information by comparing FFCs on a given watershed with nearby, similar watersheds.

A Reliable Workhorse

Designers used the index flood method of regional analysis described by Dalrymple (1960) extensively in the 1960s and early 1970s. Since the advent of USGS regional regression equations, use of the index flood method has diminished in the United States, but it is still popular in many other areas of the world and still useful in the United States.

The fundamental assumption behind the index flood method is that the shape (change in discharge from one probability value to another) of a flood frequency curve is relatively invariant within reasonable bounds of geography and watershed characteristics. The shape of an FFC is captured by selecting a base value from the FFC—the index flood discharge—and dividing each of the calculated discharges at desired probability quantiles by that value. The multiplier of the index flood itself is unity. From these ratios, the shape of the FFC is captured.

Since FFCs are monotonically increasing with decreasing probability of exceedance, quantile values with greater probability of exceedance than the index flood result in smaller discharges with flood ratios between 0 and 1. Quantile values with smaller probability of exceedance than the index flood result in discharges larger than the index flood and flood ratios greater than 1.

The base value for index flood computations can be any quantile flood but is commonly the mean annual flood. However, for highway hydrologic studies, the most common floods of interest range from 0.5 AEP (2-year) to 0.01 AEP (100-year) or larger. Choosing the mean annual flood as the base value places the index point at or near the frequent occurrence end of the curve. Uncertainty and error grow in proportion to distance from the index. Therefore, if the analyst is interested in the 0.5 AEP to 0.01 AEP part of the FFC, choosing a base value more central, e.g., the 0.1 AEP (10-year), will tend to reduce the uncertainty and error throughout that part of the FFC.

Information available on annual peak series gage analysis for regression equations suggests that standard errors of estimate often are the smallest at around the 0.1 AEP. There appears to be some loss of resolution at frequent AEP values for annual peak series that increases uncertainty for those values, while data series are seldom long enough to provide good resolution for infrequent values. Use of the 0.1 AEP (10-year return period) flood estimate as an index flood provides balance between the extremes. The 10-year flood discharge can be thought of as sufficiently rare to avoid the loss of information resolution apparent in frequent flood values obtained using annual peak series, yet sufficiently frequent as to fall well within the data range of many gage data series. The result is that using the 10-year flood as the index flood provides a balance of competing deficiencies in information.

6.3.1 General Procedure

When applying the index flood method, the hydrologic engineer can choose from a variety of methods within that process. Typical steps are:

Step 1. Develop FFCs for one or more nearby, similar gaged watersheds using statistical analysis.

The analyst estimates the existing FFC for the selected gaged site or sites by statistical analysis. In the absence of nearby gages, FFCs for nearby watersheds with similar conditions of regulation, diversion, urbanization, or land use can be estimated by any appropriate method. Statistical analysis of gage data is the preferred technique because it gives insight into specific characteristics of local watershed influences.

Step 2. Calculate the flood ratios using the 0.1 AEP as the index value. If more than one gaged watershed is analyzed, compare the flood ratios for each quantile value from the various FFCs. Develop flood ratios for the site of interest.

The analyst divides the discharge associated with each individual AEP quantile by the 0.1 AEP discharge for the same site to create a series of dimensionless ratios representing the relation of each quantile to the 0.1 AEP flood discharge. The ratio for the 0.1 AEP is 1.0. The analyst selects flood ratios for the site of interest from the individual FFCs calculated, averages them, or weights them by proximity and similarity to the site of interest. Using multiple nearby and similar gage series provides validation to prevent the use of a single, possibly anomalous, FFC. The selection of a final FFC is left to the judgment of the engineer, considering the specific needs and priorities of the project involved.

Step 3. Estimate the 0.1 AEP flood for the site of interest. If desired, the entire FFC of the site of interest may be computed to compare flood ratios derived from the selected technique with those derived from other methods.

The analyst estimates the 0.1 AEP discharge for the site of interest. The engineer chooses the method or methods appropriate for the site, conditions, information available, and project needs. For instance, if design for future urbanization or land use change is needed, the 0.1 AEP discharge developed for the future condition would be the appropriate index flood.

Step 4. Calculate the FFC for the site using the flood ratios from step 2 and the estimated 0.1 AEP discharge for the site from step 3.

The ratios for the selected FFC are from step 2 are multiplied by the 0.1 AEP flood from step 3 to create an FFC at the site of interest. The relative change in magnitude of the quantiles with respect to the index flood reflect local influences that are otherwise difficult or impossible to quantify. These steps are illustrated in the example below.

Example 6.4:	Application of the index flood method.
Objective:	Develop a flood frequency curve based on nearby gage data and compare with regional regression equation results to develop a 0.02 AEP design discharge.

Consider a culvert location in Kingfisher County, Oklahoma, with a 0.02 AEP design discharge requirement. The watershed contributing area is 23.5 square miles, of which 14.7 square miles are controlled by two small reservoirs constructed in the 1960s. Because of the presence of the reservoirs, the project team seeks to develop peak flow estimates using multiple methods.

Regression equations for Oklahoma are published in USGS Scientific Investigations Report (SIR) 2010-5137 (Lewis 2010) and use three independent variables and their values for this watershed:

- Contributing area - uncontrolled area is 8.8 square miles.
- Area-weighted mean annual precipitation (MAP) – 31.5 inches.
- Main watercourse slope calculated in the portion of the watercourse between 10 percent and 85 percent upstream of the site of interest, in feet per mile – 10.87 ft/mi.

The SIR contains a procedure for estimating discharge for watersheds controlled by reservoirs, which replaces the contributing area with uncontrolled area, but retains the entire main watercourse slope.

Step 1. Select a gage or set of gages on nearby and/or similar watersheds for analysis and develop FFCs.

Calculate an FFC for each gage using historically based statistical analysis methods. In this case, the project team selected four nearby gages based on their proximity to the site of interest and one another. The number and nature of gages selected varies with the number of gages available and the specific characteristics of the site. The design engineer may believe that similarity of characteristics is more important than proximity. In many cases, the number of suitable gages available may be a limiting factor. In cases of regionalized analyses by USGS, it may not be advisable to cross regional boundaries.

Table 6.8 summarizes the watershed characteristics that were significant in the USGS regression equations. The MAP and slope of the four gaged watersheds is close to the watershed of interest for this example. The contributing area of the design location is close to that of the Salt Creek Tributary (USGS station 07158180) and less than the other three gages.

Step 2. Calculate the historical flood ratios using the 10-year flood as the index value.

The project team computes the flood ratios using the 0.1 AEP flood as the index flood. Table 6.10 summarizes the flood ratios, with the mean and the median values for each AEP. The ratios vary among the gages with the 0.5 AEP showing ratios ranging from 0.13 to 0.46 and the 0.01 AEP showing ratios ranging from 2.07 to 5.56. However, the mean and median values for each AEP are relatively consistent.

Table 6.9 shows the FFC values resulting from Bulletin 17C analysis of the gages.

Table 6.8. USGS gages selected for example analysis for index flood method.

Gage No.	Gage Name	Contributing Area (mi^2)	MAP (inches)	Slope (ft/mi)
07158180	Salt Creek Trib. near Okeene, OK	8.37	30.9	12.71
07158400	Salt Creek near Okeene, OK	181.49	30.9	8.45
07158500	Preacher Creek near Dover, OK	14.33	32.8	14.47
07159200	Kingfisher Creek near Kingfisher, OK	165.14	31.8	6.44

Table 6.9. Estimated AEP discharges by Bulletin 17C analysis of selected USGS gages.

Gage No.	Gage Name	Discharge by AEP (ft^3/s)					
		0.50	0.20	0.10	0.04	0.02	0.01
07158180	Salt Creek Trib. near Okeene, OK	718	2,189	3,899	6,266	10,659	15,166
07158400	Salt Creek near Okeene, OK	4,677	7,620	10,066	12,825	17,074	20,830
07158500	Preacher Creek near Dover, OK	189	713	1,373	2,311	4,068	5,859
07159200	Kingfisher Creek near Kingfisher, OK	2,860	11,009	22,455	40,627	79,552	124,856

Table 6.10. Flood ratios for the selected USGS gages.

Gage No.	Gage Name	0.50	0.20	0.10	0.04	0.02	0.01
07158180	Salt Creek Trib. near Okeene, OK	0.18	0.56	1.00	1.61	2.73	3.89
07158400	Salt Creek near Okeene, OK	0.46	0.76	1.00	1.27	1.70	2.07
07158500	Preacher Creek near Dover, OK	0.14	0.52	1.00	1.68	2.96	4.27
07159200	Kingfisher Creek near Kingfisher, OK	0.13	0.49	1.00	1.81	3.54	5.56
Mean	--	0.23	0.58	1.00	1.59	2.73	3.95
Median	--	0.16	0.54	1.00	1.65	2.85	4.08

Figure 6.4 displays the same flood ratios in graphical form using a log scale on the vertical axis and a probability scale on the horizontal axis. The variation between the gages is an indication of the differences in watershed characteristics including potentially unknown and

poorly understood influences on flood frequency that may not be evident in other kinds of analyses.

The project team selects a representative set of flood ratios applicable to the watershed of interest considering the nature and criticality of the project under design. For the 0.04, 0.02, or 0.01 AEP, selection of the largest values (associated with gage 07159200) would be the conservative approach. Selection of the mean or median values, or values corresponding to gages 07158180 or 07158500 would be considered of mid-level risk, whereas the selection of values from gage 07158400 might be considered unnecessarily risky.

Because this is not a high-risk site, the project team selects the mean value of the flood ratios from Table 6.10 for the index flood analysis. The mean values are also close to the ratios for the Salt Creek Tributary which is closest in size to the design watershed and has similar slope and MAP characteristics.

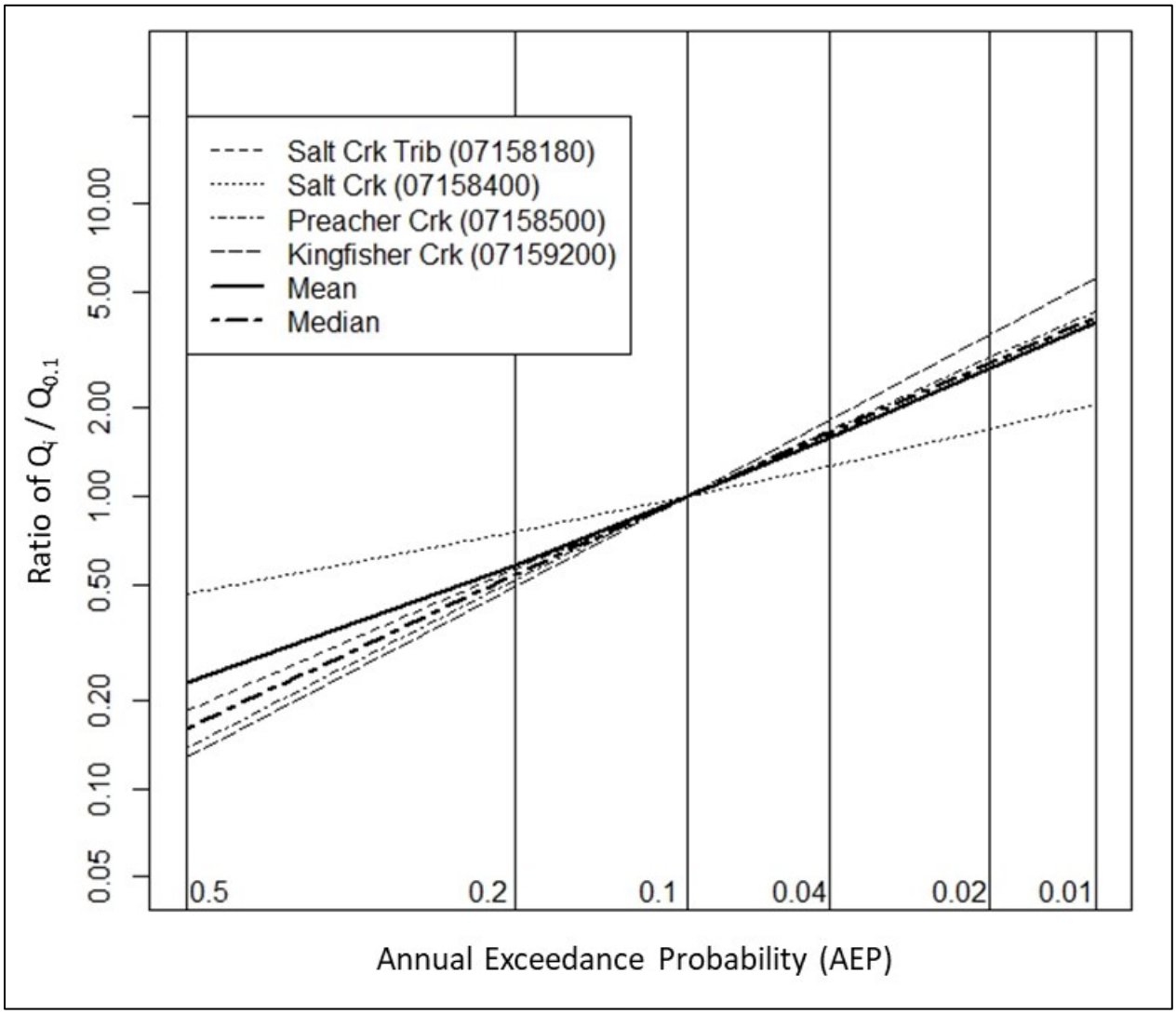

Figure 6.4. Flood ratio curves for four Oklahoma watersheds selected for comparison with the results of regression equations.

Step 3. Estimate the 0.1 AEP flood for the site.

The analyst estimates the index flood value (0.1 AEP) using any method appropriate for the site. This may include regression equations as illustrated in this example or, alternatively, a rainfall-runoff model.

Table 6.11 summarizes application of the USGS regression equations from Lewis (2010) for the site. The discharge estimated by the regression equations for the 0.1 AEP flood is 1620 ft^3/s. The table also summarizes the flood ratios computed for the site for purposes of comparison. These are not needed to perform the index adjustment method. For example, the flood ratio for the 0.02 AEP is 3420/1620 = 2.11.

Comparing this value with the ratios shown in Table 6.10 and discussed in step 2, the flood ratios developed from regression equations alone appear to represent an FFC that falls on the side of greater risk at the levels usually associated with highway structure design. Specifically, the flood ratio for the 0.02 AEP (2.11) is smaller than three of the four gages analyzed, and smaller than the mean or median values in Table 6.10. The converse is true for the more frequently occurring AEPs, e.g., the 0.5 AEP.

Table 6.11. Discharges from the regression equations and the corresponding flood ratios.

Quantity	AEP					
	0.5	0.2	0.1	0.04	0.02	0.01
Discharge (ft^3/s)	480	1050	1620	2570	3420	4360
Flood Ratio	0.30	0.65	1.00	1.59	2.11	2.69

Step 4. Calculate the FFC for the site.

Calculate the FFC for the site using flood ratios selected from step 2 and the 0.1 AEP discharge from step 3. Table 6.12 summarizes the results of multiplying the index flood from regression equations by the mean of the flood ratios from the gage analyses in Table 6.10.

Table 6.12 also compares the index flood results with the results of evaluating the regression equations alone. Flood discharges for any AEP on the FFC can then be used for hydraulic design or may be considered validation for a selected design value.

Table 6.12. Results of index method and regression equations for the site by AEP.

Quantity	AEP					
	0.5	0.2	0.1	0.04	0.02	0.01
Selected Index Flood Ratio	0.23	0.58	1.00	1.59	2.73	3.95
Index Flood FFC (ft^3/s)	370	943	1,620	2,581	4,429	6,394
Regression Equation FFC (ft^3/s)	480	1,050	1,620	2,570	3,420	4,360

Solution: For this example, the project team seeks a 0.02 AEP design value. The regression equations produced a 3,420 ft^3/s value while the index flood method produced a 4,429 ft^3/s estimate. The latter estimate may also be compared with standard error associated with the regression equation as discussed in Section 6.1.2.2.

Using the index flood method in the hydrologic design process provides a direct connection to measured flood discharges (gage data) from watersheds that are nearby geographically and/or similar in character to an ungaged watershed. Regression equations are based on gaged data but are reduced to a few explanatory variables. It is ultimately left to the judgment of the design engineer to weigh the uncertainties in estimation techniques and select a design discharge.

6.3.2 Applicability and Limitations

The index flood method applies to most watersheds when comparable gaged watersheds are available to serve as the basis for the analysis. Designers use the method to directly compute design discharges and to provide a basis for comparison with design discharges generated from other methods such as regression equations and rainfall-runoff modeling. By using gaged flow information, the index flood method reveals the shape of the FFC for watersheds similar to an ungaged watershed of interest that provides the analyst with important insights into possible behavior of the watershed of interest.

The utility of the index flood approach is that it can capture watershed conditions that contribute to the unique shape of the FFC for each watershed within reasonable bounds of geography and similarity. Whether identified or not, the approach captures watershed and meteorological conditions in the shape of the curves. Changes in watershed conditions (land use, vegetative cover, transport efficiency, etc.) could result in changes in the shape of the FFC, but can be addressed comparatively, in a similar manner.

As discussed in Section 6.1.2, regression equations developed by the USGS are the product of "pooling" information from many gages in a region considered homogeneous for flood frequency analysis. While the process of pooling information quantifies and emphasizes general relationships, it also can obscure specific aspects of the watersheds contributing to the gages. Characteristics such as flood control dams, urbanization, changes in land use or vegetation, and/or contouring/terracing of farmland may be important for some watersheds and not be reflected in the applicable regression equations. Comparing FFC shape using the index flood method to data from gages selected for similarity and proximity can provide the designer with information on how those characteristics may influence flood frequency.

This discussion has described the index flood method in conjunction with regression equations. However, designers can substitute rainfall-runoff modeling, transposition from gaged watersheds, or other methods for regression equations to estimate the index flood. The procedures outlined above can reasonably be applied to any FFC developed using methods typically used to develop design discharges. Engineers can assess the reasonability of flood ratios of an FFC developed by any method by comparing them to flood ratios for similar, nearby gaged sites, or those for watersheds with similar characteristics.

Regression equation development reports can be a source of gaged information for performing the index flood method. The results of gage analysis in regions thought to be homogeneous and used in the development of

Flood Ratios and GIS

USGS publications documenting the development of regional regression equations often contain a listing of stream gages used in the analysis, and the discharge estimates developed from statistical analysis of the gage data.

Geographical coordinates of gages are also available, occasionally in the same publications. A GIS database of estimated discharges, watershed characteristics, and flood ratios can be developed for a State, region, or DOT district. Such a database can enhance access to historically derived information and flood ratios.

regression equations are frequently available in the documentation accompanying the regression equations themselves. Flood ratios for suitable gages in a region can be calculated, tabulated, and made generally available for future reference, for use in comparison, validation, or transposition of FFC shape within a region. Summary statistics of the distribution of flood ratios for each quantile provide insight for the identification of anomalous or apparently unusual watershed behavior.

Engineers typically design highway drainage structures for a single design discharge, that is, the discharge associated with a specific AEP (or return period), and possibly for a check flood, a rare event used to assess the effects of exceedance of the design discharge. The risk of damage because of an exceeding event increases with the discharge associated with that event. Engineers can use flood ratios to compare relative risk of damage of events exceeding the design discharge. Large flood ratios imply greater potential risk and may lead a design engineer to consider damage mitigating measures; small flood ratios may be cause for less concern.

6.4 Peak Flow Envelope Curves

Design engineers may seek some assurance that a design peak flow is unlikely to occur over the design life of a project. One way to accomplish this is to compare the design peak to actual peaks of record. Crippen and Bue (1977) developed envelope curves for the conterminous U.S., with 17 regions delineated shown in Figure 6.5. They plotted maximum flood flow data from 883 sites with drainage areas less than 10,000 mi^2 versus drainage area and constructed upper envelope curves. Crippen and Bue fit the curves for the 17 regions to the logarithmic polynomial model:

$$q_{env} = K_1 A^{K_2} \left[L + A^{0.5} \right]^{K_3} \quad (6.14)$$

where:

q_{env} = Maximum flood flow envelope, ft^3/s (m^3/s)
L = Length constant, 5.0 mi (8.0 km)
A = Drainage area, mi^2 (km^2)
K_1, K_2, K_3 = Polynomial constants

Table 6.13 provides the values of the coefficients K_1, K_2, and K_3 and the upper limit on the drainage area for each region. The curves are valid for drainage areas greater than 0.1 mi^2. Crippen and Bue did not assign an exceedance probability to the flood flows used to fit the curves.

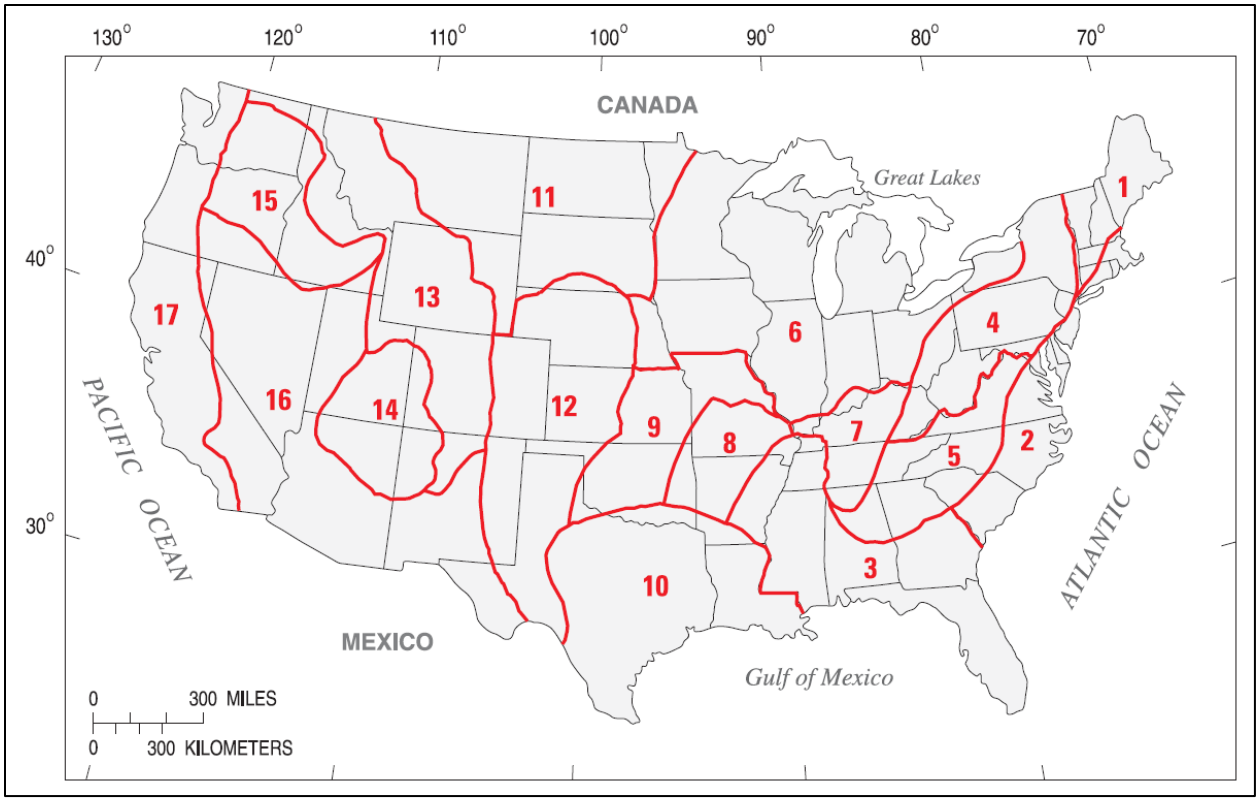

Figure 6.5. Map of the conterminous U.S. showing flood-region boundaries.

Table 6.13. Coefficients for peak flow envelope curves.

Region	Upper Limit (mi^2)	K_1	K_2	K_3
1	10,000	23,200	0.895	-1.082
2	3,000	28,000	0.770	-0.897
3	10,000	54,400	0.924	-1.373
4	10,000	42,600	0.938	-1.327
5	10,000	121,000	0.838	-1.354
6	10,000	70,500	0.937	-1.297
7	10,000	49,100	0.883	-1.352
8	10,000	43,800	0.954	-1.357
9	10,000	75,000	0.849	-1.368
10	1,000	62,500	1.116	-1.371
11	10,000	40,800	0.919	-1.352
12	7,000	89,900	0.935	-1.304
13	10,000	64,500	0.873	-1.338
14	10,000	10,000	0.710	-0.844
15	19	116,000	1.059	-1.572
16	1,000	98,900	1.029	-1.341
17	10,000	80,500	1.024	-1.461

Chapter 7 - Loss Models for Rainfall-Runoff Methods

In the design of roadway drainage structures such as culverts and bridges, the engineer typically estimates the peak flow for the stream for some designated probability. Designers have several ways of estimating discharge, each with its limitations. Gage analysis depends on the availability of a stream gage that has been in place for many years. As discussed in Section 6.1, regional regression equations generally apply to natural, nonurbanized watersheds where watershed characteristics are reasonably consistent with the data used to create the equations. The Rational Method only applies to small watersheds, usually 200 acres or less. If none of the other methods are appropriate, designers may choose to model the process of runoff resulting from rainfall. The most common method is the unit hydrograph method, detailed in Section 8.1.

Modeling a watershed using the unit hydrograph method uses empirically derived rainfall depth-duration-frequency and distribution information. However, much of the rain that falls does not become runoff but is “lost” to infiltration, evaporation, and in-watershed storage. Methods of simulating the process of estimating the portion of rainfall that does not run off are called “loss models.” That portion of rainfall that is not lost, becomes runoff. This chapter focuses on these loss models, which can then be used with unit hydrographs to create runoff hydrographs.

7.1 NRCS (SCS) Curve Number Method

For many discharge estimation methods, the important variables reflect the contributing area of the watershed, the amount of rainfall that may occur in a rainfall event, the potential for the watershed to store water, and some measure of the time response character of the watershed. The National Resources Conservation Service (NRCS) method of rainfall-runoff modeling, originally known as the Soil Conservation Service (SCS) method, is typical of many modeling methods that are based on characteristics like those described.

7.1.1 Runoff Depth Estimation

The volume of storm runoff can depend on several factors. The volume of rainfall in an event is naturally an important factor. For very large watersheds, the designer may have difficulty distinguishing the volume of runoff from one storm event from runoff attributable to rainfall from earlier storm events. However, when designers use the design storm approach, they typically assume that runoff is attributable to only the design event.

Factors other than rainfall also affect the volume of runoff. When modeling rainfall and runoff, analysts commonly use the simplifying assumption that available rainfall be separated into three categories: that which runs off, an initial lost part called the initial abstraction, and time dependent losses. Factors thought to affect the split between losses and direct runoff include the volume of rainfall, land cover and use, soil type, and antecedent moisture conditions. Land cover and land use determine the amount of depression and interception storage. See Chapter 3 for a description of abstractions.

7.1.2 Maximum Potential Retention and Curve Number

In developing its rainfall-runoff relationship, the NRCS developed the concept that each watershed retains a portion of rainfall that falls on the watershed. NRCS refers to the maximum amount of this retained rainfall as maximum potential retention, S (a depth). It is a function of soil properties, land use, land cover, and the prevailing moisture content of the soil. Within this framework, runoff from a rainfall event is a function of the depth of rainfall, initial abstraction, and

S. Depth of rainfall is separated into three components: direct runoff (Q), actual retention (F), and the initial abstraction (I_a). NRCS developed the equation:

$$Q = \frac{(P - I_a)^2}{(P - I_a) + S} \tag{7.1}$$

where:

P	=	Depth of precipitation, inches (mm)
I_a	=	Initial abstraction, inches (mm)
S	=	Maximum potential retention, inches (mm)
Q	=	Depth of direct runoff, inches (mm)

While Q and P have units of depth, they are often referred to as volumes. It is assumed that the same depths occur over the entire watershed. The actual retention for a given rainfall event is the total rainfall minus the runoff depth:

$$F = P - Q \tag{7.2}$$

where:

P	=	Depth of precipitation, inches (mm)
Q	=	Depth of direct runoff, inches (mm)
F	=	Actual retention after runoff begins, inches (mm)

NRCS proposed that initial abstraction could be estimated as a function of S:

$$I_a = \lambda S \tag{7.3}$$

where:

I_a	=	Initial abstraction, inches (mm)
S	=	Maximum potential retention, inches (mm)
λ	=	Initial abstraction ratio

Hawkins et al. (2009) generalized equation 7.3 using the initial abstraction ratio (λ) and observed that λ=0.05 worked well for the datasets they analyzed. While NRCS recognized the variability in this relation, NRCS designated λ equal to 0.2 in its formulation of the method (NRCS 2004b).

Following the NRCS formulation and substituting the initial abstraction with λ = 0.2 into the equation for runoff yields the following equation, which contains the single unknown S:

$$Q = \frac{(P - 0.2S)^2}{(P + 0.8S)} \tag{7.4}$$

where:

P	=	Depth of precipitation, inches (mm)
Q	=	Depth of direct runoff, inches (mm)
S	=	Maximum potential retention, inches (mm)

Empirical analyses to estimate the value of S found that S was related to soil type, land cover, and the hydrologic condition of the watershed. These are represented by the runoff curve number (CN), which is an index representing a combination of a hydrologic soil group and a land use and treatment class. It is used to estimate S by:

$$S = \alpha\left[\frac{1000}{CN} - 10\right] \tag{7.5}$$

where:

CN = Curve number
α = Unit conversion constant, 1.0 in CU (25.4 in SI)

7.1.3 Hydrologic Soil Group Classification

NRCS uses a soil classification system consisting of four groups, which are identified by the letters A, B, C, and D. Soil characteristics associated with each group are (NRCS 2009a):

- Group A: deep sand, deep loess, aggregated silts.
- Group B: shallow loess, sandy loam.
- Group C: clay loams, shallow sandy loam, soils low in organic content, soils usually high in clay.
- Group D: soils that swell significantly when wet, heavy plastic clays, certain saline soils.

In addition, NRCS (2009a) designated dual hydrologic soil groups to address high water table conditions. Certain wet soils are placed in group D based solely on the presence of a water table within 24 inches of the surface even though the saturated hydraulic conductivity may be favorable for water transmission. If these soils can be adequately drained, then they are assigned to dual hydrologic soil groups (A/D, B/D, and C/D). The first letter applies to the drained condition and the second to the undrained condition. For hydrologic soil group, adequately drained means that the seasonal high water table is kept at least 24 inches below the surface in a soil where it would be higher in a natural state.

Historically, engineers identify the NRCS soil group in a watershed using either soil characteristics or county soil surveys. County soil surveys made available by Soil Conservation Districts give detailed descriptions of the soils at locations within a county. Many of the reports categorize the soils into the four groups A, B, C, and D.

The NRCS Web Soil Survey provides direct access to soil properties and hydrologic soil group (HSG) data in SSURGO, the Soil Survey Geographic Database. A GIS toolbox, called the gSSURGO toolbox, uses the same database. This toolbox allows users to generate GIS maps of soil properties including HSG.

The SSURGO database and Web Soil Survey refer to the HSG dual groups. In the presence of a dual group, judgment by the analyst with respect to the effect of seasonal or intermittent water table condition is important. If high water table conditions are expected to be present under the design scenario, Group D curve numbers are used.

7.1.4 Cover Complex Classification

The NRCS cover complex classification consists of three factors: land use, treatment or practice, and hydrologic condition. The tables for estimating runoff curve numbers identify many different land uses. The tables often subdivide agricultural land uses by treatment or practices, such as contoured or straight row; this separation reflects the different hydrologic runoff potential

associated with variation in land treatment. The hydrologic condition reflects the level of land management; it is separated into three classes: poor, fair, and good. Not all the land uses are separated by treatment or condition.

7.1.5 Antecedent Conditions

The original National Engineering Handbook (NEH) Section 4 referenced Antecedent Moisture Condition (AMC) relating to rainfall in the five days preceding an event (SCS 1969). NEH-630 Chapter 10 addresses the same issue, changing the title to Antecedent Runoff Condition (ARC) and redefining the concept. Hawkins et al. (2009) discuss ARC, and state that ARC II is used for the design of structures, as it represents average conditions. Refer to NEH-630 if special circumstances warrant consideration of other conditions.

Curve Number Method Development

NRCS (formerly the SCS) published the NEH Section 4 in 1969 (SCS 1969). Subsequent additional publications such as Technical Release 20 (TR-20) and Technical Release 55 (TR-55), as well as derivative computer programs, popularized the curve number and unit hydrograph methods. NRCS has updated the method and chapters 7, 8, 9, and 10 of NEH Part 630 are available online and are helpful resources. Chapter 9 includes complete curve number tables. The development of curve numbers for local use is encouraged by NEH 630 and Hawkins et al. (2009), when possible.

7.1.6 Curve Number Tables

The NRCS has developed curve numbers for urban areas (Table 7.1), agricultural areas (Table 7.2), and arid/semiarid areas (Table 7.3). In addition, NRCS provides curve numbers for national and commercial forest areas, as well as land cover types found in Puerto Rico and Hawaii (NRCS 2004a). NRCS differentiates CN values by land cover, land, treatments, hydrologic conditions, and hydrologic soil group. For example, Table 7.2 shows that the CN for woods with good cover and soil group B is 55; for soil group C, the CN increases to 70. If the cover (on soil group B) is poor, the CN will be 66.

Table 7.1, Table 7.2, and Table 7.3 summarize CNs for average runoff conditions (ARC II) and initial abstraction equal to 0.2S. NRCS provides additional curve numbers for ARC I and III though ARC II is typically used for design (NRCS 2004b). Other conditions across the U.S., such as areas with mean annual rainfall less than 30 inches may require local calibration of CNs (Hawkins et al. 2009). Areas with lower mean annual rainfall may have lower curve numbers than presented in the tables in this manual (Thompson 2004).

Table 7.1. Runoff curve numbers for urban areas (NRCS 2004a).

Cover Description		CN for Hydrologic Soil Group [1]			
Cover Type	Subtype, Hydrologic Condition, Percent Impervious [2]	A	B	C	D
Open space (lawns, parks, golf courses, cemeteries, etc.) [3]	Poor condition (grass cover < 50%)	68	79	86	89
	Fair condition (grass cover 50% to 75%)	49	69	79	84
	Good condition (grass cover > 75%)	39	61	74	80
Various impervious areas	Paved parking lots, roofs, driveways, etc. (excluding right-of-way)	98	98	98	98
Streets and roads	Paved; curbs and storm drains (excluding right-of-way)	98	98	98	98
	Paved; open ditches (including right-of-way)	83	89	92	93
	Gravel (including right-of-way)	76	85	89	91
	Dirt (including right-of-way)	72	82	87	89
Western desert urban areas	Natural desert landscaping (pervious areas only) [4]	63	77	85	88
	Artificial desert landscaping [5]	96	96	96	96
Urban districts	Commercial and business (85% impervious)	89	92	94	95
	Industrial (72% impervious)	81	88	91	93
Residential districts by average lot size	1/8 acre or less (town houses) (65% impervious)	77	85	90	92
	1/4 acre (38% impervious)	61	75	83	87
	1/3 acre (30% impervious)	57	72	81	86
	1/2 acre (25% impervious)	54	70	80	85
	1 acre (20% impervious)	51	68	79	84
	2 acres (12% impervious)	46	65	77	82
Developing urban areas	Newly graded areas (pervious areas only, no vegetation)	77	86	91	94

1. Average runoff condition, and $I_a = 0.2S$.
2. The average percent impervious area shown was used to develop the composite CNs. Other assumptions are as follows: impervious areas are directly connected to the drainage system, impervious areas have a CN of 98, and pervious areas are considered equivalent to open space in good hydrologic condition.
3. CNs shown are equivalent to those of pasture. Composite CNs may be computed for other combinations of open space type.
4. Composite CNs for natural desert landscaping should be computed using the impervious area percentage (CN=98) and the pervious area CN. The pervious area CNs are assumed equivalent to desert shrub in poor hydrologic condition.
5. Impervious weed barrier, desert shrub with 1- to 2-inch sand or gravel mulch and basin borders.

Table 7.2. Runoff curve numbers for agricultural land cover (NRCS 2004a).

Cover Description			CN for Hydrologic Soil Group [1]			
Cover Type	Treatment [2]	Hydrologic Condition [3]	A	B	C	D
Fallow	Bare Soil	Not applicable	77	86	91	94
	Crop residue cover (CR)	Poor	76	85	90	93
		Good	74	83	88	90
Row crops	Straight row (SR)	Poor	72	81	88	91
		Good	67	78	85	89
	SR + CR	Poor	71	80	87	90
		Good	64	75	82	85
	Contoured (C)	Poor	70	79	84	88
		Good	65	75	82	86
	C + CR	Poor	69	78	83	87
		Good	64	74	81	85
	Contoured & terraced (C & T)	Poor	66	74	80	82
		Good	62	71	78	81
	C & T + CR	Poor	65	73	79	81
		Good	61	70	77	80
Small grain	SR	Poor	65	76	84	88
		Good	63	75	83	87
	SR + CR	Poor	64	75	83	86
		Good	60	72	80	84
	C	Poor	63	74	82	85
		Good	61	73	81	84
	C + CR	Poor	62	73	81	84
		Good	60	72	80	83
	C & T	Poor	61	72	79	82
		Good	59	70	78	81
	C & T + CR	Poor	60	71	78	81
		Good	58	69	77	80
Close-seeded or broadcast legumes or rotation meadow	SR	Poor	66	77	85	89
		Good	58	72	81	85
	C	Poor	64	75	83	85
		Good	55	69	78	83
	C & T	Poor	63	73	80	83
		Good	51	67	76	80
Pasture, grassland, or range- continuous forage for grazing [4]	Not applicable	Poor	68	79	86	89
		Fair	49	69	79	84
		Good	39	61	74	80

Table 7.2 (continued). Runoff curve numbers for agricultural land cover (NRCS 2004a).

Cover Description			CN for Hydrologic Soil Group [1]			
Cover Type	Treatment [2]	Hydrologic Condition [3]	A	B	C	D
Meadow-continuous grass, protected from grazing and generally mowed for hay	Not applicable	Good	30	58	71	78
Brush-brush-forbs-grass mixture with brush the major element [5]	Not applicable	Poor	48	67	77	83
		Fair	35	56	70	77
		Good	30[6]	48	65	73
Woods-grass combination (orchard or tree farm) [7]	Not applicable	Poor	57	73	82	86
		Fair	43	65	76	82
		Good	32	58	72	79
Wood [8]	Not applicable	Poor	45	66	77	83
		Fair	36	60	73	79
		Good	30	55	70	77
Farmstead-buildings, lanes, driveways, and surrounding lots	Not applicable	Not applicable	59	74	82	86
Roads (including right-of-way)	Dirt	Not applicable	72	82	87	89
	Gravel	Not applicable	76	85	89	91

1. Average runoff condition, and I_a=0.2S.
2. Crop residue cover applies only if residue is on at least 5 percent of the surface throughout the year.
3. Hydrologic condition is based on combinations of factors that affect infiltration and runoff, including (a) density and canopy of vegetative areas, (b) amount of year-round cover, (c) amount of grass or close-seeded legumes, (d) percent of residue cover on the land surface (good >20%), and (e) degree of surface toughness.
   Poor: Factors impair infiltration and tend to increase runoff.
   Good: Factors encourage average and better than average infiltration and tend to decrease runoff.
   For conservation tillage poor hydrologic condition, 5 to 20 percent of the surface is covered with residue (less than 750 pounds per acre for row crops or 300 pounds per acre for small grain).
   For conservation tillage good hydrologic condition, more than 20 percent of the surface is covered with residue (greater than 750 pounds per acre for row crops or 300 pounds per acre for small grain).
4. Poor: < 50% ground cover or heavily grazed with no mulch.
   Fair: 50 to 75% ground cover and not heavily grazed.
   Good: > 75% ground cover and lightly or only occasionally grazed.
5. Poor: < 50% ground cover.
   Fair: 50 to 75% ground cover.
   Good: > 75% ground cover.
6. If actual curve number is less than 30, use CN = 30 for runoff computation.
7. CNs shown were computed for areas with 50 percent woods and 50 percent grass (pasture) cover. Other combinations of conditions may be computed from the CNs for woods and pasture.
8. Poor: Forest litter, small trees, and brush are destroyed by heavy grazing or regular burning.
   Fair: Woods are grazed, but not burned, and some forest litter covers the soil.
   Good: Woods are protected from grazing, and litter and brush adequately cover the soil.

Table 7.3. Runoff curve numbers for arid and semiarid rangelands (NRCS 2004a).

Cover Description		CN for Hydrologic Soil Group [1]			
Cover Type	Hydrologic Condition [2]	A [3]	B	C	D
Herbaceous—mixture of grass, weeds, and low-growing brush, with brush the minor element	Poor		80	87	93
	Fair		71	81	89
	Good		62	74	85
Oak-aspen—mountain brush mixture of oak brush, aspen, mountain mahogany, bitter brush, maple, and other brush	Poor		66	74	79
	Fair		48	57	63
	Good		30	41	48
Pinyon-juniper—pinyon, juniper, or both; grass understory	Poor		75	85	89
	Fair		58	73	80
	Good		41	61	71
Sage-grass—sage with an understory of grass	Poor		67	80	85
	Fair		51	63	70
	Good		35	47	55
Desert shrub—major plants include saltbush, greasewood, creosote bush, blackbrush, bursage, paloverde, mesquite, and cactus	Poor	63	77	85	88
	Fair	55	72	81	86
	Good	49	68	79	84

1. Average runoff condition, and $I_a = 0.2S$. For range in humid regions, use Table 7.2.
2. Poor: < 30% ground cover (litter, grass, and brush overstory).
   Fair: 30 to 70% ground cover.
   Good: > 70% ground cover.
3. Curve numbers for group A have been developed only for desert shrub.

Alterations to the CN also changes S and I_a. A lower CN increases S and I_a since the latter is a function of S. The combined effects of reduction in curve numbers and reduction in rainfall may exaggerate the magnitude of the initial abstraction when $\lambda = 0.2$. Engineers may choose to use $\lambda = 0.05$ for more accurate results in such situations (Hawkins et al. 2009).

Curve Numbers May Change

NRCS is considering preparing and releasing new curve numbers based on alternative initial abstraction assumptions. New information and instructions may be released in the future.

Because CN, S, and I_a are related, changing one without considering the effects on others may result in inaccurate runoff estimates. Hawkins et. al. (2009) provides an approach to adjust CN when using $\lambda = 0.05$ rather than 0.2:

$$CN_{0.05} = \frac{100}{\left\{1.879\left[\frac{100}{CN_{0.2}} - 1\right]^{1.15} + 1\right\}} \tag{7.6}$$

where:

$CN_{0.05}$ = Curve number when λ=0.05
$CN_{0.2}$ = Curve number when λ=0.2

The adjustment of S from values for λ = 0.2 to λ = 0.05 is:

$$S_{0.05} = 1.33 S_{0.2}^{1.15} \quad (7.7)$$

Remapping of curve number and S alter the estimate of rainfall loss and, therefore, the estimate of runoff produced in a given storm. For small rainfall depths, estimates of runoff volume using λ = 0.05 will be higher than for λ = 0.2. The converse is true for rainfall depths exceeding a critical value. The critical value of rainfall, the value at which runoff for λ = 0.2 and λ = 0.05 coincide, increases with decreasing curve number. For small curve numbers and small depths of rainfall, λ=0.05 produces larger runoff depths. It is likely that designers will only use λ = 0.05 when both curve numbers and rainfall depths are small. When in doubt, comparison of the two can be performed.

Example 7.1: Curve number loss model

Objective: Compute maximum potential retention (S) and runoff depth.

Given: The curve number (from tables) of a soil is 78, and a rainfall event of 3.75 inches

CN = 78
P = 3.75 inches

Estimate maximum potential retention and runoff depth for λ = 0.2 and 0.05.

Step 1: Compute the maximum potential retention "S" using equation 7.5.

$$S = \frac{1000}{78} - 10 = [12.82 - 10] = 2.82 \text{ inches}$$

Step 2: Compute the runoff depth assuming λ = 0.2.

$$Q = \frac{(P - 0.2S)^2}{(P - 0.2S) + S} = \frac{(3.75 - (0.2 * 2.82))^2}{(3.75 - (0.2 * 2.82)) + 2.82} = 1.69 \text{ inches}$$

Step 3. Compute the runoff depth assuming λ = 0.05.

Convert S for curve number for I_a = 0.2S to S for I_a = 0.05S using equation 7.7:

$$S_{0.05} = 1.33 S_{0.2}^{1.15} = 1.33(1.69)^{1.15} = 2.43 \text{ inches}$$

$$Q = \frac{(P - 0.05S)^2}{(P - 0.05S) + S} = \frac{(3.75 - 0.05(2.43))^2}{[3.75 - 0.05(2.43)] + 2.43} = 2.17 \text{ inches}$$

Solution: Both the maximum potential retention and estimated runoff values are lower with the initial abstraction ratio equal to 0.05 compared with 0.2, as expected.

7.1.7 Estimation of CN Values for Urban Land Uses

Table 7.1 includes CN values for several urban land uses. For each of these, the CN is based on a specific percentage of imperviousness. For example, the CN values for commercial land use are based on an imperviousness of 85 percent. Curve numbers for other percentages of imperviousness can be computed using a weighted CN approach, with a CN of 98 used for the impervious areas and the CN for open space (good condition) used for the pervious portion of the area. Thus, CN values of 39, 61, 74, and 80 are used for hydrologic soil groups A, B, C, and D, respectively. These are the same CN values for pasture in good condition. Thus, the following equation can be used to compute a weighted CN:

$$CN_w = CN_p(1 - f) + f(98) \tag{7.8}$$

where:

CN_w = Weighted curve number
CN_p = Curve number of the pervious area
f = Fraction of impervious area, dimensionless

To show the use of equation 7.8, the CN values for urban districts (commercial land use) with 85 percent imperviousness are:

- A soil: 39(0.15) + 98(0.85) = 89.
- B soil: 61(0.15) + 98(0.85) = 92.
- C soil: 74(0.15) + 98(0.85) = 94.
- D soil: 80(0.15) + 98(0.85) = 95.

These are the same values shown in Table 7.1.

Equation 7.8 can be placed in graphical form (see Figure 7.1a). By entering with the percentage of imperviousness on the vertical axis at the center of the figure and moving horizontally to the pervious area CN, the composite CN can be read. The examples above for commercial land use can be used to illustrate the use of Figure 7.1a for 85 percent imperviousness. For a commercial land area with 60 percent imperviousness of a B soil, the composite CN would be:

$CN_w = 61(0.4) + 98(0.6) = 83$

The same value can be obtained from Figure 7.1a.

If the basin contains varying amounts of different covers, a weighted curve number for the entire basin can be determined as:

$$\text{Weighted CN} = \frac{\sum CN_i A_i}{A} \tag{7.9}$$

where:

CN_i = Curve number for cover type i that covers area A_i
A = Total area

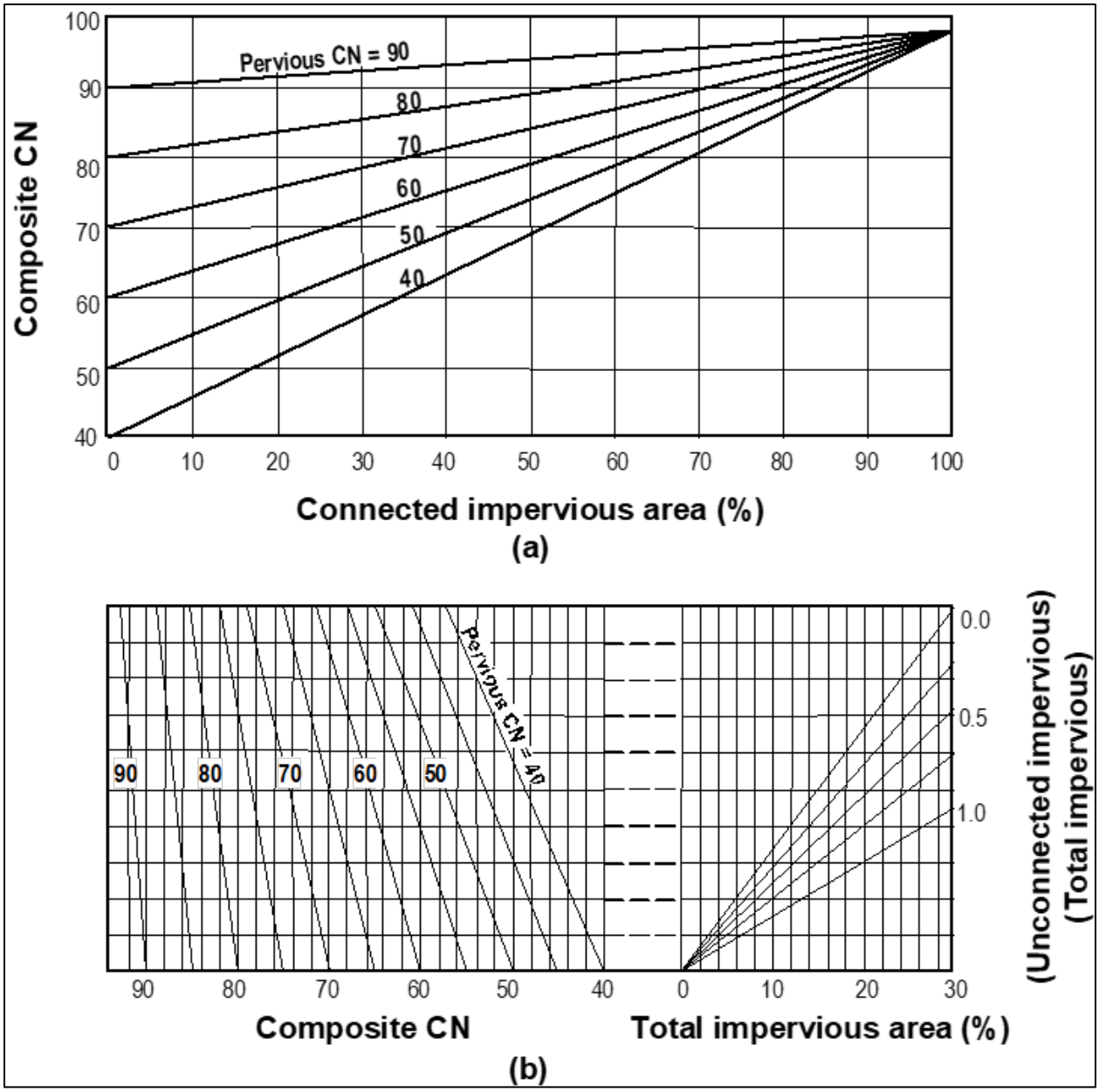

Figure 7.1. Composite curve number estimation when: (a) all imperviousness area connected to storm drains, and (b) some imperviousness area not connected to storm drain.

7.1.8 Effect of Unconnected Impervious Area on Curve Numbers

Many local drainage policies require that runoff from certain types of impervious land cover (i.e., rooftops, driveways, patios) be directed to pervious surfaces to promote infiltration rather than being connected to storm drain systems. The effect of disconnecting impervious surfaces on runoff rates and volumes can be accounted for by modifying the CN.

Three variables are involved in the adjustment: the pervious area CN, the percentage of impervious area, and the percentage of the imperviousness that is unconnected. Because Figure 7.1a for computing composite CN values is based on the pervious area CN and the percentage of imperviousness, a correction factor was developed to compute the composite CN. The correction is a function of the percentage of unconnected imperviousness (Figure 7.1b). The use

of the correction is limited to drainage areas having percentages of imperviousness that are less than 30 percent.

As an alternative to Figure 7.1b, the composite curve number (CN_c) can be computed by for a percent imperviousness less than or equal to 30 percent:

$$CN_c = CN_p + \frac{P_i}{100}\left(98 - CN_p\right)\left(1 - 0.5R\right) \tag{7.10}$$

where:

CN_c = Composite curve number
CN_p = Pervious curve number
P_i = Percent imperviousness, percent
R = Ratio of unconnected impervious area to the total impervious area.

7.2 Green-Ampt Infiltration Model

Another commonly used loss model is the Green-Ampt infiltration model (Chow et al. 1988, Maidment 1993). As the name implies, it addresses only infiltration and does not include other abstraction mechanisms.

Green-Ampt considers soil saturation and is based on a simple conceptual model of soil as discrete irregular grains of various minerals and sizes with void spaces among the grains that may contain air or water. The porosity of soil (η) is the ratio of the volume of voids to the total volume of soil:

$$\eta = \frac{V_{voids}}{V_{total}} \tag{7.11}$$

where:

η = Porosity of the soil, dimensionless
V_{voids} = Volume of voids in a known volume of soil
V_{total} = Total volume of soil

Soil is saturated when all the void space in the soil is filled with water. When water (e.g., from rainfall) is available at the ground surface of a soil that is initially relatively dry, water enters the soil at the soil surface, and moves downward under the force of gravity and of capillary attraction within the pore spaces. Figure 7.2 shows an idealized representation of the saturation of soil by infiltration. If the rainfall rate is higher than the rate of infiltration, the soil near the surface will be saturated. Water moves downward through the pores, displacing the air in the void spaces creating a wetting front through zones of transmission and wetting where moisture content diminishes with depth.

With additional water available at the ground surface, the moisture content increases at depths that are not saturated, and the wetting zone continues to move downward. The infiltration rate at the ground surface diminishes with time as the void spaces are filled with water and will reach an equilibrium infiltration rate (representing steady-state transmission of water according to Darcy's equation) if the wetting continues to move downward. Infiltration will continue unless the wetting front reaches an impermeable barrier and all voids are filled with water.

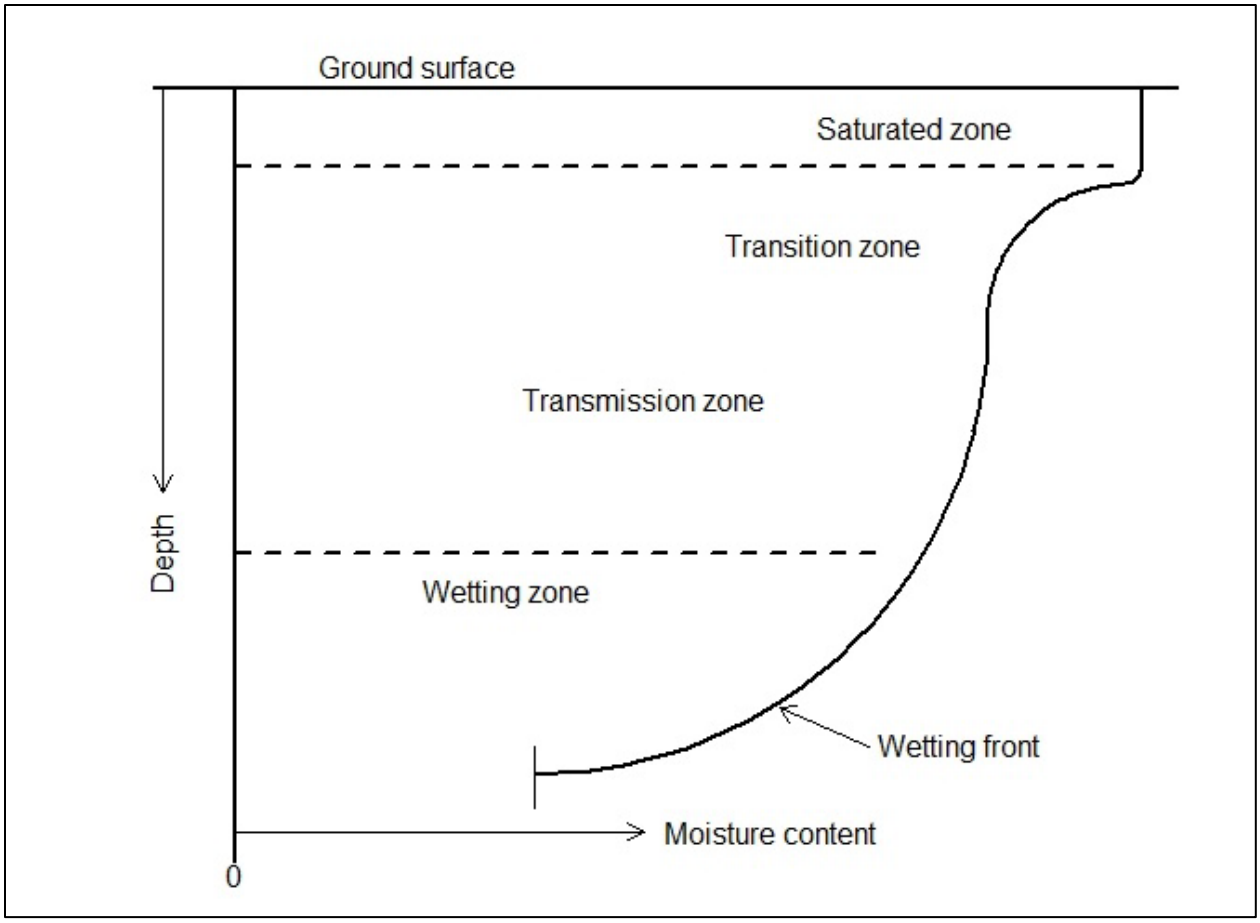

Figure 7.2. Conceptual soil saturation model.

The Green-Ampt infiltration model simplifies the model in Figure 7.2 with that shown in Figure 7.3 by assuming that flow into the soil voids is like a piston with a sharp wetting front moving downward, saturating the soil as it goes. Gravity and capillary attraction drive the downward movement of water. Therefore, the depth of infiltration (as depth of water outside of the soil pores) depends on available pore space in the soil. The available moisture storage below the wetting front is described by:

$$\Delta\theta = \eta - \theta_i \tag{7.12}$$

where:

$\Delta\theta$ = Difference between the porosity and the initial moisture content, dimensionless
θ_i = Initial moisture content, dimensionless
η = Porosity, dimensionless

The initial moisture content of a soil in place at any time ranges from a low value that represents residual moisture, θ_r, that might be present after an extended drought to a very high value that is close to or fully saturated. In the absence of a measured value, analysts can use the **wilting point** of the soil for the initial moisture content. Wilting point is the moisture content below which the soil does not support plant survival. Local, State, or Federal publications for a given area provide the wilting point for most common soils.

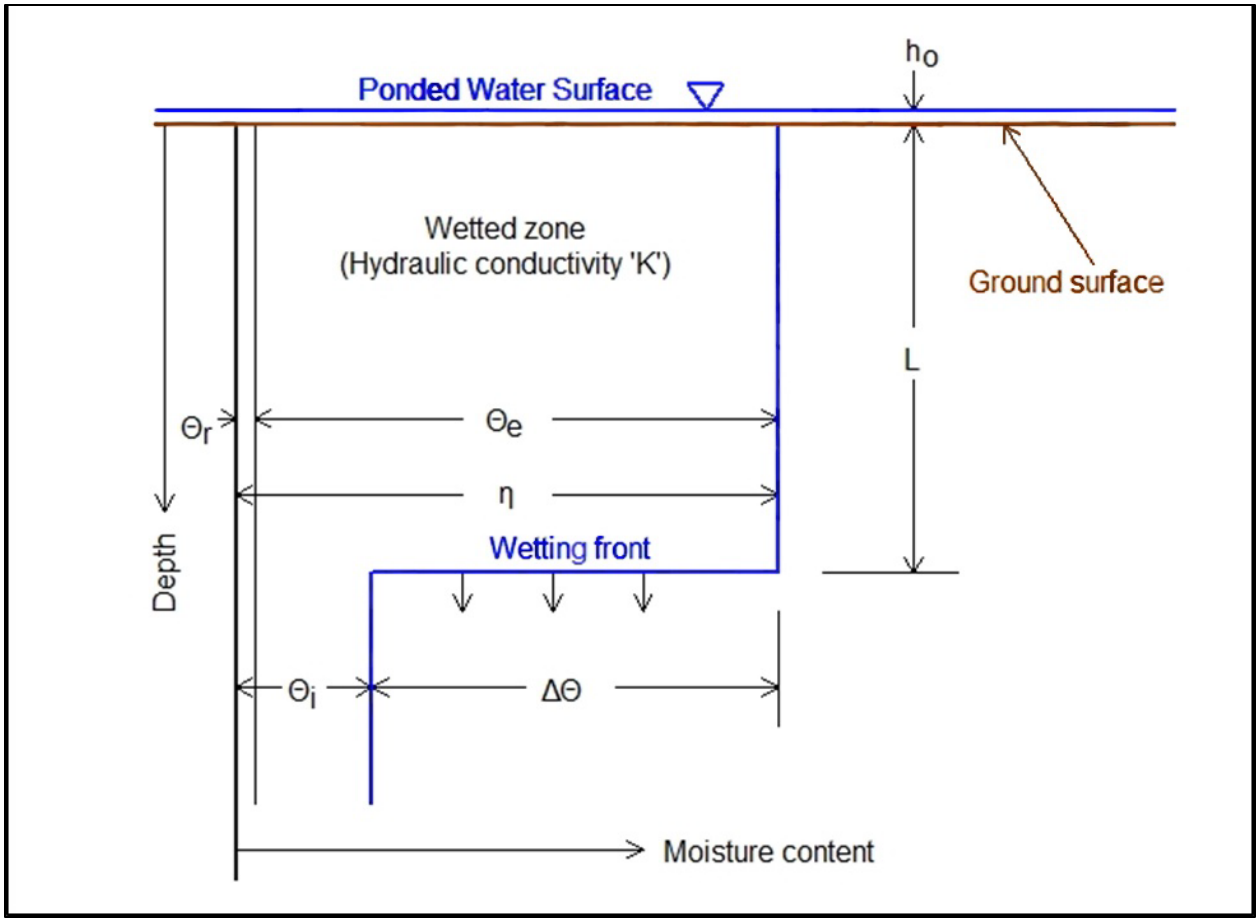

Figure 7.3. Green-Ampt infiltration model.

Water movement through the soil pores depends on both the porosity and on the size of pores. The hydraulic conductivity of a soil, denoted K, is a measure of the ability of water to flow through the soil. High hydraulic conductivity means easy movement of water; low hydraulic conductivity means more resistance to the movement of water. Hydraulic conductivity also relates to the soil particle minerals, their electrochemical properties with respect to water, and the presence of organic matter.

The rate of infiltration for Green-Ampt is calculated by:

$$f(t) = K\left[\frac{|\psi + h_0|\,\Delta\theta}{F(t)} + 1\right] \qquad (7.13)$$

where:

f(t)	=	Infiltration rate at time t, length per time (e.g., in/h)
K	=	Hydraulic conductivity, length per time (e.g., in/h)
Ψ	=	Wetting front suction head, length (e.g., inches)
h_0	=	Depth of water ponded on the ground surface, length (e.g., inches)
F(t)	=	Cumulative infiltration at time “t,” length (e.g., inches)

The wetting front suction head (Ψ) represents the capillary attractive force assisting gravity in moving water downward through the soil and is dependent on the soil characteristics. In most practical cases, the depth of ponded water h_o is negligible and is taken as zero.

The volume of infiltrated water at a given time is the length L times the available porosity, $\Delta\theta$. The difference between the porosity and θ_r is called the effective moisture, θ_e. The cumulative infiltration, with h_0 taken as zero, is calculated as:

$$F(t) = Kt + \psi\,\Delta\theta \ln\left[\left|1 + \frac{F(t)}{\psi\Delta\theta}\right|\right] \tag{7.14}$$

F(t)	=	Cumulative infiltration at time "t," length (e.g., inches)
t	=	Time, time (e.g., hours)
K	=	Hydraulic conductivity, length per time (e.g., in/h)
Ψ	=	Wetting front suction head, length (e.g., inches)
Δθ	=	Available porosity, dimensionless

This expression cannot be solved in closed form and requires an iterative solution. Many computer routines, including those found in most spreadsheet applications, readily solve such problems.

The Green-Ampt method can be calibrated to field data, if available. In the absence of field measurements, parameters can be estimated from published data. The NRCS Web Soil Survey and the gSSURGO GIS toolbox both allow ready access to saturated hydraulic conductivity (K), soil textural classification, and porosity. Tables exist relating textural classification to wetting front suction head (e.g., Maidment 1993). Agricultural data and agencies provide wilting point estimates.

Agency Recognition

To gain consistency in practice and submissions by developers and other customers, some local agencies such as cities, counties, flood control districts, and others require the Green-Ampt model for activities in their jurisdictions and may publish parameters recommended or required for use in those jurisdictions.

7.3 Other Loss Models

Numerous other loss models exist. Some are well adapted for event simulation as is typical of highway hydrology; others are better used in long-term watershed simulation. Unlike the NRCS curve number method and the Green-Ampt model, use of other loss models is constrained by a lack of general, widespread research or references for parameter estimation.

7.3.1 Initial Abstraction/Constant Loss Model

A simple model that can be adapted to design use is called the **Initial and Constant Loss (I-CL) model** (USACE 2020). This model has only two parameters: a value of the initial abstraction, which is a threshold depth of rainfall below which no runoff occurs, and a loss rate applied after the initial abstraction is satisfied. Rainfall rates greater than the loss rate produce a runoff rate that is the difference between rainfall rate and loss rate. When rainfall rate drops below the loss rate, no runoff occurs.

While the I-CL model is simple and easily applied, little information exists for the values used. Much work has been done to quantify the initial loss, but little on the constant loss. Few textbooks include recommendations on either. However, Asquith and Roussel (2007) investigated one State (Texas) and recommended procedures for both the conduct of research and values of the initial and constant losses.

The phi-index method is a special case of the I-CL model where the losses are constant throughout the storm. That is, initial losses occur at the same rate as losses later in the storm.

7.3.2 Exponential Loss

The exponential loss model is presented in commonly used software (USACE 2020) and incorporates 5 parameters for which little information exists. The USACE recommends that the exponential loss model only be used for event analyses and with calibration of the parameters.

7.3.3 Smith and Parlange

The Smith and Parlange loss model is also available in commonly used software (USACE 2020) and incorporates eight parameters for which little information exists. The Smith-Parlange model is similar to the Green-Ampt model; calibration to infiltrometer tests is feasible.

Chapter 8 - Design Hydrographs

Some highway drainage design projects may call for information beyond a peak flow. For example, designers may need not only the peak but also the runoff volume and time distribution of flow to simulate the effects of urban stormwater detention, rural farm ponds, and reservoirs in a watershed. Designers may also need information beyond a peak flow when modeling the effects of past or future urbanization on the runoff process. In such cases, designers may develop a design hydrograph—a graph or table of discharge versus time—for a rainfall event of particular characteristics. A hydrograph provides not only a peak flow, but also total volume and time distribution of runoff.

This chapter describes tools for developing design hydrographs. The first section introduces the concept of the unit hydrograph and describes several techniques for developing them. Next, the chapter describes several techniques for generating design storms that can be used as inputs to a unit hydrograph analysis to estimate a design hydrograph. These design storms can also be used as inputs to other techniques. Finally, the chapter outlines additional methods for generating design hydrographs.

8.1 Unit Hydrograph Analysis

Unit hydrograph analysis breaks down into three general and sequential processes:

1. Transforming the rainfall hyetograph to an excess rainfall hyetograph by removing rainfall lost to abstractions.
2. Developing the unit hydrograph for the watershed.
3. Computing the runoff hydrograph from the excess rainfall hyetograph and the unit hydrograph.

Figure 8.1 summarizes this conceptual process. The initial abstraction is that part of the rainfall that occurs prior to the start of direct runoff. The rainfall excess is that part of the rainfall that appears as direct runoff. The unit hydrograph, sometimes referred to as the transfer function, converts the excess rainfall to direct runoff. The direct runoff is the storm runoff that results from rainfall excess; the volumes of rainfall excess and direct runoff must be equal. The figure also shows the customary representation of the rainfall hyetograph above the hydrograph, inverted, as discrete units or pulses of rainfall aligned in time with the hydrograph.

Once engineers determine the direct runoff hydrograph, they add base flow to estimate the total hydrograph. Base flow is the water in the stream resulting from an accumulation of water in the watershed from past storm events; streamflow that is present even if the rain for the current storm event had not occurred. It results primarily from water that is temporarily stored as shallow groundwater, which enters storage during and after storm events and is returned to the surface as streamflow over an extended period of time. Figure 8.1 shows a constant base flow which is often a reasonable assumption. For some streams, zero base flow may be appropriate. Other methods for estimating base flow can also be used.

In 1932, L. K. Sherman conceived of an empirical rainfall response function that he called a “unit graph,” which he isolated by analyzing measured runoff hydrographs and estimating excess rainfall for multiple watersheds and rainfall events. Recall from Chapter 3 that excess rainfall equals the total rainfall minus abstraction losses.

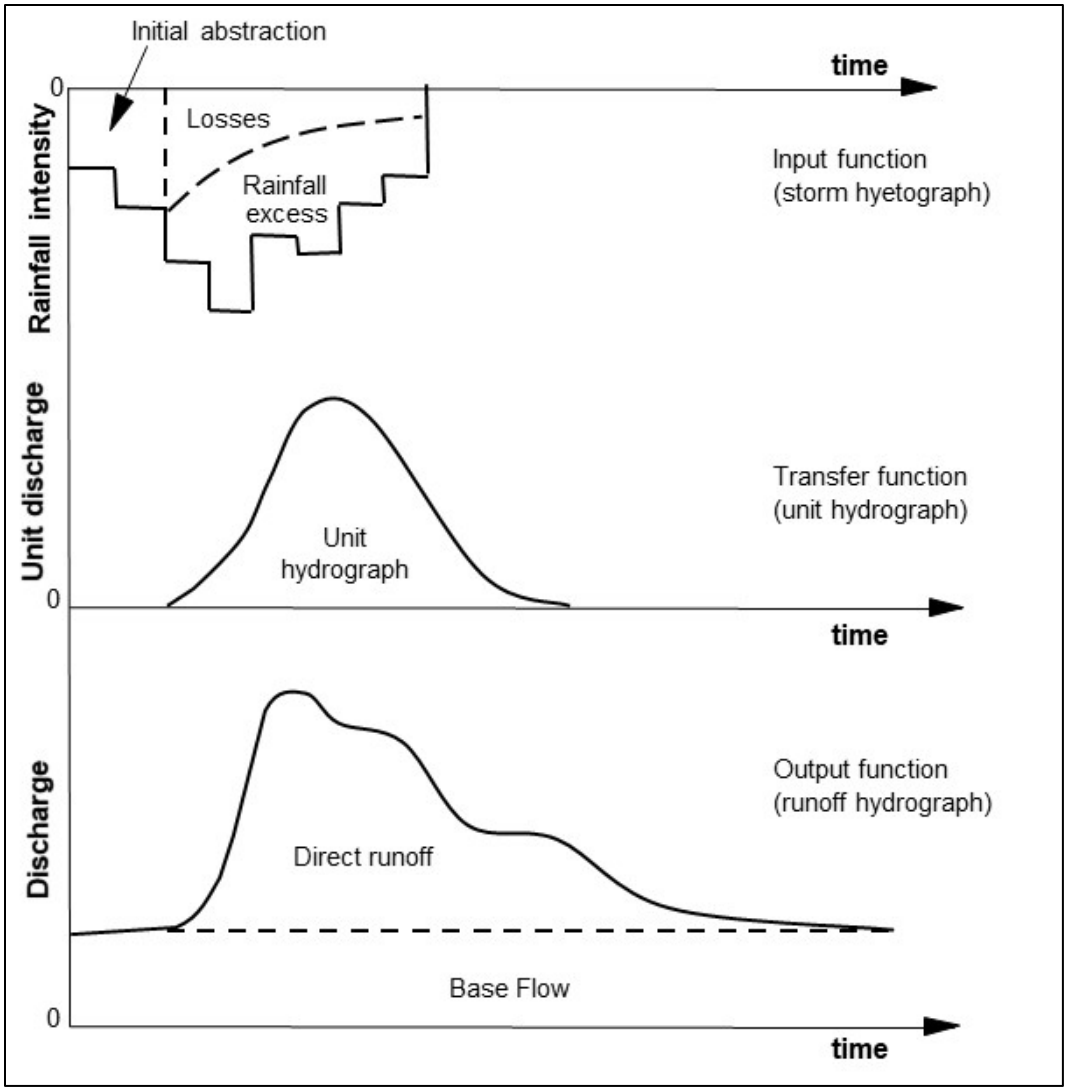

Figure 8.1. Total hydrograph using the unit hydrograph and adding base flow.

Sherman's analysis revealed that despite the differences in watershed characteristics and rainfall distributions, a watershed's temporal runoff response could be reduced to a generalized hydrograph shape in many cases. Scaled to represent a unit depth of excess rainfall, this response is generally known as a **unit hydrograph** (UH). In simple terms, a unit hydrograph is a watershed's runoff response to one unit depth, e.g., 1 inch or 1 mm, of excess rainfall occurring over a specific time interval (duration).

Figure 8.2 illustrates an example of a unit hydrograph. While the figure shows a smooth curve with the appearance of a mathematical function, engineers perform unit hydrograph calculations on discrete time steps equal to the unit hydrograph's duration. Each watershed is associated with a unique set of times, represented by:

- The time to peak (t_p): the time between the beginning of excess rainfall and the maximum outflow.
- Lag time (t_L): the time between the middle of the duration of excess rainfall and the maximum outflow.
- The total time base of runoff (t_B): the time between the beginning of excess rainfall and the end of direct runoff.

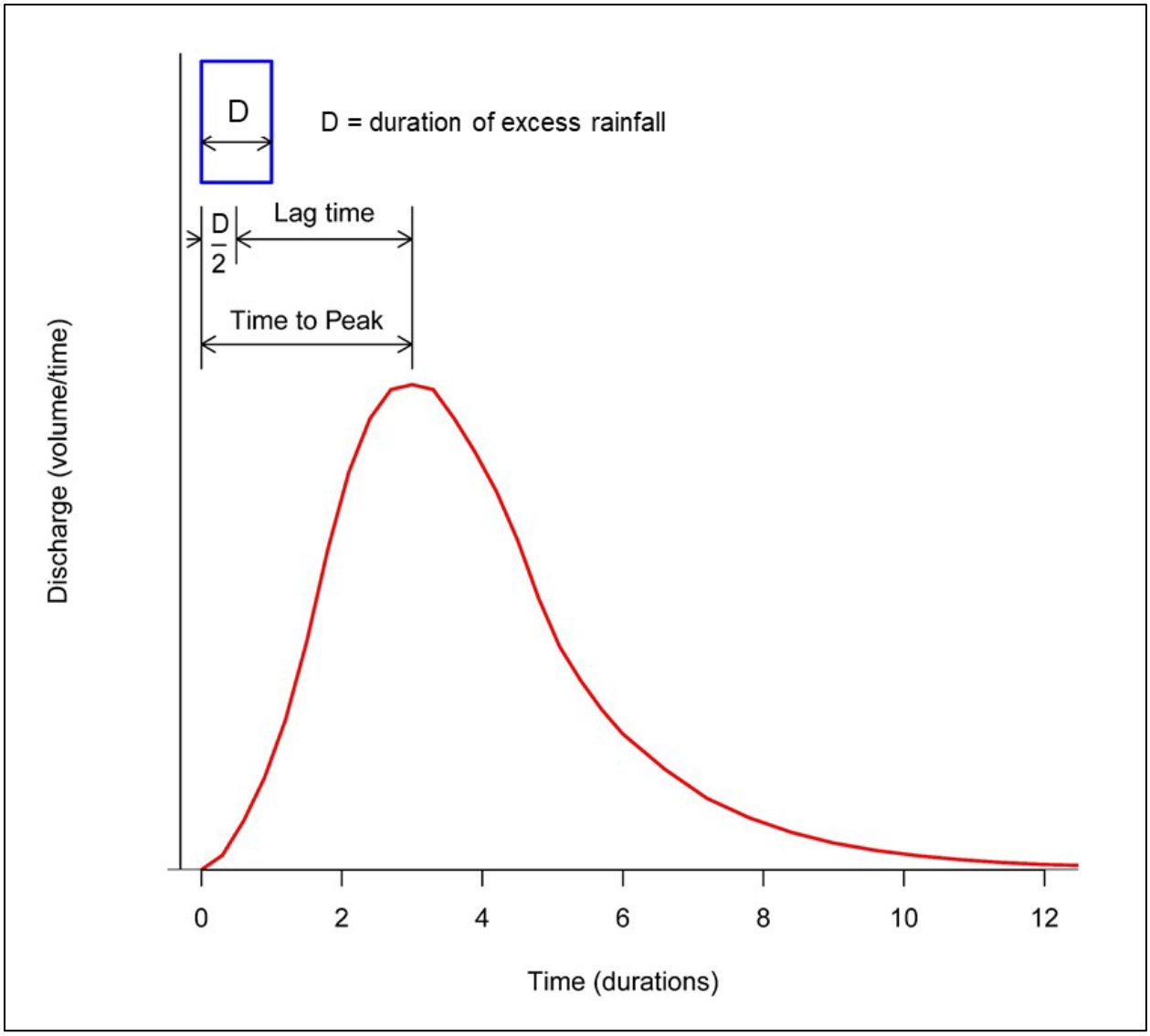

Figure 8.2. Typical unit hydrograph.

Application of the unit hydrograph to multiple pulses of excess rainfall, as shown in Figure 8.1, includes calculation of the runoff response to each pulse and then adding them together to create the direct runoff hydrograph for the storm. Three principles underlie application of unit hydrographs for a watershed:

- **Time invariance (translation)**—All time-based features on the unit hydrograph, such as the time to peak and the recession time occur at the same time relative to start of the unit hydrograph. However, the response to a particular pulse of excess rainfall is translated, i.e., shifted in time, to begin when the excess rainfall pulse begins.
- **Proportionality**—All features related to discharge on the unit hydrograph are proportional to the depth of excess rainfall by simple scaling.
- **Superposition**—At each time step of analysis, the proportional responses from each pulse of excess rainfall are added together after they have been translated in time and proportionately adjusted for magnitude.

Using the UH, designers can model watershed response to excess rainfall input. Designers can also use the UH to develop a peak flow for an ungaged watershed when data limitations or other specific conditions preclude other methods, such as regression equations. Unit hydrograph modeling conceptually represents the physical rainfall-runoff process, and it does not depend on the availability of stream gages or on watershed consistency with gaged stream characteristics. With appropriate care, designers can model virtually any watershed with the UH, making it a flexible and valuable technique.

Unit Hydrograph Flexibility

The unit hydrograph method has become commonplace in engineering practice because of its flexibility, applicability, and relative simplicity, and because of the ready availability of public domain computer programs to perform the calculations. Unit hydrograph calculations and the principle of superposition also serve as the basis for the modeling of complex watershed interactions in the presence of changing watershed conditions, reservoirs, urbanization, and diversion.

A UH analysis depends on three components:

- A **design storm** or rainfall input appropriate (hyetograph) for the analysis objectives.
- A **loss model** simulating the loss of rainfall to various abstractions, such as infiltration, which take up water, thereby reducing the amount available for runoff.
- A **watershed response model**, which describes how runoff arrives at the outlet **in time** after traveling over the watershed.

A design storm provides the distribution of rainfall over a certain period, divided into discrete depths on equal time steps. Designers generally select a design storm corresponding to hydrologic design criteria for total rainfall volume, duration, and AEP. The UH procedure can also be used for any historical or hypothetical future rainfall sequence.

A loss model is usually based on physical attributes of the watershed, such as soil type, vegetation, topography, or possibly measured properties such as infiltration. In general, designers consider time varying infiltration as the dominant process in watershed losses. In each time step, what remains of the design storm depth after applying the loss model is excess rainfall. Excess rainfall (also referred to as effective rainfall) is rainfall that becomes runoff observed at the point of interest.

Selecting a Computation Time Step

Time step size also affects the amount of rainfall used in the calculations at each step. If the time step size is very small, rainfall depth is divided into small increments, and numerical rounding of rainfall can result in mass balance errors. Time step selection can become challenging in cases of subdivided watersheds, where lag times may range widely, and software allows limited options. The shortest lag time is the appropriate basis of time step selection.

To calculate the discharge from a watershed using a UH, engineers complete calculations at time increments of the UH duration. To preserve the response represented by the unit hydrograph, engineers typically use a UH duration of no more than one-fifth of the time to peak of the UH (NRCS 2004b) to achieve reasonable resolution in the shape of the unit hydrograph and to avoid mass balance errors. Unit hydrograph computations approximate the curvilinear

shape of a hydrograph as a series of trapezoids and a large time step may contribute to mass balance errors and an underestimate of the peak flow.

The UH ordinates at each time step represent the flow rate response (volume/time) to one unit depth of excess rainfall in one time step. For each time step, the engineer scales the UH ordinate by the value of the excess rainfall (proportional to one unit) at each successive increments (D, 2D, 3D, etc.). Each ordinate on the UH represents a discharge, in volume per time. The area under the graph represents one unit depth uniformly over the surface of the watershed.

The value of each ordinate is proportional to the depth of rainfall. For 0.5 unit, each ordinate would be 0.5 of the UH's discharge. For 1.5 units, each ordinate would be 1.5 times the UH's discharge. The responses to each excess rainfall component are superimposed to create the direct runoff hydrograph.

Example 8.1:	Simple application of a unit hydrograph.
Objective:	Develop a direct runoff hydrograph from a unit hydrograph and a single rainfall pulse.

Given: A watershed with the following characteristics.

A = 856 acres (346.6 ha)

D = 0.5 h

Table 8.1 shows the unit hydrograph with a 0.5-hour duration for a watershed of 856 acres. That is, this is the unit hydrograph produced by this watershed in response to 1 inch of excess rainfall occurring over 0.5 hours. By definition, the area under the curve of this unit hydrograph equals one inch of direct runoff. The engineer confirms this with the following computation:

$$\text{Depth} = \frac{\left(\sum q\right)(D)}{A} = \frac{(1730)(0.5)}{856}\left(\frac{1\text{ac}}{43{,}560\text{ ft}^2}\right)\left(\frac{3600\text{ s}}{1\text{ h}}\right)\left(\frac{12\text{ inches}}{1\text{ ft}}\right) = 1.00\text{ inch}$$

The depth over the entire watershed area (A) is 1 inch with the duration (D) and the summation of the ordinates for flow (q) from Table 8.1.

For this example, consider a hypothetical rainfall event of 0.5-hour duration with 1.5 inches of excess rainfall on the watershed. Table 8.1 shows the discharges at each 0.5-hour interval after the rainfall occurs. Each ordinate on the unit hydrograph is scaled by the depth of rainfall (in inches); i.e., 1.5, since the UH is the watershed response to 1 inch of excess rainfall. For example, at time equal to 1 hour, 1 inch of excess rainfall produces a hydrograph with a discharge of 364 ft^3/s at that time. However, this example has 1.5 inches of excess rainfall resulting in a discharge at this time of 1.5 (364) = 546 ft^3/s. This table represents the outflow hydrograph from the watershed resulting from the single pulse of excess rainfall.

Table 8.1. Unit hydrograph for watershed and response to 1.5-inch pulse.

Time (hours)	Unit Hydrograph Discharge (ft^3/s)	Discharge from 1.5-inch pulse (ft^3/s)
0.0	0	0
0.5	30	45
1.0	364	546
1.5	500	750
2.0	405	608
2.5	242	363
3.0	118	177
3.5	50	75
4.0	14	21
4.5	4	6
5.0	2	3
5.5	1	1.5
6.0	0	0

Solution: The peak flow from the excess rainfall is the largest ordinate on the resulting hydrograph, in this case 750 ft^3/s.

Design storms and historical rainfall events are typically a series of rainfall pulses rather than a single pulse as in example 8.1. The engineer analyzes these series by repeating the UH calculations for subsequent pulses of excess rainfall of the same duration. For each pulse, the engineer determines the excess rainfall and then the proportional runoff response to those pulses. The engineer continues this process until the contributions of the entire series of pulses (the rainstorm) have been analyzed. By incrementally dividing excess rainfall into steps of the duration, excess rainfall can continue longer than the duration, simulating the response to rainfall of any length of time.

Example 8.2: A runoff hydrograph developed from a rainfall event.

Objective: Develop the direct runoff hydrograph from three rainfall pulses in an event.

Given: A contributing watershed with the following characteristics:

A = 856 acres (346.6 ha)

D = 0.5 h

P = 2.25 inches for a 1.5-hour rainfall event

The watershed receives three pulses of excess rainfall of 0.5-hour duration each. The first excess rainfall pulse is 0.5 inches, the second 1.0 inches, and the third 0.75 inches. These three blocks of excess rainfall represent an excess rainfall hyetograph (total rainfall minus the abstractions). Table 8.1 provides the 0.5-hour unit hydrograph for the watershed.

The response to each pulse is proportional to the depth of the pulse. The response to the second pulse follows the response to the first pulse one duration (time step) later; the response to the third pulse follows the first two durations later (one duration later than the second pulse), etc. Table 8.2 illustrates the progression of calculations for three pulses of excess rainfall. The engineer scales the depth of each pulse by the UH ordinates in turn (down) and then sums the resulting discharges in the appropriate time step (across).

Table 8.2. Responses to three rainfall pulses of different depths and the summation.

Time Step	Time (hours)	Effective Rainfall Depth	Time (hours)	Unit Hydrograph Discharge (ft^3/s)	Response to 1st pulse (0.5 inch) (ft^3/s)	Response to 2nd pulse (1 inch) (ft^3/s)	Response to 3rd pulse (0.75 inch) (ft^3/s)	Total Runoff (ft^3/s)
1	0	0.5	0	0	0	-	-	0
2	0.5	1.0	0.5	30	15	0	-	15
3	1	0.75	1	364	182	30	0	212
4	1.5	-	1.5	500	250	364	22.5	636.5
5	2	-	2	405	202.5	500	273	975.5
6	2.5	-	2.5	242	121	405	375	901
7	3	-	3	118	59	242	303.75	604.75
8	3.5	-	3.5	50	25	118	181.5	324.5
9	4	-	4	14	7	50	88.5	145.5
10	4.5	-	4.5	4	2	14	37.5	53.5
11	5	-	5	2	1	4	10.5	15.5
12	5.5	-	5.5	2	0.5	2	3	5.5
13	6	-	6	0	0	1	1.5	2.5
14	6.5	-	6.5	-	-	0	0.75	0.75
15	7	-	7	-	-	-	0	0

Notice that:

- The time relationship of the steps in each response are the same (time invariance).
- Each response is proportional to the depth of excess rainfall (proportionality).
- The second response follows the first by one duration (time step).
- The third response follows the second by one time step.
- The components of each response at each time step are added (superposition).
- The total number of time steps in the response is 15; the number of time steps in the unit hydrograph (13) plus the number of excess rainfall pulses minus one (3 – 1 = 2).

Figure 8.3 shows the responses from each pulse of excess rainfall and the combined total runoff hydrograph that results from the summation of the pulses at each time step. Note that the peak flow values graphically represent the corresponding values in Table 8.2.

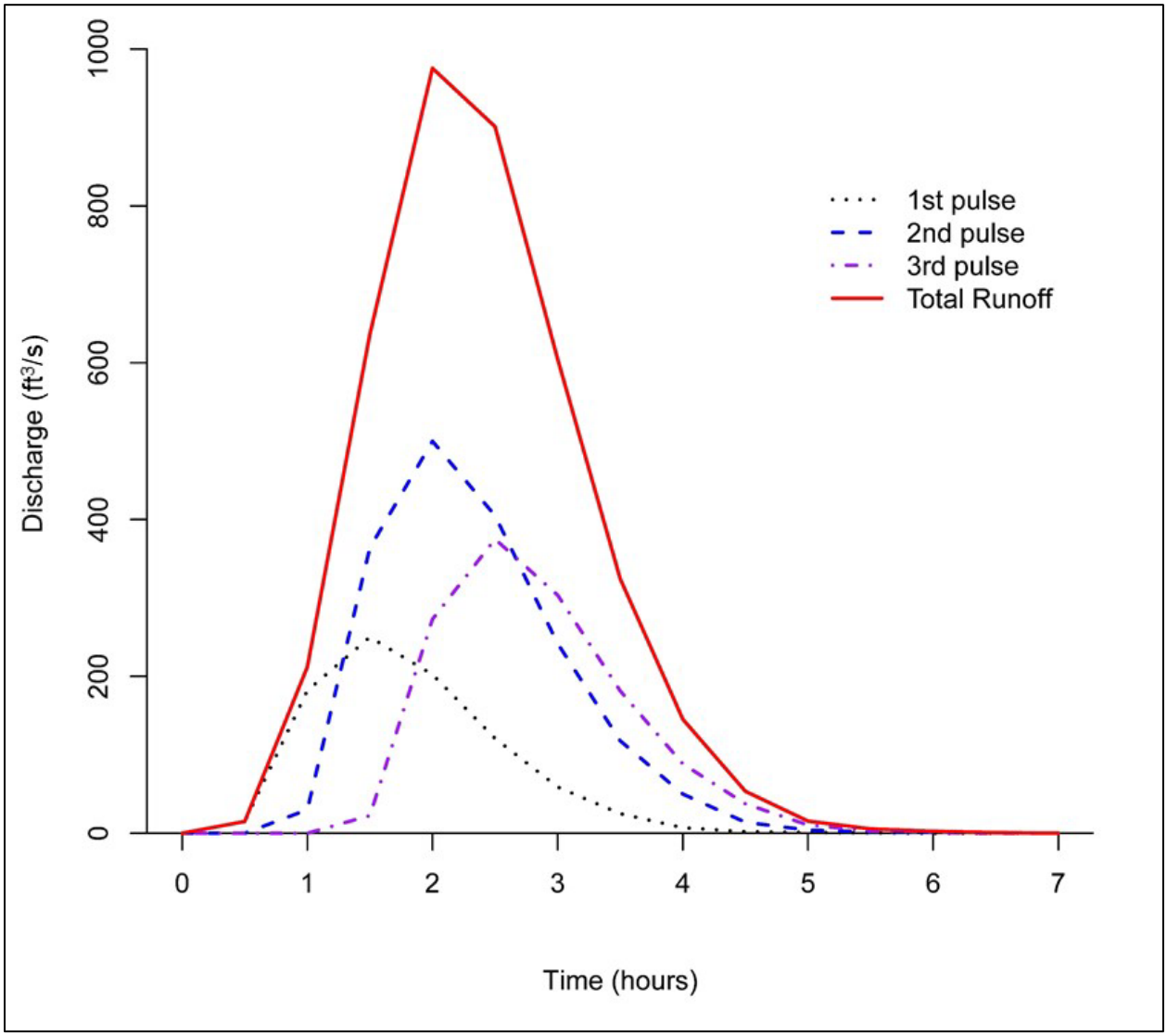

Figure 8.3. Watershed responses from each rainfall pulse and the total runoff hydrograph.

Solution:	As shown in Table 8.2 and Figure 8.3 the cumulative effect of the three pulses of excess rainfall result in a direct runoff hydrograph peak of 975.5 ft^3/s.

The peak outflow rate is a result of both the peak flow rate of the unit hydrograph and the relative depths of the pulses of excess rainfall. The example problem employed a unit hydrograph duration (0.5 hours) that was one-third of the time to peak of the unit hydrograph to show the calculations in a reasonably compact table. More commonly, engineers would select a smaller duration (time step) that is one-fifth or less of the time to peak. A smaller duration results in more time steps, and the unit hydrograph would correspondingly be divided into smaller time increments.

8.1.1 Unit Hydrograph Sources and Limitations

When site-specific data are available, engineers can obtain a unit hydrograph by analyzing synchronous rainfall and runoff data. This approach applies a loss model to the rainfall data to infer an estimate of the excess rainfall hyetograph. Several methods can calculate the ordinates of a unit hydrograph using both an excess rainfall hyetograph and an outflow hydrograph, synchronized in time. Sherman (1932) includes a simple method, appropriate for a small number of rainfall pulses. Chow et al. (1988) gives least-squares and linear programming methods for "deconvolution" of the data for use with more complex storms but warns of errors and nonlinearity. Because deconvolution methods depend on synchronous rainfall-runoff data on the watershed to obtain a UH, these methods apply to rare cases. If such data are available and the designer believes it advantageous, references such as Chow et al. (1988) and McCuen (2012) provide information on using deconvolution methods.

More commonly, engineers use unit hydrograph methods they can apply with basic information about the watershed such as basin size, shape, and response time. Described in subsequent sections, these synthetic methods include the NRCS dimensionless unit hydrograph, Snyder's unit hydrograph, and the time-area unit hydrograph.

Because of the assumptions made in the development of unit hydrograph procedures, designers should be familiar with several limitations. Uniformity of rainfall intensity and duration over the drainage basin is a simplification that is seldom true in reality. For this reason, the designer may apply areal reduction factors to rainfall for watersheds over certain sizes as described in Section 8.2.4.

In current practice, designers most commonly develop a UH for an ungaged watershed by scaling dimensionless curves published by various agencies, in particular from the U.S. Department of Agriculture Natural Resource Conservation Service (NRCS). Engineers derive the scaling factors from measurable or estimable watershed characteristics such as time of concentration and contributing area. The actual shapes are generalizations based on many rainfall-runoff studies and on the principles of UH theory.

8.1.2 NRCS Dimensionless Unit Hydrographs

The NRCS developed a synthetic unit hydrograph procedure that has been widely used in their conservation and flood control work. The method uses a dimensionless unit hydrograph based upon an analysis of a large number of natural unit hydrographs from a broad cross-section of geographic locations and hydrologic regions. The input parameters are the peak flow, the area of the watershed, and the time to peak. With these parameters, the designer can construct a standard unit hydrograph.

The NRCS evaluated unit hydrographs for a large number of actual watersheds and then made them dimensionless by dividing all discharge ordinates by the peak flow and the time ordinates by the time to peak. They then computed an average of these dimensionless UHs. The time base of the dimensionless UH was approximately 5 times the time to peak, and approximately 3/8 of the total volume occurred before the time to peak; the inflection point on the recession limb occurs at approximately 1.7 times the time to peak, and the UH has a curvilinear shape. Figure 8.4 shows the dimensionless UH and Table 8.3 summarizes the discharge ratios for selected values of the time ratios. The figure also shows the corresponding mass curve, which is the cumulative (integrated) representation of the dimensionless UH.

For purposes of comparison, the curvilinear unit hydrograph can be approximated by a triangular UH that has similar characteristics. Figure 8.5 shows a comparison of the two dimensionless unit hydrographs. It is important to recognize that the triangular UH is not a substitute for the curvilinear UH. The curvilinear UH is always used in hydrologic computations. The triangular unit hydrograph

is only used to develop an expression for computing the peak flow of the curvilinear unit hydrograph. While the time base of the triangular UH is only 8/3 of the time to peak (compared to 5 for the curvilinear UH), the areas under the rising limbs of the two UHs are the same (i.e., 37.5 percent).

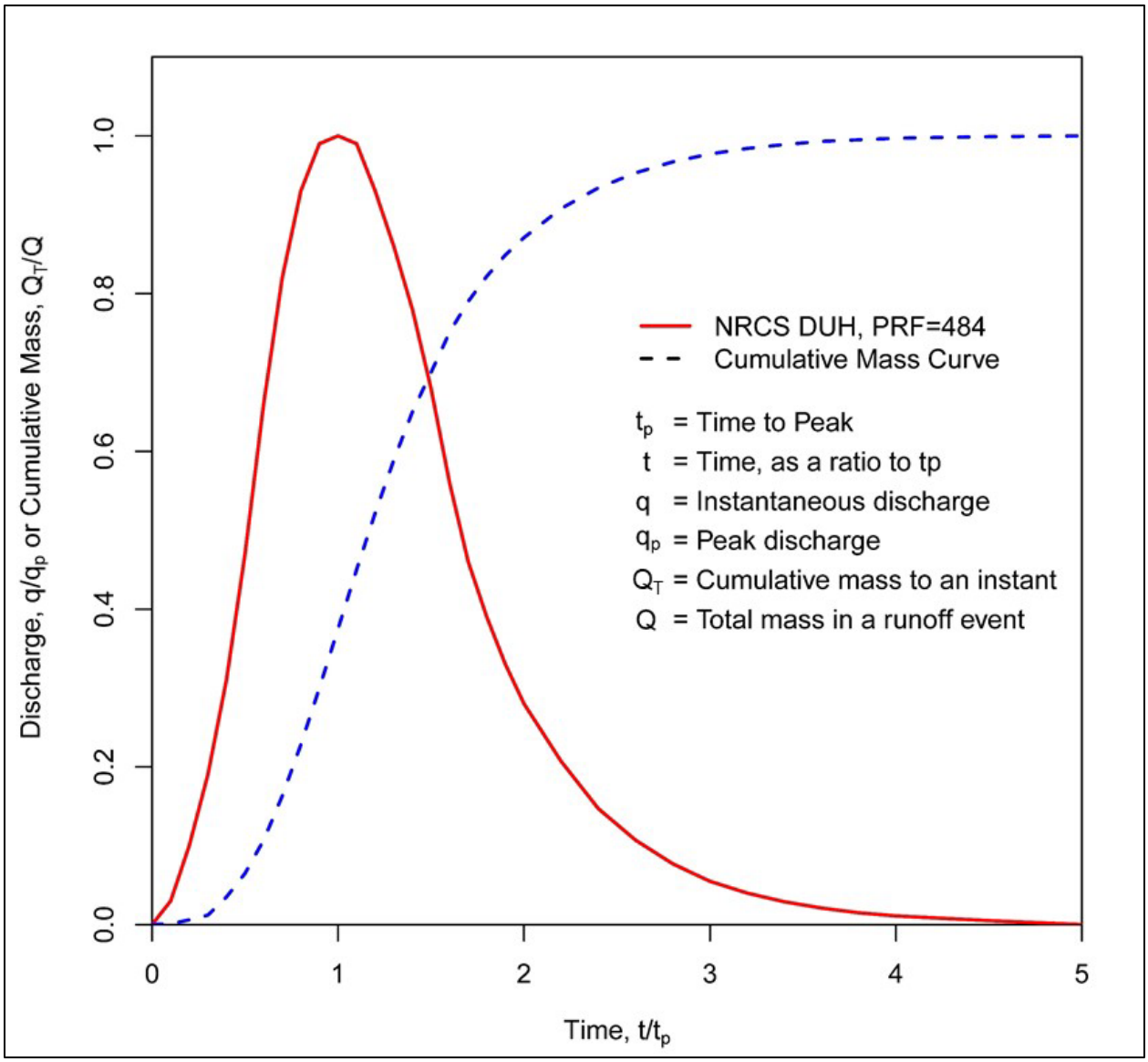

Figure 8.4. Dimensionless unit hydrograph and mass curve.

The area under a hydrograph equals the depth of direct runoff Q, which is 1 inch (1 mm) for a unit hydrograph. Based on geometry, the runoff volume is related to the characteristics of the triangular unit hydrograph by:

$$A_Q = \frac{1}{2} q_p (t_p + t_r) \qquad (8.1)$$

where:

t_p = Time to peak, s
t_r = Recession time, s
A = Watershed area, ft^2 (m^2)
Q = Direct runoff depth, ft (m)
q_p = Peak flow, ft^3/s (m^3/s)

Table 8.3. Ratios for dimensionless unit hydrograph and mass curve.

Time Ratios t/t_p	Discharge Ratios q/q_p	Mass Curve Ratios Q_t/Q
0	0.000	0.000
0.1	0.030	0.001
0.2	0.100	0.006
0.3	0.190	0.012
0.4	0.310	0.035
0.5	0.470	0.065
0.6	0.660	0.107
0.7	0.820	0.163
0.8	0.930	0.228
0.9	0.990	0.300
1.0	1.000	0.375
1.1	0.990	0.450
1.2	0.930	0.522
1.3	0.860	0.589
1.4	0.780	0.650
1.5	0.680	0.700
1.6	0.560	0.751
1.7	0.460	0.790
1.8	0.390	0.822
1.9	0.330	0.849
2.0	0.280	0.871
2.2	0.207	0.908
2.4	0.147	0.934
2.6	0.107	0.953
2.8	0.077	0.967
3.0	0.055	0.977
3.2	0.040	0.984
3.4	0.029	0.989
3.6	0.021	0.993
3.8	0.015	0.995
4.0	0.011	0.997
4.5	0.005	0.999
5.0	0.000	1.000

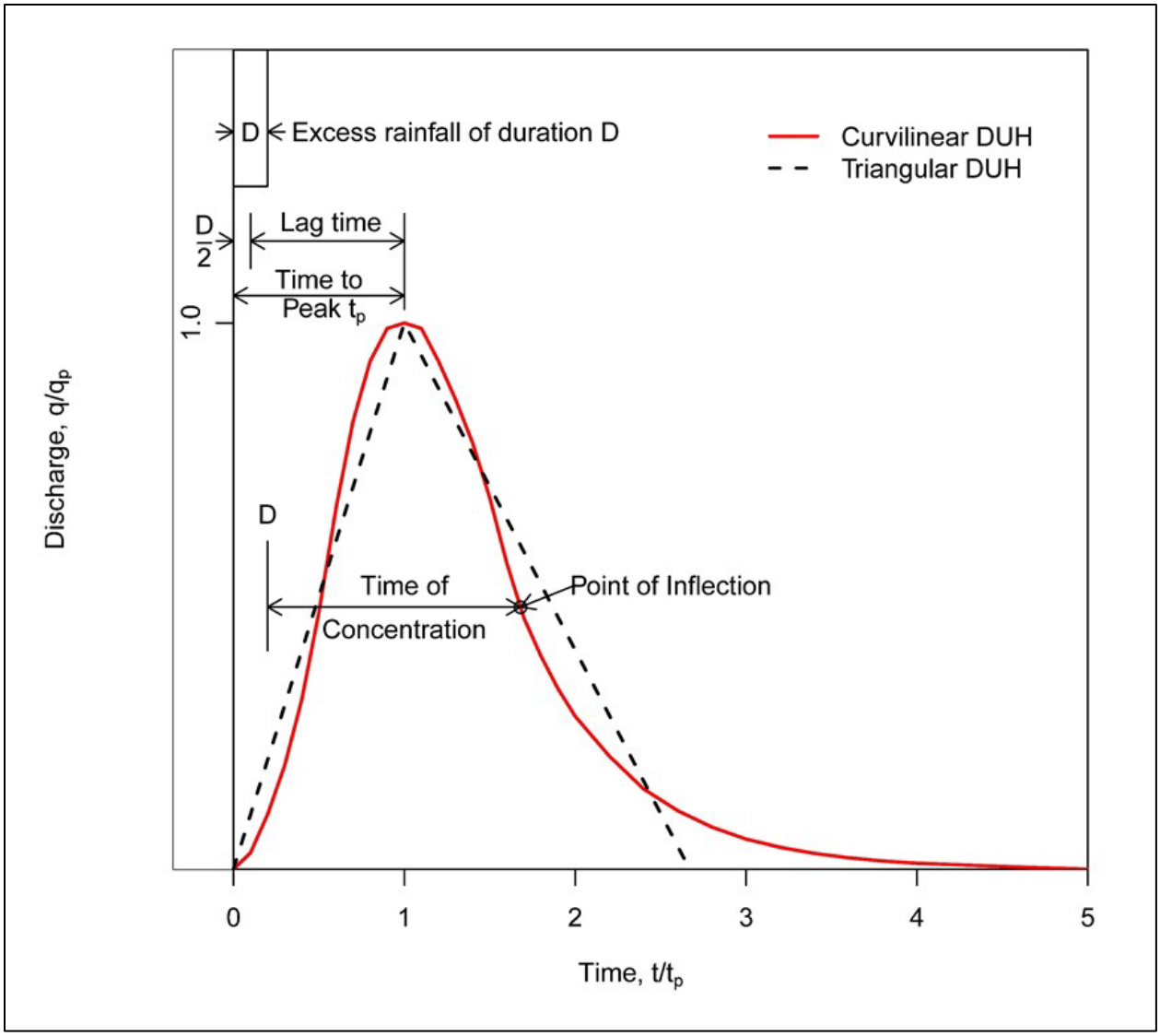

Figure 8.5. Dimensionless curvilinear unit hydrograph and equivalent triangular hydrograph.

Solving for q_p and rearranging yields:

$$q_p = \frac{A\,Q}{t_p}\left[\frac{2}{1+t_r/t_p}\right] \tag{8.2}$$

Letting K_p replace the contents within the brackets yields:

$$q_p = \frac{K_p A\,Q}{t_p} \tag{8.3}$$

Using ft^3/s for discharge, mi^2 for area, inches for runoff depth, and hours for t_p and setting $t_r = 1.67t_p$, then, K_p equals 484:

$$q_p = \frac{\alpha K_P\,A\,Q}{t_p} \tag{8.4}$$

where:

q_p	=	Peak flow, ft^3/s (m^3/s)
A	=	Watershed area, mi^2 (km^2)
Q	=	Direct runoff depth, inches (mm)
t_p	=	Time to peak, h
K_p	=	Peak rate factor equal to 484, dimensionless
α	=	Unit conversion constant, 1 in CU (0.00043 in SI)

A peak rate factor, K_p, equal to 484 reflects a hydrograph that has 3/8 of its area under the rising limb. Equation 8.4 may be applied to determine the peak of the curvilinear unit hydrograph only when K_p = 484 and Q = 1 (inch or mm). In mountainous or flat areas, it is reasonable to expect that the volume fraction under the rising limb will change. For mountainous watersheds, the volume fraction could be expected to be greater than 3/8, and therefore K_p may be near 600 while for flat, wetland areas K_p may be about 300. However, if other peak rate factors are used, a different dimensionless curve other than the one in Figure 8.4 is used to preserve the area under the curve equal to one. Section 8.1.2.1 discusses peak rate factors in more detail.

The time to peak can be expressed in terms of the unit duration of the rainfall excess and the time of concentration. Figure 8.5 provides the following two relationships:

$$t_c + D = 1.7 t_p \tag{8.5}$$

Since the NRCS sets the lag equal to 0.6 t_c, for K_p = 484, then:

$$\frac{D}{2} + 0.6 t_c = t_p \tag{8.6}$$

Solving for D yields:

$$D = \frac{2}{15} t_c = 0.133 t_c \tag{8.7}$$

Therefore, t_p can be expressed in terms of t_c:

$$t_p = \frac{D}{2} + 0.6 t_c = \frac{2}{3} t_c \cong 0.667 t_c \tag{8.8}$$

Expressing in terms of t_c rather than t_p yields:

$$q_p = \frac{\alpha K_P A Q}{0.667 t_c} \tag{8.9}$$

8.1.2.1 Peak Rate Factors

As discussed in previous section, the NRCS dimensionless unit hydrograph used was a simple triangular shape, with the peak outflow located at 3/8 of the time base. For 1 inch of excess rainfall in 1 hour duration and 1 square mile of contributing area, and time to peak of 3 hours, the resulting peak outflow rate is 484 ft^3/s. This number (484) was the original peak rate factor (PRF). The volume of runoff before the peak was 3/8 of the total, and 5/8 of the total was after the peak.

Extending the concept that a triangular shape can represent watershed response, it can be noted that at the extreme, where one-half of the volume is before the peak and the remaining one-half

after the peak, an isosceles triangle symmetric about the peak, would have a PRF of 635 ft^3/s for the same 1 inch of rainfall in 1 hour over 1 square mile. This means that PRFs under these conditions must be 635 or less.

Subsequently, the area of the triangle was redistributed to achieve a curvilinear shape but retained the same area under the curve before and after the peak. The shape was represented in a dimensionless form, with time represented relative to the time to peak (t/t_p) and discharge relative to peak flow (q/q_p). Figure 8.5 shows the curvilinear dimensionless unit hydrograph (DUH) along with the triangular unit hydrograph from which it evolved.

The standard DUH with a PRF of 484 remained unchanged as an integral part of the NRCS method for many years. Experience modeling with the method, e.g., Welle et al. (1980), showed that 484 was too large in some situations resulting in an overestimation of peak flow. The States of Delaware, Maryland, and Virginia jointly developed a DUH with a PRF of 284, called the Delmarva DUH (Welle et al. 1980). Some nearby States with similar terrain adopted the Delmarva DUH.

Acknowledging the limitations of a single PRF, the NRCS extended the concept with the publication of NEH 630 Chapter 16 (NRCS 2007a). Chapter 16 of NEH 630 contains tables and graphs for DUHs with PRFs ranging from 100 to 600. These same PRFs are available in commonly available public domain software for selection in modeling. Whereas researchers developed the original curvilinear DUH with a PRF of 484 graphically from the triangle, researchers developed the extended DUH series from a mathematical function (the gamma equation).

Little information currently exists supporting the selection of PRFs for particular watersheds. Chapter 16 of NEH 630 suggests that steeper slopes imply larger PRF and flatter slopes smaller, as the Delmarva DUH suggests. Factors other than slope likely influence the PRF (e.g., watershed shape, time-area, or stream bifurcation.) States may wish to develop defensible selection criteria based on statewide or regional studies or experience. Research in Texas (Fang et al. 2005) found a mean PRF of 370 from 1,600 events on 90 watersheds in Texas. However, no clear relationship between PRF and watershed characteristics has yet been observed.

The availability of dimensionless unit hydrographs for a wide range of PRFs provides designers with flexibility in using local knowledge or regional calibration when selecting unit hydrograph characteristics for ungaged watersheds. Figure 8.6 compares the effect of various PRFs including the original NRCS DUH with PRF of 484. The original DUH used a time base of runoff of 5 times the time to peak; other PRFs use a time base of runoff inversely proportional to the PRF. It varies from 3.4 times the time to peak for PRF of 600, to 24 times the time to peak for PRF 100.

When an engineer transforms any of these DUHs with a site-specific time to peak and peak flow, the resulting hydrographs will all represent one unit of runoff. **Those with longer time bases will also exhibit lower peaks so that the volume under the hydrograph is the same.**

8.1.2.2 Time Parameters

Figure 8.5 shows the NRCS definitions for various times pertinent to UH modeling, in particular, the lag time and the duration of excess rainfall. The lag time describes the time between the middle of the pulse of excess rainfall (D/2 on Figure 8.5) and the peak of the unit hydrograph.

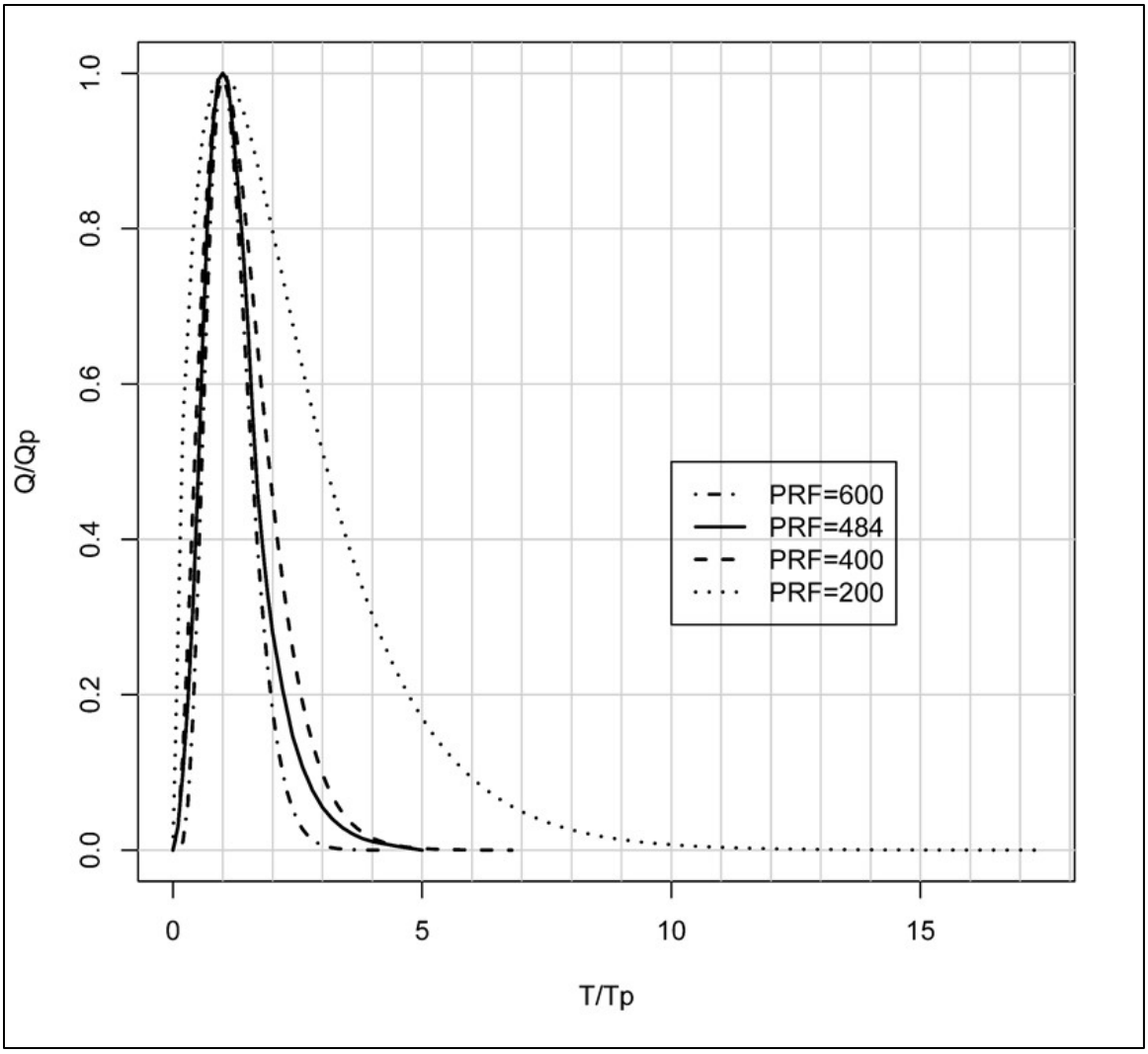

Figure 8.6. Comparison of DUH shapes and receding limbs with a range of PRFs.

A central concept in hydrology is the time of concentration (see Section 3.7). While time of concentration is a useful concept, it is not measurable. However, engineers can estimate this watershed characteristic using one of several methods. The NRCS defines time of concentration in this context as the time from the end of the rainfall pulse (time D) to the point of inflection on the receding limb of the unit hydrograph. Engineers consider the point of inflection as the point where the curve changes from being concave downward (as it approaches, crosses, and departs the peak) to being concave upward (as it diminishes and approaches zero discharge). For the original DUH with a PRF of 484 developed graphically, NRCS defines the lag time as 60 percent of the time of concentration.

Table 8.4 gives the lag time as a fraction of the time of concentration for PRFs included in NEH 630 Chapter 16, Delmarva DUH (PRF = 284), and the original DUH (PRF = 484). Since researchers graphically derived the original DUH and the subsequent PRF DUHs from a mathematical function, the points of inflection for the NEH 630 DUHs appear relatively shorter than that for the original and for the Delmarva DUH.

NEH 630 recommends that the duration of excess rainfall be 20 percent of the time to peak. It also indicates that while some variation is appropriate, it should not exceed 25 percent of t_p. NEH 630 makes no recommendation with respect to durations smaller than 20 percent of t_p. For the

nominal case of D = 20 percent of t_p, D/2 = 10 percent of t_p. Therefore, the lag time is 90 percent of t_p since lag time is the time from D/2 to the peak (100 percent minus 10 percent).

Table 8.4. Peak rate factor and lag time ratios.

PRF	Ratio of Lag Time to Time of Concentration
100	0.28
150	0.32
200	0.38
250	0.41
300	0.45
350	0.45
400	0.53
450	0.53
500	0.56
550	0.56
600	0.60
284	0.50
484	0.60

8.1.2.3 Selection of a Time Step

Equations 8.5 through 8.8 provide the relationships between time parameters based on a PRF of 484. Engineers use the information in Table 8.4 to compute values of duration (D) and time to peak from the time of concentration for other PRFs.

The nature of UH aggregation implies that the duration of each pulse of excess rainfall is the length in time of each step. Because computer programs may not allow arbitrary time step sizes, the engineer may need to round the time step size to a convenient value, according to the time step sizes allowed by the modeling software. For example, HEC-HMS allows time step sizes of 1, 2, 3, 4, 5, 6, 10, 15, 20, and 30 minutes; 1, 2, 3, 4, 6, 8, and 12 hours; and 1 day.

UH Duration and Time Step Size

For unit hydrograph calculations, the duration of excess rainfall is necessarily the same as the time step size for the analysis. The actual values used for lag time, time to peak, and time step size are coupled with one another, and are coordinated with similar values on other subwatersheds in the case of subdivision.

The use of a very fine time step causes rainfall to be divided into very small quantities and causes the convergence of lag time and time to peak. This begins to approach Instantaneous Unit Hydrograph Theory.

Regardless of the t_c and t_L times estimated for the model, the software requires that a time step of one of the available values be selected. To avoid having calculations “straddle” the peak of the UH rather than using the peak value, modelers select a time to peak, t_p, that is an integer multiple

of the time step. They then adjust t_L such that it is the integer number of time steps in t_p, minus D/2. If the process does not meet these numerical constraints, it may not produce the peak flow associated with the DUH, and mass balance of excess rainfall and outflow may not be maintained. The same general recommendations on time step size relative to t_p and t_L apply reasonably to all UH calculations.

Example 8.3:	Estimate unit hydrograph duration (time step) from a time of concentration.
Objective:	Calculate the time step size and lag time to be used for modeling a watershed.

Given a watershed:

Time of concentration = 80 minutes

Assume the NRCS DUH with PRF of 484.

Step 1. Calculate the lag time.

$t_L = 0.6\ t_c = 0.6\ (80) = 48$ minutes

Step 2. Estimate the time to peak.

Assume $D = 0.2\ t_p$.

$t_p = D/2 + t_L = (0.2\ t_p)/2 + t_L$

$0.9\ t_p = t_L$

$t_p = t_L/0.9 = 48/0.9 = 53.3$ minutes

Step 3. Estimate D.

As assumed in step 2:

$D = 0.2\ t_p = 0.2\ (53.3) = 10.7$ minutes

Assuming use of HEC-HMS, time steps of 10 or 15 minutes are available. Choose the closest available step size at 10 minutes.

Step 4. Update the time to peak and lag time for modeling.

With D = 10 minutes:

$t_p = D / 0.2 = 10 / 0.2 = 50$ minutes

$t_L = 0.9\ t_p = 0.9\ (50) = 45$ minutes

$t_c = t_L / 0.6 = 45 / 0.6 = 75$ minutes

The modeling t_c is 5 minutes shorter than the original estimate of 80 minutes. This adjustment assures that the peak of the unit hydrograph is captured by the computations. Estimating the time of concentration always involves uncertainty, making any error introduced by reasonable adaptation of time step size and lag time inconsequential.

Solution:	Providing a unit hydrograph duration (D) on an available time step of 10 minutes resulted in an adjustment of the time of concentration by 5 minutes. This is within the range of uncertainty for estimating time of concentration.

8.1.2.4 Selection of Time Steps for Subdivided Watersheds

Unit hydrograph modeling allows the engineer to subdivide watersheds into component subwatersheds, calculate the responses of the subwatersheds, and aggregate those responses in synchronous temporal alignment. However, different subwatersheds invariably have different times of concentration. The procedure above could result in different time steps appropriate for different subwatersheds that could preclude their synchronous aggregation. In these cases, the engineer modifies the procedure to assure compatibility using the following approach:

- Estimate the time of concentration of each subwatershed.
- From each time of concentration, estimate the lag time based on the multiplier for the PRF selected.
- Estimate time to peak for each subwatershed based on the assumption of lag time equal to 90 percent of time to peak.
- Identify the shortest time to peak of each of the subwatersheds.
- Select a time step based 20 to 25 percent of the shortest time to peak.
- Estimate the number of time steps to peak for the other subwatersheds. Round the number of time steps to the nearest integer.
- Adjust the time to peak, lag time, and time of concentration for the subwatersheds based on the number of time steps to peak, if appropriate.

Too Much of a Good Thing

Unit hydrograph computer models often use a time step size that was apparently arbitrarily selected to be quite small, perhaps hoping that high resolution would enhance accuracy. The designer will want to remember that dividing time into small increments also divides rainfall into small increments. In some cases, numerical truncation of the small numbers representing rainfall can result in loss of resolution and mass balance. Time step size that balances resolution with the limitations of numerical processes produces robust and stable analyses.

Example 8.4:	Estimating a common time step.
Objective:	Calculate a time step for a subdivided watershed and the resulting modeling lag times.

Given: A watershed subdivided into three subwatersheds for modeling.

Use the standard NRCS DUH with a PRF of 484 and a $t_L = 0.6\ t_c$.

Subwatershed 1: t_c = 90 minutes

Subwatershed 2: t_c = 75 minutes

Subwatershed 3: t_c = 110 minutes

Step 1. Calculate the lag time of the subwatershed with the smallest time of concentration.

Subwatershed 2 has the shortest time of concentration.

$t_L = 0.6\ (75) = 45$ minutes

Step 2. Estimate the time to peak of all watersheds.

Subwatershed 1:

$t_L = 0.6\ t_c = 0.6\ (90) = 54$ minutes

$t_p = t_L / 0.9 = 54 / 0.9 = 60$ minutes

Subwatershed 2:

$t_L = 0.6\ t_c = 0.6\ (75) = 45$ minutes

$t_p = t_L / 0.9 = 54 / 0.9 = 50$ minutes

Subwatershed 3:

$t_L = 0.6\ t_c = 0.6\ (110) = 66$ minutes

$t_p = t_L / 0.9 = 66 / 0.9 = 73.3$ minutes

Step 3. Estimate D based on the subwatershed with the shortest time to peak.

Assume $D = 0.2\ t_p$ for the shortest time to peak (subwatershed 2).

$D = 0.2\ t_p = 0.2\ (50) = 10$ minutes

Assuming use of HEC-HMS, the time step of 10 minutes is available. No adjustment is needed. The original time parameters for subwatershed 2 are unchanged.

Step 4. Estimate number of time steps to peak for other subwatersheds.

Subwatershed 1:

Number of time steps = $t_p / D = 60 / 10 = 6$

For subwatershed 1, the number of time steps is an integer, no adjustment needed.

Subwatershed 3:

Number of time steps = $t_p / D = 73.3 / 10 = 7.33$

For subwatershed 3, the number of time steps is not an integer. Round to closest value at 7.

Step 5. Update the time to peak and time of concentration for modeling.

Subwatershed 1:

No adjustment needed. Number of time steps to peak = 6. $t_p = 60$ minutes, $t_c = 90$ minutes.

$t_L = t_p – D/2 = 60 – 10/2 = 55$ minutes

Subwatershed 2:

No adjustment needed. Number of time steps to peak = 5. $t_p = 50$ minutes, $t_c = 75$ minutes.

$t_L = t_p – D/2 = 50 – 10/2 = 45$ minutes

Subwatershed 3:

Adjustment needed because the number of time steps was rounded from 7.33 to 7 in step 4. t_p = number of steps (D) = 7 (10) = 70 minutes

$t_L = t_p – D/2 = 70 – 10/2 = 65$ minutes

$t_c = t_L / 0.6 = 65 / 0.6 = 108$ minutes.

Solution:	A common time step of 10 minutes is selected for modeling all three watersheds. Minor adjustments are made to the time parameters in subwatersheds 1 and 3 to obtain internal consistency.

8.1.3 Snyder Unit Hydrograph

Snyder published his UH method in 1938, which USACE has used extensively. Snyder developed his method for relatively small watersheds in Appalachia. Subsequent studies extended the method to other regions.

In the Snyder method, the engineer uses two empirically defined terms, C_t and C_p, and the physiographic characteristics of the drainage basin to determine a D-hour unit hydrograph. This method does not explicitly determine the entire time distribution of the UH; it gives seven points through which the modeler can draw a smooth curve, interpolating other points.

The modeler evaluates certain key parameters of the unit hydrograph shown in Figure 8.7, constructing a characteristic UH from them. The key parameters are the lag time, the unit hydrograph duration, the peak flow, and the hydrograph time widths at 50 percent and 75 percent of the peak flow. Using these points, the modeler sketches a characteristic unit hydrograph and checks the volume of this hydrograph to ensure it equals 1 inch (1 mm) of runoff. If it does not, the modeler adjusts the ordinates accordingly.

A suggested procedure to develop the Snyder unit hydrograph follows:

Step 1. Data collection and determination of physiographic constants.

The engineer determines appropriate values for C_t and C_p for the watershed under consideration. Engineers can find these values from watershed studies, reference manuals, USACE district offices, or site-specific analysis of unit hydrographs from gaged streams in the same general area. The coefficient, C_t, represents the variation of UH lag time with watershed slope and storage. In his Appalachian Highlands study, Snyder found C_t to vary from 1.8 to 2.2. Further studies have shown that extreme values of C_t vary from 0.4 in Southern California to 8.0 in the Eastern Gulf of Mexico. The coefficient, C_p represents the variation of the UH peak flow with watershed slope, storage, lag time, and effective area. Values of C_p range between 0.4 and 0.94.

In addition to these empirical coefficients, the modeler estimates the watershed area, A; the length along the main channel from the outlet to the divide, L; and the length along the main channel to a point opposite the watershed centroid, L_{ca}.

Step 2. Determination of lag time.

Next, the modeler determines the lag time, T_L, of the unit hydrograph. The lag time is the time from the centroid of the excess rainfall to the hydrograph peak estimated as:

$$t_L = \alpha C_t (L\, L_c)^{0.3} \qquad (8.10)$$

where:

t_L	=	Lag time, h
C_t	=	Empirical coefficient related to lag time
L	=	Length along main channel from outlet to divide, mi (km)
L_c	=	Length along main channel from outlet to a point opposite the watershed centroid, mi (km)
α	=	Unit conversion constant, 1.0 for CU (0.75 for SI)

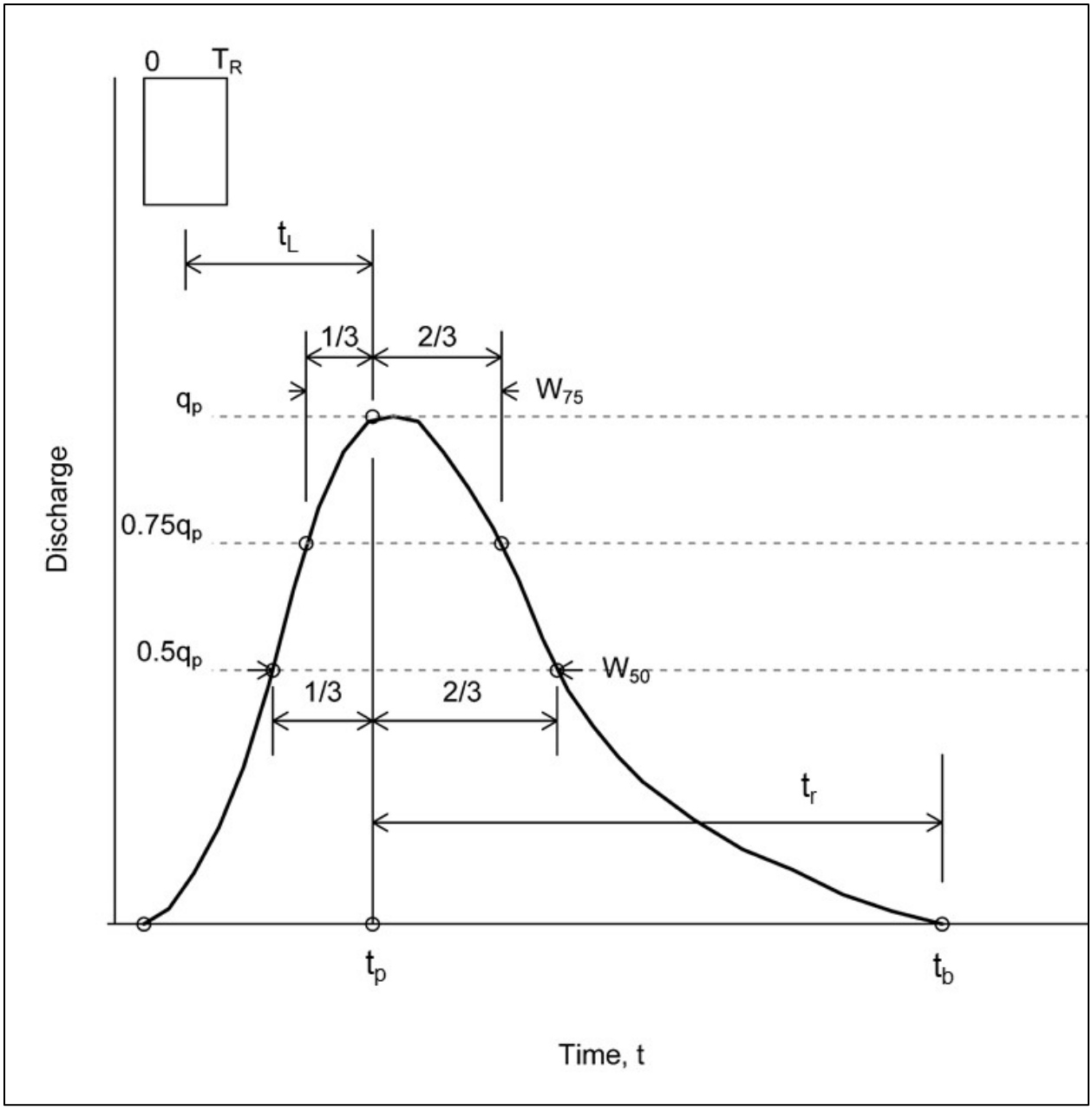

Figure 8.7. Snyder unit hydrograph definition sketch.

Step 3. Determine duration of the unit hydrograph.

Snyder developed an initial estimate of the duration of the excess rainfall, T_R:

$$T_R = \frac{t_L}{5.5} \tag{8.11}$$

where:

T_R = Unit hydrograph duration, h
t_L = Time lag, h

Because the equation may result in inconvenient values of the unit hydrograph duration, the engineer may adjust the computed lag time for other unit durations using the adjustment relationship:

$$t_{L(adj.)} = t_L + 0.25\left(T_R' - T_R\right) \quad (8.12)$$

where:

$t_{L(adj.)}$ = Adjusted lag time for the new duration, h
t_L = Initial lag time as computed above, h
T_R = Initial unit hydrograph duration, h
T_R' = Desired unit duration, h.

D versus T_R

Snyder designated the duration of excess rainfall of the unit hydrograph (called "D" elsewhere in this manual) as T_R in the development of this method. To be consistent with other references on Snyder's method, this manual uses T_R instead of D in the description of this method.

For example, if a modeler estimates an initial lag time of 12.5 hours, the corresponding unit hydrograph duration is (12.5/5.5) or 2.3 hours. Because a unit duration of 2.0 hours would be more convenient, the modeler adjusts the lag time as follows:

$$t_{L(adj)} = t_L + 0.25\left(T_R' - T_R\right) = 12.5 + 0.25\left(2.0 - 2.3\right) = 12.4\ \text{h}$$

Step 4. Estimate unit hydrograph peak flow.

Estimate the peak flow for the UH:

$$q_P = \alpha \frac{C_P A}{T_{L(adj)}} \quad (8.13)$$

where:

q_p = Unit peak flow, ft³/s/inch (m³/s/mm)
C_p = Empirical coefficient related to the peak flow
A = Watershed area, mi² (km²)
α = Unit conversion constant, 640 for CU (0.275 for SI)

Step 5. Estimate W_{50} and W_{75}.

The following equations approximate the time widths of the unit hydrograph at discharges equal to 50 percent and 75 percent of the peak flows:

$$W_{50} = \alpha_{50}\left(\frac{q_p}{A}\right)^{-1.075} \quad (8.14)$$

$$W_{75} = \alpha_{75}\left(\frac{q_p}{A}\right)^{-1.075} \quad (8.15)$$

where:

W_{50} = Time interval between the rising and falling limbs at 50 percent of peak flow, h
W_{75} = Time interval between the rising and falling limbs at 75 percent of peak flow, h
q_p = Unit peak flow, ft³/s/inch (m³/s/mm)
A = Watershed area, mi² (km²)

α_{50} = Unit conversion constant, 735 in CU (0.18 in SI)
α_{75} = Unit conversion constant, 434 in CU (0.10 in SI)

Step 6. Determine time base of unit hydrograph.

Snyder determined the time base, t_B, of the UH to be approximately:

$$t_B = 3 + \frac{t_{L(adj.)}}{8} \quad (8.16)$$

where:
t_B = Time base of the synthetic unit hydrograph, days
$t_{L(adj.)}$ = Adjusted lag time for the new duration, h

This relationship, while reasonable for larger watersheds, may not apply to smaller watersheds. A more realistic value for smaller watersheds uses 3 to 5 times the time to peak as a base for the unit hydrograph. The time to peak is the time from the beginning of the rising limb of the hydrograph to the peak.

Step 7. Construct unit hydrograph.

Using the values computed in the previous steps, the engineer sketches the unit hydrograph, remembering that the total runoff depth should equal one unit of depth (1 inch or 1 mm). A rule of thumb to assist in sketching the unit hydrograph is that the W_{50} and W_{75} time widths should be apportioned with one-third to the left of the peak and two-thirds to the right of the peak.

If adjustments are needed to the initial estimate of the unit hydrograph to correct the total runoff depth, engineers commonly preserve the time to peak and peak flow and primarily adjust the receding limb of the hydrograph up or down. If more volume is needed the engineer scales the receding limb up and may also lengthen the time base. Conversely if less volume is needed the engineer scales the receding limb down and may shorten the time base. Adjustment focuses on the receding limb because its shape is more uncertain than the rest of the hydrograph.

Example 8.5: Application of Snyder's unit hydrograph.

Objective: Construct a synthetic Snyder's unit hydrograph for a watershed.

Given a watershed with characteristics determined in step 1.

Step 1. Data collection and determination of physiographic constants.

Area = 875 mi^2 (2,266 km^2)
L = 83.6 mi (133.6 km)
L_{ca} = 40 mi (65 km)

For this region, the following apply:

C_t = 1.32
C_p = 0.63

Step 2. Determination of lag time.

$$t_L = \alpha_{75}\, C_t\, (LL_{ca})^{0.3} = 1.0(1.32)\left((83)(40)\right)^{0.3} = 15.0\,h$$

Step 3. Determine duration of unit hydrograph.

$$T_R = \frac{t_L}{5.5} = 2.7\,\text{h}$$

Select a rounded value of 3 hours. Calculate the adjusted lag time:

$$t_{L(adj.)} = t_L + 0.25\left(T_R' - T_R\right) = 15.0 + 0.25(3 - 2.7) = 15.1\text{h}$$

Step 4. Estimate the unit hydrograph peak flow.

$$q_P = \alpha\frac{C_P A}{t_{L(adj)}} = \frac{(640)(0.63)(875)}{15.1} = 23{,}000\,\text{ft}^3\text{ / s / in}$$

Step 5. Estimate W_{50} and W_{75}.

$$W_{50} = \alpha\left(\frac{q_p}{A}\right)^{-1.075} = 735\left(\frac{23{,}000}{875}\right)^{-1.075} = 22\,\text{h}$$

$$W_{75} = \alpha\left(\frac{q_p}{A}\right)^{-1.075} = 434\left(\frac{23{,}000}{875}\right)^{-1.075} = 13\,\text{h}$$

Step 6. Determine the time base of the unit hydrograph.

$$t_B = 3 + \frac{t_{L(adj.)}}{8} = 3 + \frac{15.1}{8} = 4.9\text{ days} = 118\,\text{h}$$

Compared to the hydrograph widths at 50 and 75 percent of the peak flow, a time base of 118 hours is very long. To obtain a more realistic value, assume that the time base equals 4.5 times the time to peak:

$$t_B = 4.5(t_{L(adj)} + \frac{1}{2}T_R) = 4.5\left[15.1 + \frac{1}{2}(2.7)\right] = 74.0\,\text{h}$$

Step 7. Construct unit hydrograph.

Figure 8.8 plots these points with a smooth hydrograph shape fitted with the key dimensions. Column 2 of Table 8.5 provides a tabular listing of the hydrograph with the sum of ordinates equal to 160,300 ft^3/s/in. Use the trapezoidal rule to compute the volume under the unit hydrograph:

$$\Delta t\sum_{i=1}^{25} q_{P_i} = \left(160{,}300\frac{\text{ft}^3}{\text{s / in}}\right)(3\,\text{h})\left(\frac{3600\,\text{s}}{\text{h}}\right)\left(\frac{1}{875\,\text{mi}^2}\right)\left(\frac{1\,\text{mi}}{5280\,\text{ft}}\right)^2\left(\frac{12\,\text{in}}{\text{ft}}\right)(1\,\text{in}) = 0.85\text{ inch}$$

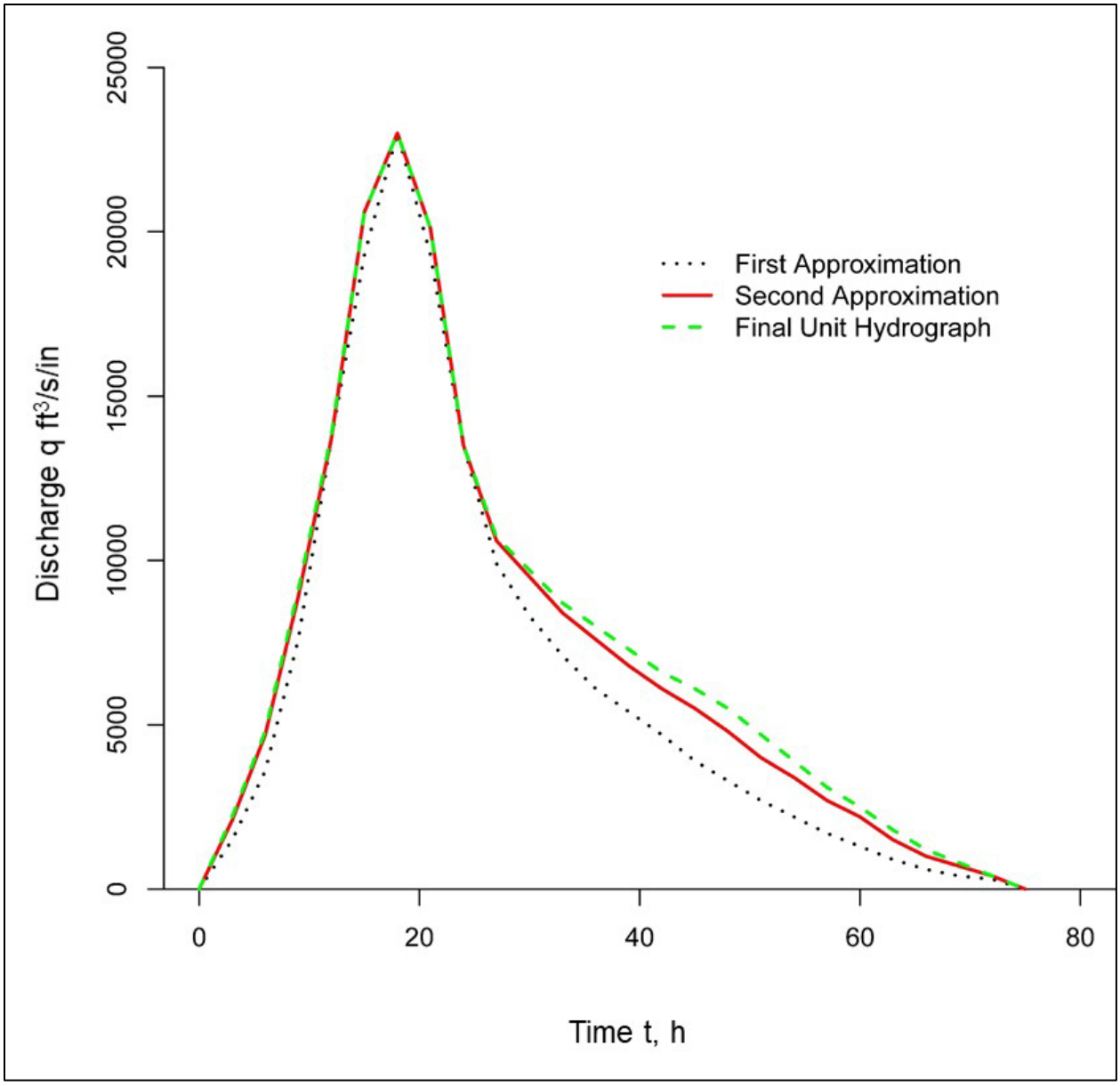

Figure 8.8. Snyder's unit hydrograph analysis.

The total volume equals 0.85 units which is less than the unit depth of 1 inch. Therefore, this initial hydrograph is not a unit hydrograph. The engineer increases the volume in a reasonable and systematic way, focusing on the receding limb of the hydrograph.

The engineer increases the receding limb for a second approximation shown in Figure 8.8 and tabulated in column 3 of Table 8.5. Again, use the trapezoidal rule to compute the volume:

$$\Delta t \sum_{i=1}^{25} q_{P_i} = \left(181{,}800 \frac{\text{ft}^3}{\text{s / in}}\right)(3\,\text{h})\left(\frac{3600\,\text{s}}{\text{h}}\right)\left(\frac{1}{875\,\text{mi}^2}\right)\left(\frac{1\,\text{mi}}{5280\,\text{ft}}\right)^2\left(\frac{12\,\text{in}}{\text{ft}}\right)(1\,\text{in}) = 0.97\ \text{inch}$$

The second approximation is about 3 percent less than the required unit depth. A third iteration is shown in Figure 8.8 and tabulated in column 4 of Table 8.5. Because the result of the trapezoidal rule computation equals one inch, this hydrograph is a 3-hour unit hydrograph for the watershed.

Table 8.5. Adjustment of ordinates of Snyder's unit hydrograph.

(1) Time (h)	(2) Initial Hydrograph ($ft^3/s/inch$)	(3) Second Hydrograph ($ft^3/s/inch$)	(4) Third Hydrograph ($ft^3/s/inch$)
0	0	0	0
3	1,500	2,100	2,200
6	3,600	4,700	4,800
9	7,600	8,900	9,100
12	13,700	13,700	13,800
15	19,300	20,600	20,600
18	23,000	23,000	23,000
21	19,300	20,100	20,100
24	13,500	13,500	13,500
27	9,900	10,600	10,700
30	8,300	9,500	9,700
33	7,100	8,400	8,700
36	6,100	7,600	8,000
39	5,400	6,800	7,300
42	4,700	6,100	6,600
45	3,900	5,500	6,100
48	3,300	4,800	5,500
51	2,700	4,000	4,700
54	2,200	3,400	3,900
57	1,700	2,700	3,100
60	1,300	2,200	2,500
63	900	1,500	1,800
66	600	1,000	1,200
69	400	700	800
72	300	400	400
75	0	0	0
Total	160,300	181,800	188,100

Solution: After three trials, a unit hydrograph for the watershed was derived.

8.1.4 Time-Area Unit Hydrographs

A time-area diagram relates runoff travel time and the fraction of the watershed contributing runoff for that travel time. The relationship of time from the beginning of runoff to cumulative contributing area is an expression of the topographic shape of a watershed. For instance, a long, narrow watershed with a single main stream would have a reasonably smooth time-area diagram with a relatively small peak. By contrast, a watershed of similar total contributing area and topography, which contributes to a confluence where two tributary streams of similar length and contributing area join would gain contributing area with time faster, resulting in a time-area diagram with a shorter time base and higher peak. The time-area graph for a watershed with two tributaries of different shapes may even exhibit two peaks. In this case, the peak is the rate of increase of contributing area with time, rather than discharge, although the two are related.

Consider an idealized watershed subdivided into of six equal subareas with subarea 1 being downstream as shown in Figure 8.9a. Subarea 1 contributes to the outlet within time equal to $t_c/3$, subareas 2, 3, and 4 contribute to the outlet within time equal to 2 times $t_c/3$, and subareas 5 and 6 contribute within time equal to t_c.

Also consider a simple rainfall hyetograph as shown in Figure 8.9b. The rainfall duration equals the time of concentration for the watershed and has an intensity i. The distribution of rainfall excess is also shown in Figure 8.9b, with a magnitude of Ci, where C is a runoff coefficient such as that for the Rational Method; thus the loss function is constant with a magnitude of i(1 - C), and the initial abstraction is assumed to be zero. Based on the assumption that the rainfall excess is uniformly distributed over the watershed, the depth of rainfall excess Ci is assumed to fall on each subarea of the watershed from time = 0 to time equal tc.

Runoff from subarea 1 begins to appear immediately as shown in Figure 8.9c. However, runoff from subareas 2, 3, and 4 will not begin to appear at the outlet until time equal to tc/3. Similarly, runoff from subareas 5 and 6 will not begin to appear until time equal to 2tc/3. In both cases, these lags represent the travel time for flow through the intervening areas.

Therefore, as shown in Figure 8.9c, at the end of time $t_c/3$, runoff from only subarea 1 will be appearing at the watershed outlet. At the end of time $2t_c/3$ subareas 1 to 4 will be contributing runoff at the outlet. At time $2t_c/3$, rains that fell on subareas 5 and 6 are not yet contributing to direct runoff at the outlet. At time t_c, all six subareas are contributing to runoff at the outlet, but the storm has ended.

During the time interval from t_c to $4t_c/3$, rain that fell during the time interval $t_c/3$ to $2t_c/3$ is still contributing runoff at the outlet from subareas 5 and 6, and rain that fell during the time interval $2t_c/3$ to t_c is contributing runoff from subareas 2, 3, and 4. Thus the runoff ordinate equals 5 units. Rain that fell during the time interval from $2t_c/3$ to t_c on subareas 5 and 6 appears as runoff at the outlet in the time interval $4t_c/3$ to $5t_c/3$. It is also important to observe that the depth of rainfall excess, Cit_c, equals the depth of direct runoff; the depths can be converted to volumes by multiplying by the drainage area, A.

This conceptual time-area analysis above simplified because the rainfall excess and direct runoff are used with a relatively large, discrete time interval, $t_c/3$. The last particle of rainfall excess falling at the upper end of subarea 5 or 6 at time t_c will require a travel time to the outlet of t_c, which means that it will appear as runoff at the outlet of time $2t_c$. The runoff hydrograph of Figure 8.9c suggests that this particle of rainfall reaches the outlet at $5t_c/3$. The difference results from the crude discretization of the calculations.

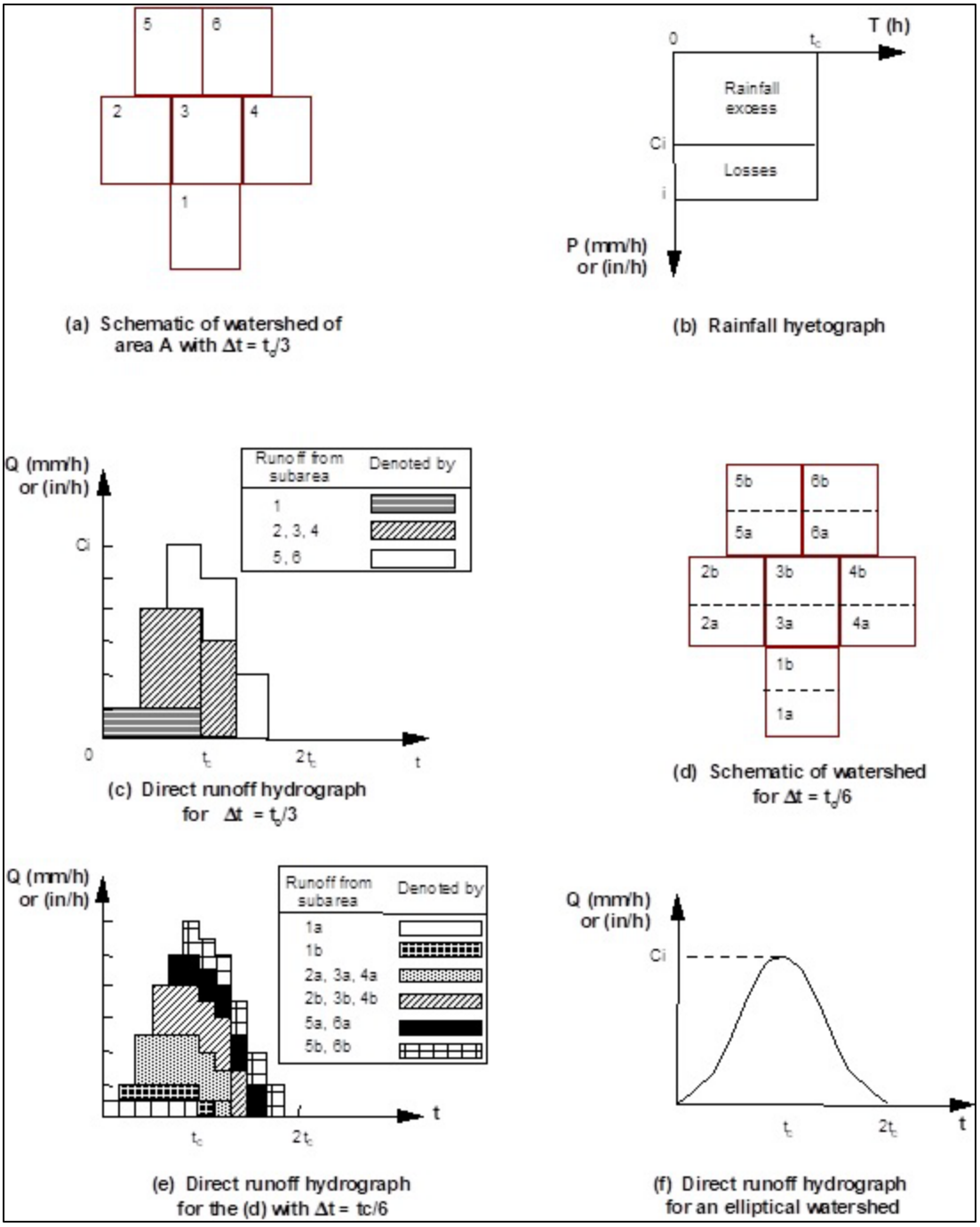

Figure 8.9. Time-area analysis.

Consider changing the time interval, Δt, from $t_c/3$ to an infinitesimally small time, the time-area analysis will yield a hydrograph with a shape similar to that of Figure 8.9f, but with a time base equal to $2t_c$. The peak still equals Ci and occurs at time t_c.

To illustrate, consider a time increment of $t_c/6$, which is one-half of the time increment used above, separate the watershed as shown in Figure 8.9d. This produces the direct runoff hydrograph shown in Figure 8.9e. In this case, the time base of the direct runoff hydrograph is $11t_c/6$; this supports the statement that the time base will approach $2t_c$ as Δt goes to zero.

For a rectangular watershed of length L and width W, the direct runoff hydrograph will have the shape of an isosceles triangle, with a peak Ci and a time base of $2t_c$. Actual watersheds do not have square edges like the schematic in Figure 8.9a, and they are not rectangular. Instead, they appear more elliptical. In such a case, the hydrograph will have a shape such as that shown in Figure 8.9f.

The Clark Unit Hydrograph

Clark adapted his unit hydrograph from the time-area relationship. He observed that in cases where simultaneous rainfall and runoff data are available, the observed response exhibits a lower peak and longer time base than the time-area histogram produces. Clark simulated the attenuation by conceptually routing the time-area response through a linear reservoir. The resulting unit hydrograph exhibits the time-area characteristics of the watershed, with attenuation.

8.2 Design Storm Development

Section 3.2 discussed the volume, duration, frequency, and intensity of storms. Some design problems only involve either the volume of rainfall or an average intensity for a specified duration and frequency. For example, the Rational Method uses the rainfall intensity for a specified AEP. Unit hydrographs can use any type of design storm. This section summarizes several methods for design storm development.

Many problems in hydrologic design, benefit from showing the variation of the rainfall volume with time. Such hydrologic design problems require that the storm input to the design method be expressed as a hyetograph and not just as a total volume for the storm. Important characteristics of a hyetograph include the peak rate of rainfall, total rainfall, time to peak, total rainfall duration, and rainfall distribution over time. The annual exceedance probability of hyetograph is also important. Because each real rainfall event has a unique time distribution of rainfall that the engineer cannot easily place in a probabilistic framework, design methods most often use a synthetic design rainfall distribution rather than an actual, measured storm hyetograph. Engineers often refer to these distributions as “storms,” even though they are artificial constructs developed for particular attributes and are not actual meteorologic events.

In developing a design storm hyetograph for any region, engineers make empirical analyses of measured rainfall records to determine the most likely arrangement of the ordinates of the hyetograph. Some storm events will have an early peak (i.e., be front-loaded), some a late peak (i.e., be back-loaded), some will peak near the middle of the storm (i.e., be center-loaded), and some will have more than one peak. Empirical analysis of measured rainfall hyetographs at a location will show the most likely of these possibilities, and engineers can use this finding to develop the design storm. However, current practice most often centers around the construction of design storms based on published depth-duration-frequency information and generalized time distributions.

An important aspect of design storms for watershed modeling is that the duration of excess rainfall matches the length of time for the watershed to become fully contributing. That is, the total length of a design storm equals or is as close as possible to the watershed time of concentration. If the entire watershed is not contributing when rainfall ceases, the maximum peak flow probable for the depth of rainfall is not observed. Conversely, because of the intensity-duration relationship discussed in Chapter 3 (intensity diminishing with duration), if excess rainfall extends further in time than the time of concentration, intensity will be lower than maximum probable for the depth of rainfall.

Consider Local Data

Where possible, engineers analyze local rainfall patterns to inform the selection of a method for developing a design storm. Rainfall and runoff records need not necessarily be for the specific drainage basin, nor do they need to all be from the same watershed. Instead, the engineer seeks an understanding of the characteristics of storms that produce large flood events including:

- The durations and time variations of intensities.
- Short, intense, convective storms or longer, more uniformly distributed cyclonic storms.

Hydrologists sometimes call the time where the duration of excess rainfall equals the watershed time of concentration the **critical duration**. Depending on the excess rainfall distribution, this duration is likely to give the maximum peak flow from a watershed for a given total precipitation depth and annual exceedance probability (AEP). The rainfall excess duration may be shorter than the total rainfall distribution if initial abstraction and other losses prevent runoff from occurring immediately. Therefore, critical duration depends somewhat on the choice and nature of the loss model as well as on rainfall distribution.

8.2.1 Constant-Intensity Design Storm

Designers frequently use the constant-intensity design storm for hydrologic designs on small urban watersheds. Commonly, engineers assume that the critical cause of flooding is the short duration, high intensity storm. In most cases, the largest peak runoff rate occurs when the entire drainage area is contributing. Therefore, engineers commonly set the duration of the design storm equal to the time of concentration of the watershed. The designer obtains the intensity of the storm from the intensity-duration curve for the location, using the frequency specified by the design standard. The total storm depth equals the intensity multiplied by the time of concentration. Designers use this approach for the Rational Method.

8.2.2 Design Hyetographs from Depth-Duration-Frequency Information

Historically, government agencies have performed large regional analyses of measured rainfall events, publishing them for use by professionals. Examples are Technical Paper #40 (TP 40) *Rainfall Frequency Atlas of the United States* (U.S. Weather Bureau 1961) and NWS HYDRO-35 (NOAA 1977). Publications such as these, or other State-sponsored analyses, provide depth- or intensity-duration information for various AEPs, often in the form of maps with rainfall isolines. Engineers can use this information to tabulate depth of rainfall for a range of durations for any given AEP.

In the 1970s, the NRCS compiled similar information and developed **type curves** for various areas of the United States (types I, IA, II, and III), all for 24-hour rainfall distributions. While little documentation exists about how the NRCS developed the curves, ample documentation exists about their application. For historical purposes, the type curves remain available in most software,

but the NRCS no longer recommends their use for design. Instead, the NRCS (2019) encourages the use of idealized distributions developed from depth-duration-frequency information. For most of the United States, the National Oceanic and Atmospheric Administration (NOAA) Atlas 14 Precipitation Frequency Data Server (PFDS) provides downloadable depth-duration-frequency (DDF) or intensity-duration-frequency (IDF) information. The following steps summarize the general procedure for developing a hyetograph.

Step 1. Acquire DDF values for the applicable AEP.

Engineers commonly use NOAA Atlas 14 as the source for DDF data for a location, but any other appropriate source of rainfall statistics is acceptable.

Step 2. Adjust the incremental intensities, if needed.

The engineer plots the incremental intensities on a log-log graph with the intensity on the vertical axis and time on the horizontal axis. The engineer checks the plot for consistency by observation, adjusting points on the line if it is not reasonably consistent and straight. A straight line on a log-log graph will result in a smooth and consistent design storm.

Step 3. Calculate beginning and end times for the rainfall blocks.

The NRCS design storm is symmetric about the midpoint in time (12 hours). The engineer constructs the design storm by "straddling" the midpoint in time with half of each time increment (e.g., for 1 hour depth, the time begins 11.5 hours and ends at 12.5 hours).

Step 4. Apportion total depth according to incremental depths.

At the center of the hyetograph, half the total 24-hour depth will have occurred. At each time computed from step 3, the engineer allocates the rainfall depth occurring in each rainfall block by straddling the midpoint in depth with half of the depth increment. That is, half occurs before the midpoint and half occurs after.

Step 5. Interpolate linearly on the time step, if needed.

For modeling by unit hydrograph methods, the design hyetograph uses uniform time increments. Data used to develop the hyetograph (from step 1) derives from increasing durations. Linear interpolation is used to "fill in" between time points on whatever time step size is needed. This produces a cumulative hyetograph, from zero to the 24-hour depth on uniform time steps.

Example 8.6:	Cumulative rainfall hyetograph using the NRCS method.
Objective:	Develop a 24-hour cumulative rainfall hyetograph on a 30-minute time step by the NRCS method.

Given: A location near Brady, Texas, with an AEP of 0.1.

Step 1. Acquire DDF values for the applicable AEP.

Download depth-duration-frequency data from NOAA Atlas 14 for the site of interest, in this case Brady, Texas. Table 8.6 summarizes the data for 5 minutes to 24 hours and Figure 8.10 displays the values graphically.

Step 2. Adjust the incremental intensities, if needed.

Adjust any inconsistencies in the data. The Brady data in Figure 8.10 are sufficiently smooth to proceed without adjustment.

Table 8.6. Data from NOAA Atlas 14 for Brady, Texas and the 0.1 AEP.

Time (min)	Depth (inches)	Intensity (in/h)
5	0.67	8.04
10	1.08	6.48
15	1.33	5.32
30	1.83	3.66
60	2.36	2.36
120	2.91	1.46
180	3.24	1.08
360	3.83	0.638
720	4.45	0.371
1440	5.13	0.214

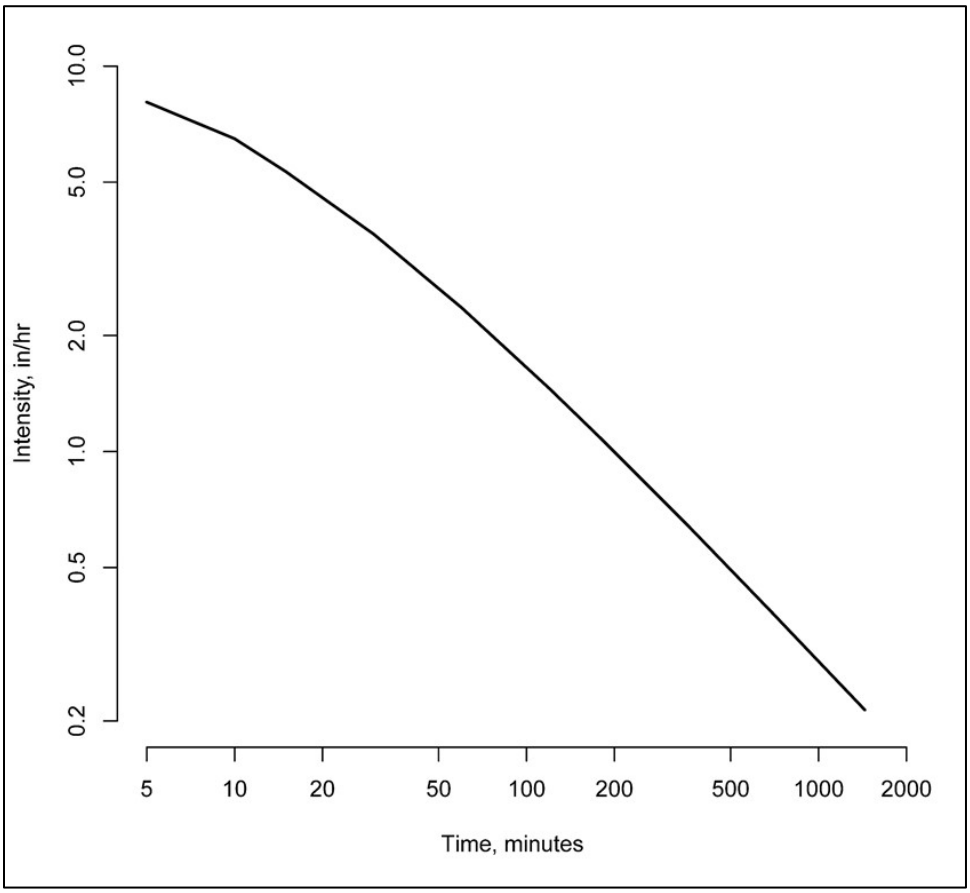

Figure 8.10. Log-log plot of time versus intensity for Brady, Texas (AEP = 0.1).

Step 3. Calculate beginning and end times for the rainfall blocks.

The hyetograph is centered in the 24-hour period and symmetrical around the center (720 minutes). The engineer centers the first (highest intensity) entry in Table 8.6 for the 5-minute duration. This intensity begins at 720 – 5/2 = 717.5 minutes and ends at 720 + 5/2 = 722.5 minutes. The engineer performs these computations for each duration in creating Table 8.7 containing all the time ordinates of the hyetograph.

Table 8.7. Time ordinates for NRCS hyetograph.

Time (Minutes)	Beginning Time (minutes)	Ending Time (minutes)
5	717.5	722.5
10	715	725
15	712.5	727.5
30	705	735
60	690	750
120	660	780
180	630	810
360	540	900
720	360	1080
1440	0	1440

Step 4. Apportion total depth according to incremental depths.

The engineer allocates the cumulative rainfall depths to the beginning and ending times shown in Table 8.7. Because the hyetograph is symmetrical, start with time equal to 720 minutes where the engineer knows that one-half of the 24-hour rainfall has fallen. In this example that value is:

5.13 / 2 = 2.565 inches

Next, the depths from each of the durations in step 2 (Table 8.6) are allocated to the time ordinates from step 3 (Table 8.7). The 5-minute duration contains 0.67 inches of rainfall. The engineer assumes that half falls before the 720-minute mark and half falls after the 720-minute mark. Therefore, at time equal to 717.5 minutes, the cumulative rainfall depth is:

2.565 – 0.67 / 2 = 2.23 inches

Similarly, at time equal to 722.5, the cumulative rainfall depth is:

2.565 + 0.67 / 2 = 2.90 inches

The engineer continues this process for each duration and compiles the results in Table 8.8. Depth at time zero is zero and depth at time 1440 is the 24-hour depth of 5.13 inches. Figure 8.11 displays the values revealing an s-shaped (sigmoidal) curve.

Table 8.8. Tabular Hyetograph from NRCS method.

Time (min)	Cumulative Depth (inches)
0	0
360	0.34
540	0.65
630	0.945
660	1.11
690	1.385
705	1.65
712.5	1.90
715	2.025
717.5	2.23
720	2.565
722.5	2.90
725	3.105
727.5	3.23
735	3.48
750	3.745
780	4.02
810	4.185
900	4.48
1080	4.79
1440	5.13

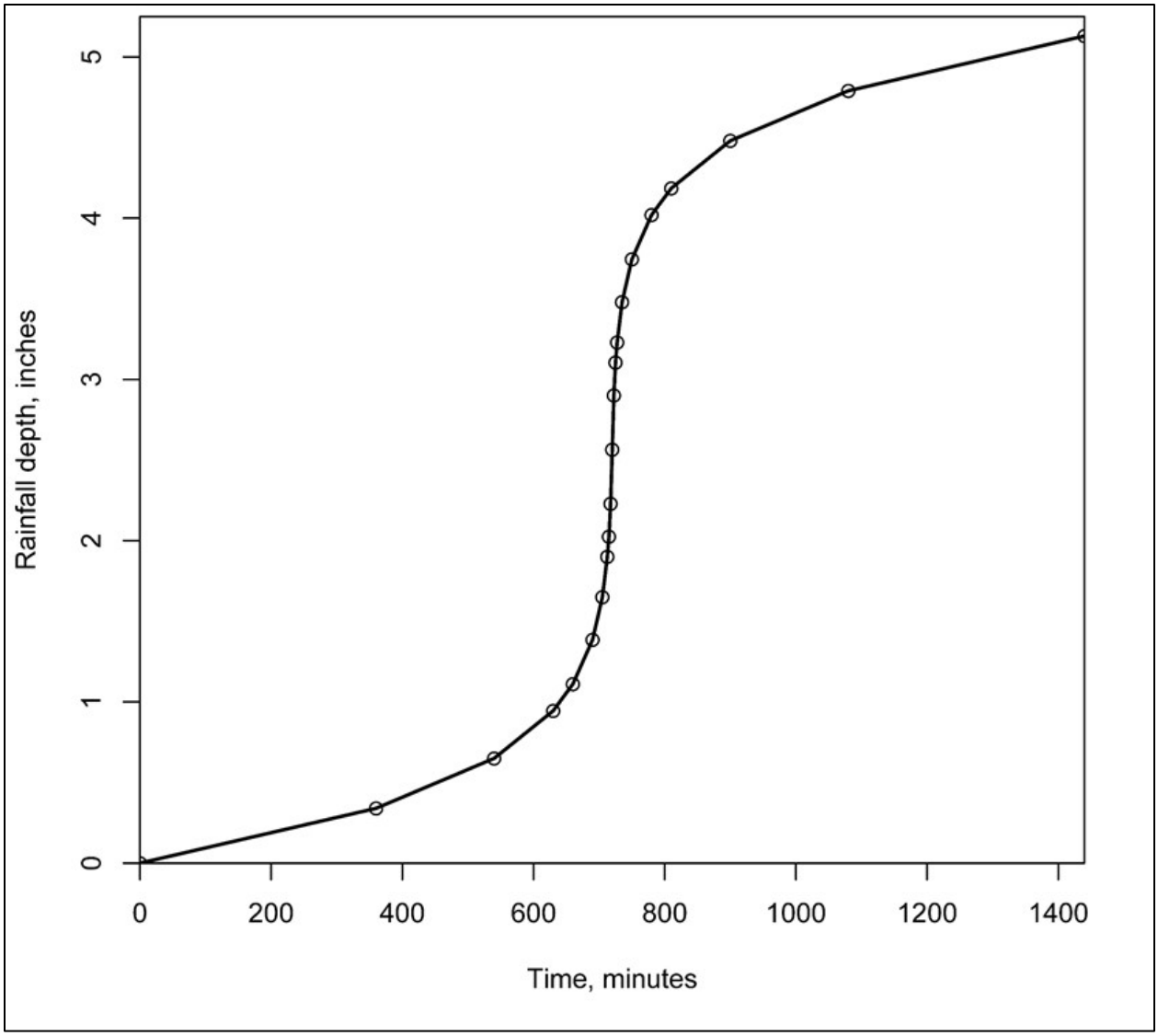

Figure 8.11. Cumulative hyetograph developed by the NRCS method from NOAA Atlas 14 data.

Step 5. Interpolate linearly on the time step, if needed.

In many cases, the engineer divides the hyetograph on the time step selected for modeling, computing an incremental rainfall hyetograph by subtracting each value from the value preceding it. The time values occur close together where curvature is large, and intensity is high; they occur further apart where the curvature changes more slowly. Linear interpolation between calculated points produces satisfactory results, considering the degree of precision involved in hydrologic modeling.

Use linear interpolation to compute rainfall depts at 30-minute time steps. The first two columns of Table 8.9 repeat the cumulative hyetograph from the previous step. The remaining two columns show the interpolated values on the uniform time step. For example, the engineer computes the cumulative depth values for times between 0 and 360 minutes from the values at 0 and 360 minutes. The engineer repeats the interpolation process to fill the remaining time steps. The table also shows that the incremental values from 705 to 718, inclusive, are not needed for a uniform 30-minute time step. Table 8.9 displays the first half of the cumulative hyetograph. **The engineer computes the second half in a similar manner**.

Table 8.9. Hyetograph interpolated to a 30-minute time step (0 to 720 minutes).

Time from Table 8.8 (min)	Depth from Table 8.8 (inches)	Time Step (min)	Cumulative Depth (inches)
0	0.00	0	0.00
[30]	-	30	0.03
[60]	-	60	0.06
[90]	-	90	0.09
[120]	-	120	0.11
[150]	-	150	0.14
[180]	-	180	0.17
[210]	-	210	0.20
[240]	-	240	0.23
[270]	-	270	0.26
[300]	-	300	0.28
[330]	-	330	0.31
360	0.34	360	0.34
[390]	-	390	0.39
[420]	-	420	0.44
[450]	-	450	0.50
[480]	-	480	0.55
[510]	-	510	0.60
540	0.65	540	0.65
[570]	-	570	0.75
[600]	-	600	0.85
630	0.95	630	0.95
660	1.11	660	1.11
690	1.39	690	1.39
705	1.65	-	-
713	1.90	-	-
715	2.03	-	-
718	2.23	-	-
720	2.57	720	2.57

Solution: Table 8.8, Table 8.9, and Figure 8.11 provide the resulting cumulative hyetograph for the 24-hour rainfall depth at Brady, Texas.

For situations calling for a hyetograph of less than 24-hour duration, extract and scale the central portion of the hyetograph. For instance, to create a 12-hour hyetograph, use the portion of the 24-hour curve lying between 6 hours and 18 hours, reducing it by subtracting the 6-hour value from all ordinates, and concluding with the 18-hour value.

For broader application to multiple projects, an engineer or transportation agency may wish to develop dimensionless cumulative hyetographs. Engineers can convert curves such as that in Figure 8.11 to dimensionless form by dividing all the ordinates by the total depth of rainfall. The engineer can check for consistency by plotting the entire "family" of curves developed in this way (for the range of AEPs commonly used in design), or by comparing them with the curves from different, nearby locations. If they are sufficiently consistent with one another, the development of characteristic regional curves may be feasible to simplify future designs. Once a dimensionless curve is developed, engineers can use it for multiple projects rather than developing a new curve for each project

A hyetograph developed by this method typically does not resemble actual, measured hyetographs, or statistical models of them. However, such a hyetograph contains rainfall depth-duration relations of the same AEP over the entire duration of the hyetograph, an advantageous generalization for many cases, particularly for subdivided watersheds. In addition, the most severe portion of the hyetograph is located centrally, giving time and depth for an initial abstraction to be satisfied.

8.2.3 Other Hyetographs

In contrast to symmetrical hyetographs developed by the NRCS, Huff (1967, 1990) analyzed numerous measured storm events to develop insight into the real-world distribution of rainfall in storms. Other authors have followed Huff's work (e.g., Williams-Sether et al. 2004, Asquith et al. 2003). These studies segregate storms into quartiles, depending on where the majority of the rainfall occurs within the duration of the storm event. Engineers describe first quartile storms as being "front-loaded," with the most intense portion of the rainfall occurring in the first ¼ of the duration, and fourth quartile storms to be "back-loaded" in the last quarter.

NOAA Atlas 14 has continued the philosophy of Huff, developing quartile-based dimensionless hyetographs for various areas of the United States including temporal distributions for 6-, 12-, 24-, and 96-hour durations. NOAA further divided each quartile into deciles of 10 percent through 90 percent. That is, NOAA created distributions for the 10 percent most front-loaded storms and for each additional decile. Therefore, for each area, there are 200 potential dimensionless rainfall distributions, scalable by depth and duration. However, NOAA has not provided recommendations on the selection of a specific distribution for modeling in most situations.

These distributions are based on measured data, and more closely resemble storms that would actually occur than the generalized NRCS procedure will produce. Figure 8.12 shows the 10 percent and 90 percent distributions for first quartile (front-loaded) and fourth quartile (back-loaded). Figure 8.13 shows selected deciles all four quartiles aggregated. As with the cumulative distributions developed by the NRCS process, engineers may need to divide them into increments using linear interpolation for modeling.

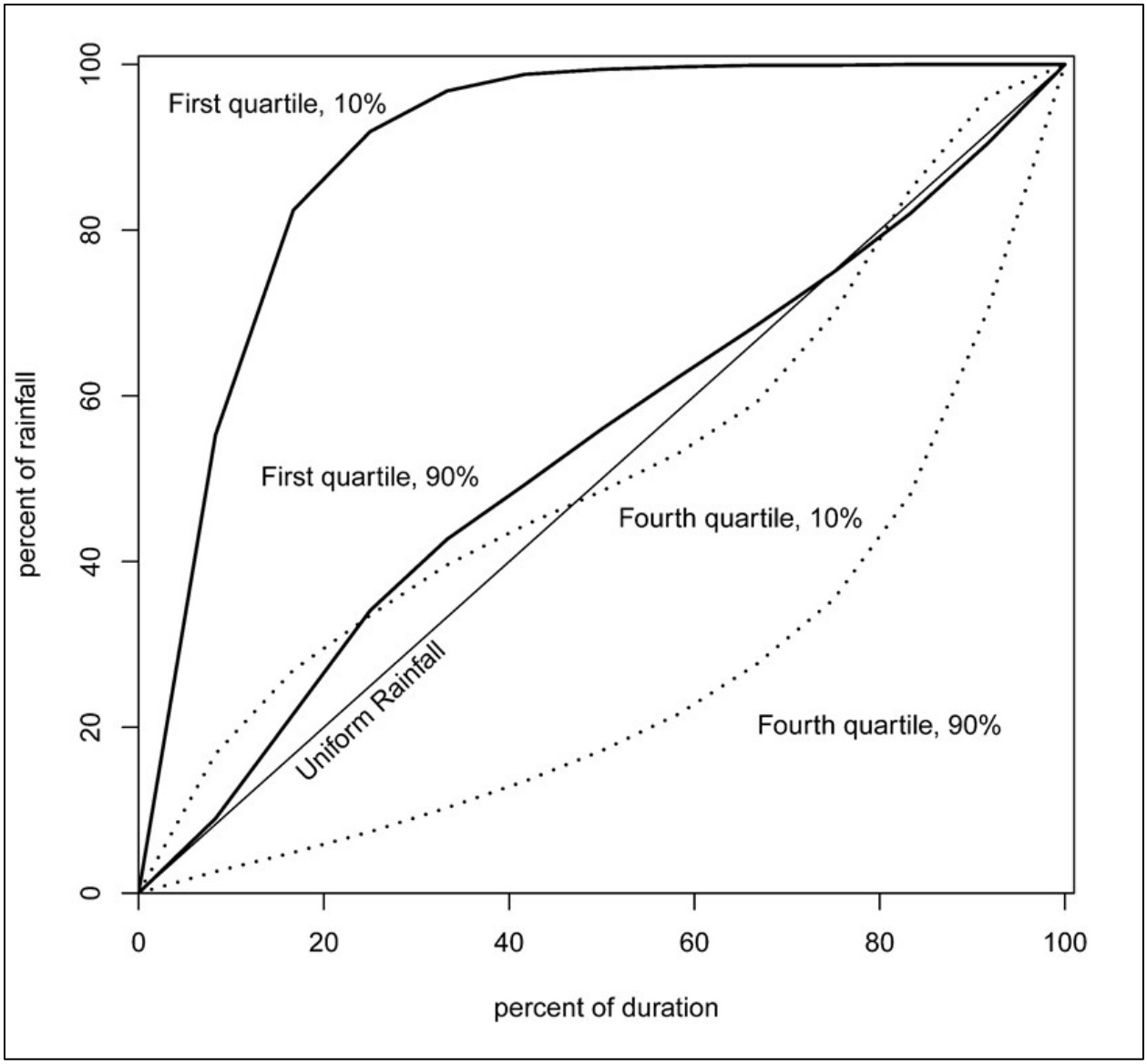

Figure 8.12. Cumulative rainfall distributions from NOAA Atlas 14 for the semiarid southwest, showing the 10 percent and 90 percent curves from both first and fourth quartiles.

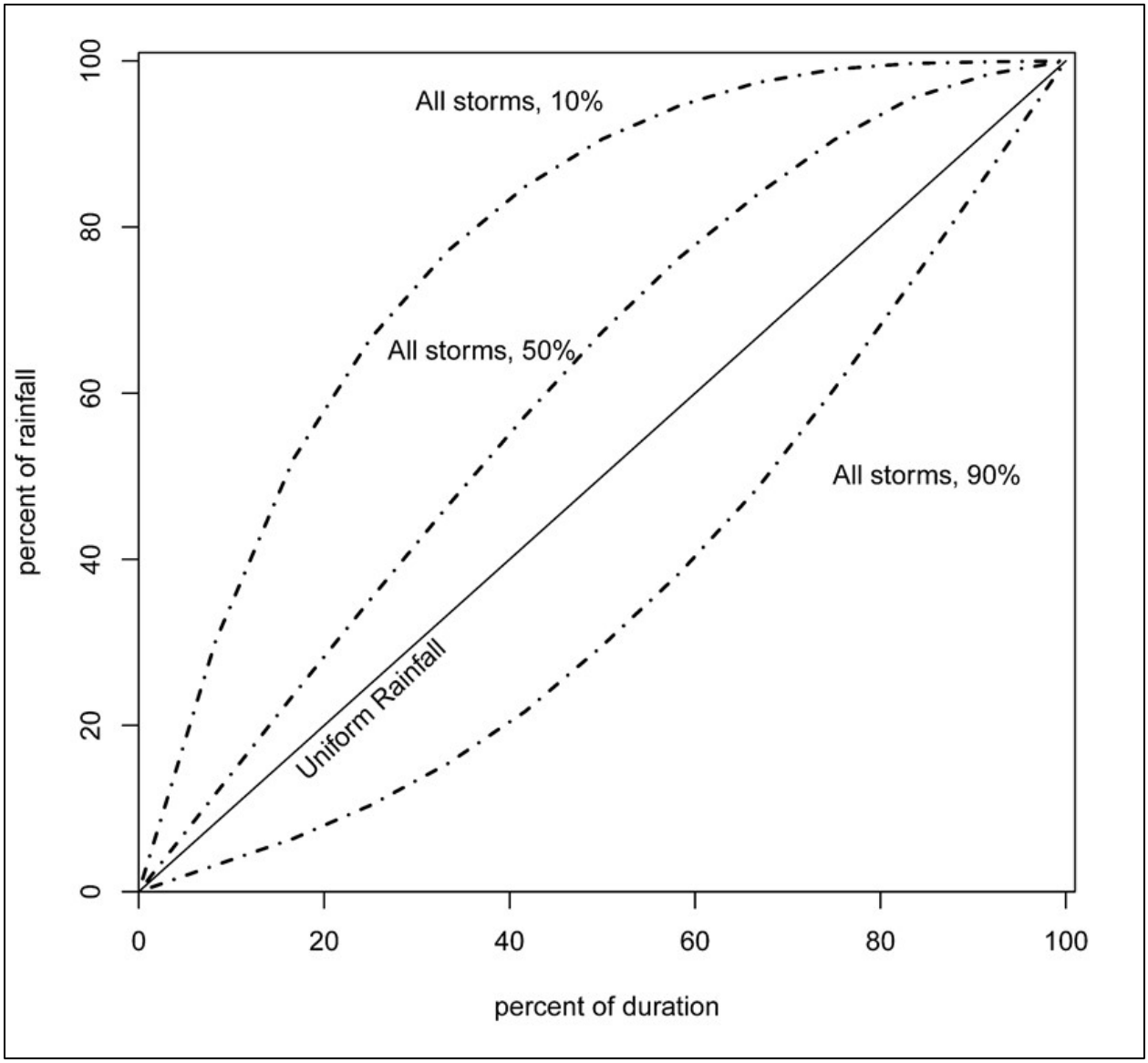

Figure 8.13. Cumulative rainfall distributions from NOAA Atlas 14 for the semiarid southwest, showing the 10 percent, 50 percent (median), and 90 percent curves from analysis of all storms, not divided into quartiles.

8.2.4 Depth-Area Adjustments

The rainfall depths from IDF curves represent point rainfall derived from rain gages. Engineers use unadjusted point rainfall for small watersheds because they assume the estimate can be uniformly applied over a small area. For designs on areas larger than a few square miles, the engineer adjusts point rainfall estimates recognizing that actual rainstorms do not have the same intensity over larger areas. As the spatial extent of a storm increases, the depth of rainfall over an area decreases rainfall depths, which depend on the total rainfall and the depth-area relationship used at the location, decrease with increasing area. In the figure, the innermost isohyet represents the greatest depth.

When selecting a point rainfall to apply uniformly over a watershed, the designer reduces the point value to account for the areal extent of the storm using a depth-area adjustment factor. The factor is a function of the drainage area and the rainfall duration. Figure 8.14 shows the depth-

area adjustment factors based on U.S. Weather Bureau Technical Paper No. 40. The engineer can use this set of curves unless specific curves derived from regional analyses are available. Figure 8.14 shows that the adjustment factor decreases from 100 percent as the watershed area increases and as the storm duration decreases. Beyond a drainage area of 300 mi^2, the adjustment factor shows little change.

Asquith (1999) developed a detailed procedure for performing areal adjustment for Texas. The procedure initially assumes an approximately circular watershed and then generalizes to watersheds that are not approximately circular but can be divided into pieces. Based on distance, the procedure calculates an adjustment factor between 0 and 1. The procedure is primarily useful within reasonable distance of the Dallas, Austin, or Houston metropolitan areas, which were the focus areas for the study. With sufficient data, other States could develop a similar analysis designers could find useful.

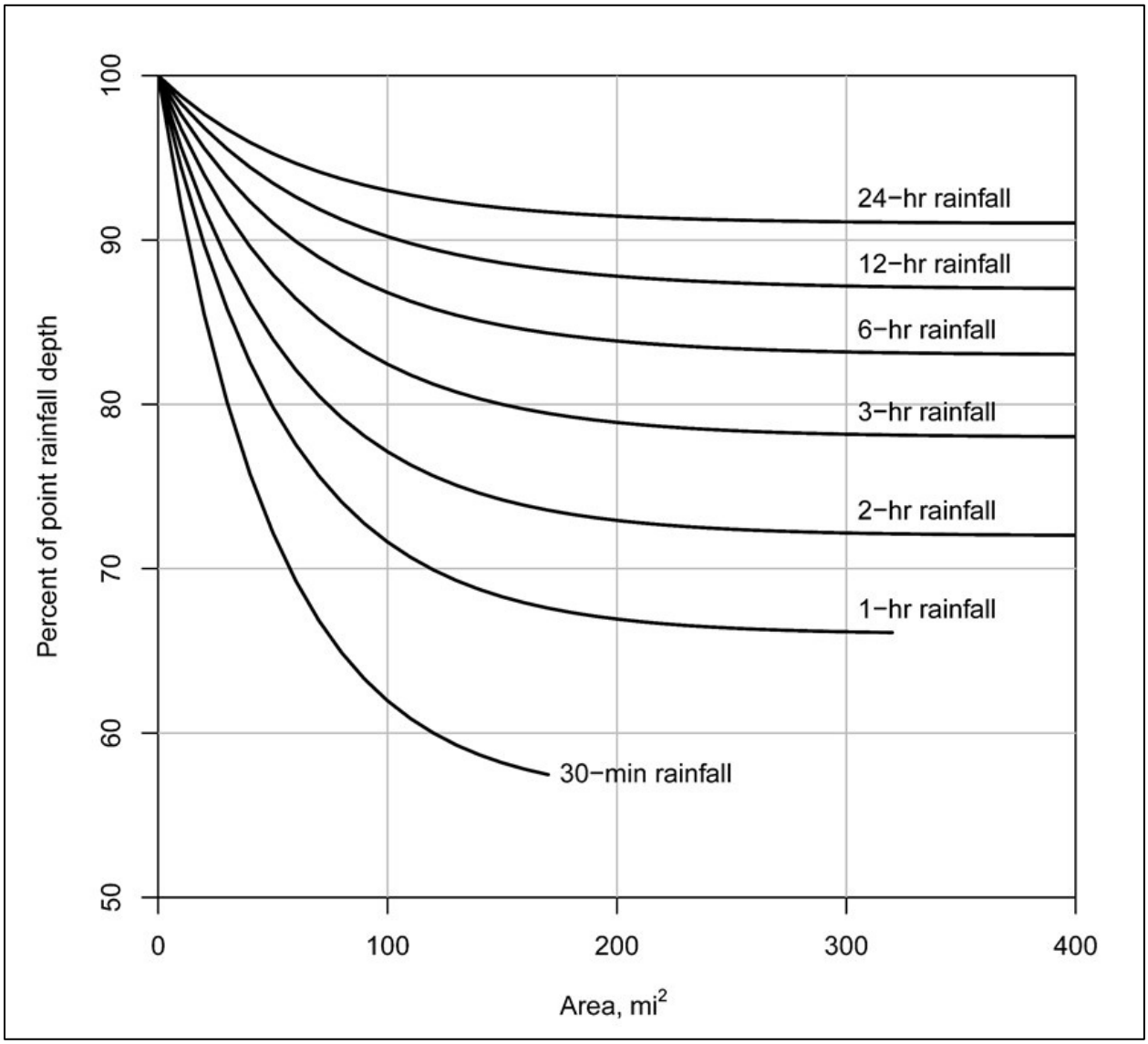

Figure 8.14. Depth-area curves for adjusting point rainfalls.

8.3 Other Hydrograph Techniques

In addition to the unit hydrograph methods described in Section 8.1, engineers use a variety of other methods for generating hydrographs that can be national in scope or regionally applicable. This section describes two methods with national applicability—the Rational Method hydrograph and hydrographs by transposition.

8.3.1 Rational Method Hydrograph

Engineers can use a modified version of the Rational Method to generate a hydrograph. Section 6.2 introduced the Rational Method as an approach to estimating peak flows and highlighted basic assumptions of the approach:

- Rainfall intensity, i, is constant over the storm duration.
- Rainfall is uniformly distributed over the watershed.
- The maximum rate of runoff occurs when runoff is being contributed to the outlet from the entire watershed.
- The peak rate of runoff equals some fraction of the rainfall intensity.
- The watershed system is linear, that is, runoff is proportionately related to rainfall.

The same assumptions apply to develop a hydrograph. In addition, engineers assume the following to create a hydrograph:

- The peak flow estimated by the Rational Method is the peak flow of the hydrograph.
- The runoff hydrograph is an isosceles triangle with a time to peak equal to t_c and a time base equal to $2t_c$.

These assumptions produce a hydrograph with 50 percent of the volume under the rising limb of the hydrograph and a total volume of $CiAt_c/\alpha$. (α = 1 in CU and 360 in SI). For small urban watersheds, designers consider that the assumption of a triangular hydrograph is reasonable for many design problems.

A hydrograph based on the Rational Method is limited by the same assumptions applicable to Rational Method use for estimating peak flow. Its benefits include its ease of development and the fact that it has sufficient accuracy for designs on small, highly urbanized watersheds.

The engineer can transform a triangular hydrograph to a unit hydrograph if needed. Since the total runoff depth of the unit hydrograph must equal one unit (1 inch or 1 mm), the engineer can determine the ordinates of the UH by multiplying each ordinate of the triangular direct runoff hydrograph by the conversion factor K:

$$K = \frac{1}{C\,i\,t_c} \tag{8.17}$$

where:

K	=	Conversion factor
t_c	=	Time of concentration, h
i	=	Rainfall intensity, in/h (mm/h)

Since the duration of the rainfall creating the hydrograph has a duration equal to the time of concentration, the resulting unit hydrograph is a t_c-h unit hydrograph.

Example 8.7:	Rational Method hydrograph.
Objective:	Estimate the conversion factor and unit hydrograph peak flow.

Given:

t_c = 0.25 h
C = 0.4
i = 2.4 in/h (60 mm/h)
A = 35 ac (14 ha)

Step 1. Estimate the Rational Method peak flow.

$Q = CiA = (0.4)(2.4)(35) = 34$ ft^3/s

Step 2. Compute the conversion factor.

$$K = \frac{1}{Cit_c} = \frac{1}{(0.4)(2.4)(0.25)} = 4.17$$

Step 3. Estimate the unit hydrograph peak flow.

Unit hydrograph peak = KQ = (4.17)(34) = 142 ft^3/s/in (0.25-h unit hydrograph)

Solution:	The conversion factor K equals 4.167 and the unit peak flow of the 0.25-h unit hydrograph is 142 ft^3/s/in. The volume under this hydrograph equals 1 inch.

8.3.2 Hydrograph Transposition

Engineers can also develop a unit hydrograph at an ungaged site by transposing unit hydrographs from other hydrologically homogeneous watersheds. Engineers use four basic factors to identify a hydrograph: the peak flow, time to peak, duration of flow or time base, and the volume of runoff.

In transposing hydrographs, the lag, or the time from the midpoint of the excess rainfall duration to the time of the peak flow, describes the time to peak. Designers can estimate lag by the equation:

$$t_L = \alpha C_t \left(\frac{LL_c}{S^{0.5}} \right)^N \qquad (8.18)$$

where:

t_L = Lag time, h
L = Length of the longest watercourse, mi (km)
L_c = Length along the longest watercourse from the outlet to a point opposite the centroid of the basin, mi (km)
S = Slope of the longest watercourse, percent
C_t = Basin coefficient determined from hydrologically homogeneous areas
N = Exponent determined from hydrologically homogeneous areas (usually equal to 0.33)
α = Unit conversion constant, 1.0 for CU (0.75 for SI)

The engineer chooses the appropriate lag time (or other time parameter) for each methodology applied. Developers of each method may define and calculate parameters differently. However, some methods are similar. For example, equation 8.18 is similar to equation 8.10 with an

exponent equal to 0.3 rather than 0.33. Selecting and using the appropriate method of estimating lag time for each method is the responsibility of the designer.

Designers can determine the coefficients in the equation for lag time for the ungaged site based on a logarithmic plot of t_L versus $(LL_c/S^{0.5})$ for similar watersheds. The same approach can determine the peak flow of the unit hydrograph by logarithmically correlating peak flow with drainage area.

To determine the duration of flow, the engineer converts each unit hydrograph from similar watersheds into a dimensionless form by dividing the flows and times by the respective peak flow and lag time for each basin. The engineer then plots these dimensionless hydrographs to obtain an average value for the time base. The engineer estimates the shape of the unit hydrograph from the transposed hydrographs and checks the volume to ensure it represents one unit (1 inch or 1 mm) of runoff from the basin of interest. If not, the engineer adjusts the shape until the volume is reasonably close to 1 inch (1 mm).

The designer rarely encounters a case with available streamflow and rainfall data for a particular site. However, data may exist at points on adjacent or nearby watersheds. When the data for developing unit hydrographs exist in nearby hydrologically similar watersheds, the transposition method can be used to obtain a design hydrograph.

Page Intentionally Left Blank

Chapter 9 - Hydrograph Routing

Commonly, engineers use routing of design hydrographs to: 1) design drainage structures accounting for detention storage and 2) analyze the effects of a channel routing and modification on peak flow. They also use routing of hydrographs to design pumping stations and to determine the time of overtopping for highway embankments. These applications generally fall into two categories: storage routing and channel routing. Designers use storage routing techniques to calculate outflow given inflow and storage characteristics. They use channel routing techniques to calculate outflow from a stream reach given inflow and channel characteristics.

9.1 Continuity Equation

Storage and channel routing methods preserve continuity of mass. The volume of water represented by an outflow hydrograph after routing equals the volume of water represented by the inflow hydrograph. Mathematically, engineers represent the continuity of mass in terms of storage as the change in storage over time equals the difference between inflow and outflow, assuming that lateral flow is insignificant:

$$\frac{dS}{dt} = I - O \tag{9.1}$$

where:

I	=	Inflow, ft^3/s (m^3/s)
O	=	Outflow, ft^3/s (m^3/s)
t	=	Time, s
S	=	Channel storage, ft^3 (m^3)

To enable numerical computations the finite difference form of the continuity equation can be rewritten in discretized terms:

$$\frac{(S_2 - S_1)}{\Delta t} = \frac{(I_1 + I_2)}{2} - \frac{(O_1 + O_2)}{2} \tag{9.2}$$

where:

Δt	=	Computational time step, s

The averaged flows, as estimated at the beginning and end of the time step, are justifiable if the time step is less than or equal to the travel time through the reach. The subscript 1 indicates the value at the beginning of a time step and the subscript 2 indicates the value at the end of the time step. The inflow hydrograph is known so the designer knows all values, I_1 and I_2. The designer selects Δt so that is known as well. In routing, the designer also knows the current values of storage (S) and outflow (O) indicated by the subscript 1. For example, in dry ponds, the initial storage and outflow, corresponding to the subscript 1, are assumed to be zero. Therefore, the equation has two unknown values, S_2 and O_2 that the designer determines through the routing process.

Storage and channel routing methods differ in how they use the continuity equation and in the additional tools employed to solve particular routing situations. As a hydrograph passes through a storage facility or a channel reach it has the potential to attenuate and translate as shown in Figure 9.1. How much attenuation and translation that occurs depends on the inflow hydrograph

and the physical characteristics of the storage facility or channel reach as discussed in the following sections.

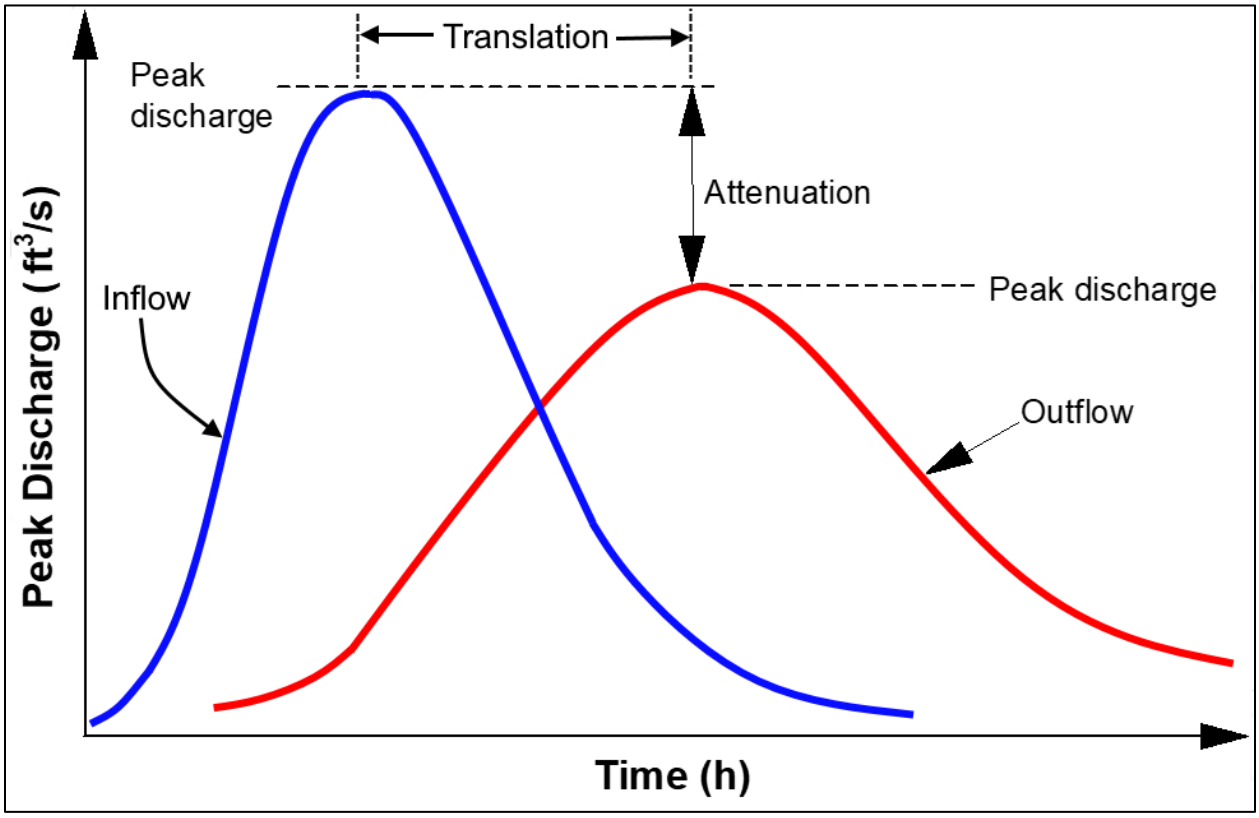

Figure 9.1. Inflow hydrograph and a routed outflow hydrograph.

9.2 *Storage Routing*

Whenever the outflow from a river channel section or body of water depends only on the storage in the reach or reservoir, designers can use storage routing techniques. These situations typically include urban stormwater detention ponds, flood control and water supply reservoirs, farm ponds, and other facilities designed to detain or retain water, which correspond to detention and retention ponds, respectively. Designers can also model backwater created by culverts and bridges using storage routing. A common characteristic for each of these situations is that the designer can reasonably approximate the water surface as level. However, the time scales of a storage routing can vary significantly from hours for stormwater and farm ponds to weeks for large reservoirs. This manual refers to storage routing as the storage-indication method, but designers refer to the same method using the terms level-pool and Modified Puls.

9.2.1 Data for Storage Routing

The objective of the storage-indication method is to derive the outflow hydrograph. The designer needs several types of data describing the inflow hydrograph and the physical characteristics of the storage:

- Inflow hydrograph.
- Stage-storage.
- Stage-discharge.

Designers develop the inflow hydrograph from procedures provided in Chapter 8 or any appropriate method for the site and application. The outflow hydrograph results from routing the inflow hydrograph through the storage facility.

Figure 9.2 provides an example of a stage-storage relationship. Each stage-storage relationship is site-specific and describes the storage volume associated with each water surface elevation (stage). The natural and constructed topographic features of the site control the relationship.

Figure 9.3 provides an example of the stage-discharge relationship. Also, site-specific, the stage-discharge relationship depends on the size and configuration of the outlet of the storage facility. The designer configures the outlet facility to satisfy applicable design criteria.

As previously discussed, equation 9.2 is a single equation with two unknowns, S_2 and O_2. Storage routing combines the stage-storage relationship of Figure 9.2 with the stage-discharge relationship of Figure 9.3 to generate the storage-discharge relationship shown in Figure 9.4. This relationship provides a second equation relating storage and outflow needed to perform the routing.

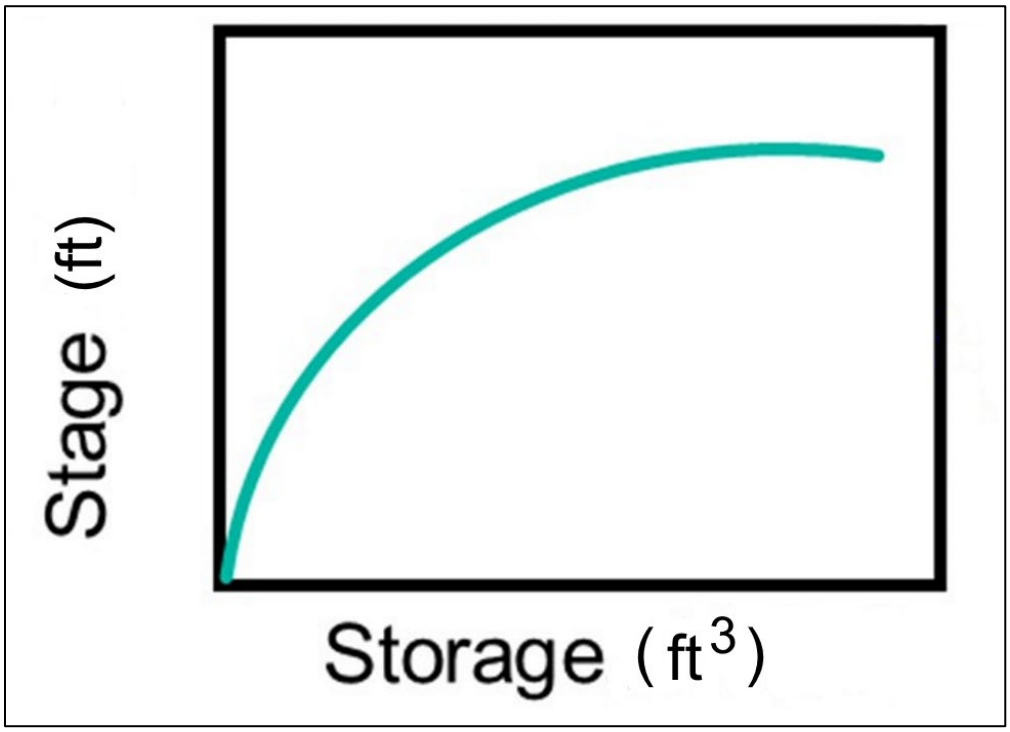

Figure 9.2. Stage-storage relationship.

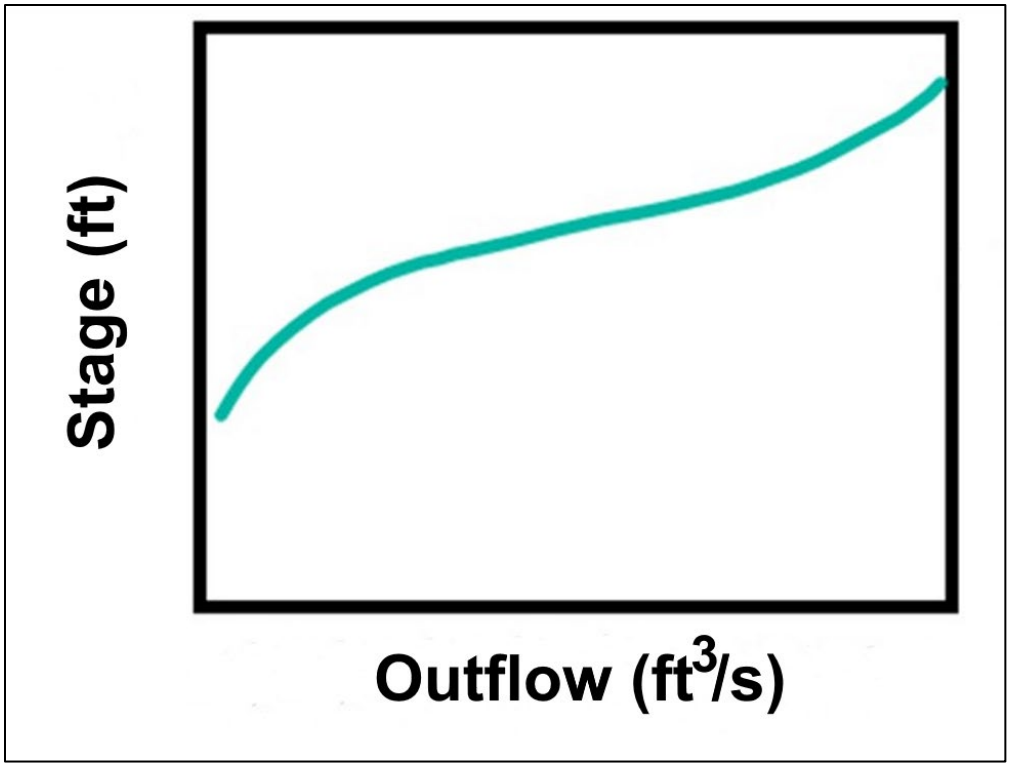

Figure 9.3. Stage-discharge relationship.

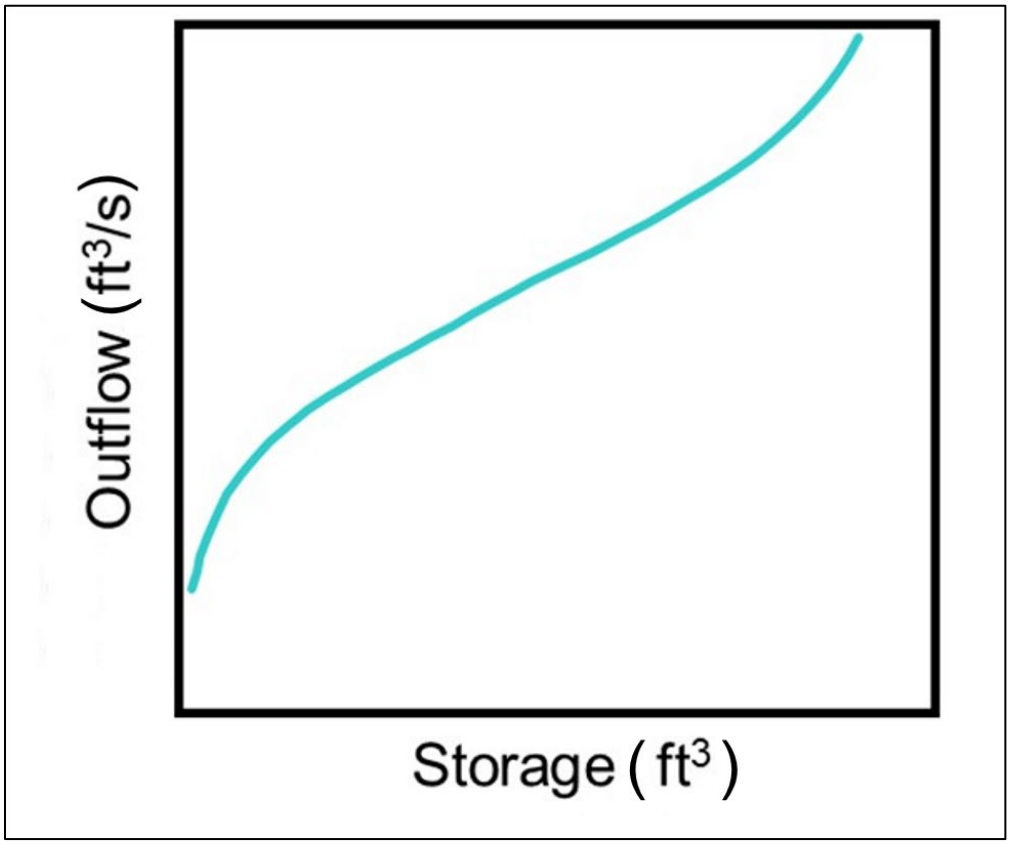

Figure 9.4. Storage-discharge relationship.

9.2.2 The Storage-Indication Curve

The storage-indication method uses the continuity equation expressed in equation 9.2 along with the input data from the previous section to perform the routing. The designer needs one more tool - the storage-indication curve - to perform storage routing. To form the storage-indication curve, algebraically transform equation 9.2 so that the knowns (I_1, I_2, S_1, and O_1) are on one side of the equation and the unknowns (S_2 and O_2) are on the other side:

$$\frac{I_1 + I_2}{2} + \left(\frac{S_1}{\Delta t} + \frac{O_1}{2}\right) - O_1 = \left(\frac{S_2}{\Delta t} + \frac{O_2}{2}\right) \tag{9.3}$$

The right-hand side of the equation, known as the storage-indication term, can be generalized, with the storage-indication relationship being graphed as O vs. ($S/\Delta t + O/2$) as shown in Figure 9.5. Use the following procedure to develop the storage-indication curve:

1. Select a value of O.
2. Determine the corresponding value of S from the storage-discharge relationship.
3. Use the values of S and O to compute ($S + O\Delta t/2$).
4. Plot a point on the storage-indication curve O versus ($S + O\Delta t/2$).

Repeat these four steps for a sufficient number of values of O to complete the storage-indication curve. Generally, linear interpolation applies when routing with the storage-indication method. To give good definition to the inflow hydrograph, select values of O at a sufficiently small interval. As a general rule of thumb, values of O only as large as the peak of the inflow hydrograph are appropriate since the ordinates of the outflow hydrograph will not exceed those of the inflow hydrograph.

To avoid numerical instabilities in the computations, choose the time step, Δt, so that at all times:

$$\frac{\Delta O}{2} \leq \frac{\Delta S}{\Delta t} \tag{9.4}$$

where:

ΔO = Change in outflow during the time step, ft^3/s (m^3/s)
ΔS = Change in storage during the time step, ft^3/s (m^3/s)

Graphically, verify this relationship by plotting a line of equal values (slope = 1) on the storage-indication curve. If equation 9.4 is true for all values, the slope of the storage-indication curve will always be less than the slope of the line of equal values, as conceptually illustrated in Figure 9.5. If not true, use a smaller time step.

The time step should also provide sufficient event detail to accurately model the inflow hydrograph and effectively capture significant points on the outflow hydrograph, most importantly the peak flow. Therefore, a successful minimum time increment will also follow:

$$\Delta t < 0.2 t_p \tag{9.5}$$

where:

Δt = Computational time step, s
t_p = Time to peak of the inflow hydrograph, s

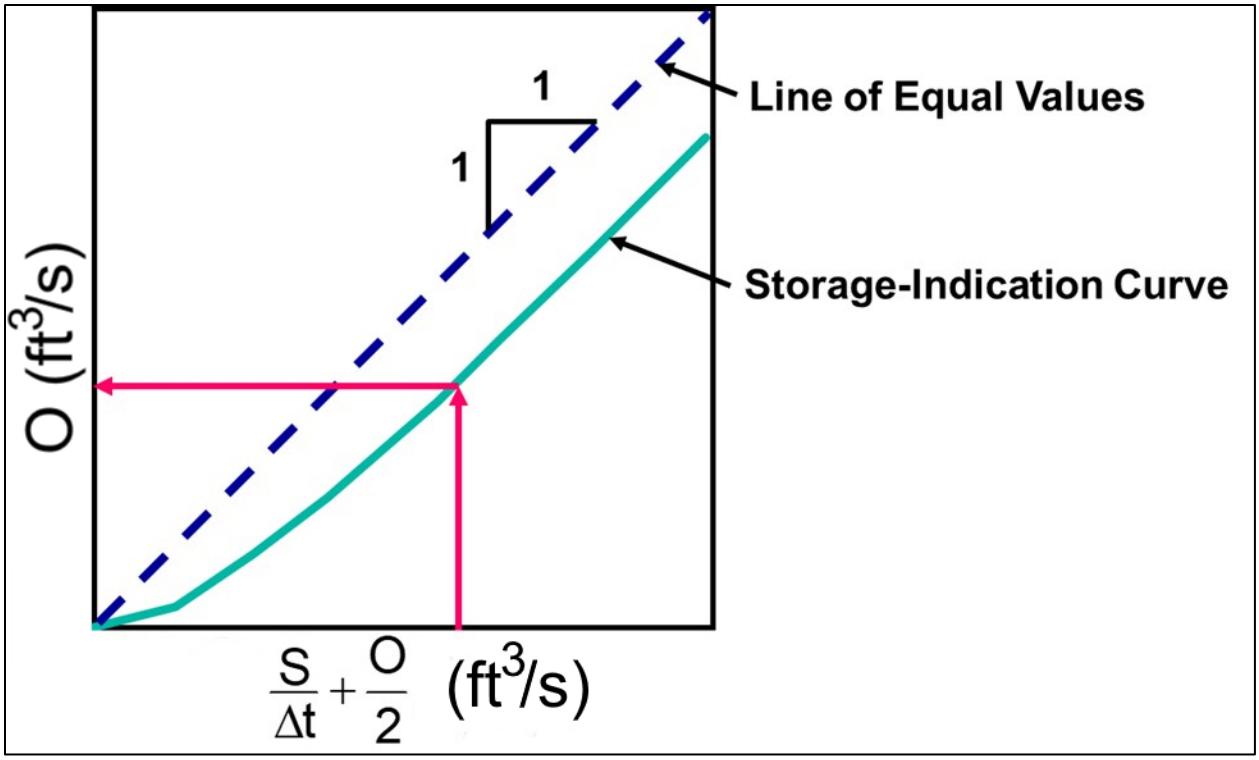

Figure 9.5. Storage-indication curve.

9.2.3 Standard Computational Procedure

Application of the storage-indication storage routing method follows a standard computational procedure using the continuity equation and developing and using the storage-indication curve to generate an outflow hydrograph. The steps are:

Step 1. Determine the storage-discharge curve.

The storage-discharge curve, e.g., Figure 9.4, incorporates site-specific physical characteristics of the storage facility and outlet works.

Step 2. Select a time step, (Δt).

The designer selects a computational time step sufficiently small using equations 9.4 and 9.5 to represent the inflow hydrograph and provide appropriate results. When using a unit hydrograph (see Section 8.1), the designer often uses the unit hydrograph duration for the time step.

Step 3. Calculate the storage-indication curve.

The designer develops the storage-indication curve as discussed in Section 9.2.2 and verifies that the slope is less than the line of equal values.

Step 4. Discretize the inflow hydrograph.

Using the time step from step 2, the designer discretizes the inflow hydrograph to prepare for the routing computations.

Step 5. Assume an initial value for O_1 and S_1.

Routing begins assuming initial conditions, that is, an initial outflow (discharge) from the storage and the initial storage volume. For dry ponds, the designer assumes the storage is empty (S = 0) and there is no outflow.

Step 6. Compute the storage-indication value, $S_1/\Delta t + O_1/2$.

The iterative part of the routing procedure begins with step 6. The designer computes the storage-indication value. For the initial computation, the initial values from step 5 are used.

Step 7. Calculate the storage-indication value at the next time step, $S_2/\Delta t + O_2/2$.

Use equation 9.3 to calculate the storage-indication value at the current the time step (subscript 1) to compute the value at the next time step (subscript 2).

Step 8. Obtain outflow from the storage-indication curve.

The designer obtains the outflow (O_2) for the storage-indication value computed in step 7 (see Figure 9.5).

Step 9. Use outflow with the storage-discharge relationship to obtain storage.

Obtain the storage that corresponds to the outflow value computed in step 8 from the storage-discharge relationship (see Figure 9.4). This outflow value is one point on the outflow hydrograph.

Step 10. Repeat routing computational process.

Repeat steps 6 through 9 for the next time increment using I_2, O_2, and S_2 as the new values of I_1, O_1, and S_1, respectively, for the duration of the inflow hydrograph.

The routing procedure results in the outflow hydrograph as the primary output and also provides the storage function (i.e., S vs. t) as another important output. The maximum value of S from the S-versus-t relationship occurs when the inflow rate equals the outflow rate. Following this point, the outflow rate exceeds the inflow rate, and the storage facility begins to empty. Graphically, this means that the peak of the outflow hydrograph crosses the receding limb of the inflow hydrograph, which corresponds to the maximum stage.

Example 9.1:	Perform storage routing of culvert system.
Objective:	Design the dimensions of a corrugated metal pipe (CMP) culvert and determine if they meet the design criteria.

A highway engineer needs to design a culvert with impoundment for a design AEP and a maximum water depth (d_{max}) and freeboard.

Given: A CMP culvert with the following design and computational parameters:

AEP	=	0.02
d_{max}	=	5.0 ft (1.5 m)
Freeboard	=	1.0 ft (0.3 m)
Δt	=	0.5 h (1,800 s)
D	=	24-inch or 36-inch (0.61-m or 0.91-m)

Step 1. Develop the storage-discharge relationship for the culvert.

Columns 1, 3, and 4 of Table 9.1 present the depth-discharge relationships for 24-inch and 36-inch CMP culverts, which are based on the culvert hydraulics. When the depth is greater than 6 ft, the embankment is overtopped, and the discharge increases significantly as the embankment begins to function as a broad crested weir. At a depth of 6.9 ft, the discharge is 87 ft^3/s due to overtopping alone.

The depth-storage relationship is site-specific, which would be based on the topography of the impoundment surface. For this example, columns 1 and 2 of Table 9.1 present the depth-storage relationship plotted in Figure 9.6.

Table 9.1. Depth-storage and depth-discharge relationships.

Depth (ft)	Storage (ft^3)	Discharge for 24-inch Culvert (ft^3/s)	Discharge for 36-inch Culvert (ft^3/s)
0.0	0	0	0
1.0	7,000	4	6
2.0	18,000	13	18
3.0	32,000	20	35
4.0	49,000	26	50
5.0	74,000	31	61
6.0	120,000	35	70
6.3	141,000	52	87
6.6	166,000	82	117
6.9	191,000	122	157

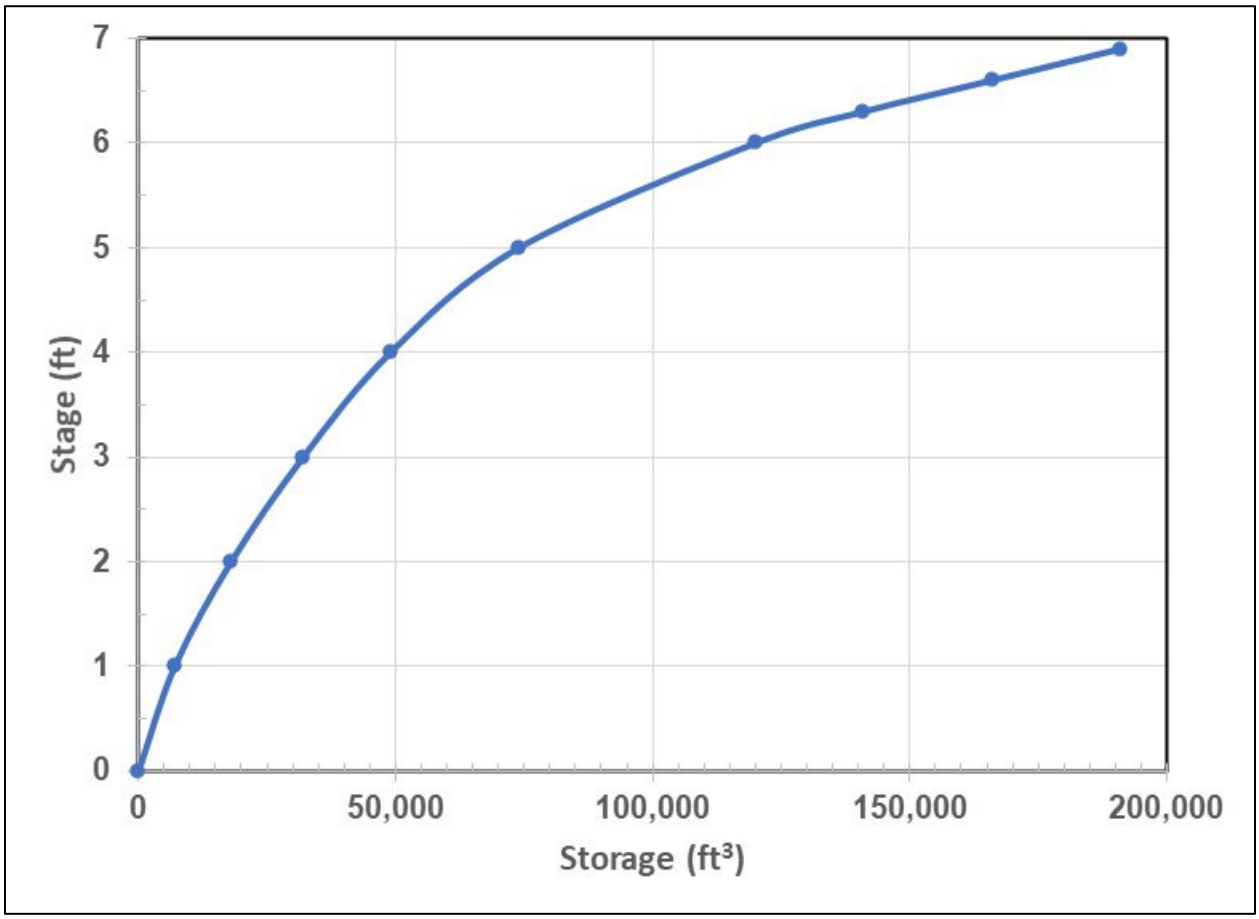

Figure 9.6. Example stage-storage curve.

Step 2. Select a time step, (Δt).

The given time step, (Δt), is 0.5 h.

Step 3. Calculate the storage-indication curve.

Using the data in Table 9.1, determine the storage-indication values, (S/Δt + O/2), for the various culvert sizes and a range of values of O. Plot the computed storage-indication values versus outflow (O), as shown in Figure 9.7. For the range depicted, the storage-indication curves for both culverts show slopes less than the line of equal values except for the 36-inch culvert curve from 20 to 40 ft^3/s. In this range, check the computations for instabilities. If higher slopes had appeared more prevalent, a smaller time step would be indicated.

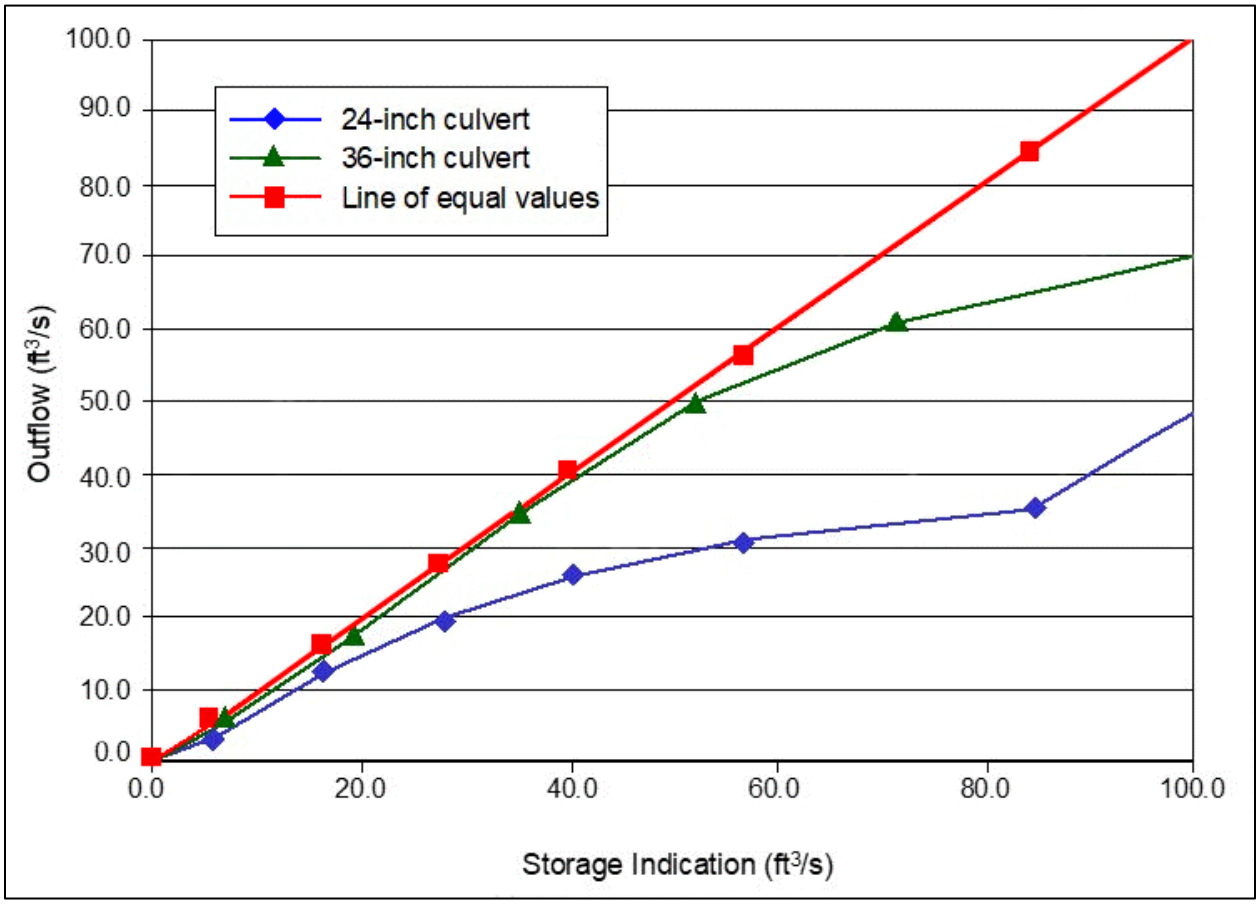

Figure 9.7. Example storage-indication curves.

Step 4. Discretize the inflow hydrograph.

Table 9.2 gives the hydrograph associated with the 0.02 AEP discharge, which is discretized to Δt = 0.5 h.

Table 9.2. Inflow hydrograph for CMP culvert storage routing example.

Time (h)	Discharge (ft^3/s)
0.0	0
0.5	11
1.0	21
1.5	30
2.0	39
2.5	49
3.0	60
3.5	49
4.0	39
4.5	30
5.0	21
5.5	11
6.0	0

Step 5. Assume an initial value for O_1 and S_1.

For a dry pond, as in this example, assume the storage is empty (S = 0) and there is no outflow (O = 0) for the initial condition.

Step 6. Compute the storage-indication value, $S_1/\Delta t + O_1/2$.

The initial storage-indication value at the beginning (t = 0 h) is:

$$\left(\frac{S_1}{\Delta t}+\frac{O_1}{2}\right)=\left(\frac{0}{0.5}+\frac{0}{2}\right)=0.0\ ft^3/s$$

Step 7. Calculate the storage-indication value at the next time step, $S_2/\Delta t + O_2/2$.

Using equation 9.3, calculate the storage-indication value at the next time step, t = 0.5 h.

$$\left(\frac{S_2}{\Delta t}+\frac{O_2}{2}\right)=\frac{I_1+I_2}{2}+\left(\frac{S_1}{\Delta t}+\frac{O_1}{2}\right)-O_1=\frac{0+11}{2}+0-0=5.5\ ft^3/s$$

Step 8. Obtain outflow from the storage-indication curve.

Using the storage-indication value from step 7, estimate the outflow from Figure 9.7.

Step 9. Use outflow with the storage-discharge relationship to obtain storage.

Using the outflow from step 7, estimate the storage by interpolation from Table 9.1.

Step 10. Repeat routing computational process.

First route the inflow hydrograph for the 24-inch diameter culvert in Table 9.3 using the relationship established by equation 9.3. This table shows a peak outflow of 51 ft^3/s and a

peak storage of 139,000 ft^3/s, which corresponds to a maximum storage depth of 6.3 ft. Since this depth exceeds the maximum depth criterion of 5 ft, this culvert size is not adequate.

Apply the same routing procedure for the 36-inch diameter culvert, shown in Table 9.4. For the 36-inch diameter culvert, the peak flow is computed to be 53 ft^3/s, corresponding to a maximum storage depth of 3.5 ft, which meets the maximum depth and minimum freeboard criteria. Figure 9.8 plots the inflow and outflow hydrographs.

Table 9.3. Hydrograph routed through 24-inch culvert.

Time (h)	Inflow (ft^3/s)	Average Inflow (ft^3/s)	$S/\Delta t + O/2$ (ft^3/s)	O (ft^3/s)	S (ft^3)
0.0	0	-	0	0	0
0.0-0.5 avg	-	5.5	-	-	-
0.5	11	-	6	4	6,540
0.5-1.0 avg	-	16.0	-	-	-
1.0	21	-	18	14	19,600
1.0-1.5 avg	-	25.5	-	-	-
1.5	30	-	29	21	34,300
1.5-2.0 avg	-	34.5	-	-	-
2.0	39	-	43	27	53,500
2.0-2.5 avg	-	44.0	-	-	-
2.5	49	-	60	32	80,100
2.5-3.0 avg	-	54.5	-	-	-
3.0	60	-	83	35	118,000
3.0-3.5 avg	-	54.5	-	-	-
3.5	49	-	103	51	139,000
3.5-4.0 avg	-	44.0	-	-	-
4.0	39	-	96	45	132,000
4.0-4.5 avg	-	34.5	-	-	-
4.5	30	-	86	36	121,000
4.5-5.0 avg	-	25.5	-	-	-
5.0	21	-	75	34	105,000
5.0-5.5 avg	-	16.0	-	-	-
5.5	11	-	57	31	75,000
5.5-6.0 avg	-	5.5	-	-	-
6.0	0	-	32	22	37,300

Table 9.4. Hydrograph routed through 36-inch culvert.

Time (h)	Inflow (ft^3/s)	Average Inflow (ft^3/s)	$S/\Delta t + O/2$ (ft^3/s)	O (ft^3/s)	S (ft^3)
0.0	0	-	0	0	0
0.0-0.5 avg	-	5.5	-	-	-
0.5	11	-	6	5	5,590
0.5-1.0 avg	-	16.0	-	-	-
1.0	21	-	17	16	15,900
1.0-1.5 avg	-	25.5	-	-	-
1.5	30	-	26	26	24,400
1.5-2.0 avg	-	34.5	-	-	-
2.0	39	-	35	35	31,900
2.0-2.5 avg	-	44.0	-	-	-
2.5	49	-	44	43	41,000
2.5-3.0 avg	-	54.5	-	-	-
3.0	60	-	56	52	54,000
3.0-3.5 avg	-	54.5	-	-	-
3.5	49	-	58	53	57,000
3.5-4.0 avg	-	44.0	-	-	-
4.0	39	-	49	47	46,000
4.0-4.5 avg	-	34.5	-	-	-
4.5	30	-	36	36	33,000
4.5-5.0 avg	-	25.5	-	-	-
5.0	21	-	26	25	24,000
5.0-5.5 avg	-	16.0	-	-	-
5.5	11	-	17	16	15,900
5.5-6.0 avg	-	5.5	-	-	-
6.0	0	-	6	6	6,600

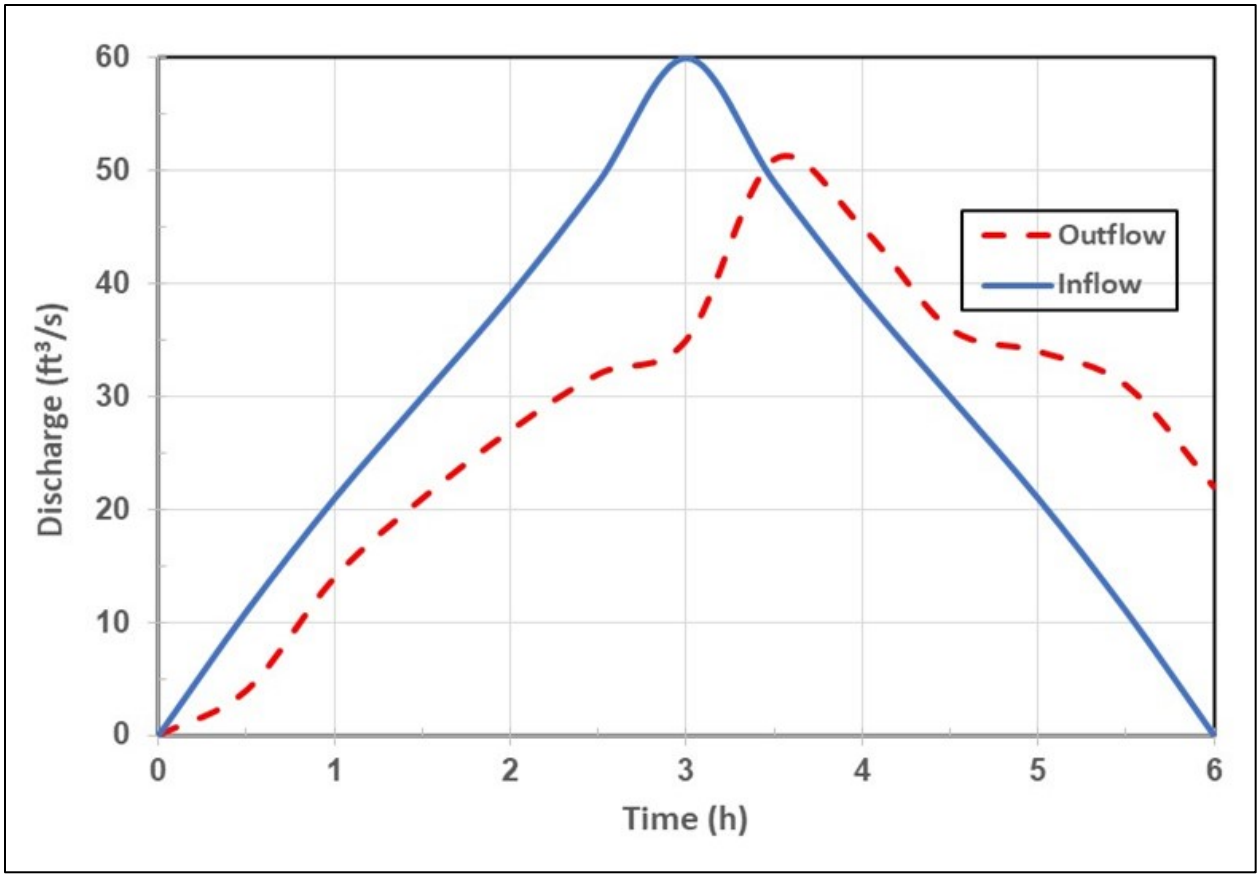

Figure 9.8. Example inflow and outflow hydrographs for 36-inch CMP.

Solution:	A 36-inch (0.91-m) diameter culvert, with a peak flow of 53 ft^3/s (1.5 m^3/s), meets the design criteria.

9.3 Channel Routing

Designers use the channel routing procedure to determine a hydrograph at any downstream point from a known hydrograph at some upstream point. As a flood hydrograph moves down a channel, flow resistance along the channel boundaries and the storage of water in the channel and floodplain modify its shape. Figure 9.1 provided an example of inflow and outflow hydrographs from a stream reach. Note that the hydrograph attenuates and translates as it moves downstream.

Like storage routing, channel routing is based on the continuity equation described in Section 9.1. If the reach is affected by lateral or tributary inflows the equation is adjusted to maintain continuity Figure 9.9 graphically represents the continuity equation with the change in time, dt, discretized as t_1 and t_2 and the change in storage, dS, represented as the wedge of water volume between the water surfaces at t_1 and t_2.

As with storage routing, the inflow hydrograph is discretized into successive time periods, Δt, of finite duration. For successful routing, the designer selects Δt to be smaller than the travel time of the hydrograph through the reach. Considering the hydrograph as a wave, the designer does not want the wave crest to completely pass through the reach during one routing period, which would preclude a numerically stable solution.

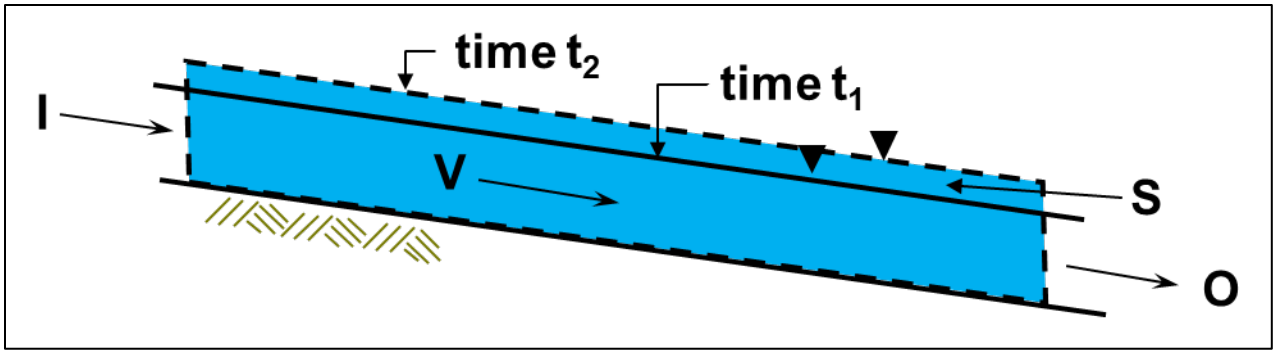

Figure 9.9. Channel routing schematic.

A number of techniques will route hydrographs through channels. This chapter presents several commonly used methods:

- Muskingum.
- Muskingum-Cunge.
- Kinematic wave.
- Modified Att-Kin.
- Lag routing.

The method to choose for a given reach depends on both the amount and type of data available and the nature of the hydrograph being routed. Table 9.5 summarizes highlights for selecting an appropriate channel routing method. For reaches with significant backwater, engineers use the storage routing method presented in section 9.2.

Table 9.5. Comparison of selected channel routing methods.

Routing Method	Attenuation	Translation	Applicability
Muskingum	✓	✓	Minimal overbank flow.
Muskingum-Cunge	✓	✓	Courant number, C ≤ 1. Useful with or without overbank flow.
Kinematic Wave		✓	Courant number, C ≤ 1
Modified Att-Kin	✓	✓	Routing coefficient ,Cm < 1
Lag Routing		✓	Useful when attenuation minimal.

9.3.1 Muskingum

The Muskingum routing method assumes the hydrograph attenuates as it moves downstream due to storage within the channel. The channel storage includes two parts: the prismatic storage, which is the water in the channel when inflow and outflow are equal, and the wedge storage, which is proportional to the difference between inflow and outflow. The Muskingum method emerges from the assumption that the storage within a given reach of river is given by:

$$S = K\left[XI + (1-X)O\right] \tag{9.6}$$

where:

S	=	Storage, ft^3 (m^3)
I	=	Inflow to the reach, ft^3/s (m^3/s)
O	=	Outflow from the reach, ft^3/s (m^3/s)
K	=	Empirical constant related to the wave travel time through the reach, s
X	=	Empirical constant balancing the relative importance of inflow versus outflow in determining the storage (varies between 0 and 0.5)

Substituting equation 9.6 into equation 9.3 yields:

$$O_2 = C_0 I_2 + C_1 I_1 + C_2 O_1 \tag{9.7}$$

where:

I_2	=	Inflow at the end of t, ft^3/s (m^3/s)
I_1	=	Inflow at the beginning of t, ft^3/s (m^3/s)
O_2	=	Outflow at the end of t, ft^3/s (m^3/s)
O_1	=	Outflow at the beginning of t, ft^3/s (m^3/s)

The following equations describe the coefficients:

$$C_0 = \frac{-K X + 0.5 \Delta t}{K - K X + 0.5 \Delta t} \tag{9.8}$$

$$C_1 = \frac{K X + 0.5 \Delta t}{K - K X + 0.5 \Delta t} \tag{9.9}$$

$$C_2 = \frac{K - K X - 0.5 \Delta t}{K - K X + 0.5 \Delta t} \tag{9.10}$$

By definition, the sum of C_0, C_1, and C_2 equals one. A difficulty with the Muskingum routing lies in determining reasonable values for K and X. The preferred method estimates K and X using measured pairs of inflow and outflow hydrographs for the site. However, because such data are rarely available engineers use more approximate methods.

When data are not available, estimate K to be the average travel time of the wave (hydrograph) through the reach. The designer estimates the travel time based on the wave celerity (speed). The discharge used in determining a value for K is the average discharge for the hydrograph. Using Manning's equation to derive an expression for wave speed (celerity) = dQ/dA and assuming a hydraulically wide channel, then celerity, $c = \beta V$, where V = flow velocity and $\beta = 5/3$. Engineers typically consider a channel where the ratio of the top width to flow depth is greater than 10 to be hydraulically wide.

The value of X ranges from 0 to 0.5. If X = 0.5, the hydrograph is translated but not attenuated. If X > 0.5, the hydrograph amplifies as it moves downstream, which does not make physical sense. In the absence of any other data, engineers typically assume X to be between 0.2 and 0.3, which results in some attenuation.

9.3.2 Muskingum-Cunge

Engineers commonly use the Muskingum-Cunge routing method. While similar to the Muskingum method, the Muskingum-Cunge routing method does not depend on extensive hydrologic data for calibration. Therefore, this method is ideal for use in ungaged streams.

The method represents a “hybrid” routing method; it has similarities to hydrologic methods but contains more physical information typical of hydraulic routing methods. The coefficients are functions of the physical parameters of the channel. The model physically accounts for the diffusion of the hydrograph as it travels through most natural channels.

The diffusion wave equation derives from the equations of continuity and momentum. The Muskingum-Cunge method is one solution of the diffusion equation. It uses the same computational equation as the Muskingum equation (equation 9.5):

$$O_2 = C_0 I_2 + C_1 I_1 + C_2 O_1 \tag{9.11}$$

However, the computation of the coefficients differs and is a function of the Courant number (C) and a diffusion coefficient (D):

$$C_0 = \frac{-1 + C + D}{1 + C + D} \tag{9.12}$$

$$C_1 = \frac{1 + C - D}{1 + C + D} \tag{9.13}$$

$$C_2 = \frac{1 - C + D}{1 + C + D} \tag{9.14}$$

By definition, the sum of C_0, C_1, and C_2 equals one. The Courant number is:

$$C = c\frac{\Delta t}{\Delta x} \tag{9.15}$$

The diffusion coefficient is:

$$D = \frac{Q_o}{c\, S_o\, T\, \Delta x} \tag{9.16}$$

where:

t	=	Time, s
x	=	Distance along the channel, ft (m)
c	=	Celerity, ft/s (m/s)
Q_o	=	Reference discharge, ft^3/s (m^3/s)
T	=	Top width of channel flow at Q_0, ft (m)
S_o	=	Slope, ft/ft (m/m)

Engineers obtain celerity, c, from a rating curve, $c = (dQ/dA)$. For wide channels, engineers can approximate it as $c = \beta V$. Engineers commonly choose the reference discharge as the average of the peak flow and base flow of the inflow hydrograph. It is intended to represent hydraulic conditions of the wave.

To capture event detail and avoid numerical dispersion, select Δt at least to meet both of the following two criteria:

$\Delta t < 0.2\ t_p$.

$\Delta t <$ wave travel time through the reach (Δx).

After selecting Δt, select Δx so that the Courant number equals 1 or slightly less. For best results, the sum of C and D will be greater than or equal to 1. Note that C_1 and C_2 can be positive or negative, unlike in the Muskingum method.

The Muskingum-Cunge method applies to most stream channels. It accounts for diffusion of the flood wave; however, if there are significant backwater effects caused by upstream or downstream controls, then this method does not apply. (Only the full dynamic equation can account for backwater effects.)

9.3.3 Kinematic Wave

A "kinematic wave" describes a wave with inertia and pressure (flow depth) gradient terms assumed to be negligible compared to the friction and gravity terms (Ponce 1989) in the full dynamic wave equation. This method is most applicable in cases where lateral flow contributes continuously to the larger flow of a channel. Neglecting inertial and pressure gradient terms reduces the momentum (or dynamic) equation to:

$$S_o = S_f \tag{9.17}$$

where:

S_o = Channel bottom slope, ft/ft (m/m)
S_f = Friction or energy slope, ft/ft (m/m)

The equation for a kinematic wave derives from the equation of continuity:

$$\frac{\partial Q}{\partial t} + c\frac{\partial Q}{\partial x} = 0 \tag{9.18}$$

where:

Q = Flow rate, ft^3/s (m^3/s)
x = Distance along the channel bottom, ft
t = Time, s
c = Wave celerity, ft/s (m/s)

Equation 9.18 assumes no lateral inflow. Using Manning's equation to derive an expression for celerity as dQ/dA and assuming a wide channel, then $c = \beta V$, where V = flow velocity and $\beta = 5/3$. Three important properties distinguish kinematic wave routing (Robeson et al. 1988):

- Kinematic waves travel only in the downstream direction.
- The wave shape does not change, and there is no attenuation of the wave height, only translation.
- The wave celerity is c = dQ/dA.

The kinematic wave equation is a nonlinear, first-order partial differential equation. To simplify application, modelers have assumed that the wave celerity can be approximated as a constant.

Then, the kinematic wave equation can then be simplified using a linear numerical scheme. Using central differences and a simplified form, kinematic routing is described by (Ponce 1989):

$$O_2 = C_0 I_2 + C_1 I_1 + C_2 O_1 \quad (9.19)$$

The coefficients have the following relationships based on the Courant number (C):

$$C_0 = \frac{C - 1}{1 + C} \quad (9.20)$$

$$C_1 = 1 \quad (9.21)$$

$$C_2 = \frac{1 - C}{1 + C} \quad (9.22)$$

The Courant number, C is:

$$C = V\beta\frac{\Delta t}{\Delta x} \quad (9.23)$$

where:

V = Average channel velocity, ft/s (m/s)

The engineer selects the spatial (Δx) and temporal (Δt) discretization so that the Courant number is less than or equal to 1 but as close to one as possible. An unsuitable Courant number results in numerical dispersion that causes errors in the numerical solutions. This means that when Δt, β, and V are specified, then the engineer will choose Δx to satisfy the Courant number criterion. Since the kinematic wave method can only translate a hydrograph, numerical dispersion produces any attenuation of the inflow hydrograph.

The kinematic wave equation applies to steep channels with little or no downstream control. It does not apply to milder slopes because the equation does not account for the significant attenuation of the hydrograph that can occur on these slopes. Input for the model primarily takes the form of a discharge-area relationship.

9.3.4 Modified Att-Kin

The modified attenuation-kinematic (Att-Kin), method provides both attenuation and kinematic translation and transforms the continuity-of-mass relationship of equation 9.2 to:

$$I_1 - \frac{O_2 + O_1}{2} = \frac{S_2 - S_1}{\Delta t} \quad (9.24)$$

Substituting S = KO into equation 9.24 and solving for O_2 yields:

$$O_2 = \left(\frac{2\Delta t}{2K + \Delta t}\right) I_1 + \left(1 - \frac{2\Delta t}{2K + \Delta t}\right) O_1 \quad (9.25)$$

Introducing the modified Att-Kin routing coefficient, C_m, as:

$$C_m = \frac{2\Delta t}{2K + \Delta t} \tag{9.26}$$

This leads to:

$$O_2 = C_m I_1 + (1 - C_m) O_1 \tag{9.27}$$

The value of K is assumed to be given by:

$$K = \frac{L}{mV} \tag{9.28}$$

where:

L = Reach length, ft (m)
V = Velocity, ft/s (m/s)

Engineers use the continuity equation to estimate velocity:

$$V = \frac{q}{A} \tag{9.29}$$

Cross-sectional area (A) relates to q by the rating curve equation:

$$q = xA^m \tag{9.30}$$

Equation 9.30 corresponds directly to the stage-discharge relationship, $O = ah^b$ since A is a function of h. Deriving the discharge using Manning's equation, then:

$$q = \frac{\alpha}{n} R_h^{2/3} A S^{1/2} = \frac{1.49}{n} S^{1/2} A \left(\frac{A}{P}\right)^{2/3} = \frac{S^{1/2}}{nP^{2/3}} A^{5/3} \tag{9.31}$$

where:

α = Unit conversion constant, 1.49 in CU (1.0 in SI)

Comparing equations 9.30 and 9.31 indicates that:

$$m = \frac{5}{3} \tag{9.32}$$

$$x = \frac{S^{1/2}}{nP^{2/3}} \tag{9.33}$$

Therefore, with these assumptions, m is a constant and x is a function of the characteristics of the cross-section. The rating curve of equation 9.30 assumes that the flow (q) and cross-sectional area (A) data measured from numerous storm events will lie about a straight line when plotted on log-log scales.

Manning's equation can be used where measured data are not available. Manning's equation can be applied for a series of depths and the rating curve constructed. The rating curve values and, thus, the coefficients are dependent on the assumptions underlying Manning's equation.

In many cases, the graph of log q versus log A will exhibit a nonlinear trend, which indicates that the model of equation 9.30 is not correct. The accuracy in using equation 9.30 to represent the rating curve will depend on the degree of nonlinearity in the plot.

The modified Att-Kin method provides for both attenuation and translation and can be summarized by the following steps:

Step 1. Evaluate the rating curve coefficients m and x.

From the channel cross-section information estimate the rating curve coefficients m and x. The engineer uses measured data or the Manning relationship for these estimates for equation 9.30.

Step 2. Compute K and then C_m.

Using the equations provided above compute K and Cm. Note that $C_m < 1$ and preferably $C_m < 0.67$.

Step 3. Route the upstream hydrograph.

The modified Att-Kin method uses equation 9.27 to perform the routings from which to derive the downstream hydrograph. This routed hydrograph represents the initial estimate of the downstream hydrograph.

Step 4. Compute initial hydrograph translation.

Compute the initial translation resulting from the routing in step 3. This time difference between the upstream and downstream hydrographs peaks is:

$$\Delta t_{pr} = t_{po} - t_{pi} \tag{9.34}$$

where:

Δt_{pr} = Initial hydrograph translation from routing
t_{po} = Time to peak of the downstream (outflow) hydrograph
t_{pi} = Time to peak of the upstream (inflow) hydrograph

Step 5. Compute the kinematic travel time.

The downstream (routed) hydrograph from step 3 is further translated when the kinematic travel time is greater than the difference in the times to peak computed in step 4. The kinematic travel time is:

$$\Delta t_{pk} = \frac{1}{3600} \frac{S_{po}}{q_{po}} \left[\frac{(q_{pi} / q_{po})^{1/m} - 1}{(q_{pi} / q_{po}) - 1} \right] \tag{9.35}$$

where:

Δt_{pk} = Kinematic travel time
q_{po} = Peak flow of the downstream hydrograph
q_{pi} = Peak flow of the upstream hydrograph
S_{po} = Maximum valley storage in the reach during the passage of, and assumed coincident with, the outflow peak

In addition:

$$S_{po} = \left(\frac{q_{po}}{k} \right)^{1/m} \tag{9.36}$$

$$k = \frac{x}{L^m} \tag{9.37}$$

Step 6. Apply additional translation, if needed.

If $\Delta t_{pk} > \Delta t_{ps}$, the storage-routed hydrograph from step 3 is translated by an additional amount equal to $\Delta t_{pk} - \Delta t_{ps}$.

9.3.5 Lag Routing

In many cases of subdivided watersheds of about 200 square miles or less, attenuation attributable to channel routing is insignificant when compared to the uncertainty in loss models, time parameters, and unit hydrograph shape. When attenuation can be ignored, the lag routing method accounts for translation but no attenuation. Engineers may choose lag routing for cases where flow in short channel segments, which are common in transportation related designs, does not vary and can be assumed to steady-state.

As the name implies, the lag method simply translates the inflow hydrograph in time. The engineer estimates the translation time based on an average flow velocity in the channel or other appropriate method such as the approach to estimating the wave travel time, K, for the Muskingum method (see Section 9.3.1).

Example 9.2:	Channel routing using four different methods.
Objective:	Estimate the outflow hydrograph by performing channel routing using the Muskingum, Muskingum-Cunge, Kinematic Wave, and modified Att-Kin methods.

Consider the river reach shown and average cross-section in Figure 9.10, where a hydrograph developed at point A is to be routed to point B. Table 9.6 summarizes the hydrograph including the peak flow of 2,966 ft^3/s (84 m^3/s).

Assume that the routing coefficients are constant and based on the reference discharge (Q_o) of 1,200 ft^3/s (34 m^3/s).

Given:

d = 6.6 ft (2.0 m)

B = 33 ft (10 m)

L = 15,750 ft (4800 m)

A = 261 ft^2 (24.2 m^2)

V = 4.6 ft/s (1.4 m/s)

c = (5/3) V = 7.7 ft/s (2.3 m/s)

Calculate the wave travel time, t_w.

t_w = 15,750 ft / [7.7 ft/s (3600 s/h)] = 0.57 hour.

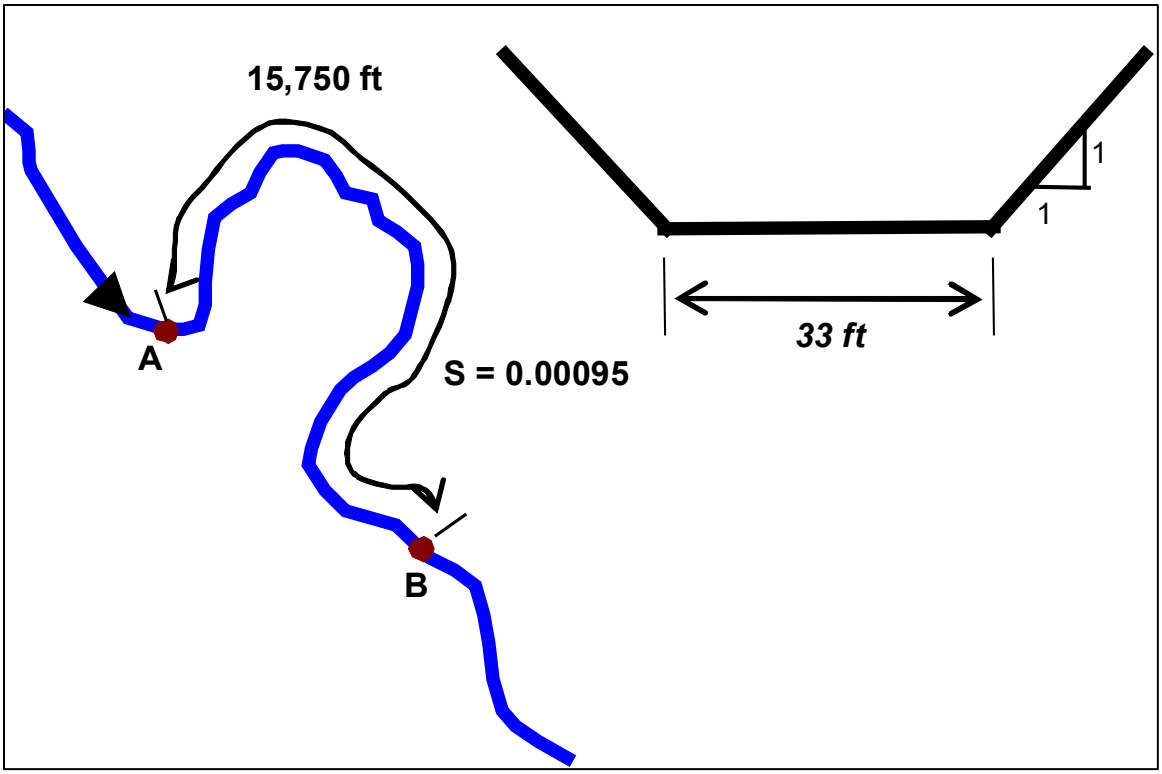

Figure 9.10. Example schematic of river reach.

Step 1. Route the hydrograph using the Muskingum method.

For the Muskingum method, first compute the coefficients C_o, C_1, and C_2 using equations 9.6, 9.7, and 9.8 and using Δt = 0.5 hour and assumed values of X = 0.2 and K = 0.57 hour as follows:

$$C_0 = \frac{-0.57(0.2) + 0.5(0.5)}{0.57 - 0.57(0.2) + 0.5(0.5)} = 0.193$$

$$C_1 = \frac{0.57(0.2) + 0.5(0.5)}{0.57 - 0.57(0.2) + 0.5(0.5)} = 0.516$$

$$C_2 = \frac{0.57 - 0.57(0.2) - 0.5(0.5)}{0.57 - 0.57(0.2) + 0.5(0.5)} = 0.291$$

The sum of the coefficients is $C_o + C_1 + C_2 = 0.193 + 0.516 + 0.291 = 1.000$.

Compute the outflow hydrograph ordinates using equation 9.5, beginning at t = 0.5 h:

$O_2 = C_0 I_2 + C_1 I_1 + C_2 O_1 = 0.193(247) + 0.516(0) + 0.291\ (0) = 48\ ft^3/s$

$O_2 = 0.193(459) + 0.516(247) + 0.291\ (48) = 230\ ft^3/s$ (at t = 1 h)

Table 9.6 presents these values along with the remaining calculations and indicates that the inflow hydrograph is translated and attenuated as shown in Figure 9.11.

Step 2. Route the inflow hydrograph using the Muskingum-Cunge method.

From equations 9.12 through 9.16, and using the given Δx and Δt:

C = 0.88

$T = B + 2zd = 33 + 2(1)(6.6) = 46.2$ ft

$D = Q_o / (cS_oT\,\Delta x) = 1{,}200 / [(7.7)(0.00095)(46.2)(15{,}750)] = 0.23$

$C_0 = (-1 + C + D) / (1 + C + D) = (-1 + 0.88 + 0.23) / (1 + 0.88 + 0.23) = 0.052$

$C_1 = (1 + C - D) / (1 + C + D) = (1 + 0.88 - 0.23) / (1 + 0.88 + 0.23) = 0.782$

$C_2 = (1 - C + D) / (1 + C + D) = (1 - 0.88 + 0.23) / (1 + 0.88 + 0.23) = 0.166$

The outflow hydrograph is computed from equation 9.11 and is given in Table 9.6. Figure 9.11 shows that the peak flow attenuates to 2,900 ft^3/s and translates to 4.5 h.

Step 3. Route the inflow hydrograph using the Kinematic Wave method.

Compute the coefficients and resulting outflow hydrograph using equations 9.17 through 9.23. The calculations proceed in the same manner as for the Muskingum method, beginning at t = 0.5 h:

$C = V\,\beta(\Delta t/\Delta x) = 4.6(5/3)(1{,}800/15{,}750) = 0.88$

$C_0 = (C - 1)/(1 + C) = (0.88 - 1)/(1 + 0.88) = -0.064$

$C_1 = 1$

$C_2 = (1 - C)/(1 + C) = (1 - 0.88)/(1 + 0.88) = 0.064$

$O_2 = C_0I_2 + C_1I_1 + C_2O_1 = -0.064(247) + 1(0) + 0.064(0) = -15\ ft^3/s$

Since a negative flow is not possible, assume a value of zero. At t = 1 h:

$O_2 = -0.064(459) + 1(247) + 0.064(0) = 218\ ft^3/s$

Table 9.6 summarizes the computations. Figure 9.11 shows that the hydrograph has been translated (i.e., the peak flow now occurs at 4.5 h) but has not been attenuated.

Step 4. Route the inflow hydrograph using the modified Att-Kin method.

Using equation 9.28:

$K = L / (mV) = 15{,}750 / [(5/3)(4.6)] = 2{,}054$ s = 0.57 h

$C_m = (2\Delta t) / ((2K + \Delta t)) = 2(1{,}800) / (2(2{,}054) + 1{,}800) = 0.609$

Using the routing equation, Table 9.6 gives the downstream hydrograph. Figure 9.11 shows that the peak outflow is 2,754 ft^3/s and has been translated from a time range of 1 h to between 4.5 and 5.0 h. Apply equation 9.35 to determine if further hydrograph translation occurs. Δt_{pk} = 0.5 h which is less than the 1-h translation shown in Table 9.6; therefore, there is no further translation.

Solution:	All four methods translate the inflow hydrograph time to peak of 4.0 to 4.5 h for the outflow hydrograph. The 2,966 ft^3/s (84 m^3/s) peak flow of the inflow hydrograph is attenuated to 2,825 ft^3/s (80 m^3/s) using Muskingum, 2,900 ft^3/s (82 m^3/s) using Muskingum-Cunge, and 2,754 ft^3/s (78 m^3/s) using modified Att-Kin methods. The kinematic wave method does not attenuate the peak. Figure 9.11 plots the inflow and routed outflow hydrographs.

Table 9.6. Inflow and outflow hydrographs for selected routing methods.

Time (h)	Inflow (ft^3/s)	Muskingum Outflow (ft^3/s)	Kinematic Wave Outflow (ft^3/s)	Muskingum-Cunge Outflow (ft^3/s)	Modified Att-Kin Outflow (ft^3/s)
0.0	0	0	0	0	0
0.5	247	48	0	13	0
1.0	459	230	218	219	150
1.5	812	461	421	438	338
2.0	1,130	772	767	766	627
2.5	1,730	1,142	1,068	1,101	933
3.0	2,401	1,690	1,645	1,660	1,418
3.5	2,684	2,250	2,334	2,293	2,017
4.0	2,966	2,614	2,644	2,634	2,423
4.5	2,754	2,825	2,959	2,900	2,754
5.0	2,507	2,730	2,783	2,765	2,754
5.5	2,119	2,500	2,549	2,530	2,604
6.0	1,836	2,178	2,165	2,172	2,308
6.5	1,624	1,897	1,871	1,881	2,021
7.0	1,412	1,664	1,653	1,656	1,779
7.5	1,271	1,460	1,436	1,445	1,556
8.0	1130	1,300	1,291	1,293	1,382
8.5	989	1,154	1,149	1,150	1,229
9.0	847	1,011	1,008	1,008	1,083
9.5	706	868	866	866	939
10.0	565	727	725	725	797
10.5	459	592	582	586	656
11.0	388	485	471	476	536
11.5	247	389	402	395	446
12.0	212	282	259	270	325
12.5	106	212	222	216	256
13.0	0	117	120	119	165
13.5	0	34	8	20	64
14.0	0	10	0	3	25
14.5	0	3	0	1	10
15.0	0	1	0	0	4
15.5	0	0	0	0	2
16.0	0	0	0	0	1
16.5	0	0	0	0	0
17.0	0	0	0	0	0

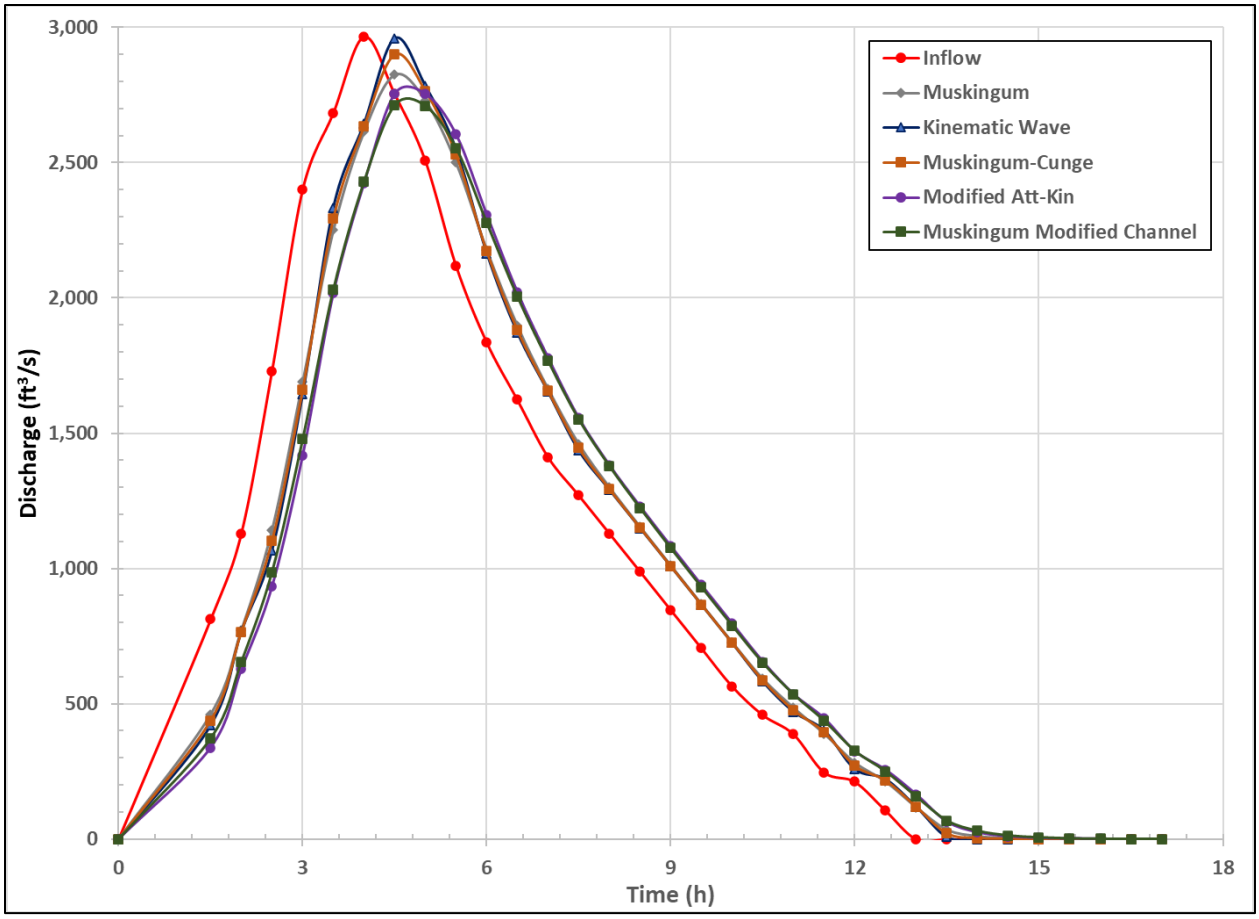

Figure 9.11. Inflow and routed hydrographs for example.

Page Intentionally Left Blank

Chapter 10 - Hydrologic Modeling

This chapter provides an overview of watershed modeling, spatial data and analysis, uncertainty, and risk analysis. A simple model, such as the Rational Method, continues to be useful to satisfactorily design many drainage structures. In many cases, however, the hydrologic aspects of drainage design have more complexity than a model as simple as the Rational Method can adequately represent. These situations include considerations of stormwater management, floodplain inundation, public safety, and broad environmental impacts. Analysis including these issues generally involves the use of a runoff hydrograph and more detailed data collection. Chapter 8 describes techniques used to develop a runoff hydrograph. Hydrologic models, as implemented in many software packages, estimate runoff hydrographs as a function of the rainfall and the spatial distribution of the land cover and soils in the watershed.

Spatially distributed models have many benefits. The hydrologist can vary the model parameters to simulate the behavior of the watershed under existing or future conditions or to examine the consequences of an array of design options. In some cases, modelers use spatial data analysis to define map-based input parameters. For example, they may use spatial data analysis to develop and store a digital database containing the land cover, soil type, and topography for a county, State, or larger area. Modelers also address uncertainty and risk in the planning and design process. This chapter discusses sources of uncertainty, nonstationarity, and risk.

10.1 Watershed Modeling

Hydrologists rely on watershed models to estimate runoff from historical and design storms. Planners and engineers use these models to simulate hydrographs or flow sequences when estimating design discharges. These design discharge estimates support decision-making regarding land use impacts, urban planning, flood control measures, water supply, and water quality. Simulation imitates a watershed through descriptive input data and mathematical formulations of natural processes.

10.1.1 The Modeling Process

Conceptually, the modeling process has three phases: identification, conceptualization, and implementation. In the identification phase, the modeler lists existing and proposed components of the watershed and collects relevant data. Pertinent information may include watershed characteristics, channel characteristics, meteorological data, water use information, streamflow data, and reservoir/storage information. For example, the modeler determines the watershed boundaries, the parts of the drainage network (e.g., pipes, channels, and storage) to explicitly represent, and the available rainfall or flow data.

During conceptualization, the modeler selects the methods for representing system components and the physical processes important in hydrologic modeling. This phase also often provides feedback for the identification phase by revealing the need for additional data useful to support modeling. In this phase, the modeler chooses the techniques to represent the system elements and selects the simulation models that provide these techniques. For example, in the conceptualization phase, the modeler will choose appropriate routing techniques for channels or storage, a technique for representing infiltration and other losses, as well as other methodological choices.

In the implementation phase, the modeler runs the model, reviews the results, and performs follow-up analyses. The modeler determines the validity of the model by demonstrating that its results represent a reasonable estimate of the actual system behavior through calibration,

validation, or sensitivity analyses. If the model output is not sufficiently valid, the modeler modifies the input data or modeling technique and reruns the model until it produces valid results.

10.1.2 Parameter Uncertainty and Sensitivity Analysis

Hydrologic models include such input parameters as precipitation, topography, land cover, soil type, and others, depending on the detail and complexity of the model. The chosen modeling technique determines how those physical characteristics translate to modeling inputs. Modelers rarely know the value of model parameters exactly as they frequently vary within a range of possible values. For example, an area might be zoned residential with lot sizes less than 0.5 acres and have a Type C Hydrologic Soil Group. However, because lot sizes, impervious areas, and soil type will vary, the modeler will be unlikely to quantify runoff characteristics with certainty.

Sensitivity analyses inform the analyst about which input parameters have the greatest effect on model outputs. Knowing the most influential inputs allows the modeler to identify the important parameters to investigate to minimize uncertainty associated with model predictions. Typically, the analyst changes the value of a particular input parameter within some specified range, running the model again to generate new results. The modeler compares the results to understand model sensitivity to the input parameters.

Figure 10.1 shows the results of a series of model runs varying input parameters to a Natural Resources Conservation Service (NRCS) approach for estimating peak flow. The modeler varied four input parameters — watershed area, time of concentration (t_c), curve number (CN), and initial abstraction (Ia) — to investigate the influence of parameter variability on peak flow estimates. The figure is normalized to an initial selection of parameters represented by the value of "1" on both axes. The lines show the change in peak flow with increases and decreases of an input variable.

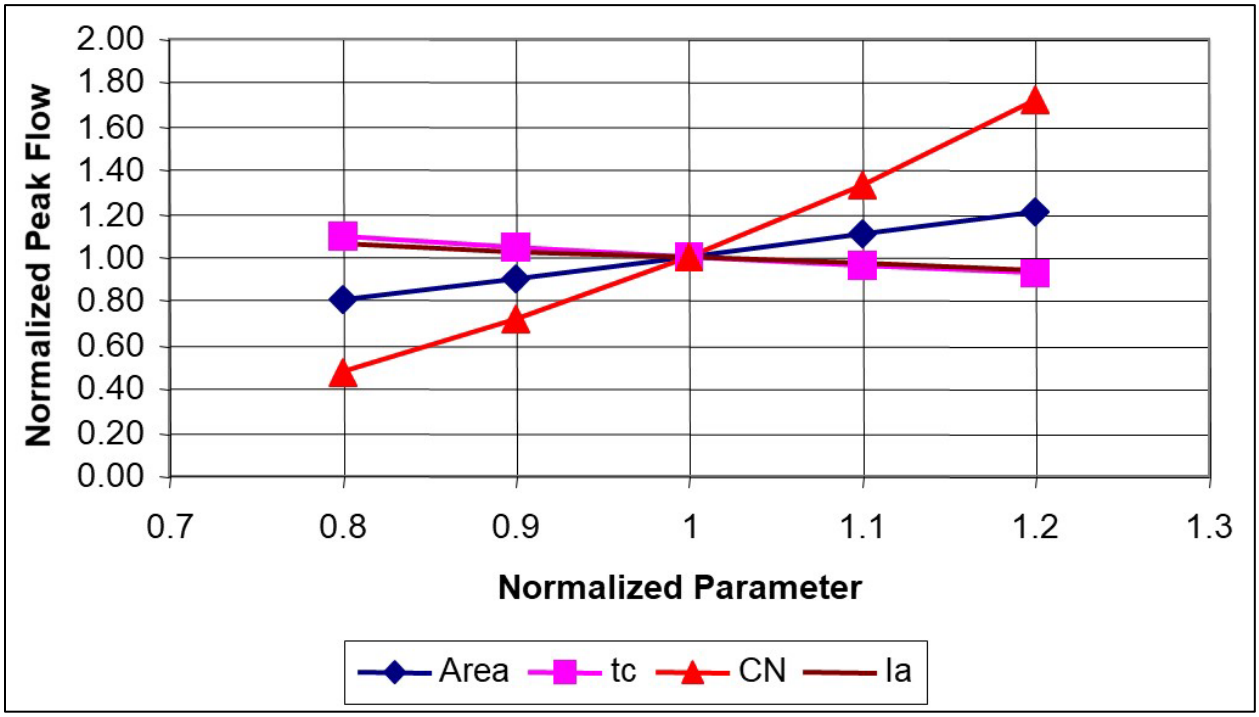

Figure 10.1. Example of sensitivity of peak flow to various input parameters.

For example, a 20 percent increase (1.2 on the x-axis) in the curve number results in a 70 percent increase (1.7 on the y-axis) in the peak flow. Similarly, a 20 percent decrease (0.8 on the x-axis) in time of concentration results in a 10 percent increase (1.1 on the y-axis) in the peak flow. For

this model and set of inputs, the modeler can observe that the output (peak flow) is most sensitive to curve number and least sensitive to time of concentration and initial abstraction. This insight can inform the modeler's efforts in data collection and analysis.

10.1.3 Model Selection

Numerous public domain and proprietary models implement the techniques described in this manual as well as many other more advanced or specialized techniques. Model selection matches analysis needs with model capabilities. This section describes categories of watershed models, their attributes, and other model selection considerations.

10.1.3.1 Lumped Parameter and Spatially Varied Models

One way analysts classify models is by the approach to describing the watershed and input parameters. A **lumped parameter** model considers the entire watershed or individual subbasins as a single unit, averaging the characteristics for that unit. For example, the land cover, soil type, and precipitation assume a single average value for each unit.

A **spatially varied** model divides the watershed into many smaller cells, often using a grid system. Each cell is described by the appropriate values of land cover, soil type, precipitation, and other inputs. Because of the differences in characterizing the watershed and meteorological inputs, spatially varied models often use different analytical methods than lumped parameter models to generate runoff, hydrographs, and peak flows.

The analyst can make lumped parameter models more detailed by subdividing the units to increasingly small subbasins. Similarly, the modeler chooses the grid size for a spatially varied model, with larger grids resulting in fewer cells. Lumped parameter models with smaller subbasins can represent a watershed with a similar level of detail to a spatially varied model using a larger grid. Some modelers refer to lumped parameter models with many subbasins as quasi-spatially varied models.

Research suggests, e.g., Thompson and Cleveland (2009), that subdivision of watersheds may not improve modeling outcomes if there are not hydrologic factors that justify subdivision. Such factors may include substantially different land uses or soil types in certain areas of the watershed, significant storage where storage routing is needed, or situations where channel routing is needed to represent hydrograph timing. In homogeneous watersheds, detailed subdivision may introduce complexity in the model by involving more parameter inputs that may or may not be supported by site-specific information but may not improve the model effectiveness.

10.1.3.2 Event-Based and Continuous Simulation Models

Analysts also classify models by the duration of the model run. An **event-based** model analyzes a single rainfall event. The event could be a historical event but is more commonly a design storm event selected to meet applicable risk-based criteria such as the 0.01 annual exceedance probability (AEP) event. An event-based application typically provides a peak flow and hydrograph associated with the design event.

A **continuous simulation** model analyzes a longer time series of rainfall, ranging from less than a year to over 10 years of data. Continuous simulation model applications can give information on low flows and typical flows, as well as high flows, by providing a longer-term continuous output hydrograph. Typically, modelers use historical time series of rainfall inputs, often altering the time series to investigate the effects of potential changes alternative rainfall scenarios. Applications include development of flow duration curves, preparation of annual or seasonal water budgets, low flow analysis, and flood flow analysis.

The FHWA's HEC-19 reference manual (FHWA 2022a) provides additional description of the differences between event-based and continuous simulation models. Modelers choose between these based on the analysis objectives.

10.1.3.3 Choosing a Watershed Model

Modelers choose a watershed model based on the analysis objectives, available data, modeler skill, and available resources. Initial considerations include the previously described distinctions — lumped parameter versus spatially varied and event-based versus continuous simulation. Beyond these, modelers consider the internal computational methods available within a watershed model including those described in this manual. These computational methods include those for converting rainfall to runoff such as the unit hydrograph (Section 8.1) and various channel (Section 9.3) and storage (Section 9.2) routing approaches.

Table 10.1 provides a matrix of watershed model attributes included in some commonly used public domain watershed models. A modeler can extend this table to include other public domain or proprietary models as well as additional attributes to support the selection of an appropriate modeling tool for a given application. Other attributes may include baseflow methodologies, infiltration approaches, water quality simulation, groundwater simulation, and automated data integration features. The table includes several watershed models:

- Hydrologic Engineering Center — Hydrologic Modeling System (HEC-HMS) developed by the U.S. Army Corps of Engineers (USACE) (USACE 2000a).
- Technical Release 20 / Technical Release 55, Windows versions (WinTR-20 / WinTR-55) developed by the NRCS (NRCS 2009b, NRCS 2015).
- Hydrologic Simulation Program — FORTRAN (HSPF) maintained by the U.S. Environmental Protection Agency (USEPA) (Bicknell et al. 2005).
- Stormwater Management Model (SWMM) developed by the USEPA (Rossman 2015).
- Gridded Surface Subsurface Hydrologic Analysis (GSSHA) developed by the USACE (Downer and Ogden 2006).

HEC-HMS simulates the precipitation-runoff processes of dendritic watershed systems. The program includes a variety of mathematical models for simulating precipitation, evapotranspiration, infiltration, excess precipitation transformation, baseflow, and open channel routing. HEC-HMS also includes a versatile parameter estimation option to aid in calibrating the various models.

WinTR-20 simulates storm events and aids in the hydrologic evaluation of flood events. Modelers can use it to analyze current watershed conditions as well as to assess the impact of proposed changes made within the watershed. Modelers can analyze multiple storms (or rainfall frequencies) within one model run. WinTR-20 computes direct runoff from watershed land areas resulting from synthetic or natural rain events and routes hydrographs through channels and/or impoundments to the watershed outlet. **WinTR-55** uses the WinTR-20 computational engine but applies to a subset of potential watersheds including only small watersheds (less than 25 mi^2), a smaller number of potential subbasins (not more than 10), and simplified routing.

HSPF simulates nonpoint source runoff and pollutant loadings for a watershed and performs flow and water quality routing in reaches. Modelers can run HSPF on a single watershed or a system of multiple hydrologically connected subwatersheds. The model depends on land use data, reach data, meteorological data, and information on the pollutants of concern in the watershed and the reaches.

Table 10.1. Watershed model selection considerations.

Attribute	HEC-HMS	WinTR-20 / TR-55	HSPF	SWMM	GSSHA
Lumped parameter vs. spatially varied	Both	Lumped parameter	Lumped parameter	Lumped parameter	Spatially varied
Event-based vs. continuous simulation	Both	Event-based	Both	Both	Both
NRCS unit hydrograph	Yes	Yes	No	No	No
Snyder unit hydrograph	Yes	No	No	No	No
Kinematic wave routing	Yes	No	Yes	Yes *	No
Muskingum-Cunge routing	Yes	Yes	No	No	No
Modified Att-Kin routing	No	No	No	No	No
Storage-indication routing	Yes	Yes	Yes	No	No
Snowmelt hydrology	Yes	No	Yes	Yes	Yes

*SWMM also provides dynamic wave routing.

SWMM simulates single events or long-term (continuous) simulation of runoff quantity and quality from primarily urban areas. The runoff component of SWMM operates on a collection of subbasin areas that receive precipitation and generate runoff and pollutant loads. The routing portion of SWMM transports this runoff through a system of pipes, channels, storage/treatment devices, pumps, and regulators. Modelers use SWMM for planning, analysis, and design related to stormwater runoff, combined sewers, sanitary sewers, and other drainage systems in urban areas.

GSSHA multidimensionally links overland, surface, and subsurface flow for watershed simulation. It is a physics-based, distributed, hydrologic, sediment and constituent fate and transport model. GSSHA includes two-dimensional (2D) overland flow and groundwater and one-dimensional (1D) streamflow and soil moisture. Analysts can use GSSHA as an event-based or continuous model where soil surface moisture, groundwater levels, stream interactions, and constituent fate are continuously simulated. The fully coupled groundwater to surface water interaction allows GSSHA to model basins in both arid and humid environments. As shown in Table 10.1, GSSHA does not use the hydrograph and routing methods described in this manual but applies computational techniques suited for 2D analysis.

10.2 Spatial Data and Analysis

At a minimum, hydrologic modeling uses input data describing precipitation, land cover, soils, and topography. As hydrologic models have become more sophisticated and integrated with geographic information systems (GIS), modelers rely more on spatial datasets. Section 4.2 provides a brief introduction to spatial datasets and GIS.

As well as providing visual outputs, spatial datasets and GIS improve the efficiency and quality of hydrologic modeling by reducing the labor intensity of data collection and analysis. By reducing the time involved in defining the input parameters, these tools reserve a larger portion of the project time to interpret results and explore alternative design strategies. Although GIS will allow a hydrologist to be more productive, it cannot replace judgment and experience. Well-designed

GIS allow the hydrologist to easily add special conditions to the database and modify pre-programmed procedures when encountering unusual watershed conditions.

A common example of spatial data and analysis in hydrology uses rainfall, watershed land cover, soil, and topographic data as model inputs. Spatial analysis of the topography provides drainage areas, stream paths, stream slopes, and watershed slopes. Spatial analysis of land cover and soil information generates infiltration and runoff parameters useful in the hydrologic model.

GIS integrate data from various sources in disparate scales and differing reference systems and stores this information in a georeferenced database. These data may include several layers such as land cover, soil type, and topography. The modeler can retrieve, analyze, and use these data to produce quantitative information to support decision-making for planning or design.

10.2.1 Multibasin Watersheds

Frequently, modelers represent watersheds as a single basin to generate peak flows and hydrographs at the watershed outlet. For many situations, modelers subdivide the watershed into multiple subbasins to better represent the hydrologic characteristics of the watershed. Situations that may call for subdivision include watersheds with:

- Large drainage areas.
- Significant differences in topographic, land cover, and soil characteristics within the watershed.
- Channels or storage where routing is important.

Figure 10.2 depicts the stream network and subbasin boundaries for a multibasin watershed. By dividing the watershed into four subbasins, the modeler can represent the watershed characteristics of each subbasin specifically rather than averaging over the entire watershed. This configuration also allows the modeler to include the effects of channel routing from the upper parts of the watershed to the lower.

This four-subbasin model qualifies as a lumped parameter model because the modeler averages the characteristics within each basin. However, the subdivision allows for a more detailed representation. Further subdivision allows greater detail and may be justified depending on the modeling objectives and the nature of the watershed.

Figure 10.3 provides a schematic network diagram illustrating the logical relationship between the subbasins for the watershed in Figure 10.2. Each box represents a subbasin and the connecting lines represent the channels connecting the subbasin. Modelers can easily see the interconnectedness of subbasins with schematic networks.

10.2.2 Spatial Computations Supporting Hydrologic Modeling

GIS and other spatial computation tools automate important tasks used to set up both lumped parameter and spatially varied watershed models. These tools include terrain analyses, parameter synthesis, and precipitation analysis.

10.2.2.1 Horizontal Coordinates, Vertical Datums, and Units

For use as inputs to watershed models, spatial data is georeferenced to a common horizontal coordinate system compatible with the selected watershed model. Similarly, spatial data including a vertical component, such as topography, reference a common vertical datum compatible with the selected model. For both horizontal and vertical data, modeling depends on knowledge of and internal compatibility with the measurement units.

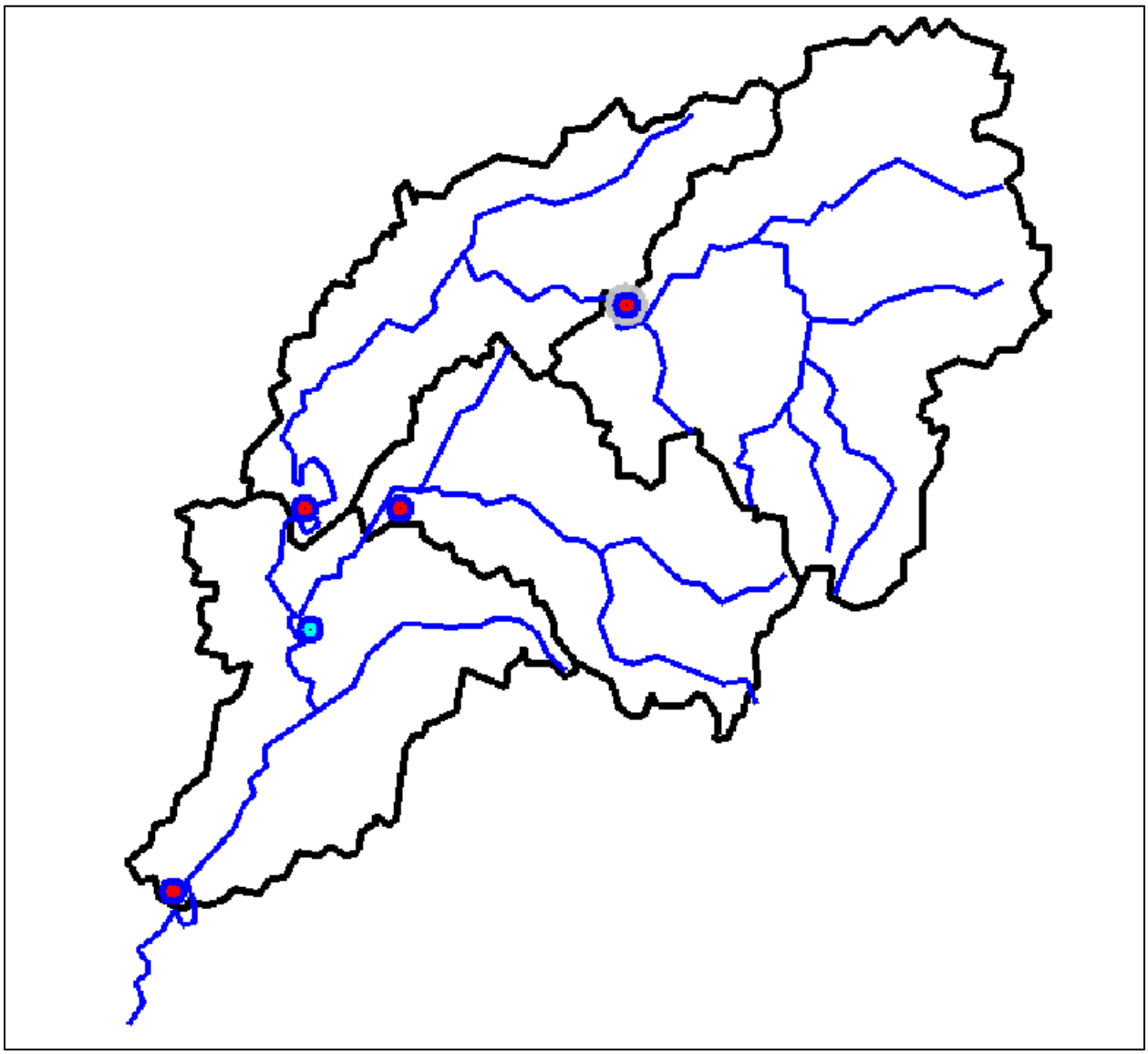

Figure 10.2. Stream network and subbasin boundaries of a multibasin watershed model.

Modelers often refer to **horizontal coordinates** as a coordinate system or projection. All coordinate systems are based on a spherical horizontal datum such as the World Geodetic System 1984 (WGS 84) and the North American Datum 1983 (NAD 83). Two common types of coordinate systems are geographic and projected. Geographic coordinate systems use a sphere to define locations on the Earth. The shape of the Earth is typically modeled as an ellipsoid. Latitude and longitude reference a point on the ellipsoid.

Elevation data references a **vertical datum**. Common vertical datums include National Geodetic Vertical Datum of 1929 (NGVD 29), the North American Vertical Datum of 1988 (NAVD 88), and local/custom vertical datums. Modelers adjust datasets with differing vertical datums so that all data references the same vertical datum.

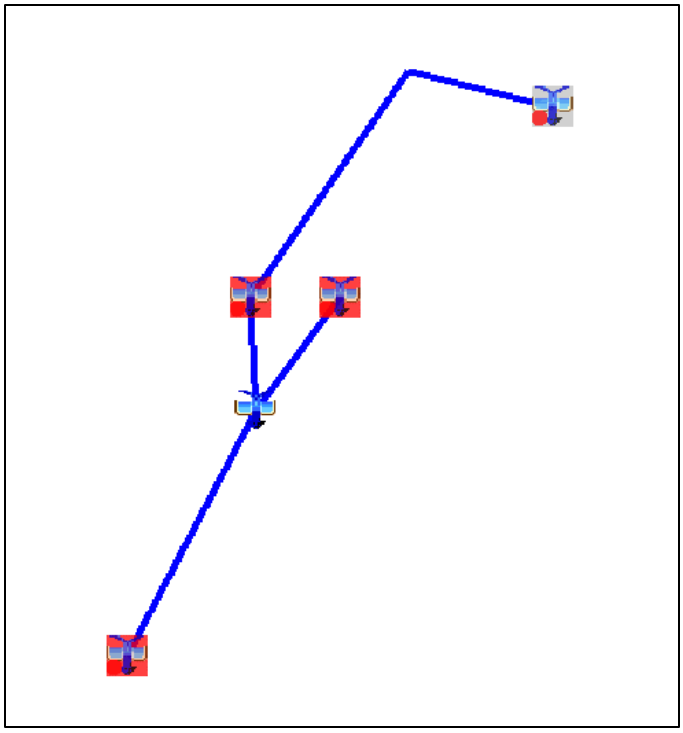

Figure 10.3. Schematic network representation of a multibasin watershed model.

10.2.2.2 Terrain Analyses

Automated terrain analyses use digital elevation models (DEMs) describing the ground surface with respect to X, Y, and Z coordinates. Most datasets are stored in gridded or triangulated formats. A **gridded** DEM typically employs a uniformly spaced X, Y grid with an elevation (Z) associated with each horizontal coordinate. A **triangulated** DEM uses a set of triangular surfaces linked to adjacent triangles at each edge to describe a surface. Modelers often call a triangulated DEM a triangulated irregular network. Modelers may find many other names for DEMs such as digital terrain models and raster datasets, but they generally refer to one of these two types of DEMS.

Hydrologic modelers use DEMs to delineate watershed and subbasin boundaries, identify stream channels and other flow paths, compute stream slopes and lengths, compute watershed slopes, estimate mean basin elevations, and many other tasks. The approach used by each watershed model or GIS preprocessor to accomplish these tasks varies, so the modeler will benefit from understanding the particular methods and datasets used by the selected application.

10.2.2.3 Parameter Synthesis

Depending on the watershed model selected, modelers can use spatial data analysis tools to estimate input parameters for both lumped parameter and spatially varied models. For example, spatial analysis tools can compute curve number for the NRCS methods discussed in Section 7.1 using geographically based layers of soil type and land cover. Another example is computing travel time in stream channels based on GIS layers of Manning's roughness and slopes generated by terrain analysis.

10.2.2.4 Precipitation Analysis

While precipitation varies spatially, for smaller basins, modelers often assume that precipitation falls uniformly across a watershed as in the Rational Method. For larger watersheds and multibasin watersheds, this assumption becomes less appropriate. Spatially distributing

precipitation over a watershed, especially for evaluation of historical events, can improve the ability of a model to accurately model the rainfall-runoff process.

Design storm or historical precipitation may be available in gridded format (e.g., radar data), analogous to DEM data, or it may be available at one or more gages. For spatially varied models, analysts convert gage-based precipitation to a spatial grid compatible with the model. For lumped parameter models, modelers adapt any precipitation dataset to each subbasin. Techniques for these adjustments include Thiessen polygons and the inverse distance method (USACE 2000a).

Modelers also consider how point precipitation data from gages, for example, apply over larger areas. Application of point precipitation over large areas overestimates total rainfall on a watershed because precipitation falls unevenly over large areas. Section 8.2.4 discusses depth-area adjustments. This adjustment is critically important when working with frequency-based design storms such as the 0.01 AEP event.

10.3 Uncertainty and Risk Analysis

For even the most detailed hydrologic modeling analysis, before finalizing the design, the modeler considers the uncertainty associated with the modeling effort and the risks associated with the design of hydraulic structures based on the modeling outputs. This section presents sources of uncertainty in hydrologic analyses and approaches for addressing the associated risks.

10.3.1 Uncertainty

Uncertainty derives from three major sources:

- Natural variability in precipitation and other meteorological and watershed characteristics.
- Simplifications used in developing the modeling tools.
- Potential changes in meteorology (climate change) and watershed characteristics (development) over time.

Hydrologic designers understand that natural variability means that sequences of flood events can follow periods of lower flow followed again by a series of flood events. Even when the modeler appropriately estimates the long-term probability of a flood event occurring in a given year, natural variability results in short-term variations to long-term patterns.

Models Are Not Reality

The quotation “All models are wrong, but some are useful” is attributed to the statistician George Box. Box’s point was that all models are simplifications of the real world and are necessarily limited. While some models include more real-world processes and phenomena than others, they remain simplifications. Analysts consider these limitations when selecting, applying, and interpreting models.

Uncertainty also derives from model simplification. For example, the Rational Method reduces the complex processes of rainfall and runoff to three parameters — runoff coefficient, rainfall intensity, and drainage area. This simplification has worked well for decades under specific circumstances. More complex watershed models incorporate more detailed representations of the watershed and more physics-based processes, but even these represent simplifications compared to the real world.

Finally, changes over time create uncertainty. While modelers often consider changes in watershed characteristics over time, such as land use, they have historically relied on stationarity of precipitation. The next section discusses stationarity and nonstationarity.

10.3.2 Nonstationarity

Most hydrologic design tools include the inherent assumption that the variables and parameters used in the models do not change over time. Stationarity means that the system does not experience temporal change. Nonstationarity could be realized as:

- A trend which occurs gradually and may result from changes in watershed land use/land cover and changes in climate.
- An abrupt change which occurs suddenly in the time series. Such a case generally involves placement or removal of dams on river systems. The construction or removal of a dam or other watershed detention facility dramatically affects the watershed response immediately downstream from the dam. The effect lessens with increasing distance from the dam (and increasing watershed drainage area). Stream diversion (for agricultural or municipal use) also represents an example of an abrupt change.
- Periodic variability, which occurs when cycles of wet and dry periods take place in the time series. These cycles usually span multiple years.

Land use and climate nonstationarity might alter the hydraulic risk of drainage structures over their service life. The discharge accommodated by the structure remains the same, but the probability of the occurrence of that discharge changes. Consequently, the risks of flooding also change. HEC-19 (FHWA 2022a) provides additional discussion of nonstationarity.

10.3.3 Risk-Based Design

Risk, as used in the context of hydrologic modeling, is the product of the probability of an event and the consequences of that event. Risk provides an overall framework for assessing or analyzing planning and design strategies and decisions. Risk analysis or assessment incorporates the concept of vulnerability and provides some measure of the costs and consequences (monetary and other) resulting from damages to and performance interruptions of the transportation asset. This facilitates the comparison of alternatives. Risk-based design refers to any procedure that considers risks associated with a project plan or design including, but not limited to thresholds, scenario analysis, and Monte Carlo analysis.

10.3.3.1 Thresholds

Engineers commonly use thresholds to design hydraulic structures. For example, the engineer may design a bridge to provide conveyance for the 0.01 AEP flood with a locally specified freeboard. The selection of both the AEP and freeboard implicitly incorporates risk. Because hydrologic design is driven by probabilities that certain events may occur during the design life of a project, planners and designers implicitly and explicitly anticipate and accept that an exceedance of design criteria (a threshold) might occur during the design life.

Although criteria exceedances may be considered a “failure” they do not always involve negative consequences in terms of public safety, asset damage, or service interruption. This fact represents one of the limitations of using thresholds as part of risk-based design. The design process does not explicitly include the consequences of exceedances. HEC-17 (FHWA 2016) provides additional discussion of the consequences of exceeding design criteria.

Even with an appropriate estimate of the long-term probability of a flood event occurring in a given year, the long-term probability does not determine the frequency of floods exceeding design criteria during the service life of a hydraulic structure. For example, while a culvert may be designed to pass the 10-year flood (i.e., the flood has an AEP of 0.1) during a planned service life of 40 years, the culvert may experience capacity-exceeding floods zero, one, two, three, four, or more times during its lifetime. A temporary coffer dam designed to withstand up to the 0.2 AEP

flood may be exceeded shortly after construction, even though the dam will only be in place for one year.

Engineers can estimate the risk of failure, or design uncertainty, using probability concepts introduced in Section 5.1. The probability of nonexceedance of a threshold value (Q_A) for n successive years equals:

$$P(\text{not } Q_A) = 1 - P(Q_A) = 1 - \text{AEP} \tag{10.1}$$

where:

$P(\text{not } Q_A)$ = Probability of not exceeding Q_A
$P(Q_A)$ = Probability of exceeding Q_A
AEP = Annual exceedance probability of Q_A

The probability that Q_A will not be exceeded for n successive years equals:

$$P(\text{not } Q_A)P(\text{not } Q_A)\cdots P(\text{not } Q_A) = [P(\text{not } Q_A)]^n = [1 - \text{AEP}]^n \tag{10.2}$$

where:

$P(\text{not } Q_A)$ = Probability of not exceeding Q_A
AEP = Annual exceedance probability of Q_A
n = Number of years

Then, it follows that the risk, R, that Q_A will be exceeded at least once in n years equals:

$$R = 1 - [P(\text{not } Q_A)]^n = 1 - [1 - \text{AEP}]^n \tag{10.3}$$

Table 10.2 summarizes the risk of exceedance based on the project life and AEP using equation 10.3. Designers can use either the table or equation to consider the likelihood that design thresholds will be exceeded during the expected project lifetime and the consequences associated with that exceedance. For example, a project designed for a 0.04 AEP with a lifetime of 50 years has an 87 percent chance of experiencing one or more floods exceeding the design discharge during its lifetime.

Table 10.2. Risk of exceedance (R) as a function of project life (n) and AEP.

Length of Service (years)	AEP				
	0.1	0.04	0.02	0.01	0.002
1	0.10	0.04	0.02	0.01	0.002
10	0.65	0.34	0.18	0.10	0.02
25	0.93	0.64	0.40	0.22	0.05
50	0.99	0.87	0.64	0.39	0.10
75	1.00	0.95	0.78	0.53	0.14
100	1.00	0.98	0.87	0.63	0.18

Example 10.1:	Risk of design threshold exceedances.
Objective:	Estimate the probability of one or more threshold exceedances over the design life of a culvert.

Given: A culvert designed to pass a 0.1 AEP design discharge maintaining the locally required freeboard. The design life of the culvert is 30 years.

Step 1. Estimate the risk of exceeding the design threshold during the culvert design life.

Use either equation 10.3 or Table 10.2 to estimate the risk. Since the table does not include an entry for a design life of 30 years, use the equation.

$$R = 1 - \left[1 - AEP\right]^{n} = 1 - \left[1 - 0.1\right]^{30} = 0.96$$

Step 2. Consider the consequences of exceedances of the design threshold.

From step 1, there is a 96 percent chance (near certainty) that the design threshold will be exceeded during the culvert design life. The designer considers the consequences of the design exceedance and evaluates whether adjustment to the design is appropriate.

Solution:	The probability of exceeding the design threshold during the design lifetime is nearly certain. Evaluation of the consequences of design exceedances determines if modifications of the design are appropriate to protect the public health, safety, and welfare, as well as the culvert and road infrastructure.

10.3.3.2 Scenario Analysis

Designers evaluate a plan or project using thresholds for a single design event, and possibly a check event, as standard practice. An extension of this practice involves consideration of a range of events that reflect uncertainty in engineering design methodologies and future scenarios. Considering a range of events represents an important tool for addressing climate change, extreme events, and the consequences of threshold exceedances.

A primary consideration in designing a resilient drainage structure is understanding how it might perform over the service life. As described in Section 10.3.3.1, a drainage structure will likely experience a wide range of flood events. In many cases, the engineer may appropriately assume that at least a few of those events will exceed the design discharge. During the design process, valid questions for consideration regarding an exceedance include what may happen, what is expected by the responsible agency, and what is expected by the public.

Specific performance parameters may target the design event specified by policy and engineering judgment (when policy allows design criteria to range over an interval). The design process does not end by satisfying these parameters. The designer may also assess performance at larger flows. Consider a culvert designed to accommodate the 0.04 AEP event, but that lies within a Special Flood Hazard Area as defined by the National Flood Insurance Program. The designer could evaluate the effect of that culvert in the context of the requirements of the base flood (0.01 AEP event). This does not necessarily imply that designers should design the culvert to accommodate the 0.01 AEP discharge, but rather that the designer could evaluate effects of the proposed structure on the water surface elevation of the base flood elevation.

Executive Order 13690 “Establishing a Federal Flood Risk Management Standard and a Process for Further Soliciting and Considering Stakeholder Input” promotes such practices that “increase resilience against flooding and helps preserve the natural values of floodplains.” (80 FR 13690 (Jan. 30, 2015), revoked by EO 13807 (Aug. 15, 2017), but reinstated by EO 14030 (May 20, 2021)).

Practitioners could also examine structures for performance at lower flow rates commensurate with more frequent flood events. For example, many hydraulic factors influence culvert performance, such as tailwater depth and barrel slope. While a culvert may perform satisfactorily at the discharge associated with the design event, a larger or smaller discharge may result in undesirable hydraulic conditions. A larger event may cause excessive velocity and the resulting erosion, while a smaller event may result in a velocity that is insufficient to support sediment transport through the reach of influence of the structure. Sediment erosion or deposition could also impair the ability of a culvert to properly perform at the design discharge because of erosion or sedimentation from earlier small discharge events.

Evaluating a range of events does not mean creating a plan or designing a project that has no damage associated with that range of events. Generally, cost and potential damage do not justify this. However, by considering this range of events, the designer could add features to a plan or project to enhance its resilience.

10.3.3.3 Monte Carlo Analysis

Monte Carlo analysis extends scenario analysis by increasing the number of scenarios and assigning probabilities to each scenario. The analyst then estimates the consequences of each scenario. The consequence has the same probability of occurrence as the scenario.

Some watershed modeling tools provide aids for implementing Monte Carlo analyses. For example, HEC-HMS provides a Markov Chain Monte Carlo analysis tool to run multiple scenarios (USACE 2020). Such aids allow the modeler to specify probability distributions for input variables. Then, the modeling tools use Monte Carlo analysis to randomly select values for each of the parameters, running the model for each combination of input parameters. The Monte Carlo analysis results in a probability distribution of hydrologic outcomes. Finally, the modeler assigns consequences to the hydrologic outcomes.

Challenges associated with Monte Carlo analysis include: 1) making reasonable estimates of the probabilities of the input parameter changes, 2) capturing changes in probabilities over time, and 3) the extensive resources needed for the analysis of multiple scenarios. However, probabilistic analysis has the potential to provide more complete information to support decision-making compared with threshold or scenario approaches.

Page Intentionally Left Blank

Chapter 11 - Special Topics in Hydrology

This chapter addresses unique situations involving more than standard methodologies: wetland mitigation, snowmelt hydrology, and arid lands hydrology.

11.1 Wetlands and Wetland Mitigation

Hydrology and biology inform the analysis of wetlands and wetland mitigation design. Therefore, successful wetland mitigation projects involve a multidisciplinary team generally including, at a minimum, a wetland scientist and a hydrologic engineer. This section addresses the role of the hydrologic engineer and the tools the engineer uses. This focus does not minimize the role of the wetland scientist; instead, it recognizes that the contributions of the wetland scientist's knowledge and tools in the mitigation process extend beyond the scope of this discussion.

11.1.1 Wetland Fundamentals

Wetlands are generally found where there is a permanent to semi-permanent surface saturation or ground saturation during the growing season. Where surface water is not present, wetlands may be sustained primarily by groundwater. Wetlands are generally characterized by permanent or seasonal inundation by water; hydrophytic plant species (adapted to growing wholly or partly submerged in water); and distinct soils that have developed in an anaerobic (saturated) environment.

Regional and local differences in climate, hydrology, topography, soils, vegetation, and water chemistry result in a broad geographic distribution of wetlands with diverse characteristics. Wetland scientists categorize wetlands into two general types: tidal and non-tidal. They further classify them as marshes, swamps, bogs, or fens, based on their vegetation and other characteristics (Zeedyk 1996, USEPA 2019).

Generally, the presence of water by ponding, flooding, or soil saturation is not always a reliable indicator of wetlands. Many wetlands are seasonally dry, particularly in the arid and semiarid West. The quantity of water present and the timing of its presence, in part, determine the functions and value of a wetland and its role in the environment.

For Federal regulatory purposes, the Code of Federal Regulations defines wetlands as "those areas that are inundated or saturated by surface or groundwater at a frequency and duration sufficient to support, and that under normal circumstances do support, a prevalence of vegetation typically adapted for life in saturated soil conditions. Wetlands generally include swamps, marshes, bogs, and similar areas" [33 CFR 328.3, 40 CFR 120.2, and 23 CFR 777.2]. In some cases, States and local governments also have wetland laws and regulations that may apply depending on the location of a project.

When the Federal definition applies, wetland scientists use this definition to determine the existence and extent of a wetland. Once they determine the location of a wetland, the multidisciplinary team evaluates the potential effects of a transportation project on the wetland and develops appropriate mitigation strategies. [*See* 40 CFR Part 230, Subpart J; 33 CFR Part 332; and 23 CFR Part 777].

Three conditions derived from the Federal definition of a wetland at 33 CFR 328.3 are used in characterizing a wetland:

- Hydrophytic vegetation dominant: vegetation adapted to wet conditions.
- Hydric soils: soil types developed under at least periodically wet conditions.
- Saturation at or near the surface, or inundation for some period of time during an average year.

Over time, the presence of the appropriate hydrology will facilitate the development of hydrophytic vegetation and hydric soils. Naturally or artificially induced changes to hydrology that increase the amount of water at a site over time will attract hydrophytic vegetation and create the conditions for the development of hydric soils, thereby potentially creating wetlands. This process has been observed, in its unintentional form, within stormwater management facilities. Unintentionally created wetlands have attracted regulatory oversight, which in turn has created maintenance issues in some locations.

Quantifying the terms used to describe wetlands presents a key challenge in the delineation, analysis, and design of wetlands. Such terms include “periodically,” “some period of time,” and “average year.” The wetland scientist plays a key role in determining the ecological needs of the desired vegetative communities, while the hydrologic engineer analyzes and designs a system to deliver the needed water.

11.1.1.1 Functions and Values

Given the diverse characteristics and functions of a wetland within an ecosystem, effective wetland mitigation goes beyond meeting the vegetative, soil, and hydrologic conditions that describe a wetland. If a transportation project affects an existing wetland, mitigation will consider the existing functions of the wetland as well as the value placed on those functions. In this way, the project team can transfer those functions and values to another location or replace them with equivalent functions and values. A functional assessment determines the functions of an existing wetland.

Wetland **functions** describe the natural processes performed by wetlands. Human society **values** those functions. Values, therefore, are subjective and may change from group to group, place to place, and over time.

Productive wetlands may offer multiple functions and significant value, while degraded wetlands may perform minimal function and therefore offer little value. Wetland functions fall into three general categories: ecological, economic, and recreational/aesthetic. These functions include:

- Ecological.
    - Floodwater storage and detention.
    - Water quality.
    - Fish and wildlife habitat and food.
- Economic.
    - Farming.
    - Timber harvest.
    - Special products.
    - Recreation revenue.
- Recreation/Aesthetic.
    - Hunting and trapping.
    - Boating.

- Bird watching.
- Photography.
- Fishing and clamming.

11.1.1.2 Mitigation Strategies

The diversity of wetland functions and the challenges of successfully mitigating the destruction of existing wetlands lead to a hierarchy of options in response to potential wetlands loss. As shown in Figure 11.1, these alternatives include—in preferential order—avoidance, minimization, and compensation. [40 CFR 230.91(c); 33 CFR Part 332.1(c); 23 CFR 777.3, 777.9].

Avoidance leaves the functions and values of an existing wetland unchanged. When feasible, planners prefer this option because it preserves known functions and avoids the uncertainties of other mitigation approaches.

When some impact cannot be avoided, planners then seek to minimize impacts to existing wetlands. Compensation may also be appropriate to complement a minimization strategy. [*See* 40 CFR Part 230, Subpart J; 33 CFR Part 332; and 23 CFR Part 777].

When project impacts call for compensation, planners consider several options, each with its own benefits and challenges. These include creation of new wetlands, restoration of degraded wetlands, or enhancement of existing wetlands. [23 CFR 230.92]. Restoration and enhancement are frequently preferred because of the higher probability of success (Marble and Riva 2002).

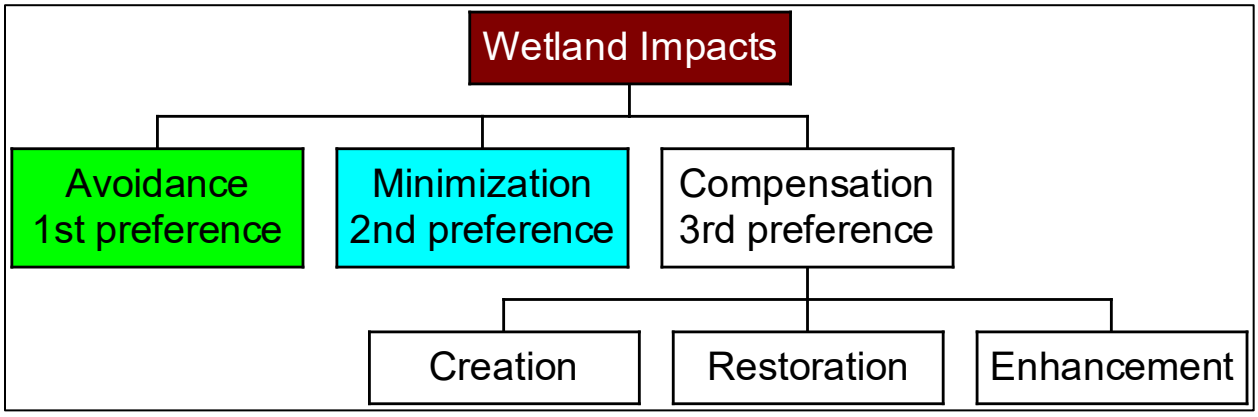

Figure 11.1. Hierarchy for addressing wetland impacts.

The variety of factors determining wetland viability complicate wetland mitigation through creation of new wetlands and restoration of impaired wetlands. The purchase of credits at a wetland bank presents an additional wetland mitigation option. Wetland banks provide access to wetlands created and maintained in anticipation of the needs of others to purchase credits for wetland losses elsewhere. If, for example, a highway project has unavoidable impacts on 1 acre of wetlands, they may provide compensatory mitigation through the purchase of credits at an approved wetland banking site.

11.1.1.3 Wetland Types

Wetlands vary in their sources of water, geology, morphology, and topography. Figure 11.2, Figure 11.3, and Figure 11.4 depict significantly different wetlands.

Wetland scientists have developed and applied several classification schemes. Wetland classifications continue to evolve as scientists learn more about wetlands and their function in the environment. For the past several decades, wetland scientists have commonly used the Cowardin

or Hydrogeomorphic (HGM) methods. The USFWS (Cowardin et al. 1992) developed a classification system that focuses on mapping wetland types and determining how the ecology of the wetland fits into the surrounding ecosystem. Though the USFWS system incorporates some aspects of hydrology and vegetation, it does not focus on these considerations. The HGM, developed by Brinson (1993), classifies wetlands by geomorphic setting, water source, and hydrodynamics. Brinson uses five HGM classes: riverine, fringe, depressional, slope, and extensive peatlands.

Figure 11.2. Schrieber Creek, Montana. Source: Montana DOT and used by permission.

Figure 11.3. Cypress Gum Swamps, North Carolina. Source: USFWS.

11.1.1.4 Hydroperiod

A “hydroperiod” describes the extent and duration of inundation or saturation of wetland systems; it differs with wetland location and type. When designing created or restored wetlands, hydrologic engineers assess the hydroperiod for existing wetlands and the target hydroperiod. For example, stormwater wetlands tend to have a hydroperiod characterized by frequent to chronic inundation by standing water. In these wetlands, hydrologic engineers typically face having too little water, though they may also encounter too much water for the desired vegetation.

In some cases, hydrologic engineers may consider the hydroperiod specifically during the growing season in addition to the full year. The growing season includes the period of most active growth for wetland vegetation. In areas of the country that experience freeze and thaw, the growing season takes place between the last freeze in the spring and the first frost in the fall based on the freeze threshold temperature of the vegetation.

Several examples depicting variation of inundation depth versus time over the course of a year illustrate the variety of hydroperiods. Figure 11.5 shows a prairie pothole in North Dakota with depths ranging from no standing water in the fall and winter to greater depths in the spring and summer. Figure 11.6 shows a northern riparian wetland in Ohio representative of a wetland adjacent to a stream or river that serves as its primary source of water. The water level in the wetland closely relates to discharge conditions in the stream. Figure 11.7 depicts a tidal marsh in Delaware with water level variations driven by the adjacent tidal variations.

Figure 11.4. Roadside wetland, Tennessee. Source: Tennessee DOT and used by permission.

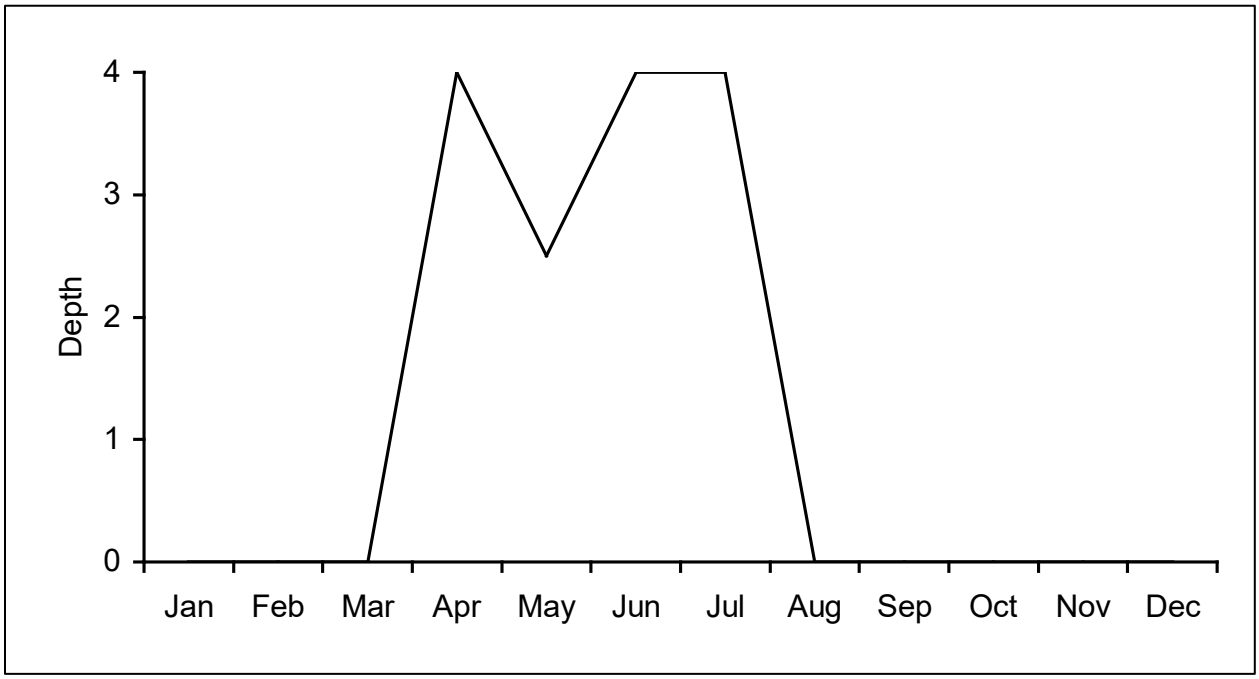

Figure 11.5. Prairie Pothole, North Dakota.

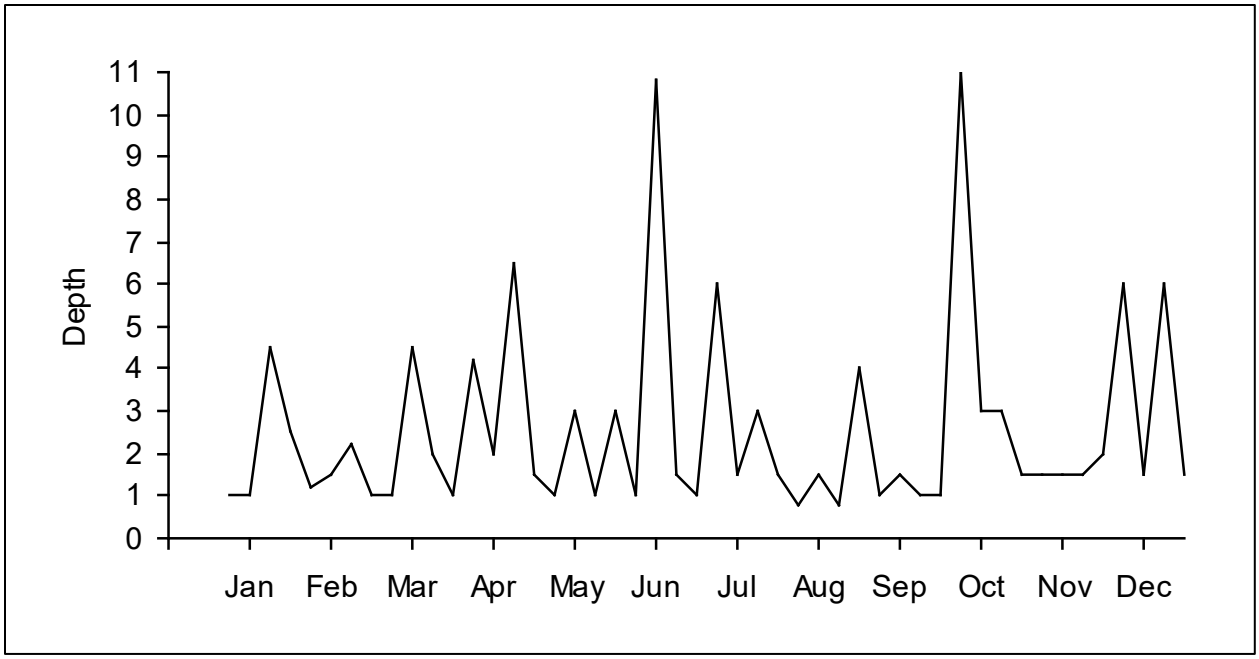

Figure 11.6. Northern Riparian, Ohio.

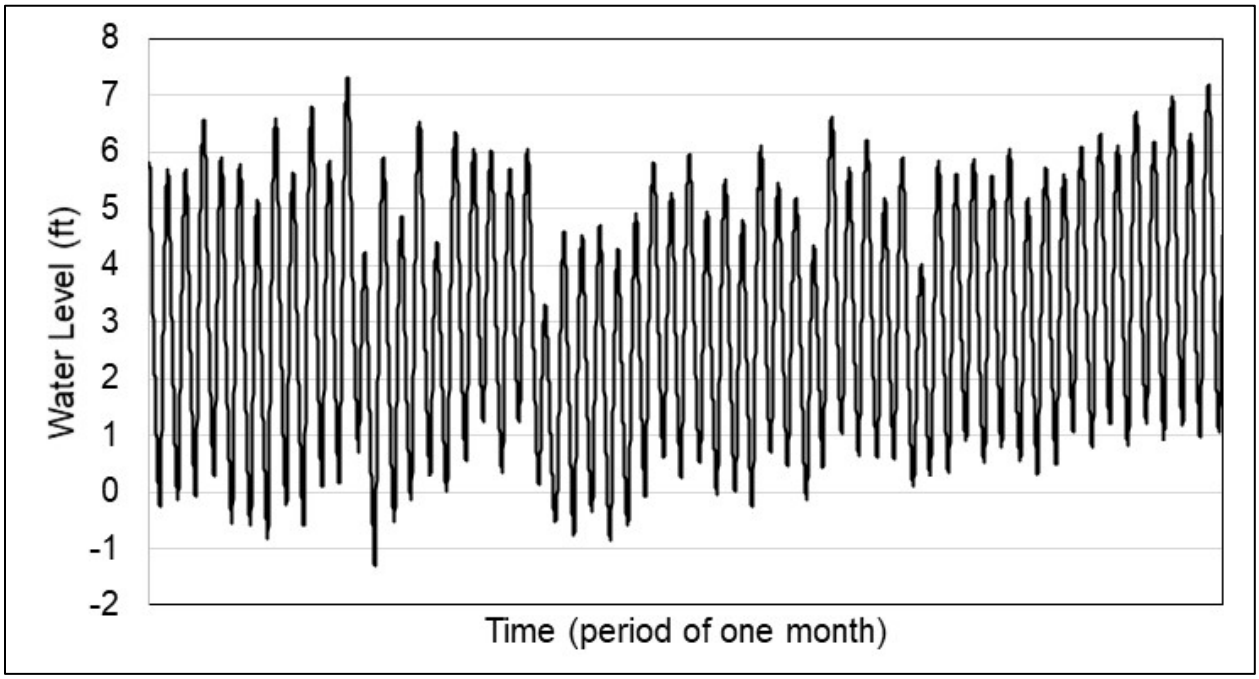

Figure 11.7. Tidal Marsh, Delaware.

The type of vegetation largely determines the design hydroperiod for wetland mitigation. The wetland scientist assists the engineer in determining the depths, durations, and timing appropriate to establish the design goals. Because the characteristics of wetlands vary significantly, these goals may also vary widely. Wetland scientists and hydrologic engineers may establish target hydroperiods based on combinations of inundation depth, inundation duration, and time of year. Table 11.1 summarizes example inundation recommendations for selected vegetation.

Table 11.1. Example inundation recommendations (USACE 2000b).

Plant Growth Form	Average Water Depth (inches)
Submergents, e.g., water celery	>20
Floating leaves, e.g., water lily	8-39
Herbaceous emergents, e.g., bulrushes	0-20
Shrubs, e.g., Buttonbush	0-8
Trees, e.g., Cypress	0-20

11.1.2 Models of Wetland Creation and Restoration

Designers can select from several types of conceptual wetland models to assist in organizing the available data and establishing goals for wetland mitigation projects. These models describe the general characteristics of the desired wetland for a given site and provide information on how to approach the design task. The models provide the basis for engineering wetlands. Classification systems explicitly addressing hydrology, such as the HGM, form the basis of these wetland models. They specify the source or sources of water, suggest water control structure design, characterize wetland setting, and guide hydroperiod criteria selection. Three major wetland model groups are surface water, groundwater, and enhancement restoration models.

Although these wetland restoration model groups are not mutually exclusive, the **surface water models** mainly apply to wetland creation rather than enhancement or restoration. As the name implies, surface water models rely on surface sources of water for the wetland. Surface water model subgroups include inline stream, offline stream, and surface categories, depending on how flows come to the site. The inline streamflow model includes placement of a water control structure in the stream. It applies only where low flows and limited debris occur, that is, in low energy locations. Engineers may find inline wetland systems difficult to implement because regulations generally discourage blocking a stream. The offline streamflow model also uses a water control structure, but to divert flows to an offline location. This approach has advantages in higher energy streams, but success depends on controlling erosion. Finally, the surface flow model is based on intercepting surface runoff through the use of berms and excavation.

Basin wetlands do not directly connect to a surface water source such as a stream, river, lake, reservoir, or estuary and rely exclusively on precipitation for their water source.

Groundwater models rely primarily on groundwater sources for water supply, but surface water sources often supplement this type of wetland creation. Groundwater models fall into two categories, spring/seepage flow and groundwater interception. Project teams create spring/seepage wetlands by excavating below a groundwater source and, possibly, using berms for containment. Groundwater interception also depends on excavation to a depth below the groundwater table. Properly characterizing the behavior of the water table over the long-term with generally short periods of monitoring observations presents the primary design challenge in this case.

The **enhancement/restoration models** build on existing water bodies and/or existing wetlands. The shared water supply model extends the use of water provided to an existing wetland by constructing additional wetlands to expand the area. Project teams using this approach will wish to avoid drying out the existing wetland when expanding the wetland area. While the shared water supply model seeks to expand area, the aquatic bed model modifies the depths in an existing

wetland to achieve alternative vegetative patterns and, in turn, alternative wetland functions and values.

The final three enhancement/restoration models build onto existing water bodies. The lake shore, island, and riparian rehabilitation models derive their sources of water from the adjacent water body, modifying depths to allow establishment of appropriate wetland vegetation.

For all restored or created wetlands, anticipating the effects of land use changes on water availability depends on understanding the source of both ground and surface water to a site.

Any of the wetland models described may involve the design and use of a control structure for water delivery and/or retention. Control structure functions may include:

- Control design depths (minimum and maximum).
- Distribute flows.
- Provide overflow capability.

The potential physical configurations can take a variety of forms depending on the site. For controlling water levels, they may include headgates, pipes/culverts, flashboard culverts, weirs, and stoplog structures. For distributing flow over a wide area within a wetland or to different wetland cells, they may include distribution headers, swales, flow splitters, and baffles/finger dikes. In almost all cases, designing control structures with adjustable features provides benefits. This permits changes to the structure after wetland construction to reflect observed versus anticipated water supply patterns and provides a means for adjustment during extreme wet or dry years. Other considerations include potential erosion, overflow, and seepage. A variety of sources, including the *Wetlands Engineering Handbook* (USACE 2000b), provide additional information on design of water control structures.

11.1.3 Water Budgets

The analytical framework of the water budget allows project teams to account for the inflow, storage, and outflow of water at a given site. Within the water budget, the engineer determines the quantitative availability of water for the wetlands along with its depth, duration, and frequency. The results of the water budget analysis inform whether the site can support the desired vegetation and wetland characteristics.

Conceptually, the water budget procedure accounts for the inflows and outflows to the wetland mitigation site resulting in an understanding of the availability of water at the site. The continuity (i.e., storage routing) equation forms the foundation for performing a water budget:

$$I - O = \frac{dS}{dt} \tag{11.1}$$

where:

I	=	Water inflow, ft^3/s (m^3/s)
O	=	Water outflow, ft^3/s (m^3/s)
dS	=	Change in storage, ft^3 (m^3)
dt	=	Change in time, s

The components of a water budget include its inflows, outflows, and storage characteristics. The choice of wetland model will influence which of the inflows and outflows the water budget will include.

11.1.3.1 Inflows

Inflows include direct precipitation (rain and snow), surface water inflow (base flow and storm runoff), and groundwater inflow. Wetland failures rarely occur because of the availability of too much water, though it is possible. Therefore, it is generally appropriate to ignore minor inputs and focus on estimating the major source of water. This conservative assumption may increase the viability of a wetland.

Direct precipitation, that is, precipitation (rain and snow) falling directly on the surface area of the wetland, provides a source of water to the wetland. However, in heavily vegetated wetlands estimates of interception range up to 35 percent. Frequently, engineers may ignore direct precipitation in water budgets because it is small compared to other water sources. Engineers will avoid double-counting direct precipitation on the wetland and stormwater runoff flowing to the wetland so that they do not overestimate the supply of water.

Surface water inflow may be in the form of base flow in a stream (potentially fed by groundwater) or in direct runoff from precipitation in the contributing watershed of the wetland. Ideally, a long-term stream gage record of daily or hourly flows will exist at a site to determine surface water contributions. If a stream gage does not exist, the engineer can generate streamflow patterns by applying a long-term precipitation record providing input to a calibrated continuous simulation model. In most cases, engineers rely on a simplified event-based modeling approach to estimate the surface water component of a water budget. Previous chapters introduced several methods. Successful application of any rainfall-runoff model involves consistency with the water budget analysis time step.

Engineers commonly estimate surface water inflows by applying the National Resources Conservation Service (NRCS) curve number method. This method produces a total volume inflow based on the precipitation, initial abstraction, and land cover as represented in the maximum potential retention variable:

$$Q = \frac{\left(P - I_a\right)^2}{\left(P + S - I_a\right)} \tag{11.2}$$

where:

Q	=	Runoff depth, inches (mm)
P	=	Rainfall depth, inches (mm)
I_a	=	Initial abstraction, inches (mm)
S	=	Maximum potential retention, inches (mm)

Since the NRCS method works with a 24-hour precipitation, engineers apply the procedure to a time series of daily rainfall data to produce a corresponding time series of daily runoff data. This approach has two potential limitations. First, it assumes that runoff for each day is independent of every other day. For example, if a precipitation event begins at 10 pm and continues until 4 am the next morning, the method will treat rainfall and runoff from 10 pm to midnight independently from that occurring between midnight and 4 am. In such a case, the method may underestimate runoff because it will treat the single storm as two smaller events with initial abstraction considered twice.

Second, the NRCS method will not show any runoff for any storm with an initial abstraction greater than or equal to precipitation. Although this may be an intuitive result, it may underestimate the total volume of runoff throughout a year. This is because the NRCS developed the method to generate runoff volumes for relatively large events, not for long-term wetland water budgets.

Recognizing these limitations, engineers may use a continuous simulation model such as the U.S. Environmental Protection Agency's (USEPA's) Stormwater Management Model (SWMM) to generate a time series of inflows (Rossman 2015). SWMM addresses the limitations of the NRCS methodology by performing a continuous accounting of infiltration, evaporation, and runoff. Starting with hourly precipitation data, the model generates hourly runoff values that account for antecedent conditions rather than assuming that each computation is independent of the previous computation.

Groundwater is the most challenging of the inflows to estimate. Typically, engineers only have access to field measurements taken from monitoring wells over a one- or two-year period for site-specific estimates of groundwater availability. Engineers interpret these data in the context of whether their collection occurred during a typical period or an atypically dry or wet period. Engineers also determine whether the groundwater comes from local versus regional aquifers and confined versus unconfined aquifers. Darcy's equation is a useful way for estimating groundwater flow to a wetland:

$$q = KA\left(\frac{dh}{dx}\right) \tag{11.3}$$

where:

q	=	Discharge, ft^3/s (m^3/s)
K	=	Hydraulic conductivity, ft/s (m/s)
A	=	Cross-sectional area orthogonal to flow, ft^2 (m^2)
dh/dx	=	Hydraulic gradient, ft/ft (m/m)

11.1.3.2 Outflows

Outflows primarily include evapotranspiration (ET), surface water outflow, and groundwater outflow (infiltration). One or more of these outflows may be small compared to the others. However, to estimate water availability conservatively, engineers consider each outflow in some manner to avoid overestimating the amount of water available in a wetland.

ET describes the combined effect of water surface evaporation and vegetative transpiration. However, vegetation reduces ET rates to 30 to 90 percent of the rates in open water. That is, the ET from a wetland would generally be less than evaporation from a lake in the same location. In some locations, ET data may be available from State climatological centers or estimated from pan evaporation rates. In the absence of site-specific data, several methods will estimate ET. Energy balance methods, such as Penman-Monteith, are complex and may rely on data unavailable for most sites. Climatological methods, such as Blaney-Criddle and Thornthwaite-Mather, rely on more commonly available climate-related variables such as solar radiation, temperature, wind speed, and relative humidity.

The Thornthwaite-Mather method (Thornthwaite and Mather 1955) uses only monthly mean air temperature and latitude to provide monthly potential evapotranspiration. Converted from tabular to equation form the potential evapotranspiration is:

$$ET_j = 0.63\left(\frac{10\left(T_j - 32\right)\left(5/9\right)}{I}\right)^a \tag{11.4}$$

where:

ET_j	=	Potential ET in month j, inches
T_j	=	Mean air temperature in month j, (°F)
I	=	Monthly heat index
a	=	Exponent, which is function of I

The monthly heat index is a function of air temperature computed over a 12-month period:

$$I = \sum_{j=1}^{12} \left(\frac{(T_j - 32)(5/9)}{5} \right)^{1.5} \tag{11.5}$$

The exponent, a, is:

$$a = 0.49 + 0.01791I - 0.0000771I^2 + 0.000000675\,I^3 \tag{11.6}$$

The method results in a monthly series of potential evapotranspiration values at the Equator (0 degrees latitude). Dunne and Leopold (1978) developed multiplicative adjustment factors for other latitudes summarized in Table 11.2.

Table 11.2. Thornthwaite-Mather latitude adjustment factors.

Latitude	Jan	Feb	Mar	Apr	May	Jun	Jul	Aug	Sep	Oct	Nov	Dec
60 N	0.54	0.67	0.97	1.19	1.33	1.56	1.55	1.33	1.07	0.84	0.58	0.48
50 N	0.71	0.84	0.98	1.14	1.28	1.36	1.33	1.21	1.06	0.90	0.76	0.68
40 N	0.80	0.89	0.99	1.10	1.20	1.25	1.23	1.15	1.04	0.93	0.83	0.78
30 N	0.87	0.93	1.00	1.07	1.14	1.17	1.16	1.11	1.03	0.96	0.89	0.85
20 N	0.92	0.96	1.00	1.05	1.09	1.11	1.10	1.07	1.02	0.98	0.97	0.96
10 N	0.97	0.98	1.00	1.03	1.05	1.06	1.05	1.04	1.02	0.99	0.97	0.96
0	1.00	1.00	1.00	1.00	1.00	1.00	1.00	1.00	1.00	1.00	1.00	1.00

A second type of outflow, surface water outflow, depends on the storage available in the wetland and the type of control structure. If a control structure is present, the elevation and configuration (weirs and orifices) will determine the outflow based on the water surface elevation in the wetland. Engineers estimate that all water volume exceeding some control elevation leaves the wetland as surface outflow during a given time step, except when using a very short time step.

Groundwater outflow represents the final departure route for water from a wetland. Like groundwater inflow, engineers can use Darcy's equation (equation 11.3) to quantify this route. However, the concept of hydraulic gradient, dh/dx, is difficult to conceptualize in the vertical direction. Therefore, engineers consider groundwater outflow as infiltration with the quantity K(dh/dx) in Darcy's equation taken as the infiltration rate for the soils underlying the wetland. Using the area of the wetland as the area in Darcy's equation provides a means for estimating groundwater outflow.

11.1.3.3 Storage

The water storage the wetland provides represents the final component of a water budget. As with stormwater management ponds, engineers often use stage-storage or stage-area curves to describe the storage of a wetland. Depth in a wetland may range from zero, where no surface inundation exists, to the maximum depth at a control location, for example, at the control structure.

Although the stage-storage relationship applies best to water budget computations, engineers may find the stage-area relationship useful for determining the extent of inundation. This stage-area relationship information helps the engineer determine the wetland areas appropriate to support certain types of vegetation. The water budget also provides key information on the hydroperiod, which project teams use to select appropriate plantings.

11.1.3.4 Routing

With the inflows, outflows, and storage information, the engineer routes water through the wetland to determine its hydrologic performance. The engineer chooses an analysis time step for the routing based on the variability of the water sources and losses, the methodologies used for estimating water availability, data availability, vegetative needs, and resources available to perform the water budget. Most water budgets use a monthly or daily time step, but they can also use an hourly time step.

A combination of depth, duration, and frequency requirements inform hydrologic design goals. Expectations for the growing season can further inform design goals. To ensure wetland survival, the design team may find it appropriate to provide for a specified number of consecutive days at a prescribed depth. Typically, surface water inflows govern selection of a time step.

At a minimum, engineers calculate surface water inflows on a daily basis. Engineers may then complete the water budget for all inflows and outflows on a daily basis, or they may aggregate the daily inflows to a monthly time step, using them in a water budget based on monthly time steps. Similarly, engineers may calculate runoff values on an hourly basis, aggregating them to daily values for water budget computations on a daily basis. Because of the unavailability of sufficient data to do so, engineers rarely calculate water budgets on a frequency of less than a day.

11.1.3.5 Period of Analysis

The engineer considers whether water budgets applied to typical or extreme conditions, or both, will best evaluate wetland performance. This decision, in consultation with a wetland scientist, relates to the frequency of inundation and long-term survivability of wetland vegetation.

Engineers often base their assessments of a typical or average year on total annual precipitation, but they may also base their determination on the number of days with measurable precipitation, total precipitation during the growing season, or other parameters. Using total annual precipitation presents the limitation that a year with many smaller storms may have a much different effect on a wetland than one with fewer large storms, despite having the same total rainfall. Therefore, distribution of rainfall throughout the year is an important consideration when selecting a typical year. Rainfall histograms are a useful tool for investigating rainfall distribution. Even though a typical year is unlikely to be the governing design event, engineers may find it useful to consider a typical year as a reference condition to compare with more extreme years.

Determining the extreme year provides essential information for evaluation of wetland performance. The extreme year describes that year during which the wetland site is stressed but survives with sufficient water. As with the typical year, the project team determines this based on total precipitation for the year, number of days of precipitation, or total precipitation during the growing season. This raises the question of how extreme the extreme year should be for design purposes. For example, if the wetland scientist determines that 9 out 10 years have sufficient

water, then, for design purposes, the extreme year the engineer selects is the one with a 10 percent (0.1) annual exceedance probability. For long records, the engineer may reasonably accomplish this by ranking the available data. For short records, the engineer fits available data to an appropriate probability distribution. Although determination of an extreme year generally only has relevance for extremely dry conditions, the engineer may use the same process to identify extremely wet years if excess water is a concern.

For design, the potential for anomalies in rainfall distribution or other parameters to cause misleading results can limit the selection of particular years (typical and extreme). Using continuous simulation to perform water budgets for all years of available data presents an alternative. Although much more computationally intensive, this approach uses the full record to evaluate a proposed wetland. Short periods of record, however, may lack extreme events or contain an uncharacteristically large percentage of extreme events. When using continuous simulation for water budgets, carefully evaluating the representativeness of a given record will address this issue.

11.1.4 Water Budget Design Procedure

Water budget design procedures vary but generally include common elements described in the following steps.

Step 1. Select wetland model.

Selecting the appropriate wetland model for the project allows the engineer to identify the important components for the water budget. Section 11.1.2 summarizes common wetland models.

Step 2. Determine design conditions.

The hydrologic engineer determines the design conditions in coordination with the wetland scientist. Jointly, they establish the hydroperiod (depth, duration, and frequency), including determining typical and extreme conditions as described in Section 11.1.1.4.

Successful wetland mitigation projects begin with clearly stated design goals. The design process may be iterative. The water budget may not support initial expectations of wetland type. This may alter the wetland design including the hydroperiod goals and perhaps even the wetland model. The water budget analysis may also demonstrate that a wetland of any kind is not viable at a given site.

Step 3. Identify inflows and outflows.

The hydrologic engineer identifies the essential inflows and outflows based on the wetland model and anticipated data availability as described in sections 11.1.3.1 and 11.1.3.2, respectively. It is conservative and appropriate (except in circumstances where too much water could be a problem) to assume one or more of the inflows to be negligible while focusing on the primary inflow source.

Step 4. Obtain data.

After establishing the wetland model and design goals, the hydrologic engineer obtains the data for the water budget. The wetland model and primary inflows and outflows will determine the emphasis to be placed on certain types of data, but generally the engineer establishes drainage area, infiltration parameters, and runoff characteristics using soils, topography, and land use/land cover data.

The engineer can establish surface water contributions either based on gaged streamflow data, if available, or through rainfall/runoff modeling based on precipitation data. The engineer can estimate evapotranspiration based on climatological data including mean monthly temperature.

Step 5. Analyze inflows.

After data collection, the engineer computes the inflows to the wetland site. Section 11.1.3.1 provides information on these computations.

Step 6. Analyze outflows.

The hydrologic engineer also computes the relevant outflows. Section 11.1.3.2 provides information on these computations.

Step 7. Characterize storage.

Next, the hydrologic engineer characterizes the storage characteristics of the wetland. Section 11.1.3.3 provides information on these computations.

Step 8. Calculate water budget.

Finally, the hydrologic engineer combines all of the components and computes the water budget. Based on the water budget, the engineer determines if the design requirements have been met. The engineer may choose to evaluate typical and extreme (dry or wet) periods to create a more complete understanding of the site and potential wetland mitigation design.

Example 11.1:	Wetland water budget application.
Objective:	Compute a monthly water budget for a created wetland for a typical rainfall year. Consider the viability of the wetland in an extreme year.

Given: A 6-acre (2.4 ha) wetland mitigation site upstream of a secondary road crossing of Clear Creek in South Carolina (example adapted from AASHTO (2000)).

Drainage area to the site: 1717 acres (695 ha)

Average spring fed baseflow: 0.0177 ft^3/s (0.00050 m^3/s)

Latitude: 34 degrees north

Soil permeability, K: 3.15 $x10^{-6}$ in/s (80 x 10^{-6} mm/s)

Step 1. Select wetland model.

For this site, the project team will create the wetland adjacent to Clear Creek with surface water being the primary water source. Therefore, the site calls for the offline stream wetland creation model.

To create a wetland using the offline stream wetland creation model involves using a control structure. The dimensions of the control structure depend on the site characteristics and the planned vegetation type. Initially, the designer assumes that the control structure will create a maximum ponded depth of 3.28 ft.

Step 2. Determine design conditions.

The wetland scientist determined that this mitigation project calls for two types of wetland vegetation:

- Submergents: Provide at least 1.64 ft of depth over a 1.2 acres area for 90 days in 9 out of 10 years.
- Emergents: Provide inundation between 0 and 1.64 ft over 4.8 acres for 90 days in 9 out of 10 years.

The design goals—specifically that the project provides sufficient water in 9 of 10 years—determine the parameters for the extreme year. Therefore, the extreme dry year has a 0.10

AEP. Based on the wetland model and the hydroperiod goals, the hydrologic engineer chooses a monthly computational time step but calculates surface runoff on a daily basis.

Step 3. Identify inflows and outflows.

The designer identifies that direct precipitation and surface water inflows are likely most important at this site and that groundwater inflow is assumed to be negligible. For the outflows, the designer determines that evapotranspiration, surface water outflows, and groundwater outflows have relevance for this water budget.

Step 4. Obtain data.

Because this site has no gaged streamflow data, the engineer will conduct rainfall/runoff modeling. A representative rainfall gage nearby includes a 47-year period of record covering the years 1949 through 1995. The designer selects the year with the median total rainfall as the typical rainfall year for this analysis, which is 1968 with 48.7 inches of precipitation. Table 11.3 summarizes the daily precipitation in 1968. The driest year on record was 1954 with 27.4 inches and the wettest was 1964 with 80 inches. All precipitation at this site was recorded as rainfall.

The designer will compute evapotranspiration based on the Thornthwaite-Mather methodology, which uses only site latitude and monthly temperatures. Table 11.4 presents average monthly temperatures for the site.

Step 5. Analyze inflows.

The inflows are direct precipitation and surface inflow. Because direct precipitation is small compared to surface inflow in this example, the engineer ignores direct precipitation.

The designer applies the NRCS runoff method, assuming average antecedent moisture conditions and that each day of rainfall generates a separate runoff event. Based on the land cover and soil types in the contributing watershed the designer estimates a curve number (CN) of 64. Maximum potential retention using equation 7.5:

$S = (1000/CN)-10 = 5.63$ inches

Assuming that initial abstraction, I_a, equals 20 percent of maximum potential retention and equation 7.3:

$I_a = 0.2(5.63) = 1.13$ inches

Therefore, only days with precipitation greater than 1.13 inches will generate runoff. Table 11.5 summarizes the runoff computations for the 14 days in 1968 generating runoff. For the monthly water budget, the engineer adds together the daily values within a month to estimate the monthly runoff summarized in Table 11.6. Calculate the direct runoff depth, Q, using equation 7.1.

The designer estimates base flow as a constant value equal to 0.0177 ft^3/s, or 47,000 ft^3/month. When available, site-specific base flow measurements inform base flow estimates.

Although the engineer has made a constant base flow assumption throughout the year in this case, such an assumption would likely be inappropriate if base flow is a significant part of the budget and significant variations are known to occur throughout the year. In this example, base flow represents a minor component of the water budget.

Table 11.3. Daily precipitation (inches) for 1968 (typical year).

Day	Jan	Feb	Mar	Apr	May	Jun	Jul	Aug	Sep	Oct	Nov	Dec
1	0.49	0.00	0.00	0.00	0.00	0.00	0.00	0.00	0.12	0.00	0.00	0.00
2	0.08	0.20	0.00	0.00	0.00	0.00	0.00	0.00	0.00	0.00	0.00	0.55
3	0.10	0.00	0.00	0.45	0.09	0.22	0.00	0.00	0.00	0.00	0.00	0.05
4	0.26	0.00	0.00	0.00	0.00	0.00	2.16	0.00	0.00	0.00	0.00	0.57
5	0.00	0.00	0.00	0.57	0.09	0.00	1.46	0.00	0.00	0.00	0.00	0.11
6	0.28	0.00	0.00	0.00	0.03	0.00	0.98	0.02	1.69	0.95	0.00	0.00
7	0.03	0.00	0.00	0.00	0.00	0.00	0.00	0.00	0.00	0.10	0.00	0.00
8	0.00	0.00	0.00	0.00	0.00	1.25	0.00	0.00	0.00	0.15	0.00	0.00
9	0.16	0.00	0.00	0.64	0.00	0.43	0.00	0.00	0.00	0.00	1.19	0.00
10	2.79	0.00	0.00	0.08	0.00	1.53	1.51	0.00	0.12	0.00	0.06	0.00
11	0.02	0.00	0.65	0.00	0.00	0.04	0.83	0.00	0.00	0.00	1.50	0.00
12	0.73	0.00	0.25	0.00	0.12	0.00	0.28	0.24	0.00	0.00	0.09	0.00
13	0.20	0.00	0.26	0.00	0.08	1.17	0.51	0.06	0.00	0.00	0.00	0.00
14	0.00	0.00	0.00	0.00	2.08	0.00	0.00	0.10	0.00	0.00	0.00	0.00
15	0.00	0.00	0.00	0.17	0.45	0.00	0.00	0.00	0.00	0.00	0.00	0.17
16	0.00	0.00	0.00	0.00	0.00	0.00	0.00	0.00	0.00	0.11	0.13	0.00
17	0.00	0.00	0.34	0.00	0.26	0.00	0.00	0.00	0.00	0.28	0.00	0.00
18	0.00	0.00	0.01	0.00	0.19	0.16	0.00	0.00	0.00	0.12	0.25	0.00
19	0.00	0.00	0.00	0.00	0.21	0.04	1.04	0.00	0.00	2.60	0.00	0.00
20	0.00	0.00	0.00	0.00	0.00	0.00	0.48	0.19	0.00	1.99	0.00	0.00
21	0.00	0.05	0.00	0.00	0.00	0.00	0.00	0.03	0.00	0.00	0.00	0.00
22	0.00	0.05	0.00	0.00	0.00	0.00	0.00	0.00	0.00	0.00	0.00	0.00
23	0.00	0.00	0.03	0.13	0.00	0.00	0.00	0.00	0.00	0.00	0.00	0.50
24	0.79	0.02	0.16	0.35	0.00	0.17	0.00	0.00	0.00	0.00	0.00	0.30
25	0.01	0.00	0.00	0.00	0.00	0.40	0.00	0.08	0.00	0.00	0.00	0.00
26	0.00	0.00	0.00	0.00	0.04	0.00	0.00	0.17	0.00	0.00	0.00	0.00
27	0.00	0.00	0.00	0.04	0.44	0.00	0.00	0.00	0.47	0.00	0.00	0.00
28	0.00	0.02	0.00	0.22	0.00	0.00	0.00	0.00	0.00	0.00	0.00	0.00
29	0.00	0.80	0.00	1.87	0.00	0.00	0.00	0.00	0.00	0.00	0.00	0.52
30	0.00		0.20	0.00	0.09	0.00	0.00	0.00	0.00	0.00	0.00	0.00
31	0.00		0.02		0.00		0.03	0.22		0.00		0.49
Total	5.9	1.1	1.9	4.5	4.2	5.4	9.3	1.1	2.4	6.3	3.2	3.3

Table 11.4. Monthly average temperatures for 1968 (typical year).

Month	Mean Temp (°F)
January	41.2
February	40.1
March	54.9
April	63.9
May	69.6
June	77.9
July	80.4
August	82.9
September	72.3
October	64.0
November	53.6
December	42.6

Table 11.5. Runoff computations for 1968.

Month / Day	Daily Precipitation, P (inches)	Q (inches)	Volume (ft^3)
January 10	2.79	0.38	2,370,161
April 29	1.87	0.09	543,063
May 14	2.08	0.14	863,889
June 8	1.25	0.00	16,937
June 10	1.53	0.03	169,539
June 13	1.17	0.00	2,226
July 4	2.16	0.16	1,002,498
July 5	1.46	0.02	117,360
July 10	1.51	0.02	153,718
September 6	1.69	0.05	321,428
October 19	2.60	0.31	1,909,865
October 20	1.99	0.12	718,562
November 9	1.19	0.00	4,628
November 11	1.50	0.02	146,079

Table 11.6. Estimated runoff for 1968 by month.

Month	Total Runoff Volume per Month (ft^3)
January	2,370,000
February	0
March	0
April	543,000
May	864,000
June	189,000
July	1,274,000
August	0
September	321,000
October	2,628,000
November	151,000
December	0

Step 6. Analyze outflows.

The designer estimates evapotranspiration using the Thornthwaite-Mather approach based on mean monthly temperature and latitude. Table 11.7 summarizes the ET computations using the monthly average temperatures for 1968. Volumetric ET outflows depend on the surface area of the wetland, which may also vary throughout the year.

The third column in Table 11.7, I_j, represents the monthly value of $[(T_j - 32)(5/9)]^{1.5}$. Summing the values in this column provides the solution to equation 11.5 and yields the monthly heat index, I:

$$I = \sum_{j=1}^{12} \left(\frac{(T_j - 32)(5/9)}{5} \right)^{1.5} = 79.8$$

Then, the designer computes the exponent in the Thornthwaite-Mather equation using equation 11.6:

$$a = 0.49 + 0.01791I - 0.0000771I^2 + 0.000000675I^3 = 1.77$$

Table 11.7. ET for 1968.

Month	Mean Temp, T_j (°F)	I_j	ET (in/month)	Correction Factor	Corrected ET (in/month)
January	41.2	1.03	0.29	0.84	0.24
February	40.1	0.85	0.23	0.91	0.21
March	54.9	4.05	1.43	1.00	1.43
April	63.9	6.66	2.58	1.08	2.79
May	69.6	8.55	3.46	1.16	4.02
June	77.9	11.52	4.93	1.20	5.91
July	80.4	12.48	5.42	1.19	6.45
August	82.9	13.47	5.93	1.13	6.70
September	72.3	9.48	3.92	1.03	4.03
October	64.0	6.72	2.61	0.95	2.48
November	53.6	3.72	1.30	0.87	1.13
December	42.6	1.28	0.37	0.82	0.30

The designer determines the surface water outflow based on a control structure designed to maintain a maximum depth of 3.28 ft. Therefore, all excess inflows stored at a depth greater than 3.28 ft will flow over the control structure as outflows. For short computational time steps, the designer may need to compute outflows using the weir equation as part of a storage routing procedure. However, in this case, the outflows are rapid compared to the monthly time step and the designer can safely assume that by the end of the month excess inflows will be released from the control structure.

Finally, groundwater outflow (infiltration) will be based on Darcy's equation with an infiltration rate of 3.15×10^{-6} in/s (0.69 ft/month).

Step 7. Characterize storage.

Figure 11.8 and Figure 11.9 illustrate the stage-storage and stage-area curves, respectively, based on the proposed grading at the site.

Step 8. Calculate water budget.

Table 11.8 summarizes the water budget over the entire year. The first row in the table establishes the starting conditions for the analysis. For this analysis, the designer estimates the starting conditions as the depth and total water volume stored in the wetland at the end of December 1967. The first column designates the month. The next two columns relate to the surface water inflows of direct runoff and base flow, estimated in volumetric terms.

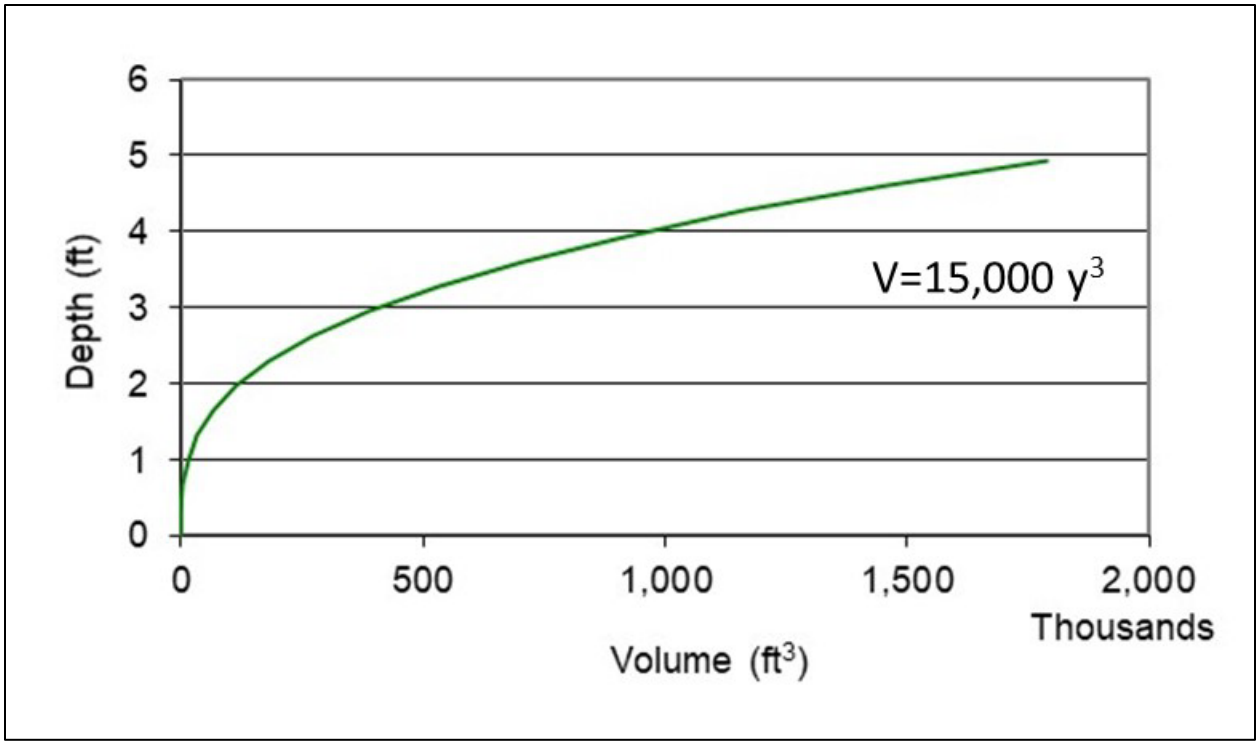

Figure 11.8. Stage-storage curve for proposed wetland.

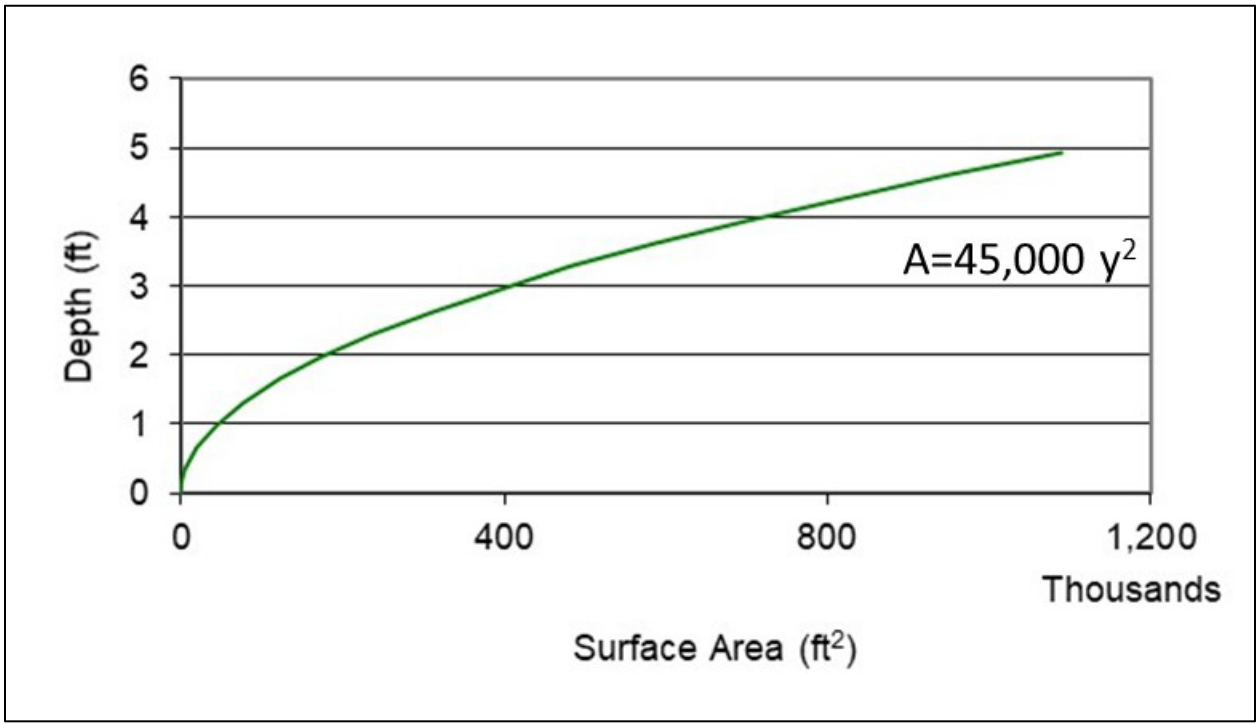

Figure 11.9. Stage-area curve for proposed wetland.

For example, in April 1968, the direct runoff of 543,000 ft^3 is combined with the 47,000 ft^3 of base flow. When added to the total volume in the wetland at the end of the prior month (168,000 ft^3) the interim volume estimate equals 758,000 ft^3. Inspection of the stage-storage curve reveals that the interim depth corresponding to this volume equals 3.69 ft after considering all inflows except direct precipitation. Deducting the outflows resulting from

potential evapotranspiration (PET) of 0.23 ft and infiltration of 0.69 ft and adding the direct precipitation of 0.377 ft yields a revised depth in the wetland of 3.15 ft. Since this is less than the 3.28 ft control depth, the month of April has no surface water outflow.

The designer contrasts the April result with the month of January, where the depth after outflows equals 5.41 ft. The designer then adjusts depth at the end of the month in January to 3.28 ft, with the difference attributed to surface water outflow.

Returning to the April computation, a depth of 3.15 ft has been determined for the end of the month. Consulting the stage-storage curve, the designer determines a volume of 468,000 ft^3 for the month-ending storage volume. The designer uses this value as the starting point for the calculations for the subsequent month.

Table 11.8. Monthly 1968 water budget.

Month	Runoff Volume (1000 ft^3)	Base Flow (1000 ft^3)	Total Volume (1000 ft^3)	Depth after inflows (ft)	PET (ft)	Infil-tration (ft)	Precip-itation (ft)	Depth after outflows (ft)	Depth at end of month (ft)	Total Volume (1000 ft^3)
Dec-67	n/a	n/a	n/a	n/a	n/a	n/a	n/a	n/a	2.62	271
Jan-68	2,370	47	2,688	5.63	0.02	0.69	0.495	5.41	3.28	530
Feb-68	0	47	577	3.37	0.02	0.69	0.095	2.76	2.76	315
Mar-68	0	47	362	2.89	0.12	0.69	0.160	2.24	2.24	168
Apr-68	543	47	758	3.69	0.23	0.69	0.377	3.15	3.15	468
May-68	864	47	1,379	4.51	0.33	0.69	0.348	3.83	3.28	530
Jun-68	189	47	766	3.71	0.49	0.69	0.451	2.97	2.97	395
Jul-68	1,274	47	1,716	4.85	0.54	0.69	0.773	4.39	3.28	530
Aug-68	0	47	577	3.37	0.56	0.69	0.093	2.22	2.22	163
Sep-68	321	47	531	3.28	0.34	0.69	0.200	2.45	2.45	222
Oct-68	2,628	47	2,897	5.77	0.21	0.69	0.525	5.40	3.28	530
Nov-68	151	47	728	3.64	0.09	0.69	0.268	3.13	3.13	459
Dec-68	0	47	506	3.23	0.03	0.69	0.272	2.78	2.78	324
Total	8,340	564	n/a	n/a	2.97	8.27	4.056	n/a	n/a	n/a

Figure 11.10 summarizes the maximum end of month depths. Note that the depth does not exceed 3.28 ft per the design criterion. Depending on the growing season, the wetland appears to have sufficient water available during the typical year.

Figure 11.11 uses the stage-area curve to display extent of inundation during each month. It shows that at the end of March and August the inundated surface area is a low of approximately 220,000 ft^2, while at the end of several other months the surface area more than doubles. Maximum surface area as determined by the control structure is 484,000 ft^2.

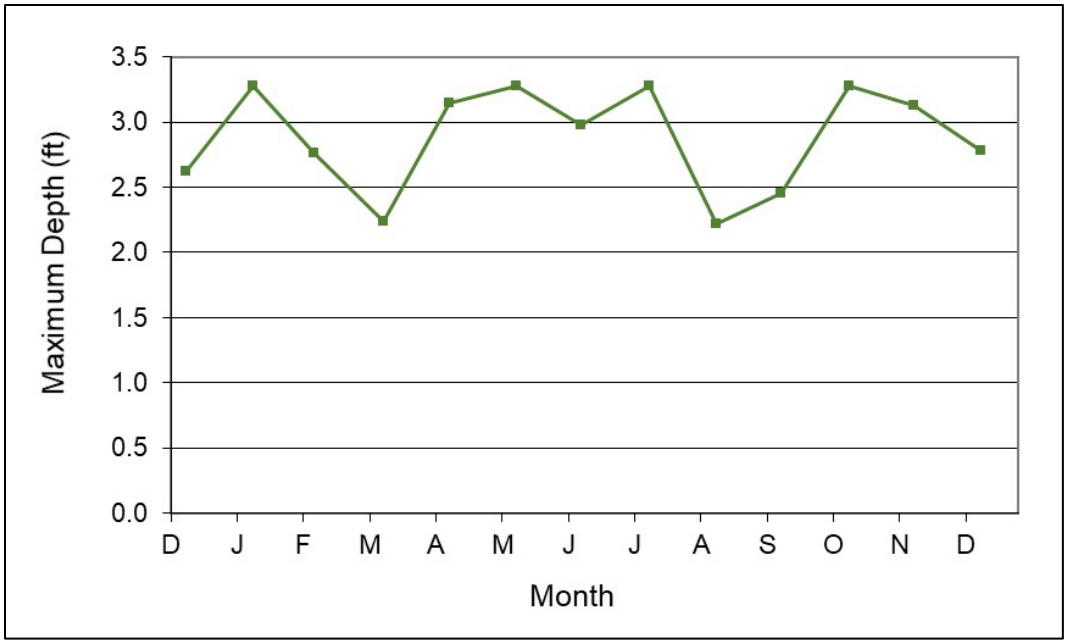

Figure 11.10. Monthly 1968 water budget.

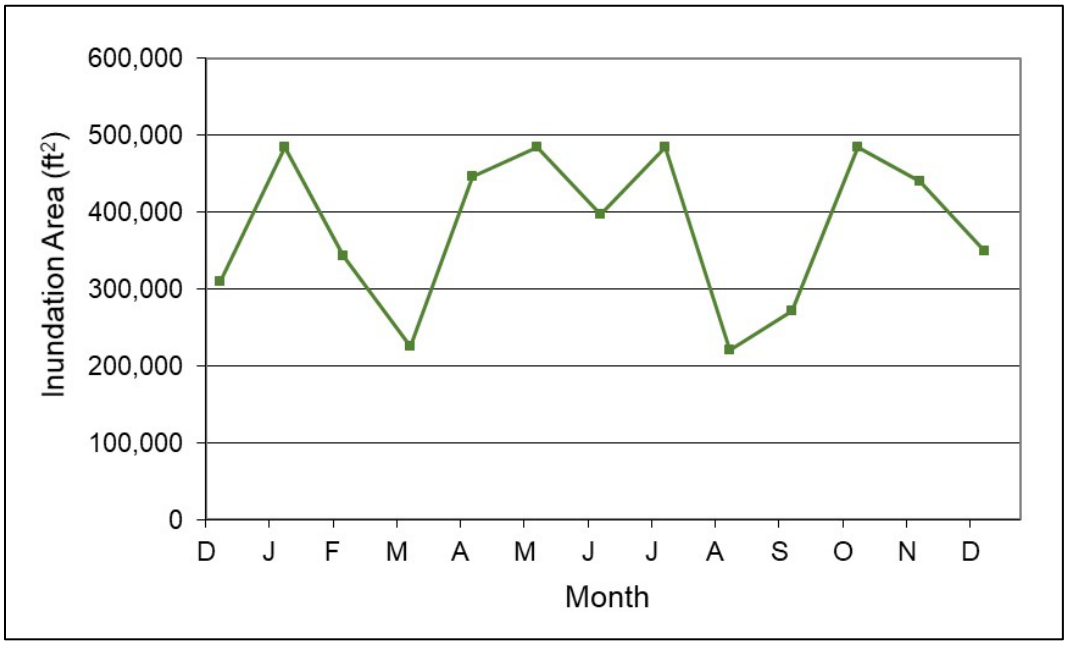

Figure 11.11. Inundation area for monthly 1968 water budget.

The designer next considers the sensitivity of these computations to the assumed starting conditions. In this case, January shows significant runoff inflows. Therefore, the designer expects the results will be insensitive to relatively wide fluctuations in starting conditions.

To determine if the design criteria have been satisfied, the designer interpolates the month-end depth values to estimate daily depth values. The designer then orders these daily values from highest to lowest and plots them as shown in Figure 11.12. From this depth-duration curve, the designer can determine what depths are being experienced over which durations. Reading off of the curve for a 90-day duration yields a maximum depth of 3.2 ft, meaning that the wetland has a depth of at least 3.2 ft at the control structure for 90 days.

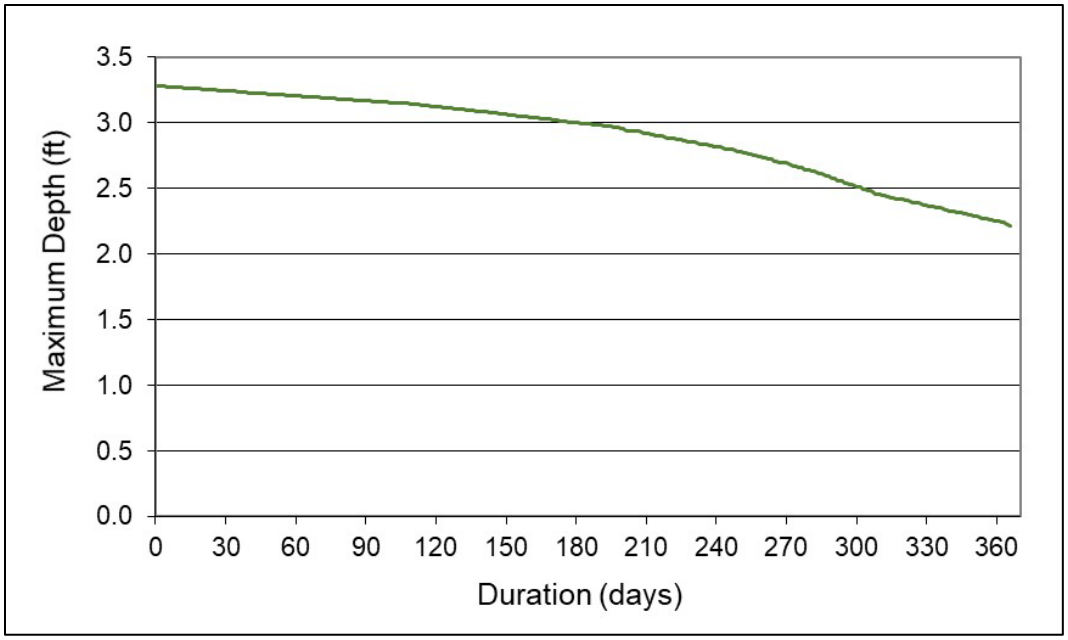

Figure 11.12. Depth-duration curve for 1968 monthly water budget.

The designer then translates the depth information to surface area to assess how much inundation occurs at certain depths throughout the wetland. Returning to the stage-area curve, the designer determines that at a maximum depth of 3.2 ft, a total area of 461,000 ft^2 or 10.6 acres is inundated for a duration of 90 days. These depths range from 0 to the maximum of 3.2 ft. Subtracting 1.64 ft from the 3.2 ft, the designer further determines that 110,000 ft^2 or 2.5 acres of area is inundated to a minimum depth of 1.64 ft with the remaining 8.1 acres inundated to depths between 0 and 1.64 ft. From this, the designer concludes that the minimum limits of 1.2 and 4.8 acres, respectively, are satisfied for the typical year.

However, the criterion is to provide sufficient water in 9 out of 10 years. The designer could identify the year within the period of record that best represents the 0.1 AEP year and perform a water budget computation for that year. Alternatively, the designer could perform water budget computations for all years and assess whether the requirements are met for 42 (90 percent) of the 47 years.

Solution:	The design criteria for inundation of the proposed vegetation were satisfied for the typical year (1968). Further analyses on other years would determine if the criteria are satisfied in 9 out of 10 years.

11.1.5 Sensitivity Analysis

Water budgets rely on many engineering judgments. Designers use sensitivity analyses to increase the chances of successful design by exploring how changes in assumptions have the potential to cause changes in design. Sensitivity analyses may also identify additional data useful for reducing uncertainty. In general, sensitivity analysis enables preparation of more robust water budgets on which to base design recommendations.

For example, if the designer initially assumes that base flow does not contribute significantly to the viability of a proposed wetland mitigation project, they may assume constant base flow. A sensitivity analysis could reduce base flow by 50 percent and increase it by 100 percent to confirm the assumption. If these changes do not alter the results in important ways, the analysis validates the reasonableness of the assumption. If, however, these scenarios result in changed

conclusions, the sensitivity indicates that more analysis and data pertaining to base flow could improve the water budget.

As described in Section 11.1.4, designers select a time step to use in preparing a water budget. Because the time step can influence the water budget, designers will consider performing a sensitivity analysis on the time step. In the example presented in the previous section, the water budget performed using a monthly time step indicated that the inundation areas suitable for submergents and emergents were 2.5 and 8.1 acres, respectively, in the typical year. Figure 11.13 shows that performing a water budget analysis on the same year using a daily time step yields a somewhat different result.

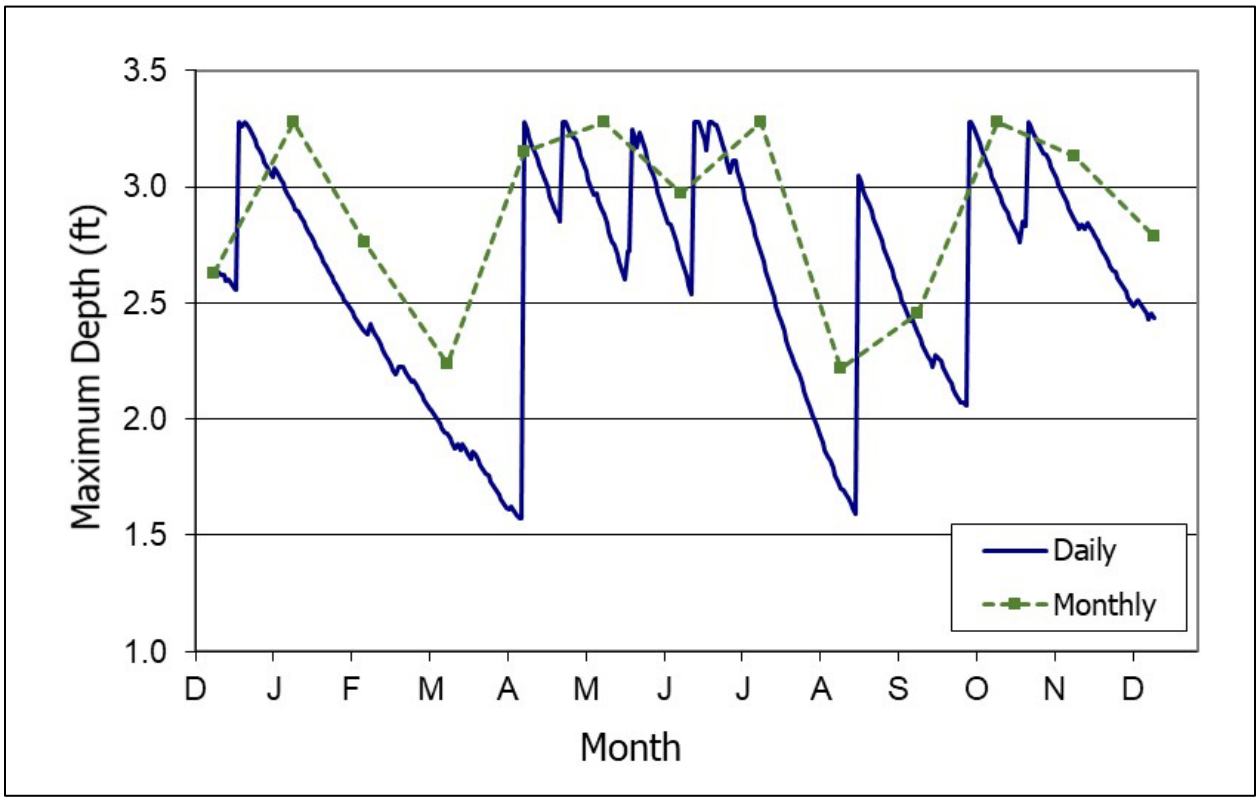

Figure 11.13. Example comparison of monthly and daily water budgets.

Creating an analogous depth-duration curve and applying the same procedures leads to the result that areas suitable for submergents and emergents are 2.0 and 7.7 acres, respectively. Based on this result, the monthly time step overestimated the available area compared with the daily time step. For the typical year, design criteria are still attained, but this may not be the case in drier years. When data are available to support the analysis, designers prefer a daily time step to a monthly time step.

11.2 Snowmelt

Snow plays an important role in annual streamflow variation in regions where it is a substantial part of the hydrologic cycle. It can cause flood damage to roads or contribute to flood hydrographs. Snowmelt experiences the same losses as rainfall, mainly infiltration. If rainfall also occurs, hydrologists combine excess rainfall with excess snowmelt to estimate the combined runoff. Hydrologists then use the runoff estimate with other hydrologic methods to generate runoff hydrographs.

The density of newly fallen snow and snowpacks can vary greatly. The snow water equivalent (SWE) is the depth of water obtained by melting the snow from a given snow event and engineers usually express it in units of an equivalent depth of water. New snow typically has a density (water content) of about 10 percent, which is equivalent to a SWE of 1 inch for a 10-inch snowfall, but it may vary from 5 percent to 25 percent. Density represents the percentage of snow volume that would be occupied by its water equivalent. The density of fallen snow generally increases over time and typically has the greatest density, e.g., 60 percent, just before the snowmelt season begins.

11.2.1 Snowmelt Runoff

The snowpack begins to melt when the temperature of the air above the snowpack exceeds freezing. Melting begins at the surface with the melt water infiltrating the snowpack. At first, the melted water only moves slightly below the surface, where it freezes again when it contacts the colder snow lying beneath. The snowpack heats slowly from energy released when melted water refreezes. Heat also comes from the overlying air and from the underlying ground. The melt water continues to infiltrate the snowpack more deeply as the temperature of the snowpack rises. Capillary films hold the water on the snow or ice crystals until the snowpack reaches its liquid water holding capacity. Hydrologists refer to the snow at this point as **ripe** and any further melting will result in runoff.

Latent Heat

Latent heat is the amount of energy needed to change the phase of a compound, such as water, with no change in temperature or pressure. Snowmelt is affected by these energy transfers. Conversion of water to ice releases energy in amounts based on the latent heat of fusion of water and the conversion of water to vapor captures energy based on the latent heat of vaporization of water.

Snowmelt occurs from the net energy (the algebraic sum) of many components of energy flux that add and subtract energy from the snowpack:

$$E_m = E_{sn} + E_{ln} + E_h + E_e + E_p + E_g + \Delta E_i \qquad (11.7)$$

where:

E_m	=	Energy available for snowmelt
E_{sn}	=	Energy from net shortwave (solar) radiation
E_{ln}	=	Energy from net longwave radiation
E_h	=	Energy from convective heat exchange
E_e	=	Energy from latent heat of condensation
E_p	=	Energy from heat convected by precipitation
E_g	=	Energy from heat conducted by ground
ΔE_i	=	Change in internal energy storage (cold content)

Melt begins when the cold content of the snowpack (also referred to as the heat deficit) reduces to zero. Cold content describes the amount of energy required to raise the temperature of the snowpack to 32 °F.

Hydrologists take two approaches to estimating snowmelt using the energy budget method. The first computes each of the contributing energy components, uses those to compute the net energy available for snowmelt, and then uses the resulting net energy to compute snowmelt. The USACE uses the second approach, which computes each component of snowmelt attributable to the

components of energy flux and then sums the resulting snowmelt to compute net snowmelt. The present chapter uses the latter approach.

The equations presented in the following discussion generally follow those used in *Runoff from Snowmelt* (USACE 1998) and *Snowmelt* (NRCS 2004c). They describe the snowmelt process for methods used by USACE and are included in HEC-1 (USACE 1990). HEC-HMS (Version 4.8) (USACE 2020) partially implements these equations but does not yet include the energy budget method. The USACE indicates they are developing an energy budget module for HEC-HMS.

Radiation, air convection, vapor condensation, warm rain (advection), and ground conduction cause snowmelt. Radiation, air convection, and vapor condensation usually represent the most important variables. Rainfall sometimes significantly affects peak flows. Ground conduction usually has a negligible effect.

11.2.1.1 Shortwave Radiation Snowmelt

Snowmelt from incident solar (shortwave) radiation converts the snowpack to water based on the daily snowmelt runoff rate estimated as:

$$M_{sw} = \frac{(1-A)E_i}{L\rho_w B} \tag{11.8}$$

where:

M_{sw} = Shortwave snowmelt, m/day
A = Albedo, dimensionless
E_i = Daily incident solar (shortwave) radiation, kJ/m^2 day
L = Latent heat of fusion for ice, 334.9 kJ/kg
ρ_w = Density of water, 1000 kg/m^3
B = Thermal quality of snow, dimensionless

Albedo describes the reflectivity of shortwave radiation of a snowpack. The albedo for snowpack ranges from about 40 percent for melting late-season snow to 80 percent to 90 percent for freshly fallen snow.

Thermal quality of snow relates to the water content in the snowpack. Hydrologists quantify it as the ratio of the weight of ice to the total weight of a snowpack sample, or alternatively, the ratio of heat required to melt a unit mass of snow to that of ice at 32 °F. Typically, thermal quality is about 0.95, but during periods of rapid melt, it may drop to 0.7 or less. A fully ripe snowpack normally contains about 3 percent to 5 percent liquid water, so the thermal quality of the snowpack would range from 0.95 to 0.97.

Adapting the previous equation for incident solar radiation in Langleys (ly) (1 ly = 41.9 kJ/m^2) leads to shortwave radiation daily snowmelt given by:

$$M_{sw} = \frac{0.00493(1-A)E_i}{B} \tag{11.9}$$

where:

M_{sw} = Shortwave snowmelt, in/day
A = Albedo, dimensionless
E_i = Daily incident solar (shortwave) radiation, ly/day
B = Thermal quality of snow, dimensionless

The intensity of solar radiation (shortwave radiation) at the edge of the Earth's atmosphere and normal to the path of radiation is a nearly constant 1.94 ly/min (1.35 kJ/m^2/s). Cloudiness, latitude, season of the year, time of day, topography, snow cover, and vegetative cover affect the amount of solar radiation that reaches the ground. Figure 11.14 supplies an estimate of the solar radiation according to season and latitude.

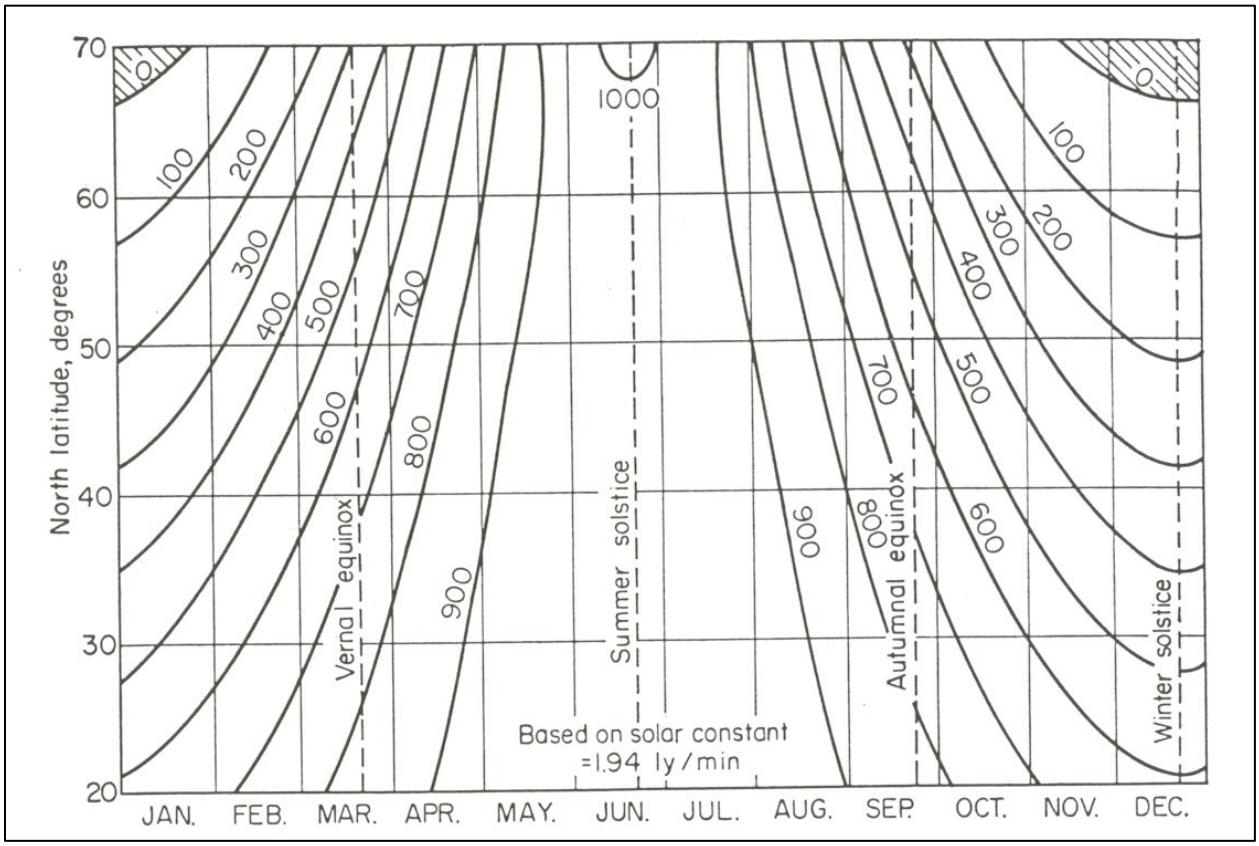

Figure 11.14. Seasonal and latitudinal variation of daily solar radiation (langleys).

11.2.1.2 Longwave Radiation Snowmelt

A portion of the net shortwave radiation might become longwave radiation. The snowpack loses longwave radiation to the atmosphere. If the atmosphere is clear, then much of the snowpack longwave radiation escapes and is lost. If the skies are cloudy or if there is a forest canopy, much of the snowpack longwave radiation reflects back to the snowpack.

Hydrologists estimate the snowpack longwave radiation loss using the Stefan-Boltzmann law for a blackbody. A blackbody is a tool physicists use for computations of energy absorption and radiation. It absorbs all radiation incident to it and emits radiation according to the Stefan-Boltzmann law.

$$E_l = \varepsilon \sigma T_s^4 \qquad (11.10)$$

where:

E_l = Longwave radiation, ly/day
ε = 0.99 for clean snow
σ = Stefan-Boltzman constant, 8.26×10^{-10} ly/(min K^4)
T_s = Snow surface temperature, K

This equation applies to longwave radiation emitted to the atmosphere from the snowpack, not net longwave radiation. It does not account for the radiation reflected back to the snowpack by clouds or forest canopy. Because back reflection longwave radiation is a complex phenomenon, USACE developed an equation for clear-sky new longwave radiation, which gives the longwave radiation melt:

$$M_l = 0.0212(T_s - 32) - 0.84 \quad (11.11)$$

where:

M_l	=	Clear-sky longwave radiation melt, in/day
T_s	=	Snow surface temperature, °F

Similarly, for melt under a cloudy sky or forest canopy, the longwave radiation melt is:

$$M_l = 0.029(T_s - 32) \quad (11.12)$$

where:

M_l	=	Clear-sky longwave radiation melt, in/day
T_s	=	Snow surface temperature, °F

Figure 11.15 and Figure 11.16 present daily snowmelt from shortwave radiation and net longwave radiation for spring and winter, respectively. The USACE created these figures based on the following relations for shortwave and reflected longwave radiation.

$$M_r = M_{rs} + M_{rl} \quad (11.13)$$

$$M_{rs} = m_s\left[1 - (0.82 - 0.024Z)N\right] \quad (11.14)$$

$$M_{rl} = m_l\left[1 - (1.0 - 0.024Z)N\right] \quad (11.15)$$

where:

M_r	=	Net radiation melt, in/day
M_{rs}	=	Shortwave radiation melt, in/day
M_{rl}	=	Longwave radiation (reflected) melt, in/day
m_s	=	Coefficient for time of year for shortwave radiation (2.0 for May 20 and 0.5 for February 15)
m_{ls}	=	Coefficient for time of year for longwave radiation (-0.41 for May 20 and -0.84 for February 15)
N	=	Amount of clouds
Z	=	Cloud height (1000s of feet)

The figures show that total radiation melt is greater in the spring than in the winter. Spring radiation melt decreases with increasing cloud cover and decreasing cloud height, but winter radiation melt increases with increasing cloud cover and decreasing cloud height. Longwave radiation has a more dominant role in the winter than spring.

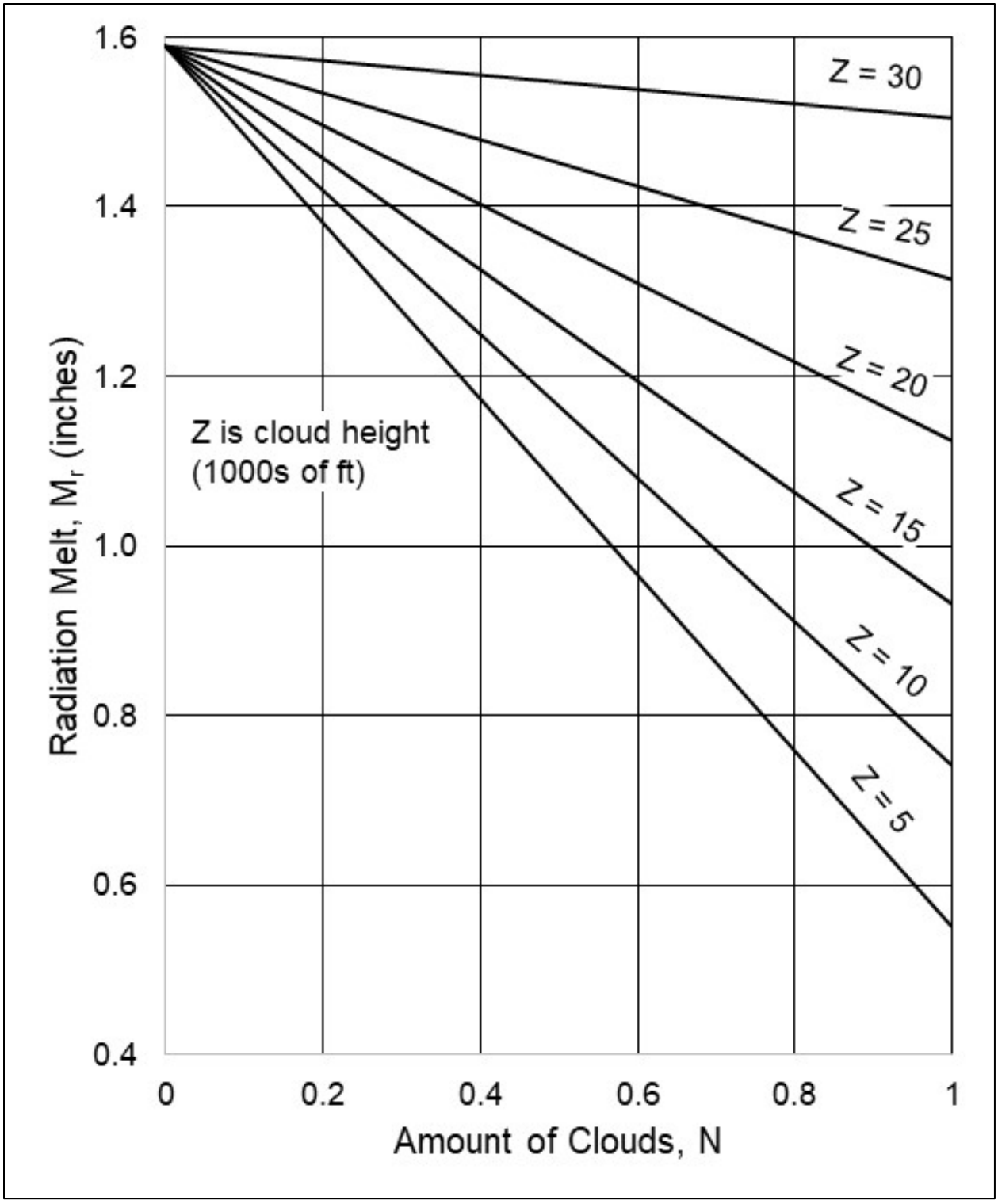

Figure 11.15. Daily snowmelt from shortwave radiation and net longwave radiation in the open with cloudy skies during spring (May 20) (USACE 1956).

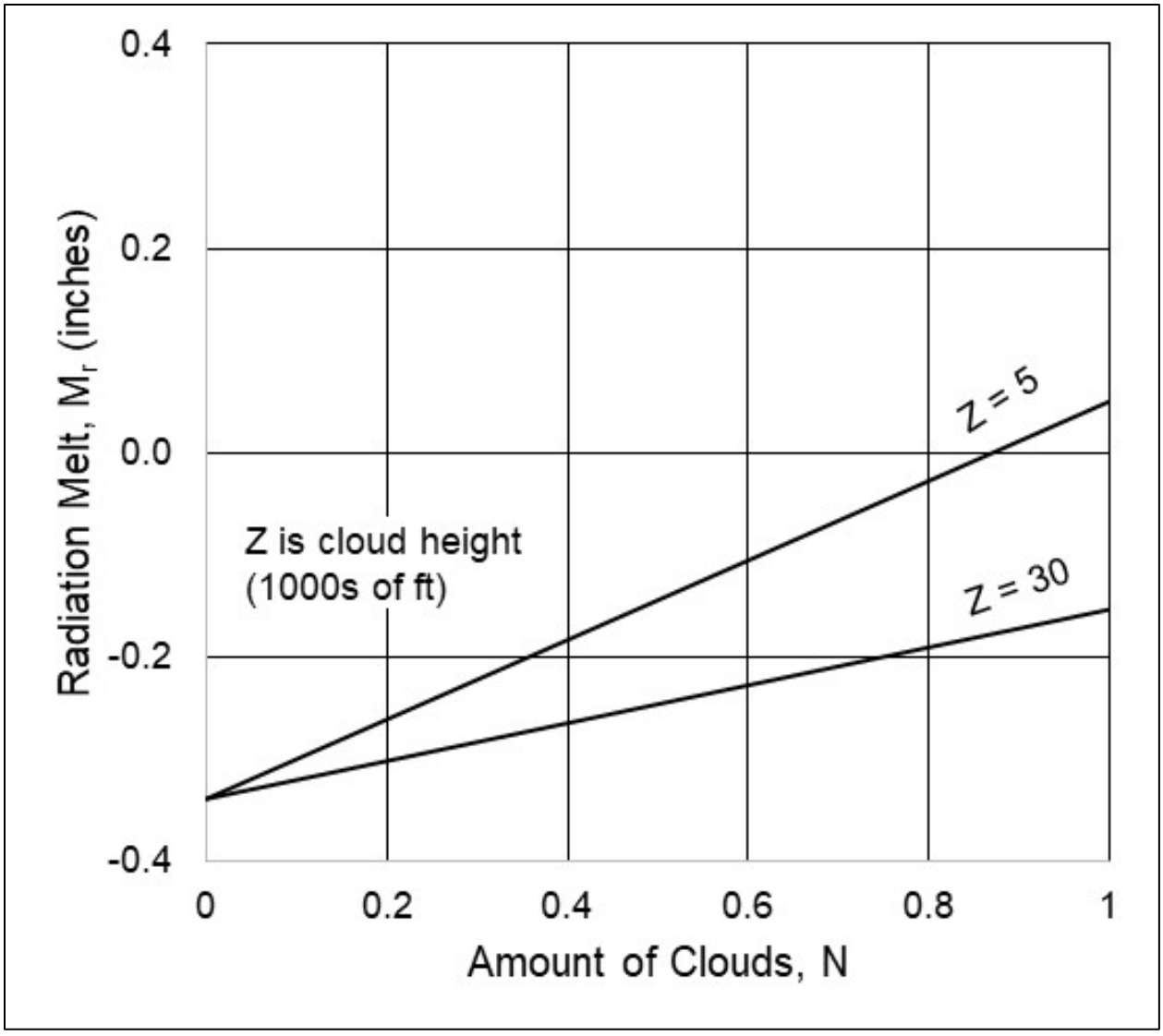

Figure 11.16. Daily snowmelt from shortwave radiation and net longwave radiation in the open with cloudy skies during winter (February 15) (USACE 1956).

11.2.1.3 Air Convection Snowmelt

Convection transfers sensible heat from the overlying air to the snowpack. The amount of snowmelt depends on wind velocity, air temperature, and the bulk heat transfer coefficient. Researchers determine the latter experimentally. As a result, the USACE conducted studies to define the bulk heat transfer coefficient. The USACE incorporated the result into the air convection heat transfer equation, with the air convection snowmelt given by:

$$M_h = 0.00179\, u_z \left(T_a - 32\right) \tag{11.16}$$

where:

M_h = Air convection snowmelt, in/day
u_z = Wind speed above snow surface, ft/s
T_a = Air temperature, °F

11.2.1.4 Vapor Condensation (Latent Heat) Snowmelt

When warmer, moisture-laden water contacts a cooler snow surface by turbulent mixing in the atmosphere, the water vapor condenses to the liquid phase on the snowpack and releases heat energy. The heat released by the water vapor is a function of atmospheric vapor pressure, vapor pressure at the snow surface, wind speed, and a bulk latent heat transfer coefficient. Similarly, to other bulk heat transfer coefficients, researchers determine the bulk latent heat transfer coefficient experimentally. The USACE studies resulted in a condensation snowmelt equation given by:

$$M_e = 0.0065 u_z (T_d - 32) \quad (11.17)$$

where:

M_e = Vapor condensation snowmelt, in/day
u_z = Wind speed above snow surface, ft/s
T_d = Dew point temperature, °F

The dew point temperature must exceed 32 °F (0 °C) for condensation melt to occur, and if the dew point temperature drops below 32 °F (0 °C), evaporation occurs at the snow surface.

11.2.1.5 Warm Rain (Advection) Snowmelt

If the temperature of the rainfall is close to freezing, the amount of energy supplied to the snowpack is small. But if the raindrop temperature is substantially greater than freezing, then raindrops are a significant heat source. Hydrologists generally assume falling raindrops are at air temperature. The USACE equation for warm rain snowmelt is:

$$M_p = 0.007 P_r (T_r - 32) \quad (11.18)$$

where:

M_p = Warm rain snowmelt, in/day
P_r = Daily rainfall, inches
T_r = Rain temperature, °F

11.2.2 Snowmelt Modeling

As described in the previous section, hydrologists estimate snowmelt processes using complex relationships with data that are generally unavailable or difficult to collect. Hydrologists developed approximations for these processes using variables that are generally easier to obtain. As with any model, hydrologists verify or validate any snowmelt analysis by comparing the results of the model with observed runoff rates whenever possible.

11.2.2.1 Energy Budget Method

The energy budget method simplifies the theoretical relationships previously discussed. The USACE developed approximations of these complex relationships using regression analyses, linearizing the equations, and using representative and easily obtained parameter values (USACE 1998). The USACE separately addressed two general conditions: rain-on-snow events and rain-free snowmelt events. Two of these equations will be presented here, those included in the USACE hydrologic model HEC-1. For the full range of equations and for a full discussion of their development see USACE (1998).

11.2.2.1.1 Rain-on-Snow Snowmelt

The USACE developed two equations to estimate snowmelt when rain is a contributing factor. Each equation applies to a different extent of forested canopy. For rain-on-snow, HEC-1 (USACE 1990) uses:

$$M = C\left[\left(0.029 + 0.00504v + 0.007P_r\right)\left(T_a - T_f\right) + 0.09\right] \quad (11.19)$$

where:

M	=	Snowmelt runoff depth, in/day
C	=	Coefficient (1 in most cases)
v	=	Wind speed 50 feet above snow, mi/h
P_r	=	Rainfall, in/day
T_a	=	Air temperature, °F
T_f	=	Temperature at which melt occurs (usually assumed to be 32 °F), °F

This equation applies to conditions where the percent of forest canopy ranges from 10 percent to 80 percent. For forest canopy conditions outside this range, the engineer may want to consider using other equations provided by the USACE (1998).

Engineers use the coefficient, C, to calibrate model results to existing data or to account for conditions that slightly differ from those assumed to develop this model. The first term in the equation accounts for net longwave radiation. The second term combines the effect of convection and condensation on snowmelt, and the third term accounts for the energy contributed by rain. The fourth and final term (a constant) accounts for shortwave radiation and ground melt. Since these equations apply to rainy days, they assume a full cloud cover.

During a rain event, convection and condensation represent the primary mechanisms for introducing heat to the snowpack causing snowmelt. This condition assumes a full cloud cover, and, therefore, slight solar radiation.

11.2.2.1.2 Rain-Free Snowmelt

The USACE (1998) developed four equations to estimate snowmelt when rain is not a contributing factor. The USACE based these equations on regression analyses with different values of percentage forest canopy. Snowmelt based on a forest canopy of 50 percent and valid for a range of 10 percent to 60 percent as used in HEC-1 (USACE 1998, NRCS 2004c) is estimated from:

$$M = C\left[0.002\, I_i\left(1 - A\right) + 0.0145\left(T_a - T_f\right) + 0.0011\, v\left(T_a - T_f\right) + 0.0039\, v\left(T_d - T_f\right)\right] \quad (11.20)$$

where:

M	=	Snowmelt runoff depth, in/day
C	=	Coefficient (1 in most cases)
v	=	Wind speed 50 feet above snow, mi/h
I_i	=	Solar radiation, ly/day
A	=	Albedo, dimensionless
T_a	=	Air temperature, °F
T_f	=	Temperature at which melt occurs (usually assumed to be 32 °F), °F
T_d	=	Dew point temperature, °F

During rain-free periods, shortwave and longwave radiation become significant, and convection and condensation are less critical. The first and second equation terms account for shortwave

radiation and longwave radiation, respectively. The third and fourth terms represent the effect of convection and condensation. The HEC-1 program uses wind speed, solar radiation, and temperature data as inputs. The current version of HEC-HMS (Version 4.10) does not include a snowmelt energy budget module.

HEC-1 calculates albedo internally. Its value reflects the number of days since the last snowfall and varies from an initial value of 0.75 to a minimum value of 0.4. The program also automatically decreases the dew point temperature with elevation at a rate of 0.2 times the temperature lapse rate.

11.2.2.2 Degree-Day Method

The degree-day method further simplifies the relationship between snowmelt and the factors affecting it by developing a correlation analysis between temperature and snowmelt. The factors affecting snowmelt either directly relate to temperature or have some degree of correlation to temperature. The atmospheric temperature reflects the extent of radiation and the air's vapor pressure, and it is sensitive to wind. In addition, air temperature is frequently the only meteorological data available.

HEC-HMS Implementation

HEC-HMS (USACE 2020) contains two methods for estimating snowmelt both based on the degree-day method, which the USACE calls the Temperature Index method. Both methods use a melt parameter and the difference between the air temperature and a reference temperature (usually freezing). A more complex application is a gridded approach, which involves more data than the lumped approach but is still based on the degree-day. HEC-HMS does not yet include the energy budget method.

A degree-day indicates the amount of heat present to create snowmelt and is defined as the deviation of the average daily temperature of 1 degree from a given datum temperature over a 24-hour period. The datum temperature for snowmelt calculations is normally 32 °F (0 °C). For example, if the average daily temperature is 5 °C, the day would have 5 degree-days above freezing. The average daily temperature is sometimes taken as the average of the daily high and low temperatures.

The degree-day method correlates temperature and the number of degree-days to snowmelt. A melt-rate coefficient links degree-days and snowmelt:

$$M = C_m \left(T_a - T_f \right) \tag{11.21}$$

where:

M	=	Snowmelt runoff depth, in/day (mm/day)
C_m	=	Melt coefficient, in/(day °F) (mm/(day °C))
T_a	=	Air temperature, °F (°C)
T_f	=	Temperature at which melt occurs (usually assumed to be 32 °F (0 °C))

The degree-day is generally valid for heavily forested areas where solar radiation and wind are less important in estimating snowmelt. Researchers report melt coefficients in the range of 0.06 to 0.09 in/°F/day (Horton 1945), 0.02 to 0.039 in/°F/day for forested areas (USACE 1956), and 0.05 to 0.10 in/°F/day (Linsley et al. 1982). Another source for estimates of the melt coefficient is the *Snowmelt Runoff Model* (Martinec et al. 2008). Modelers may use higher values of the melt coefficient for time periods with high wind or high humidity.

Example 11.2:	Snowmelt calculations.
Objective:	Estimate the watershed snowmelt for the day using the degree-day method.

Given: The data in Table 11.9.

Table 11.9. Snowmelt data for example.

Parameter	Value
Air temperature	39 °F
Melt temperature	32 °F
Melt coefficient	0.08 in/day

Step 1. Use Equation 11.12 to compute the snowmelt.

$$M = C_m\left(T_a - T_f\right) = 0.08\left(39 - 32\right) = 0.56 \text{ in / day}$$

Solution: The estimated snowmelt is 0.56 in/day.

11.2.2.3 Temperature Variation with Altitude

Air temperature generally decreases with elevation, all other factors being constant. Modelers usually assume this temperature lapse rate to be 3.3 °F per 1,000 ft. Because many snowmelt processes are temperature dependent, modelers assessing watersheds with significant relief often divide the watershed into elevation zones. The change in elevation used to define these zones usually ranges from 650 to 1300 ft. The snowmelt model in HEC-HMS can compute variable melting with altitude by providing the temperature at the bottom of the lowest elevation zone, the temperature lapse rate, and a specification of the altitude zones. The model estimates snowmelt for each elevation zone and calculates an area-weighted average snowmelt for the entire watershed.

Example 11.3:	Snowmelt computations with multiple elevation zones.
Objective:	Compute the watershed average snowmelt for a 24-hour event using the degree-day method.

Given: The data in Table 11.10.

Table 11.10. Snowmelt zone data for example.

Parameter	Zone 1	Zone 2
Drainage area	220 ac	100 ac
Air temperature	39 °F	37 °F
Melt temperature	32 °F	32 °F
Melt coefficient	0.08 in/day	0.08 in/day

Step 1. Compute snowmelt rates for each zone.

Zone 1:

$$M = C_m\left(T_a - T_f\right) = 0.08\left(39 - 32\right) = 0.56 \text{ in / day}$$

Zone 2:

$$M = C_m\left(T_a - T_f\right) = 0.08\left(37 - 32\right) = 0.40 \text{ in / day}$$

Step 2. Compute the area-weighted melt for each zone.

The total drainage area of the watershed is 320 acres. The fraction of the watershed in zone 1 is 0.69 (220/320) and the fraction in zone 2 is 0.31 (100/320). Therefore, the weighted melt for each zone is:

$$M_1 = \left(0.56 \text{ inches}\right)\left(0.69\right) = 0.39 \text{ in / day}$$

$$M_2 = \left(0.40 \text{ inches}\right)\left(0.31\right) = 0.12 \text{ in / day}$$

Step 3. Add the two weighted melts to compute the area-weighted snowmelt for the event.

$$M = 0.39 + 0.12 = 0.51 \text{ in / day}$$

Solution: The area-weighted snowmelt for the watershed using the degree-day method is 0.51 in/day.

Computation of snowmelt using the energy budget method follows the same pattern, although the computation requires additional variables and parameters. Energy budget snowmelt solutions are computed using software.

For watersheds that either experience flooding from snowmelt or rain-on-snow events or both, engineers use daily snowmelt volumes to generate hydrographs. With rain-on-snow events, the hydrographs include both the snowmelt and rainfall volumes.

11.3 Arid Lands

Scientists classify many parts of the Western United States as arid or semiarid. They base the classification, in part, on the magnitude of rainfall. Additional factors in classification include vegetation and soils. Generally speaking, arid lands have inadequate natural rainfall to support crop growth. Semiarid lands have rainfall only sufficient to support short-season crops.

Engineering hydrology characterizes arid and semiarid lands as having little rainfall, which, when it does occur, usually has high intensity with rapidly responding runoff. Flash flooding is a major concern in such areas. These events may also produce large amounts of sediment. This section describes hydrologic analyses unique to arid and semi-arid environments. These analyses include gaged flow analysis of records with zero flows; regression equations for arid regions; and methods for estimating transmission losses, assessing alluvial fans, and estimating bulked flow.

Arid and semiarid areas typically do not have hydrologic data, at least in significant quantities. Where gages exist, their records typically have years with little, infrequent, or no rainfall and, thus, no significant flooding. In other years, intense rainfalls of short duration produce high peak flows relative to the total volume of runoff. These factors make it comparatively difficult to provide estimates of flood magnitudes or probabilities.

Many arid locations also have alluvial fans. This section provides an overview of alluvial fans and their relevance for highway design.

11.3.1 Gaged Flow Analysis of Records with Zero Flows

Annual floods in arid regions often closely follow a log-normal or extreme value distribution. Log-Pearson type III curve fitting techniques also apply, provided that the annual series of peaks has non-zero values. However, arid regions commonly have annual maximum flood records that

include values of zero. Thus, development of a frequency curve based on logarithms, such as the log-Pearson type III, involves adaptation since the logarithm of zero is minus infinity. In such cases, Bulletin 17C (England et al. 2019) provides a method, termed the Multiple Grubbs-Beck Test (MGBT), for computing a frequency curve that correctly evaluates zero-flood years and identifies potentially influential low floods (PILFs). Bulletin 17C (sections 5.1.3.2 and 5.1.3.3) discusses this treatment of zero flows in more detail. The suggested procedure when analyzing records that include zero-flood years consists of five steps, as described below.

Step 1. Compute the moments.

Separate the record into two parts: all non-zero floods and zero floods. Compute the mean, standard deviation, and skew for the non-zero floods using the equations from Section 5.1.5.

Step 2. Check for outliers.

Section 5.1.3.2 discusses the test for outliers from Bulletin 17C (England et al. 2019). While low outliers occur more often than high outliers in flood records from arid regions, test for both. Bulletin 17C (Section 5.1.3.2) discusses the generalized low-outlier procedure, which is based on the MGBT approach.

Step 3. Compute the frequency curve for non-zero flows.

Use the moments of the logarithms from step 1, or from step 2 if outliers were identified, to compute the frequency curve. For this step, use station skew rather than weighted skew. For selected exceedance probabilities, obtain values of the log-Pearson type III deviates (K) from Table 5.15 for the station skew. Then, use the deviates with the log mean ($\overline{Y}$) and log standard deviation (S_y) to compute the logarithm of the discharge:

$$Y = \overline{Y} + KS_y \tag{11.22}$$

Step 4. Compute frequency curve using EMA.

Using the Expected Moments Algorithm (EMA), as prescribed in Bulletin 17C, adjust the frequency curve to correct for zero flows and outliers. Because of the complexity of the EMA, engineers use software, to develop a frequency curve that takes zero flows and outliers into account, as discussed in Section 5.1.3. Commonly applied software includes the USGS PeakFQ (Flynn et al. 2006) and the USACE HEC-SSP (Bartles et al. 2019) programs.

Step 5. Use frequency curve to make estimates.

The first four steps resulted in a frequency curve. Assess the goodness of fit by comparing the frequency curve to the measured data. Plot the frequency curve on log-probability scales using the Y values and the exceedance probabilities, P_e, to obtain the corresponding values of K. Plot the data points using a plotting position formula such as the Cunnane or Weibull.

Then, use the statistics to compute the frequency curve:

$$Q = 10^{\overline{Y}+KS_y} \tag{11.23}$$

When verifying the frequency curve, base the plotting positions for the frequency curve on either the total number of years of record or the historic record length, H, if using the historic adjustment.

Example 11.4: Frequency curves for a gaged site.

Objective: Develop unadjusted and EMA frequency curves for a gaged site.

Table 11.11 contains the annual maximum discharge record (1932-1973) for Orestimba Creek near Newman, California (USGS station 11-2745). Bulletin 17C analyzes this record and includes years with no discharge or discharges below the threshold.

Step 1. Compute the moments.

Dropping the six zero values from the record gives $n = N_t - n_z = 36$. Compute the moments of the logarithms using the Bulletin 17C method:

$\overline{Y} = 3.08$

$S_y = 0.64$

$G_y = -0.84$

Round the skew to the nearest tenth, in this case -0.8.

Step 2. Check for outliers.

Use the Bulletin 17C procedure detailed in Section 5.1.3.2. The computed MGBT PILF threshold is 782 ft^3/s. Eighteen of the 42 records fall below the PILF threshold, so 24 records remain for the frequency analysis detailed in the following steps.

Step 3. Compute the frequency curve for non-zero flows.

Compute the frequency curve using the 36 non-zero values. Table 11.11 summarizes the frequency curve based on the moments from the non-zero flows from step 1. Column 3 of the table is computed as:

$$\log Q = \overline{Y} + KS_y = 3.08 + 0.64K$$

Step 4. Compute frequency curve using EMA.

Using the statistics for the censored series with n = 24, compute the EMA frequency curve using the Bulleting 17C prescribed adjustment. Obtain Log-Pearson III deviates from Table 5.15 for a skew of -1.117 (from PeakFQ) and selected exceedance probabilities. Table 11.13 presents the results of EMA frequency curve based on the station skew, i.e., without regional skew. Column 3 of the table is computed as:

$$\log Q = \overline{Y} + KS_y = 2.89 + 0.83K$$

Apply the EMA approach again but with the inclusion of both regional and station skews to develop the frequency curve tabulated in Table 11.14. The weighted skew, based on the Bulletin 17C methodology, is -0.349. Column 3 of the table is computed using PeakFQ as:

$$\log Q = \overline{Y} + KS_y = 3.00 + 0.64K$$

Table 11.11. Annual maximum flood series, Orestimba Creek, California.

Year	Flow (ft^3/s)	Log of Flow	Exceedance Plotting Probability
1932	4,260	3.629	0.222
1933	345	low outlier	
1934	516	low outlier	
1935	1,320	3.121	0.556
1936	1,200	3.079	0.611
1937	2,180	3.338	0.417
1938	3,230	3.509	0.333
1939	115	low outlier	
1940	3,440	3.537	0.306
1941	3,070	3.487	0.361
1942	1,880	3.274	0.444
1943	6,450	3.810	0.083
1944	1,290	3.111	0.583
1945	5,970	3.776	0.111
1946	782	2.893	0.667
1947	0	na	
1948	0	na	
1949	335	low outlier	
1950	175	low oulier	
1951	2,920	3.465	0.389
1952	3,660	3.563	0.278
1953	147	low outlier	
1954	0	na	
1955	16	low outlier	
1956	5,620	3.750	0.139
1957	1,440	3.158	0.528
1958	10,200	4.009	0.028
1959	5,380	3.731	0.167
1960	448	low outlier	
1961	0	na	

Table 11.11 (continued). Annual maximum flood series, Orestimba Creek, California.

Year	Flow (ft^3/s)	Log of Flow	Exceedance Plotting Probability
1962	1,740	3.241	0.472
1963	8,300	3.919	0.056
1964	156	low outlier	
1965	560	low outlier	
1966	128	low outlier	
1967	4,200	3.623	0.250
1968	0	na	
1969	5,080	3.706	0.194
1970	1,010	3.006	0.639
1971	584	low outlier	
1972	0	na	
1973	1,510	3.179	0.500

Table 11.12. Computation of the frequency curve.

(1) Exceedance Probability P_e	(2) log-Pearson Type III Deviate (K) for G = -0.840	(3) log Q	(4) Q (ft^3/s)
0.8	-0.775524	2.579	379
0.7	-0.406770	2.817	655
0.5	0.138422	3.168	1,472
0.2	0.855346	3.630	4,262
0.1	1.158292	3.825	6,681
0.04	1.431758	4.001	10,023
0.02	1.583168	4.099	12,547
0.01	1.703630	4.176	15,002
0.002	1.905812	4.306	20,250

Table 11.13. EMA frequency curve without regional skew.

(1) Exceedance Probability P_e	(2) log-Pearson Type III Deviate (K) for G = -1.117	(3) log Q	(4) Q (ft^3/s)
0.8	-0.74319	2.271	187
0.7	-0.36171	2.588	387
0.5	0.18231	3.040	1,096
0.2	0.84734	3.593	3,913
0.1	1.10366	3.806	6,390
0.04	1.31702	3.983	9,612
0.02	1.42577	4.073	11,835
0.01	1.50641	4.140	13,809
0.002	1.62726	4.241	17,402

Table 11.14. EMA frequency curve with regional skew.

(1) Exceedance Probability P_e	(2) log-Pearson Type III Deviate (K) for G = -0.349	(3) log Q	(4) Q (ft^3/s)
0.8	-0.82022	2.470	295
0.7	-0.47941	2.689	488
0.5	0.05789	3.034	1,082
0.2	0.85392	3.546	3,515
0.1	1.23843	3.793	6,210
0.04	1.62527	4.042	11,010
0.02	1.86272	4.194	15,647
0.01	2.06813	4.326	21,208
0.002	2.46077	4.579	37,926

Step 5. Use the frequency curve to make estimates.

Figure 11.17 is the graphical representation of the EMA frequency curve using a weighted skew coefficient. The plot shows the frequency curve fitted to the 24 gage data points and the confidence limits.

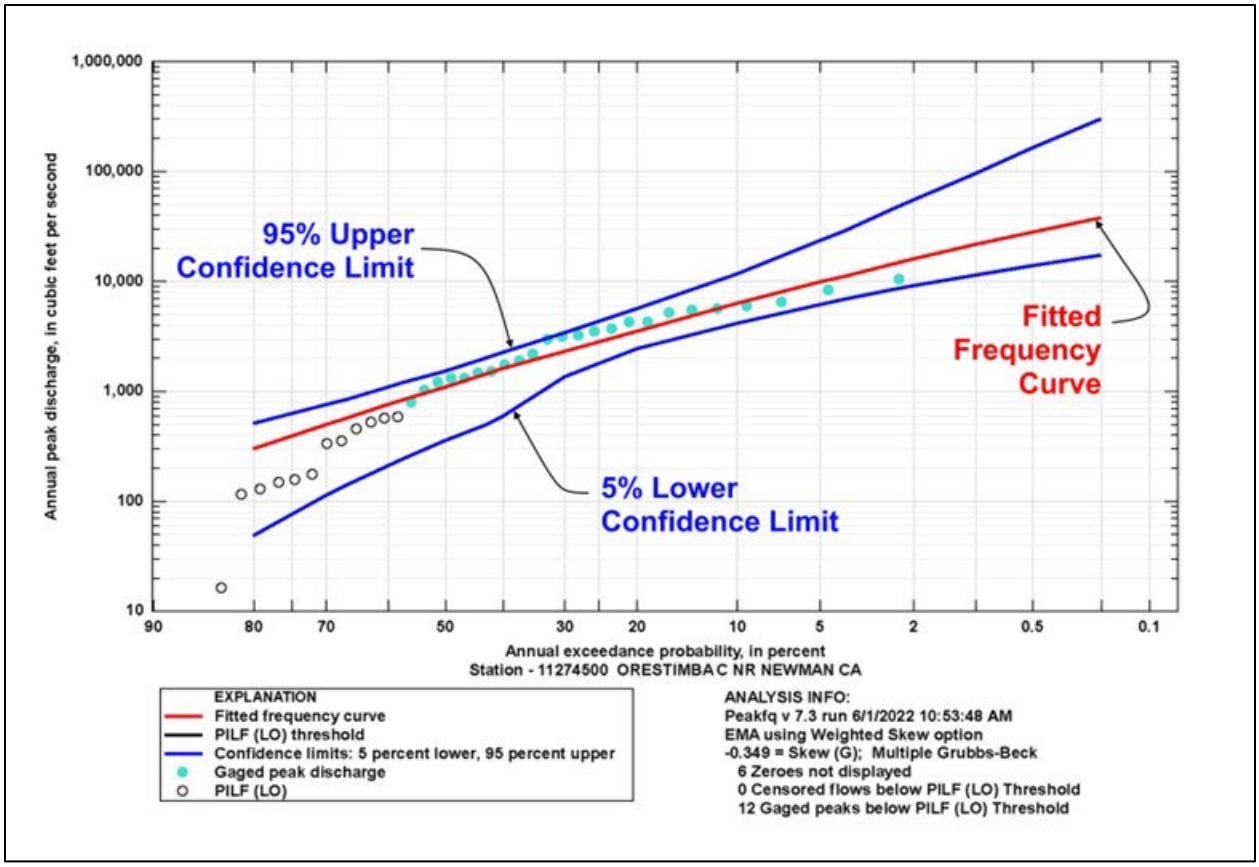

Figure 11.17. Fitted frequency curve, Orestimba Creek, California.

Solution:	The unadjusted frequency curve does not closely follow the trend in the measured data, especially in the lower tail. However, the upper portion, where design values are generally required, has reasonably good agreement. The EMA fitted curve is based, in part, on the station and generalized (regional) skews, which accounts for the regionalization of values from watersheds with different hydrologic characteristics than those of Orestimba Creek. By eliminating the zero and below-threshold flows, the fitted curve better represents the tendency of the higher magnitude flows generally relevant for typical highway drainage structures.

11.3.2 Regression Equations for the Southwestern United States

The USGS (Thomas et al. 1997) provides regression equations for the southwestern United States, which can be appropriate for arid areas in that part of the country. The general form for the equations is typical of many of the equations in the desert southwest where flow is a function of drainage area and mean annual precipitation. Section 6.1.4 provides a detailed description of these equations and their derivation.

11.3.3 Transmission Losses

To account for transmission losses, hydrologists in arid areas may adapt design hydrographs (see Chapter 8). When the initial part of a runoff hydrograph enters and flows through a dry stream channel, significant amounts of water can seep into the bed and banks of the stream, creating a transmission loss. Transmission loss rates vary widely over the duration of a flood hydrograph

and throughout a region. Such losses are important because they can significantly change the shape of a hydrograph, the total runoff volume, and the peak at downstream channel sections.

The losses depend on the material characteristics of the stream cross-section, the surface area of the beds and banks of the reach, the location of the ground water table, antecedent moisture of the cross-section, and the existence and type of vegetation in the stream. Designers generally do not consider antecedent moisture and vegetation because these can easily change.

Engineers can use the following methodology to estimate transmission losses for conditions with observed inflow and outflow data, no uniform lateral inflow, and no out-of-bank flow. Chapter 19 of the National Engineering Handbook discusses in detail this methodology and its assumptions and limitations (NRCS 2007b).

This method estimates the outflow volume Q_d at the end of a reach given the volume at the upper end of the reach, Q_u. Where measured data from previous storm events are available, a linear water yield model is used:

$$Q_d = \begin{cases} 0 & \text{for } Q_u \le Q_o \\ a + bQ_u & \text{for } Q_o < Q_u < Q_1 \\ Q_u - V & \text{for } Q_1 \le Q_u \end{cases} \quad (11.24)$$

where:

a, b	=	Regression coefficients
V	=	Maximum potential loss
Q_1	=	Maximum loss threshold volume
Q_o	=	Minimum loss threshold volume

Q_o is computed as:

$$Q_o = \frac{-a}{b} \quad (11.25)$$

This method includes the following constraints on the regression coefficients:

$$a \le 0 \le b \le 1 \quad (11.26)$$

If the regression coefficients do not meet these constraints, examine the data to detect data points that may cause the irrationality. Graphical analysis is useful for identifying potentially questionable data points.

The corresponding peak flow is computed by:

$$q_d = \begin{cases} 0 & \text{if } Q_d = 0 \\ \frac{(Q_d - Q_u)}{D} + b' q_u & \text{if } Q_d > 0 \end{cases} \quad (11.27)$$

where:

b’	=	Adjusted regression slope (b’ = b if $Q_u<Q_1$)
D	=	Duration of the inflow, s
q_u	=	Peak rate of inflow at the upper reach, ft^3/s (m^3/s)

Estimate the linear regression parameters from the measured data as:

$$a = \bar{Q}_d - b\bar{Q}_u \tag{11.28}$$

$$b = \frac{\sum_{i=1}^{n}\left[\left(Q_{di} - \bar{Q}_d\right)\left(Q_{ui} - \bar{Q}_u\right)\right]}{\sum_{i=1}^{n}(Q_{ui} - \bar{Q}_u)^2} \tag{11.29}$$

where:

$\bar{Q}_d$ = Mean outflow volume, ft^3/s (m^3/s)

$\bar{Q}_u$ = Mean inflow volume, ft^3/s (m^3/s)

NRCS (2007b) provides extensions of this method to account for lateral inflow and for sites lacking gaged data.

11.3.4 Alluvial Fans

Common in arid and semi-arid environments, alluvial fans are fan-shaped deposits of material at the place where a stream issues from a narrow valley of high slope onto a plain or broad valley of low slope. An alluvial cone is made up of the finer materials suspended in flow while a debris cone is a mixture of all sizes and kinds of materials. To understand the processes occurring in the formation of alluvial fans, designers draw on knowledge and expertise in hydrology, open channel hydraulics, geology, sediment transport, and geomorphology.

Alluvial fan creation depends on a source of sediment and debris and the means to convey this material to the depositional area. In the depositional area, increased flow area reduces the sediment carrying capacity of the stream.

Fan features include the topographic apex, which is the head of highest point on an active alluvial fan, and the hydrographic apex, which is the highest point on an alluvial fan where flow is least confined. An active alluvial fan has uncertain flow paths that may diverge and/or rejoin, as shown in Figure 11.18.

Flow paths may shift during each flow event and between flow events. Flows may be debris flows, water flows, or a mixture. These shifts and complex flows add significant design challenges for the highway designer crossing an alluvial fan.

Assessment of the hydrologic and hydraulic characteristics of alluvial fans consists of three phases. The first phase identifies the presence of alluvial fans within the project area from soils maps, geologic maps, topographic maps, and aerial photographs. A site visit also contributes invaluable information for identifying alluvial fans and their characteristics.

The second phase identifies the active and inactive regions of the alluvial fan. Inactive regions on the alluvial fans may be covered with vegetation and the channel will be incised and capable of carrying the design flow under the given conditions. Active areas will have newer sediment deposits and a relative lack of vegetation. Larger flows or different conditions may allow the flow to break out of the channel in a process called avulsion. The flow and new channel may cross the project area at a new location.

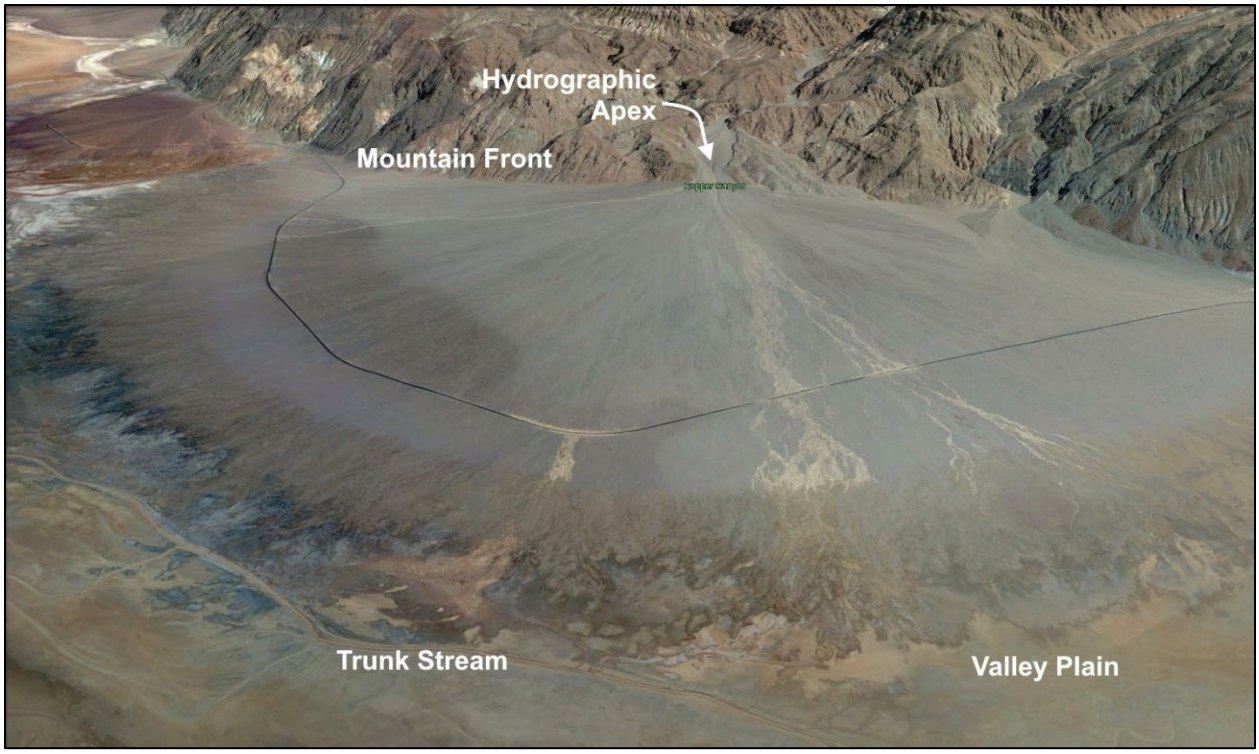

Figure 11.18. Example of an alluvial fan, Copper Canyon, California. Source: Google Earth.

The third phase of assessing alluvial fans describes the design flow at a given point on the fan. This is a function of not only the precipitation and factors affecting runoff, but also the probability of flooding at any location on the active portion of the fan. The sediment content of a flow may vary from negligible sediment to more than 50 percent sediment and debris, bulking the flow, and creating the need to design channel crossings and other structures for this increased flow volume. See Section 11.3.5 for bulked flow. An assessment of the conditional probability of flooding at all locations across the active portion of the fan will assist in determining the appropriate annual exceedance probability (AEP) flood at a particular location.

The reader may wish to consult the following resources for further information on alluvial fans:

- HEC-16 (FHWA 2023) presents an overview of analytical methods and hazard mitigation measures for alluvial fans.
- The Federal Emergency Management Agency's (FEMA's) *Guidance for Flood Risk Analysis and Mapping – Alluvial Fans* (FEMA 2016) discusses the three stages for identification and mapping of alluvial fan flooding, which are consistent with the aforementioned three phases of alluvial fan assessment.
- The U.S. Army Corps of Engineers (USACE) has developed a methodology and computer program that uses the principles of risk-based analyses to estimate flood hazards on alluvial fans. *Guidelines of Risk and Uncertainty Analysis in Water Resources Planning* (USACE 1992) discusses the methodology.
- FEMA developed a computer program called FAN that analyzes alluvial fans. It is provided and discussed in *FAN, An Alluvial Fan Flooding Computer Program User's Manual and Program Disk* (FEMA 1990), which is available by request from the FEMA Library.
- Two-dimensional modeling programs, such as SRH-2D (USBR 2008), may also be used to model flow on alluvial fans. These models can estimate the characteristics of flows with

a large amount of sediment, unconfined flow, split flow, mud and debris flow, and complex urban flooding.

- The USACE's *Assessment of Structural Flood-Control Measures on Alluvial Fans* (USACE 1993) lists several types of flood control measures used on alluvial fans and their advantages and disadvantages, and it provides several case studies of their application.

11.3.5 Bulked Flow

Bulking and bulked flow combines clear-water flow and high concentrations of sediment. This phenomenon occurs more often in mountainous terrain in arid and semiarid regions prone to wildfires that incinerate vegetation cover on the surfaces of soil. Bulking also occurs in mountainous regions where soil can be readily transported.

Estimating sediment concentrations and debris has a high degree of uncertainty due to the variability of sediment transport characteristics. In practical design, the clear-water assumption can underpredict flows by neglecting the consideration of sediment and debris loads, which can be significant in highly alluvial systems and recent burn areas. Therefore, bulked flows provide a factor of safety for the design of hydraulic structures with adequate capacity. Bulked flow is estimated from clear-water flow:

$$Q_B = c_{BF} Q_C \tag{11.30}$$

where:

Q_B = Bulked flow, ft^3/s (m^3/s)
c_{BF} = Bulking factor
Q_C = Clear-water flow, ft^3/s (m^3/s)

An equation for bulking factor is:

$$c_{BF} = \frac{(Q + Q_S)}{Q} = 1 + \frac{C_V}{(1 - C_V)} = 1 + \frac{C_W}{S_g(1 - C_W)} \tag{11.31}$$

where:

C_{BF} = Bulking factor
Q = Water discharge, ft^3/s (m^3/s)
Q_s = Sediment discharge, ft^3/s (m^3/s)
C_v = Concentration by volume (sediment volume/total volume)
S_g = Sediment specific gravity
C_w = Concentration by weight (sediment weight/total weight)

In some hydrologic regions, empirical relationships from historical observed sediment laden flood events establish the bulking factors. In burn prone zones, sediment and debris production can be significant enough to potentially block or clog downstream hydraulic structures.

HEC-19 (FHWA 2022a) provides more detailed information on sediment bulking, as well as countermeasures to protect downstream hydraulic structures. HEC-16 (FHWA 2023) also provides additional information on sediment bulking.

Example: Bulking Factor Application

In San Bernardino, California, engineers developed designs for the replacement of two adjacent bridges over City Creek, Boulder Avenue, and Base Line Street. The engineers designed both bridges to accommodate a 100-year discharge of 10,470 ft^3/s. The bridges are located in an area prone to high sediment concentration, and historically, bridges have washed out in the reach. To account for the potential increased flow volume the sediment loading would cause, the engineers adjusted the design discharge by a bulking factor of 1.5, consistent with the sediment concentration reflecting a mud flood. This resulted in a 100-year bulked discharge equal to 10,470 ft^3/s x 1.5 = 15,705 ft^3/s.

Page Intentionally Left Blank

Literature Cited

AASHTO 2000. *Model Drainage Manual*, Metric Edition, Appendices 7-E and 15-G American Association of State Highway and Transportation Officials, Washington, DC.

AASHTO 2014. *Drainage Manual*, 1st Edition, American Association of State Highway and Transportation Officials, Washington, DC.

ASCE 1960. *Design Manual for Storm Drainage*, American Society of Civil Engineers, New York.

Asquith, W.H. 1999. *Areal-Reduction Factors for the Precipitation of the 1-Day Design Storm in Texas*, U. S. Geological Survey, Water Resources Investigations Report 99-4267.

Asquith, W.H., J.R. Bumgarner, and L.S. Fahlquist 2003. "A Triangular Model of Dimensionless Runoff Producing Rainfall Hyetographs in Texas," *Journal American Water Resources Association*, 39(4), 911-921.

Asquith, W.H. and M. Roussel 2007. *An Initial Abstraction, Constant-Loss Model for Unit Hydrograph Modeling for Applicable Watersheds in Texas*, U.S. Geological Survey Scientific Investigations Report 2007-5243.

Asquith, W.H. and D.B. Thompson 2008. *Alternative Regression Equations for Estimation of Annual Peak-Streamflow Frequency for Undeveloped Watersheds in Texas using PRESS Minimization*, Scientific Investigations Report 2008-5084, USGS.

Asquith, W. and M. Roussel 2009. *Regression Equations for Estimation of Annual Peak-Streamflow Frequency for Undeveloped Watersheds in Texas Using an L-moment-Based, PRESS-Minimized, Residual-Adjusted Approach*, USGS Scientific Investigations Report 2009–5087.

Asquith 2021. Personal communication with Dr. William Asquith, Research Hydrologist, USGS on April 12, 2021.

Bartles, M., G. Brunner, M. Fleming, B. Faber, G. Karlovits, and J. Slaughter 2019. HEC-SSP Software Package, Version 2.2. U.S. Army Corps of Engineers, Hydrologic Engineering Center, Davis, CA.

Beard, Leo R. 1962. *Statistical Methods in Hydrology*, U.S. Army Engineer District, Corps of Engineers, Sacramento, CA.

Bicknell, B.R., J.C. Imhoff, J.L. Kittle Jr., T.H. Jobes, and A.S. Donigian, Jr. 2005. *Hydrological Simulation Program - Fortran (HSPF) User's Manual for Release 12.2*, USEPA National Exposure Research Laboratory, Athens, GA, in cooperation with U.S. Geological Survey, Water Resources Division, Reston, VA.

Biden, Joseph R. "Executive Order on Tackling the Climate Crisis at Home and Abroad (EO 14008), "Washington, DC.

Biden, Joseph R. "Executive Order on Advancing Racial Equity and Support for Underserved Communities Through the Federal Government (EO 13985)," January 2021.

Blum, A.G., P.J. Ferraro, S.A. Archfield, K.R. Ryberg 2020. "Causal Effect of Impervious Cover on Annual Flood Magnitude for the United States," *Geophysical Research Letters*, 47(5).

Brinson, M.M. 1993. *A Hydrogeomorphic Classification for Wetlands*, U.S. Army Corps of Engineers, technical report WRP-DE-4.

Capesius, J.P. and V.C. Stephens 2009. *Regional Regression Equations for Estimation of Natural Streamflow Statistics in Colorado*, U. S. Geological Survey Scientific Investigations Report 2009-5136.

Chow, V.T., D.R. Maidment, and L.W. Mays 1988. *Applied Hydrology*, McGraw-Hill, Inc., New York, NY.

Cowardin, l.M., V. Carter, F.C. Golet, and E.T. LaRoe 1992. *Classification of Wetlands and Deep Water Habitats in the United States*, U.S. Fish and Wildlife Service, FWS/OBS-79/31 (first printing 1979).

Crippen, J.R. and Bue, C.D. 1977. Maximum Floodflows in the Conterminous United States. U.S. Geological Survey Water-Supply Paper 1887.

Dalrymple, T. 1960. *Flood Frequency Analysis*. U. S. Geological Survey, Water Supply Paper 1543-A.

Downer, C.W. and F.L. Ogden 2006. *Gridded Surface Subsurface Hydrologic Analysis (GSSHA) User's Manual*, Version 1.43 for Watershed Modeling System 6.1, ERDC/CHL SR-06-1, USACE.

Dudley, R.W., S.A. Archfield, G.A. Hodgkins, B. Renard, K.R. Ryberg 2018. *Peak-Streamflow Trends and Change-Points and Basin Characteristics for 2,683 U.S. Geological Survey Streamgages in the Conterminous U.S.*, (ver. 3.0, April 2019), U.S. Geological Survey data release.

Dunne, T. and L. Leopold 1978. *Water in Environmental Planning*, W. H. Freeman & Co., San Francisco.

England, J.F., Jr., T.A. Cohn, B.A. Faber, J.R. Stedinger, W.O. Thomas, Jr., A.G. Veilleux, J.E. Kiang, and R.R. Mason, Jr. 2019. Guidelines for Determining Flood Flow Frequency—Bulletin 17C (ver. 1.1): U.S. Geological Survey Techniques and Methods, book 4, chap. B5.

Fang, X., K. Prakash, T. Cleveland, D. Thompson, and P. Pradhan 2005. "Revisit of NRCS Unit Hydrograph Procedures, " in *Proceedings of the ASCE Texas Section Spring Meeting,* Austin, Texas.

FEMA 1990. *FAN, An Alluvial Fan Flooding Computer Program User's Manual and Program Disk*, September.

FHWA 2002. *Highway Hydrology*, Hydraulic Design Series No. 2 (HDS-2), Second Edition, FHWA-NHI-02-001, Federal Highway Administration, Washington, DC.

FEMA 2016. *Guidance for Flood Risk Analysis and Mapping, Alluvial Fans*, Federal Emergency Management Agency, November.

FHWA 2014. "FHWA Order 5520: Transportation System Preparedness and Resilience to Climate Change and Extreme Weather Events," Federal Highway Administration, Washington, DC.

FHWA 2017. *Synthesis of Approaches for Addressing Resilience in Project Development*, Publication No. FHWA-HEP-17-082, Federal Highway Administration, Washington, DC.

FHWA 2015. *FHWA Environmental Justice Reference Guide*, Federal Highway Administration, Washington, DC, available online: http://www.ncfrpc.org/mtpo/FullPackets/MTPO/2021/ej_guide_fhwahep15035.pdf.

FHWA 2016. *Highways in the River Environment — Floodplains, Extreme Events, Risk, and Resilience,* Hydraulic Engineering Circular No. 17 (HEC-17), 2nd edition, FHWA-HIF-16-018, Federal Highway Administration.

FHWA 2021. “Policy on Using Bipartisan Infrastructure Law Resources to Build a Better America,” Federal Highway Administration, Washington, DC.

FHWA 2021. *Highways in the River Environment: Roads, Rivers, and Floodplains*, Hydraulic Engineering Circular No. 16 (HEC-16), FHWA-HIF-23-004, Federal Highway Administration.

FHWA 2022a. *Highway Hydrology: Evolving Methods, Tools and Data*, Hydraulic Engineering Circular No. 19 (HEC-19), FHWA-HIF-23-050, Federal Highway Administration.

FHWA 2022b. “Sustainable Highways Initiative, Overview” (website), Federal Highway Administration, Washington, DC, available online: https://www.sustainablehighways.dot.gov/overview.aspx#quest1, last accessed June 1, 2022.

FHWA 2022c, “FHWA State Asset Management Plan Under BIL,” May 5, 2022, Federal Highway Administration, Washington, DC.

Flynn, K.M., W.H. Kirby, and P.R. Hummel 2006. *User’s manual for program PeakFQ, Annual Flood Frequency Analysis Using Bulletin 17B Guidelines*, U.S. Geological Survey Techniques and Methods Book 4, Chapter B4.

Gotvald, A.J. and A.E. Knaak 2011. *Magnitude and Frequency of Floods for Urban and Small Rural Streams in Georgia, 2008*, Scientific Investigations Report 2011-5042.

Gumbel, E.J. 1941. “The Return Period of Flood Flows,” *Annals of Mathematical Statistics*, 12(2), 163-190.

Hawkins, R.H., T.J. Ward, D.E. Woodward, and J.A. Van Mullem 2009. *Curve Number Hydrology: State of the Practice*, American Society of Civil Engineers, Reston, VA.

Hedgecock, T.S. and K.G. Lee 2007. *Magnitude and Frequency of Floods for Urban Streams in Alabama*, Scientific Investigations Report 2010-5012, USGS.

Hecht, J.S. and R.M. Vogel 2020. “Updating Urban Design Floods for Changes in Central Tendency and Variability using Regression,” *Advances in Water Resources*, 136.

Helsel, D.R., R.M. Hirsch, K.R. Ryberg, S.A. Archfield, and E.J. Gilroy 2020. “Statistical Methods in Water Resources: U.S. Geological Survey Techniques and Methods,” chapter A3, *Book 4, Hydrologic Analysis and Interpretation*, U.S. Geological Survey.

Hodgkins, G. 1999. *Estimating the Magnitude of Peak Flows for Streams in Maine for Selected Recurrence Intervals*, USGS Water-Resources Investigations Report 99-4008.

Horton, R.E. 1945. “Infiltration and Runoff During the Snow-melting Season, with Forest-cover,” *Eos Transactions,* AGU, 26(1), 59-68.

Hosking, J.R.M. 1990. “L-moments: Analysis and estimation of distributions using linear combinations of order statistics,” *Journal of the Royal Statistical Society*, 52(1),105–124.

Hosking, J.R.M. 1992. “Moments or L-moments: An example comparing two measures of distributional shape,” *The American Statistician*, 46(3),186-189.

Huff, F.A. 1967. “Time Distribution of Rainfall in Heavy Storms,” *Water Resources Research*, 3(4), 1007-1019.

Huff, F.A. 1990. *Time Distributions of Heavy Rainstorms in Illinois*, Illinois State Water Survey Circular 173, Champaign, Illinois.

Kite, G.W. 1988. *Frequency and Risk Analyses in Hydrology*, Water Resources Publications, Littleton, CO.

Lewis, J.M. 2010. *Methods for Estimating the Magnitude and Frequency of Peak Streamflows for Unregulated Streams in Oklahoma*, U.S. Geological Survey Scientific Investigations Report SIR 2010-5137.

Linsley, Jr, R.K., M.A. Kohler, and J.L.H. Paulhus 1982. *Hydrology for Engineers*, McGraw-Hill.

Lombard, P.J. and G.A. Hodgkins 2015. *Peak Flow Regression Equations for Small, Ungaged Streams in Maine—Comparing Map-based to Field-based Variables*, U.S. Geological Survey Scientific Investigations Report 2015–5049.

Maidment, D.R., ed., 1993. *Handbook of Hydrology*, McGraw-Hill, Inc., New York, NY.

Marble, A.D. and X Riva 2002. *Guidelines for Selecting Compensatory Wetlands Mitigation Options*, NCHRP Report 182.

Martinec, J., A. Rango, and R.T. Roberts 2008. *Snowmelt Runoff Model (SRM) User's Manual*. New Mexico State University, Las Cruces, NM, February.

Mastin, M.C., C.P. Konrad, A.G. Veilleux, and A.E. Tecca 2016. *Magnitude, Frequency, and Trends of Floods at Gaged and Ungaged Sites in Washington, Based on Data through Water Year 2014* (ver 1.2, November 2017), U.S. Geological Survey Scientific Investigations Report 2016–5118.

McCuen, R.H. 1993. *Microcomputer Applications in Statistical Hydrology*, Prentice-Hall, Inc., Englewood Cliffs, NJ.

McCuen, R.H. 2012. *Hydrologic Analysis and Design,* fourth edition, Pearson Higher Education, Inc., Hoboken, NJ.

McCuen, R.H. and B.S. Levy 2000. "Evaluation of Peak Discharge Transposition," *Journal of Hydrologic Engineering*, ASCE, July.

Moglen, G.E. and D.E. Shivers 2006. *Methods for Adjusting U.S. Geological Survey Rural Regression Peak Discharges in an Urban Setting, Reston, Virginia*, U.S. Geological Survey, Scientific Investigations Report 2006-5270.

NOAA 1977. *Five- to 60-Minute Precipitation Frequency for the Eastern and Central United States*, NOAA Technical Memorandum NWS HYDRO-35, Silver Spring, Maryland.

NRCS 2002. "Treatment Classes," *National Engineering Handbook,* Part 630 Hydrology, Chapter 8.

NRCS 2004a. "Hydrologic Soil-Cover Complexes," *National Engineering Handbook,* Part 630 Hydrology, Chapter 9.

NRCS 2004b. "Estimation of Direct Runoff from Storm Rainfall," *National Engineering Handbook,* Part 630 Hydrology, Chapter 10.

NRCS 2004c. "Snowmelt," *National Engineering Handbook*, Part 630 Hydrology, Chapter 11.

NRCS 2007a. "Hydrographs," *National Engineering Handbook*, Part 630 Hydrology, Chapter 16.

NRCS 2007b. "Transmission Losses," *National Engineering Handbook*, Part 630 Hydrology, Chapter 19.

NRCS 2009a. "Hydrologic Soil Groups," *National Engineering Handbook,* Part 630 Hydrology, Chapter 7.

NRCS 2009b. *Small Watershed Hydrology WinTR–55 User Guide*, Natural Resources Conservation Service.

NRCS 2010. “Time of Concentration,” *National Engineering Handbook*, Part 630 Hydrology, Chapter 15.

NRCS 2015. *WinTR-20 User Guide (Version 3.10)*, Natural Resources Conservation Service.

NRCS 2019. “Storm Rainfall Depth and Distribution,” *National Engineering Handbook*, Part 630 Hydrology, Chapter 4.

Maidment, D.R., ed., 1993. *Handbook of Hydrology*, McGraw-Hill, Inc., New York, NY.

Over, T.M., R.J. Saito, A.G. Veilleux, J.B. Sharpe, D.T. Soong, and A.L. Ishii 2017. *Estimation of Peak Discharge Quantiles for Selected Annual Exceedance Probabilities in Northeastern Illinois* (ver. 2.0, November 2017), U.S. Geological Survey Scientific Investigations Report 2016–5050.

Paretti, N.V., J.R. Kennedy, L.A. Turney, and A.G. Veilleux 2014. *Methods for Estimating Magnitude and Frequency of Floods in Arizona, Developed with Unregulated and Rural Peak-flow Data through Water Year 2010*, U.S. Geological Survey Scientific Investigations Report 2014-5211.

Ponce, V.M. 1989. *Engineering Hydrology: Principles and Practices*, Prentice-Hall, Inc., Englewood Cliffs, NJ.

Ragan, R.M. 1971. *A Nomograph Based on Kinematic Wave Theory for Determining Time of Concentration for Overland Flow*, Report Number 44, Civil Engineering Department, University of Maryland at College Park.

Ries, K.G. 2006. “The National Streamflow Statistics Program: A Computer Program for Estimating Streamflow Statistics for Ungaged Sites,” Chapter A6, U.S. Geological Survey Techniques and Methods Report TM, Book 4, *Hydrologic Analysis and Interpretation*.

Ries, K.G., and J.A. Dillow 2006. *Magnitude and Frequency of Floods on Nontidal Streams in Delaware*, U.S. Geological Survey Scientific Investigations Report 2006-5146.

Riggs, H.C. 1968. “Some Statistical Tools in Hydrology,” Chapter A1, Techniques of Water Resources Investigations of the United States, Geological Survey, Book 4, *Hydrologic Analysis and Interpretation*.

Robeson, L.A., Aldrich, J.A., and Dickinson, R.E. 1988. Storm Water Management Model, Version 4 - Part B: EXTRAN Addendum, EPA/600/3-88/001b, NTIS, Springfield, VA, June.

Rossman, L.A. 2015. *Storm Water Management Model User’s Manual Version 5.1*, EPA- 600/R-14/413b, National Risk Management Research Laboratory, Office of Research and Development, USEPA.

Roussel, M.C., D.B. Thompson, X. Fang, T.G. Cleveland, and C.A. Garcia 2005. *Time-Parameter Estimation for Applicable Texas Watersheds*, Texas Department of Transportation Research Project Number 0–4696.

Sanders, T.G. (Editor) 1980. *Hydrology for Transportation Engineers*. U.S. Department of Transportation, Federal Highway Administration.

Sauer, V.B.,1974. *Flood Characteristics of Oklahoma Streams, Techniques for Calculating Magnitude and Frequency of Floods in Oklahoma with Compilations of Flood Data through 1971*, WRI Report 52-73, U.S. Geological Survey, Oklahoma City, OK.

Sauer, V.B., Thomas, W. O., Stricker, V. A., and Wilson, K. V. 1983. *Flood Characteristics of Urban Watersheds in the United States*. U.S. Geological Survey, Water Supply Paper 2207, Washington, DC.

SCS 1969. “Storm Rainfall Data,” *National Engineering Handbook,* Section 4 Hydrology, Chapter 4.

SCS 1986. *Urban Hydrology for Small Watersheds,* Technical Release No. 55, U.S. Department of Agriculture, Washington, DC.

Sherman, L.K. 1932. “Streamflow from Rainfall by the Unit-graph Method,” *Engineering News Record*, 108, 501-505.

Sherwood, J.M. 1994. *Estimation of Peak-Frequency Relations, Flood Hydrographs, and Volume-Duration-Frequency Relations of Ungaged Small Urban Streams in Ohio*, Water-Supply Paper 2432, USGS.

Snyder, F.M.1938. “Synthetic Unit Graphs.” *Trans., American Geophysical Union*, 19.

Thomas, B.E., H.W. Hjalmarson, and S.D. Waltemeyer 1997. *Methods of Estimating Magnitude and Frequency of Floods in the Southwestern United States*, USGS Water Supply Paper 2433.

Thomas, Jr., W.O. 1985. “A Uniform Technique for Flood Frequency Analysis.” *J. Water Resources Planning and Management*, ASCE, 111(3), 321-330.

Thomas, W.O. 1987. “The Role of Flood-Frequency Analysis in the U.S. Geological Survey,” in *Applications of Frequency and Risk in Water Resources* (V.P. Singh, ed.), D. Reidel Publ. Co., 463-484.

Thompson, D.B. 2004. *Climatic Adjustment of NRCS Curve Numbers*, TXDOT Project 2104-F, Texas Tech University.

Thompson, D.B. and T.G. Cleveland 2009. *Subdivision of Texas Watersheds for Hydrologic Modeling*, Texas Department of Transportation, FHWA/TX -0–5822–01–2.

Thornthwaite, C.W. and J.R. Mather 1957. “Instructions and Tables for Computing Potential Evapotranspiration and the Water Balance,” Laboratory of Climatology, *Publications in Climatology*, 8(1), Centerton, New Jersey.

USACE 1956. *Snow Hydrology*, NTIS PB 151 660, North Pacific Division. Portland, Oregon. June.

USACE 1990. *HEC-1 Flood Hydrograph Package, User’s Manual*, Hydrological Engineering Center.

USACE 1992. *Guidelines for Risk and Uncertainty Analysis in Water Resources Planning*, Report 92-R-1, Fort Belvoir, VA.

USACE 1993. *Assessment of Structural Flood-Control Measures on Alluvial Fans*, October.

USACE 1998. *Runoff from Snowmelt*, Engineering Manual 1110-2-1406, U.S. Army, Washington, DC, March.

USACE 2000a. *Hydrologic Modeling System HEC-HMS: Technical Reference Manual*, U.S. Army Corps of Engineers, Hydrological Engineering Center.

USACE 2000b. *Wetlands Engineering Handbook*, Environmental Laboratory, ERDC/EL TR-WRP-RE-21, U.S. Army Engineer Research and Development Center, compiled by Trudy J. Olin, Craig Fischenich, Michael R. Palermo, and Donald F. Hayes, March.

USACE 2020. *HEC-HMS User’s Manual,* Version 4.8. U.S. Army Corps of Engineers, Hydrologic Engineering Center.

USBR 2008. *SRH-2D version 2: Theory and User’s Manual*, Sedimentation and River Hydraulics – Two-Dimensional River Flow Modeling, U.S. Bureau of Reclamation.

USEPA 2019. “How Wetlands are Defined and Identified under CWA Section 404” (website), U.S. Environmental Protection Agency, Washington, DC, available online: www.epa.gov/cwa-404/how-wetlands-are-defined-and-identified-under-cwa-section-404, last accessed March 25, 2022.

USDOT 2021. “Climate Action Plan: Revitalizing Efforts to Bolster Adaptation and Increase Resilience, U.S. Department of Transportation, Washington, DC.

USDOT 2022. *Equity Action Plan*, U.S. Department of Transportation, Washington, DC, available online: https://www.transportation.gov/sites/dot.gov/files/2022-04/Equity_Action_Plan.pdf.

U.S. Weather Bureau, Office of Climatology 1960. “National Atlas of the United States, Mean Annual Total Snowfall (inches).”

U.S. Weather Bureau 1961. *Rainfall Frequency Atlas of the United States,* Technical Paper No. 40, U.S. Department of Commerce, Washington, DC.

Water Resources Council 1967. *A Uniform Technique for Determining Flood Flow Frequencies*, Bulletin 15, Washington, DC.

Water Resources Council 1982. *Guidelines for Determining Flood Flow Frequency, Bulletin 17B,* Interagency Advisory Committee of Water Data, U.S. Geological Survey, Reston, VA.

Welle, P., D.E. Woodward, and H.F. Moody 1980. *A Dimensionless Unit Hydrograph for the Delmarva Peninsula,* American Society of Agricultural Engineers Paper Number 80–2013, St. Joseph, MI.

Williams-Sether, T., W.H. Asquith, D.B. Thompson, T.G. Cleveland, and X. Fang 2004. *Empirical, Dimensionless, Cumulative-Rainfall Hyetographs Developed From 1959–86 Storm Data for Selected Small Watersheds in Texas*, U. S. Geological Survey Scientific Investigations Report 2004-5075.

Zeedyk, W.D. (1996). *Managing Roads for Wet Meadow Ecosystem Recovery,* FHWA-FLP-96-016, USDA Forest Service in Coordination with U.S. Department of Transportation, Federal Highway Administration.

Page Intentionally Left Blank

Appendix - Units

SI* (MODERN METRIC) CONVERSION FACTORS

APPROXIMATE CONVERSIONS TO SI UNITS

Symbol	When You Know	Multiply By	To Find	Symbol
		LENGTH		
in	inches	25.4	millimeters	mm
ft	feet	0.305	meters	m
yd	yards	0.914	meters	m
mi	miles	1.61	kilometers	km
		AREA		
in^2	square inches	645.2	square millimeters	mm^2
ft^2	square feet	0.093	square meters	m^2
yd^2	square yard	0.836	square meters	m^2
ac	acres	0.405	hectares	ha
mi^2	square miles	2.59	square kilometers	km^2
		VOLUME		
fl oz	fluid ounces	29.57	milliliters	mL
gal	gallons	3.785	liters	L
ft^3	cubic feet	0.028	cubic meters	m^3
yd^3	cubic yards	0.765	cubic meters	m^3
		NOTE: volumes greater than 1000 L shall be shown in m^3		
		MASS		
oz	ounces	28.35	grams	g
lb	pounds	0.454	kilograms	kg
T	short tons (2000 lb)	0.907	megagrams (or "metric ton")	Mg (or "t")
		TEMPERATURE (exact degrees)		
°F	Fahrenheit	5 (F-32)/9 or (F-32)/1.8	Celsius	°C
		ILLUMINATION		
fc	foot-candles	10.76	lux	lx
fl	foot-Lamberts	3.426	$candela/m^2$	cd/m^2
		FORCE and PRESSURE or STRESS		
lbf	poundforce	4.45	newtons	N
lbf/in^2	poundforce per square inch	6.89	kilopascals	kPa

APPROXIMATE CONVERSIONS FROM SI UNITS

Symbol	When You Know	Multiply By	To Find	Symbol
		LENGTH		
mm	millimeters	0.039	inches	in
m	meters	3.28	feet	ft
m	meters	1.09	yards	yd
km	kilometers	0.621	miles	mi
		AREA		
mm^2	square millimeters	0.0016	square inches	in^2
m^2	square meters	10.764	square feet	ft^2
m^2	square meters	1.195	square yards	yd^2
ha	hectares	2.47	acres	ac
km^2	square kilometers	0.386	square miles	mi^2
		VOLUME		
mL	milliliters	0.034	fluid ounces	fl oz
L	liters	0.264	gallons	gal
m^3	cubic meters	35.314	cubic feet	ft^3
m^3	cubic meters	1.307	cubic yards	yd^3
		MASS		
g	grams	0.035	ounces	oz
kg	kilograms	2.202	pounds	lb
Mg (or "t")	megagrams (or "metric ton")	1.103	short tons (2000 lb)	T
		TEMPERATURE (exact degrees)		
°C	Celsius	1.8C+32	Fahrenheit	°F
		ILLUMINATION		
lx	lux	0.0929	foot-candles	fc
cd/m^2	$candela/m^2$	0.2919	foot-Lamberts	fl
		FORCE and PRESSURE or STRESS		
N	newtons	0.225	poundforce	lbf
kPa	kilopascals	0.145	poundforce per square inch	lbf/in^2

*SI is the symbol for the International System of Units. Appropriate rounding should be made to comply with Section 4 of ASTM E380. (Revised March 2003)